DISSERTATION

SPATIOTEMPORAL VARIABILITY OF FLOODPLAIN SEDIMENT AND ORGANIC CARBON RETENTION IN MOUNTAIN STREAMS OF THE COLORADO FRONT RANGE

Submitted by

Nicholas A. Sutfin

Department of Geosciences

In partial fulfillment of the requirements

For the Degree of Doctor of Philosophy

Colorado State University

Fort Collins, Colorado

Spring 2016

Doctoral Committee:

Adviser: Ellen Wohl

Sara Rathburn
Stephanie Kampf
Thomas Borch

ABSTRACT

SPATIOTEMPORAL VARIABILITY OF FLOODPLAIN SEDIMENT AND ORGANIC CARBON RETENTION IN MOUNTAIN STREAMS OF THE COLORADO FRONT RANGE

Organic carbon retention along river corridors is an important regulator of ecosystem processing and a growing body of research indicates that carbon storage in floodplains can be a significant component of the terrestrial carbon cycle. The first part of this dissertation reviews the literature on carbon storage along floodplains and presents a conceptual model that highlights how sediment accumulation on floodplains in cool, high-elevation mountainous environments could result in some of the highest organic carbon per area among rivers in diverse regions. Investigation of floodplain sediment along three study reaches of mountain streams in the Colorado Front Range indicates that depth-averaged mean soil organic carbon content of ~3 – 5 % is accurately estimated using systematic random sample at ~10 sampling locations. Sediment samples from an additional 21 study reaches indicate correlations between organic carbon content and soil moisture, sample depth, grain size, relative elevation of the floodplain surface, thickness of soil at the sampling location, and valley confinement. Older mean pooled-radiocarbon ages of charcoal in floodplain sediment at two study reaches above 2900 m (>1200 y BP) compared to ages at two study reaches below 2400 m (<700 y) suggest an elevational control on floodplain disturbance regime in the Front Range. Observations of floodplain disturbance, which occurred during regional floods in September 2013, indicated an exponential increase in the amount of floodplain area disturbed with decreasing elevation and increasing

distance downstream. These results suggest potential correspondence with a previously documented shift in hydroclimatic disturbance regime at ~2300 m. Investigation of landscape-scale controls on organic carbon storage per area through comparisons of five different valley types (24 total study reaches) indicated that unconfined valleys may store more carbon per area and the dynamic environment in valley segments with multiple sub-parallel channels limits the capacity of floodplains to store sediment and associated carbon. The occurrence of multithread channels is dependent upon the presence of beavers or persistent logjams as biotic rivers of channel planform. Floodplains of single thread channels in unconfined valleys tend to be saturated and dominated by grasses and sedges, lacking the density of trees necessary to ensure continued recruitment of wood to the channel and into logjams. These results indicate that mountain streams are an important component of the terrestrial carbon cycle through carbon storage in unconfined single thread channels and ecosystem processing in more complex multithread channels.

ACKNOWLEDGEMENTS

This dissertation was made possible by many groups and individuals, but most importantly my wife, Marissa Sutfin. She continues to provide logistical, emotional, nutritional, and intellectual, support and inspiration during this great adventure. Her passion, awareness, and excitement inspire me intellectually, creatively, and artistically, and help in driving my desire to contribute meaningful science to the world. I am fortunate to witness the world around us partly through her eyes, which encourages me to keep balance and harness my own creativity in all that I do. I would dedicate this to her, but that seems a bit awkward, because this is her dissertation too. She is the light that guides me, and the song that keeps me going. Thank you, Marissa, for walking this path with me and enduring the struggles along the way.

Another person that was critical to making this dissertation possible is my adviser, Ellen Wohl. I certainly could not have completed this research and dissertation without her. I affirm what can be seen with all sincerity in the eyes of every one of Ellen's graduate students I've met, when they say, Ellen is the best adviser they could ever have. That is certainly the case for me. I aspire to keep up with her in the field and on paper. She seems to glide across the landscape and soar through publications. I cannot express enough gratitude for all her hard work, time, insight, guidance, trust, encouragement, and support that has made all this possible. Most of all, I am grateful for all the opportunities you have provided, Ellen. Thank you for helping to show me the world by literally providing opportunities to travel across oceans, move mountains (of soil), and encouraging questions regarding the processes I see in the landscape around me.

Many individuals in my fluvial family within the fluvial geomorphology group have provided encouragement, support, advice, and insight into graduate research methods and funding, life balance, and moving beyond graduate school. I am greatly appreciative to Sara Rathburn for her time, energy, and guidance in so many things academic and non-academic including opportunities in research and funding as well as advice regarding a future career in research and academia. Specifically, I want to thank Natalie Kramer-Anderson, Heidi Klingel, Katherine Lininger, Bridget Livers, JoJo Mangano, Derek Schook, Dan Scott, Lina Polvi, and Kris Jaeger for their friendship, time, energy, opinions, advice, encouragement and insight. I am especially grateful for open ears, collaboration, and support from Bridget, Katherine, and Derek. Your smiles and welcoming demeanor helped create a positive and productive atmosphere. Thanks for the great company in the field, Bridget, and allowing me to distract you, Katherine, with discussions regarding methods and interpretation. There is truly no better Flamily or fluvial geomorphic lineage of which I could be a part.

The CSU I-WATER program was also responsible for shaping my graduate experience throughout the course of my PhD, and thus influencing this dissertation. I am grateful to the PI's, Jorge Ramirez, LeRoy Poff, Scott Denning, and Niel Grigg for many great opportunities associated with the program. Other I-WATER faculty, including Brian Bledsoe and Tim Covino, have provided additional opportunities and expertise from which I have gathered valuable knowledge. A big thank you to Karleene Schindler for her organizational efforts and being the glue that helps hold I-WATER together. My fellow I-WATER Fellows helped create our experiences, particularly some of the leaders and fellow collaborators including Joel Sholtes, David Martin, Laurel Lynch, Dylan Harrison-Atlas, Rosie Records, Bella Oleksy, Whitney Beck, and Rod Lammers, and although not an official I-WATER Fellow, Tim Fegel. In particular, thank you Tim and Laurel for opening my eyes to the unseen, microbes! I am especially grateful for the leadership and sincere friendship of Joel, who has helped me keep balance and get more out of this experience. Thanks to you all.

I have many individuals to thank, who have helped me with my research in the field and in the laboratory including Ben Von Thaden, Dean Anderson, John Harris, Bryce Johnson, Joel Sholtes, Jon Garber, Laurel Lynch, Fernando Ugalde, Matheus Cruz Lima, Pam Wegener, and Michaela Woerndl. Thank you for enduring long hours either hiking, in many cases somewhat treacherously, while carrying heavy loads of soils or standing for long hours to help sieve soils.

I thank the Department of Geosciences and the Warner College of Natural Resources at Colorado State University including many individuals who offered support and opportunities. Thank you, Sharon Gale, who would drop anything to help me, or at least effectively multitask to do so. I express gratitude to Robin Reich for his insight and expertise regarding spatial statistics and for use of his unpublished Rspatial package. I thank Lee MacDonald for an amazing opportunity and his mentorship and camaraderie in a life-changing experience in Vietnam, which certainly influence how I think about teaching and my research.

I express gratitude to my PhD committee, including Sara Rathburn, Stephanie Kampf, and Thomas Borch for helping to guide my efforts and research questions. Your insight, conversation, encouragement, and questions help make me a better scientist and improve my interpretations of the work presented here and in future manuscripts. I also thank Tim Covino for filling in on my PhD committee during my preliminary exams and his guidance with other collaborative research.

This paper is based upon work supported by: National Science Foundation Grant No. DGE-0966346 "I-WATER: Integrated Water, Atmosphere, Ecosystems Education and Research Program" at Colorado State University; NSF Doctoral Research Dissertation Improvement Grant

#1536186; two research grants from the Geological Society of America; a research grant from the Colorado Scientific Society, and two research grants along with several scholarships and grants through the Department of Geosciences and Warner College of Natural Resources at Colorado State University.

DEDICATION

I dedicate this dissertation to my nephew, Kyson. Your energy and excitement invigorates my youthful nature. May you continue to follow your interests and utilize your magnificent intellect and talents to realize your dreams. In doing so, I am certain you will live a life that makes this world a better place and honors your kind and considerate heart.

TABLE OF CONTENTS

LIST OF TABLES

LIST OF FIGURES

Chapter 1: Introduction

Knowledge of physical processes in river corridors is crucial for understanding how rivers shape the landscape and support aquatic and riparian ecosystems and ecosystem services that societies depend upon. Understanding of riverine processes grows increasingly important as human population growth continues to encroach upon river corridors, land-use practices and flow regulation within rivers alter natural flow and sediment regimes (Poff et al., 1997; Wohl et al., 2015), and hydroclimatic regimes shift with a changing climate (Bates et al., 2008; Alexander, 2014). Although factors that influence the distribution and transport of organic matter and carbon in river corridors are important for aquatic and riparian ecosystems (Naiman et al., 2005; Allan and Castillo, 2007), they also have implications for global carbon cycling and terrestrial carbon reservoirs. Rivers have received considerable attention recently as significant components of global carbon budgets, partly because inland waters may serve as a medium for carbon storage within the geosphere (Cole et al., 2007; Battin et al., 2009; Aufdenkampe et al., 2011; Wohl et al., 2012). Understanding the spatial and temporal variability of floodplain sediment and associated organic carbon retention thus provides insight into hotspots for ecosystem processing of carbon and potential for long-term storage.

Projected warming, decreased snowpack, earlier annual snowmelt, increased frequency of severe wildfire (Westerling et al., 2006), insect infestation (Kurz et al., 2008), increased likelihood of severe storms (Bates et al., 2008), altered flow regimes, decline in hydrologic connectivity (Alexander, 2014), and land-use disturbances (Wohl, 2006) make relatively unaltered, small mountain streams at high elevations in the western United States especially vulnerable to future climate and land-use changes. As the primary sources of allochthonous organic matter to rivers, headwater streams provide the foundation for riverine food webs (Allan and Castillo, 2007). The spatial distribution of organic carbon in river corridors also depends upon localized physical characteristics and geomorphology of rivers and valley bottoms. I discuss river channel complexity in the context of spatial variations in bedforms, channel planform, and valley-bottom geometry, and examine how these variations influence organic carbon retention and distribution.

To investigate the spatial and temporal variability of organic carbon in riverine corridors, I investigate the role of hydroclimatically driven fluvial disturbance regime, elevation, longitudinal position within a watershed, reach-scale (10^1-10^2 m lengths) valley geometry, floodplain topography, and biogeomorphic drivers of channel planform along floodplains of mountain streams in the Colorado Front Range. My research focused on North Saint Vrain Creek and its tributaries and also included study reaches along Mill Creek, Big Thompson River, the South Fork Cache La Poudre River, and numerous reaches along Glacier Creek in Rocky Mountain National Park. Extensive fieldwork to survey floodplains and sample floodplain sediment and charcoal along 24 study reaches provides insight into floodplain sediment dynamics and associated organic carbon retention in mountain streams. Extreme precipitation and widespread floods across the Colorado Front Range in September of 2013 provided a unique opportunity to combine data that represent average long-term conditions in floodplain sediment and charcoal with direct observations of floodplain sediment dynamics.

This research, which developed as a continuation of a small pilot study, investigates additional hypotheses and tests our original findings by increasing the sample size and expanding the coverage of study sites across multiple basins. In an examination of carbon storage per area along 8 different combinations of valley types and forest stand age, Wohl et al. (2012) found that relatively unconfined valley segments that hosted streams with multiple, subparallel channels (multithread channels) across the valley bottom stored a disproportionately large amount of carbon per area as standing biomass, litter, humus, and especially, sediment and downed wood. Multithread channels stored 85% of the estimated carbon across valley bottoms, but constituted only 25% of the total river kilometers in North Saint Vrain Creek watershed. Although earlier work had not distinguished river corridors when estimating regional carbon stocks (e.g., Bradford et al., 2008), Wohl et al. (2012) estimated that rivers could store as much as 25% of the carbon in uplands within only 1% of the surface area of a watershed. These inferences, however, were based on a single study reach for each of the eight categories of valley and channel geometry.

I begin by synthesizing other studies that quantify carbon storage in rivers to compare these results to current work on rivers in other regions. Chapter 2, *Banking Carbon*, provides an extensive introduction, background, and literature review of organic carbon storage and the physical factors influencing retention in floodplains and riparian ecosystems. In this chapter, I outline the significance of carbon in rivers and highlight the potential importance of mountain rivers in terrestrial carbon budgets. Previous research on carbon storage in floodplains does not provide guidelines for sampling floodplain sediment to estimate reach-average global mean organic carbon content, so I examine this topic in chapter 3.

Based on extensive sampling of floodplain sediment along three study reaches in North Saint Vrain Creek watershed, I assess the variability in the estimate of mean organic carbon content along each study reach using depth-averaged arithmetic mean, inverse distance weighting, and kriging in chapter 3. I then conduct a statistical analysis to determine how many samples are needed to reduce variability and bias of the estimated mean organic carbon content along each study reach using the preferred method. Additionally, I investigate soil characteristics and spatial relationships across the floodplain as covariates and potential predictors of soil organic carbon content at all study sites.

Recognizing that organic carbon content of floodplain soil may have little significance in long-term storage if the residence time of the host sediment is very short, I investigate floodplain disturbance regime in chapter 4. Using radiocarbon ages of charcoal from floodplain sediment, observed floodplain disturbance from the 2013 flood, and volume estimates of net erosion and deposition at two study reaches along North Saint Vrain Creek, I examine the potential implications for floodplain sediment transit time associated with a hydroclimatic shift and distinct change in magnitude and frequency of peak flows and debris flows at 2300 m elevation (Jarrett, 1990). I test the hypothesis that floodplain sediment transit time is positively and non-linearly correlated with elevation. The rationale behind this hypothesis is that extreme events resulting from large convective thunderstorms below 2300 m on the Colorado Front Range result in lower transit time of floodplain sediment compared to higher elevation sites where extreme events are not documented as exceeding snowmelt-dominated hydrographs.

Placing floodplain disturbance and organic carbon content of floodplain soils into a spatial context, chapter 5 examines the potential role of valley geometry and channel complexity on organic carbon storage per area of valley bottom. I test two a hypotheses valley confinement and floodplain sediment transit time. The first hypothesis states that floodplain sediment transit time is positively correlated with valley confinement. The second hypothesis is that channel avulsion and erosion associated with multithread channels (Collins et al., 2012) limits the mean age of floodplain sediment, resulting in shorter transit times compared to single thread channels in unconfined valley segments. In presenting my results and differences among the study reaches, I provide a conceptual model to explain the observations and importance of geomorphic drivers of organic carbon storage in mountain streams. Finally, I conclude by placing these findings into perspective and providing insights into floodplain carbon storage and suggestions for future work.

References

Alexander L. 2014. Connectivity of Streams and Wetlands to Downstream Waters: A Review and Synthesis of the Scientific Evidence (External Review Draft) . US EPA National Center for Environmental Assessment. Environmental Protetion Agency: Washington DC [online] Available from: http://cfpub.epa.gov/ncea/cfm/recordisplay.cfm?deid=238345 (Accessed 26 January 2015)

Allan JD, Castillo MM. 2007. Stream Ecology . Second Edition. Springer: Dordrecht, The Netherlands

Aufdenkampe AK, Mayorga E, Raymond PA, Melack JM, Doney SC, Alin SR, Aalto RE, Yoo K. 2011. Riverine coupling of biogeochemical cycles between land, oceans, and atmosphere. Frontiers in Ecology and the Environment **9** : 53–60. DOI: 10.1890/100014

Bates BC, Kundzewicz ZW, Palutikof JP. 2008. Climate change and water . Technical Report. IPCC: IPCC Secretariat, Geneva

Battin TJ, Luyssaert S, Kaplan LA, Aufdenkampe AK, Richter A, Tranvik LJ. 2009. The boundless carbon cycle. Nature Geoscience **2** : 598–600. DOI: 10.1038/ngeo618

Cole JJ, Prairie YT, Caraco NF, McDowell WH, Tranvik LJ, Striegl RG, Duarte CM, Kortelainen P, Downing, JA Middelburg JJ, Melack J. 2007. Plumbing the Global Carbon Cycle: Integrating Inland Waters into the Terrestrial Carbon Budget. Ecosystems **10** : 172–185. DOI: 10.1007/s10021-006-9013-8

Collins BD, Montgomery DR, Fetherston KL, Abbe TB. 2012. The floodplain large-wood cycle hypothesis: A mechanism for the physical and biotic structuring of temperate forested alluvial valleys in the North Pacific coastal ecoregion. Geomorphology **139–140** : 460–470. DOI: 10.1016/j.geomorph.2011.11.011

Jarrett RD. 1990. Paleohydrologic techniques used to define the spatial occurrence of floods. Geomorphology **3** : 181–195. DOI: 10.1016/0169-555X(90)90044-Q

Kurz WA, Dymond CC, Stinson G, Rampley GJ, Neilson ET, Carroll AL, Ebata T, Safranyik L. 2008. Mountain pine beetle and forest carbon feedback to climate change. Nature **452** : 987–990. DOI: 10.1038/nature06777

Naiman RJ, Decamps H, McClain ME, Likens GE. 2005. RIparia: Ecology, conservation, and management of streamside communities . Academic Press: Burlington, MA

Poff NL, Allan JD, Bain MB, Karr JR, Prestegaard KL, Richter BD, Sparks RE, Stromberg JC. 1997. The natural flow regime. BioScience **47** : 769–784.

Westerling AL, Hidalgo HG, Cayan DR, Swetnam TW. 2006. Warming and Earlier Spring Increase Western U.S. Forest Wildfire Activity. Science **313** : 940–943. DOI: 10.1126/science.1128834

Wohl E. 2006. Human impacts to mountain streams. Geomorphology **79** : 217–248. DOI: 10.1016/j.geomorph.2006.06.020

Wohl E, Bledsoe BP, Jacobson RB, Poff NL, Rathburn SL, Walters DM, Wilcox AC. 2015. The Natural Sediment Regime in Rivers: Broadening the Foundation for Ecosystem Management. BioScience : biv002. DOI: 10.1093/biosci/biv002

Wohl E, Dwire K, Sutfin N, Polvi L, Bazan R. 2012. Mechanisms of carbon storage in mountainous headwater rivers. Nature Communications **3** : 1263. DOI: 10.1038/ncomms2274

Chapter 2: A review of organic carbon storage and physical factors influencing retention in floodplains and riparian ecosystems

Summary

Rivers are dynamic components of the terrestrial carbon cycle and provide important functions in ecosystem processes. Although rivers act as conveyers of carbon to the oceans, rivers also retain carbon within riparian ecosystems along floodplains, with potential for long-term (> 10^2 y) storage. Research in ecosystem processing emphasizes the importance of organic carbon (OC) in river systems, and estimates of OC fluxes in terrestrial freshwater systems indicate that a significant portion of terrestrial carbon is stored within river networks. Studies have examined soil OC on floodplains, but research that examines the potential mechanistic controls on OC storage in riparian ecosystems and floodplains is more limited. I emphasize three primary OC reservoirs within fluvial systems, 1) standing riparian biomass, 2) dead biomass as large wood (LW) in the stream and on the floodplain, and 3) OC on and beneath the floodplain surface, including litter, humus, and soil organic carbon (SOC). This review focuses on studies that have framed research questions and results in the context of OC retention, accumulation and storage within the three primary pools along riparian ecosystems. In this paper, I (i) discuss the various reservoirs for OC storage in riparian ecosystems, (ii) discuss physical conditions that facilitate carbon retention and storage in riparian ecosystems, (iii) provide a synthesis of published OC storage in riparian ecosystems, (iv) present a conceptual model of the conditions that favor OC storage in riparian ecosystems, (v) briefly discuss human impacts on OC storage in riparian ecosystems, (vi) and highlight current knowledge gaps.

2.1 Introduction: Why does river organic matter matter?

Rivers distribute and deliver sediment and organic carbon through the landscape. Spatial distribution of carbon within riparian ecosystems regulates delivery to the ocean and atmosphere, retention and storage within the geosphere, and ecosystem processing for the foundation of foodwebs (Vannote et al., 1980; Allan and Castillo, 2007; Aufdenkampe et al., 2011). I frame this discussion regarding distribution and retention of organic carbon in rivers around floodplains and riparian ecosystems.

I refer to floodplains as the relatively flat topographic surfaces adjacent to rivers that experience inundation on annual to decadal time scales, to be distinguished from adjacent uplands that are not regularly inundated. Floodplains are estimated to cover between 0.8 x 10^6 and 2 x 10^6 km^2 globally (Leopold et al., 1964; Tockner and Stanford, 2002; Mitsch and Gosselink, 2015). I refer to riparian ecosystems as the biota and biogeochemical processes occurring at the interface of terrestrial and freshwater ecosystems along floodplains (Gregory et al., 1991; Naiman et al., 2005). Riparian ecosystems provide ecological and societal benefits such as flood attenuation and denitrification, which is largely dependent on carbon content (Devito et al., 2000; Hill et al., 2000; Wohl, 2000a, 2000b; Craig et al., 2008), but this discussion focuses on the physical attributes of rivers and factors that regulate retention of OC as influenced by climate, geology, hydrology, and geomorphology. First, I briefly review relevant aspects of riparian ecosystems and the services they provide to create the context for more detailed discussion of OC dynamics in rivers including ecosystem processing of OC and terrestrial carbon budgets.

2.1.1 Physical complexity and river ecosystem processing of OC

Position along river networks and resulting channel and floodplain characteristics regulate components of riparian ecosystems, the local source of OC inputs, distribution and transportation (Tank et al., 2010) of OC, biogeochemical processing (Battin et al., 2008), and resulting ecosystem services.

I adopt the river-centric convention of stream ecologists when referring to allochthonous organic matter (OM) as that which is derived from outside of the channel including riparian vegetation (e.g., leaves, needles, wood), and autochthonous organic matter as that which is produced through primary production in the stream (e.g., algae, periphyton). Allochthonous and autochthonous OM provide the trophic foundation for river ecosystems (Vannote et al., 1980; Allan and Castillo, 2007). Organic matter is the primary source for organic carbon (OC) within rivers when compared with fossilized carbon (kerogen; Allan and Castillo, 2007). Approximately 45-50% of OM by mass, depending on species, is OC (Allan and Castillo, 2007). Usage of OM and OC throughout this manuscript is not interchangeable, but instead specifically refers to one or the other.

Terrestrial allochthonous detrital material entering headwater streams is the primary source of OM input to river systems (Vannote et al., 1980; Gomi et al., 2002; Allan and Castillo, 2007; Hilton et al., 2008; Chapin III et al., 2011). These OM inputs are a major source of OC and provide the foundation for biogeochemical processing and foodwebs in aquatic and terrestrial environments (Allan and Castillo, 2007). Narrow headwater channels receive high inputs of plant debris as coarse particulate organic matter (CPOM, > 1 mm) from riparian ecosystems and uplands, which is broken down into fine particulate organic matter (0.5 μm < FPOM < 1 mm) by aquatic invertebrates and microbes within the channel, on the floodplain, and within the subsurface (Wagener et al., 1998; Allan and Castillo, 2007; Chapin III et al., 2011). Dissolved organic carbon (DOC; < 0.5 μm) can be derived from living biomass or leached from POM, and can remain in channel and floodplain sediment through adsorption to mineral grains, constituting a significant amount of OC in sediment and soil (Allan and Castillo, 2007). Downed large wood (LW; >10 cm in diameter and 1m in length) also provides a significant source of particulate organic matter (POM; including CPOM and FPOM) to river systems (Ward and Aumen, 1986). In larger rivers that receive more abundant sunlight, autochthonous primary production is a more significant source of OM present in the channel.

The degree of physical channel complexity along a river segment influences the distribution and concentration of POM and OC. I refer to channel complexity qualitatively as the (1) magnitude of channel boundary irregularities, (2) sinuosity, radius of curvature and wave length of channel meanders and bends, (3) number of channels across the valley bottom, (4) number and spacing of flow obstructions, (5) variation in bed slope and bedforms, (6) size and variation in bed material, (7) type, abundance, and density of aquatic and riparian vegetation, and the (8) number and spacing of steps, pools and riffles for any stream or river segment. Many factors of channel complexity are analogous to Manning's channel roughness coefficient (Arcement and Schneider, 1989), which incorporates roughness components as well as slope, planform, and bedforms. Thus, a highly incised, straight channel lined by concrete would have a very low complexity. In contrast, a sinuous headwater stream of the same size with channel spanning logjams approximately every few meters, 4-5 threads of channelized flow across the valley bottom, abundant steps and backwater pools, channel substrate alternating from boulders and cobbles, and lined with abundant willows and trees would have a very high degree of channel complexity.

Rivers with a high degree of channel complexity (1) increase the residence time of water, sediment, large wood, and POM within sites of flow separation and off-channel areas such as the floodplain and hyporheic zone, (2) maintain biological hotspots that facilitate breakdown of OM, and (3) effectively filter excess nutrients and DOC from surface and shallow subsurface waters (Bilby, 1981; Stallard, 1998; Kasahara and Wondzell, 2003; Battin et al., 2008, 2009; Hilton et al., 2008). Riparian ecosystems, particularly those with high degrees of channel complexity, facilitate retention and complex biogeochemical processing of pollutants and excess nutrients (Devito et al., 2000; Battin et al., 2008; Tank et al., 2010), which can be present in high concentrations in highly impacted watersheds (Devito et al., 2000; Allan and Castillo, 2007; Craig et al., 2008). High dissolved organic carbon (DOC) concentrations in surface waters create potential risks for human consumption because carcinogenic disinfectant byproducts are produced when DOC is combined with chlorine at water treatment plants (Trussell and Umphres, 1978; Coffin et al., 2000; Sapkal and Valunjkar, 2013). In watersheds with a substantial proportion of agricultural land use, C content of riparian soils is an important factor for water quality and amelioration of high nitrate concentrations because denitrification can be C limited (Hill, 1996; Hill et al., 2000) and is largely dependent on availability of OM in riparian soils (Devito et al., 2000).

River fluxes of OM and thus OC exert an important control on freshwater and nearshore ecosystems and the ecosystem services they provide. Physical and biological processes in rivers influence OC retention over varying time scales (Battin et al., 2008, 2009; Aufdenkampe et al., 2011; Wohl et al., 2012a), and understanding these processes is crucial for determining potential impacts of global climate change, land use, and land-cover changes on OC dynamics within river systems. Improved understanding of the distribution and retention of OC in river systems can continue to inform river management practices and foster opportunities for ecosystem processing of excess nutrients.

2.1.2 Rivers and the global carbon cycle

Global C budgets, which estimate the annual exchange of C between short-term reservoirs (i.e., atmosphere, vegetation, soil, near-surface sea water), do not fully account for CO_2 released to the atmosphere annually. A significant portion of OC (~ 2 Pg C yr^{-1}) is assumed to be taken up by terrestrial sources (Le Quéré et al., 2009; Ballantyne et al., 2012). However, current estimates of oceanic and terrestrial C sinks do not fully account for the total C released annually to the atmosphere through burning of fossil fuels.

The terrestrial C component contains the largest uncertainty of all aspects of the global C cycle (Gregory et al., 2009), yet appears to be able to absorb an increasing amount of CO_2 (Ballantyne et al., 2012). Battin et al. (2009a) and Aufdenkampe et al. (2011) estimate that a significant portion (~22%) of C entering headwater streams is unaccounted for by delivery to the oceans or CO_2 outgassing from metabolism by aquatic biota. This suggests that C is being stored somewhere within the terrestrial environment along river systems (Figure 2.1; Stallard, 1998; Battin et al., 2009; Aufdenkampe et al., 2011; Hoffmann et al., 2013). This represents a potential C reservoir previously unaccounted for in C stock estimates, which may help to close the missing terrestrial C sink (Cole et al., 2007). Wetlands have been identified as significant C reservoirs (Kayranli et al., 2010) and the largest source of net ecosystem productivity among land surface types (Schulze et al., 2005), but forest inventories of vegetation and soil organic carbon (SOC) have not examined surfaces adjacent to rivers as distinct landforms with different SOC content than those of the adjacent uplands. Despite being a dynamic component of the terrestrial C cycle, river systems are among the least investigated freshwater landscape features as potential long-term C reservoirs (Cole et al., 2007). Limited research conducted to date, however, suggests that river networks might store a significant proportion of terrestrial C (Jaramillo et al., 2003; Walter and Merritts, 2008; Cierjacks et al., 2010; Wohl et al., 2012b; Hoffmann et al., 2013, 2014a).

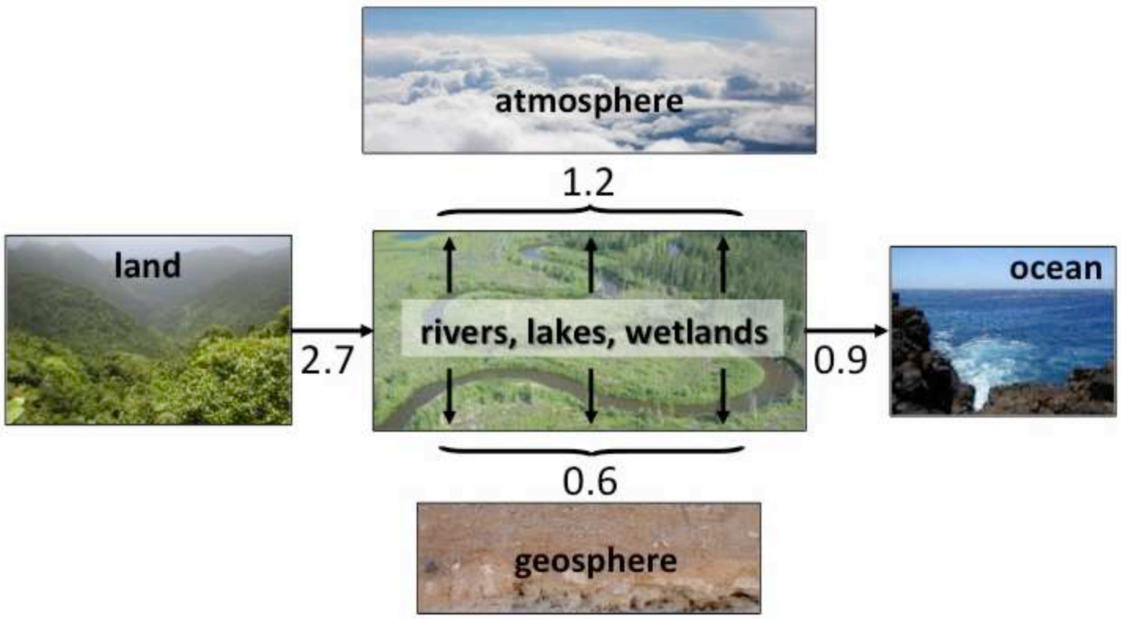

Figure 2.1. Modified from Aufdenkampe et al. (2011; Figure 3). Values represent carbon fluxes in petagrams of carbon per year (Pg C yr^{-1}) based on calculations from Battin et al. (2009). Surface water facilitates fluxes between terrestrial carbon reservoirs, delivering carbon to the atmosphere and the ocean. Recent research has shown that only a relatively small proportion of carbon makes it to the ocean after i) outgassing to the atmosphere following metabolism by biota and ii) sinks to the geosphere. This suggests that rivers facilitate terrestrial carbon storage.

The objectives of this paper are to (i) summarize the primary reservoirs for OC in river systems, (ii) discuss differences in fluvial environments that can influence OC storage with respect to landscape- and local-scale controls, (iii) summarize published data of OC stocks in riparian ecosystems, and (iv) discuss gaps in existing knowledge of OC in fluvial systems. Although human activities very likely strongly affect OC dynamics in fluvial environments, I address these potential effects only briefly in this review.

2.2 Organic carbon reservoirs in riparian ecosystems

Organic carbon is stored along river networks in four primary reservoirs: (1) Standing riparian biomass, (2) large downed wood, (3) sediment, including OM, litter and humus on or beneath the surface within the channel and across the floodplain, and (4) instream biomass (Figure 2.2). Work to quantify and compare autochthonous net primary production in stream and allochthonous litter inputs indicates wide differences among climatic regions, such that OC values per area are dominated by primary productivity in warmer climates and allochthonous OM in cooler climates (Allan and Castillo, 2007). Comparison of values from sediment, wood, and above-ground biomass with those of instream biomass (i.e., benthic invertebrates, filamentous algae, fine benthic organic matter, and fish) of boreal streams from Naiman et al. (1987) shows that storage within instream OC stocks per area is relatively insignificant (Figure 2.2; 0.8-4.8 Mg C ha-1). Comparison with values from work by Findlay et al. (2002) in arid, temperate, and tropical streams indicates similar low values for instream biomass (0.21-1.9 Mg C ha-1). Organic carbon delivered by streams can contribute to riparian ecosystems during high flows (Pinay et al., 1992; Hall et al., 2009; Tank et al., 2010) and when physically removed from the channel by biotic activities. However, because OC fluxes from the channel to the floodplain are incorporated into surface and subsurface sediment and instream biomass values are small compared to the other three reservoirs, I do not focus on OC within active channels as a major reservoir for OC in river ecosystems. Additionally, instream biomass and OC fluxes are variable spatially and temporally, making instream OC reservoirs extremely transient. Standing biomass in riparian ecosystems, on the other hand, is much larger (7 - 2794 Mg C ha^{-1}) and can include trees that store carbon for 10^2 – 10^4 years. For these reasons, I focus in this paper on the largest and most persistent OC reservoirs in riparian ecosystems: (1) standing riparian biomass, (2) large downed wood (LW), and (3) floodplain sediment and OM.

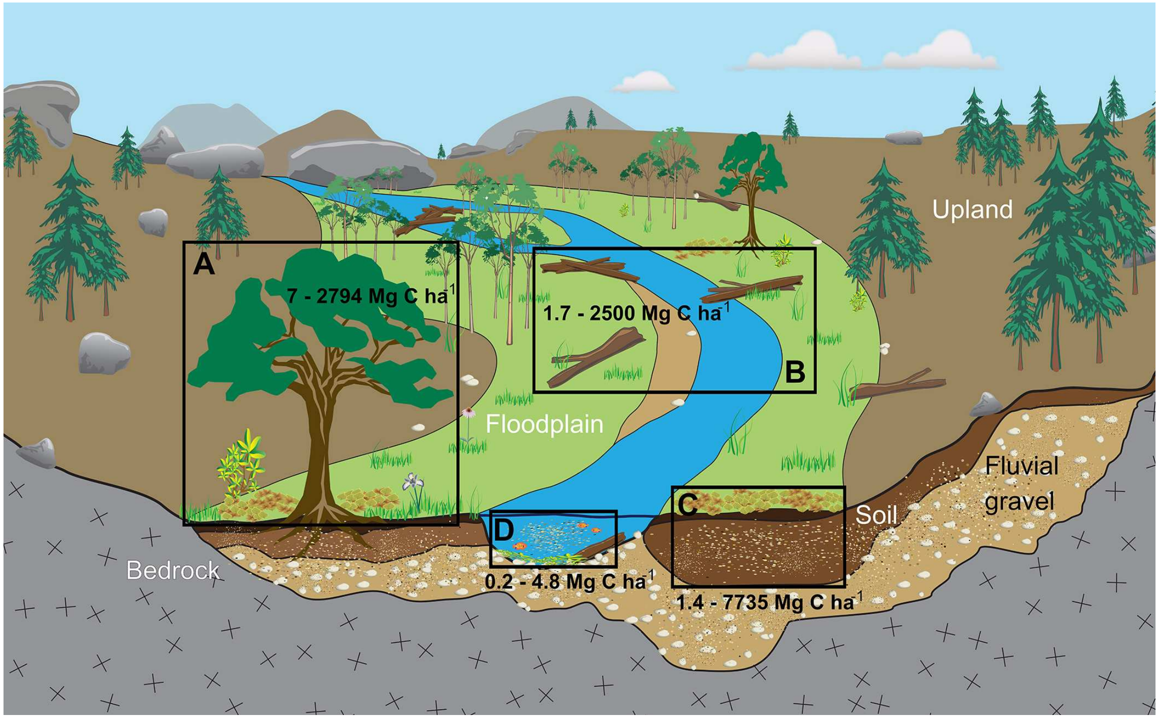

Figure 2.2. Organic carbon is stored within four primary reservoirs in river systems: above- and belowground standing biomass as riparian vegetation (A), large instream and downed wood on the floodplain (B), sediment on the floodplain surface and in the shallow subsurface, including soil organic carbon, litter and humus (C), and in-stream biomass including filamentous algae, periphyton, benthic invertebrates, fish, and particulate organic matter (D). Values indicate the estimated range of organic carbon per area (Mg C ha^{-1}) from studies cited in this review. Values from Naiman et al. (1987) and Findlay et al. (2002) show that instream biomass (D) accounts for a relatively small portion of carbon stored in river systems per area when compared to the other three reservoirs.

River valleys, floodplains, and riparian ecosystems funnel water, sediment, and associated OC through the landscape. Geologic, climatic, hydrologic, and geomorphic characteristics of the landscape influence the travel time and retention of water, sediment, and OC along this journey and provide opportunities for storage. Riparian ecosystems tend to contain more moisture than adjacent uplands, and commonly exhibit distinct vegetation types. This means that riparian ecosystems may store more OC per area than other, more thoroughly examined components of the landscape such as upland forests, grasslands, and agricultural plots. Work in tropical regions, for example, indicates that floodplains store more OC than drier, adjacent uplands (Jaramillo et al., 2003).

Quantitative comparisons among sites will be discussed later, following a review of OC storage in riparian ecosystems. First, I discuss potential controls on OC retention along river systems (Figure 2.3). I discuss factors that dictate OC storage in a variety of settings, which can result in widely different magnitude or direction of influence, depending on the region.

2.3 Landscape-scale controls on organic carbon in riparian ecosystems

The distribution of OC at the landscape scale (10^2-10^6 km^2) depends largely upon factors that influence gross primary production and the decay, transport, and accumulation of OM (Dodds et al., 2015). These large-scale drivers include geologic setting and ecoregion (Figure 2.3). Geologic setting refers to tectonic history, lithology, and geologic structure. Ecoregions or biomes characterize biogeographic regions by climate, soil type, and biotic communities. Differences in climate influence physical and chemical weathering of rocks and sediment, available moisture, vegetation communities within a given biome, soil development, and decomposition of organic matter.

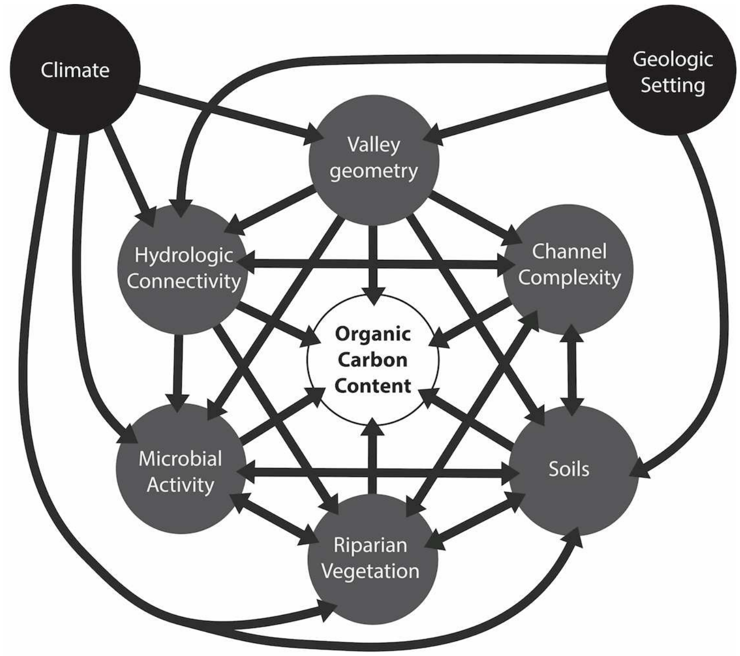

Figure 2.3. A conceptual diagram of regional and local controls on organic carbon reservoirs in riverine systems. Potential influences are highlighted here, but the mechanism, direction, and magnitude of each influence varies greatly across different geologic settings and climatic regions.

Ecoregions are characterized by distinct vegetation on regional scales, but they do not differentiate vegetation in riparian ecosystems from adjacent uplands. Riparian vegetation communities, however, vary in association with each ecoregion and differ in rates of gross primary production (Naiman et al., 2010). Vegetation type regulates the form, quality, and seasonality of OM inputs available for breakdown or storage in riparian ecosystems (Schulze et al., 2005; Chapin III et al., 2011). Decomposition of OM is highly dependent on temperature and moisture, which also control the rate of chemical and physical weathering of soil and rock. Grain size distributions in rivers affect the availability of mineral facies for adsorption of OC, and thus influence relative differences in rates of OC mineralization by microbes and aquatic invertebrates (Schulze et al., 2005; Allan and Castillo, 2007).

Together with climate, geologic setting controls topography, elevation, and drainage basin and valley characteristics. These factors in turn influence local climate, hydrologic disturbance regime, aqueous and soil chemistry, soil type, and rates of primary production (Figure 2.3). Thus, the direction and magnitude of the influences on OC sources, retention, and fluxes in riparian ecosystems vary greatly across Earth's surface depending on both regional and local characteristics.

2.3.1 Climatic influences of organic carbon in riparian ecosystems

As a source of energy and water, regional climate plays a crucial role in regulating primary productivity, decomposition, and disturbance, thus determining sources, transport, accumulation, and breakdown of OM. Globally, the major control of climate is solar energy, and thermally defined zones can be broadly delineated by latitude (Bailey, 2009). I define hydroclimatic differences in river systems across broad climatic regions including (1) boreal or subarctic, (2) temperate, (3) arid, and (4) tropical. It becomes apparent when classifying published values of OC in riparian ecosystems using even these generalized climatic regions that large gaps are present in all but the temperate regions. Using data from temperate regions, Woodall and Liknes (2008) identified the highest OC stocks occurring in areas with cool summers, suggesting temperature-limited decay rates, whereas the lowest OC stocks are found in semi-arid areas, suggesting water-limited primary productivity and OM inputs. Carbon reservoirs are positively correlated with available moisture and negatively correlated with maximum temperature (Woodall and Liknes, 2008). Flow variability of rivers influences riparian vegetation community structure and the sources and distribution of OM along floodplains (Camporeale and Ridolfi, 2006). For these reasons, I briefly cover climatic controls on OC accumulation and mobilization, including general trends in regional flow regimes. Flow regimes specific to each climatic region regulate (i) riparian vegetation recruitment and survival, (ii) aggradation and degradation of floodplain sediment, and (iii) transport and recruitment of large wood to the stream and on the floodplain.

Tropical regions

Relatively constant annual temperatures characterize tropical regions, with seasonal variations dominated by precipitation. The year-round growing season results in high productivity and abundant vegetation in uplands and riparian areas, with high POM inputs to streams (Lyons et al., 2002; Alin et al., 2008; Hilton et al., 2008; West et al., 2011; Wohl and Ogden, 2013). Low variability in temperatures are accompanied by low monthly and interannual variability of discharge in tropical rivers (Wohl, 2007), providing a regulated environment for primary production, OM inputs, and exports of OC. Variations in precipitation, however, may create distinct seasons of increased moisture and peak discharge in some rivers (Wohl et al., 2012a), which likely influence OC storage along extensive floodplains and riparian ecosystems in lowland, tropical river systems. Flood pulses deliver sediment and OM to the floodplain and riparian wetland ecosystems, creating potential for high OC reservoirs. Abundant moisture and warm temperatures in tropical regions, however, facilitate rapid decomposition of organic matter. In addition to high decomposition rates, monsoons and heavy precipitation leach soils of nutrients and OM in tropical environments, resulting in little-to-no organic O- and A-horizons in soils, which commonly have a litter layer atop B-horizons (Birkeland, 1999).

Processes in steep tropical uplands deliver OC to lowland environments (Ramos Scharrón et al., 2012). Slope failures in steep uplands of tropical regions likely flush organic matter through riparian ecosystems relatively rapidly compared to other regions (Lyons et al., 2002; Hilton et al., 2008, 2010; Ramos Scharrón et al., 2012), perhaps simply supplying flatter lowlands with OC inputs. Climatic patterns such as the El Nino Southern Oscillation can be responsible for rapid deposition of 20 – 80 cm of sediment in a single event on the floodplains of the Amazon River (Aalto et al., 2003) and aggradation of 2.8 – 3.7 mm yr^{-1} has been calculated for the Amazon River floodplains during 9500 – 3000 y Bp (Mertes and Dunne, 2007). Although conditions exist for rapid decomposition of C along floodplains in the tropics, work by Alin et al. (2008) and Goni et al. (2008) suggest that recalcitrant terrigenous OC and aged soil OM can persist along floodplains for 10^2 – 10^3 years without being metabolized. Their work along floodplains of the Fly and Strickland rivers in Papua New Guinea used radiogenic carbon isotopes in surface water and floodplain and delta sediment to determine that OC from headwaters does consist of highly processed OM, but the majority is very old and dominated by terrigenous sources in streams and on floodplains (Alin et al., 2008) and on the subaqueous Fly river delta, where marine sources of C were not detected (Goni et al., 2008).

Temperate regions

Distinct seasonality in temperature and discharge within temperate regions is responsible for consistent annual patterns of productivity, OM inputs, and OC retention in riparian ecosystems. Temperate regions encompass a range of dominant vegetation types, including evergreen and deciduous forests, shrublands, and grasslands. Consistent seasonal trends in OM inputs and temperature regulate biogeochemical processing of OM, such that OC accumulates more rapidly in soils compared to tropical regions. Moderate interannual variability and low monthly variability in discharge of temperate rivers (Wohl, 2007), likely dampen variability in the aggradation and degradation of floodplain sediment and large wood. However, local climate — and C processing — can be highly variable depending on topography, latitude, and location relative to the oceans. Temperate regions encompass the most variability in temperature, precipitation, discharge and floodplain disturbance regime among the climatic regions covered here. Consequently, I distinguish arid regions within the temperate latitudes as a separate category.

Arid regions

Riparian ecosystems typically have increased moisture and greater vegetation density compared to adjacent uplands, and this trend in generally more pronounced in arid regions (Friedman and Lee, 2002). Limited primary production, as a result of potential evaporation exceeding precipitation, limits OM inputs to riparian ecosystems in arid regions. Although a large portion of vegetation in arid regions includes cacti, succulents, and woody perennial plants and trees with photosynthetic stems that appear to create limited plant litter, riparian ecosystems receive a significant amount of OM from seasonal flowers, grasses, seed casings, small leaves, and wood (Sponseller and Fisher, 2006). Low moisture availability in arid regions limits productivity, but also hinders decomposition of OM and thus increases opportunities for OC storage in riparian ecosystems (Harms and Grimm, 2008).

Reservoirs of OC in arid-region riparian ecosystems are highly influenced by timing of precipitation and flooding, which can occur sporadically throughout the year. Subtropical deserts, however, typically receive the majority of their moisture as monsoons. This strong seasonality in precipitation affects productivity, decay rates, local transport and redistribution of OM more greatly than in temperate regions (Merritt and Wohl, 2003; Stromberg et al., 2010). High spatial and temporal (i.e., daily, monthly, and annual) variability of discharge in many arid rivers (Wohl, 2007) is likely to provide little predictability of mobility and aggradation of sediment, wood, and

OM. Flash floods, common in arid regions, redistribute OC in sediment among channels and floodplains (Valett et al., 2005). Thus, storage of OC is likely highly variable, spatially and temporally, in arid region riparian ecosystems.

Boreal regions

Boreal or subarctic regions experience large temperature variation between seasons. The short summers are generally warm and humid, with very long days, resulting in high levels of seasonal productivity of forest and wetland vegetation in the summer and significant OM inputs in the autumn months. Rivers in subarctic and boreal regions experience low interannual variability and large monthly variability in hydrograph peaks as a result of snowmelt and ice breakup during the spring and early summer months (Wohl, 2007), However, lower snowpack and earlier snowmelt as a result of increased warming may alter the magnitude of annual peaks (Costard and Gautier, 2007). Timing of peak flows remains relatively consistent, with the potential for secondary peaks as ice breakup migrates downstream (Costard and Gautier, 2007). This seasonal hydrologic disturbance regime is responsible for consistent transport of OC onto and from floodplains.

Subarctic soils may contain significant amounts of OC in peatlands, permafrost, and from terrestrial OM inputs (Schuur et al., 2008; Tarnocai et al., 2009). Long, cold winters and shallow water tables perched above permafrost facilitate saturated conditions that limit aerobic microbial activity and metabolism of OC pools, contributing to extensive OC storage in soils. Throughflow in the active layer of periglacial environments, however, causes seasonal flushing during snowmelt (Koch et al., 2013), which may mobilize shallow SOC in subarctic regions (Striegl et al., 2005), particularly in floodplains. This mobilization promotes a distinct seasonality of OC flushing from the active layer, which may limit OC storage. Ice- and logjams, however, are common and promote overbank flow, sometimes increasing flow stage by 8-10 m on major rivers such as the Lena in Russia (Costard and Gautier, 2007).

Permafrost serves as a significant reservoir and source of OC from soils in boreal river networks, and may include large wood frozen into floodplain deposits (Wohl, 2013a). Bank erosion and collapse, which are increasingly common with climate change and melting of permafrost (Costard and Gautier, 2007), may transport OC that has been stored for significant periods of time (i.e., $>10^3$ y). Because (1) permafrost constitutes the highest observed values of SOC in upland soils (Schuur et al., 2008; Tarnocai et al., 2009), (2) seasonal melt flushes OC from the active layer (Striegl et al., 2005; Koch et al., 2013), and (3) riparian soils experience increased depth of melting, abundant hyporheic exchange, and higher magnitude and longer duration of throughflow, boreal environments may exhibit a reversal of SOC trends in riparian areas, such that riparian soils have lower OC content compared to surrounding upland soils.

Highlands and mountainous regions

Mountainous terrain within all climatic zones can assume characteristics of other climatic regions. Topographic influences can alter precipitation regimes, create meso-climates, and change hydrologic disturbance regimes (Jong et al., 2005). Increased elevation can induce orographic precipitation such that highlands receive more rain than surrounding lowland regions (Loukas et al., 2000; Jong et al., 2005). Lower temperatures at higher elevations may result in seasonal snowpack and limit microbial activity. In general, mountainous environments tend to change the hydroclimatic regime by decreasing temperature and increasing precipitation, thus shifting toward a wetter and cooler climate, providing more consistency in hydrologic response and disturbance regime (Jong et al., 2005), slowing decomposition of OC, and potentially increasing retention of OC. Exceptions exist, including steep mountainous environments which experience rapid denudation, hillslope erosion, and channel incision (Hilton et al., 2008). These characteristics are regulated by and discussed further in the context of geologic setting.

2.3.2 Geologic Setting

Geologic setting includes tectonic setting, rock type, weathering rates, sediment production, and ultimately the availability of minerals and nutrients, which can all influence OC retention along riparian ecosystems. Tectonic setting broadly includes active and passive tectonic plate boundaries in continental interiors and along continental margins. Active uplift, whether within the interior or along the margins of continents, encourages steep hillslopes and streams, more frequent mass wasting, and potential mobilization and subsequent breakdown/mineralization of OC downslope, with less opportunity for storage along headwater streams (Hilton et al., 2008; Wohl and Ogden, 2013). Transport of sediment by rivers toward lower gradient interiors of continents, as in the Amazon and Mississippi River basins, may result in significant aggradation and storage of sediment (Meade, 2007) and associated OC. Mountain ranges with steep rivers along continental margins are more likely to transport sediment and OC to the ocean more rapidly (Hilton et al., 2008, 2010; Leithold et al., 2006).

The tectonic nature of continental margins plays an important role in determining the duration of storage of OC. Tectonically passive continental margins create potential to store OC in sediment of deltaic deposits or within estuaries. Riverine environments along low-elevation coasts constitute potential storage for 10^2-10^4 y, but are subject to tides, changes in sea level rise, and storm surges (Mertes and Dunne, 2007). Tectonically active margins provide potential for much longer storage periods of 10^5-10^9 y, particularly those that occur where subduction of oceanic tectonic plates beneath continental plates moves sediment and OC into the mantle to be recycled through volcanic processes (Dasgupta and Hirschmann, 2010). Although it is important to note differences in potential storage between continental interiors and active and passive continental margins, I do not cover additional details regarding the fate or storage of OC once it reaches the ocean.

Geologic setting controls topography and influences local climate and hydroclimatic disturbance regime. Topography influences potential transport and storage of sediment, soil, and OM. In rivers flowing through low-lying, relatively flat regions, floodplains are likely to retain OM for longer periods of time (Noe and Hupp, 2009) compared to steep, mountainous terrain with more rapid downstream movement of OM (Benda et al., 2005; Hilton et al., 2010). Similarly, geologic setting dictates the energy gradient between any given point along a river and base level, which influences channel slope and the balance between water and sediment inputs, and thus channel incision and floodplain and channel aggradation (Lane, 1955; Schumm, 1977; Leopold and Bull, 1979; Schumm, 1993).

Geologic and climatic controls on base level play a major role in whether rivers aggrade or incise the landscape through which they flow and thus potential for OC storage along floodplains. Local base level associated with knick points, lakes, inland seas, reservoirs, and sea level influences stream gradients, erosion, and aggradation. Changes in local base level and sea level have the ability to influence OC storage in riparian ecosystems because active uplift and steep slopes facilitate hillslope mass wasting and floodplain erosion (Hilton et al., 2010). Limited research suggests that floodplains in low-relief environments within the interior United States (Guyette et al., 2008), and even smaller, steep streams in the tectonically passive interior U.S.

Rocky Mountains (Wohl et al., 2012a), are more likely to retain OM within the terrestrial environment for a longer period than streams in regions of active tectonic uplift. Thus, tectonic, topographic, and climatic setting creates the template for local characteristics and factors such as channel form and complexity, which influence distribution and fluxes of OM within river systems.

2.4 Localized controls on the distribution of organic matter in riparian ecosystems

As with the landscape scale, the distribution of OC at the local scale of individual valley segments 10^1-10^3 m in length depends on factors that influence gross primary production and the decay, transport, and accumulation of OM. At the local scale, these factors include valley and channel geometry as well as biotic influences.

2.4.1. Valley and channel geometry

Climate interacts with geology to create the topography that influences fluxes of water, sediment, and OM through the landscape (Schumm, 1977; Benda et al., 2005). Channel form changes downstream along an idealized progression from primarily erosive, steep, coarse-grained headwater streams toward lower-gradient channels with finer-grained substrate (Schumm, 1977; Montgomery and Buffington, 1997). However, this downstream progression may take the form of spatially discrete zones, with distinctly different hillslope processes, degrees of sediment and water connectivity between hillslope and channels, and channel characteristics that influence OM dynamics, so that downstream changes in OC reservoirs can be characterized via geomorphic process domains (Montgomery, 1999). Process domains help to identify the relative degree of connectivity between hillslopes and channels and categorize spatially distinct regions by the dominant geomorphic processes responsible for sediment dynamics and ecosystem disturbances (Wohl, 2010a; Polvi et al., 2011; Bellmore and Baxter, 2014).

Hillslope-river connectivity, valley confinement and channel geometry (i.e., cross-sectional geometry, planform, bedforms, bank irregularities) influence fluxes of water, sediment, living biomass, POM, and OC (Schumm, 1977; Montgomery, 1999; Gomi et al., 2002; Benda et al., 2005; Hilton et al., 2008). Although river and hillslope coupling of water and sediment may be expected to decrease with increasing distance downstream (Montgomery, 1999; Brierley and Fryirs, 2005), spatial heterogeneity of lithology and geomorphic processes interrupt this idealized progression (Benda et al., 2005). Spatial heterogeneity in bedrock jointing, for example, facilitates longitudinal heterogeneity in valley geometry (Ehlen and Wohl, 2002; Wohl, 2008), as does glaciation (Amerson et al., 2008).

Valley confinement regulates the distribution of hydraulic forces responsible for sediment transport and resulting channel form (Dunne and Leopold, 1978; Leopold et al., 1964; Montgomery, 1999; Wohl et al., 2012b). Narrowly confined valleys concentrate flow and promote rapid increases in hydraulic force with increasing discharge, which limits deposition of sediment and OM. Broad, unconfined valleys dissipate transport energy during flood flows, facilitate deposition and storage of OM, and promote the development of multithread channel planforms (Wohl, 2000a; Naiman et al., 2005; Wohl, 2013a). Multithread channels increase channel complexity and create positive feedbacks as flow diverges around channel obstructions, islands and bars, resulting in accumulation of OM (Bilby, 1981; Montgomery et al., 2003; Quinn et al., 2007; Richardson et al., 2009; Wohl and Cadol, 2011; Camporeale et al., 2013; Polvi and Wohl, 2013; Wohl, 2013a; Beckman and Wohl, 2014a; Wohl and Beckman, 2014). Hydraulic backwaters and pools immediately downstream of obstructions delay downstream transport of OM and provide the physical complexity that facilitates biological hotspots in which microbes and aquatic biota mineralize OC and nutrients (Battin et al., 2008). These types of channel structures are particularly important in headwater streams with high inputs of OM (Conners and Naiman, 1984; Baron et al., 1991; Richardson et al., 2009; Tank et al., 2010).

Characteristics of riparian soils and plant communities correlate strongly with valley form, the catchment hydrologic regime, hillslope and floodplain geomorphic processes, and distribution of geomorphic surfaces (e.g., floodplains, berms, banks) across the valley bottom (Sollins et al., 1985; Gregory et al., 1991). Heterogeneity in riparian vegetation and soils is closely linked to connectivity of water on and beneath the stream bed and floodplain, which is influenced by valley geometry, channel planform, gradients in soil moisture, and redox potential in the riparian corridor (Tabacchi et al., 1998; Polvi et al., 2011). Thus, the amount of OC stored, and the relative contribution of different OC pools, may vary considerably in different portions of a given watershed. Heterogeneity of drainage networks, the natural disturbance regime, process domain, and land management activities affect channel form and influence the variability of riparian vegetation community structure (National Council for Air and Stream Improvement, 2005). Riparian vegetation plays a key role in the distribution of OM throughout a watershed by contributing OM to riparian ecosystems as instream and floodplain wood, leaf litter, and decaying roots, and by influencing flow characteristics and channel geometry.

For the purpose of our discussion, I define hydrologic connectivity as fluxes of water i) longitudinally within channels, ii) laterally between floodplains and channels, and iii) vertically between surface water, hyporheic flow, and groundwater (Wainwright et al., 2011; Bracken et al., 2013). While hydrologic connectivity influences the connectivity of sediment, I refer to these concepts separately and refer to sediment connectivity primarily as the downstream transport of sediment and lateral exchange and potential storage on the floodplain (Fryirs, 2013; Hoffmann et al., 2009). Each of these facets of connectivity influences the distribution and biogeochemical processing of OM in river systems (Stanford and Ward, 1993; Pringle, 2003; Wohl, 2010b, 2014b). Lateral and longitudinal hydrologic connectivity, for example, facilitate the transport, accumulation, retention, and breakdown of OM (Bilby, 1981; Montgomery et al., 2003; Battin et al., 2008; Wohl, 2013a). Increased lateral and vertical connectivity facilitate saturated conditions in floodplains, thus increasing vegetative production but limiting decomposition of OM. Saturated conditions limit microbial metabolism and mineralization of SOC (Falloon et al., 2011; Moyano et al., 2012) and foster the accumulation and long-term storage of OC (Polvi and Wohl, 2012; Wohl, 2013b). Hyporheic exchange promotes aeration, microbial metabolism of OC (Edwards, 1998; Zarnetske et al., 2011), and adsorption of DOC onto soil mineral facies (Schulze et al., 2005).

Precipitation and flow regimes influence all forms of hydrologic connectivity, as does the topography that governs water routing through a catchment (Dunne and Leopold, 1978; Benda et al., 2005). Hydrologically flashy systems that respond quickly to rainfall flush OM and OC through the catchment quickly (Dunne and Leopold, 1978), limiting opportunities for decomposition (Battin et al., 2008) and potential for long-term storage (Aufdenkampe et al., 2011; Wohl et al., 2012b). Conversely, catchments with significant interception, high infiltration, and high channel complexity, produce longer flow paths and increase lag times for hydrograph response (Dunne and Leopold, 1978). This delay in downstream conveyance of water facilitates accumulation of fine sediment and POM (Montgomery et al., 2003; Sear et al., 2010; Wohl, 2013a; Wohl and Beckman, 2014), hyporheic exchange, mineral adsorption of DOC (Schulze et al., 2005), and fosters hotspots for decomposition of OM (Battin et al., 2008).

2.4.2. Biotic influences on channel geometry

Biotic influences on channel geometry include: (1) riparian vegetation (Tabacchi et al., 1998; Camporeale et al., 2013; Merritt, 2013), (2) riparian grazing and browsing (Kauffman et al., 1983; Clary, 1999), (3) large wood (Abbe and Montgomery, 2003; Collins et al., 2012; Wohl, 2013a), (4) beavers (Ives, 1942; Persico and Meyer, 2013; Polvi and Wohl, 2013; Westbrook et al., 2013; Wohl, 2013b), and (5) aquatic biota (Butler, 1995; Montgomery et al., 1996; Statzner et al., 2000, 2003; Jones, 2012). In this discussion, I focus on major changes to channel form that influence the major reservoirs of OC by biotic drivers including riparian vegetation, large wood, and beavers. Although fauna can influence channel geometry through grazing, major changes to channel form are typically a function of intensive grazing associated with livestock and thus are related to land use, which is discussed in section 7.

Interactions between channel geometry and riparian vegetation affect channel cross-sectional form, planform, spatial variations in flow velocity (Trimble, 2004; Nepf and Ghisalberti, 2008; Camporeale et al., 2013; Merritt, 2013), and therefore the distribution and fluxes of OM. Lateral connectivity to the floodplain, for example, partly reflects channel geometry and significantly influences germination, establishment, and survival of many riparian species (Cooper et al., 1999; Merritt and Poff, 2010; Camporeale et al., 2013). Some riparian plant species are adapted to tolerate high shear stress during high flows (Camporeale et al., 2013) and provide stability to channel banks by increasing soil cohesion through root tensile strength (Abernethy and Rutherfurd, 2001). This resistance to bank erosion creates a positive feedback:

flow velocity decreases along banks and vegetated islands, and this facilitates sediment deposition immediately downstream and creates new germination sites for riparian plants, which then contribute to bank stability and continued aggradation (Tabacchi et al., 1998; Naiman et al., 2005; Camporeale et al., 2013; Merritt, 2013).

In forested environments of the northern hemisphere, beavers can play an important role in storage of OM along riparian ecosystems (Naiman et al., 1986; Correll et al., 2000; Wohl, 2013b). Alligators and hippopotamuses can also influence channel form by constructing canals and small water holes or ponds to aid their travel, predation, and foraging, but these effects are still relatively insignificant compared to the extensive geomorphic engineering of the beaver (Butler, 1995). Beavers greatly alter channel geometry and valley bottoms in what has been termed the beaver meadow complex (Ives, 1942). Beavers engineer an extensive series of terraced dams, ponds, and canals, which greatly increase channel complexity, promote lateral connectivity to the floodplain, encourage floodplain aggradation, raise riparian water tables, and thus contribute to the rapid colonization and growth of wetland riparian plant species (Westbrook et al., 2006; Polvi and Wohl, 2013; Westbrook et al., 2013; Wohl, 2013b). In Rocky Mountain National Park, USA, valleys with beaver meadows (Morgan, 1868) contain deeper accumulations of fine sediment and higher OC content than valleys without beaver activity (Kramer et al., 2012; Wohl et al., 2012b). These beaver-influenced sediments can persist for thousands of years (Persico and Meyer, 2009, 2013; Polvi and Wohl, 2012). The geomorphic effects of beaver activities on the distribution of OM and associated OC storage are similar to those created by instream wood and logjams.

Channel planform, disturbance regime, and riparian vegetation dynamics impact the wood load in channels and floodplains, and the resulting OC dynamics. Feedbacks between hydraulics and vegetation mentioned above also apply to wood with regard to the dissipation of energy and accumulation of sediment (Montgomery et al., 2003; Sear et al., 2010; Wohl, 2013a; Beckman and Wohl, 2014; Wohl and Beckman, 2014). Instream wood not only facilitates channel complexity and flow divergence, but also provides refugia for aquatic invertebrates and microbes that break down and metabolize CPOM and FPOM (Allan and Castillo, 2007). Channel-spanning logjams create pools and trap sediment and POM for time periods of 10^0-10^1 years (Montgomery et al., 2003; Sear et al., 2010; Wohl, 2013a; Beckman and Wohl, 2014; Wohl and Beckman, 2014). Large pieces of wood and abundant wood associated with old-growth forests, in particular, can form persistent channel-spanning logjams that facilitate the development of multithread channels (Brummer et al., 2006; Collins et al., 2012; Wohl et al., 2012b). Continuous avulsion and shifting of channels occur partly as a response to undercutting of standing trees during high flows, which ensures continued recruitment of instream wood (Collins et al., 2012; Wohl, 2013a). Increased channel complexity as a result of riparian vegetation, beaver dams, and persistent logjams increases sediment deposition, accumulation and retention of OM (Polvi and Wohl, 2012; Wohl et al., 2012b; Wohl, 2013a, 2013b; Polvi and Wohl, 2013; Wohl and Beckman, 2014).

2.5 A review of organic carbon stocks in riparian ecosystems

In this section, I discuss influential factors and relative differences in three primary pools for OC storage in river systems: 1) standing riparian biomass, 2) dead biomass as LW in the stream and on the floodplain, and 3) floodplain surface (i.e., litter) and subsurface (i.e., humus and soil) sediment and OM. In this context, I summarize existing knowledge of floodplain and riparian components of river systems. I do not include specific discussion of other wetland environments, lakes, reservoirs, alluvial fans, estuaries, and deltas, even though these depositional environments are likely substantial storage areas for OC (Chmura et al., 2003; Cole et al., 2007; Bianchi and Allison, 2009; Kayranli et al., 2010). Reported values of OC specific to riparian ecosystems and floodplains are published in journals of diverse disciplines and do not necessarily frame findings as carbon storage in riparian ecosystems or floodplains. I gather this information and present it in a way that highlights the primary reservoirs and influential factors for potential long-term (10^2 - 10^4 y) storage.

2.5.1 Riparian vegetation

Vegetation constitutes a significant OC reservoir in riparian ecosystems and provides the source for much of the LW and CPOM that is stored on the floodplain. A limited number of studies have examined OC pools in riparian biomass (Table 2.1; Figure 2.4), each with specific objectives that influenced the biomass components measured (e.g., Fierke and Kauffman, 2005). Reported values for total riparian biomass OC, which includes vegetation and LW in some studies, are wide-ranging (<1 to 2794 Mg C ha^{-1}), and directly reflect the vegetation structure and successional stage (Table 2.1). Published research has largely focused on temperate regions (Table 2.1; Figure 2.4), including several studies that examined streams impacted by disturbance (Giese et al., 2000, 2003; Fierke and Kauffman, 2005; Ruffing et al., in press). Highest values were observed for mesic, old growth, conifer-dominated riparian forests in the Southern Rocky Mountains (Figure 2.4, Wohl et al., 2012), while lowest values occurred in early successional cottonwood stands (Fierke and Kauffman, 2005), herbaceous-dominated meadows (Dwire et al., 2004; Cierjacks et al., 2010; Wohl et al., 2012b), and willow shrub stands (Wohl et al. 2012). At disturbed temperate sites, alteration or removal of riparian vegetation resulted in notably lower

OC pools (Giese et al., 2000, 2003; Fierke and Kauffman, 2005; Ruffing et al., in press). Mature temperate hardwood forests include a wide diversity of tree and understory species, yet total OC storage in riparian biomass consistently ranges from ~100 – 300 Mg C ha^{-1} (Table1)

Studies of estimated riparian biomass were limited primarily to temperate regions, leaving few data for other climatic regions. No published estimates of riparian biomass OC were found for arid regions. However, pioneer species of willow and cottonwood trees are common in the floodplains of many desert rivers in North America (Stromberg et al., 2013), and values may be comparable to those reported for mature cottonwood forests in Oregon (190 -218 Mg C ha^{-1}; Fierke and Kauffman, 2005). In tropical floodplain forests, total biomass OC values appear at the higher end of those in temperate riparian ecosystems (Figure 2.4; Jaramillo et al., 2003). To improve understanding of riverine OC storage, more riparian vegetation types in different ecoregions need to be sampled for a complete suite of biomass components.

Field-based estimation of OC pools in riparian vegetation involves intensive sample collection and processing. To facilitate more rapid assessment of riverine biomass and OC stocks, different remote sensing techniques have been applied (Filippi et al., 2014). Suchenwirth et al. (2012, 2014) distinguished riparian vegetation types and used high spatial resolution remote sensing data to estimate carbon stocks along the Danube River, Austria, which proved comparable to field-based estimates (Figure 2.4; Cierjacks et al., 2010). With increased focus on regional carbon budgets, development of remote sensing tools holds promise for estimating OC stocks for different vegetation types globally, including riparian floodplains.

Table 2.1. Published values of organic carbon pools from biomass and carbon inputs via litterfall in alluvial riparian ecosystems.

Location	**Climate**	**Biomass Components Measured**	**Riparian vegetation type**	**Total Biomass Carbon (Mg C ha^{-1})**	**Reference**
Chamela Biological Station, Jalisco, Mexico	Tropical	Trees (live), vines, seedlings, roots	Tropical floodplain forest (combination of evergreen and deciduous species)	119-188[a]	Jaramillo et al. 2003
Pen Branch Fourmile Branch Meyer's Branch (3rd order tributaries to Savannah River, South Carolina, USA)	Temperate	Trees, shrubs, herbaceous, litterfall, forest floor, fine roots, submerged aquatic vegetation	Bottomland hardwood forest (different seral stages; deciduous species)	7.5 – 108.8	Giese et al. 2000, 2003
Meyer's Branch Savannah River South Carolina, USA	Temperate	Trees, shrubs, herbaceous	Cypress-tupelo forest	174 - 192[a]	Muzika et al. 1987
Danube River, Austria	Temperate	Trees, shrubs	Mature hardwood, conifer & cottonwood forests; Young reforestations	160 – 280 35	Cierjacks et al. 2010
Williamette River, Oregon, USA	Temperate	Trees (live & dead)	Black cottonwood (chronosequence of 5 successional stages)	<1 – 218[a]	Fierke and Kauffman 2005
6 streams, SE Wyoming USA (1st and 2nd order)	Temperate (mountains)	Trees, shrubs, herbaceous, forest floor	Conifer-dominated	53-166	Ruffing et al., in press
North St. Vrain & Big Thompson Rivers, Colorado, USA	Temperate (mountains)	Trees, shrubs, herbaceous, forest floor	Conifer-dominated; willow-dominated; herbaceous meadow	194-360 57 42	Wohl et al. 2012
West Chicken Creek Limber Jim Creek, northeast Oregon, USA	Temperate (mountains)	Herbaceous (above & below ground)	Herbaceous meadow	7 – 21.5[a]	Dwire et al. 2004

[a] Estimated from reported biomass values using a conversion factor of 0.5 (assuming 50% C content).

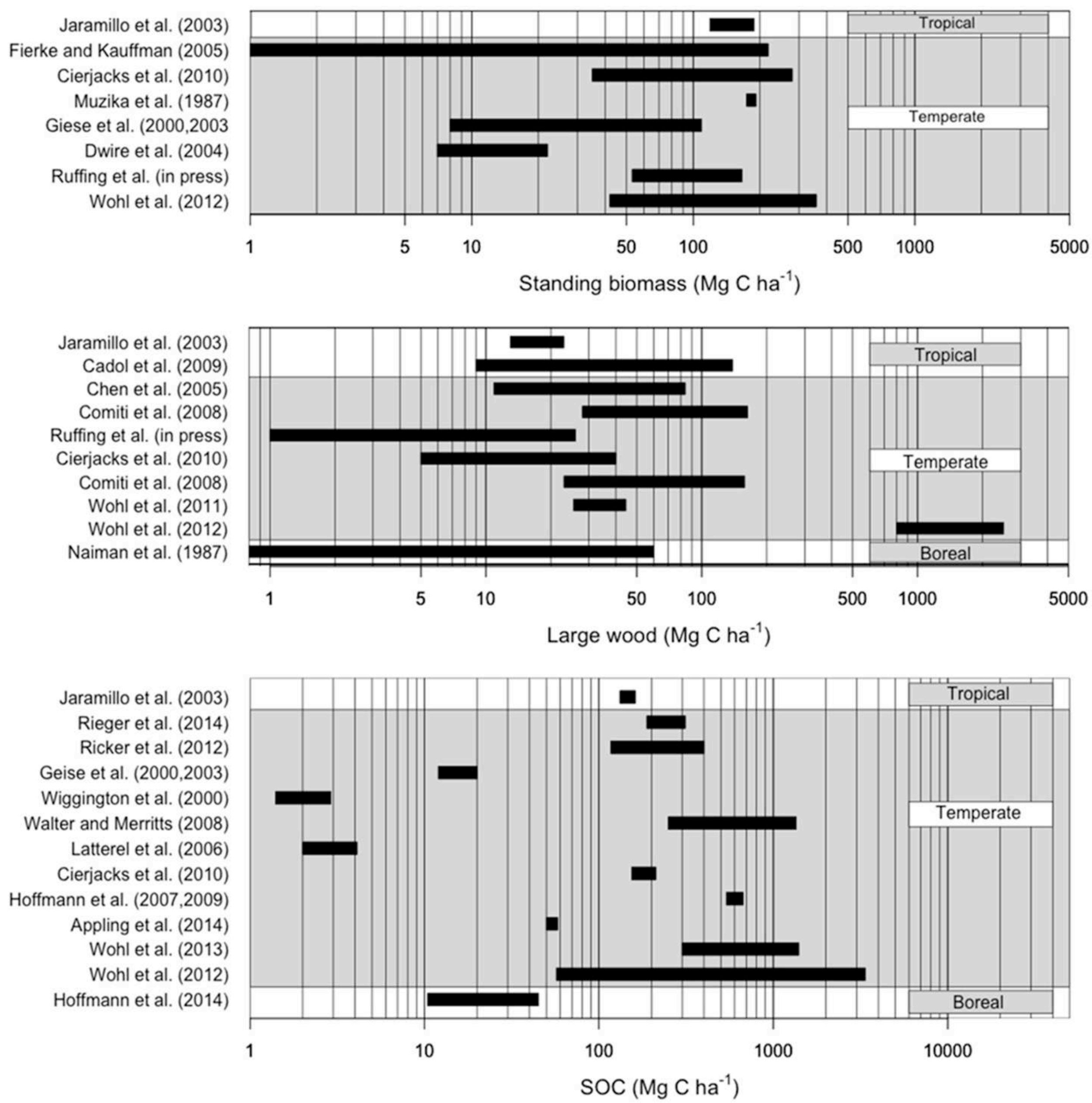

Figure 2.4. Studies cited here that quantify carbon reservoirs in riparian ecosystems and floodplains. Black bars indicate ranges of values reported by each study of organic carbon storage in biomass, large downed wood, and soil organic carbon. Note the different scale on x-axis of SOC figure. More details described in Tables 1-3.

2.5.2 Large downed wood

Large downed wood (LW) provides an important source of OM to river systems and floodplains. In a tropical Costa Rican forest, large dead wood accounted for a third of the OC in above-ground woody biomass within the entire watershed (Clark et al., 2002). Dead wood in subalpine forests in the Colorado and Wyoming Rocky Mountains ranged from 2.8 – 60 % (1.3 - 34.3 Mg ha^{-1}; Kueppers et al., 2004) and 12.9 – 56% (Bradford et al., 2008) of that in above-ground woody biomass. Long residence times of LW in streams and on the floodplain provide potential for long-term storage of OC and sources of POM. Numerous factors influence the volume and residence time of stored wood in river systems, including characteristics of the riparian forest stand age, stem density, species, wood decay rate, hydroclimatic disturbance regime and floods, and wood recruitment mechanisms, which include individual tree topple, disturbance-related mortality, bank and floodplain erosion, and transport from adjacent uplands and channels (Benda and Sias, 2003; Collins et al., 2012). Thus, the recruitment, residence time, and stored volume of floodplain and instream wood are largely dictated by climate, geologic setting, and local controls on channel form.

Table 2.2. Published values of ages and carbon storage as downed wood on floodplains and in active channels

Location	Climate	Ages of wood (y)	OC content (Mg C ha^{-1})	OC content (Mg C 100m^{-1})	Reference
			Floodplains		
Southeastern Australia	Temperate	240 ± 40			Webb & Erskine, 2003
Ontario, Canada	Temperate	350-800			Guyette et al., 2002
Missouri, USA	Temperate	3515 [a]			Guyette et al., 2008
Colorado, USA	Temperate		800-2500		Wohl et al., 2012
South Carolina, USA	Temperate		25.5 - 44.5 [b]		Wohl et al. 2011
Quebec, Canada	Temperate		57.3		Naiman, 1987
Central Chili	Temperate		23 – 158 [b]		Comiti et al., 2008
Tierra del Fuego, Argentina	Temperate		30 [b]		Comiti et al., 2008
Danube River, Austria	Temperate		5-40		Cierjacks et al. 2010
SE Wyoming USA (1st and 2nd order)	Temperate		1-26		Ruffing et al., this issue
Chamela Biological Station, Jalisco, Mexico	Tropical		13-23 [e]		Jaramillo et al. 2003
			Active channels		
Quebec, Canada	Boreal		0.8 - 60, 23.2[f]		Naiman et al., 1987
British Columbia, Canada	Temperate		10.9 - 83.9[c]		Chen et al. (2005)
Washington, USA	Temperate	19[c], >1400 [d]			Hyatt and Naiman, 2002
Washington, USA	Temperate			0.75 - 35.5 [b] 0 - 21.8 [b]	Fox & Bolton, 2007
Italy	Temperate			0.1 - 0.7 [b]	Comiti et al., 2006
Central Chili Tierra del Fuego, Argentina	Temperate		28 – 163 [b] 28 [b]		Comiti et al., 2008
La Selva, Costa Rica	Tropical		9-139 [b]	1.4-15.8 [b]	Cadol et al., 2009

[a] wood buried by floodplain aggradation
[b] estimated from reported values and wood density for reported species assuming 50% of mass as C
[c] reported median value
[d] maximum age reported
[e] estimated range from reported wood volumes, reported mean wood densities, and reported error
[f] calculated mean from published values

The amount of OC stored on the floodplain and in the channel as wood varies with drainage area, ecoregion, forest stand characteristics, and valley and channel characteristics. Limited research suggests that in smaller rivers (i.e., drainage areas <1000 km^2) downed instream and floodplain wood can constitute the primary reservoir of stored OC (Naiman et al., 1987), particularly in unconfined valley segments wider than ten times the bankfull channel width (Wohl et al., 2012a). Larger rivers (i.e., >1000 km^2), in which channel width typically exceeds the length of individual pieces of wood, historically had substantial wood accumulations in the form of wood rafts (Triska, 1984; Wohl, 2014a), although wood rafts are now rare because of systematic wood removal from rivers.

Volumes of instream wood tend to be greatest in temperate environments, which have larger trees than boreal regions, but longer decay times than tropical regions (Table 2.2, Figure 2.4; Cadol et al., 2009; Wohl, 2013a). Although studies of decay rates within rivers are almost non-existent, decay rates for logs on a forest floor vary from 50 to 100 years in dry climates (O'Connell, 1997; Ellis et al., 1999), 10 to 100 years in humid temperate climates (Boyce, 1961; Harmon, 1982), and less than 10 years in the tropics (Delaney et al., 1998; Clark et al., 2002; Lewis et al., 2004). These differences between regions correspond to the potential for long residence times of LW in temperate rivers and the relative mass of OC stored in living vegetation and Hyatt and Naiman (2001) documented LW that had been in the Queets River of Washington for up to 1400 years, although most pieces were < 50 years old. In the redwood forests of northwestern California, LW residence times can exceed 200 years (Keller et al., 1995). In old growth, conifer-dominated riparian forests of the Southern Rocky Mountains, standing trees account for only 7-22% of the total stored OC, whereas downed wood accounts for 77-93% (Figure 2.4; Wohl et al. 2012). Although tropical floodplain forests also store notable amounts of OC (Figure 2.4), over 90% comes from standing riparian biomass (trees and vines), whereas downed wood contributes only about 8%, presumably due to rapid decay rates (Jaramillo et al. 2003).

Forest stand characteristics that influence the storage of OC as LW include species composition and stand age. Species composition and stand age influence susceptibility to disturbances such as wildfire, blowdowns, and insects (Turner, 2010). Species composition and stand age also influence piece size and shape of LW, and therefore mobility and residence time of LW on floodplains and in channels (Montgomery et al., 2003; Wohl et al., 2011). Finally, species composition and stand age influence mortality rate and rates of LW decay and abrasion (Keim et al., 2000; Hyatt and Naiman, 2001; Latterell and Naiman, 2007; Wohl and Goode, 2008).

Channel geometry and instream wood play an important role in the retention and ecosystem processing of OC because wood obstructing channelized flow can facilitate complex flow paths and hydrologic connectivity to the floodplain and floodplain retention of OM (Sear et al., 2010; Wohl et al., 2011; Collins et al., 2012; Polvi and Wohl, 2013; Wohl, 2013a; Beckman and Wohl, 2014), delay the downstream transport of POM (Bilby, 1981; Montgomery et al., 2003; Quinn et al., 2007; Battin et al., 2008; Sear et al., 2010; Wohl et al., 2011; Polvi and Wohl, 2013; Wohl, 2013a; Beckman and Wohl, 2014a), and create biological hotspots that provide opportunities for biota to metabolize OC (Gomi et al., 2002; Allan and Castillo, 2007; Hilton et al., 2008; Tank et al., 2010).

Large instream and floodplain wood can persist for thousands of years (Guyette et al., 2002, 2008; Webb and Erskine, 2003), can constitute the majority of the OC stored on floodplains (Wohl et al., 2012b). Persistent large downed wood can also serve as a continued source of POM for riparian and aquatic ecosystems (Ward and Aumen, 1986; Guyette et al., 2002, 2008; Webb and Erskine, 2003). Accurate estimates of the natural range of variability in contribution of wood to OC reservoirs are impractical because a long history of human modification has resulted in substantial reductions in wood loads (Wohl, 2014a).

2.5.3 Litter, POM, humus, and soil organic carbon

The floodplain surface and shallow subsurface host a large reservoir for OC, including surface organic layers and soil organic carbon (SOC). Surface organic layers, frequently termed the forest floor, consist of plant litter in various stages of decay (Perry et al., 2008). Litter is the OM that comprises the top layer of the forest floor, and is composed of small branches, twigs, and recently fallen needles and leaves that are still identifiable and little altered by decomposition (Naiman et al., 2005; Lutes et al., 2006). The litter layer may also include OM from shrubs, grasses, and forbs that have recently died. Litterfall is the OM that falls to the floodplain forest floor or the allochthonous material that enters streams from riparian vegetation. On the forest floor, the humus layer underlies the litter layer and is comprised of partially decomposed OM and litter, which is no longer recognizable as discrete plant parts.

Floodplain litter and humus layers reflect riparian vegetation type, successional stage, local productivity of vegetation, and the climatic and edaphic factors that regulate decomposition (Benfield, 1997). In uplands, the highest litterfall rates are found in tropical equatorial forests (~5.3 Mg C ha^{-1} yr^{-1}; Vitousek, 1984; Vitousek and Sanford, 1986), followed by tropical montane (~3.1 Mg C ha^{-1} yr^{-1}; Veneklaas, 1991) and warm temperate forests (Table 2.3; ~2.5 Mg C ha^{-1} yr^{-1}; Bray and Gorham, 1964; Naiman et al., 2005). The lowest litterfall rates have been observed in boreal and cool temperate forests (<1 to ~1.5 Mg C ha^{-1} yr^{-1};Bray and Gorham, 1964; Naiman et al., 2005). Reviews of allochthonous litterfall to rivers show the same geographical trends as litterfall to the forest floor and reveal an inverse relationship between riparian litter production and latitude (Xiong and Nilsson, 1997) and a positive relationship between litterfall and annual precipitation (Benfield, 1997). Riparian vegetation is generally characterized by higher plant diversity, biomass, and higher rates of litter production than adjacent upland vegetation (Xiong and Nilsson 1997).The majority of published information on litterfall by riparian vegetation is limited to warm, temperate forest floodplains in North America, where annual litter inputs range from approximately 2.8 to 4 Mg C ha^{-1} (Table 2.3), indicating higher productivity in riparian forests relative to uplands.

In most riparian areas, however, the forest floor organic layers, especially the litter layer, are much more dynamic than in upland environments. During high flows, OM from upstream riparian sources and instream primary productivity can be deposited and local floodplain OM redistributed (Pinay et al., 1992; Hall et al., 2009). Hillslope erosion and debris flows can deliver OM from upslope and bury riparian OM under mineral sediment (Ramos Scharrón et al., 2012). Erosional and depositional disturbances contribute to the mosaic of OC distribution in riparian areas and the creation of biogeochemical hotspots (McClain et al., 2003), partly through the redistribution of litter and POM by fluvial processes.

Riparian vegetation litter is a major source for POM for lotic foodwebs, particularly along headwater streams where channels are narrow and allochthonous inputs are high (Vannote et al., 1980; Conners and Naiman, 1984; and Aumen, 1986; Gomi et al., 2002; Allan and Castillo, 2007; Hilton et al., 2008; Richardson et al., 2009; Tank et al., 2010). Discontinuities due to tributary variation in valley form, and anthropogenic and natural disturbances, disrupt an idealized downstream pattern in which autochthonous C inputs grow progressively more important than allochthonous inputs (Tabacchi et al., 1998; Allan and Castillo, 2007).

Table 2.3. Published values for carbon accumulation rates and total storage on floodplains.

Location	Climate	Drainage area (km^2)	Accumulation rate (Mg C ha^{-1} y^{-1})	Sediment organic carbon content (Mg C ha^{-1})	Reference
Alberta, Canada	Boreal	----	----	10.4-45, 23.6[g]	Hoffmann et al. (2014)
Ichauwaynochaway Creek, Georgia, USA	Temperate	2600	0.18 (over 30 y)[b] 1.07 (over 100 y)	---	Craft and Casey (2000)
Headwaters in southern New England, USA	Temperate	≤ 600 ha	0.03 0.007 pre-colonial	262, (117-400)	Ricker et al. (2012)
Rhine River, Germany	Temperate	185,000	0.034-0.254	538-671	Hoffmann et al. (2009, 2007)
Chickahominy, Virginia, USA Choptank Dragon Run Mattaponi Pamunkey Patuxent Pocomoke	Temperate	1210 290 360 2360 2800 900 970	1.4 0.7 0.9 1.4 0.7 0.7 0.3	---	Noe and Hupp (2009)
Atchafalaya River, Louisiana, USA	Temperate	5670	8	---	Hupp et al. (2008)
Tar River, North Carolina, USA	Temperate	8056	2.8	---	Brinson et al. (1980)
North St. Vrain & Big Thompson Rivers, Colorado, USA	Temperate	20-36	---	57-622 [c] 224-3365 [d] 1014 [e]	Wohl et al. (2012)
Beaver Brook and Upper Poudre River, Colorado, USA	Temperate	3.8 - 110		300 - 400 [f] 1150 - 1400 [e]	Wohl (2013)
6 rivers southwestern England	Temperate	276-1124	0.7-1.1	---	Walling et al. (2006)
20 streams, mid-Atlantic Piedmont, USA	Temperate	11-1230	---	250-1350	Walter and Merritts (2008)
Savannah River, South Carolina, USA	Temperate	51-57	---	1.4-2.9	Wigginton et al. (2000)
Middle Fork Flathead River, MT, USA	Temperate	2300	---	7735	Appling (2012)
Queets River, WA, USA	Temperate	1153	----	2-4.1	Latterell et al. (2006)
Danube River, Austria	Temperate	104,000	2.9	----	Tockner et al. (1999)
Ebro River, Spain	Temperate	40,434	1.4-3	---	Cabezas et al. (2009)

Kankakee River, Illinois, USA	Temperate	---	0.6	---	Mitsch et al. (1979)
Cache River, Illinois, USA	Temperate	---	0.6	---	Mitsch et al. (1977)
Appalachicola River, Florida, USA	Temperate	----	0.2	----	Mulholland (1981)
Danube River, Austria	Temperate	----	----	154-186 176 212	Cierjacks et al. 2010
Pen Branch Fourmile Branch Meyer's Branch (3rd order tributaries to Savannah River, South Carolina, USA)	Temperate	----	----	12-20[d]	Giese et al., 2000, 2003
Danube, Austria	Temperate	----	----	188-313	Rieger et al. (2014)
Jalisco, Mexico	Tropical	----	----	132-162[c]	Jaramillo et al. (2003)
Amazon River, Brazil	Tropical	3660	1-2.5	---	Moreira-Turcq et al. (2004)

[a] Mean (range in parentheses, when available)
[b] Greater historical rates are interpreted to reflect land use and lack of soil conservation practices in the past
[c] floodplain sediment; forested site
[d] floodplain sediment and downed, dead wood; forested site
[e] active beaver meadow
[f] relict/abandoned beaver meadow
[g] calculated mean of reported means

The distribution, accumulation, and type of POM influence the rate of decomposition and mineralization of nutrients (Vannote et al., 1980; Gomi et al., 2002; Allan and Castillo, 2007; Hilton et al., 2008; Tank et al., 2010). Allochthonous carbon inputs in headwater streams are composed primarily of CPOM in the form of pieces of wood, litter, and humus (Vannote et al., 1980; Ward and Aumen, 1986; Allan and Castillo, 2007; Richardson et al., 2009; Tank et al., 2010). Microbes and aquatic invertebrates break down CPOM to FPOM, contributing OC and nutrients to aquatic and terrestrial foodwebs that include numerous vertebrate, invertebrate, and microbial taxa (Vannote et al., 1980; Wagener et al., 1998; Allan and Castillo, 2007). Litter and redistributed POM pools can be dynamic by means of hydraulic redistribution, but continued aggradation can facilitate decomposition and storage as humus and SOC.

Soils are the third largest reservoir in the global carbon cycle after the deep ocean and geologic storage, and store more carbon than living biomass and the atmosphere combined (Ruddiman, 2001). Abundant research has examined SOC content in various landscapes, but work focusing on river systems is limited (Figure 2.4). The majority of research has occurred in temperate and subtropical regions, whereas boreal, arid, and tropical regions have received considerably less attention. Although OC studies in floodplain sediment are very limited in tropical regions, Moreira-Turcq et al. (2004) and Jaramillo et al., (2003) suggest that tropical riparian ecosystems contain SOC values comparable to the lower end of values in temperate regions (Table 2.3). Cabezas et al. (2009) indicate that Mediterranean temperate climates may have similar trends, whereas temperate and subtropical climates appear to have much variability in SOC storage.

Hydrologic disturbance, particle sorting and potential accumulation of fine sediment make riparian ecosystems a dynamic component of the terrestrial carbon cycle, with implications for SOC processing and potential long-term storage. Soil moisture and percent clay content are positively correlated with SOC content (Pinay et al., 1992; Jobbágy and Jackson, 2000; Wigginton et al., 2000; Hoffmann et al., 2009; Moyano et al., 2012), so that dry, coarser textured soils typically contain less OC. Dissolved organic carbon (DOC) transported through riparian soils may be adsorbed to clay mineral surfaces (Schulze et al., 2005).Typical soil chronosequences exhibit a decrease in SOC content with depth (Birkeland, 1999; Jobbágy and Jackson, 2000). This relationship does not appear as strong in floodplain soils (Cole et al., 2007; Gurwick et al., 2008b), although it can be present (Walling, 2006).

SOC distribution in riparian ecosystems can be complex because surface and subsurface microbial activity and mineralization of OC can be disconnected. Much OC can be stored as roots and in buried A-horizons (Blazejewski et al., 2009) and SOC content may become more stable with burial (Cole et al., 2007) because it is farther from intense microbial activity at the surface (Gurwick et al., 2008a; Ricker et al., 2012). Because microbial activity is regulated by temperature, seasonal and diurnal variations influence microbial metabolism of OC. The moist conditions of riparian soils facilitate increased metabolism of SOC by microbes (Billings et al., 1998), whereas saturated conditions associated with shallow water tables decrease metabolism and increase potential for long-term storage (Falloon et al., 2011). Continued aggradation and burial of floodplain soils may contribute to high rates of OC sequestration (Gurwick et al., 2008a).

Potential for long-term storage of SOC depends on the source and form of the OC (Gurwick et al., 2008b) and the residence time of floodplain sediment (Oost et al., 2012). DOC may travel through river networks in ~10 – 10^2 years, whereas POM may take much longer (i.e., >10^3 years; Raymond and Bauer, 2001), presumably being stored within floodplain sediment.

Residence time of SOC is influenced by biologic and physical factors. Our discussion is framed primarily within the context of physical drivers that influence residence time of sediment and organic debris on floodplains in riparian ecosystems, with only limited mention of the biogeochemical factors that influence metabolism. The biologically-driven residence times typically of interest to ecologists and biogeochemists, however, are dependent on other factors discussed above, including moisture content, temperature, and characteristics of riparian vegetation communities.

Although researchers have examined OC storage and dynamics in river systems, work investigating mechanistic and geomorphic controls on OC storage in riparian ecosystems is limited. Pinay et al. (1992) were among the first to examine carbon storage in riparian soils, with explicit distinction of geomorphic influence on sediment size distributions and associated SOC (Figure 2.4.). Examination of three segments of the Garonne River in France indicated that confined, erosional segments dominated by sandy soils contained less SOC than less confined, depositional segments dominated by silty clay soils (Pinay et al., 1992). However, a much larger fraction of the OC in the erosional, sandy soil reach was available for biological uptake. Fine–grained sediments can serve as nutrient and OC sinks, whereas sandy soils readily release available carbon during high flows (Pinay et al., 1992).

Channel geometry and the degree of valley confinement and relative width of the floodplain to the channel can play a crucial role in the aggradation of sediment and accumulation of POM and SOC (Fryirs et al., 2007). Several studies indicate that wider valley bottoms and lower-gradient channels store more fine sediment, POM, and SOC compared to steeper and more laterally confined valley segments (Blazejewski et al., 2009; Noe and Hupp, 2009; Wohl et al., 2012b).

Reach characteristics associated with hydroclimate, flow regime, and valley geometry, including riparian valley width, duration of inundation, sediment sources, distance from the active channel, and flow velocity, may also account for significant differences in POM and SOC storage (Hupp et al., 2008). Although floodplains have received some attention as sites of OC accumulation, less frequently inundated surfaces such as terraces should also be evaluated for OC content (Latterell et al., 2006). Spatial differences in OC content among geomorphic surfaces in various landscapes will likely depend on climate, vegetation type, distance from the channel, and land use before, during, and after the time of aggradation and abandonment. Gurwick et al. (2008a) emphasize the importance of the abundance of OC at the time of deposition, rather than the time since deposition, with regard to controls on current OC content.

2.6 Regional comparisons of floodplain OC storage and a first-order estimate of global floodplain OC storage

Reported accumulation rates and mass of OC calculated per area within riparian ecosystems (Figure 2.4) reveal that OC reservoirs in riparian ecosystems are highly variable across and within particular climatic regions. This indicates that other factors such as geologic setting and local-scale variables play an important role in OC storage within riparian ecosystems. Temperate regions exhibit the most variability, but this could reflect the fact that most of the work done to quantify OC storage in riparian ecosystems comes from temperate regions, as well as the diversity of temperature, moisture, and meso-climate conditions within temperate latitudes. Highlands in various climatic regions, for example, suggest the potential for large OC reservoirs along small mountainous streams (Aguado and Burt, 2007), which might have OC storage per unit area at least an order of magnitude higher than most lowland rivers (Wohl et al., 2012b;

Wohl, 2013b; Hoffmann et al., 2014a, 2014b), except for those highly impacted by land use and legacy sedimentation (Walter and Merritts, 2008).

Drawing on the literature cited in Tables 1- 3 and Figure 2.4, I propose a conceptual model of the conditions under which OC retention is maximized in riparian ecosystems (Figure 2.5). Although these conditions encompass the regional and local characteristics discussed above and in Figure 2.3 and their influence on the three primary reservoirs for moderate-to-long-term OC retention and storage, Figure 2.5 does not capture the full complexity of OC dynamics associated with all potential factors. The most notable of these complexities are moisture and temperature. As discussed above, an intermediate level of moisture provides optimal conditions for the decomposition of OC, such that saturation of limited moisture hinders decomposition (Jobbágy and Jackson, 2000; Falloon et al., 2011). Rivers in tropical forests provide an example. Although higher temperatures facilitate increased growth of riparian vegetation in the tropics, they also increase decomposition rate, which lowers OC storage as indicated in Figure 2.3 and the optimal conditions captured in Figure 2.5. This is why I suggest that colder environments store more carbon. Cold and wet environments provide another example of the complexity of influences on OC storage: wet conditions are required to produce vegetation, but cold conditions regulate decomposition. The combined factors of wet and cold environments increase OC storage. The schematic illustration in Figure 2.5 is not meant to imply linear relationships between OC storage and temperature, moisture, or other factors, but rather to illustrate the directional trends in these relationships and the optimal conditions for OC storage.

Currently, limited data in most climatic regions constrain our ability to examine potential differences across Earth's surface. From the studies cited here, it appears that large primary productivity in tropical regions results in large reservoirs of standing biomass, but high rates of decomposition limit large wood and SOC reservoirs compared to temperate regions (Figure 2.4; Jaramillo et al., 2003). Although work indicates large SOC reserves in boreal regions outside of riparian areas (Tarnocai et al., 2009), the limited work cited here (Hoffmann et al., 2014a) does not indicate these difference along boreal floodplains. I emphasize that inferences are constrained by currently published work, but I draw on this work to discuss potential conditions for optimal OC storage.

Warmer temperatures and increased moisture increase decomposition rates and metabolism of OC (Trumbore and Czimczik, 2008; Falloon et al., 2011). Although warm moist tropical climates have high primary productivity and standing biomass, high decomposition rates and the lack of distinct seasonal fluxes of litter timed with redistribution from seasonal flow regimes likely limit total carbon storage in soil, litter, and large wood (Clark et al., 2002; Cadol et al., 2009). Conversely, metabolism of riparian ecosystems in boreal regions is temperature limited. Moisture controls are more complicated because microbial respiration increases with increasing moisture content, but saturated conditions limit aerobic respiration and metabolism of OC. Abundant moisture and saturated conditions from snowmelt and shallow water tables overlying permafrost in alpine and boreal regions also limit metabolism. Low primary productivity in boreal regions, however, limits potential uptake of OC to soils and storage within large trees and large wood. Limited work along boreal and alpine floodplains indicates a relatively small range of SOC storage in riparian ecosystems (1.8 - 234.6 Mg C ha^{-1}; Hoffmann et al., 2014a, 2014b), but very high SOC contents in boreal peatlands and permafrost (322 – 696 Mg C ha^{-1}; Tarnocai et al., 2009) suggest that the limited work on boreal floodplains (Table 2.3; Figure 2.4) may not capture the true range of variability in subarctic rivers.

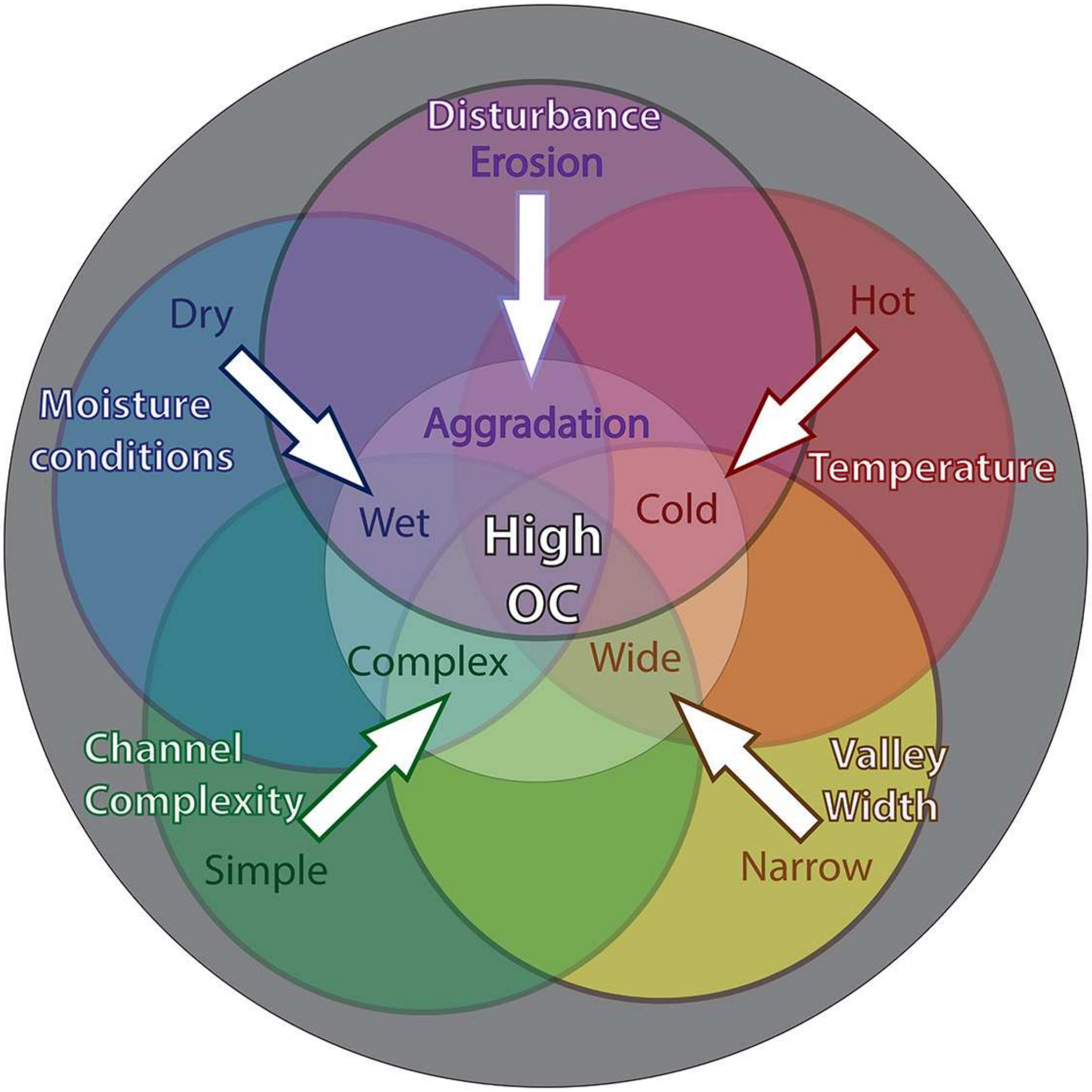

Figure 2.5 Optimal conditions for high organic carbon (OC) retention (in the center of the diagram) in river systems based on relationships between regional and local controls in Figure 2.3. Arrows denote the gradient toward optimal conditions with regard to valley width, channel complexity, moisture, temperature, and disturbance. Figure 2.3 illustrates the interrelations between other factors that influence these optimal conditions. Channel complexity, for example, is influenced by biotic drivers such as vegetation, beavers, and large downed wood; whereas moisture conditions are influenced by ecoregion, valley characteristics, channel complexity, and soil type. This model indicates that optimal conditions for organic carbon retention are low gradient river segments in broad unconfined valleys with high levels of channel complexity — which facilitates hydrologic connectivity, saturated conditions, and sediment aggradation — in cooler climates. Each component in this conceptual model can be influence by various factors is Figure 2.3. For example, moisture conditions can be influences by climate, valley geometry, channel form, and hydrologic connectivity.

Valley geometry influences available space for energy dissipation and the aggradation of alluvial sediment, which can influence primary productivity, abundance of riparian vegetation, and complexity of channel geometry. With room to move in relatively wide valleys and atop alluvial plains, channels can adjust their bedforms, width:depth ratio and cross sectional form, slope, channel planform, and grain size distribution (Leopold et al., 1964; Knighton, 1998; Wohl, 2014b) to develop complex geometries and floodplains that help to slow the movement of water, and facilitate moist conditions and deposition of sediment, OM, and OC.

Increased lateral and vertical hydrologic connectivity should ensure increased OC storage, as reflected in the highest SOC contents listed in this review (Wohl et al., 2012b; Wohl, 2013b), but this is dependent on the magnitude and frequency of hydrologic and geomorphic disturbances and the variability of moisture conditions. As long as connectivity between the floodplain and the channel facilitates aggradation, continued accumulation and storage of OC is ensured. Erosion of the floodplain during high magnitude floods can displace OC stored in floodplain sediment and remove riparian vegetation, hence the significance of wide valleys and open plains, which can dissipate energy and limit erosion of the floodplain.

I expect that low gradient, wide floodplains in old-growth forests with complex channel geometry, a high degree of lateral hydrologic connectivity between channels and floodplains, saturated soil conditions, and slow rates of organic decay associated with relatively cold temperatures will have the greatest per unit area storage of OC. Although the data presented in this review do not necessarily support this, I hypothesize that boreal, alpine, and cool temperate regions that exhibit the above-mentioned physical attributes are likely to store more OC per unit area compared to other regions, primarily because of low temperatures and rates of decomposition. Additional, field-based quantifications of OC storage are needed to examine the validity of this conceptual model and our proposed optimal conditions of OC storage in riparian ecosystems.

An accurate approximation of global carbon storage in riparian ecosystems requires additional information in under-represented regions, the use of common metrics for sampling and reporting values, and utilization of advanced computational resources capable of analyzing large quantities of remotely sensed data and modeling the various influential factors discussed here. Because temperate regions have received the large majority of attention with regard to OC in riparian ecosystems, the ability to extrapolate values across Earth's surface is limited. Despite the paucity of data and shortcomings in the state of reported OC values, a first order approximation can be made. Floodplains are estimated to cover approximately 0.8 x 10^6 to 2 x 10^6 km ^{2} globally (Leopold et al., 1964; Tockner and Stanford, 2002; Mitsch and Gosselink, 2015). As a conservative estimate across all climatic regions, and using the median for both the minimum and maximum values of organic carbon stored in riparian ecosystems (i.e., 202 – 386 Mg C ha^{-1}) from each study cited above, riverine ecosystems could store as much as 16 - 125 Pg C globally. Because SOC is the largest reservoir of OC in riparian ecosystems (Figure 2.4), I use the same method to estimate that floodplain SOC may account for 12 - 80 Pg C globally. When compared with modeled estimates of potential OC in soils globally (991 – 2469 Pg C; Hiederer and Kochy, 2011), our rough estimate suggests that riparian ecosystems could account for 0.5-8% of global SOC storage, even though they cover only 0.5-1% of the land surface. I emphasize that this is a first order approximation that must be refined with additional quantification from less represented climatic regions, as well as better use of remote sensing data to quantify total floodplain area and proportions of that total area associated with differing sizes of rivers and differing valley geometry and flow regime.

2.7 Human influences on OC reservoirs in riparian ecosystems

In this section, I briefly review human alterations of OC dynamics in river systems. Although human-induced changes in process and form within uplands and river corridors have likely exerted a substantial influence on OC transport to, and processing and storage within, rivers, this topic has received minimal attention. This section is intended to highlight the major categories of human influence and emphasize the need for more focused research on this topic.

Land use and land cover changes are transforming landscapes at an accelerating rate throughout the world and are recognized as a critical gap in the current understanding of the terrestrial carbon cycle (Houghton, 1994; Tappeiner et al., 2008). Land use can play a significant role in sediment and carbon supply to rivers, as well as accumulation rates within riparian ecosystems. Although largely undocumented, the conversion of fertile floodplains to other land uses, particularly agriculture, has likely caused significant carbon releases, reducing the amount of stored carbon (Mitra et al., 2005). Land use can also influence biomass and SOC by altering the age of riparian forests (Giese et al., 2000, 2003). SOC increases with stage of forest succession (Wigginton et al., 2000), although rates of OC accumulation can decline with time (Zehetner et al., 2009).

Land use can increase floodplain accumulation of OC, particularly forest harvest and agricultural practices that accelerate erosion and downslope movement of sediment (Noe and Hupp, 2005; McCarty et al., 2009). In a study of land-use trends in watersheds of southern New England, USA, Ricker et al. (2012) related patterns of riparian sedimentation and carbon sequestration rates to three major land-use periods: precolonial, colonial-agrarian, and modern. Although results varied across watersheds, they found that most of the stored sediment and SOC in riparian soils originated during the postcolonial period, and that net SOC sequestration rates have increased nearly 200-fold since precolonial times (pre-1800), likely due to regional deforestation and conversion to agricultural use. In contrast, Norton et al. (2011) found that degraded montane riparian meadows of the Sierra Nevada Mountains of California, USA, stored lower amounts of SOC than meadows in 'properly functioning condition'. Degradation was attributed to logging, a legacy of heavy, unregulated livestock grazing, and more recently, recreational vehicle use. Loss of biodiversity in riparian ecosystems (Tockner and Stanford, 2002) can greatly influence OM inputs to riverine ecosystems and potential carbon stocks.

Flow regulation can also influence OC dynamics within riparian ecosystems. Structures such as dams and diversions interrupt downstream transport of OM and DOC. Walter and Merritts (2008) document legacy sediment and OC storage of 250-1350 Mg C/ha behind thousands of abandoned milldams in Pennsylvania and Maryland, USA. Bank erosion of this legacy sediment redistributes OC along downstream floodplains (Schenk et al., 2013). Sediment aggradation in inland lentic waters including lakes and man-made reservoirs can store as much as 33% of the carbon moving through fluvial systems (Tranvik et al., 2009). Flow diversion also alters flow characteristics that support riparian vegetation and entrain and transport OM. In an examination of temporal effects of hydrologic connectivity on nutrient dynamics along a floodplain in the Danube River within Austria, for example, Tockner et al. (1999) determined that accumulation of OM occurred primarily during large flood pulses, whereas export of DOC occurred primarily during moderate flood levels with limited connectivity to the floodplain.

Channel manipulation in the form of channelization, straightening, dredging, bank stabilization, and construction of levees can influence OC dynamics by encouraging incision and altering longitudinal and lateral fluxes of water and fine sediment, OM, and DOC. These types of channel manipulation are commonly done to reduce flooding and to more efficiently convey water. By increasing longitudinal connectivity, these types of channel manipulations increase downstream fluxes and decrease vertical connectivity between the channel and hyporheic zone, and lateral connectivity between the channel and floodplain. This alters fluxes of dissolved and particulate OC by reducing retention of water and sediment in riparian areas and entire watersheds. Decreased retention of water and sediment reduces biological uptake and storage of OC within riparian ecosystems (Naiman et al., 1986). Current efforts in process-based channel restoration, however, aim to increase lateral connectivity of water and sediment to the floodplain and facilitate increased hyporheic exchange (Collins and Montgomery, 2002; Beechie et al., 2010; Burchsted et al., 2010).

2.8 Knowledge gaps and discussion

Although OC retention in floodplains and riparian areas is important for OC reservoirs and ecosystem processing, many gaps exist within our collective understanding of riparian OC pools. Gaps in knowledge include: (i) the magnitude of differences across regions and biomes, (ii) effects of a changing climate, (iii) residence time, and (v) human influences.

2.8.1 Data paucity

The most notable knowledge gap, apparent from this review, is the lack of global coverage of studies across diverse climates and geologic settings. Most studies, including surveys of OC in standing biomass, downed large wood, and soil in riparian ecosystems, lie within temperate climates, and few to no studies have been conducted in boreal, tropical, and arid regions. Most studies have been conducted in North America and Europe, but it is difficult in these regions to study landscapes that have not been highly impacted by human activities. Examining the natural processes responsible for OC retention in river systems requires working in less human-altered regions before these natural processes become too highly impacted. Work in these areas may also provide a baseline for future restoration. Additionally, data are limited in (i) more tectonically active landscapes, including the South American Andes and the Himalaya, (ii) areas which are difficult to study, such as large tropical rivers like the Amazon, and boreal rivers, (iii) mountainous environments, which are particularly sensitive to climate change, and (iv) arid and semi-arid regions, which may represent future conditions for many regions of the world following desertification and over-comsumption of freshwater resources. Although I propose general patterns of climatic and landscape controls on OC retention in riparian ecosystems, more research is needed to examine these relationships, test proposed influences, understand relevant processes, and establish baseline conditions for OC retention along river networks. This is important not only for the terrestrial carbon cycle and storage, but also for ecosystem processing, food webs, ecosystem integrity, and ecosystem services.

2.8.2 A changing climate

As climate change alters precipitation regimes, changes in seasonal hydrologic connectivity will likely influence the ability of individual landscapes to retain OC. Rising mean annual temperatures, declining snowpack, and earlier snowmelt in mountainous regions (Bates et al., 2008; Pederson et al., 2011) are expected to decrease hydrologic connectivity (Allison et al., 1990; Schulze and Walker, 1997; Alexander, 2014), and thus may impact ecosystem processing of OC and nutrients. Organic carbon with potential for long-term storage becomes more bioavailable as wetland soils dry completely or for longer periods throughout the year. This loss of moisture impacts soil microbial activity and the productivity of aquatic biota by altering connectivity, as well as changes in surface water temperature. Similarly, loss of connectivity causes shifts in riparian vegetation community structure and resulting leaf litter and POM. The directional shift caused by specific changes in processing of OC within riparian ecosystems is uncertain because of higher global average temperatures (Trumbore and Czimczik, 2008) and potential increase in the frequency of extreme storms (Bates et al., 2008). Increased intensity of feedbacks between riparian vegetation and channel planform impacts the natural ability of the landscape to delay, filter, and store POM, nutrients, and DOC from surface waters.

Projected sea level rise as a response to climate change has the potential to influence floodplain aggradation through changes in base level. Decline in the elevation of base level encourages channel incision, decreases lateral hydrologic connectivity, and may promote the decline of local water tables and abandonment of floodplain surfaces (Mertes and Dunne, 2007; Wohl, 2015). Periods of aggradation and degradation along the Mississippi River floodplain, for example, are closely tied to glacial cycles that regulate sea level (Knox, 2007). A rising sea level may mean less erosion of river channel beds, banks, and floodplains, and thus potentially more OC storage in riparian ecosystems.

Although disturbances such as insect infestations and wildfire occur naturally, their frequency and intensity are increasing with climate change (Westerling et al., 2006; Bentz et al., 2010). These factors influence the age, size, and abundance of wood available for recruitment and sources of CPOM (Amiro et al., 2010; Turner, 2010). Increased loss of old-growth forest as a result of increased frequency of these disturbances limits CPOM inputs, decreases standing biomass, and limits the size of large trees that can facilitate persistent, channel-spanning log jams (Wohl, 2013a).

2.8.3 Residence time

As mentioned above, residence time of OC in riparian ecosystems is regulated by the residence time of floodplain sediment and OM, as well as by microbial metabolism. Quantification of floodplain sediment turnover rates can help determine how long OM and associated OC remain in riparian ecosystems, but understanding rates of decomposition and mineralization of OC is required to fully quantify potential OC storage. The form in which OC is retained in riparian ecosystems influences potential for ecosystem processing or long-term storage. Recalcitrant and more stable forms of SOC may be retained for longer periods of time within the terrestrial carbon reservoir, whereas more labile and more easily processed forms of SOC serve as a source for metabolism by soil and aquatic biota (Blazejewski et al., 2005; Gurwick et al., 2008a). Hoffmann et al. (2013) identify three components of OC fluxes in sediment that warrant attention: i) increases in bioavailable OC following disaggregation, ii) adsorption of OC to mineral facies, and iii) increased stability of OC following aggradation and burial. These topics beg the question; Which factor most limits OC storage in floodplains, residence time of floodplain sediment or rate of microbial metabolism? These topics may become increasingly important as riparian soils dry and sea levels rise. More research is also needed to understand how and when the composition of microbial communities changes and how shifts in microbial communities influence processing of OC. It is also important to emphasize the large-scale and local influences on potential aggradation, long-term storage, and fate of OC in river systems. What are the tradeoffs between OC storage along complex channels, for example, versus increased hotspots for microbial mineralization of OC?

2.8.4 Land use in the Anthropocene

Although geologic setting and a changing climate regulate conditions for OC retention in riparian ecosystems, human activities that decrease channel complexity and hydrologic connectivity have the ability to greatly decrease OC retention in river systems. However, the relative magnitude of these human-induced effects is undetermined for diverse regions and biomes. As I establish a baseline understanding the natural processes of OC storage along river networks, I can begin to examine the impacts of land use more thoroughly. Work in human-altered areas is needed to determine whether process-based river restoration (Collins and Montgomery, 2002; Wohl et al., 2005, 2015; Beechie et al., 2010) and the use of green infrastructure in urban watersheds could mimic natural processes to increase carbon retention in riparian ecosystems.

The challenges facing freshwater sustainability under a warming climate are exacerbated by growing populations and increasing demand for freshwater as land-use managers continue to increase freshwater reservoirs and flow diversions. Flow alterations and unsustainable groundwater pumping may also lower the elevation of groundwater tables connected to rivers and streams and induce drying of riparian wetlands. Uncertainties regarding changes to the hydrologic regime, population growth, and land use leave many questions regarding the future of carbon in river systems.

Berhe et al. (2007) and Oost et al. (2012) suggest that erosion following disturbance increases the capacity of the landscape to take up carbon by removing vegetation and OC stored in soils. Uptake then increases as vegetation grows more rapidly and soils begin to develop. Thus, if human activities such as agriculture and urbanization increase erosion rates (Wolman, 1967) or severe storms and floods occur more frequently with the onset of climate change (Bates et al., 2008), more rapid terrestrial OC uptake may occur. If the transported sediment and associated OC is eventually delivered to a floodplain, delta, estuary, or subduction zone for longer-term storage, this provides space for more sediment and associated OC to accumulate, and therefore could provide a net increase in OC storage. If erosion simply makes the OC more available for decomposition and metabolism, storage capacity of OC would decrease following the disturbance.

2.9 Conclusion

Current research suggests that rivers play a significant, albeit currently poorly quantified, role in the global carbon cycle. Limited studies indicate that riparian ecosystems and floodplains can store a significantly larger amount of carbon per area compared to surrounding uplands. The primary reservoirs for OC in riparian ecosystems are i) aboveground standing biomass, ii) large downed wood, iv) OM and sediment on and beneath the floodplain surface. The relative importance of these pools varies with scale, ecoregion, and geologic setting to the extent that no significant patterns have yet emerged. Land use, flow regulation, and channel manipulation greatly impact i) water and sediment regime, ii) hydrologic connectivity, iii) channel complexity, and iv) inputs and accumulation of OM that control retention of OC in riparian ecosystems. I propose that broad unconfined valleys with complex channel geometry and wet conditions in cool regions are optimal conditions for OC retention and storage in riparian ecosystems. Further investigation of a wide range of rivers across various scales and climates is necessary to determine global significance of river systems in the terrestrial carbon budget. Not all river systems are created equal — some types of rivers and some portions of each river are likely disproportionately important with respect to OC storage — but we need additional basic field data to begin to understand these differences. If research quantifies these differences, and particularly if we can identify hot spots of OC storage, such knowledge can be used to inform river management and restoration, not least because OC storage zones are also likely to be highly biologically productive for instream and riparian communities (Bellmore and Baxter, 2014).

Recognition

This paper is based upon work supported by National Science Foundation Grant No. DGE-0966346 "I-WATER: Integrated Water, Atmosphere, Ecosystems Education and Research Program" at Colorado State University. I thank two anonymous reviewers for useful comments on the paper.

References

Aalto R, Maurice-Bourgoin L, Dunne T, Montgomery DR, Nittrouer CA, Guyot J-L. 2003. Episodic sediment accumulation on Amazonian flood plains influenced by El Niño/Southern Oscillation. Nature 425 : 493–497. DOI: 10.1038/nature02002

Abbe TB, Montgomery DR. 2003. Patterns and processes of wood debris accumulation in the Queets river basin, Washington. Geomorphology 51 : 81–107. DOI: 10.1016/S0169-555X(02)00326-4

Abernethy B, Rutherfurd ID. 2001. The distribution and strength of riparian tree roots in relation to riverbank reinforcement. Hydrological processes 15 : 63–79.

Aguado E, Burt JE. 2007. Understanding Weather and Climate . 4th ed. Prentice Hall [online] Available from: http://www.abebooks.com/Understanding-Weather-Climate-4th-Edition-Edward/12725764606/bd (Accessed 29 August 2014)

Alexander L. 2014. Connectivity of Streams and Wetlands to Downstream Waters: A Review and Synthesis of the Scientific Evidence (External Review Draft) . US EPA National Center for Environmental Assessment. Environmental Protetion Agency: Washington DC [online] Available from: http://cfpub.epa.gov/ncea/cfm/recordisplay.cfm?deid=238345 (Accessed 26 January 2015)

Alin SR, Aalto R, Goni MA, Richey JE, Dietrich WE. 2008. Biogeochemical characterization of carbon sources in the Strickland and Fly rivers, Papua New Guinea. Journal of Geophysical Research 113 DOI: 10.1029/2006JF000625 [online] Available from: http://doi.wiley.com/10.1029/2006JF000625 (Accessed 6 May 2014)

Allan JD, Castillo MM. 2007. Stream Ecology . Second Edition. Springer: Dordrecht, THe Netherlands

Allison GB, Cook PG, Barnett SR, Walker GR, Jolly ID, Hughes MW. 1990. Land clearance and river salinisation in the western Murray Basin, Australia. Journal of Hydrology 119 : 1–20. DOI: 10.1016/0022-1694(90)90030-2

Amerson BE, Montgomery DR, Meyer G. 2008. Relative size of fluvial and glaciated valleys in central Idaho. Geomorphology 93 : 537–547. DOI: 10.1016/j.geomorph.2007.04.001

Amiro BD, Barr AG, Barr JG, Black TA, Bracho R, Brown M, Chen J, Clark KL, Davis KJ, Desai AR, Dore S, Engel V, Fuentes JD, Goldstein AH, Goulden ML, Kolb TE, Lavigne MB, Law BE, Margolis HA, Martin T, McCaughey JH, Misson L, Montes-Helu M, Noormets A, Randerson JT, Starr G, Xiao J. 2010. Ecosystem carbon dioxide fluxes after disturbance in forests of North America. Journal of Geophysical Research 115, G00K02, doi:10.1029/2010JG001390.

Appling AP. 2012. Connectivity drives function: carbon and nitrogen dynamics in a floodplain-aquifer ecosystem. PhD dissertation, Duke University, Durham, North Carolina.

Arcement GJ, Schneider VR. 1989. Guide for selecting Manning's roughness coefficients for natural channels and flood plains . US Government Printing Office [online] Available from: http://mosfet.isu.edu/classes/Sato/ENVE615/S13/Manning%20n.pdf (Accessed 1 May 2014)

Aufdenkampe AK, Mayorga E, Raymond PA, Melack JM, Doney SC, Alin SR, Aalto RE, Yoo K. 2011. Riverine coupling of biogeochemical cycles between land, oceans, and atmosphere. Frontiers in Ecology and the Environment 9 : 53–60. DOI: 10.1890/100014

Bailey RG. 2009. Ecosystem Geography: From Ecoregions to Sites . 2nd ed. Springer

Ballantyne AP, Alden CB, Miller JB, Tans PP, White JWC. 2012. Increase in observed net carbon dioxide uptake by land and oceans during the past 50 years. Nature 488 : 70–72. DOI: 10.1038/nature11299

Baron J, McKnight D, Denning AS. 1991. Sources of dissolved and particulate organic material in Loch Vale watershed, Rocky Mountain National Park, Colorado, USA. Biogeochemistry 15 : 89–110.

Bates BC, Kundzewicz ZW, Palutikof JP. 2008. Climate change and water . Technical Report. IPCC: IPCC Secretariat, Geneva

Battin TJ, Kaplan LA, Findlay S, Hopkinson CS, Marti E, Packman AI, Newbold JD, Sabater F. 2008. Biophysical controls on organic carbon fluxes in fluvial networks. Nature Geoscience 1 : 95–100. DOI: 10.1038/ngeo101

Battin TJ, Luyssaert S, Kaplan LA, Aufdenkampe AK, Richter A, Tranvik LJ. 2009. The boundless carbon cycle. Nature Geoscience 2 : 598–600. DOI: 10.1038/ngeo618

Beckman ND, Wohl E. 2014. Carbon storage in mountainous headwater streams: The role of old-growth forest and logjams. Water Resources Research 50 : 2376–2393. DOI: 10.1002/2013WR014167

Beechie TJ, Sear DA, Olden JD, Pess GR, Buffington JM, Moir H, Roni P, Pollock MM. 2010. Process-based Principles for Restoring River Ecosystems. BioScience 60 : 209–222. DOI: 10.1525/bio.2010.60.3.7

Bellmore JR, Baxter CV. 2014. Effects of Geomorphic Process Domains on River Ecosystems: A Comparison of Floodplain and Confined Valley Segments. River Research and Applications 30 : 617–630. DOI: 10.1002/rra.2672

Benda LE, Sias JC. 2003. A quantitative framework for evaluating the mass balance of in-stream organic debris. Forest Ecology and Management 172 : 1–16. DOI: 10.1016/S0378-1127(01)00576-X

Benda L, Hassan MA, Church M, May CL. 2005. Geomorphology of Steepland Headwaters: The Transition from Hillslopes to Channels1. JAWRA Journal of the American Water Resources Association 41 : 835–851. DOI: 10.1111/j.1752-1688.2005.tb03773.x

Benfield EF. 1997. Comparison of litterfall input to streams. Journal of the North American Benthological Society 16 : 104. DOI: 10.2307/1468242

Bentz BJ, Régnière J, Fettig CJ, Hansen EM, Hayes JL, Hicke JA, Kelsey RG, Negrón JF, Seybold SJ. 2010. Climate Change and Bark Beetles of the Western United States and Canada: Direct and Indirect Effects. BioScience 60 : 602–613. DOI: 10.1525/bio.2010.60.8.6

Berhe AA, Harte J, Harden JW, Torn MS. 2007. The Significance of the Erosion-induced Terrestrial Carbon Sink. BioScience 57 : 337–346. DOI: 10.1641/B570408

Bianchi TS, Allison MA. 2009. Large-river delta-front estuaries as natural "recorders" of global environmental change. Proceedings of the National Academy of Sciences 106 : 8085–8092. DOI: 10.1073/pnas.0812878106

Bilby RE. 1981. Role of organic debris dams in regulating the export of dissolved and particulate matter from a forested watershed. Ecology 62 : 1234–1243.

Billings SA, Richter DD, Yarie J. 1998. Soil carbon dioxide fluxes and profile concentrations in two boreal forests. Canadian Journal of Forest Research 28 : 1773–1783.

Birkeland PW. 1999. Soils and geomorphology . 3rd ed. Oxford University Press: New York, NY

Blazejewski GA, Stolt MH, Gold AJ, Groffman PM. 2005. Macro- and Micromorphology of Subsurface Carbon in Riparian Zone Soils. Soil Science Society of America Journal 69 : 1320. DOI: 10.2136/sssaj2004.0145

Blazejewski GA, Stolt MH, Gold AJ, Gurwick N, Groffman PM. 2009. Spatial Distribution of Carbon in the Subsurface of Riparian Zones. Soil Science Society of America Journal 73 : 1733. DOI: 10.2136/sssaj2007.0386

Boyce JS. 1961. Forest Pathology . 1961 Third Edition edition. McGraw: N.Y.; Toronto

Bracken LJ, Wainwright J, Ali GA, Tetzlaff D, Smith MW, Reaney SM, Roy AG. 2013. Concepts of hydrological connectivity: Research approaches, pathways and future agendas. Earth-Science Reviews 119 : 17–34. DOI: 10.1016/j.earscirev.2013.02.001

Bradford JB, Birdsey RA, Joyce LA, Ryan MG. 2008. Tree age, disturbance history, and carbon stocks and fluxes in subalpine Rocky Mountain forests. Global Change Biology 14 : 2882–2897. DOI: 10.1111/j.1365-2486.2008.01686.x

Bray JR, Gorham E. 1964. Litter production in forests of the world. Advances in ecological research : 101–157.

Brierley GJ, Fryirs KA. 2005. Geomorphology and River Management: Applications of the River Styles Framework . 1st ed. Blackwell: Oxford, UK [online] Available from: http://www.wiley.com/WileyCDA/WileyTitle/productCd-1405115165.html

Brinson MM, Bradshaw HD, Holmes RN, Elkins JB. 1980. Litterfall, stemflow, and throughfall nutrient fluxes in an alluvial swamp forest. Ecology 61 : 827-835.

Brummer CJ, Abbe TB, Sampson JR, Montgomery DR. 2006. Influence of vertical channel change associated with wood accumulations on delineating channel migration zones, Washington, USA. Geomorphology 80 : 295–309. DOI: 10.1016/j.geomorph.2006.03.002

Burchsted D, Daniels M, Thorson R, Vokoun J. 2010. The River Discontinuum: Applying Beaver Modifications to Baseline Conditions for Restoration of Forested Headwaters. BioScience 60 : 908–922. DOI: 10.1525/bio.2010.60.11.7

Butler DR. 1995. Zoogeomorphology: Animals as Geomorphic Agents . Cambridge University Press

Cabezas A, Comín FA, Walling DE. 2009. Changing patterns of organic carbon and nitrogen accretion on the middle Ebro floodplain (NE Spain). Ecological Engineering 35 : 1547–1558. DOI: 10.1016/j.ecoleng.2009.07.006

Cadol D, Wohl E, Goode JR, Jaeger KL. 2009. Wood distribution in neotropical forested headwater streams of La Selva, Costa Rica. Earth Surface Processes and Landforms 34 : 1198–1215. DOI: 10.1002/esp.1800

Camporeale C, Perucca E, Ridolfi L, Gurnell AM. 2013. Modeling the interactions between river morphodynamics and riparian vegetation: River morphodynamics and riparian zones. Reviews of Geophysics 51 : 379–414. DOI: 10.1002/rog.20014

Camporeale C, Ridolfi L. 2006. Riparian vegetation distribution induced by river flow variability: A stochastic approach. Water Resources Research 42 : W10415. DOI: 10.1029/2006WR004933

Chapin III FS, Matson PA, Vitousek PM. 2011. Principles of terrestrial ecosystem ecology . 2nd ed. Springer: New York

Chen X, Wei X, Scherer R. 2005. Influence of wildfire and harvest on biomass, carbon pool, and decomposition of large woody debris in forested streams of southern interior British Columbia. Forest Ecology and Management 208 : 101–114. DOI: 10.1016/j.foreco.2004.11.018

Chmura GL, Anisfeld SC, Cahoon DR, Lynch JC. 2003. Global carbon sequestration in tidal, saline wetland soils. Global Biogeochemical Cycles 17 : 1111. DOI: 10.1029/2002GB001917

Cierjacks A, Kleinschmit B, Babinsky M, Kleinschroth F, Markert A, Menzel M, Ziechmann U, Schiller T, Graf M, Lang F. 2010. Carbon stocks of soil and vegetation on Danubian floodplains. Journal of Plant Nutrition and Soil Science 173 : 644–653. DOI: 10.1002/jpln.200900209

Clark DB, Clark DA, Brown S, Oberbauer SF, Veldkamp E. 2002. Stocks and flows of coarse woody debris across a tropical rain forest nutrient and topography gradient. Forest Ecology and Management 164 : 237–248. DOI: 10.1016/S0378-1127(01)00597-7

Clary WP. 1999. Stream Channel and Vegetation Responses to Late Spring Cattle Grazing. Journal of Range Management 52 : 218–227. DOI: 10.2307/4003683

Coffin JC, Ge R, Yang S, Kramer PM, Tao L, Pereira MA. 2000. Effect of Trihalomethanes on Cell Proliferation and DNA Methylation in Female B6C3F1 Mouse Liver. Toxicological Sciences 58 : 243–252. DOI: 10.1093/toxsci/58.2.243

Cole JJ, Prairie YT, Caraco NF, McDowell WH, Tranvik LJ, Striegl RG, Duarte CM, Kortelainen P, Downing, JA Middelburg JJ, Melack J. 2007. Plumbing the Global Carbon Cycle: Integrating Inland Waters into the Terrestrial Carbon Budget. Ecosystems 10 : 172–185. DOI: 10.1007/s10021-006-9013-8

Collins BD, Montgomery DR. 2002. Forest Development, Wood Jams, and Restoration of Floodplain Rivers in the Puget Lowland, Washington. Restoration Ecology 10 : 237–247. DOI: 10.1046/j.1526-100X.2002.01023.x

Collins BD, Montgomery DR, Fetherston KL, Abbe TB. 2012. The floodplain large-wood cycle hypothesis: A mechanism for the physical and biotic structuring of temperate forested alluvial valleys in the North Pacific coastal ecoregion. Geomorphology 139–140 : 460–470. DOI: 10.1016/j.geomorph.2011.11.011

Comiti F, Andreoli A, Lenzi MA, Mao L. 2006. Spatial density and characteristics of woody debris in five mountain rivers of the Dolomites (Italian Alps). Geomorphology 78 : 44-63.

Comiti F, Andreoli A, Mao L, and Lenzi MA. 2008. Wood storage in three mountain streams of the southern Andes and its hydro-morphological effects. Earth Surface Processes and Landforms 33 : 244-262.

Conners ME, Naiman RJ. 1984. Particulate allochthonous inputs: Relationships with stream size in an undisturbed watershed. Canadian Journal of Fisheries and Aquatic Sciences 41 : 1473–1484. DOI: 10.1139/f84-181

Cooper DJ, Merritt DM, Andersen DC, Chimner RA. 1999. Factors controlling the establishment of Fremont cottonwood seedlings on the Upper Green River, USA. Regulated Rivers: Research & Management 15 : 419–440. DOI: 10.1002/(SICI)1099-1646(199909/10)15:5<419::AID-RRR555>3.0.CO;2-Y

Correll DL, Jordan TE, Weller DE. 2000. Beaver pond biogeochemical effects in the Maryland Coastal Plain. Biogeochemistry 49 : 217–239. DOI: 10.1023/A:1006330501887

Costard F, Gautier E. 2007. The Lena River: Hydromorphodynamic features in a deep permafrost zone. In Large Rivers: Geomorphology and Management , Gupta A (ed). John Wiley & Sons: West Sussex, England; 225–232.

Craft CB, Casey WP. 2000. Sediment and nutrient accumulation in floodplain and depressional freshwater wetlands of Georgia, USA. Wetlands 20 : 323-332.

Craig LS, Palmer MA, Richardson DC, Filoso S, Bernhardt ES, Bledsoe BP, Doyle MW, Groffman PM, Hassett BA, Kaushal SS, Mayer PM, Smith SM, Wilcock PR. 2008. Stream restoration strategies for reducing river nitrogen loads. Frontiers in Ecology and the Environment 6 : 529–538. DOI: 10.1890/070080

Dasgupta R, Hirschmann MM. 2010. The deep carbon cycle and melting in Earth's interior. Earth and Planetary Science Letters 298 : 1–13. DOI: 10.1016/j.epsl.2010.06.039

Delaney M, Brown S, Lugo AE, Torres-Lezama A, Quintero NB. 1998. The Quantity and Turnover of Dead Wood in Permanent Forest Plots in Six Life Zones of Venezuela1. Biotropica 30 : 2–11. DOI: 10.1111/j.1744-7429.1998.tb00364.x

Devito KJ, Fitzgerald D, Hill AR, Aravena R. 2000. Nitrate dynamics in relation to lithology and hydrologic flow path in a river riparian zone. Journal of Environmental Quality 29 : 1075–1084.

Dodds WK, Gido K, Whiles MR, Daniels Melinda D., Grudzinski BP. 2015. The Stream Biome Gradient Concept: factors controlling lotic systems across broad biogeographic scales. Freshwater Science 34 : 1–19. DOI: 10.1086/679756

Dunne T, Leopold LB. 1978. Water in Environmental Planning . Macmillan

Dwire KA, Kauffman JB, Brookshire ENJ, Baham JE. 2004. Plant biomass and species composition along an environmental gradient in montane riparian meadows. Oecologia 139 : 309–317. DOI: 10.1007/s00442-004-1498-2

Edwards RT. 1998. The hyporheic zone. In River ecology and management , Naiman RJ and Bilby RE (eds). Springer-Verlag: New York; 399–429.

Ehlen J, Wohl EE. 2002. Joints and landform evolution in bedrock canyons. Transactions, Japanese Geomorphological Union 23 : 237–255.

Ellis LM, Molles MC, Crawford CS. 1999. Influence of Experimental Flooding on Litter Dynamics in a Rio Grande Riparian Forest, New Mexico. Restoration Ecology 7 : 193–204. DOI: 10.1046/j.1526-100X.1999.72012.x

Falloon P, Jones CD, Ades M, Paul K. 2011. Direct soil moisture controls of future global soil carbon changes: An important source of uncertainty. Global Biogeochemical Cycles 25 : 1–14. DOI: 10.1029/2010GB003938

Fierke MK, Kauffman JB. 2005. Structural dynamics of riparian forests along a black cottonwood successional gradient. Forest Ecology and Management 215 : 149–162. DOI: 10.1016/j.foreco.2005.06.014

Filippi AM, Güneralp İ, Randall J. 2014. Hyperspectral remote sensing of aboveground biomass on a river meander bend using multivariate adaptive regression splines and stochastic gradient boosting. Remote Sensing Letters 5 : 432–441. DOI: 10.1080/2150704X.2014.915070

Findlay SEG, Tank J, Dye S, Valett HM, Mulholland PJ, McDowell WH, Johnson SL, Hamilton SK, Edmonds J, Dodds WK, and Bowden WB. 2002. A cross-system comparison of bacterial and fungal biomass in detritus pools of headwater streams. Microbial Ecology 43 : 55-66.

Fox M, Bolton S. 2007. A regional and geomorphic reference for quantities and volumes of instream wood in unmanaged forested basins of Washington State. North American Journal of Fisheries Management 27, 342-359.

Friedman JM, Lee VJ. 2002. Extreme floods, channel change, and riparian forests along ephemeral streams. Ecological Monographs 72 : 409–425.

Fryirs K. 2013. (Dis)Connectivity in catchment sediment cascades: a fresh look at the sediment delivery problem. Earth Surface Processes and Landforms 38 : 30–46. DOI: 10.1002/esp.3242

Fryirs KA, Brierley GJ, Preston NJ, Spencer J. 2007. Catchment-scale (dis)connectivity in sediment flux in the upper Hunter catchment, New South Wales, Australia. Geomorphology 84 : 297–316. DOI: 10.1016/j.geomorph.2006.01.044

Giese LA, Aust WM, Trettin CC, Kolka RK. 2000. Spatial and temporal patterns of carbon storage and species richness in three South Carolina coastal plain riparian forests. Ecological Engineering 15, Supplement 1 : S157–S170. DOI: 10.1016/S0925-8574(99)00081-6

Giese LAB, Aust WM, Kolka RK, Trettin CC. 2003. Biomass and carbon pools of disturbed riparian forests. Forest Ecology and Management 180 : 493–508. DOI: 10.1016/S0378-1127(02)00644-8

Gomi T, Sidle RC, Richardson JS. 2002. Understanding Processes and Downstream Linkages of Headwater Systems. BioScience 52 : 905. DOI: 10.1641/0006-3568(2002)052[0905:UPADLO]2.0.CO;2

Goni MA, Monacci N, Gisewhite R, Crockett J, Nittrouer C, Ogston A, Alin SR, Aalto R. 2008. Terrigenous organic matter in sediments from the Fly River delta-clinoform system (Papua New Guinea). Journal of Geophysical Research: Earth Surface 113 : F01S10. DOI: 10.1029/2006JF000653

Gregory JM, Jones CD, Cadule P, Friedlingstein P. 2009. Quantifying Carbon Cycle Feedbacks. Journal of Climate 22 : 5232–5250. DOI: 10.1175/2009JCLI2949.1

Gregory SV, Swanson FJ, McKee WA, Cummins KW. 1991. An Ecosystem Perspective of Riparian Zones. BioScience 41 : 540–551. DOI: 10.2307/1311607

Gurwick NP, Groffman PM, Yavitt JB, Gold AJ, Blazejewski G, Stolt M. 2008a. Microbially available carbon in buried riparian soils in a glaciated landscape. Soil Biology and Biochemistry 40 : 85–96. DOI: 10.1016/j.soilbio.2007.07.007

Gurwick NP, McCorkle DM, Groffman PM, Gold AJ, Kellogg DQ, Seitz-Rundlett P. 2008b. Mineralization of ancient carbon in the subsurface of riparian forests. Journal of Geophysical Research 113 DOI: 10.1029/2007JG000482 [online] Available from: http://doi.wiley.com/10.1029/2007JG000482 (Accessed 1 May 2014)

Guyette RP, Cole WG, Dey DC, Muzika R-M. 2002. Perspectives on the age and distribution of large wood in riparian carbon pools. Canadian Journal of Fisheries and Aquatic Sciences 59 : 578–585. DOI: 10.1139/f02-026

Guyette RP, Dey DC, Stambaugh MC. 2008. The Temporal Distribution and Carbon Storage of Large Oak Wood in Streams and Floodplain Deposits. Ecosystems 11 : 643–653. DOI: 10.1007/s10021-008-9149-9

Hall R, Baker M, Arp C, Koch B. 2009. Hydrologic control of nitrogenremoval, storage and export in a mountain stream. Limnology and Oceanography 54 : 2128–2142.

Harmon ME. 1982. Decomposition of standing dead trees in the southern Appalachian Mountains. Oecologia 52 : 214–215. DOI: 10.1007/BF00363839

Harms TK, Grimm NB. 2008. Hot spots and hot moments of carbon and nitrogen dynamics in a semiarid riparian zone. Journal of Geophysical Research: Biogeosciences 113 : G01020. DOI: 10.1029/2007JG000588

Hiederer R, Kochy M. 2011. Global soil organic carbon estimates and the Harmonized World Soil Database . JRC Scientific and Technical Report. European Union European Joint Commission Centre: Luxembourg

Hill AR. 1996. Nitrate Removal in Stream Riparian Zones. Journal of Environment Quality 25 : 743. DOI: 10.2134/jeq1996.00472425002500040014x

Hill AR, Devito KJ, Campagnolo S, Sanmugadas K. 2000. Subsurface denitrification in a forest riparianzone: interactions between hydrology and supplies ofnitrate and organic carbon. Biogeochemistry 51 : 193–223.

Hilton RG, Galy A, Hovius N. 2008. Riverine particulate organic carbon from an active mountain belt: Importance of landslides: LANDSLIDE MOBILIZED POC. Global Biogeochemical Cycles 22 : n/a–n/a. DOI: 10.1029/2006GB002905

Hilton RG, Galy A, Hovius N, Horng M, Chen H. 2010. Efficient transport of fossil organic carbon to the ocean by steep mountain rivers: Retaining carbon in the lithosphere. 0290 pp. [online] Available from: http://adsabs.harvard.edu/abs/2010AGUFM.B41A0290H (Accessed 4 May 2014)

Hoffmann T, Mudd SM, van Oost K, Verstraeten G, Erkens G, Lang A, Middelkoop H, Boyle J, Kaplan JO, Willenbring J, Aalto R. 2013. Short Communication: Humans and the missing C-sink: erosion and burial of soil carbon through time. Earth Surface Dynamics Discussions 1 : 93–112. DOI: 10.5194/esurfd-1-93-2013

Hoffmann T, Glatzel S, Dikau R. 2009. A carbon storage perspective on alluvial sediment storage in the Rhine catchment. Geomorphology 108 : 127–137. DOI: 10.1016/j.geomorph.2007.11.015

Hoffmann U, Hoffmann T, Johnson EA, Kuhn NJ. 2014a. Assessment of variability and uncertainty of soil organic carbon in a mountainous boreal forest (Canadian Rocky Mountains, Alberta). CATENA 113 : 107–121. DOI: 10.1016/j.catena.2013.09.009

Hoffmann U, Hoffmann T, Jurasinski G, Glatzel S, Kuhn NJ. 2014b. Assessing the spatial variability of soil organic carbon stocks in an alpine setting (Grindelwald, Swiss Alps). Geoderma 232–234 : 270–283. DOI: 10.1016/j.geoderma.2014.04.038

Houghton RA. 1994. The Worldwide Extent of Land-Use Change. BioScience 44 : 305–313. DOI: 10.2307/1312380

Hupp CR, Demas CR, Kroes DE, Day RH, Doyle TW. 2008. Recent sedimentation patterns within the central Atchafalaya Basin, Louisiana. Wetlands 28 : 125–140. DOI: 10.1672/06-132.1

Hyatt TL, Naiman RJ. 2001. The residence time of large woody debris in the Queets River, Washington, USA. Ecological Applications 11 : 191–202. DOI: 10.1890/1051-0761(2001)011[0191:TRTOLW]2.0.CO;2

Ives RL. 1942. The beaver-meadow complex. Journal of Geomorphology 5 : 191–203.

Jaramillo VJ, Kauffman JB, Rentería-Rodríguez L, Cummings DL, Ellingson LJ. 2003. Biomass, Carbon, and Nitrogen Pools in Mexican Tropical Dry Forest Landscapes. Ecosystems 6 : 609–629. DOI: 10.1007/s10021-002-0195-4

Jobbágy EG, Jackson RB. 2000. The vertical distribution of soil organic carbon and its relation to climate and vegetation. Ecological applications 10 : 423–436.

Jones CG. 2012. Ecosystem engineers and geomorphological signatures in landscapes. Geomorphology 157–158 : 75–87. DOI: 10.1016/j.geomorph.2011.04.039

Jong C de, Collins D, Ranzi R (eds). 2005. Climate and Hydrology in Mountain Areas. In Climate and Hydrology in Mountain Areas , . John Wiley & Sons, Ltd; i–xvii. [online] Available from: http://onlinelibrary.wiley.com/doi/10.1002/0470858249.fmatter/summary (Accessed 25 June 2015)

Kasahara T, Wondzell SM. 2003. Geomorphic controls on hyporheic exchange flow in mountain streams: Geomorphic controls on hyporheic exchange. Water Resources Research 39 : SBH 3–1–SBH 3–14. DOI: 10.1029/2002WR001386

Kauffman JB, Krueger WC, Vavra M. 1983. Impacts of Cattle on Streambanks in Northeastern Oregon. Journal of Range Management 36 : 683–685. DOI: 10.2307/3898184

Kayranli B, Scholz M, Mustafa A, Hedmark Å. 2010. Carbon Storage and Fluxes within Freshwater Wetlands: a Critical Review. Wetlands 30 : 111–124. DOI: 10.1007/s13157-009-0003-4

Keim F, Skaugset E, Bateman S. 2000. Dynamics of Coarse Woody Debris Placed in Three Oregon Streams. Forest Science 46 : 13–22.

Keller EA, MacDonald A, Tally T, Merrirr NJ. 1995. Effects of large organic debris on channel morphology and sediment storage in selected tributaries of Redwood Creek, northwestern California . USGS Professional Paper 1454

Knighton D. 1998. Fluvial Forms and Processes: A New Perspective . 2 edition. Routledge: London ; New York

Knox JC. 2007. The Mississippi River system. In Large Rivers: Geomorphology and Management , Gupta A (ed). John Wiley & Sons: West Sussex, England; 145–177.

Koch JC, Ewing SA, Striegl R, Mcknight DM. 2013. Rapid runoff via shallow throughflow and deeper preferential flow in a boreal catchment underlain by frozen silt (Alaska, USA). Hydrogeology Journal 21 : 93–106. DOI: http://dx.doi.org.ezproxy2.library.colostate.edu:2048/10.1007/s10040-012-0934-3

Kramer N, Wohl EE, Harry DL. 2012. Using ground penetrating radar to “unearth” buried beaver dams. Geology 40 : 43–46. DOI: 10.1130/G32682.1

Kueppers LM, Southon J, Baer P, Harte J. 2004. Dead Wood Biomass and Turnover Time, Measured by Radiocarbon, along a Subalpine Elevation Gradient. Oecologia 141 : 641–651.

Lane EW. 1955. Design of Stable Channels. Transactions of the American Society of Civil Engineers 120 : 1234–1260.

Latterell JJ, Naiman RJ. 2007. Sources and dynamics of large logs in a temperate floodplain river. Ecological Applications 17 : 1127–1141. DOI: 10.1890/06-0963

Latterell JJ, Scott Bechtold J, O’keefe TC, Van Pelt R, Naiman RJ. 2006. Dynamic patch mosaics and channel movement in an unconfined river valley of the Olympic Mountains. Freshwater Biology 51 : 523–544. DOI: 10.1111/j.1365-2427.2006.01513.x

Leithold EL, Blair NE, Perkey DW. 2006. Geomorphologic controls on the age of particulate organic carbon from small mountainous and upland rivers: AGE OF POC. Global Biogeochemical Cycles 20 : n/a–n/a. DOI: 10.1029/2005GB002677

Leopold LB, Bull WB. 1979. Base Level, Aggradation, and Grade. Proceedings of the American Philosophical Society 123 : 168–202.

Leopold LB, Wolman MG, Miller JP. 1964. Fluvial Processes in Geomorphology . Courier Dover Publications

LeQuere C, Raupach MR, Canadell JG, Marland G, Bopp L, Ciais P, Conway TJ, Doney SC, Feely RE, Foster R, Friedlingstein P, Gurvey K, Houghton RA, House JI, Huntingford C, Levy PE, Lomas MR, Majkut J, Metzl N, Ometto JP, Peters GP, Prentice IC, Randerson JT, Running SW, Sarmiento JL, Schuster U, Sitch S, Takahashi T, Viovy N, van der Werf GR, Woodward FI. 2009. Trends in the sources and sinks of carbon dioxide. Nature Geoscience 2 : 831–836. DOI: 10.1038/ngeo689

Lewis SL, Phillips OL, Sheil D, Vinceti B, Baker TR, Brown S, Graham AW, Higuchi N, Hilbert DW, Laurance WF, Lejoly J, Malhi Y, Monteagudo A, Vargas PN, Sonke B, Supardi MNN, Terborgh JW, Martinez RV. 2004. Tropical forest tree mortality, recruitment and turnover rates: calculation, interpretation and comparison when census intervals vary. Journal of Ecology 92 : 929–944. DOI: 10.1111/j.0022-0477.2004.00923.x

Loukas A, Vasiliades L, Dalezios NR. 2000. Flood producing mechanisms identification in southern British Columbia, Canada. Journal of Hydrology 227 : 218–235. DOI: 10.1016/S0022-1694(99)00182-1

Lutes DC, Keane RE, Caratti JF, Key CH, Benson N., Sutherland S, Gangi LJ. 2006. Fire effects monitoring and inventory systems . General Technical Report. U.S. Department of Agriculture, Forest Service, Rocky Mountain Research Station: Fort Collins, CO

Lyons WB, Nezat CA, Carey AE, Hicks DM. 2002. Organic carbon fluxes to the ocean from high-standing islands. Geology 30 : 443–446. DOI: 10.1130/0091-7613(2002)030<0443:OCFTTO>2.0.CO;2

McCarty G, Pachepsky Y, Ritchie J. 2009. Impact of Sedimentation on Wetland Carbon Sequestration in an Agricultural Watershed. Journal of Environment Quality 38 : 804. DOI: 10.2134/jeq2008.0012

McClain ME, Boyer EW, Dent CL, Gergel SE, Grimm NB, Groffman PM, Hart SC, Harvey JW, Johnston CA, Mayorga E, McDowell WH, Pinay G. 2003.. Biogeochemical Hot Spots and Hot Moments at the Interface of Terrestrial and Aquatic. Ecosystems 6 : 301–312. DOI: 10.1007/s10021-003-0161-9

Meade RH, 2007. Transcontinental moving and storage: the Orinoco and Amazon Rivers transfer the Andes to the Atlantic. In, A. Gupta, ed., Large Rivers: Geomorphology and Management, John Wiley and Sons, Chichester, 45-63.

Merritt DM. 2013. Recipricol relations between riparian vegetation, fluvial landforms, and channel process. In Treatise on geomorphology , Wohl EE (ed). Academic Press: Poland;

Merritt DM, Poff NLR. 2010. Shifting dominance of riparian Populus and Tamarix along gradients of flow alteration in western North American rivers. Ecological Applications 20 : 135–152.

Merritt DM, Wohl EE. 2003. Downstream hydraulic geometry and channel adjustment during a flood along an ephemeral, arid-region drainage. Geomorphology 52 : 165–180. DOI: 10.1016/S0169-555X(02)00241-6

Mertes AK, Dunne T. 2007. Effects of tectonism, climate change, and sea-level change on the form and behavior of the modern Amazon River and its floodplain. In Large Rivers: Geomorphology and Management , Gupta A (ed). John Wiley & Sons: West Sussex, England; 115–140.

Mitra S, Wassmann R, Vlek PL. 2005. An appraisal of global wetland area and its organic carbon stock. Current Science 88 : 25.

Mitsch WJ, Dorage CL, Wiemhoff JR. 1979. Ecosystem dynamics and a phosphorus budget of an alluvial cypress swamp in southern Illinois. Ecology 60 : 1116-1124.

Mitsch WJ, Dorage CL, Wiemhoff JR. 1977. Forested wetlands for water resource management in southern Illinois. Research Report No. 132, Illinois Water Resources Center, Urbana, Illinois.

Mitsch WJ, Gosselink JG. 2015. Wetlands . 5th ed. Wiley: Hoboken

Montgomery DR. 1999. Process domains and the river continuum. Journal of the American Water Resources Association 35 : 397–410.

Montgomery DR, Buffington JM. 1997. Channel-reach morphology in mountain drainage basins. Geological Society of America Bulletin 109 : 596–611. DOI: 10.1130/0016-7606(1997)109<0596:CRMIMD>2.3.CO;2

Montgomery DR, Buffington JM, Peterson NP, Schuett-Hames D, Quinn TP. 1996. Stream-bed scour, egg burial depths, and the influence of salmonid spawning on bed surface mobility and embryo survival. Canadian Journal of Fisheries and Aquatic Sciences 53 : 1061–1070. DOI: 10.1139/f96-028

Montgomery DR, Collins BD, Buffington JM, Abbe TB, others. 2003. Geomorphic effects of wood in rivers. American Fisheries Society Symposium [online] Available from: http://www.treesearch.fs.fed.us/pubs/23945 (Accessed 15 July 2014)

Moreira-Turcq P, Jouanneau JM, Turcq B, Seyler P, Weber O, Guyot JL. 2004. Carbon sedimentation at Lago Grande de Curuai, a floodplain lake in the low Amazon region: insights into sedimentation rates. Palaeogeography, Palaeoclimatology, Palaeoecology 214 : 27–40. DOI: 10.1016/j.palaeo.2004.06.013

Morgan LH. 1868. The American Beaver and His Works . J.B. Lippincott & Company

Moyano FE, Vasilyeva N, Bouckaert L, Cook F, Craine J, Curiel Yuste J, Don A, Epron D, Formanek P, Franzluebbers A, Ilstedt U, Katterer T, Orchard V, Reichstein M, Rey A, Ruamps L, Subke J-A, Thomsen IK, Chenu C. 2012. The moisture response of soil heterotrophic respiration: interaction with soil properties. Biogeosciences 9 : 1173–1182. DOI: 10.5194/bg-9-1173-2012

Mulholland PJ. 1981. Organic Carbon Flow in a Swamp-Stream Ecosystem. Ecological Monographs 51 : 307–322. DOI: 10.2307/2937276

Muzika RM, Gladden JB, Haddock JD. 1987. Structural and functional aspects of succession in southeastern floodplain forests following a major disturbance. American Midland Naturalist 117 : 1-9.

Naiman RJ, Bechtold JS, Beechie TJ, Latterell JJ, Pelt RV. 2010. A Process-Based View of Floodplain Forest Patterns in Coastal River Valleys of the Pacific Northwest. Ecosystems 13 : 1–31.

Naiman RJ, Decamps H, McClain ME, Likens GE. 2005. RIparia: Ecology, conservation, and management of streamside communities . Academic Press: Burlington, MA

Naiman RJ, Melillo JM, Hobbie JE. 1986. Ecosystem Alteation of Boreal Forest Streams by Beaver (Castor Canadensis). Ecology 67 : 1254–1269. DOI: 10.2307/1938681

Naiman RJ, Melillo JM, Lock MA, Ford TE, Reice SR. 1987. Longitudinal Patterns of Ecosystem Processes and Community Structure in a Subarctic River Continuum. Ecology 68 : 1139. DOI: 10.2307/1939199

National Council for Air and Stream Improvement. 2005. Riparian zone management and the protection of biodiversity: A problem analysis . Technical Bulletin

Nepf H, Ghisalberti M. 2008. Flow and transport in channels with submerged vegetation. Acta Geophysica 56 : 753–777. DOI: 10.2478/s11600-008-0017-y

Noe GB, Hupp CR. 2005. Carbon, nitrogen, and phosphorus accumulation in floodplains of Atlantic Coastal Plain rivers, USA. Ecological Applications 15 : 1178–1190.

Noe GB, Hupp CR. 2009. Retention of Riverine Sediment and Nutrient Loads by Coastal Plain Floodplains. Ecosystems 12 : 728–746. DOI: 10.1007/s10021-009-9253-5

Norton JB, Jungst LJ, Norton U, Olsen HR, Tate KW, Horwath WR. 2011. Soil Carbon and Nitrogen Storage in Upper Montane Riparian Meadows. Ecosystems 14 : 1217–1231. DOI: 10.1007/s10021-011-9477-z

O'Connell AM. 1997. Decomposition of Slash Residues in Thinned Regrowth Eucalpt Forest in Western Australia. Journal of Applied Ecology 34 : 111–122. DOI: 10.2307/2404852

Oost KV, Verstraeten G, Doetterl S, Notebaert B, Wiaux F, Broothaerts N, Six J. 2012. Legacy of human-induced C erosion and burial on soil–atmosphere C exchange. Proceedings of the National Academy of Sciences 109 : 19492–19497. DOI: 10.1073/pnas.1211162109

Pederson GT, Gray ST, Woodhouse CA, Betancourt JL, Fagre DB, Littell JS, Watson E, Luckman BH, Graumlich LJ. 2011. The Unusual Nature of Recent Snowpack Declines in the North American Cordillera. Science 333 : 332–335. DOI: 10.1126/science.1201570

Perry DA, Oren R, Hart SC. 2008. Forest Ecosystems . JHU Press

Persico L, Meyer G. 2009. Holocene beaver damming, fluvial geomorphology, and climate in Yellowstone National Park, Wyoming. Quaternary Research 71 : 340–353. DOI: 10.1016/j.yqres.2008.09.007

Persico L, Meyer G. 2013. Natural and historical variability in fluvial processes, beaver activity, and climate in the Greater Yellowstone Ecosystem. Earth Surface Processes and Landforms 38 : 728–750. DOI: 10.1002/esp.3349

Pinay G, Fabre A, Vervier P, Gazelle F. 1992. Control of C, N, P distribution in soils of riparian forests. Landscape Ecology 6 : 121–132.

Polvi LE, Wohl E. 2012. The beaver meadow complex revisited - the role of beavers in post-glacial floodplain development. Earth Surface Processes and Landforms 37 : 332–346. DOI: 10.1002/esp.2261

Polvi LE, Wohl EE, Merritt DM. 2011. Geomorphic and process domain controls on riparian zones in the Colorado Front Range. Geomorphology 125 : 504–516. DOI: 10.1016/j.geomorph.2010.10.012

Polvi L, Wohl EE. 2013. Biotic Drivers of Stream Planform: Implications for Understanding the Past and Restoring the Future. BioScience 63 : 439–452. DOI: 10.1525/bio.2013.63.6.6

Pringle C. 2003. What is hydrologic connectivity and why is it ecologically important? Hydrological Processes 17 : 2685–2689. DOI: 10.1002/hyp.5145

Quinn JM, Phillips NR, Parkyn SM. 2007. Factors influencing retention of coarse particulate organic matter in streams. Earth Surface Processes and Landforms 32 : 1186–1203. DOI: 10.1002/esp.1547

Ramos Scharrón CE, Castellanos EJ, Restrepo C. 2012. The transfer of modern organic carbon by landslide activity in tropical montane ecosystems. Journal of Geophysical Research: Biogeosciences 117 : G03016. DOI: 10.1029/2011JG001838

Raymond PA, Bauer JE. 2001. Riverine export of aged terrestrial organic matter to the North Atlantic Ocean. Nature 409 : 497–500. DOI: 10.1038/35054034

Richardson JS, Hoover TM, Lecerf A. 2009. Coarse particulate organic matter dynamics in small streams: towards linking function to physical structure. Freshwater Biology 54 : 2116–2126. DOI: 10.1111/j.1365-2427.2009.02279.x

Ricker MC, Donohue SW, Stolt MH, Zavada MS. 2012. Development and application of multi-proxy indices of land use change for riparian soils in southern New England, USA. Ecological Applications 22 : 487–501.

Rieger I, Lang F, Kowarik I, Cierjacks A. 2014. The interplay of sedimentation and carbon accretion in riparian forests. Geomorphology 214 : 157-167.

Ruddiman WF. 2001. Earth’s Climate: Past and Future. Macmillan

Ruffing C, Dwire KA, Daniels MD. In press. Carbon pools in stream-riparian corridors; legacy of disturbance along mountain streams of southeastern Wyoming. Earth Surface Processes and Landforms

Sapkal RS, Valunjkar SS. 2013. Development and sensitivity analysis of water quality index for evaluation of surface water for drinking purpose. International Journal of Civil Engineering and Technology 4 : 119–134.

Schenk ER, Hupp CR, Gellis A, Noe G. 2013. Developing a new stream metric for comparing stream function using a bank-floodplain sediment budget: a case study of three Piedmont streams. Earth Surface Processes and Landforms 38 : 771–784. DOI: 10.1002/esp.3314

Schulze DJ, Walker KF. 1997. Riparian eucalypts and willows and their significance for aquatic invertebrates in the River Murray, South Australia. Regulated Rivers: Research & Management 13 : 557–577. DOI: 10.1002/(SICI)1099-1646(199711/12)13:6<557::AID-RRR485>3.0.CO;2-Q

Schulze E-D 1941-, Beck E, Müller-Hohenstein K. 2005. Plant ecology . Springer

Schumm SA. 1977. The Fluvial System . John Wiley & Sons Inc: New York

Schumm SA. 1993. River Response to Baselevel Change: Implications for Sequence Stratigraphy. The Journal of Geology 101 : 279–294.

Schuur EAG, Bockheim J, Canadell JG, Euskirchen E, Field CB, Goryachkin SV, Hagemann S, Kuhry P, Lafleur PM, Lee H, Mazhitova G, Nelson FE, Rinke A, Romanovsky VE, Shiklomanov N, Tarnocai C, Venevsky S, Vogel JG, Zimov SA. 2008. Vulnerability of Permafrost Carbon to Climate Change: Implications for the Global Carbon Cycle. BioScience 58 : 701–714. DOI: 10.1641/B580807

Sear DA, Millington CE, Kitts DR, Jeffries R. 2010. Logjam controls on channel:floodplain interactions in wooded catchments and their role in the formation of multi-channel patterns. Geomorphology 116 : 305–319. DOI: 10.1016/j.geomorph.2009.11.022

Sollins P, Glassman CA, Dahm CN. 1985. Composition and Possible Origin of Detrital Material in Streams. Ecology 66 : 297–299. DOI: 10.2307/1941331

Sponseller RA, Fisher SG. 2006. Drainage Size, Stream Intermittency, and Ecosystem Function in a Sonoran Desert Landscape. Ecosystems 9 : 344–356. DOI: 10.1007/s10021-005-0167-6

Stallard RF. 1998. Terrestrial sedimentation and the carbon cycle: Coupling weathering and erosion to carbon burial. Global Biogeochemical Cycles 12 : 231–257. DOI: 10.1029/98GB00741

Stanford JA, Ward JV. 1993. An Ecosystem Perspective of Alluvial Rivers: Connectivity and the Hyporheic Corridor. Journal of the North American Benthological Society 12 : 48–60. DOI: 10.2307/1467685

Statzner B, Fièvet E, Champagne J-Y, Morel R, Herouin E. 2000. Crayfish as geomorphic agents and ecosystem engineers: Biological behavior affects sand and gravel erosion in experimental streams. Limnology and Oceanography 45 : 1030–1040. DOI: 10.4319/lo.2000.45.5.1030

Statzner B, Peltret O, Tomanova S. 2003. Crayfish as geomorphic agents and ecosystem engineers: effect of a biomass gradient on baseflow and flood-induced transport of gravel and sand in experimental streams. Freshwater Biology 48 : 147–163. DOI: 10.1046/j.1365-2427.2003.00984.x

Striegl RG, Aiken GR, Dornblaser MM, Raymond PA, Wickland KP. 2005. A decrease in discharge-normalized DOC export by the Yukon River during summer through autumn. Geophysical Research Letters 32 : L21413. DOI: 10.1029/2005GL024413

Stromberg JC, Lite SJ, Dixon MD. 2010. Effects of stream flow patterns on riparian vegetation of a semiarid river: Implications for a changing climate. River Research and Applications 26 : 712–729. DOI: 10.1002/rra.1272

Stromberg JC, Mccluney KE, Dixon MD, Meixner T. 2013. Dryland Riparian Ecosystems in the American Southwest: Sensitivity and Resilience to Climatic Extremes. Ecosystems 16 : 411–415. DOI: http://dx.doi.org.ezproxy2.library.colostate.edu:2048/10.1007/s10021-012-9606-3

Suchenwirth L, Förster M, Cierjacks A, Lang F, Kleinschmit B. 2012. Knowledge-based classification of remote sensing data for the estimation of below- and above-ground organic carbon stocks in riparian forests. Wetlands Ecology and Management 20 : 151–163. DOI: 10.1007/s11273-012-9252-8

Suchenwirth L, Stümer W, Schmidt T, Förster M, Kleinschmit B. 2014. Large-Scale Mapping of Carbon Stocks in Riparian Forests with Self-Organizing Maps and the k-Nearest-Neighbor Algorithm. Forests 5 : 1635–1652. DOI: 10.3390/f5071635

Tabacchi E, Correll DL, Hauer R, Pinay G, Planty-Tabacchi A-M, Wissmar RC. 1998. Development, maintenance and role of riparian vegetation in the river landscape. Freshwater Biology 40 : 497–516. DOI: 10.1046/j.1365-2427.1998.00381.x

Tank JL, Rosi-Marshall EJ, Griffiths NA, Entrekin SA, Stephen ML. 2010. A review of allochthonous organic matter dynamics and metabolism in streams. Journal of the North American Benthological Society 29 : 118–146. DOI: 10.1899/08-170.1

Tappeiner U, Tasser E, Leitinger G, Cernusca A, Tappeiner G. 2008. Effects of Historical and Likely Future Scenarios of Land Use on Above- and Belowground Vegetation Carbon Stocks of an Alpine Valley. Ecosystems 11 : 1383–1400. DOI: 10.1007/s10021-008-9195-3

Tarnocai C, Canadell JG, Schuur EAG, Kuhry P, Mazhitova G, Zimov S. 2009. Soil organic carbon pools in the northern circumpolar permafrost region. Global Biogeochemical Cycles 23 DOI: http://dx.doi.org/10.1029/2008GB003327 [online] Available from: http://search.proquest.com/docview/20677682?accountid=10223 (Accessed 5 June 2015)

Tockner K, Pennetzdorfer D, Reiner N, Schiemer F, Ward JV. 1999. Hydrological connectivity, and the exchange of organic matter and nutrients in a dynamic river–floodplain system (Danube, Austria). Freshwater Biology 41 : 521–535. DOI: 10.1046/j.1365-2427.1999.00399.x

Tockner K, Stanford JA. 2002. Riverine flood plains: present state and future trends. Environmental Conservation 29 : 308–330. DOI: 10.1017/S037689290200022X

Tranvik LJ et al. 2009. Lakes and reservoirs as regulators of carbon cycling and climate. presented at the American Geophysical Union Chapman Conference Office on Abrupt Climate Change. 2298–2314 pp. [online] Available from: http://cat.inist.fr/?aModele=afficheN&cpsidt=22279829 (Accessed 19 May 2014)

Trimble SW. 2004. Effects of Riparian Vegetation on Stream Channel Stability and Sediment Budgets. In Riparian Vegetation and Fluvial Geomorphology , Bennett SJ and Simon A (eds). American Geophysical Union; 153–169. [online] Available from: http://onlinelibrary.wiley.com/doi/10.1029/008WSA12/summary (Accessed 3 June 2015)

Triska FJ. 1984. Role of wood debris in modifying channel geomorphology & riparian areas of a large lowland river under pristine conditions: a historical case study. Verhand. Internat. Verein Limnol 22 : 1876–1892.

Trumbore SE, Czimczik CI. 2008. GEOLOGY: An Uncertain Future for Soil Carbon. Science 321 : 1455–1456. DOI: 10.1126/science.1160232

Trussell RR, Umphres MD. 1978. The Formation of Trihalomethanes. American Water Works Association Journal 70 : 604–12.

Turner MG. 2010. Disturbance and landscape dynamics in a changing world. Ecology 91 : 2833–2849. DOI: 10.1890/10-0097.1

Valett HM, Baker MA, Morrice JA, Crawford CS, Molles MC, Dahm CN, Moyer DL, Thibault JR, Ellis LM. 2005. Biogeochemical and metabolic responses to the flood pulse in a semiarid floodplain. Ecology 86 : 220–234. DOI: 10.1890/03-4091

Vannote RL, Minshall GW, Cummins KW, Sedell JR, Cushing CE. 1980. The river continuum concept. Canadian journal of fisheries and aquatic sciences 37 : 130–137.

Veneklaas EJ. 1991. Litterfall and nutrient fluxes in two montane tropical rain forests, Colombia. Journal of Tropical Ecology 7 : 319–336. DOI: 10.1017/S0266467400005587

Vitousek PM. 1984. Litterfall, Nutrient Cycling, and Nutrient Limitation in Tropical Forests. Ecology 65 : 285–298. DOI: 10.2307/1939481

Vitousek PM, Sanford RL Jr. 1986. Nutrient Cycling in Moist Tropical Forest. Annual Review of Ecology and Systematics 17 : 137–167.

Wagener SM, Oswood MW, Schimel JP. 1998. Rivers and soils: parallels in carbon and nutrient processing. BioScience : 104–108.

Wainwright J, Turnbull L, Ibrahim TG, Lexartza-Artza I, Thornton SF, Brazier RE. 2011. Linking environmental régimes, space and time: Interpretations of structural and functional connectivity. Geomorphology 126 : 387–404. DOI: 10.1016/j.geomorph.2010.07.027

Walling DE. 2006. Human impact on land–ocean sediment transfer by the world's rivers. Geomorphology 79 : 192–216. DOI: 10.1016/j.geomorph.2006.06.019

Walter RC, Merritts DJ. 2008. Natural Streams and the Legacy of Water-Powered Mills. Science 319 : 299–304. DOI: 10.1126/science.1151716

Ward GM, Aumen NG. 1986. Woody debris as a source of fine particulate organic matter in coniferous forest stream ecosystems. Canadian Journal of Fisheries and Aquatic Sciences 43 : 1635–1642.

Webb AA, Erskine WD. 2003. Distribution, recruitment, and geomorphic significance of large woody debris in an alluvial forest stream: Tonghi Creek, southeastern Australia. Geomorphology 51 : 109–126.

West AJ, Lin CW, Lin TC, Hilton RG, Liu SH, Chang CT, Lin KC, Galy A, Sparkes RB, Hovius N. 2011. Mobilization and transport of coarse woody debris to the oceans triggered by an extreme tropical storm. Limnology and Oceanography 56, 77-85.

Westbrook CJ, Cooper DJ, Baker BW. 2006. Beaver dams and overbank floods influence groundwater-surface water interactions of a Rocky Mountain riparian area. Water Resources Research 42 : n/a–n/a. DOI: 10.1029/2005WR004560

Westbrook CJ, Veatch W, Morrison A. 2013. Is ecohydrology missing much of the zoo? Ecohydrology 6 : 1–7. DOI: 10.1002/eco.1365

Westerling AL, Hidalgo HG, Cayan DR, Swetnam TW. 2006. Warming and Earlier Spring Increase Western U.S. Forest Wildfire Activity. Science 313 : 940–943. DOI: 10.1126/science.1128834

Wigginton JD, Lockaby BG, Trettin CC. 2000. Soil organic matter formation and sequestration across a forested floodplain chronosequence. Ecological Engineering 15, Supplement 1 : S141–S155. DOI: 10.1016/S0925-8574(99)00080-4

Wohl E. 2007. Hydrology and Discharge. In Large Rivers: Geomorphology and Management , Gupta A (ed). John Wiley & Sons: West Sussex, England; 29–41.

Wohl E. 2008. The effect of bedrock jointing on the formation of straths in the Cache la Poudre River drainage, Colorado Front Range. Journal of Geophysical Research 113 DOI: 10.1029/2007JF000817 [online] Available from: http://doi.wiley.com/10.1029/2007JF000817 (Accessed 4 May 2014)

Wohl E. 2010a. A brief review of the process domain concept and its application to quantifying sediment dynamics in bedrock canyons. Terra Nova 22 : 411–416. DOI: 10.1111/j.1365-3121.2010.00950.x

Wohl E. 2010b. Mountain rivers revisited . American Geophysical Union [online] Available from: http://www.agu.org/books/wm/v019/ (Accessed 4 May 2014)

Wohl E, Barros A, Brunsell N, Chappell NA, Coe M, Giambelluca T, Goldsmith S, Harmon R, Hendrickx JMH, Juvik J, McDonnell J, Ogden F. 2012a. The hydrology of the humid tropics. Nature Climate Change 2 : 655–662. DOI: 10.1038/nclimate1556

Wohl E. 2013a. Floodplains and wood. Earth-Science Reviews 123 : 194–212. DOI: 10.1016/j.earscirev.2013.04.009

Wohl E. 2013b. Landscape-scale carbon storage associated with beaver dams. Geophysical Research Letters 40 : 3631–3636. DOI: 10.1002/grl.50710

Wohl E. 2014a. A legacy of absence Wood removal in US rivers. Progress in Physical Geography 38 : 637–663. DOI: 10.1177/0309133314548091

Wohl E. 2014b. Rivers in the Landscape: Science and Management . 1 edition. Wiley-Blackwell: Hoboken, NJ

Wohl E. 2015. Particle dynamics: The continuum of bedrock to alluvial river segments. Geomorphology 241 : 192–208. DOI: 10.1016/j.geomorph.2015.04.014

Wohl E, Angermeier PL, Bledsoe B, Kondolf GM, MacDonnell L, Merritt DM, Palmer MA, Poff NL, Tarboton D. 2005. River restoration. Water Resources Research 41 : W10301. DOI: 10.1029/2005WR003985

Wohl E, Beckman ND. 2014. Leaky rivers: Implications of the loss of longitudinal fluvial disconnectivity in headwater streams. Geomorphology 205 : 27–35. DOI: 10.1016/j.geomorph.2011.10.022

Wohl E, Cadol D. 2011. Neighborhood matters: Patterns and controls on wood distribution in old-growth forest streams of the Colorado Front Range, USA. Geomorphology 125 : 132–146. DOI: 10.1016/j.geomorph.2010.09.008

Wohl E, Dwire K, Sutfin N, Polvi L, Bazan R. 2012b. Mechanisms of carbon storage in mountainous headwater rivers. Nature Communications 3 : 1263. DOI: 10.1038/ncomms2274

Wohl EE. 2000a. Geomorphic effects of flooding. In Inland flood hazards, Wohl EE (ed). New York, NY; 167–187.

Wohl EE. 2000b. Inland Flood Hazards. In Inland flood hazards, Wohl EE (ed). Cambridge University PRess: New York, NY; 3–27.

Wohl E, Goode JR. 2008. Wood dynamics in headwater streams of the Colorado Rocky Mountains. Water Resources Research 44 : W09429. DOI: 10.1029/2007WR006522

Wohl, E, Ogden FL. 2013. Organic carbon export in the form of wood during an extreme tropical storm, Upper Rio Chagres, Panama. Earth Surface Processes and Landforms 38, 1407-1416.

Wohl E, Polvi LE, Cadol D. 2011. Wood distribution along streams draining old-growth floodplain forests in Congaree National Park, South Carolina, USA. Geomorphology 126 : 108–120. DOI: 10.1016/j.geomorph.2010.10.035

Wolman MG. 1967. A cycle of sedimentation and erosion in urban river channels. Geografiska Annaler 49A : 385–395.

Woodall CW, Liknes GC. 2008. Climatic regions as an indicator of forest coarse and fine woody debris carbon stocks in the United States. Carbon Balance and Management 3 : 5. DOI: 10.1186/1750-0680-3-5

Xiong S, Nilsson C. 1997. Dynamics of leaf litter accumulation and its effects on riparian vegetation: a review. The Botanical Review 63 : 240–264.

Zarnetske JP, Haggerty R, Wondzell SM, Baker MA. 2011. Labile dissolved organic carbon supply limits hyporheic denitrification. Journal of Geophysical Research 116 DOI: 10.1029/2011JG001730 [online] Available from: http://doi.wiley.com/10.1029/2011JG001730 (Accessed 1 May 2014)

Zehetner F, Lair GJ, Gerzabek MH. 2009. Rapid carbon accretion and organic matter pool stabilization in riverine floodplain soils. Global Biogeochemical Cycles 23 : GB4004. DOI: 10.1029/2009GB003481

Chapter 3: Quantifying soil carbon content along floodplains of mountain streams in the Colorado Front Range, USA

Summary

River corridors along small mountain streams have the potential to store substantial organic carbon in floodplain sediment, but quantifying this storage can be time- and labor-intensive, given the spatial heterogeneity of floodplain stratigraphy and organic carbon content within and between successive valley segments. Here, I use a dataset consisting of 660 sediment samples from three intensively sampled primary valley segments and 21 less intensively sampled secondary valley segments to (i) assess the variability in three spatial statistical techniques to estimate global mean organic carbon content, (ii) quantify the minimum number of systematic random samples needed to estimate mean floodplain soil organic carbon (SOC) content, (iii) identify potential covariates of SOC content based on spatial position with respect to the channel and soil state variables, (iv) and examine SOC patterns across various floodplain geomorphic features to identify potential hotspots for OC content in the study area and along similar mountain streams. Reach-average floodplain SOC content of ~3-5% can be accurately estimated by collecting only 15 randomly selected samples at various depths and locations or all depths at 10 sampling locations across the floodplains in this study area. Regression analyses indicate that SOC content correlates with soil moisture, grain size distributions, soil depth, elevation of the floodplain surface, and valley confinement. Principle component analysis indicates that the geomorphic floodplain features and topography could regulate distribution of predictors of soil organic carbon content. I find that mean floodplain soil organic carbon (6.1 ± 7%) is greater than

those in uplands of the study area (1.5 ± 0.08% to 2.2 ± 0.14%) and greater than other studies along floodplains in other regions.

3.1 Introduction

Soils are the third largest reservoir for organic carbon (OC) on Earth, exceeded only by the ocean and deep geologic storage, and the largest terrestrial reservoir (Jobbágy and Jackson, 2000; Ruddiman, 2001). Thus, soils are a significant component of the terrestrial carbon cycle, but feedbacks among Earth's surface, atmosphere, and biosphere make quantification of terrestrial carbon reservoirs difficult and ridden with the greatest uncertainty among the primary OC reservoirs (i.e., surface ocean, deep ocean, atmosphere, deep geologic storage) (Ballantyne et al., 2012). The mechanistic source of an increasing uptake of atmospheric carbon occurring at the land surface has yet to be identified and has been termed the terrestrial carbon sink (Ballantyne et al., 2012; IPCC 2007 et al., 2007).

Terrestrial carbon budgets identify freshwater systems as a mediator to storage within the geosphere (Cole et al., 2007; Battin et al., 2009; Aufdenkampe et al., 2011; Hoffmann et al., 2013) and recent work has identified the potential for at least some riparian ecosystems and floodplain soils, previously unaccounted for in carbon stocks, to be a component of the missing terrestrial carbon sink (Hoffmann et al., 2009; Wohl et al., 2012; Sutfin et al., 2015). Furthermore, current understanding and quantification of the vertical distribution of global soil OC (SOC) (Jobbágy and Jackson, 2000) do not take into account dynamic fluvial environments and discontinuities in SOC content with increasing depth along floodplains.

Recent reviews of soil organic carbon in floodplains indicate that cool, wet conditions are likely to result in the highest per unit values of OC storage along river networks (Sutfin et al., 2015). Optimal conditions occur in cold, wet environments because available moisture supports vegetation growth and high organic matter inputs, whereas the potential for saturated conditions and cooler temperatures are likely to limit decomposition and microbial metabolism of OC (Falloon et al., 2011; Jobbágy and Jackson, 2000). These conditions are met at high latitudes and high altitudes, particularly where wetlands are present. Because small headwater streams account for the majority of river kilometers globally, small mountain streams could be a significant component of OC storage along river networks.

Because of the strong relationship among soil moisture, temperature, and carbon content, future changes in SOC stocks associated with global climate change are complicated by uncertainty in anticipated changes in moisture as well as temperature (Falloon et al., 2011; Trumbore and Czimczik, 2008). Uncertainty associated with these changes in moisture is particularly large for floodplain soils and sediment, which may experience extreme shifts in erosional and depositional patterns as a response to changes in hydroclimatic disturbance regime and more frequent or extreme storms (Alexander, 2014; Bates et al., 2008). Snowmelt-dominated mountain streams are highly susceptible to these changes in hydroclimatic regime because of decreased annual average snowpack and earlier timing of snowmelt, which could leave floodplain sediment drier for longer periods of time throughout the year (Alexander, 2014).

Identifying variability, spatial patterns, and statistical relationships with other sedimentation characteristics across floodplain soils is a necessary step to quantifying the amount of carbon stored in these mountainous environments and the accuracy of estimates of OC storage based on limited sampling. Hoffmann et al. (2014) analyzed spatial variability of OC within an alpine catchment including floodplains, but did not examine spatial relationships and differences in SOC across specific geomorphic floodplain features. Examining spatial patterns of sediment and OC accumulation associated with hydrologic and geomorphic floodplain features across transects on the Atchafalaya River (5, 670 km^2) in the southeastern US, Hupp et al. (2008) found the highest sediment accumulation rates at topographic lows that were frequently inundated for long periods of time with multiple sources of sediment-laden water. However, they did not examine spatial relationships and differences in SOC in the context of geomorphic surfaces. Hoffmann et al. (2009) found an increase in organic carbon content from the channel bed, up the sloped river bank, in the overbank, and in channel fill, respectively, along the Rhine river, Germany (>20,000 km^2). Questions remain regarding the variation in SOC among floodplain features of small rivers (<500 km^2) and the number of samples needed to accurately estimate mean SOC content of floodplains, particularly where limited work has been conducted, as in small mountain streams.

I address these issues by examining spatial statistical patterns in SOC across floodplains of small, steep mountain streams and relationships between SOC and specific geomorphic floodplain features such as stream banks, overbank channels, and beaver meadows. Exhaustive systematic sampling of floodplain soils, which can be highly variable in OC content (Sutfin et al., 2015), is costly and time- and labor-intensive. Identifying the minimum number of soil samples needed to minimize bias and accurately estimate mean OC content saves time and money when quantifying potential SOC reservoirs in floodplains. The objectives of this study are to (1) quantify the minimum number of systematic random samples needed to estimate mean floodplain SOC content along three primary study reaches, (2) identify potential covariates of SOC content based on spatial position with respect to the channel and soil state variables, (3) and examine SOC patterns across various floodplain geomorphic features to identify potential hotspots for OC content in the study area and along similar mountain streams.

3.2 Study area

The study area in north-central Colorado, USA lies primarily within Rocky Mountain National Park (RMNP). Established in 1915, RMNP has limited development and has preserved natural conditions along mountainous streams. The underlying geology of RMNP is a core of granite and schistic gneiss (Braddock and Cole, 1990), containing little to no $CaCO_3$ with few outliers (~0.01- 12.7%, mean = 0.43%, median = 0.33%, and standard deviation = 0.6%), as evidenced in sediment and soil analysis analyses along study reaches.

Study reaches are located along streams on the eastern side of the continental divide, where Pleistocene alpine glaciation extended down-valley to as low as 2300 m in elevation (Anderson et al., 2006). Vegetation differs with elevation. Forests in the subalpine zone (3500 – 2850 m elevation) are dominated by Engelmann spruce (*Picea englemannii*), subalpine fir (*Abies lasiocarpa*), lodgepole pine (*Pinus contorta*), aspen (*Populus tremuloides*), and limber pine (*Pinus flexilis*). Forests in the montane zone (2850 – 1750 m elevation) are dominated by ponderosa pine (*Pinus ponderosa var. scopulorum*) and Douglas-fir (*Pseudotsuga menziesii*) (Veblen and Donnegan, 2005). Vegetation in riparian areas differs from adjacent uplands and includes willow (*Salix* spp.), blue spruce (*Picea pungens*), aspen (*Populus tremuloides*), river birch (*Betula fontinalis*), grasses and sedges (*Carex* spp.) (Veblen and Donnegan, 2005). Distinct vegetation communities are located within fluvial process domains in the study area, with process domains defined by elevation and lateral valley confinement (Polvi et al., 2011).

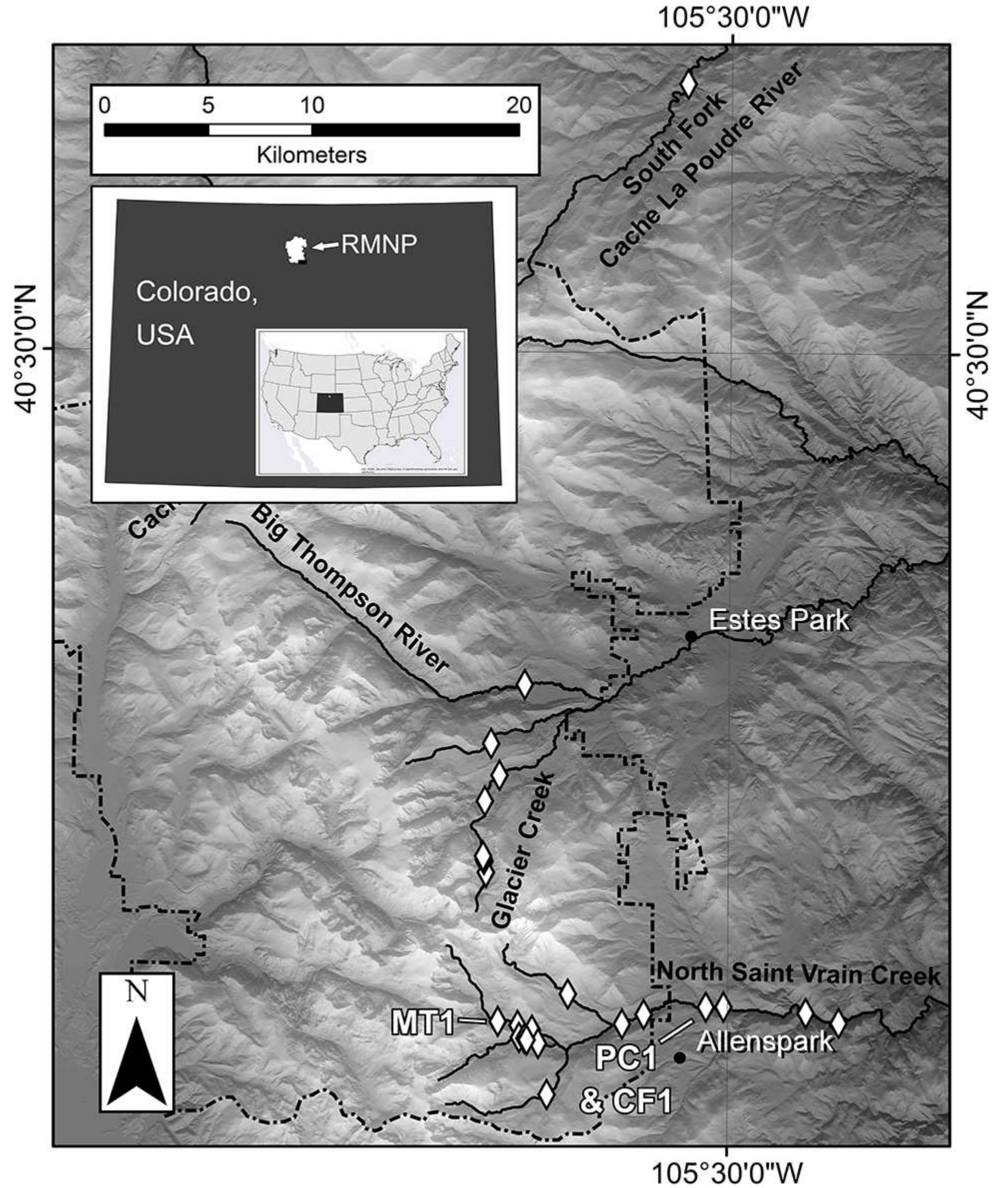

Figure 3.1 Twenty-four study reaches are concentrated in the southeastern portion of Rocky Mountain National Park in northern Colorado, USA and located within two primary study basins. A single study reach (SFPAB6), located approximately 20 km to the north in another basin, is not indicated on this map. The three primary study sites (CF1, PC1, and MT1) are labeled

Nineteen study reaches are located in the southeastern portion of RMNP along North Saint Vrain (NSV) and Glacier Creeks (Figure 3.1), and five additional study reaches extend eastward outside of the park and downstream along NSV, and into other drainages in the region. All study reaches are located in the subalpine and montane vegetation zones and encompass a range of drainage areas (10 – 180 km^2) and channel gradients (1 – 15%). Although dynamic conditions along floodplains of the mountainous study area interrupt the stability required to develop well-defined soil horizons, shifts in seasonal and inter-annual erosional and depositional patterns leave organic-rich deposits and lenses, including buried wood, beneath the surface of floodplains.

3.3 Methods

3.3.1. Field-based data collection

Twenty-four study reaches were defined by 11 transects spaced one bankfull channel width apart (Figure 3.2). Channels surveyed included primarily straight, single-thread channels, but three study reaches had complex channel planform with multiple subparallel, or anabranching, channels (Nanson and Knighton, 1996) that spread across the valley bottom and contain flow throughout the year around semi-stable, vegetated islands. Disturbances such as tree throw from high velocity winds and bank erosion create dynamic environments with channel avulsions and periodic shifts in island configuration, channel planform and cross sectional profiles (Collins et al., 2012; Polvi and Wohl, 2013). These shifts in channel geometry are also facilitated by the presence of large, abundant logjams that persist for years to decades. I refer to these sites as multithread channels. Where beaver (*Castor canadensis*) are present in the study area, they engineer dams to obstruct flow, which may result in changes in channel planform and sedimentation patterns analogous to those associated with logjams (Ives, 1942; Persico and Meyer, 2009; Polvi and Wohl, 2013). I refer to logjams and beaver dams as biotic drivers of channel planform.

Stratification across categories of valley confinement and the influence of biotic drivers of channel planform was conducted to capture the variability in floodplain hydrologic conditions and connectivity of water and sediment between the channel and the floodplain (Bracken et al., 2013; Wainwright et al., 2011). For the sake of this study, I consider floodplains or valley bottoms to be regularly inundated at least every decade, as indicated by riparian vegetation species in the study area (Merritt et al., 2010; Veblen and Donnegan, 2005). I define mean valley confinement as the width of the valley (w_v) or floodplain divided by the width of the channel (w_c). I define valley segments as confined ($w_v < 2 \times w_c$), partly confined ($w_v = 2$ to $5 \times w_c$), unconfined ($w_v > 5 \times w_c$), as having a multithread channel planform induced by logjams, or as influenced by past or contemporary presence of beaver.

Topography of the floodplain was surveyed at each study reach along 11 transects perpendicular to the down-valley direction using a Laser Technology TruPulse 360B laser rangefinder. The rangefinder is accurate to $\pm$ 0.1 m and was used to calculate relative elevation, horizontal distance of each transect point from the active channel, and soil sampling location. I distinguished three primary study reaches in which soils were sampled more extensively, and 21 secondary study reaches for which sample size was minimized.

The three primary study reaches were located within a confined, partly confined, and multithread valley segment. At these reaches, soils were sampled more extensively in order to examine bias in sampling associated with sample size. At the multithread reach, which had an average valley width of 60 m, soil samples were collected every 20 m. Where sampling locations fell into an active channel, samples were not collected or were shifted to a random selection on either bank of the channel. This resulted in a total of 31 sampling locations across the valley bottom and a total of 51 soil samples at various depths. At the confined and partly confined sites (16.5 and 32 m wide, respectively), one sample was taken at a random location on the left and right bank of the channel (12-18 m wide) where possible, resulting in 15 and 14 sampling locations and 38 and 34 soil samples, respectively.

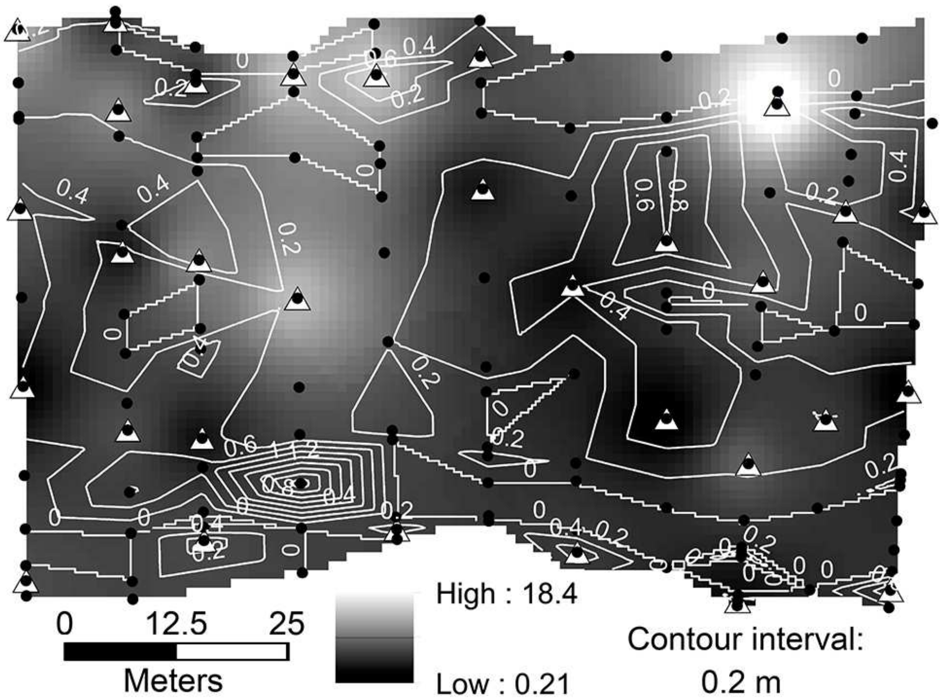

Figure 3.2 Example of a study reach with multiple channels of flow from frame left to right across the valley bottom (multithread reach; MT1) with eleven transects ~8-10 m apart and perpendicular to the down-valley direction. Black dots represent survey points along each transect and white triangles represent soil sampling locations, in this case approximately every 20 m where soil or sediment was present. The black and white underlay is the result of inverse distance weighting of soil organic carbon (OC) content where the lightest and darkest colors represent OC contents of ~18% (in the top right corner of the figure) and 0.2%, respectively. White contour lines indicate soil depth.

At the 21 secondary study reaches, systematic random sampling was used, such that a random location was selected for a soil sample along each transect (Figure 3.2). This was done by measuring the width of the valley bottom in the field using the laser range finder or by estimating the width between two points on either side of the valley using a GPS. The width was then divided into segments of a meter and a random location was selected by increments of a meter from the valley edge using a random number generator in the field. Where random locations fell within the channel, another location was selected randomly. Where sediment or soil was not present along an entire transect (primarily within highly confined valleys), an additional randomly located sample was collected on a different transect with greater floodplain area. Where possible, each secondary study reach had 11 sampling locations, but in some reaches confined by bedrock, samples were collected at as little as five sampling locations.

Random samples were collected from a total of 294 locations along the 24 study reaches. At each sampling location, litter (identifiable organic matter such as leaves, cones, needles) and humus (unidentifiable and partially decomposed organic matter) were removed from the surface of the soil profile before sampling. I do not include litter and humus (organic horizon) in this analysis because they are relatively transient and vary greatly in thickness within this dynamic fluvial environment. Sediment below the organic horizon captures the long-term average of organic matter and OC. At all sampling locations, soils were sampled at 15-cm depth increments using a 2.5-inch (~6.4 cm) diameter stainless steel hand auger. Augering penetrated to the depth of bedrock or gravel or to a maximum depth of 180 cm in finer sediment. A total of 660 collected soil samples were frozen until analyzed for SOC content by the Colorado State University Soil and Water Testing Laboratory. Once dried, soil samples were homogenized and subsampled for SOC analysis using a LECO TruSpec CN furnace. Each sample was then analyzed for CO_3-C by treating the sample with 0.4 N HCl and measuring the CO_2 loss gravimetrically. Total organic carbon content by weight was calculated as total carbon minus CO_3-C.

Grain-size analysis was conducted on a subset of samples for all depths at randomly selected sampling locations for each study reach. Four soil sampling locations were selected from each study reach and all depth increments for each location were processed. A total of 186 samples were sieved for grain size analysis to determine percent gravel >2mm, coarse sand (0.5 – 2mm), medium-to-fine sand (0.062 – 0.5 mm), and silt and clay finer than sand (< 0.062 mm) by weight.

3.3.2 Statistical analyses

General statistics and correlations between study reaches, SOC content, and grains size were examined using R statistical software [R Core Team, 2009]. Pairwise t-tests were conducted using the *stats* package in R, for which correction for unequal sample size uses the Holm method.

Estimate reach-average SOC

To determine differences between methods for estimating reach-average soil organic carbon content and determine the best method, I (1) calculated the arithmetic mean of all samples along each study reach, (2) calculated arithmetic depth-averaged mean, (3) conducted ordinary kriging, and (4) conducted inverse distance weighting at the three primary study reaches. Depth-averaged mean was calculated by averaging the samples at all depths for each sampling location before taking an average of those means. The number of neighbors and ordinary kriging method used were determined by minimizing the mean squared error prediction (MSEP) for all study reaches. Leave-one-out analysis was conducted to determine MSEP with increasing number of neighbors for Gaussian, spherical, and exponential models in R. Kriging was then conducted using the kriging model output of the range, sill, and nugget in the *advanced* option parameters of the *kriging* tool in ESRI ArcMap GIS software. Similarly, the best parameters for inverse distance weighting (IDW) were determined by simultaneously minimizing bias and MSEP using leave-one-out validation for the nearest number of neighbors and using a distance decay exponent of 1 and 2. Inverse distance weighting was conducted in ESRI ArcMap GIS software. I compare results of these methods of estimating mean SOC, the global arithmetic mean of all samples regardless of sampling location and sample depth, and the arithmetic mean of depth-averaged samples at each sampling location for the three primary study reaches in order to choose the best possible method to represent the "true" population mean for additional statistical analyses.

Determine sample size to minimize bias

To determine the minimum number of samples needed to accurately estimate mean OC content of floodplains soils for each reach, I examined bias by conducting random bootstrap sampling with replacement along each of the three primary study reaches using a total of 122 soil samples from 60 sampling locations (Table 3.1). In doing this, I calculated the bias for each bootstrapped mean. Bias is the difference of the modeled or estimated mean, in this case the bootstrapped mean, from the "true" mean. Bootstrap trials varied by the total number of randomly selected samples, such that the number of random samples increased incrementally by one for each trial, up to the total number of samples collected at each reach. Bootstrap resampling was conducted 10,000 times for each trial, for which the mean, bias, and variance of the mean SOC content were calculated from each of the 10,000 bootstrap samples. The same bootstrap analysis was conducted for each study reach using randomly selected individual samples and a separate analysis was conducted using depth-averaged values from each sampling location along each reach.

In completing this analysis, I use the results from estimating the reach-average organic carbon content described above as an estimate of the true mean. The best estimate of the true mean, however, would be one based on an infinite number of samples until all sediment along each study reach has been analyzed for OC content to determine the true mean. This can be seen in a plot of bias as a result of sample size, such that the estimated mean and bias converge toward the true population mean (Figure 3.3). Analyzing this many samples is impractical and costly, so I conduct this analysis to determine the number of samples at which bias and variance converge within a reasonable sample size based on a subset of study reaches with higher sampling density than I planned to conduct for additional reaches.

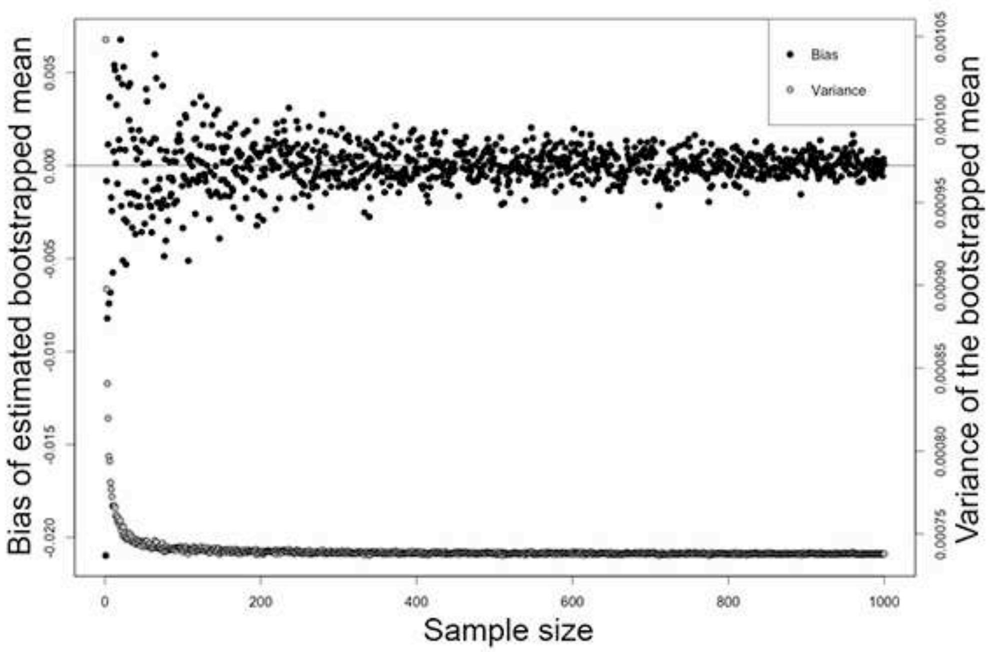

Figure 3.3 Bias (deviation of the estimated mean from the true population mean) and variance are reduced with increasing sample size, converging toward a single value.

Multiple linear regression

Multiple linear regressions were conducted using the *stats* package in R statistical software (R Core Team, 2012) on two datasets to examine potential relationships between SOC and other variables in two separate analyses. In regression analysis 1, soil sample data for all 24 study reaches were used to examine spatial relationships including horizontal distance from the active channel (DFC), valley confinement (VC), total maximum soil depth or thickness at a sampling location (ST), relative floodplain surface elevation along the sampling transect (SE), relative elevation of the sample from the active channel (EFC), and average sample depth of each 15-cm long soil sample (SD). Soil moisture content (M) was also used in regression 1 because the data were available for all samples and M is largely dependent on position within the floodplain. Regression analysis 2 was conducted using the subset of soil analyzed for grain size to examine relationships between SOC and soil moisture, grain size, and all the spatial variables listed above. Soil characteristic inputs included all the spatial relationships listed above and the various size fractions of gravel (>2 mm), coarse sand (0.5 – 2 mm), fine sand 0.062 – 0.5 mm), total sand 0.062 – 2 mm), and finer than sand (i.e., silt and clay, <0.062 mm).

For each of the two regression analyses, multiple linear regression including all variables was conducted to examine the relative significance of each variable and stepwise multiple linear regression (a combination of backward and forward regression) was used to determine the best possible regression model. The optimal number of variables used in each regression model was identified, in order to choose the most important variables, by determining at what point there was no significant reduction of the Akaike information criteria (AIC) with inclusion of additional variables. In both regression analyses, the number of variables indicated using the AIC as described above agreed with the number of variables selected by the stepwise multiple linear regression models. This resulted in five variables in regression 1 and eight variables in regression 2. In the regression 2 model, elevation from the channel was eliminated as a variable because of co-linearity with average sample depth and surface elevation (r^2 = 0.43 and 0.86, respectively).

Principle component analysis

Principle component analysis was conducted on the two separate datasets described above to examine the potential for differences in soil characteristics and spatial relationships with floodplain geomorphic features. The *lm* and *step* functions of the *stats* package in R statistical software were used to conduct multiple linear regression and stepwise multiple linear regression (R Core team). Inputs included spatial and soil characteristic variables described above that were identified as significant in the regression models. These inputs are depicted in principle component space to provide qualitative interpretation and comparison of potential patterns in floodplain geomorphic surfaces with regard to controls on SOC content. Geomorphic floodplain features identified in the field and included in this analysis are stream banks (BK), overbank channels (OB), grassy meadows (GM), elevated tree berms or hummocks (HM), beaver meadows (BM), standing water (SW), islands (IS), the valley edge (VE), and the generic classification of floodplains (FP).

3.4. Results

3.4.1 Reach-average soil organic carbon content

Results for estimating reach-average SOC content indicated that the arithmetic mean consistently underestimated, whereas kriging overestimated, reach-average SOC content for all three primary study reaches, resulting in relative error (bias from the mean of means for all methods; Table 3.1). Depth-average arithmetic mean and IDW resulted in values within the range of the latter two methods and depth-average mean resulted in the lowest overall error. In a more detailed comparison of spatial averaging methods to calculate mean SOC content, Hoffman et al. (2014) found similar results, such that no significant difference existed among IDW, ordinary kriging, and regression kriging.

Table 3.1. Percent soil organic carbon content for the three primary study reaches calculated (i) as the mean of all soil samples in each study reach regardless of sample depth; (ii) as depth-averaged mean at each sampling location; (iii) using ordinary kriging; and (iv) using inverse distance weighting (IDW). Kriging and IDW were calculated using the listed optimized parameters, where *p* is the exponential parameter in IDW and *n* is the number of nearest neighbors. Error indicates the percent difference of the estimated mean for each method and the mean of all means. This is used to identify the least biased method from the three primary study reaches. Depth-average arithmetic mean was identified as the best estimate with the least variations from all other estimation methods (highlighted in dark grey).

Study reach	Method of estimating mean	Min	Max	Mean	Std	Error
CF1 (confined)	Mean across all samples	0.41	6.85	2.72	1.82	6%
	Depth-average mean	1.22	4.90	3.02	1.29	4%
	IDW (p=2, n=10)	1.23	4.90	2.93	0.78	1%
	Kriging (Gaussian, n=5)	2.16	4.08	2.93	0.54	1%
PC1 (partly confined)	Mean across all samples	0.44	20.94	3.16	3.50	27%
	Depth-average mean	0.88	20.94	4.38	4.99	1%
	IDW (p=1, n=8)	1.20	19.04	4.71	1.68	9%
	Kriging (exponential, n=10)	0.81	17.55	5.10	3.21	18%
MT1 (multithread)	Mean across all samples	0.18	18.49	4.80	3.87	6%
	Depth-average mean	0.18	18.49	5.22	4.12	2%
	IDW (p= 1 , n=15)	0.18	16.31	5.14	1.40	1%
	Kriging (Gaussian, n= 26)	0.18	17.98	5.25	3.16	3%

Comparison of soil organic carbon (SOC) content from 660 soil samples, across 24 study reaches, and between five valley types indicates a wide range of reach average values, but significant differences only between unconfined and other valley types (Table 3.2). Depth-average SOC contents for study reaches ranged from 2.31% along a beaver meadow to 18.96% along a single-thread channel in an unconfined valley (Table 3.2). A pairwise t-test of depth-averaged mean SOC content for all 24 study reaches indicated that SOC content of only unconfined valleys varied significantly from confined, partly confined, beaver influenced, and multithread channels ($p < 0.0012$).

Based on the results from various methods in estimating reach-average mean organic carbon content, depth-averaged arithmetic mean was chosen to represent the "true" population mean in the following analysis of bias with sample size.

Table 3.2. Description of 24 study reaches including valley type, sample size, basic statistics for soil organic carbon content, and size fraction based on grain-size analysis of a subset of samples. Sample size indicates the number of sampling locations at each study reach (Location), total number of soil samples collected at various depths for each location (Total n), and the subset of samples from various depths sieved for grain-size analysis (Grain size). Calculated values for SOC content include the minimum (Min), median (Med), maximum (Max), and standard deviation (SD). Three study reaches highlighted in grey indicate the three primary study reaches.

		Sample size			Depth-averaged arithmetic mean SOC					Grain size fraction (%)		
Study Reach	Valley Type	Location	Total n	Grain size	Min	Med	Max	Mean	SD	> 2mm (gravel)	0.062 -0.2 mm (sand)	< 0.062 mm (silt & clay)
AB1	Beaver meadow	12	28	6	0.6	12.1	27.4	11.7	7.9	7.4	81.4	9.8
AB2	Beaver meadow	10	18	4	5.3	12.9	18.3	12.5	4.5	1.5	75.4	22.8
AB4	Beaver meadow	13	49	9	3.0	4.2	9.1	5.2	2.0	8.5	70.0	20.7
AB5	Beaver meadow	11	49	27	1.2	2.3	3.4	2.3	0.7	4.2	80.2	15.1
AB6	Beaver meadow	11	39	11	1.2	2.9	4.0	2.8	0.8	9.1	75.5	15.3
CF1	Confined	15	38	8	1.2	3.2	4.9	3.0	1.3	3.1	88.8	7.4
CF2	Confined	9	11	2	3.5	6.5	10.6	6.6	2.0	15.0	69.1	15.7
CF3	Confined	5	10	3	1.8	5.2	41.9	14.4	16.8	22.6	70.8	5.0
CF4	Confined	8	16	3	2.7	7.2	29.5	9.7	8.8	7.5	81.9	10.6
CF5	Confined	8	19	4	0.3	2.7	5.5	2.6	1.7	1.0	89.0	9.4
CF7	Confined	9	10	6	1.2	8.9	17.8	8.7	5.2	13.0	73.0	13.6
MT1	Multithread	31	51	16	0.2	3.8	18.5	5.2	4.1	10.7	68.5	20.8
MT2	Multithread	11	24	5	0.2	6.8	29.0	9.6	10.0	2.2	83.0	14.7
MT3	Multithread	11	15	4	2.6	6.7	20.0	8.9	6.3	0.9	83.6	15.3
PC1	Partly Confined	14	34	5	0.9	2.8	20.9	4.4	5.0	17.2	73.7	8.6
PC2	Partly Confined	8	11	4	0.3	6.3	33.1	9.2	10.6	12.7	74.5	12.8
PC3	Partly Confined	14	22	6	1.1	2.8	14.5	4.1	3.4	10.7	81.1	7.3
PC4	Partly Confined	10	20	5	1.0	2.5	6.1	3.2	1.8	17.5	77.3	4.7
PC5	Partly Confined	11	30	7	1.1	2.8	5.7	3.0	1.3	3.3	88.4	7.0
PC6	Partly Confined	11	36	8	3.0	10.4	42.5	13.2	12.0	12.1	62.8	25.0
PC7	Partly Confined	10	34	16	1.5	2.4	11.5	3.4	3.02	5.5	84.8	9.1
UC1	Unconfined	11	22	6	3.1	18.0	47.6	19.0	13.2	15.7	62.1	20.8
UC2	Unconfined	11	35	13	3.7	10.0	26.5	13.5	7.3	15.1	61.0	23.6
UC3	Unconfined	9	39	17	3.6	4.8	13.3	5.5	3.1	3.4	75.3	21.2

3.4.2 Sample size, bias, and variance

Bootstrap analysis indicates that bias, which is the distance between the bootstrap-estimated mean and the population mean, decreases with increasing sample size for all three primary study reaches, as expected (Figure 3.4). Similarly, variance of the bootstrapped means decreases as sample size increases. The bias values in these plots are not fixed values representative of the bias for each consecutive number of samples, because the bias was calculated as a mean of 10,000 bootstrapped means (Figure 3.4). These plots can, however, be used to interpret at what point sampling bias becomes constrained within a specific range from the number of samples analyzed. Similarly, these plots indicate at what sample size variance of the mean converges to a minimum or levels out based on our estimate of the population depth-averaged mean.

Although bias is still present throughout all trials, based on the number of samples analyzed in this study, bias and variance level out for both the bootstrapped mean of all individual samples and the bootstrapped depth-average means from all sampling locations. The bias of bootstrapped means from all samples collected (three plots on the left, Figure 3.4) level out from values as high as 0.04 to a range of 0.02 at approximately 15 samples for all reaches. Bias of the bootstrapped depth-averaged mean SOC content (three plots on the right; Figure 3.4) displayed the same convergence toward the estimated true mean, such that at approximately 8 - 10 sampling locations, the bias is constrained within some bounds and the variance of estimated means levels out.

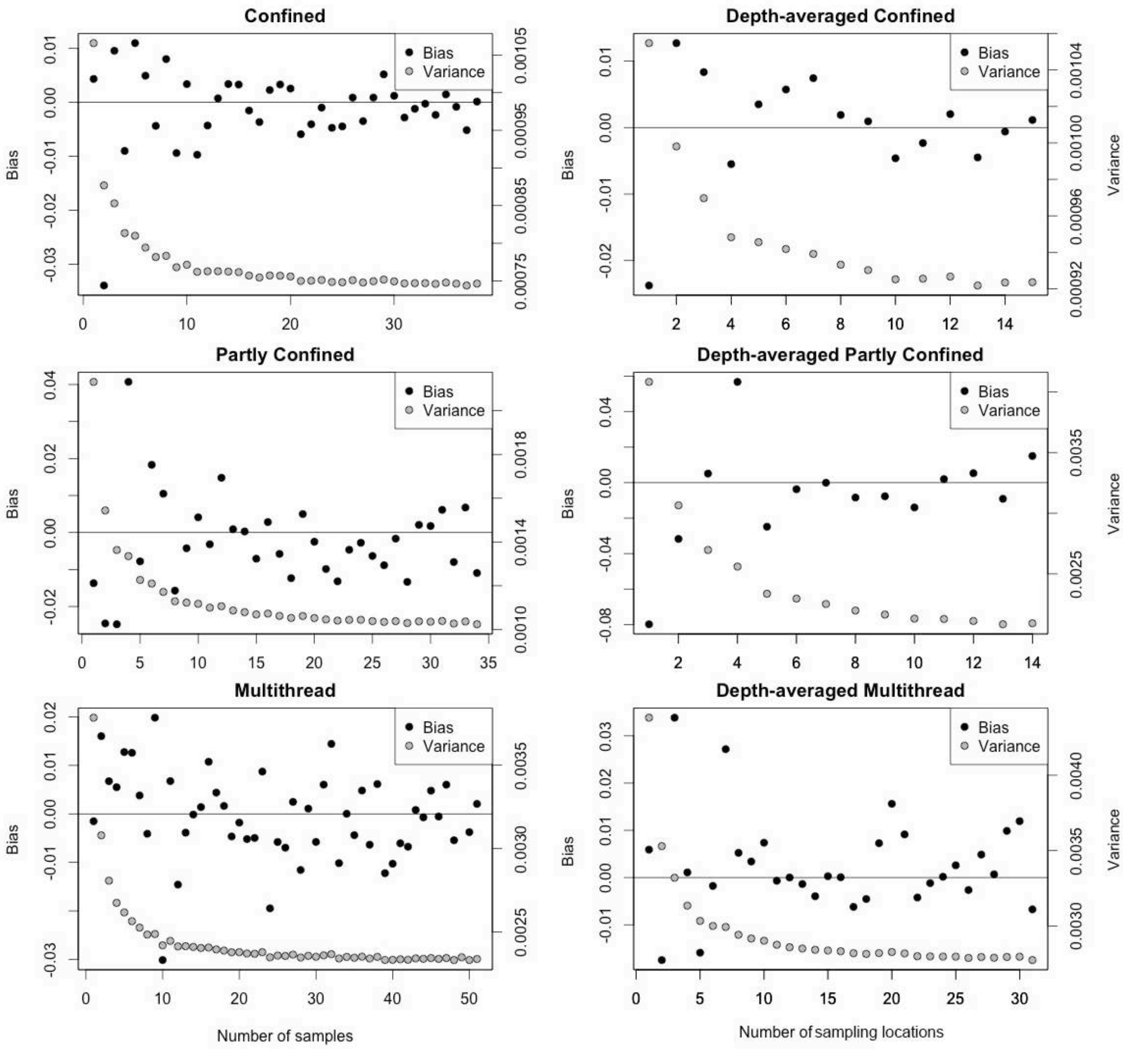

Figure 3.4 Differences between the bootstrapped mean and the population mean (bias) for soil organic carbon content as a result of the number of random samples selected for each trial iteration. The bias was calculated as the mean of 10,000 bootstrapped means for each consecutive number of randomly selected samples. The population mean, from which the bootstrapped means deviate and which is indicated by the horizontal line where bias = 0 in each plot, was estimated by the arithmetic depth-averaged mean. The variance represents the variance of bootstrapped means for each trial. The three plots on the left were based on bootstrapped means of every sample along each reach, regardless of sample depth and location, whereas the three plots on the right are bootstrapped depth-averaged means. Thus, the plots on the left represent the total number of samples randomly selected at various depths along each transect, whereas the plots on the right represent the number of sampling locations at which soil samples are collected at all incremental depths.

These results indicate that, given the possibility of collecting 34 - 51 samples at various random depths and locations or 15-cm incremental samples at all depths for 14 - 31 sampling locations across the floodplains of the study area, approximately the same bias and variance would be achieved by sampling only 15 samples at random depth and locations or sampling at every depth at ~10 randomly selected sampling locations along systematically spaced transects.

3.4.3 Predictors of SOC content: Regression analysis

As expected, SOC content correlates with moisture content (r^2 = 0.66) and silt and clay content (r^2 = 0.54), but correlation with depth is less than those found in upland soils (r^2 = -0.32; Table 3.3). Grain size analysis indicates that all study reaches are dominated by sand (>60% sand; Table 3.1). Unconfined valley segments contain on average more clay than other channel types, although the difference is not significant (Table 3.3).

Table 3.3 Correlation matrix among all possible predictors used in regression analysis (with the exception of elevation from the channel, which was eliminated due to co-linearity with sample depth and surface elevation).

	Elevation from the channel (m)	Confinement (m/m)	Surface elevation (m)	Maximum soil thickness (m)	Distance from channel (m)	Sample depth (cm)	Gravimetric moisture content (%)	Silt and clay, <0.062 mm (%)	Fine sand (%)	Sand (%)	Coarse sand (%)	Greater than 2mm (%)	Total organic carbon content (%)
Elevation from the channel (m)	1	-0.8	-0.17	-0.55	-0.28	-1	0.06	0.12	0.05	0	-0.06	-0.11	0.32
Confinement (m/m)	-	1	0.27	0.21	0.58	0.09		0.15	0.14	-0.05	-0.22	-0.08	-0.05
Surface elevation (m)	-	-	1	0.27	0.54	0.18	-0.2	-0.2	-0.03	-0.01	0.03	0.02	-0.06
Maximum soil thickness (m)	-	-	-	1	0.46	0.55	0.18	0.17	-0.1	-0.12	-0.1	-0.02	-0.07
Distance from channel (m)	-	-	-	-	1	0.29	-0.05	0.12	0.07	-0.01	-0.1	-0.09	-0.14
Sample depth (cm)	-	-	-	-	-	1	-0.07	-0.12	-0.05	0	0.06	0.11	-0.32
Moisture content (%)	-	-	-	-	-	-	1	0.65	0.02	-0.27	-0.28	-0.28	0.33
Silt and clay, <0.062 mm (%)	-	-	-	-	-	-	-	1	0.13	-0.39	-0.52	-0.44	0.54
Fine sand (%)	-	-	-	-	-	-	-	-	1	0.59	-0.66	-0.68	-0.06
Sand (%)	-	-	-	-	-	-	-	-	-	1	0.22	-0.66	-0.35
Coarse sand (%)	-	-	-	-	-	-	-	-	-	-	1	0.21	-0.23
Greater than 2mm (%)	-	-	-	-	-	-	-	-	-	-	-	1	-0.12
Total organic carbon content (%)	-	-	-	-	-	-	-	-	-	-	-	-	1

Multiple linear regression 1 included all 660 soil observations to investigate relationships between SOC content, soil moisture, and position across floodplains of the 24 study reaches. Regression 1 analysis including all variables indicated that only valley confinement (VC) and soil moisture (M) were significant ($p < 0.001$) variables in predicting SOC content when all possible variables were included. After the addition of approximately five variables, the AIC no longer decreased significantly. This result agreed with the best model selection from step-wise multiple linear regression (in which moisture was expressed as %, confinement was a dimensionless ratio, and all other variables were in m), which resulted in equation 3.1,

$$\text{SOC} = -1.8464 + 0.2693(M) - 0.0399(SD) + 2.9267(EFC) - 0.2154(VC) + 0.4536(ST) \tag{3.1}$$

where *SD* is the sample depth, *EFC* is the elevation from the channel, and *ST* is the total maximum soil depth or thickness at the sampling location.

Regression analysis 2 conducted on a subset of samples, which included all spatial variables and grain size, indicated that soil moisture content ($p < 0.001$), floodplain surface elevation (*SE*; $p = 0.003$), gravel content ($p = 0.003$), sample depth ($p = 0.005$), silt and clay content ($p = 0.006$), valley confinement ($p = 0.018$), and soil thickness at the sampling location ($p = 0.081$) were all significant in predicting SOC content when including all variables in the regression model. The AIC agreed with stepwise multiple linear regression in identifying eight variables for the best regression model.

$$\text{SOC} = 96.052 + 0.203(M) - 0.047(SD) - 0.991(\text{Sand}) - 0.143(VC) - 2.310(SE) - 0.912(\text{Gravel}) - 0.839(\text{Silt-Clay}) - 2.005(ST) \tag{3.2}$$

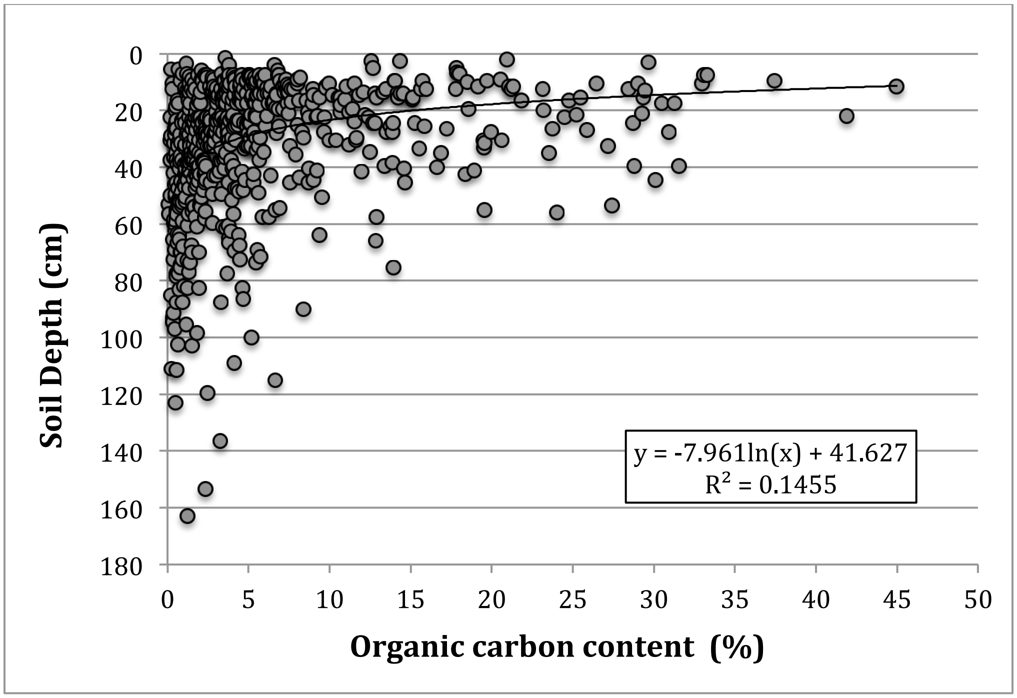

Figure 3.5 Percent soil organic carbon content generally decreases with depth, but the best fit logarithmic regression line explains only ~%15 of the variability in this relationship.

Although the best model from multiple linear regression includes soil depth as a predictor, it only explains a small portion of the variability in SOC content (Figure 3.5). Greater variability and maximum values of SOC content are present at shallow depths, but depth explains only ~15% of the variability in SOC content. Standardizing organic carbon content by the depth average mean at each sampling location yielded a similar relationship with an increase in r^2 by only ~0.03. Considering other predictors, however, such as elevation of the floodplain surface and grain size, the seemingly weak relationship may be significant across floodplains of mountain streams.

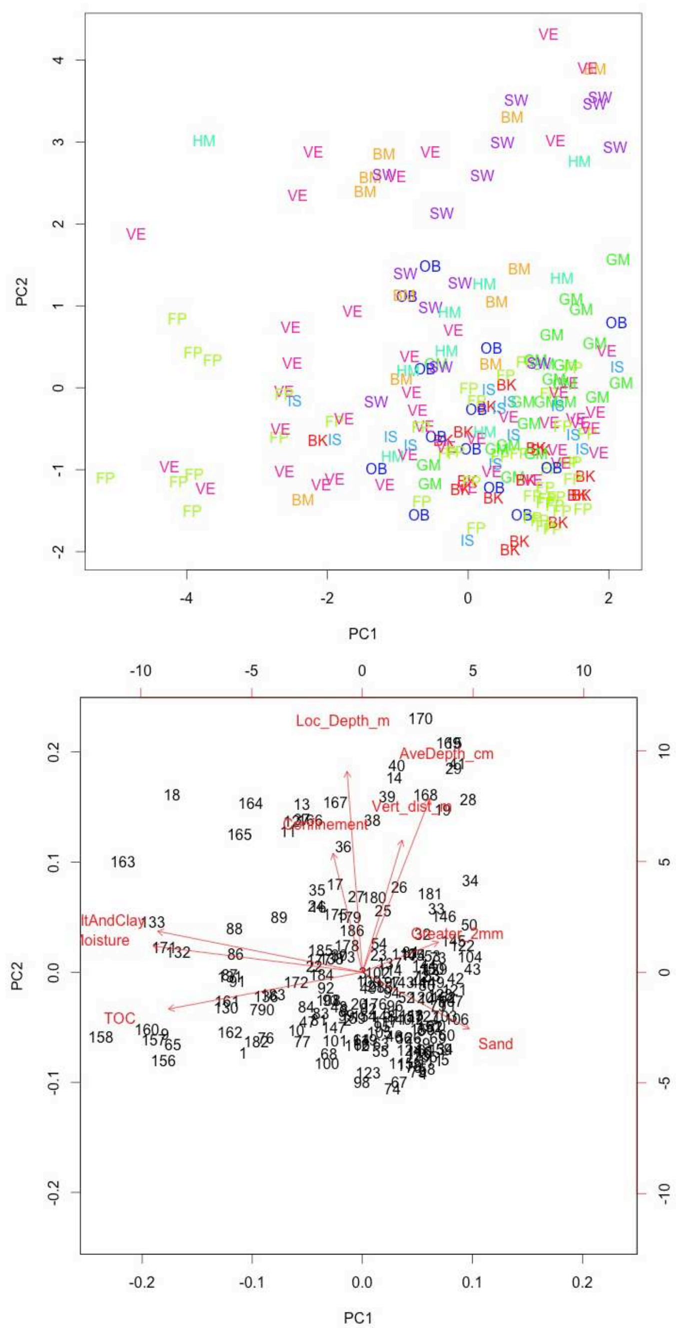

Figure 3.6 Principle component analysis of spatial and grain size variables identified as significant from regression 2, which include soil moisture, sample depth, percent sand, valley confinement, surface elevation, gravel content, percent silt and clay, and total soil depth at the sampling location. The upper plot is each observation plotted by the first two principle components using an abbreviation and different color for each geomorphic floodplain feature, as follows: banks (BK), overbank channels (OB), grassy meadows (GM), hummocks (HM), elevated tree berms or hummocks (HM), beaver meadows (BM), standing water (SW), islands (IS), valley edge (VE), and the generic classification of floodplains (FP). The lower plot is a biplot indicating the magnitude and direction of each variable on the first two principle components axes.

To summarize, multiple linear regression analysis indicated that soil moisture, soil sample depth, percent sand, valley confinement, floodplain surface elevation, gravel content, silt and clay content, and the maximum soil depth of thickness at each sampling location are potential predictors of soil organic carbon content. Using these significant variables as an input to principle components analysis, I investigate potential differences across geomorphic floodplain features.

3.4.4 Linking floodplain geomorphic features with SOC

Principle component analysis (PCA) using only spatial data identified as significant from regression 1 plus SOC content did not separate significant groups according to floodplain geomorphic feature. More clear groupings are illustrated, however, with inclusion of grain size from the variables identified as significant from stepwise linear regression 2 into PCA (Figure 6). Although grouping on a plot of the first two principle components and an explanatory biplot do not indicate that total organic carbon content (TOC) is distinct among geomorphic features alone, clustering of some groups suggest that variables with which OC is correlated may be organized by geomorphic floodplain features. Notable distinctions include samples from channel banks (BK, at the lower right) and grassy meadows (GM, just beside BK toward the upper left). From the biplot at the bottom of Figure 6, this can be interpreted as differences in percent sand content. The more general class of floodplain samples (FP) are concentrated in the lower right as well, but contain more spread across the plot. The location of overbank channels (OB) in the bottom right quadrant indicates coarser material, which is in agreement with boxplots of grain size fractions by geomorphic feature (Figure 7). Samples located in wet beaver meadows (BM) and where standing water was present (SW) seem to be constrained within the right portion of the plot and generally not overlap with more dry, grassy meadows or samples from the channel banks. Examination of the biplot alone (Figure 7) illustrates the strongest correlations with OC content, including a positive correlation with moisture and percent silt and clay content, and an inverse correlation with percent sand and percent gravel.

Results from this PCA do not clearly define groups such that particular geomorphic features exhibit distinct differences in SOC content or capture the variables identified as predictors for organic carbon content. Close examination of plots of the first two principle components and the biplot, however, display grouping of some geomorphic features, suggesting differences in at least some predictors of SOC across floodplain geomorphic surfaces.

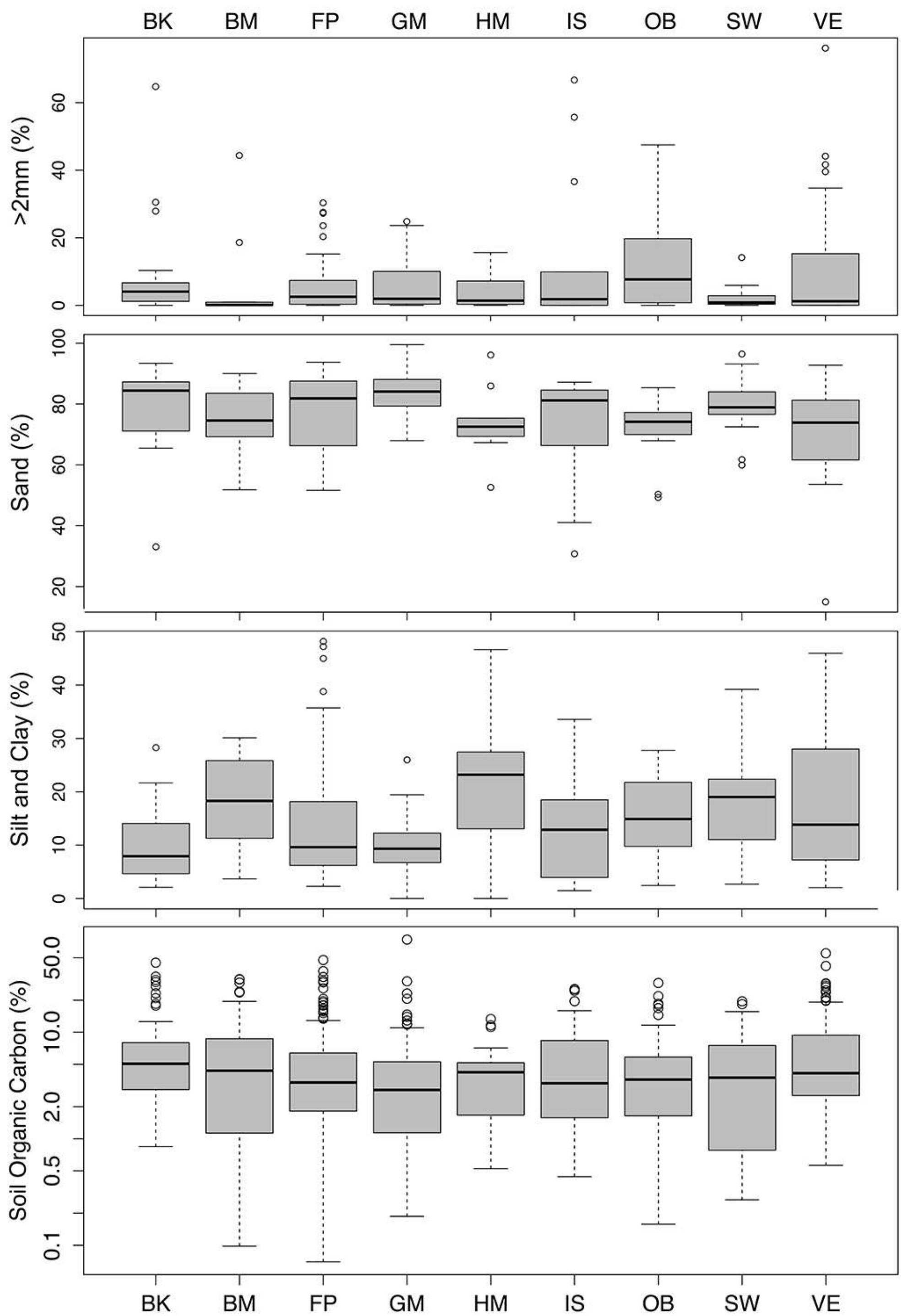

Figure 3.7 Boxplots of grain size fractions and soil organic carbon content across different geomorphic features as follows: banks (BK), overbank channels (OB), grassy meadows (GM), hummocks (HM), elevated tree berms or hummocks (HM), beaver meadows (BM), standing water (SW), islands (IS), valley edge (VE), and the generic classification of floodplains (FP).

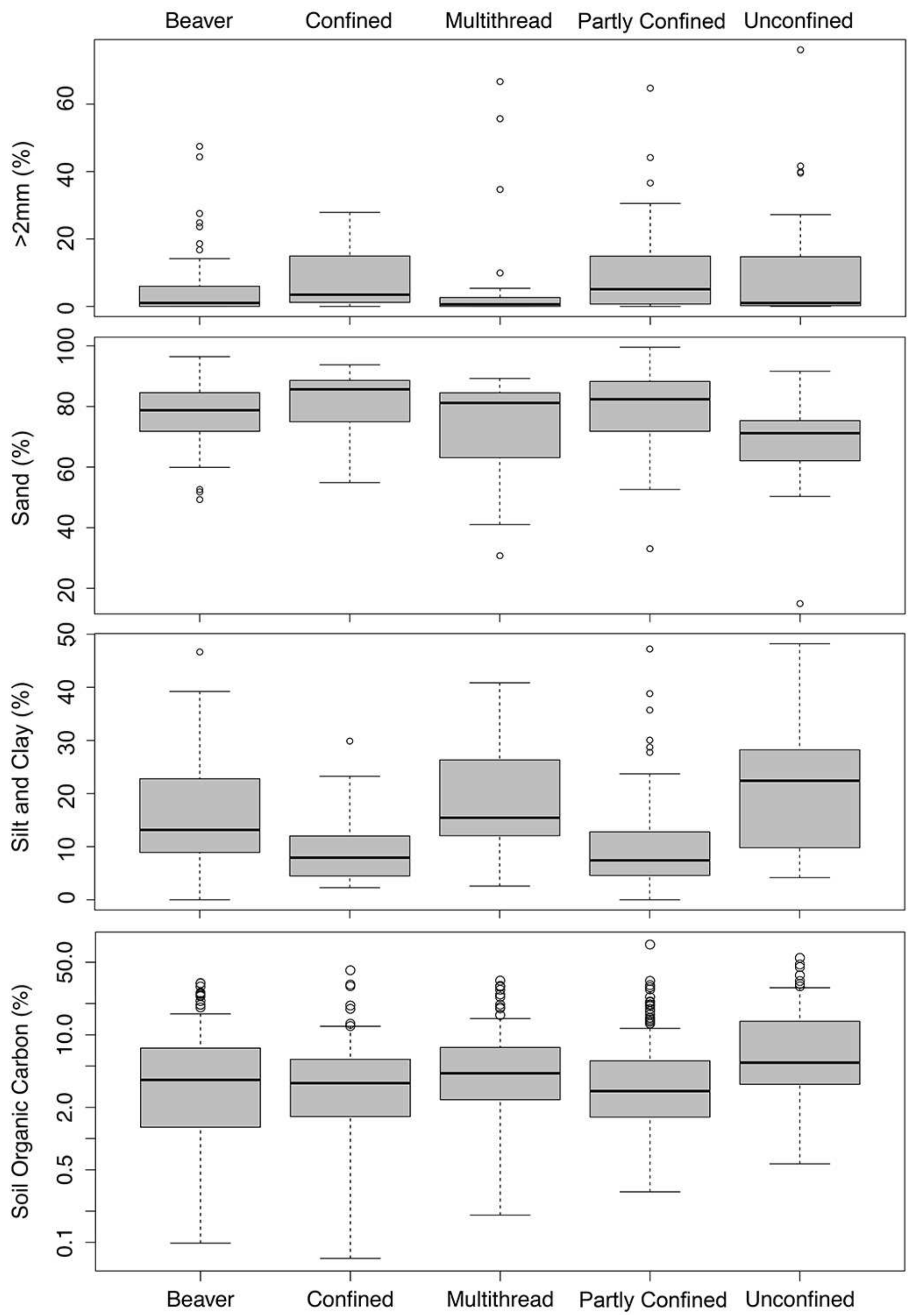

Figure 3.8 Boxplots of grain size fractions and soil organic carbon across the different valley types.

Differences in grain size distributions among valley types are not significant, although channels in unconfined valleys (beaver meadows, multithread, and single thread unconfined channels) accumulated greater silt and clay content, whereas confined and partly confined valleys contain more sand and gravel (Figure 8). Although not significantly different, single thread channels in unconfined valleys have the highest mean organic carbon content.

3.5 Discussion

Although I find that depth-average arithmetic mean provides the best estimate of the global reach-average mean over other spatial statistical methods, depending on the goals of other studies, these methods may be preferred. If reducing the bias of mean SOC content is crucial in other studies and a greater number of samples is an option, for example, kriging and IDW may result in more accurate estimates given a more intensitve sampling campaigns than those presented here.

Spatial statistical methods of estimating mean SOC content across floodplain surfaces of this study area (~3-5%) fall within an acceptable range (~1%) required to estimate SOC stocks. Bootstrap random sampling analysis and bias plots in which bias and variance converge indicate that the reach-average mean SOC content estimated using approximately 15 soil samples selected at random depths and locations or all incremental sampling depths at 10 randomly selected sampling locations would fall within the same range of estimates as those using up to 50 samples and 30 sampling locations, respectively. This means that unless more than 50 samples are going to be analyzed, an investigator can capture the variability of the mean SOC content without an increase in bias by collecting only 15 randomly selected samples at various depths and systematic locations across the floodplains in this study area and perhaps other mountainous streams as well. Alternatively, sampling all depths at approximately 10 sampling locations should provide a similar estimate of the mean, at least within the accuracy provided by 30 sampling locations.

Regression analysis supports the general understanding that OC content is largely correlated with moisture content, grain size distributions, and soil depth. Relationships with soil depth in previous studies, however, are generally stronger than those presented here (Jobbágy and Jackson, 2000). This is likely a result of the dynamic fluvial environment of mountainous floodplains along which surfaces are rarely stable for the long periods of time that lower relief, stable environments can experience. Understanding more specifically the mechanistic influences of how and where carbon is stored on floodplains could provide more insight into carbon storage along river corridors and potential importance of rivers in terrestrial carbon stocks and the global carbon budget.

Our principle components analysis suggests that geomorphic floodplain features could play a significant role in controlling the spatial variability of SOC content in floodplain soils, although these results did not define distinct features with significantly higher carbon content over others. Regression analysis indicates that floodplain surface elevation relative to the cross valley direction and surface water elevation correlates strongly with SOC content, which supports findings by *(Hupp et al., 2008)* along the much larger and lower-gradient Atchafalaya River. Soil characteristics, however, dominate the controls on OC content and it is not obvious that spatial attributes play a very strong role. The relative effect of spatial variables on organic carbon content blended with and is perhaps overshadowed by covariates of grain size distribution, as indicated from the biplot.

Our results indicate potential differences in the variables that correlate with OC content across geomorphic features. The subset sample size on which grain size analysis was conducted was relatively small and does not provide the large dataset needed to investigate these relationships thoroughly or identify distinct differences. Further work with stratified random sampling of grain size across geomorphic floodplain features could determine the minimum sample size needed, as I have done here, but constrain bias of estimated means with more certainty than resulted from this study.

Observed differences in SOC content across valley type and the potential for differences among geomorphic floodplain features highlight the presence of localized controls on SOC content in floodplains of mountain streams. Single-thread channels in unconfined valleys, for example, exhibit significantly higher organic carbon content than all other stream types (Holm-corrected $p < 0.001$) and accumulate finer sediment, likely as a result of decreased flow velocity across relatively wider floodplains (Figure 8). This work provides guidelines for sampling regarding the number of samples and suggests that stratifying sampling across geomorphic floodplain features may provide greater detail in differences associated with drivers of SOC content in floodplains of mountain rivers.

Our results indicate a significant difference in soil organic carbon content of floodplains (6 ± 7%) relative to those of uplands in the study area (Table 3.4). Licata and Sanford (2012) examined upland soil carbon content along a gradient from the foothills to the subalpine zones in the Colorado Front Range, including ponderosa forests to spruce and subalpine fir forests (which encompasses our study area), and found SOC contents of 1.5 ±0.08 to 2.2 ± 0.14%. Our values, however, are much smaller than those from *(Wohl et al., 2012)*, who found organic carbon contents along floodplains in the Colorado Front Range of 10 – 14%. Much higher mean SOC contents could have been a result of fewer study sites in the earlier study. Our systematic random sampling scheme and greater number of study sites provide a more accurate estimate of SOC content along floodplains of the Front Range.

Table 3.4. Values of soil organic carbon content of floodplains from studies in other regions and uplands and floodplains (including this study) of the Colorado Front Range

Location	Mean SOC (%)	Std dev (%)	Study
Colorado, USA (uplands)[a]	1.5 to 2.3	± 0.08 to 0.14	Licata and Sanford, 2012
Colorado, USA	10 to 14	-	Wohl et al., 2012
Colorado, USA*	6	± 7	This study
MidAtlantic USA (piedmont floodplains)			Walters and Merritts, 2008
-mineral top soil	1 to 2	-	
-buried organic horizon	2 to 9	-	
Alberta, Canada [b]	1.3 to 1.5	± 0.14 to 5.8	Hoffmann et al., 2014
Chamela, Mexico	1.6 to 3.1	-	Jaramillo et al., 2003
Rhine River, Germany	0.2 to 2	-	Hoffman et al., 2009

* values from this study
[a] values from uplands in the study area
[b] only selected values from floodplains cited

Mean organic carbon content at our study sites fall within the higher range of those from other studies examining floodplain carbon content (Table 3.3). Our results are comparable to organic horizons in the MidAtlantic region of the US (2 -9%) buried by milldam sedimentation during the industrial period (Walter and Merritts, 2008). This implies that humans have greatly altered carbon storage along river corridors with alterations of the sediment regime (Wohl et al., 2015; Wolman, 1967).

3.6 Conclusion

Quantifying OC retention and storage along floodplains may significantly contribute to identifying the missing terrestrial carbon sink. Floodplain sediment in mountain streams of the Colorado Front Range have higher organic carbon content than those in adjacent uplands and those in floodplains in other regions. Identifying how and where rivers retain OC is important for understanding ecosystem processing of carbon, aquatic and riparian foodwebs, and potential long-term storage of carbon in fluvial systems. Our analysis shows that depth average means should estimate SOC content relatively accurately. I outline methods to reduce the number of samples required to estimate floodplain OC content and provide values from 24 study reaches with various characteristics, which indicate higher OC content in floodplain soils compared to adjacent uplands. A limited subset of samples on which grain size analysis was conducted suggests that geomorphic floodplain features correspond to grain size distribution and resulting SOC content. Further investigation may prioritize stratified random sampling to investigate these relationships in greater detail.

Recognition

This paper is based upon work supported by: National Science Foundation Grant No. DGE-0966346 "I-WATER: Integrated Water, Atmosphere, Ecosystems Education and Research Program" at Colorado State University; NSF Doctoral Research Dissertation Improvement Grant #1536186; two research grants from the Geological Society of America; a research grant from the Colorado Scientific Society, and two research grants along with several scholarships through the Department of Geosciences and Warner College of Natural Resources at Colorado State University. I express gratitude to Robin Reich for use of his R code and to colleagues Katherine Lininger, Dan Scott, and Derek Schook for conversations and insight regarding soil sampling, coding, and spatial modeling. I also thank Ben Von Thaden, Dean Anderson, Joel Shotles, Fernando Ugalde, Jon Garber, Laurel Lynch, Timothy Fegel, John Harris, and Bryce Johnson for their company and assistance in the laboratory and the field.

References

Alexander L. 2014. Connectivity of Streams and Wetlands to Downstream Waters: A Review and Synthesis of the Scientific Evidence (External Review Draft) . US EPA National Center for Environmental Assessment. Environmental Protetion Agency: Washington DC [online] Available from: http://cfpub.epa.gov/ncea/cfm/recordisplay.cfm?deid=238345 (Accessed 26 January 2015)

Anderson RS, Riihimaki CA, Safran EB, MacGregor KR. 2006. Facing reality: Late Cenozoic evolution of smooth peaks, glacially ornamented valleys, and deep river gorges of Colorado's Front Range. In Special Paper 398: Tectonics, Climate, and Landscape Evolution , . Geological Society of America; 397–418. [online] Available from: http://specialpapers.gsapubs.org/cgi/doi/10.1130/2006.2398(25) (Accessed 1 May 2014)

Aufdenkampe AK, Mayorga E, Raymond PA, Melack JM, Doney SC, Alin SR, Aalto RE, Yoo K. 2011. Riverine coupling of biogeochemical cycles between land, oceans, and atmosphere. Frontiers in Ecology and the Environment 9 : 53–60. DOI: 10.1890/100014

Ballantyne AP, Alden CB, Miller JB, Tans PP, White JWC. 2012. Increase in observed net carbon dioxide uptake by land and oceans during the past 50 years. Nature 488 : 70–72. DOI: 10.1038/nature11299

Bates BC, Kundzewicz ZW, Palutikof JP. 2008. Climate change and water . Technical Report. IPCC: IPCC Secretariat, Geneva

Battin TJ, Luyssaert S, Kaplan LA, Aufdenkampe AK, Richter A, Tranvik LJ. 2009. The boundless carbon cycle. Nature Geoscience 2 : 598–600. DOI: 10.1038/ngeo618

Bracken LJ, Wainwright J, Ali GA, Tetzlaff D, Smith MW, Reaney SM, Roy AG. 2013. Concepts of hydrological connectivity: Research approaches, pathways and future agendas. Earth-Science Reviews 119 : 17–34. DOI: 10.1016/j.earscirev.2013.02.001

Braddock WA, Cole JC. 1990. Geologic map of Rocky Mountain National Park and vicinity, Colorado

Cole JJ et al. 2007. Plumbing the Global Carbon Cycle: Integrating Inland Waters into the Terrestrial Carbon Budget. Ecosystems 10 : 172–185. DOI: 10.1007/s10021-006-9013-8

Collins BD, Montgomery DR, Fetherston KL, Abbe TB. 2012. The floodplain large-wood cycle hypothesis: A mechanism for the physical and biotic structuring of temperate forested alluvial valleys in the North Pacific coastal ecoregion. Geomorphology 139–140 : 460–470. DOI: 10.1016/j.geomorph.2011.11.011

Falloon P, Jones CD, Ades M, Paul K. 2011. Direct soil moisture controls of future global soil carbon changes: An important source of uncertainty. Global Biogeochemical Cycles 25 : 1–14. DOI: 10.1029/2010GB003938

Hoffmann T et al. 2013. Short Communication: Humans and the missing C-sink: erosion and burial of soil carbon through time. Earth Surface Dynamics Discussions 1 : 93–112. DOI: 10.5194/esurfd-1-93-2013

Hoffmann T, Glatzel S, Dikau R. 2009. A carbon storage perspective on alluvial sediment storage in the Rhine catchment. Geomorphology 108 : 127–137. DOI: 10.1016/j.geomorph.2007.11.015

Hoffmann U, Hoffmann T, Jurasinski G, Glatzel S, Kuhn NJ. 2014. Assessing the spatial variability of soil organic carbon stocks in an alpine setting (Grindelwald, Swiss Alps). Geoderma 232–234 : 270–283. DOI: 10.1016/j.geoderma.2014.04.038

Hupp CR, Demas CR, Kroes DE, Day RH, Doyle TW. 2008. Recent sedimentation patterns within the central Atchafalaya Basin, Louisiana. Wetlands 28 : 125–140. DOI: 10.1672/06-132.1

IPCC 2007, Core Writing Team, Pachauri RK, Reisinger A. 2007. Climate Change 2007: Synthesis Report. Contribution of Working Groups I, II and III to the Fourth Assessment Report of the Intergovernmental Panel on Climate Change . IPCC: Geneva, Switzerland

Ives RL. 1942. The beaver-meadow complex. Journal of Geomorphology 5 : 191–203.

Jobbágy EG, Jackson RB. 2000. The vertical distribution of soil organic carbon and its relation to climate and vegetation. Ecological applications 10 : 423–436.

Licata C, Sanford R. 2012. Charcoal and Total Carbon in Soils from Foothills Shrublands to Subalpine Forests in the Colorado Front Range. Forests 3 : 944–958. DOI: 10.3390/f3040944

Merritt DM, Scott ML, LeROY POFF N, Auble GT, Lytle DA. 2010. Theory, methods and tools for determining environmental flows for riparian vegetation: riparian vegetation-flow response guilds. Freshwater Biology 55 : 206–225. DOI: 10.1111/j.1365-2427.2009.02206.x

Nanson GC, Knighton AD. 1996. Anabranching Rivers: Their Cause, Character and Classification. Earth Surface Processes and Landforms 21 : 217–239. DOI: 10.1002/(SICI)1096-9837(199603)21:3<217::AID-ESP611>3.0.CO;2-U

Persico L, Meyer G. 2009. Holocene beaver damming, fluvial geomorphology, and climate in Yellowstone National Park, Wyoming. Quaternary Research 71 : 340–353. DOI: 10.1016/j.yqres.2008.09.007

Polvi LE, Wohl EE, Merritt DM. 2011. Geomorphic and process domain controls on riparian zones in the Colorado Front Range. Geomorphology 125 : 504–516. DOI: 10.1016/j.geomorph.2010.10.012

Polvi L, Wohl EE. 2013. Biotic Drivers of Stream Planform: Implications for Understanding the Past and Restoring the Future. BioScience 63 : 439–452. DOI: 10.1525/bio.2013.63.6.6

R Core Team. 2012. R: A language and environment for statistical computing. . R Foundation for Statistical Computing.: Vienna, Austria

Ruddiman WF. 2001. Earth's Climate: Past and Future . Macmillan

Sutfin NA, Wohl EE, Dwire KA. 2015. Banking carbon: A review of organic carbon storage and physical factors influencing retention in floodplains and riparian ecosystems. Earth Surface Processes and Landforms : n/a–n/a. DOI: 10.1002/esp.3857

Trumbore SE, Czimczik CI. 2008. GEOLOGY: An Uncertain Future for Soil Carbon. Science 321 : 1455–1456. DOI: 10.1126/science.1160232

Veblen TT, Donnegan JA. 2005. Historical range of variability for forest vegetation of the national forests of the Colorado Front Range . USDA Forest Service, Rocky Mountain Region [online] Available from: https://129.82.112.12/docs/frs/cfri/VeblenHRVFrontRange.pdf (Accessed 26 January 2015)

Wainwright J, Turnbull L, Ibrahim TG, Lexartza-Artza I, Thornton SF, Brazier RE. 2011. Linking environmental régimes, space and time: Interpretations of structural and functional connectivity. Geomorphology 126 : 387–404. DOI: 10.1016/j.geomorph.2010.07.027

Walter RC, Merritts DJ. 2008. Natural Streams and the Legacy of Water-Powered Mills. Science 319 : 299–304. DOI: 10.1126/science.1151716

Wohl E, Bledsoe BP, Jacobson RB, Poff NL, Rathburn SL, Walters DM, Wilcox AC. 2015. The Natural Sediment Regime in Rivers: Broadening the Foundation for Ecosystem Management. BioScience : biv002. DOI: 10.1093/biosci/biv002

Wohl E, Dwire K, Sutfin N, Polvi L, Bazan R. 2012. Mechanisms of carbon storage in mountainous headwater rivers. Nature Communications 3 : 1263. DOI: 10.1038/ncomms2274

Wolman. 1967. A cycle of sedimentation and erosion in urban river channels. Geografiska Annaler 49A : 385–395.

Chapter 4: An elevational-driven shift in floodplain disturbance regime

Summary

The extreme flooding of September 2013 in the Colorado Front Range presents an opportunity to examine the geomorphic implications of elevational differences in floodplain disturbance regime. At eight study reaches along North Saint Vrain Creek, Colorado, I used radiocarbon ages of charcoal as a proxy for floodplain sediment residence time to examine differences in floodplain dynamics between high-elevation sites dominated by snowmelt peak flows and lower elevation sites below 2300 m that also have rainfall floods. Of the ~16 ha of floodplain disturbed during the 2013 flood, >85% were below 2300 m. Cumulative area of disturbed floodplain increased exponentially with increasing drainage area, rising dramatically below 2300 m. Detailed surveys of a site above 2300 m indicate net deposition (830 m^3), whereas the site below 2300 m had net erosion (670 m^3). Reach-average, pooled mean radiocarbon ages are an order of magnitude higher at high elevation sites (> 1200 y BP) compared to low elevation sites (< 700 y BP), indicating shorter sediment residence times in low elevation floodplains. Results suggest that similar elevational controls may influence floodplain sediment dynamics in other mountainous regions with longitudinal differences in hydroclimatic regime.

4.1 Introduction

The role of extreme precipitation and floods in the riverine transport of sediment through the landscape has been emphasized in paleohydrologic studies (Jarrett, 1990; McCain and Shroba, 1979) and recently highlighted by the occurrence of anomalous precipitation and river flooding (e.g., (Magilligan et al., 2015). The magnitude and frequency of such extreme events are predicted to increase with global climate change (Bates et al., 2008). This may be particularly important in high-relief terrains in which elevation limits between predominantly snowmelt versus rainfall runoff could change. Rainfall runoff can generate higher magnitude, shorter duration flood peaks with substantial erosive potential, so shifts in the location of rainfall flooding could alter the stability of river corridors, with consequences for sediment yield, water quality, natural hazards, and river ecosystems.

Floodplains are a particularly important component of river response during floods. Beyond attenuating peak flows, floodplains can serve as sediment sources during extreme events, but also as sediment reservoirs, even in steep mountain streams (Lancaster et al., 2010; Lancaster and Casebeer, 2007). This complicates comparison of denudation rates and sediment yield. Floodplain sediment storage and transit time are poorly understood (Hoffmann, 2015), but are recognized as interruptions to longitudinal sediment connectivity (Fryirs, 2013) that provide opportunities for sediment storage and closing sediment budgets (Schenk et al., 2013). Quantifying floodplain sediment residence time and identifying spatial patterns and the role of hydrologic disturbance in mountain streams provides information critical to modeling landscape evolution and predicting flood hazards and contaminant transport.

Previous work on large river floodplains has demonstrated that floodplain dynamics (sedimentation and erosion) significantly influence sediment storage (Aalto et al., 2008; Dunne et al., 1998) and riverine sediment budgets (Dunne et al., 1998; Schenk et al., 2013), and are influenced by climate forcing (Aalto et al., 2003). Few studies, however, have examined how elevational differences in disturbance regimes in high-relief environments influence floodplain dynamics. Floodplain sediment mean residence time is expected to increase downstream with increasing drainage area and average width and longitudinal extent of floodplains (Wohl, 2013). I examine the differences in floodplain sediment residence time along mainstem and tributary basins (10 - 20 km^2) nested within a 200-km^2 drainage. Floodplain study reaches are located along a longitudinal gradient across a distinct elevation boundary at 2300 m in the Colorado Front Range (CFR), which has well-documented implications for flood magnitude and duration (Jarrett, 1991). Here, I present the first quantification of floodplain sediment age and the geomorphic implications for floodplain dynamics associated with this hydroclimatic boundary.

I use randomly collected radiocarbon ages of charcoal in floodplain sediment to estimate floodplain sediment residence time along a gradient with decreasing elevation and increasing drainage area to test the hypothesis that high-elevation mountain streams exhibit increased sediment residence time relative to lower elevation sites in the CFR. I estimate floodplain sediment erosion and deposition at two study sites and the area of floodplain disturbance in the study catchment as a result of the 2013 CFR storm. Finally, I discuss the implications of the results for understanding floodplain dynamics in the context of sediment yield, natural hazards, and climate change in mountainous regions where similar elevational controls exist.

4.2 Regional Setting

A Precambrian core of granite, gneiss, and schist makes up the Colorado Front Range (Braddock and Cole, 1990). The range was uplifted during the Laramide orogeny (Dickinson et al., 1988) and has ^{210}Be- derived denudation rates of 20-30 mm/ky (Dethier and Lazarus, 2006; Foster et al., 2015). Rapid exhumation rates (Anderson et al., 2006) have recently been attributed to widespread hillslope and bank erosion following extreme events (Anderson et al., 2015) using observations and LiDAR analysis after the September 2013 storm, which caused >1138 debris flows along the northern CFR (Coe et al., 2014).

The CFR is characterized by an elevation-driven shift in precipitation and hydroclimatic disturbance regime, as reflected in paleohydrologic indicators of large floods (Grimm et al., 1995), gage records (Jarrett, 1990), and indirect discharge estimates from recent large floods (McCain and Shroba, 1979) (Ogden et al., 2000). Hydrographs at elevations above 2300 m are dominated by seasonal snowmelt with peak unit discharge up to 1.1 $m^3/s/km^2$, whereas sites at lower elevations have a secondary peak resulting from large convective thunderstorms that can produce peak unit discharge up to 40 $m^3/s/km^2$ {Citation}(Jarrett, 1990).

Localized response, including floodplain sediment residence time, to these extreme precipitation and floods depends largely on geology and geomorphic process domains associated with longitudinal variation in lateral valley confinement (Polvi et al., 2011; Wohl, 2010). Relatively unconfined valley segments, which tend to be located in the CFR where rivers cut across densely spaced bedrock joints (Wohl, 2008), dissipate flood energy and accumulate sediment (Wohl et al., 2012).

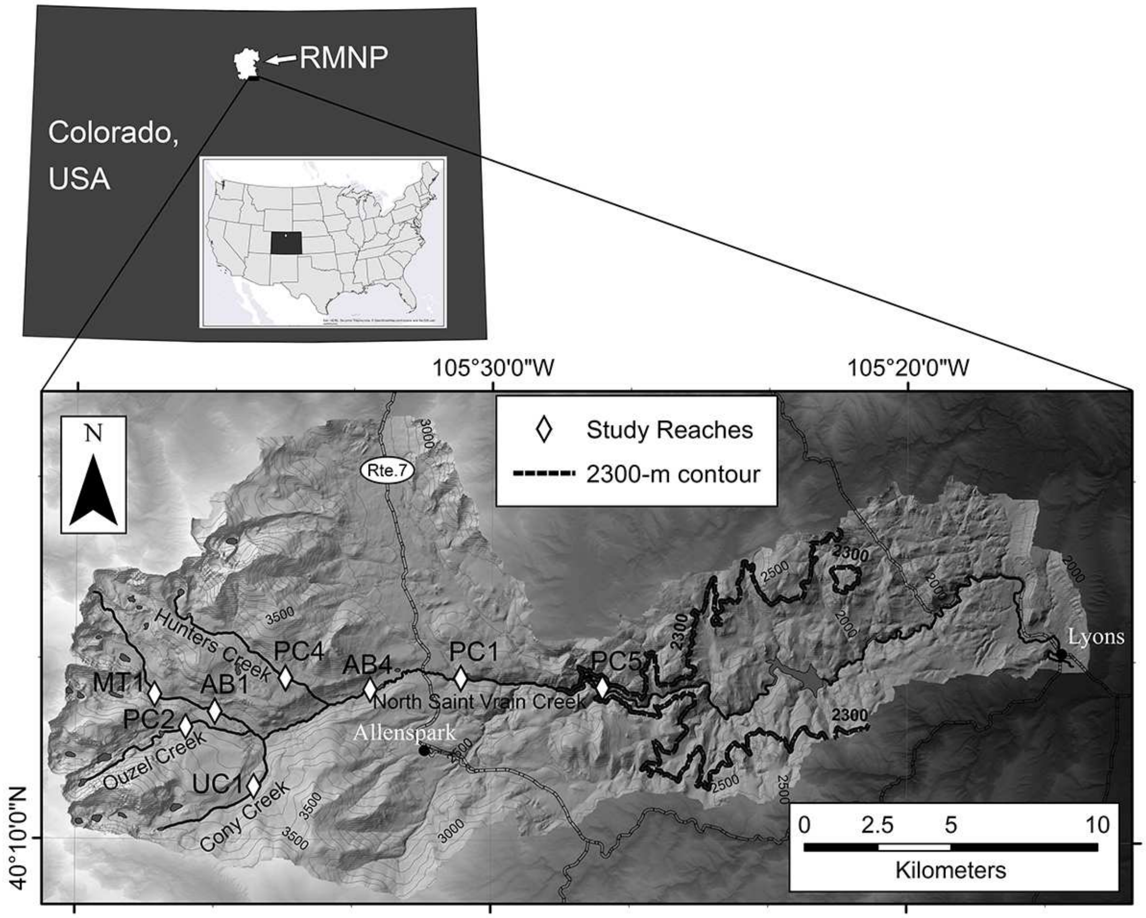

Figure 4.1 Eight study reaches within the North Saint Vrain Creek watershed in the southeastern portion of Rocky Mountain National Park (RMNP), Colorado, USA.

The study area lies within the North Saint Vrain Creek (NSV) watershed, extending from Ralph Price Reservoir upstream to headwaters at the continental divide. Radiocarbon analysis focuses on two study sites above Route 7 (PC4 at 3027 m and AB1 at 2905 m) and two study reaches ~2 and 7 km downstream of Route 7 and ~ 150 and 80 m above and below the 2300-m elevation contour, respectively (Figure 4.1). The NSV watershed has limited anthropogenic disturbance relative to other watersheds in the region. Estimated recurrence intervals from the 2013 flood on NSV are ~2 and >200 years at Allenspark and Lyons, respectively (Figure 4.1; (Yochum, 2015). Three study reaches (PC1, PC4, PC5) have a floodplain width (w_v) between 2 and 5 times the bankfull channel width (w_c), whereas w_v is nearly nine times w_c at AB1.

4.3 Methods

Remotely sensed photography from USDA NAIP aerial imagery collected in 2012 and 2013 before and after the 2013 flood was used with field observations and surveys to estimate the area of floodplain surfaces disturbed during the flood along NSV downstream from State Route 7. Interpreted disturbance here does not distinguish between erosion and deposition, but only observable differences as indicated by changes in vegetation in NAIP aerial imagery from 2012 and 2013. Post-event LiDAR collected by FEMA was used to verify the contemporary position of the channel and floodplain, which reduced uncertainty where the valley was heavily shadowed in the imagery. Heavy shadows limited detection of floodplain disturbance, particularly at higher elevations and small drainage areas where channels are very narrow. Field observations verified floodplain disturbance at higher elevations, but these results are presented as order of magnitude estimates primarily as a method of comparison at different elevations. Reconditioned NHD flowlines of the NSV main stem (Nagel et al., 2014) were segmented into 100-m segments in ArcMap and the corresponding elevation from the DEM and cumulative area of disturbed floodplain surfaces was obtained for each point that intersected a 50-m buffer of the floodplain polygons.

Each study reach was defined by 11 transects spaced one bankfull channel width apart. The topographic floodplain surface was surveyed along each transect using a Laser Technology TruPulse 360B laser range finder. The depth of floodplain sediment was measured using the depth of penetration of a 1-cm diameter rebar pounded into sediment until refusal at bedrock or clasts larger than coarse sand, which typically have an abrupt boundary with overlying finer sediment. Sediment volumes were estimated from measured depths using irregular triangular networks (TINs) in ESRI ArcMap. Total mass of sediment along each study reach was calculated using mean bulk density (0.9 g/cm^3) estimated from 23 measurements across floodplains in the study area.

Pre-event, 2013 topographic surveys along each transect of the two study reaches farthest downstream (PC1 and PC5) allowed me to anchor post-event surveys along the valley endpoints of at least 6 transects observed to have experienced little to no change after the flood. The differences between pre-event surveys and post-event LiDAR were calculated to estimate net change in floodplain surface topography. The volume of net displacement from the previous floodplain was estimated by cutting out the location of the active channel and using TINs in ERSI ArcMap to calculate the volume of the difference between pre-event ground surveys and post-event LiDAR. Although estimated values are rough approximations with inherent error, relative values provide information about net erosion or deposition. Positive values indicate a decrease in floodplain surface elevation and are interpreted as net erosion. Negative values indicate an increase in floodplain surface elevation and are interpreted as net deposition.

Systematic random sampling of floodplain sediment was conducted along 8 study reaches for the full depth of the floodplain soil profile until refusal using a stainless steel hand auger. A single sampling location was randomly selected along each transect using a random number generator to select the number of meters from the valley edge for each sample location. Where charcoal samples were limited, all possible charcoal samples collected from each reach were processed by accelerated mass spectrometer of ^{14}C. After selection of the 5 deepest samples along study reach PC1, random selection of four samples was conducted out of a remaining 11 samples. Where charcoal and sample size were limited, additional sampling locations were selected where sediment depths were greatest. Individual radiocarbon ages were calibrated using OxCal software (Bronk Ramsey, 2001) and the IntCal13 calibration curve (Reimer et al., 2004) and summed probabilities were normalized for all samples from each study reach. Pooled mean radiocarbon ages for each study reach were calibrated using Calib software (Stuiver and Reimer, 1993) and the IntCal13 curve. These calibration methods result in standard deviations for pooled mean radiocarbon ages based on the probability distribution for each radiocarbon age. Pooled mean radiocarbon age of charcoal in floodplain sediment was used to constrain a maximum value for mean floodplain sediment residence time of floodplain sediment.

4.4 Results

Of floodplain area disturbed by the 2013 flood, approximately 16.1 ha were eroded during the event and ~85% of the disturbed floodplain area occurred below 2300 m (Figure 4.2). Cumulative area of disturbed floodplain increases with decreasing elevation and increasing cumulative drainage area by a non-linear relationship (Figure 4.2). As elevation decreased along the mainstem NSV, the relative area of disturbed floodplain following the 2013 flood increased by a power of ~17.4. Noticeable increases in floodplain disturbance occur at the confluence of NSV and significant tributaries including Rock Creek, Cabin Creek, and Dry Saint Vrain Creek. Floodplain disturbance remains constant for short distances along NSV where the valley is highly confined by steep canyons walls and no floodplain was present prior to the flood.

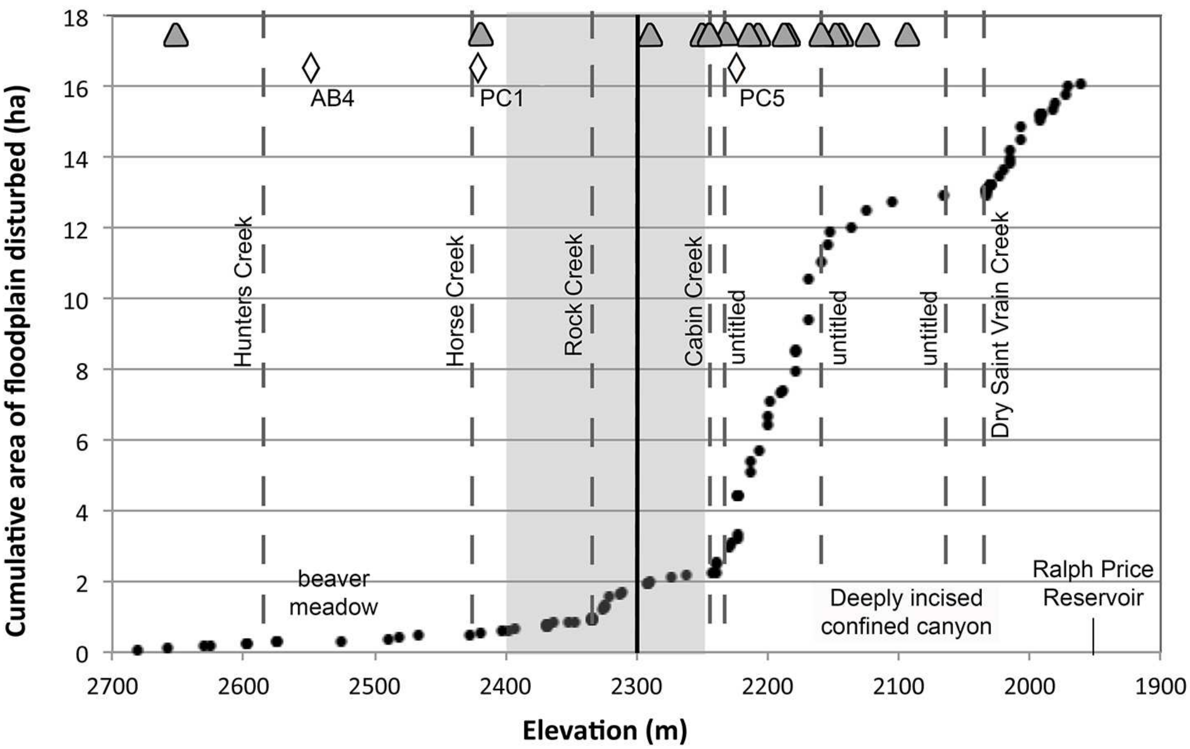

Figure 4.2 Cumulative area of disturbed floodplains with decreasing elevation along North Saint Vrain Creek following the 2013 flood indicate a power-law relationship ($r^2 = 0.94$) captures more of the variability than a linear regression ($r^2 = 0.81$). Gray triangles indicate locations of significant debris flows from adjacent hillslopes and tributaries (indicated as dashed vertical lines) and white diamonds indicate the location of study reaches. The vertical black line indicates the location of 2300 m elevation, and the shaded area indicates what I interpret as the long-term average transitional zone for floodplain disturbance regime in the study basin.

Estimated net erosion and deposition along the floodplains of study reaches PC1 and PC5 indicate significant mobilization and change in the volume of floodplain sediment during the 2013 flood (Table 4.1, Figure 4.3, 4.4). Both study reaches were impacted by debris-flow sediment input. PC1 experienced net deposition, whereas PC5 experienced net erosion, although the channel experienced significant erosion and deposition, respectively, in each reach

Table 4.1 Net change in elevation of floodplain surfaces following the 2013 event from difference in pre-event field surveys and post-event FEMA LiDAR.

Change	PC1	PC5
Erosion (m^3)	259	828
Deposition (m^3)	1090	150
Net change (m^3)	Deposition (830 m^3)	Erosion (678 m^3)

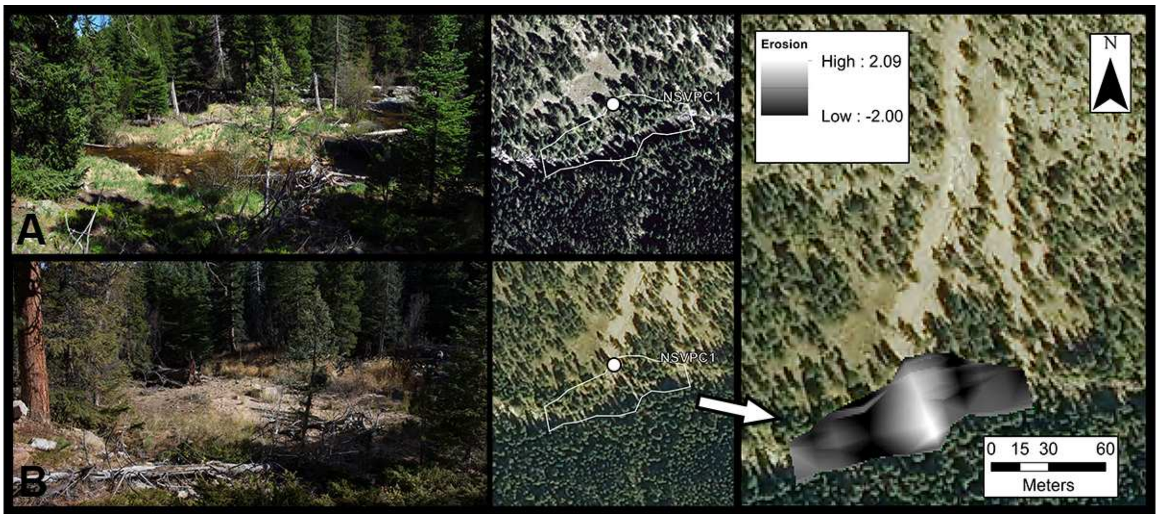

Figure 4.3 Before and after (A and B, respectively) photographs of effects of the 2013 flood on study reach PC1 (~2470 m elevation), illustrating net deposition from a debris flow that filled a side channel from valley left. Photographs were taken looking downstream from the white dot on valley left indicated in the middle frame, where flow is from west to east. The debris-flow scar is visible in the right frame, with a raster file indicating change in floodplain topography. Light colors and positive values indicate a decrease in floodplain surface elevation and net erosion, whereas dark colors and negative values indicate an increase in floodplain surface elevation and net deposition. Erosion from the debris flow

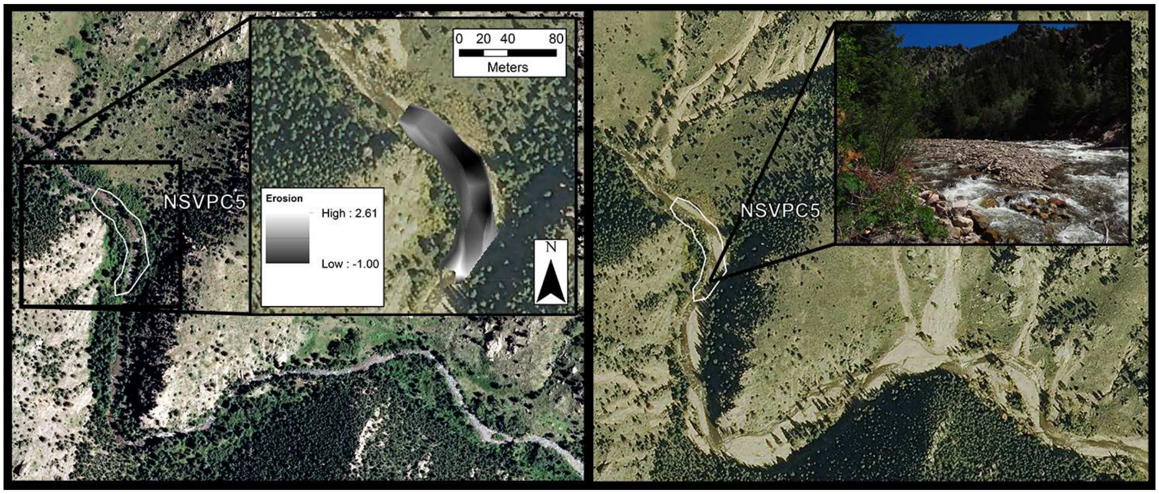

Figure 4.4 Numerous debris flows greatly impacted the lower elevations of North Saint Vrain Creek in the 2013 event and are visible in these pre- and post- event aerial images used to delineate the area of impacted floodplains along the river corridor. White outlines study reach NSVPC5, in both photographs. Light colors and positive values of the inset raster images indicate a decrease in floodplain surface elevation and net erosion, whereas dark colors and negative values indicate an increase in floodplain surface elevation and net deposition. The inset photograph in the lower frame illustrates in-channel deposition of gravels and boulders that encouraged erosion of the floodplain.

Summed probabilities of all samples from each study reach indicate decreasing variability of calibrated radiocarbon ages with decreasing elevation, with the exception of the highest elevation study reach (PC4; Figure 4.5). Residence time of floodplain sediment reflects the same pattern, such that a positive correlation exists between maximum floodplain sediment residence time and study reach elevation, with the exception of PC4. A distinct difference exists between high elevation (>2500 m) and low elevation (<2500 m) study reaches, resulting in residence times >1355 y BP and <700 y BP, respectively (Figure 4.5, Table 4.2). Coefficient of determination from linear regression of pooled mean radiocarbon age indicates a significant power-law relationship with elevation and contributing drainage area (r^2 = 0.82 and 0.79, respectively; Figure 4.6).

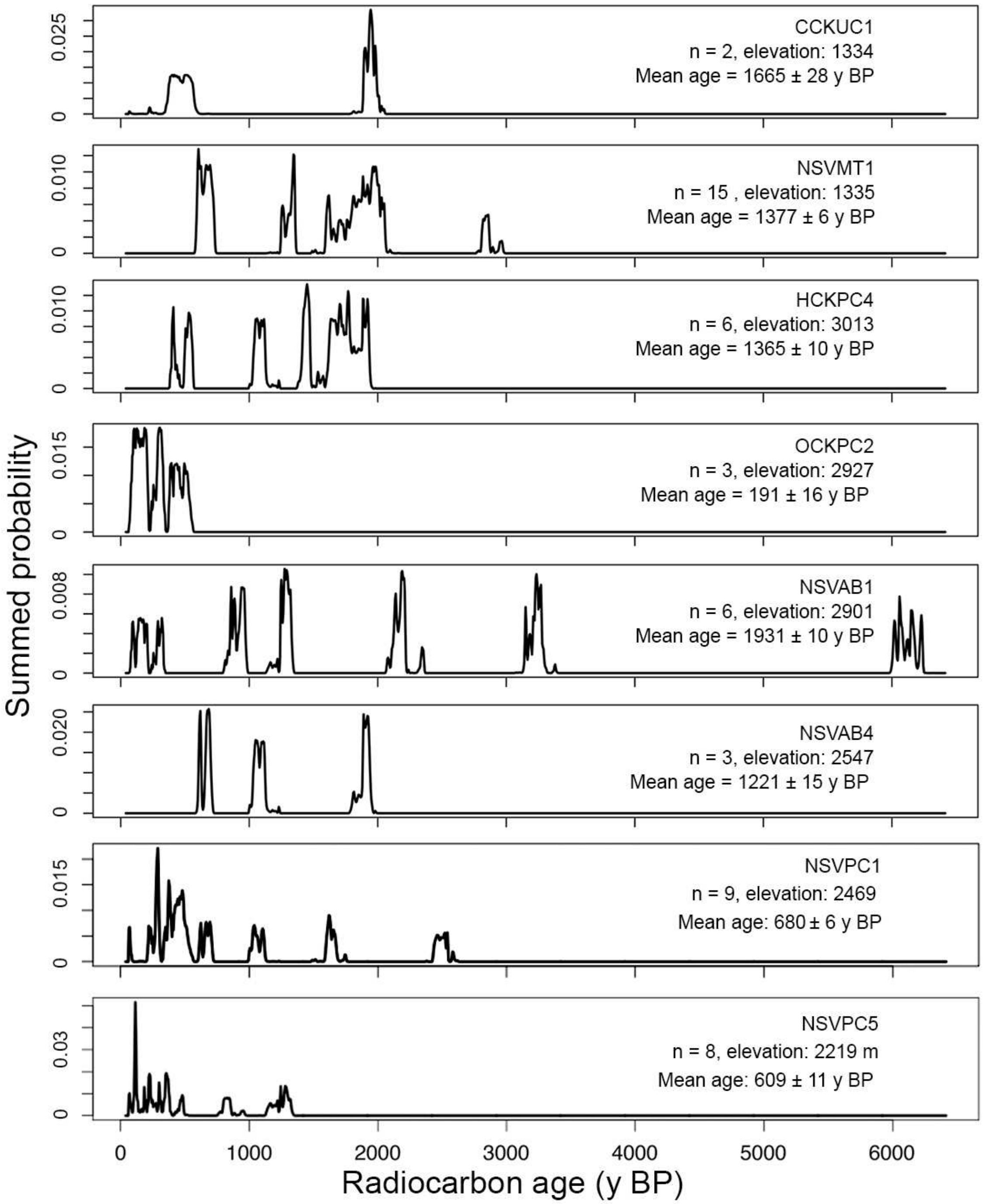

Figure 4.5 Summed probabilities of all samples from each study reach. The variability or spread in ages between each charcoal sample indicates potential for storage or lack of storage of old sediment. Although UC1 and AB4 have very small sample sizes (2 and 3, respectively), pooled mean ages for all study reaches indicate two separate populations above and below 2500 m elevation with pooled mean ages >1200 y BP and <700 y BP, respectively.

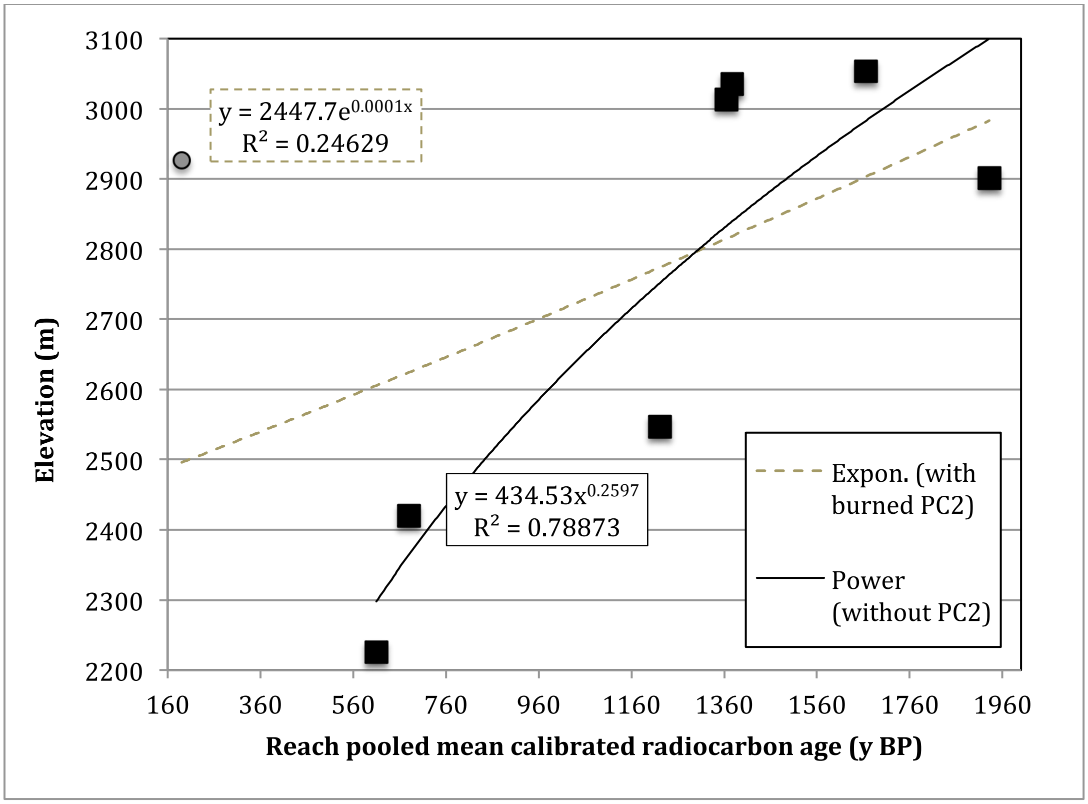

Figure 4.6 Pooled reach-averaged mean radiocarbon age indicates two distinct populations with different residence times. Floodplains above 2500 m in elevation have residence times > 1200 y BP (with the exception of a reach burned in 1978), whereas 2 study sites below 2500 m have ages < 600 y BP. The best fit regression line excluding the study reach recently burned in 1978 (OCKPC2) indicates a power-law relationships with elevation and drainage area (r^2 = 0.79) .

Table 4.2 Site characteristics, pooled mean radiocarbon age, and calculated values used to estimate floodplain sediment residence time.

Study Reach	Mean residence time (y BP)		Drainage Area (km^2)	Elevation (m)	Valley Confinement (m/m)	Stream Gradient (m/m)
CCKUC1	1665	± 28	12.7	3054	4.7	0.028
NSVMT1	1377	± 6	14.8	3035	10.3	0.063
HCKPC4	1365	± 10	10.1	3013	4.1	0.069
OCKPC2	191	± 16	11.1	2927	2.9	0.063
NSVAB1	1931	± 10	19.1	2901	10.4	0.037
NSVAB4	1221	± 15	82.2	2547	21.7	0.012
NSVPC1	680	± 6	96.4	2469	2.3	0.037
NSVPC5	609	± 11	200.0	2219	2.2	0.023

4.5 Discussion

Pooled mean radiocarbon ages do not differ in relation to valley confinement or stream gradient, but do reflect two distinct groups differing in elevation. This suggests an elevation control on floodplain sediment residence time, such that higher elevations store sediment for much longer periods than lower elevation reaches, with a threshold occurring somewhere between 2300 and 2500 m. Even with a higher number of samples at the lower elevation sites and increasing probability of re-worked charcoal and carbon that provide only a maximum limiting age for floodplain sediment, the higher elevation sites have much greater ages. These differences are interpreted as more rapid turnover of floodplain sediment at lower elevations because even deeper samples at the lower elevation sites include only younger charcoal (i.e., 46 and 69 cm at PC5 and PC1, respectively). Additionally, even small sample sizes at high elevations yield much older pooled mean ages.

An abrupt increase in floodplain disturbance during the 2013 flood occurred just below 2300 m elevation, which suggests a shift in fluvial disturbance regime at the same elevation as the previously identified shift in hydroclimatic regime (Jarrett, 1990; Figure 4.2). Estimated changes in floodplain sediment area and inferred erosion and deposition at two study reaches during the 2013 flood suggest greater event-driven floodplain change at lower elevations because PC1 was dominated by deposition at 2469-m elevation, whereas PC5 was dominated by erosion at 2219-m elevation. Although both reaches were affected by debris-flows initiated from adjacent hillslopes, increased unit stream power accompanying larger discharge at lower elevations appears to have mobilized sediment inputs at PC5, whereas the relatively lower magnitude of stream power at PC1 did not mobilize debris-flow sediment.

Erosion and deposition at NSVPC1 and NSVPC5 can, however, also be influenced by the relative confinement and channel planform at each reach, although both reaches are located along bends in the channel. There appears to be a downstream trend in the mean age of floodplain sediment, but inference of a distinct shift in sediment residence time associated with the disturbance regime may require analysis of additional sites below 2300 m. However, substantially greater anthropogenic impacts to the channel and floodplain at lower elevations limit the ability to perform such an analysis.

Although distinct zonation of flood magnitudes has been attributed to upper elevation limits on convective thunderstorms in the CFR (Gochis et al., 2014; McCain and Shroba, 1979), other transitions along this boundary may influence floodplain disturbance and sediment dynamics. The shift from lower montane to upper montane vegetation communities occurring at ~2350 m includes an increase in the abundance of Douglas-fir relative to the ponderosa pine forests of the lower montane zone, as well as more persistent snowpack and greater return intervals for wildfires (Veblen and Donnegan, 2005) and associated debris flows.

Anderson et al. (2015) state that debris flows during extreme events may be responsible for the majority of floodplain erosion in the Front Range, but Coe et al. (2014) suggest no significance differences in spatial frequency of debris flow initiation at the 2300 m elevation hydroclimatic transition. Data presented here, however, suggest that differences in floodplain disturbance regime occurring between 2300 and 2500 m may result in different responses to debris-flow sediment inputs. These observations illustrate potential mechanisms of floodplain evolution through filling of side channels and creation of new islands in PC1 and PC5, respectively. Greater hydraulic force at lower elevations may be the driver needed to evacuate debris-flow deposits from floodplains on the Front Range.

These results provide insight into the importance of floodplain sediment storage in sediment budgets of mountain streams. Discrepancies between basin-wide erosion rates and sediment yield can be reduced by considering significant loss of longitudinal sediment connectivity by floodplains (Fryirs, 2013), even in small mountain streams. Elevational differences in floodplain dynamics of mountain streams can result in substantially greater floodplain erosion, sediment yields, and natural hazards at lower elevations during extreme storms, as well as decreased retention of organic carbon and nutrients in floodplain sediment (Wohl et al., 2012; Sutfin et al., 2015). If changing climate results in upward shifts in the elevational boundary between snowmelt and rainfall floods, floodplains that are relatively stable, retentive sediment reservoirs at time spans of 10^2-10^3 years under existing climate could become net sediment sources.

4.6 Conclusion

I test potential differences in floodplain disturbance regime and sediment residence time along an elevational gradient in the Colorado Front Range. Estimated floodplain disturbance and calculated net change in floodplain sediment volume along North St. Vrain Creek (NSV) during the 2013 flood support the geomorphic record from radiocarbon ages of charcoal in floodplain sediment. These results suggest that high elevation streams with relatively smaller drainage areas experience less floodplain disturbance and exhibit longer residence times, compared to lower elevation sites with much larger drainage areas in the NSV watershed, contrary to trends in floodplain dynamics with increasing drainage area documented for river networks in other regions. Because many mountain ranges experience topographic-controlled boundaries in hydroclimatic and hydrologic runoff regimes, similar differences in fluvial disturbance likely influence floodplain sediment dynamics and storage in high elevation stream networks of other mountain regions.

Recognition

This paper is based upon work supported by: National Science Foundation Grant No. DGE-0966346 "I-WATER: Integrated Water, Atmosphere, Ecosystems Education and Research Program" at Colorado State University; NSF Doctoral Research Dissertation Improvement Grant #1536186; and research grants from the Geological Society of America, the Colorado Scientific Society, and several scholarships through the Department of Geosciences and Warner College of Natural Resources at Colorado State University.

References

Aalto R, Lauer JW, Dietrich WE. 2008. Spatial and temporal dynamics of sediment accumulation and exchange along Strickland River floodplains (Papua New Guinea) over decadal-to-centennial timescales. Journal of Geophysical Research: Earth Surface (2003–2012) 113 DOI: 10.1029/2006JF000627 [online] Available from: http://onlinelibrary.wiley.com/doi/10.1029/2006JF000627/abstract (Accessed 27 October 2015)

Aalto R, Maurice-Bourgoin L, Dunne T, Montgomery DR, Nittrouer CA, Guyot J-L. 2003. Episodic sediment accumulation on Amazonian flood plains influenced by El Niño/Southern Oscillation. Nature 425 : 493–497. DOI: 10.1038/nature02002

Anderson RS, Riihimaki CA, Safran EB, MacGregor KR. 2006. Facing reality: Late Cenozoic evolution of smooth peaks, glacially ornamented valleys, and deep river gorges of Colorado's Front Range. In Special Paper 398: Tectonics, Climate, and Landscape Evolution , . Geological Society of America; 397–418. [online] Available from: http://specialpapers.gsapubs.org/cgi/doi/10.1130/2006.2398(25) (Accessed 1 May 2014)

Anderson SW, Anderson SP, Anderson RS. 2015. Exhumation by debris flows in the 2013 Colorado Front Range storm. Geology 43 : 391–394. DOI: 10.1130/G36507.1

Bates BC, Kundzewicz ZW, Palutikof JP. 2008. Climate change and water . Technical Report. IPCC: IPCC Secretariat, Geneva

Braddock WA, Cole JC. 1990. Geologic map of Rocky Mountain National Park and vicinity, Colorado

Bronk Ramsey C. 2001. Development of the radiocarbon calibration program OxCal. Radiocarbon 43 : 355 – 363.

Coe JA, Kean JW, Godt JW, Baum RL, Jones ES, Gochis DJ, Anderson GS. 2014. New insights into debris-flow hazards from an extraordinary event in the Colorado Front Range. GSA Today 24 : 4–10. DOI: 10.1130/GSATG214A.1

Dickinson WR, Klute MA, Hayes MJ, Janecke SU, Lundin ER, McKITTRICK MA, Olivares MD. 1988. Paleogeographic and paleotectonic setting of Laramide sedimentary basins in the central Rocky Mountain region. Geological Society of America Bulletin 100 : 1023–1039. DOI: 10.1130/0016-7606(1988)100<1023:PAPSOL>2.3.CO;2

Dunne T, Mertes LAK, Meade RH, Richey JE, Forsberg BR. 1998. Exchanges of sediment between the flood plain and channel of the Amazon River in Brazil. Geological Society of America Bulletin 110 : 450–467. DOI: 10.1130/0016-7606(1998)110<0450:EOSBTF>2.3.CO;2

Fryirs K. 2013. (Dis)Connectivity in catchment sediment cascades: a fresh look at the sediment delivery problem. Earth Surface Processes and Landforms 38 : 30–46. DOI: 10.1002/esp.3242

Gochis D et al. 2014. The Great Colorado Flood of September 2013. Bulletin of the American Meteorological Society DOI: 10.1175/BAMS-D-13-00241.1 [online] Available from: http://journals.ametsoc.org/doi/abs/10.1175/BAMS-D-13-00241.1 (Accessed 20 March 2015)

Grimm MM, Wohl EE, Jarrett RD. 1995. Coarse-sediment distribution as evidence of an elevation limit for flash flooding, Bear Creek, Colorado. Geomorphology 14 : 199–210. DOI: 10.1016/0169-555X(95)00037-6

Hoffmann T. 2015. Sediment residence time and connectivity in non-equilibrium and transient geomorphic systems. Earth-Science Reviews 150 : 609–627. DOI: 10.1016/j.earscirev.2015.07.008

Jarrett RD. 1990. Paleohydrologic techniques used to define the spatial occurrence of floods. Geomorphology 3 : 181–195. DOI: 10.1016/0169-555X(90)90044-Q

Lancaster ST, Casebeer NE. 2007. Sediment storage and evacuation in headwater valleys at the transition between debris-flow and fluvial processes. Geology 35 : 1027–1030. DOI: 10.1130/G239365A.1

Lancaster ST, Underwood EF, Frueh WT. 2010. Sediment reservoirs at mountain stream confluences: Dynamics and effects of tributaries dominated by debris-flow and fluvial processes. Geological Society of America Bulletin 122 : 1775–1786.

Magilligan FJ, Buraas EM, Renshaw CE. 2015. The efficacy of stream power and flow duration on geomorphic responses to catastrophic flooding. Geomorphology 228 : 175–188. DOI: 10.1016/j.geomorph.2014.08.016

McCain JF, Shroba RR. 1979. Storm and flood of July 31-August 1, 1976, in the Big Thompson River and Cache la Poudre River basins, Larimer and Weld Counties, Colorado . USGS Numbered Series. U.S. Govt. Print. Off., [online] Available from: http://pubs.er.usgs.gov/publication/pp1115AB (Accessed 26 January 2015)

Nagel DE, Buffington JM, Parkes SL, Wenger S, Goode JR; 2014. A landscape scale valley confinement algorithm: Delineating unconfined valley bottoms for geomorphic, aquatic, and riparian applications [online] Available from: http://www.treesearch.fs.fed.us/pubs/45825 (Accessed 16 April 2015)

Ogden FL, Sharif HO, Senarath SUS, Smith JA, Baeck ML, Richardson JR. 2000. Hydrologic analysis of the Fort Collins, Colorado, flash flood of 1997. Journal of Hydrology 228 : 82–100. DOI: 10.1016/S0022-1694(00)00146-3

Polvi LE, Wohl EE, Merritt DM. 2011. Geomorphic and process domain controls on riparian zones in the Colorado Front Range. Geomorphology 125 : 504–516. DOI: 10.1016/j.geomorph.2010.10.012

Reimer PJ et al. 2004. IntCal04 terrestrial radiocarbon age calibration, 0-26 cal kyr BP. Radiocarbon 46 : 1029–1058. DOI: 10.2458/azu_js_rc.46.4167

Schenk ER, Hupp CR, Gellis A, Noe G. 2013. Developing a new stream metric for comparing stream function using a bank-floodplain sediment budget: a case study of three Piedmont streams. Earth Surface Processes and Landforms 38 : 771–784. DOI: 10.1002/esp.3314

Stuiver M, Reimer J. 1993. Extended 14C data base and revised CALIB 3.014 C age calibration program. Radiocarbon 35 : 215–230.

Wohl E. 2008. The effect of bedrock jointing on the formation of straths in the Cache la Poudre River drainage, Colorado Front Range. Journal of Geophysical Research 113 DOI: 10.1029/2007JF000817 [online] Available from: http://doi.wiley.com/10.1029/2007JF000817 (Accessed 4 May 2014)

Wohl E. 2010. A brief review of the process domain concept and its application to quantifying sediment dynamics in bedrock canyons. Terra Nova 22 : 411–416. DOI: 10.1111/j.1365-3121.2010.00950.x

Wohl E. 2013. Floodplains and wood. Earth-Science Reviews 123 : 194–212. DOI: 10.1016/j.earscirev.2013.04.009

Yochum SE. 2015. COlorado Front Range Flood of 2013: Peak flows and flood frequencies. presented at the 5th Federal Interagency Hydrologic Modeling Conference. Peppermill Hotel, Reno, Nevada USA. 537–548 pp. 19 April

Chapter 5: Geologic and geomorphic controls on spatial variability of organic carbon retention along mountain streams

Summary

I quantify storage of organic carbon in downed wood, litter and humus on the floodplain surface, and floodplain sediment along valley segments of diverse geometry in the Southern Rockies. My objectives are to: investigate the roles of valley geometry, channel planform, contributing drainage area, and elevation on reach-scale organic carbon storage; identify mechanisms that facilitate or limit organic carbon storage; and present a conceptual model to explain spatial and temporal variability of organic carbon stocks. I find that floodplain sediment is the primary reservoir for organic carbon along river corridors of 24 study reaches in the study area. Based on 660 sediment samples from 273 locations, laterally unconfined valley segments with a single channel store significantly more carbon than either confined valley segments or unconfined valleys with multiple, subparallel channels. Elevation and stream gradient are the most significant predictors of organic carbon per unit area, and I infer that these relationships reflect differences in hydroclimatic disturbance regime and soil temperature. I interpret the observed patterns of organic carbon storage via a conceptual model that focuses on how differences in spatial density of bedrock joints influence valley geometry and riparian water tables, which in turn influence riparian vegetation, bank erodibility, and channel planform. These differences in channel form facilitate either frequent channel avulsion, floodplain erosion, and limited organic carbon content of soils in valley segments with multiple channels, or relatively stable single channels, floodplain deposition, and higher carbon content.

5.1 Introduction

Storage of organic carbon within sediments of river corridors and lakes has been increasingly recognized as a significant component of the terrestrial carbon cycle (Aufdenkampe et al., 2011; Battin et al., 2009; Cole et al., 2007; Hoffmann et al., 2013; Tranvik et al., 2009). A river corridor includes the active channel and floodplain. Organic carbon can be stored within diverse reservoirs in river corridors, including living biomass, downed wood, and floodplain sediment of sand size and finer, although sediment organic carbon has received the most attention and constitutes the largest reservoir in most studies (Sutfin et al., 2015). Quantifying spatial variations in organic carbon storage within river networks and identifying how geomorphic processes influence spatial variations may help to constrain terrestrial carbon budgets and provide insight into carbon dynamics in river systems. This in turn has implications for understanding riverine food webs and biogeochemical cycles (Battin et al., 2008; Gurwick et al., 2008) and potential changes in floodplain carbon storage associated with land use, river restoration, and climate change (Cole et al., 2007).

Because upland erosion has been linked to increased potential for new sediment storage, burial of organic carbon, and rapidly growing carbon sinks in depositional environments (Berhe et al., 2007; Oost et al., 2012), erosion and sedimentation along dynamic river corridors may promote increased rates of carbon uptake by the geosphere. These processes may be shifted in either direction by land-use and river manipulation (Hoffmann et al., 2010) or restoration (Bullinger-Weber et al., 2014) and anticipated increases in storm severity as a result of climate change (Bates et al., 2008). This erosion-induced carbon storage may help to account for the growing terrestrial carbon sink (Ballantyne et al., 2012; Le Quéré et al., 2009) and high uncertainty in terrestrial global carbon budgets (Gregory et al., 2009). Continued floodplain aggradation and burial remove particulate and dissolved organic carbon from physical breakdown and active microbial communities, creating potential for storage over time spans of 10^2-10^3 years (Blazejewski et al., 2005). Floodplain carbon retention is also important for aquatic and riparian ecosystems, particularly along headwater streams and small mountain rivers with limited floodplain area and net primary productivity (Allan and Castillo, 2007; Battin et al., 2008; Naiman et al., 2005).

Small mountainous streams are particularly important because they receive the majority of allochthonous terrestrial OC (Vannote et al., 1980; Battin et al., 2008). Riparian corridors receive significant organic litter-fall into relatively narrow streams (Vannote et al., 1980) and retain OC derived from surficial hillslope erosion and landslides that release ancient OC in sedimentary bedrock (Hilton et al., 2008, 2010; Gomez et al., 2010). The U.S. Rocky Mountains are a focus of high carbon uptake, with 70% of the carbon sink at elevations above 750 m, which comprises 20-40% of the total uptake for the lower 48 states (Schimel and Braswell, 2005). However, many aspects of carbon dynamics in the U.S. Rocky Mountains remain poorly understood, including the role of mountain streams. Studies thus far (Bradford et al., 2008) have likely underestimated carbon stocks because values are derived from upland soils and vegetation only, while headwater stream processes have been ignored. The research described here addresses this underestimation by quantifying organic carbon storage in diverse channel segments in the Southern Rocky Mountains.

The majority of existing work on floodplain organic carbon storage focuses on shallow sediment organic carbon reservoirs along floodplains of large rivers (Hoffmann et al., 2009; Jaramillo et al., 2003; Noe and Hupp, 2005, 2009). Limited work has investigated (i) relationships between floodplain sediment carbon content and grain-size distributions (Bullinger-

Weber et al., 2014; Hoffmann et al., 2009; Wigginton et al., 2000), and (ii) spatial variability of estimated carbon content, accumulation rates, and stocks across floodplain surfaces (Noe and Hupp, 2009). Although (Sutfin et al., 2015) suggest potential landscape-scale controls on spatial variation in floodplain organic carbon storage, most existing work has not quantified differences in carbon storage in relation to valley and channel geometry or sediment connectivity. However, the longitudinal disconnectivity of sediment (Fryirs, 2013; Fryirs et al., 2007) and residence time on the floodplain (Hoffmann, 2015), which are influenced by hydroclimatic disturbance regime (Chapter 4 of this dissertation) and lateral valley confinement, largely control the potential for organic carbon storage.

In a pilot study of mountain stream networks of the northern Colorado Front Range, Wohl et al. (2012) identified laterally unconfined valley segments as storing disproportionately large amounts of organic carbon in downed wood and floodplain sediment relative to higher gradient, laterally confined portions of the river network. The pilot study found that the majority of the organic carbon was stored in downed wood in laterally unconfined valley segments flowing through old-growth forest in which numerous channel-spanning logjams created multithread (anabranching) channels. Floodplain sediment accounted for the majority of organic carbon storage in beaver meadows in which beaver dams created multithread channels. The pilot study left numerous unanswered questions, however, regarding spatial variability in organic carbon storage. The more extensive and detailed research summarized here addresses these questions.

I quantify organic carbon stocks in three primary floodplain carbon reservoirs – downed wood, litter and humus, and floodplain sediment finer than sand size – in multiple valley segments classified into five types based on lateral valley confinement and channel planform.

My objectives were to: investigate the roles of valley geometry, channel planform, contributing drainage area, and elevation on organic carbon storage at the reach scale; identify mechanisms that facilitate or limit organic carbon storage in mountain streams; and present a conceptual model to explain variability of organic carbon stocks in diverse valley segments. In doing so, I test the hypothesis that valley and channel geometry exert a significant influence on floodplain sediment organic carbon storage. I hypothesize that valley segments above 2500 m elevation and with multithread channels store more carbon compared to single-thread unconfined valley segments at similar elevations. The dynamic fluvial environment of multithread channel segments, which are characterized by development of logjams, beaver dams, islands, and channel avulsion, may limit organic storage capacity and be largely responsible for the pattern observed in the pilot study, in which multithread valley segments had shallower accumulations of organic-rich fine sediment than single-thread channels in unconfined valleys.

I address the research objectives by calculating average organic carbon storage per area across diverse valley segments; testing differences between valley types using corrected t-tests; and conducting multiple linear regression to examine relations between potential control variables and organic carbon storage per floodplain area. I conclude with a conceptual model that explains observed spatial variation in floodplain organic carbon storage as a function of valley geometry, forest stand age, geomorphic channel complexity, position in the watershed, and fluvial disturbance regime.

5.2 Study Area

The Colorado Front Range is composed of an igneous and metamorphic Precambrian core of granite, gneiss, and schist (Braddock and Cole, 1990), within which spatial variation in bedrock jointing facilitates longitudinal variation in lateral valley confinement and the formation of strath terraces (Wohl, 2008). Rivers along the Front Range have incised deep canyons on the flanks of the mountain range and through tilted sedimentary strata at the eastern margin of the Precambrian core (Anderson et al., 2006). Pleistocene glaciation on the eastern side of the Front Range extended downslope to elevations of approximately 2300 – 2500 m, marked by terminal moraines.

With increasing elevation above the plains, steppe vegetation transitions into montane forest (1830-2740 m elevation), subalpine forest (2740-3400 m), and eventually alpine vegetation (Veblen and Donnegan, 2005). This study focuses on the subalpine and montane zones. The subalpine zone is dominated by subalpine fir (*Abies lasiocarpa*), lodgepole pine (*Pinus contorta*), limber pine (*Pinus flexilis*), Engelmann spruce (*Picea englemannii*), and aspen (*Populus tremuloides*), whereas the montane zone primarily includes ponderosa pine (*Pinus ponderosa var. scopulorum*) and Douglas-fir (*Pseudotsuga menziesii*) (Veblen and Donnegan, 2005). Riparian communities in both zones also include large numbers of aspen, willow, and river birch. The primary, stand-killing disturbances in the region are wild fires, insect infestations, and blowdowns (Veblen and Donnegan, 2005). Fire severity and coverage are positively correlated, and frequency is inversely correlated, with elevation, ranging from > 100 y between stand-replacing fires in the subalpine to 5-30 y between ground-surface fires in the lower montane zone (Veblen and Donnegan, 2005). Stand-killing disturbances affecting different portions of the study area date prior to 1654, 1676, 1695, 1730, 1748, 1859, 1880, 1900, 1902, 1915, and 1978 CE (Sibold et al., 2006). A major infestation of mountain pine beetles is currently causing widespread die-off of lodgepole pines in the region, but is not yet resulting in substantial increases in tree mortality or topple within riparian zones.

Mean annual precipitation of ~ 50 cm in the foothills increases with elevation to ~ 100 cm at the continental divide (Barry, 1973). Most of the study sites are within Rocky Mountain National Park (RMNP). The primary drainages on the eastern side of RMNP are the Big Thompson River (BTR), North Saint Vrain Creek (NSV), and the extensive tributary network for these two trunk streams. Snowmelt runoff during May-July dominates the annual hydrograph of rivers within RMNP. At elevations below ~2300 m, summer convective storms can create flash floods with much larger discharge per unit drainage area (Jarrett, 1990), as seen in substantial floods across the Front Range in Sept. 2013.

Although flash floods from convective storms have recurrence intervals of ~300 years, they can result in extensive floodplain reworking (McCain and Shroba, 1979). Analysis of the 2013 floods along rivers of the Colorado Front Range indicate a power-law relationship between drainage area and floodplain disturbance along North Saint Vrain Creek, such that floodplain disturbance increases exponentially with decreasing elevations below 2300 m (Chapter 4 of this dissertation). Radiocarbon ages of charcoal from floodplain sediment along four study reaches on North Saint Vrain Creek also indicated much longer reach-average residence times of floodplain sediment at elevations above 2500 m (1365 ± 10 and 1931 ± 10 y BP) compared to sites near and below 2500 m (680 ± 6 and 609 ± 11 y BP). Channel morphology is predominantly cobble- to boulder-bed step-pool and pool-riffle sequences (Livers and Wohl, 2015), and floodplain deposits are dominated by the sand fraction (Chapter 3 of this dissertation). Floodplain development is longitudinally discontinuous and most floodplain segments are < 100 m wide. Substantial longitudinal variability in wood loads and downstream spacing of channel-spanning jams reflects variability in valley geometry and forest age (Wohl and Cadol, 2011).

I define the relative confinement of valleys in the study area by the ratio between the width of the valley bottom or floodplain (w_v) and the bankfull channel width (w_c), to include confined ($w_v < 2\ w_c$), partly confined ($2\ w_c < w_v < 5\ w_c$), and unconfined ($w_v > 5\ w_c$). In unconfined valleys, beaver dams and persistent channel-spanning logjams can facilitate multiple, subparallel channels across the valley bottom in a form of anabranching (Nanson and Knighton, 1996), which I refer to as multithread channels. These multithread systems exhibit increased channel complexity, defined primarily as high variability in streambed profiles and irregular channel boundaries. Beavers engineer floodplains and increase channel complexity to create beaver meadows (Ives, 1942; Polvi and Wohl, 2012), which raises riparian water tables (Westbrook et al., 2006) and facilitates saturated sediments and organic carbon storage (Falloon et al., 2011). Although channels incise and transition back to single-thread channels when beaver dams fall into disrepair, these valley bottoms still have potential for organic carbon storage (Wohl, 2013b). Logjam-forced development of multithread channels occurs only in unconfined valley segments with dense old-growth forest stands where downed trees are large and numerous enough to create persistent, closely spaced, channel-spanning logjams (Beckman and Wohl, 2014b; Wohl, 2013a).

Prior work by Wohl et al. (2012) and my field observations indicate multithread channels do not occur in unconfined valleys where old-growth forests are not present or where old-growth trees do not densely populate the floodplain. Unconfined single-thread channel segments occur within old-growth forests of the study area where grassy meadows dominate the floodplain and forest stands are not sufficiently dense to ensure continued recruitment of wood to the channel.

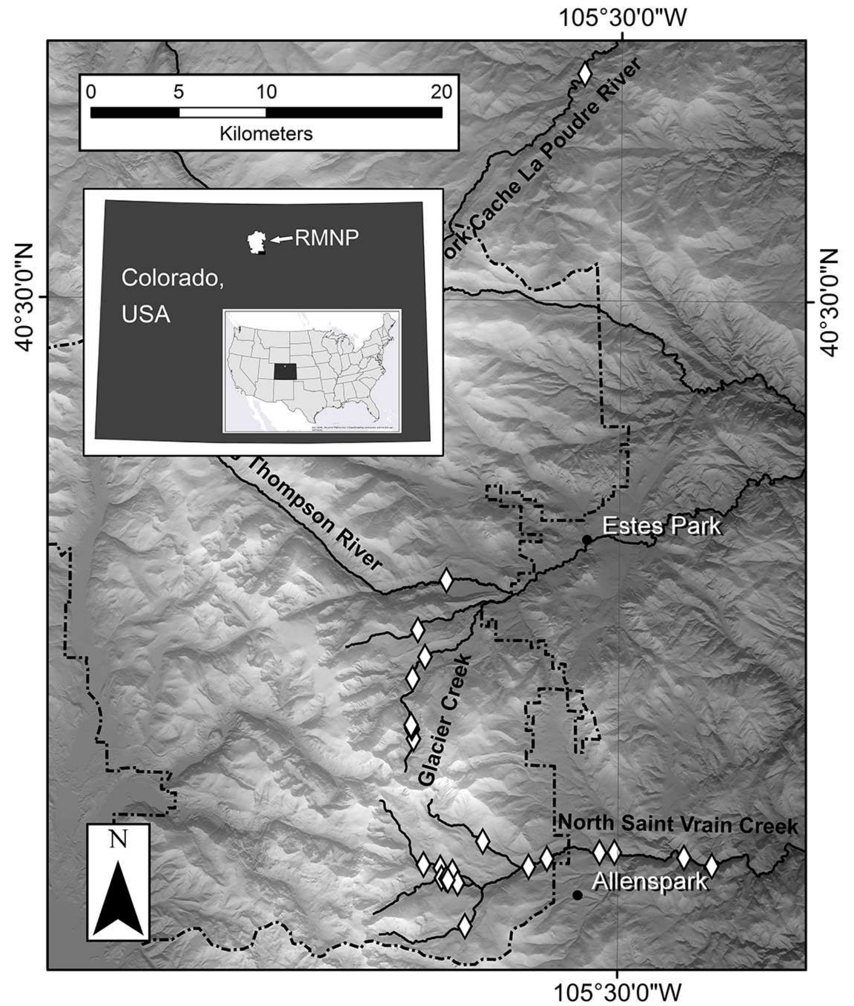

Figure 5.1 Study area in Northern Colorado includes 24 study reaches indicated by white diamond markers in and near Rocky Mountain National Park. Most reaches are focused on the main stem and tributaries of North Saint Vrain Creek with other reaches located along Glacier Creek and other tributaries to Big Thompson River, as well as South Fork Cache La Poudre River.

5.3 Methods

I surveyed 24 study reaches along the main stem and tributaries of North Saint Vrain Creek, Glacier Creek, Big Thompson River, and the South Fork Cache La Poudre River (Figure 5.1, Table 5.1). At each study reach, 11 transects were oriented perpendicular to the down-valley direction and spaced one bankfull-width apart. Topographic surveys of the floodplain surface were conducted along each transect using a stadia rod and a Laser Technologies TruPulse 360B laser rangefinder at points of topographic change with spacing between each point being less than 11 m. At each survey point, the depth of soil and fine sediment was measured using a 3/8-inch diameter rebar until refusal at bedrock or gravel. Systematic random sampling of sediment was conducted such that one sampling location was selected along each transect for most study reaches. More intensive sampling and prior bootstrap analysis indicated that bias in estimates of reach-average mean was reduced at approximately 10-11 sampling locations (Chapter 3 of this dissertation). A random number generator was used in the field to select the sampling location by distance in meters starting from the valley edge, for a total of 273 sampling locations.

Volumetric samples of organic matter, which was partially decomposing but identifiable or decomposed to a degree beyond recognition (litter and humus, respectively), were collected as a single sample of the organic horizon at each sampling location using an aluminum can. A total of 660 mineral soil samples were collected at 15-cm depth increments at the same sampling location beneath the litter and humus using a stainless steel hand auger until refusal or depths exceeded 180 cm, which occurred at only 3 sampling locations. Volumetric soil samples were collected horizontally in small trenches excavated along the floodplain to estimate bulk density where possible using a soil sampling tube 7 cm in diameter. Abundant roots made sampling difficult and most bulk density samples were determined to be unreliable, resulting in 21 total samples. Refer to Chapter 3 of this dissertation for additional details regarding soil sampling and characteristics.

Table 5.1. Mean values for characteristics and covariates of 24 study reaches. Valley and channel width and valley confinement were calculated as means of the surveyed and calculated values along 11 transects. Elevation and drainage area represent values derived from the down-stream most portion of each study reach.

Study Reach	Valley type	Valley width (m)	Channel width (m)	Valley confinement (m/m)	Gravimetric soil moisture content (%)	Stream Gradient (m/m)	Elevation (m)	Drainage Area (km^2)
NSVAB1	Beaver	67	6.8	10	55	0.037	2901	19.1
OCKAB2	Beaver	43	7.0	8	65	0.04	2978	10.6
NSVAB4	Beaver	247	14.1	22	40	0.012	2547	82.2
BTRAB5	Beaver	180	17.3	11	29	0.006	2462	93.7
SFPAB6	Beaver	77	10.6	7	25	0.011	2410	180.6
NSVCF1	Confined	18	13.0	1	16	0.032	2385	9.8
OCKCF2	Confined	9	5.3	2	35	0.095	2971	10.7
GCKCF3	Confined	12	8.5	3	34	0.13	2845	21.0
NSVCF4	Confined	11	6.2	2	38	0.085	2951	17.9
NSVCF5	Confined	19	14.1	1	20	0.026	2162	20.5
GCKCF7	Confined	10	5.6	2	42	0.09	3071	9.7
NSVMT1	Multithread	61	6.5	10	44	0.063	3035	14.8
GCKMT2	Multithread	34	6.7	6	39	0.03	3068	9.8
OCKMT3	Multithread	53	5.2	10	53	0.033	2990	10.5
NSVPC1	Partly confined	33	17.1	2	21	0.037	2420	96.4
OCKPC2	Partly confined	14	5.1	3	38	0.063	2927	11.1
GCKPC3	Partly confined	33	8.5	4	25	0.027	2701	33.2
HCKPC4	Partly confined	15	3.7	4	30	0.069	3013	10.1
NSVPC5	Partly confined	27	12.7	2	23	0.023	2226	20.0
NSVPC7	Partly confined	43	14.5	3	48	0.016	2573	77.4
GCKPC6	Partly confined	14	4.2	4	34	0.02	3118	7.1
CCKUC1	Unconfined	26	5.6	5	58	0.028	3054	12.7
GCKUC2	Unconfined	32	5.1	7	54	0.013	3053	10.3
MCKUC3	Unconfined	47	7.8	10	41	0.01	2797	3.0

Contributing drainage area for each study reach was calculated using USGS digital elevation models (DEMs) and the watershed tool in ERSI ArcMap. Stream gradient was calculated as the slope of the linear regression line between horizontal and vertical distance down stream. Values for stream gradient were derived for 2 reaches using USGS 10-m digital elevation models (i.e., AB1, PC3) and 2 reaches using FEMA LiDAR (i.e., CF1, AB4). For all other study reaches, surface water slope was measured in the field using the laser range finder. Triangular irregular networks (TINs) were created in ArcMap to estimate the volume of sediment along each study reach. Average bulk density across all reaches ($\rho_b = 0.9 \pm 0.24$ g/cm^3) was multiplied by the volume of floodplain sediment to determine the mass of sediment along each study reach.

Soil samples were frozen until analyzed for SOC content by the Colorado State University Soil and Water Testing Laboratory. Once dried, soil samples were homogenized and subsampled for SOC analysis using a LECO TruSpec CN furnace. Each sample was then analyzed for CO_3-C by treating the sample with 0.4 N HCl and measuring the CO_2 loss gravimetrically. Total organic carbon content by weight was calculated as total carbon minus CO_3-C. The difference between the total mass of soil after drying at 105° C for 24 hours and the pre-dried soil mass was used to determine the gravimetric soil moisture content. Mean carbon contents of samples averaged across all depths at each sampling location were used to calculate organic carbon storage at each reach because prior analysis indicated that the results are comparable to estimates of mean organic carbon content derived from inverse distance weighting and ordinary kriging (Chapter 3 of this dissertation). Total mass of sediment along each study reach was multiplied by the depth-averaged gravimetric soil carbon content along each reach to calculate the total mass of organic carbon storage.

Litter and humus samples were dried at 105° C for 24 hours, weighed, burned in a muffle furnace at 550° C for 24 hours, and then weighed again. Organic matter content was calculated as the difference in pre-burned and post-burned weight, 50% of which was interpreted as organic carbon. Total reach volume of litter and humus was calculated by multiplying the average depth measured at each reach by the TIN-derived surface area. Averages across all reaches for bulk density (0.20 ± 0.17 g/cm^3) and organic carbon content ($24 \pm 13\%$) of litter and humus were used to estimate mass of organic matter and carbon stored, respectively, along each study reach.

The length and diameter of downed floodplain wood greater than 1-m in length and 10-cm in diameter was surveyed and wood volumes were calculated as the volume of a cylinder using the average diameter of the two end measurements. The mass of carbon stored in each piece was estimated using 400 g/cm^3 for softwood species in the area (Forest Service Products Laboratory and USDA Forest Service, 2010) and assuming 50% carbon by mass. Total mass of carbon in all floodplain reservoirs (i.e., sediment, litter and humus, and wood) was divided by the surface area of each TIN to estimate total carbon storage per area along each study reach.

Prior research using multiple regression analyses showed that organic carbon content of soils in the study area is correlated with percent silt and clay fraction, sand fraction, and size fraction greater than 2 mm as well as soil moisture, degree of valley confinement, maximum depth of sediment deposits at the sampling location, the relative elevation of the floodplain surface, and soil sample depth (Chapter 3 of this dissertation). Although moisture content and silt and clay fraction had the only individual r^2 values greater than 0.5 ($r^2 = 0.66$ and 0.54, respectively), multiple regression indicated significance at the 99% confidence level for all but valley confinement and maximum soil depth at the sampling location ($p = 0.018$ and 0.081, respectively).

I tested differences between valley types using Holm-corrected t-tests, and conducted multiple linear regression to examine potential drivers in organic carbon storage per area. Potential predictors in multiple linear regression included reach-averaged valley confinement, stream gradient, drainage area, and elevation. Although drainage area and elevation are correlated and both covariates are linked to floodplain hydrologic disturbance regime in the study area (Chapter 4 of this dissertation), these two variable are not equivalent ($r^2 = 0.30$) because study reaches are spread along tributaries with similar drainage areas at different elevations and vice versa. The rationale for using all four covariates is to capture factors that influence the supply and movement of water and sediment, and by extension organic matter and carbon, for each reach within a relatively homogenous geologic setting (Bracken et al., 2013; Fryirs, 2013; Hoffmann, 2015; Wainwright et al., 2011).

5.4 Results

Mean carbon storage per area as downed wood does not differ significantly across the five valley types (Figure 5.2; $p > 0.57$), and litter and humus differ significantly only between multithread and partly confined channels ($p = 0.10$). Approximately equal or more carbon is stored in litter and humus as in wood across all valley types. The amounts of variability across each valley type are wide and show little distinction, except that multithread valley segments generally store abundant wood with little variation (~40 – 45 MgC ha^{-1}; Table 5.2), and store more OC as litter and humus compared to all other reaches. Although differences are not significant, beaver-influenced valleys generally store less organic carbon in litter and humus relative to unconfined single-thread and multithread channels in unconfined valleys (Table 5.2; Figure 5.2).

Table 5.2. Carbon storage in sediment, duff, and wood along 24 study reaches

Study Reach	Valley type	Valley area (ha)	Wood		Litter and humus		Sediment				Total
			Volume (m^3)	Carbon (MgC ha^{-1})	Volume (m^3)	Carbon (MgC ha^{-1})	Mean SOC (%)	Mean depth (cm)	Volume (m^3)	Carbon (MgC ha^{-1})	Carbon (MgC ha^{-1})
NSVAB1	Beaver	0.58	23.0	7.9	546.1	55.1	11.6	54	3126.2	565.1	628.1
OCKAB2	Beaver	0.30	79.5	53.4	265.5	55.7	12.5	26	773.7	292.5	401.6
NSVAB4	Beaver	5.04	14.7	0.6	2109.6	18.1	5.2	57	28798.5	266.3	285.1
BTRAB5	Beaver	3.27	16.4	1.0	1090.6	6.5	2.3	60	19501.1	124.0	131.6
SFPAB6	Beaver	0.81	14.6	3.6	91.5	1.9	2.8	51	4187.5	130.4	135.9
NSVCF1	Confined	0.09	16.8	36.5	82.4	22.7	3.0	25	229.8	67.7	147.7
OCKCF2	Confined	0.02	6.6	61.7	19.3	32.4	6.6	22	47.3	130.8	237.0
GCKCF3	Confined	0.01	0.6	14.1	7.3	35.8	14.4	9	7.9	112.3	162.1
NSVCF4	Confined	0.03	2.1	14.7	26.1	43.5	9.7	15	41.4	128.8	187.0
NSVCF5	Confined	0.04	0.8	3.8	18.0	6.5	2.6	21	90.3	50.5	60.8
GCKCF7	Confined	0.04	0.9	4.6	27.6	33.0	8.7	16	59.4	124.5	162.1
NSVMT1	Multithread	0.49	103.1	42.0	558.5	58.1	5.2	26	1269.3	121.5	221.6
GCKMT2	Multithread	0.12	26.8	45.5	106.0	41.9	9.6	23	268.6	196.9	284.4
OCKMT3	Multithread	0.37	74.1	39.9	452.4	73.0	8.9	24	881.7	190.7	303.6
NSVPC1	Partly confined	0.30	17.5	11.5	209.9	14.7	4.4	19	590.0	76.7	102.9
OCKPC2	Partly confined	0.06	15.8	55.5	47.4	32.8	9.2	18	100.6	146.3	234.6
GCKPC3	Partly confined	0.26	28.2	21.4	200.3	23.4	4.0	19	509.2	70.2	115.0
HCKPC4	Partly confined	0.05	10.7	42.2	40.0	47.7	3.2	33	169.1	96.9	186.8
NSVPC5	Partly confined	0.26	3.5	2.7	51.8	4.4	3.0	32	815.6	85.0	92.1
GCKPC6	Partly confined	0.05	1.1	4.7	14.4	25.2	13.2	42	193.0	492.8	522.7
NSVPC7	Partly confined	0.43	17.7	8.3	299.6	14.5	3.4	46	1966.3	139.0	161.8
CCKUC1	Unconfined	0.13	18.4	27.8	47.1	21.4	19.0	30	402.4	516.9	566.1
GCKUC2	Unconfined	0.15	5.0	6.7	80.1	41.0	13.5	49	729.5	595.7	643.5
MCKUC3	Unconfined	0.21	7.4	7.1	173.6	55.1	5.4	57	1186.3	279.1	341.2

By a significant majority, the primary component of organic carbon storage in floodplains of the study area is sediment (Table 5.2, 5.3; Figure 5.2). Unconfined single-thread valley segments store a larger amount of organic carbon per area than other valley types, on average (Table 5.3, Figure 5.2) and significantly more carbon than confined and partly confined valley segments at the 95% confidence level (p = 0.02 and 0.04, respectively). Although single-thread channels in unconfined valleys store more OC per area on average compared to beaver meadows and multithread channels, these differences are not significant (p = 0.46 and 0.36, respectively).

Figure 5.2. Average total organic carbon storage by valley type as proportions of wood, litter and humus, and sediment.

Table 5.3. Mean values and standard deviations of organic carbon reservoirs in sediment, duff, wood, and total storage per area for 5 valley types. All values are in Mg ha^{-1}.

Planform	Valley type	Mean SOC		Duff		Downed wood		Total C	
Multithread	Old growth multithread	170	± 42	58	± 16	42	± 3	270	± 43
	Beaver meadow	276	± 179	27	± 26	13	± 23	316	± 407
Single thread	Unconfined	464	± 165	39	± 17	14	± 12	517	± 157
	Partly confined	158	± 151	23	± 14	21	± 20	152	± 62
	Confined	102	± 35	29	± 13	23	± 23	146	± 62

Examination of channel and watershed characteristics as potential control variables for total carbon storage per area indicates that elevation is a key factor ($r^2 = 0.61$, $p < 0.002$; Table 5.4). Although not significant ($r^2 > \pm 0.21$), elevation, drainage area, and confinement are all weakly correlated with TOC storage per area. Multiple linear regression using all possible variables indicates that elevation and stream gradient are the most significant predictors of OC storage per area ($p < 0.01$) and multiple stepwise linear regression identifies the best regression model as having only elevation and stream gradient.

Table 5.4. Matrix of correlation coefficients for channel and watershed characteristics and total organic carbon storage per area

	Confinement (m/m)	Stream gradient (%)	Drainage area (km^2)	Elevation (m)	Total Carbon (MgC ha^{-1})
Confinement (m/m)	1	-0.4	0.27	0.04	0.31
Stream gradient (%)	-	1	-0.36	0.4	-0.21
Drainage area (km^2)	-	-	1	-0.54	-0.34
Elevation (m)	-	-	-	1	**0.61**
Total Carbon (MgC ha^{-1})	-	-	-	-	1

5.5 Discussion

Drainage area and elevation are correlated, as expected ($r^2 = 0.59$), and both are the most significant predictors of TOC storage per unit area among the study reaches. The significance of elevation in predicting OC storage per area of floodplain may reflect two factors. The first is hydroclimatic disturbance regime. As detailed in Chapter 4, larger magnitude rainfall floods at lower elevations likely decrease floodplain sediment transit time and limit the abundance and duration of OC storage in floodplain sediment.

The second factor related to elevation is air temperature and associated differences in snow and canopy cover that could influence temperature-dependent microbial activity and fixation of organic carbon in soil (Trumbore and Czimczik, 2008). Soil temperatures below freezing for a greater portion of the year and potential saturated conditions during snowmelt may limit microbial consumption at high elevations, making high elevation mountain streams potential hotspots for organic carbon storage (Sutfin et al., 2015). Similar conditions regulate differences in microbial metabolism and carbon content between highly shaded (multithread or confined) and un-shaded (single-thread unconfined) floodplains.

Stream gradient, indicated in multiple regression as significant along with elevation, drives the hydraulic forces on the floodplain and banks. Critical stream power is driven by stream gradient and facilitates erosion or allows deposition, such that low stream gradient is likely to facilitate accumulation of sediment and organic matter on the floodplain. Greater depth of sediment and higher soil organic carbon content, as well as increased organic carbon storage per area, are reasonable results of low hydraulic forces on the floodplain where stream gradient is low.

Recent research emphasizes the efficiency with which microbes fix carbon as the dominant factor for soil carbon retention. This is not a matter of whether microbial activity is high or low, but rather the ratio between how much carbon microbes consume and how much they fix into the soil (Cotrufo et al., 2015). Thus, if soil development and burial (Gurwick et al., 2008) and moisture regimes (Falloon et al., 2011; Trumbore and Czimczik, 2008) influence microbial efficiency and soil organic carbon, the greater erosion in valley segments with multithread channels or at lower elevations may explain not only decreased mean soil depth, but also lower organic carbon content relative to unconfined, single-thread channels at higher elevations.

5.5.1 Potential long-term storage of organic carbon

Mean residence time of floodplain sediment along rivers in the Front Range is associated with a shift in floodplain disturbance regime occurring between 2300 – 2500 m, such that elevations below the boundary exhibit maximum floodplain sediment residence times <700 y BP (chapter 4 of this dissertation). This shift correlates with and is likely related a documented shift in hydroclimatic regime, such that large convective thunderstorms below ~2300 m result in high magnitude floods (Jarrett, 1990). Smaller streams at higher elevations do not experience such high magnitude floods and have longer floodplain sediment residence times (>1500 y BP). Long residence time of floodplain sediment at high-elevation, partly confined and unconfined streams of various channel form may translate to long-term OC storage at high elevations, but this is also regulated by other factors controlling residence time of soil OC. The stability of floodplain surfaces and the available moisture associated with each valley type could influence the efficiency of microbes and their ability to fix or respire carbon as CO_2: stable, consistently moist floodplain sediments would be expected to result in carbon storage rather than respiration.

5.5.2 Biogeomorphic limitations on floodplain carbon retention

Although mountainous streams are commonly thought of as erosive systems, floodplain deposition constitutes a significant component of organic carbon storage and creates much higher organic carbon concentrations in floodplain sediments compared to upland sediments (Wohl et al., 2012). The dynamic environment of floodplains may result in atypical relationships of organic carbon with depth (Gurwick et al., 2008). This is true in mountain streams, in particular, as seen in this study area (Chapter 4 of this dissertation).

My results suggest that geologic controls on valley geometry significantly influence carbon storage along river corridors because unconfined valley segments tend to store more carbon than more confined valleys. However, carbon storage in unconfined valleys is significantly greater than confined and partly confined valleys only where single-thread channels are present. This raises the question of why unconfined valley segments with old-growth forest and single-thread channels store more organic carbon per area than those with multithread channels that result from either beaver activity or persistent, channel-spanning logjams. In this context, I consider other local controls on floodplain organic carbon storage.

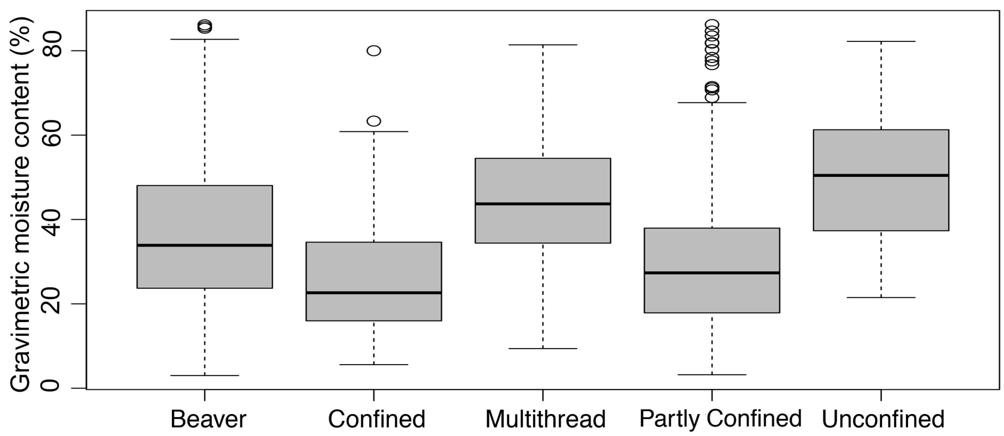

Figure 5.3 Moisture content of soil samples along the study reaches in the study indicate that single thread channels in unconfined valleys have significantly higher moisture content ($p < 0.001$).

Unconfined valleys with single-thread channels differ from those with logjam-induced, multithread channels in having abundant grassy meadows, lower tree density, lower gradients (0.03-0.06% and 0.01-0.03%, respectively), saturated soils, less active channel area, deeper average maximum floodplain sediment (45 cm compared to 24 cm), and higher reach-average organic carbon content (12.7% compared to 7.9%; Table 5.1; Figure 5.3, 5.6). From these observations, I develop a conceptual model of how geomorphic processes associated with floodplain and instream wood limit the capacity of multithread-channel valley segments to store sediment and organic carbon over longer time periods.

Widely spaced riparian trees, as observed in unconfined single-thread valley segments (Figure 5.4), limit large wood (LW) recruitment to the channel and the capacity to develop channel-spanning logjams that are closely spaced along the channel (Wohl, 2013a). Although sediment deposition upstream of logjams in multithread reaches stores organic matter and carbon (Beckman and Wohl, 2014a), logjams also facilitate overbank flow and channel avulsion (Collins et al., 2012). This locally erodes the preexisting floodplain, undercuts banks, and recruits more wood to the channel, analogous to processes documented in larger rivers in low-relief environments (Collins et al., 2012). Additionally, multiple channels effectively maximize surface area available for bank erosion. Other disturbances that disproportionately affect the tallest old-growth trees, such as microbursts (Wohl, 2013c) and beetle kill, uproot trees abruptly or over time and create large depressions in the surface adjacent to channels, facilitating concentration of overbank flow and channel avulsion. Because extreme floods do not appear to completely excavate floodplain sediment at high elevations where multithread channels are present, unlike lower elevations (Chapter 4 of this dissertation), typical annual snowmelt peak flows over time likely result in continuous reworking of channel configuration and erosion of valley bottom sediment. This limits the depth of accumulated sediment across the valley bottom, as well as duration and volume of organic carbon storage per area.

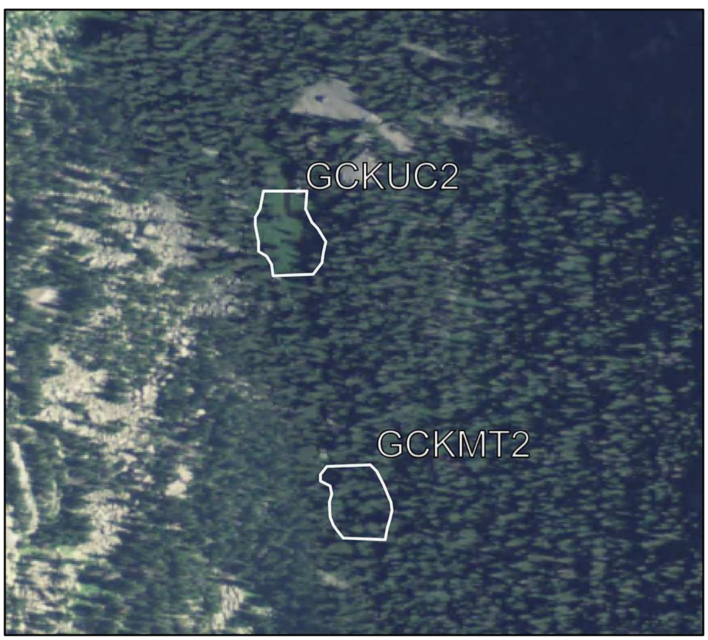

Figure 5.4 An example of the differences in stem density of trees along the floodplain at multithread (GCKMT2) and single thread (GCKUC2) channels in unconfined valleys.

Laterally unconfined valley segments in the study area are associated with more closely spaced bedrock joints (Ehlen and Wohl, 2002) and observations following rainfall and during snowmelt indicate that joints form important conduits for subsurface flow in the study area. This suggests that unconfined valley segments could have greater subsurface flow inputs from adjacent uplands than do confined valley segments. However, during periods of base flow, the relatively coarse-grained floodplain sediment and multiple channels spaced at comparatively small lateral distances across a valley bottom likely contribute to floodplain drainage and lower riparian water tables in multithread channel reaches.

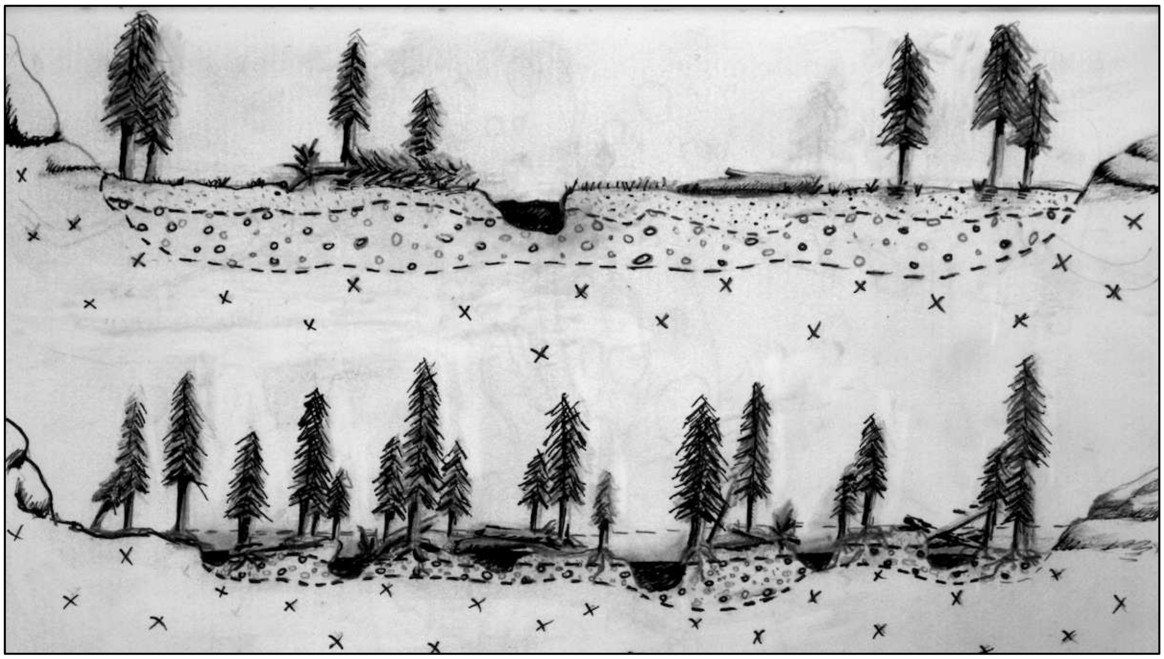

Figure 5.5 Conceptual model of controls on the formation and limited sediment storage of multithread channels (lower row) compared to single-thread channels (upper row) in unconfined valleys. Multithread channels form only in old-growth forests where trees are large enough to create persistent channel-spanning logjams and closely spaced enough to encourage continued recruitment to the channel (lower row). Along single-thread channels in unconfined valleys, the greater root density of grasses and higher silt and clay content limit bank erosion (upper row). Fine stippling in subsurface indicates sand and finer sediment, open circles indicate cobbles and boulders, and x marks indicate bedrock.

Densely growing tussock grasses, sedges, and rushes are abundant in valley segments with younger or less abundant trees. These non-woody plants form laterally continuous root mats that increase bank resistance to erosion (Polvi et al., 2014) and create substantial hydraulic roughness during shallow overbank flows, encouraging floodplain deposition of fine sediment and organic matter (Nepf and Ghisalberti, 2008). The greater erosional resistance of stream banks and floodplain surfaces, and limited wood recruitment to the channel, likely result in formation of a single channel rather than a multithread channel planform. Limited lateral erosion of this single channel, relative to multiple channels, facilitates vertical floodplain accretion and accumulation of relatively thick sequences of fine sediment. I have also observed that these meadow areas remain saturated throughout the year, even during periods of drought. This suggests relatively abundant groundwater inputs from adjacent uplands and limited drainage of the floodplain during periods of base flow, presumably as the result of relatively fine-grained floodplain sediment and the presence of only one channel. Saturated sediments help to maintain reducing conditions and enhance organic carbon storage in floodplain sediment (Moyano et al., 2012).

Using these concepts, I adapt the large-wood floodplain cycle hypothesis developed by Collins et al. (2012) for larger, floodplain rivers in the Pacific Northwest. Abundant logjams and dispersed LW in mountain streams of the Colorado Front Range facilitate channel avulsion and erosion of the floodplain and vegetated islands, and limit accumulation of fine sediment and organic matter along some segments of the valley bottom (Figure 5.5). Where tree stand density is low in unconfined valley segments, possibly as a result of groundwater inputs that create saturated conditions and hinder tree growth, LW recruitment is not sufficient to create logjams and multithread channels. Thus, high flows have very different effects in unconfined valley segments with single thread river segments and grassy floodplains versus multithread river segments with dense forests. High flows in single-thread channels overtop the banks and disperse energy across a grassy meadow floodplain, which may result in bank erosion, but likely facilitates floodplain aggradation. High flows in a multithread channel segment dissipate energy through bank erosion and hydraulic roughness from LW. Increased channel complexity and diversion of flow around logjams within multithread channel segments exposes stream banks to flow energy available for erosion and undercutting, which facilitates continued recruitment of LW, more logjams and multithread channels.

The low density of trees and high percent of sediment organic carbon content in unconfined single thread valley segments may also be related to available moisture and chemistry. Average sediment organic carbon content is much higher in single-thread unconfined segments compared to multithread channels, but this is primarily driven by two study reaches, GCKUC2 and CCKUC1, which have wet grassy meadows with saturated conditions that may limit tree growth and metabolism of organic carbon. A partly confined reach, GCKPC6, also contains wet grassy meadows along both sides of the valley and has anomalously high organic carbon content (13.2%) compared to the mean of other partly confined reaches (4.5 ± 2.3 %). The third unconfined single-thread study reach, MCKUC3, contains groups of more densely-packed trees, greater wood loads per floodplain area, significantly lower sediment organic carbon content, and has significantly higher $CaCO_3$ values than all other stream types ($P < 0.001$).

Unconfined valley segments with beaver dams are also likely to be more changeable environments than unconfined valleys with single-thread channels. Although active beaver dams commonly maintain high riparian water tables, beavers allow some dams to fall into disrepair and build new dams elsewhere, creating more spatial and temporal fluctuations in the riparian water table than appear to occur in groundwater-fed grassy valley bottoms. Beavers also excavate canals across the floodplain, locally enhancing bank erosion and the formation of secondary channels. The combined effects of greater bank erosion and greater fluctuations in the riparian water table relative to single channels in unconfined valley segments may limit organic carbon storage in beaver meadows. It is important to note, however, that beaver meadows formed upstream from Pleistocene glacial moraines can store significant total amounts of organic carbon because of their very large surface areas and greater soil depths (Wohl, 2013b). Additionally, total OC storage per area in beaver meadows could be underestimated here with regard to wood volumes. Only large wood visible on the floodplain surface was surveyed in this study, but abundant downed wood partly buried beneath grasses and floodplain sediment in various stages of decomposition is likely to be present in beaver meadows. Although only large pieces of wood (> 1 m in length and >10 cm in diameter) were surveyed, the abundance of smaller wood likely to be concentrated in buried beaver dams and lodges may be significant.

Table 5.5. Mean (and range) organic carbon storage per area along floodplains and in adjacent uplands of the study reaches and from other work cited in subalpine regions of the study area in the northern Colorado Rocky Mountains. All values are in units of Mg C ha^{-1}.

	Above-ground biomass	Wood	Litter and humus	Mineral soil	Total	Reference
Upland	71 (16-89)	35 (2-78)	34 (12-74)	63	132 (77-215)	Arthur and Fahey, 1992
Upland	111 (94-136)	37 (17-60)	72 (62-84)	61 (51-73)	170 (140-217)	Bradford et al., 2008
Riparian	161 (18-219)	---	34 (1-67)	---	---	Wohl et al., 2012
Riparian	---	22 (1-62)[a]	32 (2-73)	208 (51-596)	260 (61-644)	This study

In summary, the conceptual model in Figure 5.5 illustrates how multiple geologic and biotic variables interact to influence floodplain organic carbon storage in streams of the Southern Rocky Mountains. These variables include (i) valley geometry, which largely reflects joint geometry and glacial history, (ii) elevation, which correlates with hydroclimatic disturbance regime, soil temperature, soil microbial activity, and riparian vegetation, (iii) riparian vegetation, which reflects disturbance history (fires, insects, blowdowns) and groundwater inputs, and (iv) channel planform, which reflects wood recruitment, beaver activity, and erosional resistance of stream banks. These variables interact in complex, nonlinear fashion to facilitate or limit organic carbon storage in floodplain sediment. The patterns and interactions that I document for streams of the Colorado Front Range are likely to apply to mountainous stream networks in other regions. Mountain streams across diverse lithologies and biomes commonly exhibit substantial longitudinal variation in valley geometry, channel planform, riparian vegetation, and wood loads, as well as elevational gradients in disturbance regime (e.g. Wohl, 2010). These findings suggest that multithread channels could be a significant component of ecosystem processing of carbon, because aquatic and riparian biota can more easily access carbon retained within the floodplain compared to otherwise analogous valley segments with single channels.

Total carbon storage per area is higher in floodplains and association riparian ecosystems (261 ± 172 Mg C ha^{-1}) compared to adjacent uplands (Bradford et al., 2008; Table 5.5). Although uplands have higher OC storage per area as wood, litter and humus, floodplains constitute a much higher storage per area in mineral soil. This is likely a result, in part, of much deeper soils along floodplains compared to hillslopes and the tendency of river corridors to accumulate sediment, debris, and coarse particulate organic matter from uplands and adjacent hillslopes. Hydraulic forces that redistribute litter, humus, and large wood along floodplains, however, may limit accumulation or simply result in higher temporal variability such that conditions at the time of the survey do not reflect the long-term average. Regardless of these potential mechanisms, riverine corridors of the study area store a significant portion of carbon per area, which exceeds that of the greater uplands in the study region. This suggests that floodplains of mountain streams are a significant component of aquatic and riparian ecosystem processing of organic carbon and terrestrial carbon reservoirs.

Organic carbon reservoirs in floodplains along an elevational gradient are likely to respond differently to climate change. Study reaches below 2500 m tend to store much less OC per area as wood, litter, and humus compared to other study reaches at higher elevations. As noted above, this may be a result of increased hydraulic forces in more confined valleys, which mobilize wood and sediment during high flows. Anticipated warming and increased frequency of severe storms are likely to increase the elevation of the floodplain disturbance transitional zone, which could reduce surficial OC retention at increasingly higher elevations. Additionally, anticipated increases in global average atmospheric temperature are likely to decrease snowpack, cause earlier snowmelt, and increased mean annual soil temperature at high elevations. As soils warm and remain saturated for shorter durations throughout the year, microbial activity could increase substantially and decrease SOC content. The supply of litter and duff to floodplains along high-elevation mountain streams may increase as a result of increased productivity in a warmer climate, but decomposition of wood, litter, and humus as well as metabolism of SOC is likely to occur more rapidly. This may result in a decrease in OC storage at high elevations.

5.6 Conclusion

Further collaboration is needed across disciplines to effectively link watershed- to reach-scale geomorphic and biogeochemical processes. Although these links have commonly been ignored, current research emphasizes the need for such collaborations (Viles, 2012). Mountain streams in the Colorado Front Range store a significant amount of carbon per area and I investigate potential controls on the variability of that storage. Unconfined valleys have the capacity to store sediment for >1000 y even in small erosive mountain streams, and associated carbon is higher than adjacent upland storage in the Colorado Front Range. Carbon retention is largely dependent upon valley confinement and local biogeomorphic drivers of channel planform. Single-thread channels in unconfined valleys segments store a significantly larger amount of carbon per area than those with multiple sub-parallel channels across the valley bottom. I present a conceptual model that explains how the dynamic environment along valley bottoms where logjams and beavers are present, including fluctuations in local water tables and increased erosion, may limit the capacity of floodplains to store organic carbon storage.

Recognition

This paper is based upon work supported by: National Science Foundation Grant No. DGE-0966346 "I-WATER: Integrated Water, Atmosphere, Ecosystems Education and Research Program" at Colorado State University; NSF Doctoral Research Dissertation Improvement Grant #1536186; two research grants from the Geological Society of America; a research grant from the Colorado Scientific Society, and two research grants along with several scholarships through the Department of Geosciences and Warner College of Natural Resources at Colorado State University. I express gratitude to Robin Reich for use of his R code and to colleagues Katherine Lininger, Dan Scott, and Derek Schook for conversations and insight regarding soil sampling, coding, and spatial modeling. I also thank Ben Von Thaden, Dean Anderson, Joel Shotles, Fernando Ugalde, Jon Garber, Laurel Lynch, Timothy Fegel, John Harris, and Bryce Johnson for their company and assistance in the laboratory and the field.

References

Allan JD, Castillo MM. 2007. Stream Ecology . Second Edition. Springer: Dordrecht, THe Netherlands

Anderson RS, Riihimaki CA, Safran EB, MacGregor KR. 2006. Facing reality: Late Cenozoic evolution of smooth peaks, glacially ornamented valleys, and deep river gorges of Colorado's Front Range. In Special Paper 398: Tectonics, Climate, and Landscape Evolution , . Geological Society of America; 397–418. [online] Available from: http://specialpapers.gsapubs.org/cgi/doi/10.1130/2006.2398(25) (Accessed 1 May 2014)

Aufdenkampe AK, Mayorga E, Raymond PA, Melack JM, Doney SC, Alin SR, Aalto RE, Yoo K. 2011. Riverine coupling of biogeochemical cycles between land, oceans, and atmosphere. Frontiers in Ecology and the Environment 9 : 53–60. DOI: 10.1890/100014

Ballantyne AP, Alden CB, Miller JB, Tans PP, White JWC. 2012. Increase in observed net carbon dioxide uptake by land and oceans during the past 50 years. Nature 488 : 70–72. DOI: 10.1038/nature11299

Barry RG. 1973. A Climatological Transect on the East Slope of the Front Range, Colorado. Arctic and Alpine Research 5 : 89–110. DOI: 10.2307/1550251

Bates BC, Kundzewicz ZW, Palutikof JP. 2008. Climate change and water . Technical Report. IPCC: IPCC Secretariat, Geneva

Battin TJ, Kaplan LA, Findlay S, Hopkinson CS, Marti E, Packman AI, Newbold JD, Sabater F. 2008. Biophysical controls on organic carbon fluxes in fluvial networks. Nature Geoscience 1 : 95–100. DOI: 10.1038/ngeo101

Battin TJ, Luyssaert S, Kaplan LA, Aufdenkampe AK, Richter A, Tranvik LJ. 2009. The boundless carbon cycle. Nature Geoscience 2 : 598–600. DOI: 10.1038/ngeo618

Beckman ND, Wohl E. 2014a. Carbon storage in mountainous headwater streams: The role of old-growth forest and logjams. Water Resources Research 50 : 2376–2393. DOI: 10.1002/2013WR014167

Beckman ND, Wohl E. 2014b. Effects of forest stand age on the characteristics of logjams in mountainous forest streams. Earth Surface Processes and Landforms 39 : 1421–1431. DOI: 10.1002/esp.3531

Berhe AA, Harte J, Harden JW, Torn MS. 2007. The Significance of the Erosion-induced Terrestrial Carbon Sink. BioScience 57 : 337–346. DOI: 10.1641/B570408

Blazejewski GA, Stolt MH, Gold AJ, Groffman PM. 2005. Macro- and Micromorphology of Subsurface Carbon in Riparian Zone Soils. Soil Science Society of America Journal 69 : 1320. DOI: 10.2136/sssaj2004.0145

Bracken LJ, Wainwright J, Ali GA, Tetzlaff D, Smith MW, Reaney SM, Roy AG. 2013. Concepts of hydrological connectivity: Research approaches, pathways and future agendas. Earth-Science Reviews 119 : 17–34. DOI: 10.1016/j.earscirev.2013.02.001

Braddock WA, Cole JC. 1990. Geologic map of Rocky Mountain National Park and vicinity, Colorado

Bradford JB, Birdsey RA, Joyce LA, Ryan MG. 2008. Tree age, disturbance history, and carbon stocks and fluxes in subalpine Rocky Mountain forests. Global Change Biology 14 : 2882–2897. DOI: 10.1111/j.1365-2486.2008.01686.x

Bullinger-Weber G, Le Bayon R-C, Thébault A, Schlaepfer R, Guenat C. 2014. Carbon storage and soil organic matter stabilisation in near-natural, restored and embanked Swiss floodplains. Geoderma 228–229 : 122–131. DOI: 10.1016/j.geoderma.2013.12.029

Cole JJ et al. 2007. Plumbing the Global Carbon Cycle: Integrating Inland Waters into the Terrestrial Carbon Budget. Ecosystems 10 : 172–185. DOI: 10.1007/s10021-006-9013-8

Collins BD, Montgomery DR, Fetherston KL, Abbe TB. 2012. The floodplain large-wood cycle hypothesis: A mechanism for the physical and biotic structuring of temperate forested alluvial valleys in the North Pacific coastal ecoregion. Geomorphology 139–140 : 460–470. DOI: 10.1016/j.geomorph.2011.11.011

Cotrufo MF, Soong JL, Horton AJ, Campbell EE, Haddix ML, Wall DH, Parton WJ. 2015. Formation of soil organic matter via biochemical and physical pathways of litter mass loss. Nature Geoscience 8 : 776–779. DOI: 10.1038/ngeo2520

Ehlen J, Wohl EE. 2002. Joints and landform evolution in bedrock canyons. Transactions, Japanese Geomorphological Union 23 : 237–255.

Falloon P, Jones CD, Ades M, Paul K. 2011. Direct soil moisture controls of future global soil carbon changes: An important source of uncertainty. Global Biogeochemical Cycles 25 : 1–14. DOI: 10.1029/2010GB003938

Forest Service Products Laboratory RJ, USDA Forest Service FPL. 2010. Wood handbook : wood as an engineering material . Technical Report. US Department of Agriculture, Forest Service: Madison, Wisconsin [online] Available from: http://www.treesearch.fs.fed.us/pubs/37440 (Accessed 3 September 2014)

Fryirs K. 2013. (Dis)Connectivity in catchment sediment cascades: a fresh look at the sediment delivery problem. Earth Surface Processes and Landforms 38 : 30–46. DOI: 10.1002/esp.3242

Fryirs KA, Brierley GJ, Preston NJ, Spencer J. 2007. Catchment-scale (dis)connectivity in sediment flux in the upper Hunter catchment, New South Wales, Australia. Geomorphology 84 : 297–316. DOI: 10.1016/j.geomorph.2006.01.044

Gomez B, Baisden WT, Rogers KM. 2010. Variable composition of particle-bound organic carbon in steepland river systems. Journal of Geophysical Research 115 DOI:

10.1029/2010JF001713 [online] Available from: http://doi.wiley.com/10.1029/2010JF001713 (Accessed 1 May 2014)

Gregory JM, Jones CD, Cadule P, Friedlingstein P. 2009. Quantifying Carbon Cycle Feedbacks. Journal of Climate 22 : 5232–5250. DOI: 10.1175/2009JCLI2949.1

Gurwick NP, Groffman PM, Yavitt JB, Gold AJ, Blazejewski G, Stolt M. 2008. Microbially available carbon in buried riparian soils in a glaciated landscape. Soil Biology and Biochemistry 40 : 85–96. DOI: 10.1016/j.soilbio.2007.07.007

Hilton RG, Galy A, Hovius N. 2008. Riverine particulate organic carbon from an active mountain belt: Importance of landslides: LANDSLIDE MOBILIZED POC. Global Biogeochemical Cycles 22 : n/a–n/a. DOI: 10.1029/2006GB002905

Hilton RG, Galy A, Hovius N, Horng M, Chen H. 2010. Efficient transport of fossil organic carbon to the ocean by steep mountain rivers: Retaining carbon in the lithosphere. 0290 pp. [online] Available from: http://adsabs.harvard.edu/abs/2010AGUFM.B41A0290H (Accessed 4 May 2014)

Hoffmann T et al. 2013. Short Communication: Humans and the missing C-sink: erosion and burial of soil carbon through time. Earth Surface Dynamics Discussions 1 : 93–112. DOI: 10.5194/esurfd-1-93-2013

Hoffmann T. 2015. Sediment residence time and connectivity in non-equilibrium and transient geomorphic systems. Earth-Science Reviews 150 : 609–627. DOI: 10.1016/j.earscirev.2015.07.008

Hoffmann T, Glatzel S, Dikau R. 2009. A carbon storage perspective on alluvial sediment storage in the Rhine catchment. Geomorphology 108 : 127–137. DOI: 10.1016/j.geomorph.2007.11.015

Hoffmann T, Thorndycraft VR, Brown AG, Coulthard TJ, Damnati B, Kale VS, Middelkoop H, Notebaert B, Walling DE. 2010. Human impact on fluvial regimes and sediment flux during the Holocene: Review and future research agenda. Global and Planetary Change 72 : 87–98. DOI: 10.1016/j.gloplacha.2010.04.008

Ives RL. 1942. The beaver-meadow complex. Journal of Geomorphology 5 : 191–203.

Jaramillo VJ, Kauffman JB, Rentería-Rodríguez L, Cummings DL, Ellingson LJ. 2003. Biomass, Carbon, and Nitrogen Pools in Mexican Tropical Dry Forest Landscapes. Ecosystems 6 : 609–629. DOI: 10.1007/s10021-002-0195-4

Jarrett RD. 1990. Paleohydrologic techniques used to define the spatial occurrence of floods. Geomorphology 3 : 181–195. DOI: 10.1016/0169-555X(90)90044-Q

Le Quéré C et al. 2009. Trends in the sources and sinks of carbon dioxide. Nature Geoscience 2 : 831–836. DOI: 10.1038/ngeo689

Livers B, Wohl E. 2015. An evaluation of stream characteristics in glacial versus fluvial process domains in the Colorado Front Range. Geomorphology 231 : 72–82. DOI: 10.1016/j.geomorph.2014.12.003

McCain JF, Shroba RR. 1979. Storm and flood of July 31-August 1, 1976, in the Big Thompson River and Cache la Poudre River basins, Larimer and Weld Counties, Colorado . USGS Numbered Series. U.S. Govt. Print. Off., [online] Available from: http://pubs.er.usgs.gov/publication/pp1115AB (Accessed 26 January 2015)

Moyano FE et al. 2012. The moisture response of soil heterotrophic respiration: interaction with soil properties. Biogeosciences 9 : 1173–1182. DOI: 10.5194/bg-9-1173-2012

Naiman RJ, Decamps H, McClain ME, Likens GE. 2005. RIparia: Ecology, conservation, and management of streamside communities . Academic Press: Burlington, MA

Nanson GC, Knighton AD. 1996. Anabranching Rivers: Their Cause, Character and Classification. Earth Surface Processes and Landforms 21 : 217–239. DOI: 10.1002/(SICI)1096-9837(199603)21:3<217::AID-ESP611>3.0.CO;2-U

Nepf H, Ghisalberti M. 2008. Flow and transport in channels with submerged vegetation. Acta Geophysica 56 : 753–777. DOI: 10.2478/s11600-008-0017-y

Noe GB, Hupp CR. 2005. Carbon, nitrogen, and phosphorus accumulation in floodplains of Atlantic Coastal Plain rivers, USA. Ecological Applications 15 : 1178–1190.

Noe GB, Hupp CR. 2009. Retention of Riverine Sediment and Nutrient Loads by Coastal Plain Floodplains. Ecosystems 12 : 728–746. DOI: 10.1007/s10021-009-9253-5

Oost KV, Verstraeten G, Doetterl S, Notebaert B, Wiaux F, Broothaerts N, Six J. 2012. Legacy of human-induced C erosion and burial on soil–atmosphere C exchange. Proceedings of the National Academy of Sciences 109 : 19492–19497. DOI: 10.1073/pnas.1211162109

Polvi LE, Wohl E. 2012. The beaver meadow complex revisited - the role of beavers in post-glacial floodplain development. Earth Surface Processes and Landforms 37 : 332–346. DOI: 10.1002/esp.2261

Polvi LE, Wohl E, Merritt DM. 2014. Modeling the functional influence of vegetation type on streambank cohesion. Earth Surface Processes and Landforms 39 : 1245–1258. DOI: 10.1002/esp.3577

Schimel D, Braswell BH. 2005. The Role of Mid-latitude Mountains in the Carbon Cycle: Global Perspective and a Western US Case Study. In Global Change and Mountain Regions , Huber UM, Bugmann HKM, and Reasoner MA (eds). Springer Netherlands; 449–456. [online] Available from: http://link.springer.com/chapter/10.1007/1-4020-3508-X_45 (Accessed 26 January 2015)

Sibold JS, Veblen TT, González ME. 2006. Spatial and temporal variation in historic fire regimes in subalpine forests across the Colorado Front Range in Rocky Mountain National Park, Colorado, USA. Journal of Biogeography 33 : 631–647. DOI: 10.1111/j.1365-2699.2005.01404.x

Sutfin NA, Wohl EE, Dwire KA. 2015. Banking carbon: A review of organic carbon storage and physical factors influencing retention in floodplains and riparian ecosystems. Earth Surface Processes and Landforms : n/a–n/a. DOI: 10.1002/esp.3857

Tranvik LJ et al. 2009. Lakes and reservoirs as regulators of carbon cycling and climate. presented at the American Geophysical Union Chapman Conference Office on Abrupt Climate Change. 2298–2314 pp. [online] Available from: http://cat.inist.fr/?aModele=afficheN&cpsidt=22279829 (Accessed 19 May 2014)

Trumbore SE, Czimczik CI. 2008. GEOLOGY: An Uncertain Future for Soil Carbon. Science 321 : 1455–1456. DOI: 10.1126/science.1160232

Vannote RL, Minshall GW, Cummins KW, Sedell JR, Cushing CE. 1980. The river continuum concept. Canadian journal of fisheries and aquatic sciences 37 : 130–137.

Veblen TT, Donnegan JA. 2005. Historical range of variability for forest vegetation of the national forests of the Colorado Front Range . USDA Forest Service, Rocky Mountain Region [online] Available from: https://129.82.112.12/docs/frs/cfri/VeblenHRVFrontRange.pdf (Accessed 26 January 2015)

Viles HA. 2012. Microbial geomorphology: A neglected link between life and landscape. Geomorphology 157-158 : 6–16. DOI: 10.1016/j.geomorph.2011.03.021

Wainwright J, Turnbull L, Ibrahim TG, Lexartza-Artza I, Thornton SF, Brazier RE. 2011. Linking environmental régimes, space and time: Interpretations of structural and functional connectivity. Geomorphology 126 : 387–404. DOI: 10.1016/j.geomorph.2010.07.027

Westbrook CJ, Cooper DJ, Baker BW. 2006. Beaver dams and overbank floods influence groundwater-surface water interactions of a Rocky Mountain riparian area. Water Resources Research 42 : n/a–n/a. DOI: 10.1029/2005WR004560

Wigginton JD, Lockaby BG, Trettin CC. 2000. Soil organic matter formation and sequestration across a forested floodplain chronosequence. Ecological Engineering 15, Supplement 1 : S141–S155. DOI: 10.1016/S0925-8574(99)00080-4

Wohl E. 2008. The effect of bedrock jointing on the formation of straths in the Cache la Poudre River drainage, Colorado Front Range. Journal of Geophysical Research 113 DOI: 10.1029/2007JF000817 [online] Available from: http://doi.wiley.com/10.1029/2007JF000817 (Accessed 4 May 2014)

Wohl E. 2010. Mountain rivers revisited . American Geophysical Union [online] Available from: http://www.agu.org/books/wm/v019/ (Accessed 4 May 2014)

Wohl E. 2013a. Floodplains and wood. Earth-Science Reviews 123 : 194–212. DOI: 10.1016/j.earscirev.2013.04.009

Wohl E. 2013b. Landscape-scale carbon storage associated with beaver dams. Geophysical Research Letters 40 : 3631–3636. DOI: 10.1002/grl.50710

Wohl E. 2013c. Redistribution of forest carbon caused by patch blowdowns in subalpine forests of the Southern Rocky Mountains, USA. Global Biogeochemical Cycles 27 : 2013GB004633. DOI: 10.1002/2013GB004633

Wohl E, Cadol D. 2011. Neighborhood matters: Patterns and controls on wood distribution in old-growth forest streams of the Colorado Front Range, USA. Geomorphology 125 : 132–146. DOI: 10.1016/j.geomorph.2010.09.008

Wohl E, Dwire K, Sutfin N, Polvi L, Bazan R. 2012. Mechanisms of carbon storage in mountainous headwater rivers. Nature Communications 3 : 1263. DOI: 10.1038/ncomms2274

Chapter 6: Synthesis

Research that quantifies organic carbon storage in riparian ecosystems and floodplains is limited, particularly in regions outside of the temperate latitudes (Sutfin et al., 2015). The role of river carbon dynamics in foodwebs and ecosystem processing has been well documented and the importance of rivers in carbon dynamics has recently received considerable attention (Cole et al., 2007; Battin et al., 2009; Tranvik et al., 2009; Aufdenkampe et al., 2011; Hoffmann et al., 2013; Regnier et al., 2013; Galy et al., 2015; Hilton et al., 2015), but the majority of this work focuses on the flux of carbon to the ocean via rivers. Although some researchers have investigated carbon storage along river networks and emphasized this role in terrestrial carbon cycling (Hoffmann et al., 2009; Wohl et al., 2012), the number of these studies is limited (Sutfin et al., 2015).

Existing studies and the work presented here show floodplains store significantly more carbon per area than adjacent uplands. Although drainage topography and networks act as funnels for water and carbon, rivers are not simply conduits for these components crucial to life. Physical channel complexity, as defined by high spatial variability in channel boundaries, planform, and bedforms, is likely to facilitate conditions that encourage at least temporary storage of sediment and coarse particulate organic matter. Gravity and hillslope hydrologic processes deliver organic matter from uplands to valley bottoms, where high primary productivity of riparian vegetation, relative to adjacent uplands, further concentrates organic carbon along river corridors. Increased hydrologic connectivity and shallow water tables provide mobilization and available moisture for the physical and biological breakdown of organic matter, although saturated conditions can limit microbial metabolism of OC. Similarly, longer seasonal durations of cooler temperatures and snow pack in mountainous regions may limit microbial activity. This means that mountain stream corridors may provide a significant carbon sink, and are highly vulnerable to changes in temperature and moisture conditions anticipated under a changing climate.

6.1 Summary of work presented

The results of this study indicate that mountain rivers may store a significant amount of OC previously unaccounted for in carbon stocks. Multiple linear regression indicated that soil moisture and depth, grain size distribution, valley confinement, the elevation of the floodplain surface, and the total thickness of floodplain sediment at the sampling location are significant predictors of soil organic carbon content. Although there are no distinct relationships between geomorphic floodplain features and soil organic carbon content, principle components analysis suggests that geomorphic features may influence the variables that regulate soil organic carbon content along floodplains in the Colorado Front Range. This means that the spatial variability of carbon storage along river corridors may reflect geologic, hydrologic, and geomorphic processes along valley bottoms.

Radiocarbon ages and analysis of effects from the 2013 floods in the Colorado Front Range show that floodplain sediment residence time is longer in high elevation streams, as a result of floodplain disturbance regime. This may be driven in part by a shift in hydroclimatic regime at ~2300 m, such that large convective thunderstorms create extreme floods at low elevations that erode floodplain sediment and result in shorter floodplain sediment residence times. Analysis of floodplain disturbance during the 2013 Front Range flood along North Saint Vrain Creek suggests a relatively abrupt boundary at which floodplains become more intensively disturbed at ~2300 m. Radiocarbon ages, however, suggest a transitional boundary between 2300-2500 m along which floodplain sediment captures a long-term average of flood characteristics and impacts. Floodplain sediment residence times at elevations above 2500 m indicate potential long-term storage of sediment and associated organic carbon.

Investigation of carbon storage per area in downed wood, litter and humus, and sediment indicate that floodplains and riparian ecosystems may be a significant terrestrial reservoir for carbon storage previously unaccounted for in carbon stock estimates of adjacent uplands. Reach-average carbon storage per area (260 Mg ha^{-1}) at my study reaches is significantly higher than values of carbon stocks per area in uplands of the region (170 Mg ha^{-1}; (Bradford et al., 2008). These results suggest that floodplain carbon storage may help fill the missing terrestrial carbon sink (Ballantyne et al., 2012; Hoffmann et al., 2013) and constrain the estimated value of carbon storage within the geosphere via rivers, lakes, and wetlands (Tranvik et al., 2009; Aufdenkampe et al., 2011). Battin et al. (2008) and Aufdenkampe et al. (2011) proposed that rivers account for an estimated storage of 0.9 Pg C yr^{-1} within the geosphere via floodplains, lakes, and wetlands, but (Tranvik et al., 2009)) suggest a broad range of uncertainty between ~0.2 and 1.6 Pg C yr^{-1}. Because work investigating potential carbon storage in floodplains is relatively new and focuses primarily on large rivers, storage within small streams, primarily those in mountainous environments, may constitute a largely overlooked component of floodplain storage. Work presented here indicates significant storage along mountainous floodplains and suggests terrestrial carbon storage within the geosphere is likely on the higher end of the range (1.6 Pg C yr^{-1}) estimated by (Tranvik et al., 2009)).

In Chapter 2, I presented a conceptual model for the optimal conditions for organic carbon storage in floodplains, which include relatively cool, wet, unconfined valleys, with high channel complexity and conditions that favor aggradation over erosion. Because these conditions are met in high elevation mountain streams with snowmelt-driven hydrographs, I expected to find higher carbon storage per area in the mountain streams of the Colorado Front Range compared to floodplains of other regions. Comparison of carbon storage along other floodplains indicates that carbon storage per area in mountain streams of the study area (146-517 Mg C ha^{-1}) is on the higher end of storage along floodplains from other studies in lower relief environments (Sutfin et al., 2015). The geomorphic conditions optimal for carbon storage, however, may need to be adjusted.

Although I suggested that high channel complexity would result in the highest carbon content per area, multithread channel reaches in this study did not store the highest OC per area. Single-thread channels in unconfined valleys stored the highest amount of OC per area. Although observations and results show that greater silt and clay content and higher soil moisture are correlated with higher SOC content and that deeper floodplain sediment in unconfined valley segments are likely the causes of higher OC storage per area, questions remain regarding why. Evidence of ground water inputs in grassy meadows within the study area, and work in other regions indicating grasslands have relatively higher SOC content, suggests that these differences need to be investigated further. These differences, however, do not appear to be driven by the residence time of floodplain sediment.

Organic carbon storage per area at elevations above 2500 m is regulated by valley confinement, channel planform, and biotic drivers. Unconfined valleys in young forests or where floodplains are dominated by grasses rather than densely spaced trees, host single-thread channels and wet meadows that store almost twice the amount of carbon per area on average as other valley types. In old-growth forests with densely spaced trees large enough to create persistent, channel-spanning logjams, multiple sub-parallel channels may develop, which limit sediment storage and organic carbon storage per area. The seasonal wetting and drying of multithread channels likely facilitate rapid decomposition of organic matter and soil organic carbon. Similarly, beaver activity, which diverts flow to different portions of a valley bottom, creates a dynamic environment for water and sediment that may increase the metabolism of organic carbon. These unconfined valleys still store a significantly large amount of carbon per area. Although the dynamic environment of multithread channels limits the capacity to store carbon long term, these valley segments likely serve vital functions in ecosystem processing and sustaining food webs by creating hotspots for metabolism of organic carbon.

6.2 Recommendations for future work

Carefully focused future work can help to answer additional questions regarding carbon storage along river corridors in mountainous regions. Questions of particular importance include the relative influence of individual drivers of higher organic carbon content along single-thread channels in unconfined valleys, and how valley-bottom dynamics control the residence time of organic carbon in floodplain sediment of mountain streams. With regard to my study in particular, an additional study reach on an unconfined single-thread channel for intensive sampling used to determine the necessary number of samples needed to estimate mean SOC content could have provided more insight into spatial variation in organic carbon in this valley type. More extensive sampling across a beaver meadow could also be beneficial in identifying variation across the valley and the appropriate number of samples necessary to accurately estimate sediment organic carbon, as well as potential differences in geomorphic floodplain features. Because the spatial density of trees along floodplains drives channel form and the apparent potential to store organic carbon, surveying basal density of the floodplain forest and locating more unconfined single-thread channels is highly recommended. In surveying the floodplain topography, I now acknowledge that continuing the survey across the active channel (rather than not surveying the active channel) would have provided the data necessary to estimate hydraulic forces, such as bed shear stress and stream power, in the channel and floodplain during large floods. This could provide beneficial insight and facilitate quantitative analysis of sediment dynamics across floodplains with changes in elevation.

With regard to future directions and research in other regions, increased understanding of many aspects of sediment and carbon dynamics is needed to fully quantify carbon storage in floodplains globally and to integrate floodplains into the terrestrial carbon budget. Of significant importance is quantifying differences in OC inputs, metabolism, and storage across various climatic regions and biomes. Storage and flux of carbon along floodplains are largely regulated by sediment dynamics with regard to hydroclimatic regime, floodplain accretion, and bank erosion. Quantification of carbon accretion on floodplains and understanding the implications of carbon dynamics associated with the rate of bank erosion on larger rivers, in particular, are necessary to fully quantify riverine carbon storage and flux.

The role of biogeochemistry and microbial efficiency is a crucial component to understanding carbon dynamics along river corridors and the potential for long-term storage of organic carbon. Although quantifying sediment residence times and flux provide a basis for understanding potential for long-term carbon storage, more work needs to be done to investigate carbon dynamics associated with the stability of floodplain environments. Interdisciplinary collaboration to investigate the form of carbon stored in floodplains, the relative likelihood that the carbon will be metabolized, and the residence time of carbon, are necessary to fully understand the importance of small streams in the terrestrial carbon cycle and the role of geology, geomorphology, and hydrology in the biogeochemical processing of organic carbon along river networks.

Quantifying natural processes that store carbon along river corridors in various regions is the first step, but identifying anthropogenic impacts on these processes is crucial for estimating storage and flux of carbon in global rivers and predicting changes in river carbon dynamics. Anthropogenic impacts on river corridors, including sediment dynamics in particular, are superimposed over natural processes that regulate carbon flux in rivers. Alteration of rivers likely influences the ability of rivers to retain carbon along floodplains. Land-use changes and channelization of rivers reduce channel complexity and opportunities for metabolism of organic carbon in rivers, hindering ecosystem functioning (Battin et al., 2008). This may be an underlying cause in the observed decline in ecosystem integrity of highly impacted streams. Similarly, a historic decline in beaver populations and forest stand disturbances such as deforestation, wildfire, and beetle kill limit the age and size of trees, hindering the development of multithread channels. Where rivers are channelized and artificial levees prevent overbank flow, aggradation of floodplain sediment and accumulation of stored carbon are limited.

6.3 River carbon and climate change

Controls on organic carbon retention along river corridors, which are regulated by temperature, moisture, and hydraulic disturbance, are likely to change substantially with projected increase in global average temperature, snowpack and snowmelt, and the frequency of extreme events. Projected changes in hydroclimatic regime and frequency of extreme events associated with climate change (Bates et al., 2008) are likely to alter sediment dynamics and the stability of floodplains (Sutfin et al., 2015). Extreme events, for example, could result in shorter residence time of sediment. This could be significant for extreme floods on large rivers in low-relief environments as well as increasing elevation of hydroclimatic boundaries in mountainous regions, as suggested by work presented here. Results from this study indicating higher OC storage along single-thread versus multithread channels suggest that short-term stability of floodplain surfaces and hydrologic connectivity regulate floodplain carbon storage. Although all high-elevation sites are stable for long durations (i.e., residence times >1200 y), multithread channels store less carbon even though they experience short-term instability through channel avulsions, bank erosion, and increased lateral hydrologic connectivity, as inferred from shallower water tables. Anticipated decreases in hydrologic connectivity anticipated with climate change (Alexander, 2014), in addition to those resulting from land use and flow regulation, are likely to influence carbon dynamics in rivers (Sutfin et al., 2015). The direction of these potential changes is uncertain and requires investigation.

6.4 Conclusion

Whether through long-term storage or ecosystem processing of organic carbon, mountain streams provide important functions and services in carbon dynamics. Differences in hydroclimatic regime associated with mountainous areas and those of low relief are likely to create similar conditions in floodplain sediment dynamics in other regions. Floodplains in cooler mountain regions, particularly where glaciers and snow are primary drivers of moisture regimes, are likely to store significantly larger amounts of organic carbon per area compared to adjacent uplands. Because moisture and hydroclimatic regime are significant drivers of organic carbon storage at the landscape scale, carbon dynamics are highly susceptible to changes as a result of anticipated changes in snowpack, snow melt, and increased intensity and frequency of extreme storms and floods.

References

Alexander L. 2014. Connectivity of Streams and Wetlands to Downstream Waters: A Review and Synthesis of the Scientific Evidence (External Review Draft) . US EPA National Center for Environmental Assessment. Environmental Protetion Agency: Washington DC [online] Available from: http://cfpub.epa.gov/ncea/cfm/recordisplay.cfm?deid=238345 (Accessed 26 January 2015)

Aufdenkampe AK, Mayorga E, Raymond PA, Melack JM, Doney SC, Alin SR, Aalto RE, Yoo K. 2011. Riverine coupling of biogeochemical cycles between land, oceans, and atmosphere. Frontiers in Ecology and the Environment 9 : 53–60. DOI: 10.1890/100014

Ballantyne AP, Alden CB, Miller JB, Tans PP, White JWC. 2012. Increase in observed net carbon dioxide uptake by land and oceans during the past 50 years. Nature 488 : 70–72. DOI: 10.1038/nature11299

Bates BC, Kundzewicz ZW, Palutikof JP. 2008. Climate change and water . Technical Report. IPCC: IPCC Secretariat, Geneva

Battin TJ, Kaplan LA, Findlay S, Hopkinson CS, Marti E, Packman AI, Newbold JD, Sabater F. 2008. Biophysical controls on organic carbon fluxes in fluvial networks. Nature Geoscience 1 : 95–100. DOI: 10.1038/ngeo101

Battin TJ, Luyssaert S, Kaplan LA, Aufdenkampe AK, Richter A, Tranvik LJ. 2009. The boundless carbon cycle. Nature Geoscience 2 : 598–600. DOI: 10.1038/ngeo618

Bradford JB, Birdsey RA, Joyce LA, Ryan MG. 2008. Tree age, disturbance history, and carbon stocks and fluxes in subalpine Rocky Mountain forests. Global Change Biology 14 : 2882–2897. DOI: 10.1111/j.1365-2486.2008.01686.x

Cole JJ et al. 2007. Plumbing the Global Carbon Cycle: Integrating Inland Waters into the Terrestrial Carbon Budget. Ecosystems 10 : 172–185. DOI: 10.1007/s10021-006-9013-8

Galy V, Peucker-Ehrenbrink B, Eglinton T. 2015. Global carbon export from the terrestrial biosphere controlled by erosion. Nature 521 : 204–207. DOI: 10.1038/nature14400

Hilton RG, Galy V, Gaillardet J, Dellinger M, Bryant C, O'Regan M, Gröcke DR, Coxall H, Bouchez J, Calmels D. 2015. Erosion of organic carbon in the Arctic as a geological carbon dioxide sink. Nature 524 : 84–87. DOI: 10.1038/nature14653

Hoffmann T et al. 2013. Short Communication: Humans and the missing C-sink: erosion and burial of soil carbon through time. Earth Surface Dynamics Discussions 1 : 93–112. DOI: 10.5194/esurfd-1-93-2013

Hoffmann T, Glatzel S, Dikau R. 2009. A carbon storage perspective on alluvial sediment storage in the Rhine catchment. Geomorphology 108 : 127–137. DOI: 10.1016/j.geomorph.2007.11.015

Regnier P et al. 2013. Anthropogenic perturbation of the carbon fluxes from land to ocean. Nature Geoscience 6 : 597–607. DOI: 10.1038/ngeo1830

Sutfin NA, Wohl EE, Dwire KA. 2015. Banking carbon: A review of organic carbon storage and physical factors influencing retention in floodplains and riparian ecosystems. Earth Surface Processes and Landforms : n/a–n/a. DOI: 10.1002/esp.3857

Tranvik LJ et al. 2009. Lakes and reservoirs as regulators of carbon cycling and climate. presented at the American Geophysical Union Chapman Conference Office on Abrupt Climate Change. 2298–2314 pp. [online] Available from: http://cat.inist.fr/?aModele=afficheN&cpsidt=22279829 (Accessed 19 May 2014)

Wohl E, Dwire K, Sutfin N, Polvi L, Bazan R. 2012. Mechanisms of carbon storage in mountainous headwater rivers. Nature Communications 3 : 1263. DOI: 10.1038/ncomms2274

Chapter 7: Appendices

7.1 Appendix A. Survey data

Table 7.1. Topographic floodplain surveys along each transect of 24 study reaches. Vertical and horizontal distances are respective differences between each consecutive point.

Study Reach	Transect	Depth (cm)	Vertical (m)	Horizontal (m)	X_UTM	Y_UTM	Notes
NSVAB1	T1	13	0.8	62	447947.00	4450819.00	VR edge, S1.0 (0-6, duff), S1.1 (6-13)
NSVAB1	T1	13	0.4	61.6	447947.00	4450820.00	BF, spruce
NSVAB1	T1	19	0.2	61.4	447947.00	4450820.00	FP, overbank channel
NSVAB1	T1	16	0.3	60	447947.00	4450821.00	FP bar
NSVAB1	T1	0	0	58.6	447948.00	4450823.00	REW
NSVAB1	T1	0	0	52.1	447950.00	4450829.00	LEW
NSVAB1	T1	45	0.3	52	447950.00	4450829.00	BF, ToC
NSVAB1	T1	20	0.5	48.6	447951.00	4450832.00	veg island, Doug fir
NSVAB1	T1	23	0.2	46.6	447952.00	4450834.00	edge of standing water, OB channel
NSVAB1	T1	3	0.8	42.1	447953.00	4450838.00	berm, Douglas and Engleman spruce
NSVAB1	T1	11	1.1	36.4	447955.00	4450844.00	berm, Douglas and Engleman spruce
NSVAB1	T1	46	1	32.7	447956.00	4450847.00	berm, Douglas and Engleman spruce
NSVAB1	T1	22	1	27.9	447957.00	4450852.00	FP, OB channel
NSVAB1	T1	66	1.3	19.5	447960.00	4450860.00	grasy wet meadow
NSVAB1	T1	46	1.1	9.8	447963.00	4450869.00	grasy wet meadow
NSVAB1	T1	31	1.2	0	447966.00	4450879.00	VL edge, NSVAB1 T1vl
NSVAB1	T10	49	-0.5	66.7	448015.17	4450785.34	VR edge
NSVAB1	T10	37	0.1	60.8	448017.81	4450790.62	FP, OB channel
NSVAB1	T10	45	0.4	57.5	448019.29	4450793.57	FP berm
NSVAB1	T10	14	0.1	55.3	448020.27	4450795.54	standing water, OB channel
NSVAB1	T10	14	0.2	51.6	448021.92	4450798.85	FP

NSVAB1	T10	14	0.2	50.9	448022.24	4450799.47	BF
NSVAB1	T10	0	0	50.8	448022.28	4450799.56	REW
NSVAB1	T10	0	0	44.3	448025.19	4450805.38	LEW
NSVAB1	T10	15	0.8	43.9	448025.37	4450805.73	ToC
NSVAB1	T10	25	0.6	40.6	448026.84	4450808.69	berm w/ E and SP1
NSVAB1	T10	44	0.5	36	448028.90	4450812.80	wet BM, W
NSVAB1	T10	25	0.8	25.7	448033.51	4450822.01	wet BM, W, S10
NSVAB1	T10	52	1.4	17.5	448037.17	4450829.35	wet BM, W, E, SP1
NSVAB1	T10	35	1.9	8.9	448041.02	4450837.04	wet BM, W, E, SP1
NSVAB1	T10	28	2.1	0	448045.00	4450845.00	wet BM, VL edge
NSVAB1	T11	48	0.5	59.3	448023.88	4450782.76	VR edge
NSVAB1	T11	12	0.1	57.1	448024.85	4450784.74	standing water, OB channel
NSVAB1	T11	51	0.7	55.4	448025.60	4450786.26	OB, berm, Douglas fir
NSVAB1	T11	9	0.3	51.6	448027.27	4450789.67	FP
NSVAB1	T11	16	0.2	49	448028.42	4450792.01	BF
NSVAB1	T11	0	0	48.4	448028.68	4450792.55	side channel
NSVAB1	T11	14	0.2	46.9	448029.34	4450793.89	BF
NSVAB1	T11	0	0	46.8	448029.39	4450793.98	REW
NSVAB1	T11	0	0	40	448032.38	4450800.09	LEW
NSVAB1	T11	18	0.3	38.7	448032.96	4450801.26	BF, W hell
NSVAB1	T11	25	0.7	37.5	448033.48	4450802.33	berm, W on cobble levee, mostly litter and duff
NSVAB1	T11	10	0	32.8	448035.55	4450806.55	BM, spruce, W, grass
NSVAB1	T11	22	-0.1	27.3	448037.98	4450811.49	wet BM on edge of tree berm, W
NSVAB1	T11	21	0.5	25.4	448038.81	4450813.20	tree berm w/ SP1
NSVAB1	T11	14	0.2	23.6	448039.61	4450814.81	wet BM with spruce
NSVAB1	T11	20	0.2	20	448041.19	4450818.04	wet BM, S11
NSVAB1	T11	57	1.1	10	448045.60	4450827.02	grassy BM w/ spruce, S12
NSVAB1	T11	63	1.7	0	448050.00	4450836.00	grassy BM w/ spruce, VL edge
NSVAB1	T2	17	0.4	61.9	447956.18	4450817.46	VR edge
NSVAB1	T2	29	-0.1	61.1	447956.48	4450818.20	BF
NSVAB1	T2	0	-0.3	61	447956.51	4450818.30	REW
NSVAB1	T2	0	-0.3	52.9	447959.50	4450825.83	LEW

NSVAB1	T2	0	0	52.7	447959.57	4450826.01	BF, cutbank
NSVAB1	T2	18	0.2	52.4	447959.68	4450826.29	upland FP
NSVAB1	T2	32	0.4	45.7	447962.15	4450832.52	OB channel, standing water
NSVAB1	T2	28	0	41.6	447963.67	4450836.33	FP upland, S4.0
NSVAB1	T2	52	0.6	38.4	447964.84	4450839.30	FP, grassy wet meadow, willow, grasses
NSVAB1	T2	52	0.8	32.6	447966.98	4450844.70	FP berm
NSVAB1	T2	51	1.3	23.2	447970.45	4450853.43	FP berm
NSVAB1	T2	28	1.2	15.8	447973.18	4450860.31	grassy wet meadow
NSVAB1	T2	73	1.3	5.8	447976.86	4450869.61	grassy wet meadow
NSVAB1	T2	59	1.1	0	447979.00	4450875.00	grassy wet meadow, VL edge
NSVAB1	T3	51	0.5	67.6	447962.98	4450813.95	VR edge
NSVAB1	T3	0	0.3	67.5	447963.02	4450814.04	BF, ToC
NSVAB1	T3	0	0	67.5	447963.02	4450814.04	REW
NSVAB1	T3	0	0	61.5	447965.59	4450819.46	LEW
NSVAB1	T3	11	0.2	60.1	447966.20	4450820.72	BF, island, willow, grassy, D on log berm
NSVAB1	T3	38	0	58.9	447966.71	4450821.81	side channel edge
NSVAB1	T3	28	0.2	56.8	447967.61	4450823.70	berm
NSVAB1	T3	49	0	51.5	447969.89	4450828.49	BM, W
NSVAB1	T3	37	0.2	45.5	447972.46	4450833.91	BM, berm with E
NSVAB1	T3	27	0.6	38	447975.68	4450840.68	E and D island in BM
NSVAB1	T3	62	1	30.1	447979.08	4450847.82	BM
NSVAB1	T3	75	1.2	22.5	447982.34	4450854.68	BM
NSVAB1	T3	86	1.3	14.9	447985.60	4450861.54	BM
NSVAB1	T3	121	1.2	8.6	447988.31	4450867.23	BM
NSVAB1	T3	75	1.5	0	447992.00	4450875.00	VL edge
NSVAB1	T4	33	0.5	67	447972.25	4450812.48	VR edge, FP
NSVAB1	T4	44	0.4	66.3	447972.57	4450813.10	FP, S2.0 (0-8, duff), S2.1 (8-23), S2.2 (23-44)
NSVAB1	T4	55	0.4	64.5	447973.39	4450814.70	FP
NSVAB1	T4	30	0.2	64	447973.62	4450815.14	BF, ToC, moss spruce
NSVAB1	T4	0	0.4	64	447973.62	4450815.14	REW
NSVAB1	T4	0	0.4	59.1	447975.87	4450819.49	LEW
NSVAB1	T4	6	0.6	58.7	447976.06	4450819.85	BF

NSVAB1	T4	27	0.9	56.7	447976.97	4450821.63	FP berm, E & D
NSVAB1	T4	14	0.6	54.1	447978.17	4450823.94	OB channwl, standing water
NSVAB1	T4	57	0	49	447980.51	4450828.47	tree berm in BM, E
NSVAB1	T4	29	0.2	39.8	447984.73	4450836.64	BM
NSVAB1	T4	22	0.7	31.6	447988.49	4450843.93	BM
NSVAB1	T4	92	0.6	24.6	447991.71	4450850.14	BM, willow
NSVAB1	T4	100	1.3	14.6	447996.30	4450859.03	
NSVAB1	T4	93	1.2	5.5	448000.48	4450867.11	
NSVAB1	T4	15	1.3	0	448003.00	4450872.00	VL edge
NSVAB1	T5	33	0.2	79	447978.31	4450805.57	VR edge
NSVAB1	T5	20	0	78	447978.79	4450806.45	FP, OB channel
NSVAB1	T5	49	0.4	76.2	447979.65	4450808.03	FP, veg berm, pine
NSVAB1	T5	37	0.5	75.6	447979.93	4450808.56	BF, RR
NSVAB1	T5	0	0.7	75.6	447979.93	4450808.56	REW
NSVAB1	T5	0	0.7	69.8	447982.70	4450813.66	LEW
NSVAB1	T5	20	0.9	69.4	447982.89	4450814.01	BF, W, E
NSVAB1	T5	39	1.1	64.6	447985.18	4450818.23	BM, hummock berm with E and grass
NSVAB1	T5	48	1.8	57.3	447988.66	4450824.64	BM tree berm
NSVAB1	T5	15	1.7	50.4	447991.95	4450830.71	BM
NSVAB1	T5	43	1.9	43	447995.49	4450837.21	BM
NSVAB1	T5	37	2.1	35.1	447999.25	4450844.15	BM, tall willow hell
NSVAB1	T5	122	1.9	27.5	448002.88	4450850.83	tall willow hell, S5
NSVAB1	T5	86	2	20	448006.46	4450857.42	BM, willow hell
NSVAB1	T5	127	1.9	8.6	448011.90	4450867.44	BM, willow hell
NSVAB1	T5	25	1.9	0	448016.00	4450875.00	VL edge
NSVAB1	T6	40	0.2	76.7	447985.92	4450802.86	VR edge
NSVAB1	T6	13	0	75.2	447986.65	4450804.17	FP, OB channel
NSVAB1	T6	39	0.5	70.6	447988.87	4450808.20	FP, veg island, spruce
NSVAB1	T6	40	0.4	70.2	447989.06	4450808.55	ToC, undercut
NSVAB1	T6	0	0.2	70.2	447989.06	4450808.55	BF, cutbank
NSVAB1	T6	0	0	70.2	447989.06	4450808.55	REW
NSVAB1	T6	0	0	64.7	447991.72	4450813.36	LEW

NSVAB1	T6	12	0.2	63.9	447992.11	4450814.06	BF, FP, willow, E
NSVAB1	T6	68	0.1	61	447993.51	4450816.60	FP, willow, side channel, wet meadow
NSVAB1	T6	38	0.4	58.1	447994.91	4450819.14	berm w/E & D
NSVAB1	T6	22	0.2	56.5	447995.69	4450820.54	BM
NSVAB1	T6	22	0.7	50.2	447998.73	4450826.06	BM next to tree island
NSVAB1	T6	60	0.9	47.4	448000.09	4450828.51	S6
NSVAB1	T6	91	1.1	43.9	448001.78	4450831.57	wet BM
NSVAB1	T6	60	1.1	34.4	448006.37	4450839.89	willow hell, wet
NSVAB1	T6	136	1.1	30.5	448008.26	4450843.30	willow hell, wet
NSVAB1	T6	170	1.4	22.3	448012.22	4450850.48	berm w/ S in BM
NSVAB1	T6	50	1.5	13.9	448016.28	4450857.83	Wet BM w/ spruce and W
NSVAB1	T6	84	1.5	6.7	448019.76	4450864.13	Wet BM w/ spruce and W
NSVAB1	T6	27	1.5	0	448023.00	4450870.00	Wet BM, VL edge
NSVAB1	T7	9	0	72.1	447993.17	4450800.33	VR edge, side channel
NSVAB1	T7	38	0	69.8	447994.25	4450802.36	FP, OB side channel
NSVAB1	T7	70	0.4	66	447996.04	4450805.71	FP berm w/ logs & Engelmean spruce
NSVAB1	T7	34	0.3	62	447997.91	4450809.25	BF
NSVAB1	T7	0	0.1	61.7	447998.05	4450809.51	REW
NSVAB1	T7	0	0.1	55.4	448001.01	4450815.08	LEW
NSVAB1	T7	12	0.3	54.3	448001.52	4450816.05	FP, grassy berm with W
NSVAB1	T7	9	0.2	52.1	448002.56	4450817.99	FP, OB channel, S7
NSVAB1	T7	28	0.1	51.3	448002.93	4450818.70	FP, OB channel
NSVAB1	T7	30	0.3	50.8	448003.17	4450819.14	FP berm, E and W
NSVAB1	T7	37	0.4	43.5	448006.59	4450825.58	wet BM
NSVAB1	T7	58	0.8	39.2	448008.61	4450829.38	wet BM, W
NSVAB1	T7	37	1	35.6	448010.30	4450832.56	wet BM, W
NSVAB1	T7	70	1.3	32.1	448011.94	4450835.65	berm w/ E & D island, S8
NSVAB1	T7	119	1.4	24.3	448015.60	4450842.54	wet BM
NSVAB1	T7	113	1.4	15.7	448019.63	4450850.14	wet BM
NSVAB1	T7	112	1.6	6.5	448023.95	4450858.26	wet BM, willow hell
NSVAB1	T7	47	1.6	0	448027.00	4450864.00	wet BM, VL edge
NSVAB1	T8	12	0.2	69.6	447999.53	4450796.97	VR edge

NSVAB1	T8	11	0	67.1	448000.74	4450799.17	FP, OB channe;
NSVAB1	T8	30	0.2	64.1	448002.18	4450801.80	FP
NSVAB1	T8	10	0.4	59.4	448004.44	4450805.92	FP
NSVAB1	T8	11	0.2	58.7	448004.78	4450806.53	BF
NSVAB1	T8	0	0	58.5	448004.87	4450806.71	REW
NSVAB1	T8	0	0	46.9	448010.45	4450816.88	LEW
NSVAB1	T8	32	0.3	46.5	448010.64	4450817.23	BF, FP, BM
NSVAB1	T8	90	0.8	39.4	448014.06	4450823.45	FP, sloping wet BM, W
NSVAB1	T8	55	1.1	29.9	448018.62	4450831.78	wet BM, W, E, S9
NSVAB1	T8	92	1.4	22.9	448021.99	4450837.92	wet BM, W,
NSVAB1	T8	106	1.6	17.3	448024.68	4450842.83	wet BM, W,
NSVAB1	T8	99	1.5	12.3	448027.09	4450847.22	wet BM, W,
NSVAB1	T8	82	1.6	6.8	448029.73	4450852.04	wet BM, W, E
NSVAB1	T8	27	1.6	0	448033.00	4450858.00	wet BM, VL edge
NSVAB1	T9	24	0.5	56.4	448010.73	4450800.09	VR edge
NSVAB1	T9	30	0.1	54.9	448011.43	4450801.42	OB channe, S3.0 (0-8, duff), S3.1(8-23), S3.2(23-
NSVAB1	T9	47	0.6	53.3	448012.18	4450802.83	veg island
NSVAB1	T9	10	0.7	48.8	448014.27	4450806.82	veg island
NSVAB1	T9	0	0.2	47.7	448014.78	4450807.79	BF, cutbank
NSVAB1	T9	0	-0.1	47.7	448014.78	4450807.79	toe of cutbank, veg island
NSVAB1	T9	23	0.2	45.7	448015.72	4450809.56	BF
NSVAB1	T9	0	0	45.3	448015.90	4450809.91	REW
NSVAB1	T9	0	0	39	448018.84	4450815.49	LEW
NSVAB1	T9	0	0.2	39	448018.84	4450815.49	BF, RL, cutbank
NSVAB1	T9	25	0.5	39	448018.84	4450815.49	RL ToC
NSVAB1	T9	18	0.4	34.8	448020.79	4450819.20	Tree berm, E and spruce1
NSVAB1	T9	31	0.1	34.1	448021.12	4450819.82	wet BM
NSVAB1	T9	42	0.2	28.7	448023.63	4450824.60	wet BM, W, SP1
NSVAB1	T9	72	0.6	20.2	448027.59	4450832.12	wet BM, W, SP1
NSVAB1	T9	130	0.8	14.3	448030.34	4450837.35	wet BM, W, SP1
NSVAB1	T9	132	1	6	448034.21	4450844.69	wet BM, W, SP1
NSVAB1	T9	22	0.9	0	448037.00	4450850.00	wet BM, VL edge

NSVCF1	T1	26	1	15	457128.05	4451872.87	VR edge
NSVCF1	T1	38	0.8	14.5	457127.88	4451873.34	inactive side channel
NSVCF1	T1	70	1	13	457127.37	4451874.76	S11.0 (0-13, duff), S11.1 (13-28), S11.2 (28-43),
NSVCF1	T1	28	0.7	12.4	457127.17	4451875.32	
NSVCF1	T1	22	0.4	11.7	457126.94	4451875.98	BF, ToC
NSVCF1	T1	0	0	11.4	457126.83	4451876.26	REW
NSVCF1	T1	0	0	1.1	457123.37	4451885.96	LEW
NSVCF1	T1	0	0.1	0.4	457123.13	4451886.62	BF
NSVCF1	T1	0	0.3	0	457123.00	4451887.00	VL edge
NSVCF1	T2	32	0.5	13.9	457141.99	4451880.03	VR edge
NSVCF1	T2	32	0.4	13.1	457141.70	4451880.77	S10.0 (0-6, duff), S10.1 (6-21), 10.2 (21-36),
NSVCF1	T2	53	0.3	12.4	457141.45	4451881.43	BF
NSVCF1	T2	0	0	11.8	457141.24	4451881.99	REW
NSVCF1	T2	0	0	0.7	457137.25	4451892.35	LEW
NSVCF1	T2	19	0.2	0.2	457137.07	4451892.81	BF
NSVCF1	T2	0	0.4	0	457137.00	4451893.00	VL edge
NSVCF1	T3	58	0.4	14.9	457154.01	4451882.97	VR edge
NSVCF1	T3	32	0.2	14.2	457153.78	4451883.63	S9.0 (0-8), S9.1 (8-23), S9.2 (23-32), bank
NSVCF1	T3	69	0.2	13.2	457153.44	4451884.57	BF, RR
NSVCF1	T3	0	0	12.5	457153.20	4451885.23	REW
NSVCF1	T3	0	0	1.7	457149.57	4451895.40	LEW
NSVCF1	T3	39	0.2	1.5	457149.50	4451895.59	BF
NSVCF1	T3	24	0.3	0.7	457149.24	4451896.34	FP, S5.0(0-12, duff), S5.1 (12-24)
NSVCF1	T3	56	0.4	0	457149.00	4451897.00	VL edge
NSVCF1	T4	64	0.8	17.8	457166.93	4451885.44	VR edge
NSVCF1	T4	68	0.7	16.1	457166.65	4451887.12	S8.0 (0-7), S8.1 (7-22), S8,2 (22-37), S8.3 (37-
NSVCF1	T4	61	0.5	14.2	457166.33	4451888.99	BF, ToC
NSVCF1	T4	0	0	13.6	457166.24	4451889.59	REW
NSVCF1	T4	0	0	1.7	457164.28	4451901.32	LEW
NSVCF1	T4	0	0.5	0.5	457164.08	4451902.51	BF, Boulder
NSVCF1	T4	0	0.8	0	457164.00	4451903.00	VL edge, Boulder
NSVCF1	T5	43	0.3	18.1	457182.84	4451888.56	VR edge, toe of cutbank

NSVCF1	T5	39	0.3	16.9	457182.52	4451889.72	S7.0 (0-4), S7.1 (4-19), S7.2 (19-34), S7.3 (34-39)
NSVCF1	T5	18	0.2	15.7	457182.20	4451890.87	
NSVCF1	T5	9	0.1	15.3	457182.09	4451891.26	
NSVCF1	T5	0	0	13.8	457181.69	4451892.70	REW
NSVCF1	T5	0	0	1.9	457178.51	4451904.17	LEW
NSVCF1	T5	26	0.1	1.6	457178.43	4451904.46	ToC
NSVCF1	T5	31	0.2	0.7	457178.19	4451905.33	BF, S4.0 (0-6), S4.1 (6-21), S4.2 (21-31)
NSVCF1	T5	13	0.4	0	457178.00	4451906.00	VL edge
NSVCF1	T6	62	0.6	22.4	457198.89	4451889.39	VR edge
NSVCF1	T6	38	0.3	21.2	457198.58	4451890.55	S6.0 (0-8), S6.1 (8-23), S6.3 (23-38)
NSVCF1	T6	66	0.3	20.5	457198.39	4451891.22	BF, ToC
NSVCF1	T6	0	0	20.2	457198.31	4451891.51	REW
NSVCF1	T6	0	0	3.8	457194.00	4451907.33	LEW
NSVCF1	T6	71	0.2	3.1	457193.82	4451908.01	BF
NSVCF1	T6	75	0.2	1.9	457193.50	4451909.17	S3.0 (0-6, duff), S3.1 (6-23), S3.2 (23-41), S3.3
NSVCF1	T6	48	0.2	0.8	457193.21	4451910.23	FP
NSVCF1	T6	13	0.3	0	457193.00	4451911.00	VL edge
NSVCF1	T7	50	1.1	24.5	457214.00	4451891.01	VR edge, toe of hillslope
NSVCF1	T7	22	0.9	23	457213.69	4451892.48	S5.0 (0-7), S5.1 (7-22), FP
NSVCF1	T7	0	0.4	21.2	457213.32	4451894.25	REW
NSVCF1	T7	0	0.4	16.4	457212.34	4451898.94	right edge of bar
NSVCF1	T7	0	0	14.4	457211.94	4451900.90	Left edge of vegetated island
NSVCF1	T7	0	0	1.9	457209.39	4451913.14	LEW
NSVCF1	T7	29	0.4	1.1	457209.22	4451913.92	BF
NSVCF1	T7	43	0.5	0.5	457209.10	4451914.51	S2.0(0-9, duff), S2.1 (9-24), S2.2 (24-39), S2.3
NSVCF1	T7	81	0.5	0	457209.00	4451915.00	VR edge Toe of hillslope
NSVCF1	T8	66	0.7	20.6	457228.66	4451897.19	VR edge
NSVCF1	T8	49	0.5	19	457228.22	4451898.73	S4.0 (0-8), S4.1 (8-24), S4.2 (24-39), S4.3 (39-
NSVCF1	T8	47	0.5	17.4	457227.78	4451900.27	BF, ToC
NSVCF1	T8	21	0	16.7	457227.59	4451900.94	REW
NSVCF1	T8	0	0	2.2	457223.60	4451914.88	LEW
NSVCF1	T8	0	0.7	0.9	457223.25	4451916.13	BF, cobs>B

NSVCF1	T8	23	0.9	0.5	457223.14	4451916.52	S1.0 (0-10, duff), S1.1 (10-23), bank
NSVCF1	T8	0	1.1	0	457223.00	4451917.00	VL edge at base of talus
NSVCF1	T9	51	0.3	12.4	457240.01	4451902.97	VR
NSVCF1	T9	29	0.3	11.2	457239.72	4451904.13	S3.0 (0-18), S3.1 (18-29), bank
NSVCF1	T9	0	0	10	457239.43	4451905.30	REW
NSVCF1	T9	0	0	0.9	457237.22	4451914.13	LEW
NSVCF1	T9	0	0.5	0	457237.00	4451915.00	BF on talus slope, VL edge
NSVCF1	T10	17	0.5	9.9	457250.99	4451905.15	VR edge top of cutbank, S2,0 (0-9, duff), S2.1
NSVCF1	T10	28	0.3	9.6	457250.96	4451905.45	BF, toe of cutbank
NSVCF1	T10	0	0	8.4	457250.84	4451906.64	REW
NSVCF1	T10	0	0	0	457250.00	4451915.00	LEW
NSVCF1	T10	0	0.5	0	457250.00	4451915.00	VL edge
NSVCF1	T11	23	0.5	13.1	457262.00	4451902.94	VR edge
NSVCF1	T11	27	0.3	12.6	457261.97	4451903.44	BF RR
NSVCF1	T11	48	0.3	11.5	457261.88	4451904.53	S1.0 (0-12), S1.1 (12-27), S1.2 (27-42), S1.3 (42-
NSVCF1	T11	0	0	9.9	457261.76	4451906.13	REW
NSVCF1	T11	0	0	0	457261.00	4451916.00	LEW
NSVCF1	T11	0	0.5	0	457261.00	4451916.00	VL edge
NSVMT1	T11	36	0	67.2	446381.01	4451225.07	VL
NSVMT1	T11	79	0	65.2	446381.18	4451227.06	S14 (0-7, duff), S15 (7-22), S16 (22-37), S17 (37-
NSVMT1	T11	0	0	63.1	446381.37	4451229.15	RL, BF
NSVMT1	T11	0	0	60.7	446381.59	4451231.54	RR, BF, veg island
NSVMT1	T11	0	0	57.4	446381.88	4451234.83	RL, BF
NSVMT1	T11	0	0	53.5	446382.23	4451238.71	RR, BF
NSVMT1	T11	44	0	52.8	446382.29	4451239.41	veg island
NSVMT1	T11	0	0	52.1	446382.35	4451240.11	RL, BF
NSVMT1	T11	0	0	47.7	446382.75	4451244.49	RR, BF
NSVMT1	T11	35	0	42.8	446383.18	4451249.37	S20 (9-0, duff), S21 (8-15), S22 (15-25), island
NSVMT1	T11	0	0	35.3	446383.85	4451256.84	RL, BF
NSVMT1	T11	0	0	30.7	446384.26	4451261.42	RR, BF
NSVMT1	T11	47	0	22.6	446384.98	4451269.49	S23 (0-19, duff), S24 (19-35), S25 (35-40), island
NSVMT1	T11	49	0	12.6	446385.88	4451279.45	N/A

NSVMT1	T11	0	0	7.8	446386.30	4451284.23	RL (BF)
NSVMT1	T11	0	0	0	446387.00	4451292.00	RR (BF), VR edge
NSVMT1	T10	0	0	62.2	446372.10	4451227.08	VR edge, RR, BF
NSVMT1	T10	0	0	53	446372.98	4451236.24	RL, BF
NSVMT1	T10	41	0	43	446373.92	4451246.19	S10 (0-18, duff), S11 (18-32), FP island
NSVMT1	T10	0	0	33	446374.87	4451256.15	RR, BF, side channel, marshl wetland
NSVMT1	T10	0	0	23	446375.82	4451266.10	RL, BF
NSVMT1	T10	25	0	19.5	446376.15	4451269.59	S12 (0-11, duff), S13 (11-25), island
NSVMT1	T10	0	0	16.1	446376.47	4451272.97	RR, BF
NSVMT1	T10	0	0	13.1	446376.76	4451275.96	RL, BF
NSVMT1	T10	62	0	8.5	446377.19	4451280.54	N/A
NSVMT1	T10	0	0	6.5	446377.38	4451282.53	RR, BF, mainstem
NSVMT1	T10	0	0	0	446378.00	4451289.00	RL, BF, main stem, VL edge
NSVMT1	T9	0	0	63.9	446363.94	4451225.30	VL edge
NSVMT1	T9	32	0	63.4	446363.98	4451225.80	S1 (0-4, duff), S2 (4-14)
NSVMT1	T9	0	0	62.7	446364.04	4451226.50	RL, BF
NSVMT1	T9	0	0	58.4	446364.38	4451230.78	RR, BF
NSVMT1	T9	53	0	57.9	446364.42	4451231.28	veg island
NSVMT1	T9	0	0	57.3	446364.47	4451231.88	RL, BF
NSVMT1	T9	0	0	54.3	446364.70	4451234.87	RR, BF
NSVMT1	T9	26	0	47.9	446365.21	4451241.25	FP, S3 (0-14, duff), S4 (14-24)
NSVMT1	T9	36	0	37.9	446366.00	4451251.22	
NSVMT1	T9	0	0	34.7	446366.25	4451254.41	RL, BF, side channel
NSVMT1	T9	0	0	30.2	446366.61	4451258.89	RR, BF, side channel
NSVMT1	T9	50	0	27.4	446366.83	4451261.69	S5 (0-12, duff), S6 (12-27), S7 (27-38), island
NSVMT1	T9	25	0	17.4	446367.62	4451271.65	
NSVMT1	T9	16	0	7.4	446368.41	4451281.62	S8 (0-5), S9(5-15) , RL, BF
NSVMT1	T9	0	0	6	446368.53	4451283.02	RL, BF
NSVMT1	T9	0	0	0	446369.00	4451289.00	RR, BF, VR
NSVMT1	T8	0	0	57.4	446356.00	4451229.60	VR edge, RR BF
NSVMT1	T8	0	0	50.7	446356.00	4451236.30	RL, BF
NSVMT1	T8	60	0	40.7	446356.00	4451246.30	S21 (0-15, duff), S22 (15-30), CHARCOAL, FP

NSVMT1	T8	60	0	30.7	446356.00	4451256.30	
NSVMT1	T8	0	0	28.2	446356.00	4451258.80	RR side channel
NSVMT1	T8	0	0	26.6	446356.00	4451260.40	RL, side channel
NSVMT1	T8	81	0	20.7	446356.00	4451266.30	S23 (0-11), S24 (11-26), S25 (26-41)
NSVMT1	T8	86	0	10.7	446356.00	4451276.30	
NSVMT1	T8	0	0	6.9	446356.00	4451280.10	RR, BF
NSVMT1	T8	0	0	0	446356.00	4451287.00	RL, BF
NSVMT1	T7	27	0	58.2	446346.00	4451228.81	VL edge
NSVMT1	T7	55	0	55.7	446345.96	4451231.31	S15 (0-16, duff), S16 (16-31), S17 (31-45), VL
NSVMT1	T7	0	0	53.2	446345.92	4451233.81	BF, RL active channel
NSVMT1	T7	0	0	47.7	446345.82	4451239.31	BF, RR active channel
NSVMT1	T7	15	0	45.7	446345.79	4451241.31	active floodplain
NSVMT1	T7	0	0	35.7	446345.62	4451251.31	active side channel
NSVMT1	T7	45	0	25.7	446345.44	4451261.30	tree berm, S18 (0-12, duff), S19 (12-27), S20
NSVMT1	T7	27	0	15.7	446345.27	4451271.30	berm, tree island
NSVMT1	T7	0	0	8.1	446345.14	4451278.90	BF, RL, active channel
NSVMT1	T7	0	0	0	446345.00	4451287.00	RR, BF and VR edge
NSVMT1	T6	0	0	56.2	446336.00	4451234.81	VR edge
NSVMT1	T6	0	0	55.6	446335.99	4451235.41	BF, RR
NSVMT1	T6	0	0	51.9	446335.93	4451239.11	BF, RL
NSVMT1	T6	33	0	48.9	446335.87	4451242.11	veg island
NSVMT1	T6	0	0	47.9	446335.86	4451243.11	BF (RR)
NSVMT1	T6	0	0	41.7	446335.74	4451249.31	BF (RL)
NSVMT1	T6	37	0	38.9	446335.69	4451252.11	S8 (0-10, duff), Charcoal!, island
NSVMT1	T6	38	0	28.9	446335.52	4451262.10	rocky berm
NSVMT1	T6	33	0	18.9	446335.34	4451272.10	adjacent to small side channel, S9 (0-10), S10
NSVMT1	T6	0	0	10.4	446335.19	4451280.60	BF, RR
NSVMT1	T6	0	0	7	446335.12	4451284.00	BF, RL
NSVMT1	T6	34	0	4	446335.07	4451287.00	FP, S12 (0-8, duff), S13(8-25), S14 (25-34)
NSVMT1	T6	19	0	0	446335.00	4451291.00	VL edge
NSVMT1	T5	0	0	60.3	446325.70	4451232.76	Valley left
NSVMT1	T5	33	0	59.2	446325.65	4451233.86	S1 (0-17, duff), S2(17-32), S3 (32-40)

NSVMT1	T5	0	0	57.8	446325.59	4451235.26	BF, LEW
NSVMT1	T5	0	0	49.1	446325.20	4451243.95	BF, REW
NSVMT1	T5	35	0	48.1	446325.15	4451244.95	
NSVMT1	T5	19	0	38.1	446324.70	4451254.94	S4 (0-13, duff), no samples
NSVMT1	T5	7	0	28.1	446324.26	4451264.93	dry side channel
NSVMT1	T5	0	0	21.8	446323.98	4451271.22	BF, RL
NSVMT1	T5	0	0	18.1	446323.81	4451274.92	inactive channel
NSVMT1	T5	0	0	16.1	446323.72	4451276.92	BF, RR
NSVMT1	T5	64	0	8.1	446323.36	4451284.91	S5 (0-5, duff), S6(5-20), S7(20-35), veg island
NSVMT1	T5	0	0	5.7	446323.25	4451287.31	BF, RL
NSVMT1	T5	0	0	2.4	446323.11	4451290.60	BF, RR
NSVMT1	T5	10	0	0	446323.00	4451293.00	VR edge
NSVMT1	T4	0	0	58	446315.04	4451229.01	REW, VR edge
NSVMT1	T4	0	0	53	446314.95	4451234.01	LEW
NSVMT1	T4	175	0	48	446314.86	4451239.01	
NSVMT1	T4	0	0	42.5	446314.76	4451244.51	REW
NSVMT1	T4	0	0	37.2	446314.66	4451249.81	LEW
NSVMT1	T4	14	0	27.2	446314.49	4451259.80	S14 (aka, S13), (0-14, duff), S14.2 (15-30), S14.3
NSVMT1	T4	0	0	11.4	446314.20	4451275.60	REW
NSVMT1	T4	0	0	4	446314.07	4451283.00	LEW
NSVMT1	T4	0	0	2	446314.04	4451285.00	S15, VL
NSVMT1	T4	0	0	0	446314.00	4451287.00	VL
NSVMT1	T3	52	0	55.4	446303.97	4451232.61	S9 (0-14, duff), (14-29), (29-44), (44-51), VL
NSVMT1	T3	0	0	53.9	446303.95	4451234.11	LEW
NSVMT1	T3	0	0	52.2	446303.92	4451235.81	REW
NSVMT1	T3	46	0	47.2	446303.83	4451240.81	
NSVMT1	T3	25	0	43.9	446303.77	4451244.11	S10 (0-1-, duff), (10-25), island
NSVMT1	T3	47	0	33.9	446303.59	4451254.11	
NSVMT1	T3	0	0	31.6	446303.55	4451256.40	LEW
NSVMT1	T3	0	0	26.1	446303.46	4451261.90	REW
NSVMT1	T3	57	0	23.9	446303.42	4451264.10	S11 (0-15, duff), (15-30), island
NSVMT1	T3	38	0	13.9	446303.24	4451274.10	

NSVMT1	T3	0	0	12.4	446303.22	4451275.60	LEW
NSVMT1	T3	0	0	10.1	446303.18	4451277.90	REW
NSVMT1	T3	36	0	3.9	446303.07	4451284.10	island, S12 (0-9, duff), (9-24), (24-28)
NSVMT1	T3	0	0	3.1	446303.05	4451284.90	LEW
NSVMT1	T3	0	0	0	446303.00	4451288.00	REW
NSVMT1	T3	0	0	0	446303.00	4451288.00	There is no S13, VR
NSVMT1	T2	0	0	66	446295.97	4451226.03	Valley right, VR
NSVMT1	T2	0	0	64	446295.91	4451228.03	REW
NSVMT1	T2	0	0	58.6	446295.75	4451233.43	LEW
NSVMT1	T2	63	0	54	446295.61	4451238.02	
NSVMT1	T2	28	0	47	446295.40	4451245.02	S5 (0-10, duff), (10-25), (25-28), island
NSVMT1	T2	26	0	44	446295.31	4451248.02	REW
NSVMT1	T2	0	0	38.4	446295.15	4451253.62	LEW, side channe;
NSVMT1	T2	0	0	34	446295.01	4451258.02	
NSVMT1	T2	12	0	27	446294.81	4451265.01	S6 (no duff), (0-12), FP
NSVMT1	T2	39	0	24	446294.72	4451268.01	
NSVMT1	T2	21	0	14	446294.42	4451278.01	
NSVMT1	T2	15	0	11	446294.33	4451281.00	S7 (0-10, duff), (10-15), FP
NSVMT1	T2	0	0	4.3	446294.13	4451287.70	REW
NSVMT1	T2	0	0	1.3	446294.04	4451290.70	LEW
NSVMT1	T2	30	0	1	446294.03	4451291.00	FP, S8 (0-13, duff), 13-30
NSVMT1	T2	43	0	0	446294.00	4451292.00	VL edge
NSVMT1	T1	10	0	63.6	446283.99	4451226.41	RL valley edge
NSVMT1	T1	20	0	61.9	446283.97	4451228.11	S1 (0-10, duff) (10-20), VL
NSVMT1	T1	0	0	60.2	446283.94	4451229.81	LEW
NSVMT1	T1	0	0	56.1	446283.88	4451233.91	REW
NSVMT1	T1	8	0	50.1	446283.78	4451239.91	
NSVMT1	T1	37	0	40.1	446283.63	4451249.90	S2 (0-3, duff) (3-8), island
NSVMT1	T1	51	0	30.1	446283.47	4451259.90	
NSVMT1	T1	44	0	20.1	446283.31	4451269.90	S3 (0-3, duff) (3-18), (18-33), (33-44), island
NSVMT1	T1	31	0	10.1	446283.16	4451279.90	
NSVMT1	T1	0	0	9.8	446283.15	4451280.20	LEW

NSVMT1	T1	0	0	6	446283.09	4451284.00	REW
NSVMT1	T1	34	0	0	446283.00	4451290.00	S4 (0-27 , duff), (27-34), VR, Valley right, upland
NSVPC1	T1	18	0.8	23	456293.68	4451860.92	VR edge
NSVPC1	T1	39	0.6	21.9	456293.47	4451862.00	S1.0 (0-7, duff), S1.1 (7-22), S1.2 (22-37), S1.3
NSVPC1	T1	74	0.5	20.7	456293.24	4451863.18	BF, ToC
NSVPC1	T1	0	0	20.5	456293.21	4451863.38	REW
NSVPC1	T1	0	0	5.5	456290.35	4451878.10	LEW
NSVPC1	T1	68	0.2	3.9	456290.05	4451879.67	BF, STEEP CHANNEL GRADIENT CREATES
NSVPC1	T1	63	0	2.7	456289.82	4451880.85	FP, S1.0 (0-11, DUFF), S1.1 (11-25)
NSVPC1	T1	31	0.4	0	456289.31	4451883.50	VL
NSVPC1	T2	0	0.1	22.9	456306.06	4451867.72	VR edge, cobs, toe of cutbank
NSVPC1	T2	0	0	21.9	456305.84	4451868.69	REW
NSVPC1	T2	0	0	10.8	456303.41	4451879.52	LEW
NSVPC1	T2	21	0.3	8.7	456302.95	4451881.57	BF
NSVPC1	T2	23	0.2	4.2	456301.96	4451885.96	S2.0 (0-12, DUFF), S2.1 (12-23), FP
NSVPC1	T2	34	0.6	0	456301.04	4451890.06	VL EDGE
NSVPC1	T3	9	0.3	30.7	456319.03	4451869.20	VR edge, toe of the slope
NSVPC1	T3	22	0.3	30.3	456318.92	4451869.58	S2.0 (0-6, duff), S2.1 (6-22), FP VR edge
NSVPC1	T3	43	0.3	30	456318.83	4451869.87	BF, ToC
NSVPC1	T3	0	0	29.5	456318.69	4451870.35	REW
NSVPC1	T3	0	0	20.5	456316.10	4451878.97	LEW
NSVPC1	T3	0	0.6	18.3	456315.47	4451881.07	BF, duff on Bs
NSVPC1	T3	0	0.8	17.5	456315.24	4451881.84	potential veg island w/ Bs
NSVPC1	T3	11	0.8	15.4	456314.63	4451883.85	FP, OB island
NSVPC1	T3	10	0.6	12.3	456313.74	4451886.82	FP
NSVPC1	T3	9	0.4	9	456312.79	4451889.98	S3.0 (0-9, duff)
NSVPC1	T3	45	0.6	3.9	456311.32	4451894.86	trib channel
NSVPC1	T3	9	0.8	0	456310.20	4451898.60	VL edge
NSVPC1	T4	0	2	32.6	456335.31	4451875.05	on B, VR edge
NSVPC1	T4	0	0	32.4	456335.26	4451875.24	REW on large boulder
NSVPC1	T4	0	0	21.4	456332.56	4451885.90	LEW
NSVPC1	T4	12	0.4	21.4	456332.56	4451885.90	ToC

NSVPC1	T4	37	0.5	20.4	456332.31	4451886.87	BF
NSVPC1	T4	31	0.1	12.4	456330.34	4451894.63	FP, OB channel
NSVPC1	T4	1	-0.1	10.7	456329.93	4451896.27	FP, S4.0 (0-1, duff)
NSVPC1	T4	37	0	8.5	456329.39	4451898.41	Next to B
NSVPC1	T4	0	1.5	7.5	456329.14	4451899.38	on large B
NSVPC1	T4	0	1.9	5.3	456328.60	4451901.51	on large B
NSVPC1	T4	0	0.4	3.4	456328.13	4451903.35	on large B
NSVPC1	T4	44	0.3	1.7	456327.71	4451905.00	FP
NSVPC1	T4	19	0.7	0	456327.30	4451906.65	VL edge
NSVPC1	T5	0	0.9	39	456352.89	4451876.28	VR edge, ToC, edge of terrace
NSVPC1	T5	0	0.3	38.6	456352.79	4451876.66	BF
NSVPC1	T5	0	0	37.7	456352.56	4451877.53	REW
NSVPC1	T5	0	0	1.6	456343.41	4451912.45	LEW, Transect falls on split in side channel, flow
NSVPC1	T5	40	0.2	0.7	456343.18	4451913.32	S5.0 (0-18), S5.1 (18-33), S5.2 (33-40), BF VL
NSVPC1	T5	37	0.3	0	456343.00	4451914.00	Bf, VL edge
NSVPC1	T6	7	0.6	52.1	456369.46	4451879.06	VR edge
NSVPC1	T6	4	0.7	51.6	456369.27	4451879.53	ToC, S3.0(0-4, NO duff)
NSVPC1	T6	30	0.5	51.2	456369.12	4451879.90	BF
NSVPC1	T6	0	0	49.9	456368.63	4451881.10	REW
NSVPC1	T6	0	0	43.3	456366.13	4451887.21	right edge of island
NSVPC1	T6	0	0	37.3	456363.86	4451892.76	left edge of island
NSVPC1	T6	0	0	22.1	456358.09	4451906.83	LEW
NSVPC1	T6	0	0.2	22.1	456358.09	4451906.83	ToC
NSVPC1	T6	52	0.2	20.6	456357.53	4451908.21	BF, veg island
NSVPC1	T6	41	0.6	12.1	456354.30	4451916.08	FP island, S6.0 (0-9, duff), S6.1 (9-24), S6.2 (24-
NSVPC1	T6	85	0.6	8.5	456352.94	4451919.41	cutbnak on RR side of channel island
NSVPC1	T6	0	0.2	8.4	456352.90	4451919.50	REW of side channel
NSVPC1	T6	0	0.2	3.9	456351.20	4451923.67	LEW of side channel
NSVPC1	T6	16	0.4	3.2	456350.93	4451924.32	ToC, BF, FP
NSVPC1	T6	33	0.5	0	456349.72	4451927.28	VL edge
NSVPC1	T7	24	0.3	39.8	456375.03	4451892.06	VR edge
NSVPC1	T7	13	0.1	39.3	456374.88	4451892.54	BF, S4.0(0-3, duff), S4.1 (3-31)

NSVPC1	T7	0	0	38.7	456374.70	4451893.11	REW
NSVPC1	T7	0	0	28.7	456371.67	4451902.64	LEW
NSVPC1	T7	0	0.9	28.7	456371.67	4451902.64	
NSVPC1	T7	0	0.9	26.2	456370.92	4451905.03	
NSVPC1	T7	37	1.5	25.2	456370.62	4451905.98	BF, FP
NSVPC1	T7	47	1.8	21.5	456369.50	4451909.51	S7.0 (0-7, duff), S7.1 (7-22), S7.2 (22-35), S7.3
NSVPC1	T7	23	1.9	19.3	456368.83	4451911.60	edge of FP island
NSVPC1	T7	0	2.1	16.4	456367.96	4451914.37	top of island
NSVPC1	T7	17	2.1	10.4	456366.14	4451920.09	edge of island, FP
NSVPC1	T7	30	2	9.4	456365.84	4451921.04	FP
NSVPC1	T7	28	2	7.9	456365.39	4451922.47	BF on RR of side channel
NSVPC1	T7	0	1.7	7.7	456365.33	4451922.66	REW island
NSVPC1	T7	0	1.7	2.8	456363.85	4451927.33	LEW island
NSVPC1	T7	54	2.1	2.7	456363.82	4451927.43	BF, ToC
NSVPC1	T7	15	2.2	0	456363.00	4451930.00	VL edge
NSVPC1	T8	47	0.4	32.6	456383.55	4451897.83	VR edge, ToC
NSVPC1	T8	0	0.1	32.1	456383.42	4451898.32	BF, ToC
NSVPC1	T8	0	0	31.3	456383.23	4451899.10	REW
NSVPC1	T8	0	0	20	456380.51	4451910.06	LEW, island, FP
NSVPC1	T8	52	0.3	19.3	456380.34	4451910.74	BF, island
NSVPC1	T8	60	0.3	18.3	456380.10	4451911.71	S8.0 (0-9, duff), S8.1 (9-24), S8.2 (24-39), S8.3
NSVPC1	T8	67	0.3	17.1	456379.81	4451912.88	FP edge, toe of veg island, valley edge
NSVPC1	T8	22	0.7	16	456379.55	4451913.95	top island edge
NSVPC1	T8	74	0.4	10.6	456378.25	4451919.19	island, FP, OB channel
NSVPC1	T8	25	0.7	7.1	456377.41	4451922.58	island, FP, OB channel
NSVPC1	T8	5	0.2	6.3	456377.22	4451923.36	BF at RL of island
NSVPC1	T8	0	-0.1	6	456377.14	4451923.65	REW side channel
NSVPC1	T8	0	-0.1	1.6	456376.08	4451927.92	REW
NSVPC1	T8	31	0.3	1.4	456376.04	4451928.12	BF
NSVPC1	T8	19	0.5	0	456375.70	4451929.48	VL edge
NSVPC1	T9	31	0.7	29.2	456395.37	4451896.69	VR edge
NSVPC1	T9	79	0.5	28.3	456395.15	4451897.56	S5.0 (0-6, duff), S5.1 (6-22), S5.2 (22-37), S5.3

NSVPC1	T9	55	0.4	27.4	456394.93	4451898.43	
NSVPC1	T9	0	0.1	26.7	456394.76	4451899.11	REW
NSVPC1	T9	0	0.1	14.3	456391.72	4451911.14	LEW
NSVPC1	T9	22	0.2	14.2	456391.70	4451911.23	ToC
NSVPC1	T9	3	0	10.4	456390.77	4451914.92	FP, OB channel, S9.0 (0-3, duff)
NSVPC1	T9	6	0.5	7.6	456390.08	4451917.63	top of island
NSVPC1	T9	27	0.2	5.9	456389.67	4451919.28	BF, RR side channel
NSVPC1	T9	0	0	5.7	456389.62	4451919.47	REW
NSVPC1	T9	0	0	2	456388.71	4451923.06	LEW
NSVPC1	T9	10	0.3	1.8	456388.66	4451923.25	BF
NSVPC1	T9	19	0.7	0	456388.22	4451925.00	VL edge
NSVPC1	T10	33	0.7	25.9	456406.54	4451898.72	VR
NSVPC1	T10	33	0.5	25.2	456406.39	4451899.41	S6.0 (0-7, duff), S6.1 (7-22), S6.2 (22-33), VR
NSVPC1	T10	56	0.4	24.6	456406.26	4451900.00	BF
NSVPC1	T10	18	0.2	23.5	456406.03	4451901.07	
NSVPC1	T10	0	0	22.7	456405.87	4451901.85	REW
NSVPC1	T10	0	0	3.9	456401.95	4451920.24	LEW
NSVPC1	T10	41	0.2	3.9	456401.95	4451920.24	BF, grassy FP
NSVPC1	T10	69	0.3	2	456401.55	4451922.10	S10.0 (0-8, duff), S10.1 (8-23), S10.2 (23-38),
NSVPC1	T10	30	0.4	0	456401.13	4451924.05	VL edge
NSVPC1	T11	55	0.6	20.8	456417.91	4451901.52	VR edge
NSVPC1	T11	25	0.4	19.9	456417.68	4451902.39	S7.0 (0-7, duff), S7.1 (7-22), S7.2 (22-25), VR
NSVPC1	T11	33	0.3	19.1	456417.48	4451903.17	BF
NSVPC1	T11	69	0	17.8	456417.16	4451904.43	inactive side channel
NSVPC1	T11	30	0.2	16.2	456416.76	4451905.98	~BF elevation
NSVPC1	T11	0	0	15.8	456416.66	4451906.36	REW
NSVPC1	T11	0	0	1.1	456413.00	4451920.60	LEW
NSVPC1	T11	0	0.3	0.3	456412.80	4451921.38	BF, cobs
NSVPC1	T11	0	0.6	0	456412.73	4451921.67	VL edge, ToC
CCKUC1	T1	0	0.4	12.1	448692.45	4447650.44	VR edge
CCKUC1	T1	10	0.2	10.1	448690.89	4447651.69	BF, S1
CCKUC1	T1	0	0	8.9	448689.95	4447652.44	REW

CCKUC1	T1	0	0	4.1	448686.20	4447655.44	LEW
CCKUC1	T1	32	0.4	3.9	448686.05	4447655.56	BF
CCKUC1	T1	32	0.5	0	448683.00	4447658.00	VL edge
CCKUC1	T2	45	0.6	20.1	448701.69	4447650.29	VR edge
CCKUC1	T2	12	0.2	13.1	448696.58	4447655.06	S2, FP
CCKUC1	T2	9	0.2	11.8	448695.63	4447655.95	BF, FP
CCKUC1	T2	0	0	11.6	448695.48	4447656.09	REW
CCKUC1	T2	0	0	6.7	448691.90	4447659.43	LEW
CCKUC1	T2	68	0.3	6.6	448691.82	4447659.50	BF
CCKUC1	T2	100	0.8	0	448687.00	4447664.00	VL edge
CCKUC1	T3	49	0.4	20.1	448706.69	4447654.29	VR edge
CCKUC1	T3	59	0.5	16	448703.70	4447657.08	FP
CCKUC1	T3	46	0.4	12.7	448701.28	4447659.33	ToC, BF
CCKUC1	T3	0	0	12.7	448701.28	4447659.33	REW
CCKUC1	T3	0	0	6	448696.39	4447663.91	LEW
CCKUC1	T3	21	0.2	2.6	448693.90	4447666.23	BF
CCKUC1	T3	57	0.6	0	448692.00	4447668.00	S10. meadow, VL edge
CCKUC1	T4	16	0.2	25.7	448714.15	4447656.86	VR edge
CCKUC1	T4	50	0.5	18.2	448708.56	4447661.86	FP, Tree hummock
CCKUC1	T4	54	0.1	13.9	448705.36	4447664.73	BF, S3
CCKUC1	T4	21	0	11.9	448703.87	4447666.07	REW
CCKUC1	T4	0	0	6.1	448699.55	4447669.93	LEW
CCKUC1	T4	17	0.4	2.7	448697.01	4447672.20	BF RL
CCKUC1	T4	73	0.6	0	448695.00	4447674.00	VL ege
CCKUC1	T5	28	0	24.3	448716.16	4447662.86	VR edge
CCKUC1	T5	31	0.1	21	448713.70	4447665.05	S4, FP
CCKUC1	T5	48	0.6	13.7	448708.24	4447669.90	tree hummock
CCKUC1	T5	25	0.3	12.1	448707.04	4447670.96	BF, ToC
CCKUC1	T5	49	0	9.1	448704.80	4447672.95	REW
CCKUC1	T5	0	0	2.7	448700.02	4447677.21	LEW
CCKUC1	T5	24	0.4	2.6	448699.94	4447677.27	ToC, BF
CCKUC1	T5	99	0.5	0	448698.00	4447679.00	VL edge

CCKUC1	T6	0	-0.1	26.7	448721.24	4447667.82	VR edge, rock side channel
CCKUC1	T6	24	0.2	21.1	448716.78	4447671.21	FP
CCKUC1	T6	21	0	19.3	448715.35	4447672.30	FP, S5
CCKUC1	T6	30	0.1	13.2	448710.50	4447676.00	BF
CCKUC1	T6	37	0	8.4	448706.68	4447678.91	grassy REW
CCKUC1	T6	0	0	1.8	448701.43	4447682.91	LEW
CCKUC1	T6	28	0.3	1.7	448701.35	4447682.97	ToC, BF
CCKUC1	T6	85	0.4	0	448700.00	4447684.00	VL edge
CCKUC1	T7	22	0.1	30.6	448727.32	4447673.40	VR ege
CCKUC1	T7	39	0.5	21.5	448719.50	4447678.04	FP, tree hummock
CCKUC1	T7	24	0.4	9.6	448709.26	4447684.11	FP, S6
CCKUC1	T7	26	0.4	8.1	448707.97	4447684.87	ToC, BF
CCKUC1	T7	0	0	8.1	448707.97	4447684.87	REW
CCKUC1	T7	0	0	2.9	448703.49	4447687.52	LEW
CCKUC1	T7	51	0.4	2.9	448703.49	4447687.52	BF, ToC
CCKUC1	T7	55	0.7	0	448701.00	4447689.00	VL edge
CCKUC1	T8	42	0	34	448732.41	4447677.79	VR edge
CCKUC1	T8	30	0	25.2	448724.54	4447681.73	FP
CCKUC1	T8	29	0.3	19.6	448719.53	4447684.23	FP
CCKUC1	T8	0	0.3	15.1	448715.51	4447686.25	S7, FP
CCKUC1	T8	20	0.3	11.5	448712.29	4447687.86	ToC, BF
CCKUC1	T8	0	0	11.4	448712.20	4447687.90	REW
CCKUC1	T8	0	0	7	448708.26	4447689.87	LEW
CCKUC1	T8	68	0.4	6.8	448708.08	4447689.96	ToC, BF
CCKUC1	T8	95	0.9	0	448702.00	4447693.00	VL edge
CCKUC1	T9	40	0	33.2	448733.69	4447683.15	VR edge
CCKUC1	T9	23	-0.2	30.2	448731.01	4447684.49	S8, OB channel
CCKUC1	T9	14	0.1	24.6	448726.00	4447687.00	
CCKUC1	T9	27	0.3	13.8	448716.34	4447691.83	BF, ToC
CCKUC1	T9	0	0	13.7	448716.25	4447691.87	REW
CCKUC1	T9	0	0	8.4	448711.51	4447694.24	LEW
CCKUC1	T9	65	0.3	8.4	448711.51	4447694.24	BF ToC

CCKUC1	T9	59	0.5	0	448704.00	4447698.00	VL edge
CCKUC1	T10	11	-0.2	28.8	448731.95	4447688.51	VR edge
CCKUC1	T10	9	0.1	22.8	448726.54	4447691.11	FP
CCKUC1	T10	11	0.5	17.5	448721.77	4447693.41	FP
CCKUC1	T10	12	0.5	14.5	448719.06	4447694.71	ToC
CCKUC1	T10	0	0	14.4	448718.97	4447694.75	REW
CCKUC1	T10	0	0	7.8	448713.03	4447697.62	LEW
CCKUC1	T10	12	0.3	7.6	448712.85	4447697.70	BF, ToC
CCKUC1	T10	31	0.4	5.6	448711.05	4447698.57	FP side channel, S11
CCKUC1	T10	47	0.3	0	448706.00	4447701.00	VL edge
CCKUC1	T11	28	0	26	448733.05	4447691.97	VR edge
CCKUC1	T11	12	0.1	23.4	448730.75	4447693.18	S9, FP
CCKUC1	T11	41	0.5	14	448722.41	4447697.52	FP, Tree hummock
CCKUC1	T11	29	0.3	9.4	448718.33	4447699.65	BF, ToC
CCKUC1	T11	0	0	9.3	448718.25	4447699.70	REW
CCKUC1	T11	0	0	4.7	448714.17	4447701.83	LEW
CCKUC1	T11	42	0.4	3.1	448712.75	4447702.57	BF, ToC
CCKUC1	T11	30	0.3	0	448710.00	4447704.00	VL edge
GCKMT2	T1	32	0.8	25.8	445720.78	4458972.01	VR edge, wet mossy
GCKMT2	T1	0	-0.2	20.5	445715.48	4458972.21	side channel, sd-pebs
GCKMT2	T1	49	0.3	18.8	445713.79	4458972.28	S1, vegetated island with SAF, ES
GCKMT2	T1	24	0.6	15	445709.99	4458972.42	vegetated island with SAF, ES
GCKMT2	T1	0	0	12.4	445707.39	4458972.52	REW
GCKMT2	T1	0	0	1.1	445696.10	4458972.96	LEW
GCKMT2	T1	0	0.8	0	445695.00	4458973.00	VL edge
GCKMT2	T2	7	2.1	31.1	445722.08	4458978.97	VR edge
GCKMT2	T2	18	1.6	28.6	445719.59	4458978.89	low point
GCKMT2	T2	0	2.3	26.4	445717.39	4458978.82	top of B with trees
GCKMT2	T2	0	0.2	24	445714.99	4458978.75	side channel
GCKMT2	T2	57	0.5	22.4	445713.39	4458978.70	tall grassy bank
GCKMT2	T2	0	0	20	445710.99	4458978.62	dry OB channel, sd-cobs
GCKMT2	T2	27	0.7	18.4	445709.39	4458978.57	root wad, soil slopes to river

GCKMT2	T2	0	1.3	17.4	445708.39	4458978.54	REW, main stem
GCKMT2	T2	0	1.3	11.7	445702.69	4458978.37	LEW main stem
GCKMT2	T2	27	1.9	11.7	445702.69	4458978.37	ToC
GCKMT2	T2	80	2.2	10.6	445701.59	4458978.33	Top of island, S2
GCKMT2	T2	0	2.1	9.2	445700.20	4458978.29	REW side channel
GCKMT2	T2	0	2.1	4.1	445695.10	4458978.13	LEW side channel
GCKMT2	T2	5	2.4	1.9	445692.90	4458978.06	RL, FP
GCKMT2	T2	3	2.6	0	445691.00	4458978.00	VL edge
GCKMT2	T3	83	1.6	34.7	445723.57	4458983.96	VL edge
GCKMT2	T3	28	1.4	32.2	445721.08	4458983.75	OB channel, tree island
GCKMT2	T3		1.5	31.7	445720.58	4458983.71	S3, flowing water
GCKMT2	T3	56	1.6	30.9	445719.79	4458983.64	RL bank
GCKMT2	T3	0	1.3	30.8	445719.69	4458983.63	LEW
GCKMT2	T3	0	1.1	26	445714.91	4458983.22	REW, side channel
GCKMT2	T3	7	0.5	20.3	445709.23	4458982.73	across side channel
GCKMT2	T3	5	0.4	18.7	445707.63	4458982.60	grassy islandwith surface flow
GCKMT2	T3	0	0	18.4	445707.33	4458982.57	LEW
GCKMT2	T3	0	0	14.2	445703.15	4458982.21	REW
GCKMT2	T3	0	0	12.6	445701.55	4458982.08	side channel
GCKMT2	T3	59	0.9	12.5	445701.45	4458982.07	ToC
GCKMT2	T3	34	1.3	10.7	445699.66	4458981.91	ToB
GCKMT2	T3	8	2.3	7	445695.97	4458981.60	duff, large B
GCKMT2	T3	0	1.6	3.1	445692.09	4458981.26	trib
GCKMT2	T3	36	2.3	0	445689.00	4458981.00	VR edge, grassy meadow
GCKMT2	T4	13	0.7	38.2	445724.99	4458990.00	VR edge
GCKMT2	T4	0	-0.1	36.5	445723.30	4458989.82	Tributary, sd_peb, water
GCKMT2	T4	68	0.1	34	445720.81	4458989.56	ToC of trib
GCKMT2	T4	12	0.2	30.9	445717.73	4458989.23	grassy FP
GCKMT2	T4	0	0	29.9	445716.74	4458989.13	REW, main stem
GCKMT2	T4	0	0	25	445711.86	4458988.62	LEW
GCKMT2	T4	36	0.3	22.4	445709.28	4458988.34	Top of grassy island, ES
GCKMT2	T4	0	0	20.6	445707.49	4458988.16	side channel with 13 cm depth

GCKMT2	T4	65	0.4	18.2	445705.10	4458987.91	hummocky log terrace
GCKMT2	T4	0	0.1	11	445697.94	4458987.15	REW, side channel
GCKMT2	T4	0	0.1	6.2	445693.17	4458986.65	LEW side channe;
GCKMT2	T4	220	2.3	6	445692.97	4458986.63	uprooted wad on stream bed, S4
GCKMT2	T4	47	0.8	4.1	445691.08	4458986.43	top of root wad
GCKMT2	T4	22	-0.1	2	445688.99	4458986.21	side channel
GCKMT2	T4	38	0.9	0	445687.00	4458986.00	VL edge
GCKMT2	T5	17	1.1	36.6	445724.38	4458995.04	VL edge
GCKMT2	T5	0	0	34.2	445721.99	4458994.78	side channel, sd-pebs, 40cm deep channel
GCKMT2	T5	39	0.7	32.4	445720.20	4458994.58	base of root wad
GCKMT2	T5	270	2.9	30.4	445718.21	4458994.36	top of root wad
GCKMT2	T5	0	0.2	30.4	445718.21	4458994.36	LEW
GCKMT2	T5	0	0.2	26.2	445714.04	4458993.89	REW
GCKMT2	T5	27	0.4	26.1	445713.94	4458993.88	ToC
GCKMT2	T5	17	0.5	25	445712.85	4458993.76	Top of island
GCKMT2	T5	24	0.4	23.6	445711.46	4458993.61	S5, island
GCKMT2	T5	0	0.1	22.3	445710.16	4458993.46	OB channel, sd-pebs
GCKMT2	T5	49	0.6	18.5	445706.39	4458993.04	top of island, FP with grass/trees
GCKMT2	T5	47	0.6	15.7	445703.60	4458992.73	top of island, FP with grass/trees
GCKMT2	T5	0	0.4	12.7	445700.62	4458992.40	LEW side channel
GCKMT2	T5	0	0.4	11.3	445699.23	4458992.25	REW side channel, left edge of island
GCKMT2	T5	10	0.5	10.4	445698.34	4458992.15	top of island
GCKMT2	T5	0	0.4	9.6	445697.54	4458992.06	LEW
GCKMT2	T5	0	0.4	2.4	445690.39	4458991.27	REW
GCKMT2	T5	46	0.7	2.3	445690.29	4458991.25	ToC
GCKMT2	T5	15	1.1	0	445688.00	4458991.00	VR edge
GCKMT2	T6	0	2.3	36.8	445722.59	4458998.96	VR edge
GCKMT2	T6	21	1.8	35.4	445721.19	4458998.80	ToC RR
GCKMT2	T6	0	1.6	35.3	445721.10	4458998.79	REW
GCKMT2	T6	0	1.6	28.2	445714.04	4458998.03	LEW
GCKMT2	T6	34	1.9	26.4	445712.25	4458997.84	base of root wad
GCKMT2	T6	35	2.1	23.9	445709.76	4458997.57	upland FP w? grass

GCKMT2	T6	21	1.8	20.2	445706.08	4458997.17	OB channel
GCKMT2	T6	84	1.4	19	445704.89	4458997.04	top of island
GCKMT2	T6	12	0.6	16.5	445702.40	4458996.77	OB channel
GCKMT2	T6	24	0.9	13.8	445699.72	4458996.48	S6, FP grassy island
GCKMT2	T6	43	0.6	9.6	445695.54	4458996.03	ToC, RR
GCKMT2	T6	0	0.2	9.5	445695.44	4458996.02	REW side channel
GCKMT2	T6	0	0.2	7.6	445693.56	4458995.82	LEW
GCKMT2	T6	52	0.5	7.3	445693.26	4458995.78	ToC, RL
GCKMT2	T6	5	0.5	4.9	445690.87	4458995.53	duff on B
GCKMT2	T6	31	0	4	445689.98	4458995.43	OB channel
GCKMT2	T6	26	0.3	0.5	445686.50	4458995.05	FP w? grass
GCKMT2	T6	39	0.4	0	445686.00	4458995.00	VL edge
GCKMT2	T7	61	1.5	31.2	445719.14	4459001.95	VR edge
GCKMT2	T7	0	0.7	29.2	445717.14	4459001.82	REW on B
GCKMT2	T7	0	0.4	24.7	445712.65	4459001.54	LEW
GCKMT2	T7	32	0.7	23.9	445711.85	4459001.49	ToC, RL, S7
GCKMT2	T7	67	0.9	20.1	445708.06	4459001.25	veg FP
GCKMT2	T7	10	0.1	12.2	445700.18	4459000.76	OB channel
GCKMT2	T7	33	0.4	10.2	445698.18	4459000.64	Top of bank
GCKMT2	T7	3	0.2	6.4	445694.39	4459000.40	ToC, RR
GCKMT2	T7	0	0	6.3	445694.29	4459000.39	REW
GCKMT2	T7	0	0	2.1	445690.10	4459000.13	LEW
GCKMT2	T7	6	0.2	1.9	445689.90	4459000.12	ToC, RL
GCKMT2	T7	54	0.6	0	445688.00	4459000.00	sloped FP, VL edge
GCKMT2	T8	60	0.4	32.8	445719.78	4459005.99	VL edge
GCKMT2	T8	0	0	31.6	445718.59	4459005.96	LEW, side
GCKMT2	T8	0	0	29.3	445716.29	4459005.89	REW, side
GCKMT2	T8	35	0.4	29.2	445716.19	4459005.88	ToC, RR
GCKMT2	T8	26	0.5	25.5	445712.49	4459005.77	FP island, S8
GCKMT2	T8	0	0.1	23.1	445710.09	4459005.70	OB channel
GCKMT2	T8	0	0.1	19.8	445706.79	4459005.60	OB channel
GCKMT2	T8	33	0.7	15.5	445702.49	4459005.47	tree hummock on veg island

GCKMT2	T8	43	0.5	9.2	445696.20	4459005.28	veg island
GCKMT2	T8	15	0.2	6.5	445693.50	4459005.20	ToC RL main stem
GCKMT2	T8	0	0	6.4	445693.40	4459005.19	LEW, main
GCKMT2	T8	0	0	0.9	445687.90	4459005.03	REW main
GCKMT2	T8	2	0.4	0.8	445687.80	4459005.02	litter on rock
GCKMT2	T8	8	0.6	0	445687.00	4459005.00	VR edge
GCKMT2	T9	50	0.9	36.1	445717.05	4459009.95	VR edge
GCKMT2	T9	37	0.5	33.3	445714.25	4459009.80	ToC, RR
GCKMT2	T9	0	0.2	33.2	445714.15	4459009.79	REW
GCKMT2	T9	0	0.2	25.1	445706.06	4459009.35	LEW
GCKMT2	T9	50	0.8	24.8	445705.76	4459009.34	ToC, RL, tree thrown root wad
GCKMT2	T9	43	0.7	20.3	445701.27	4459009.10	veg grassy island, tree hummock
GCKMT2	T9	0	0.1	17.3	445698.27	4459008.93	OB channel
GCKMT2	T9	6	0.4	14.4	445695.38	4459008.78	S9, small grassy island on B
GCKMT2	T9	0	0	13.2	445694.18	4459008.71	REW, side channel
GCKMT2	T9	0	0	10.9	445691.88	4459008.59	LEW side
GCKMT2	T9	33	0.5	10.6	445691.58	4459008.57	ToC island
GCKMT2	T9	29	1.5	6.6	445687.59	4459008.36	ToC RR side channel
GCKMT2	T9	0	1.1	6.3	445687.29	4459008.34	REW side chan
GCKMT2	T9	0	1.1	2.1	445683.10	4459008.11	LEW side chan
GCKMT2	T9	35	1.4	1.9	445682.90	4459008.10	ToC RL
GCKMT2	T9	10	1.7	0	445681.00	4459008.00	VL edge
GCKMT2	T10	19	0.4	34.7	445715.64	4459013.98	VL edge
GCKMT2	T10	35	0.3	30.4	445711.35	4459013.73	ToB
GCKMT2	T10	0	0	30.1	445711.05	4459013.72	LEW side chan
GCKMT2	T10	0	0	27.8	445708.75	4459013.59	REW side chan
GCKMT2	T10	31	0.3	27.5	445708.46	4459013.57	ToC RR island
GCKMT2	T10	42	0.5	22.2	445703.16	4459013.27	ToC
GCKMT2	T10	0	0.1	22	445702.96	4459013.26	LEW side chan'
GCKMT2	T10	0	0.1	16.8	445697.77	4459012.96	REW side chan
GCKMT2	T10	12	0.3	16.5	445697.47	4459012.94	TOC RR side chan
GCKMT2	T10	21	0.5	10.7	445691.68	4459012.61	ToC RL main stem, S10

GCKMT2	T10	0	0.2	10.6	445691.58	4459012.60	LEW main
GCKMT2	T10	0	0.2	4	445684.99	4459012.23	REW main
GCKMT2	T10	35	0.6	3.8	445684.79	4459012.22	ToC RR main
GCKMT2	T10	69	1	0	445681.00	4459012.00	VR edge
GCKMT2	T11	0	0	26.8	445711.78	4459017.99	LEW, VL edge on B
GCKMT2	T11	0	0	0	445685.00	4459017.00	REW, VR edge on other side of very wide main
OCKPC2	T1	27	0.9	17	448259.98	4450159.09	Vr edge
OCKPC2	T1	0	0.4	16.3	448259.79	4450159.77	BF, RR on B
OCKPC2	T1	0	0	15.6	448259.61	4450160.44	REW
OCKPC2	T1	0	0.2	10.5	448258.29	4450165.37	LEW
OCKPC2	T1	0	0.4	10.4	448258.26	4450165.46	BF RL cutbank
OCKPC2	T1	41	0.5	10.3	448258.23	4450165.56	ToC
OCKPC2	T1	55	0.7	8.4	448257.74	4450167.39	FP, S1
OCKPC2	T1	19	0.7	0	448255.56	4450175.51	VL edge
OCKPC2	T2	8	1	17.2	448264.96	4450161.22	VR edge
OCKPC2	T2	6	0.7	15.9	448264.72	4450162.49	BF, RR
OCKPC2	T2	0	0.2	15.2	448264.60	4450163.18	REW
OCKPC2	T2	0	0	9.7	448263.60	4450168.59	LEW
OCKPC2	T2	35	0.2	9.3	448263.53	4450168.98	BF RL
OCKPC2	T2	30	0.5	8.5	448263.38	4450169.77	ToC, S2
OCKPC2	T2	12	0.8	0	448261.84	4450178.13	VL ege, FP toe of terrace
OCKPC2	T3	7	0.4	12	448269.99	4450164.48	VR edge
OCKPC2	T3	21	0.3	11.8	448269.97	4450164.68	BF RR
OCKPC2	T3	0	0	11.4	448269.92	4450165.07	REW
OCKPC2	T3	0	0.2	6.4	448269.31	4450170.04	LEW
OCKPC2	T3	20	0.4	6.2	448269.28	4450170.24	BF RL, ToC
OCKPC2	T3	29	0.5	3.1	448268.90	4450173.31	S3, FP
OCKPC2	T3	29	0.8	0	448268.52	4450176.39	VL edge, toe of terrace
OCKPC2	T4	46	0.6	11.3	448275.64	4450164.32	VR edge
OCKPC2	T4	35	0.4	9.7	448275.64	4450165.92	BF, ToC
OCKPC2	T4	0	0.1	9.5	448275.64	4450166.12	REW
OCKPC2	T4	0	0	4.5	448275.64	4450171.12	LEW

OCKPC2	T4	0	0.2	4.3	448275.64	4450171.32	BF RL on B
OCKPC2	T4	32	0.4	3.6	448275.64	4450172.02	ToC
OCKPC2	T4	12	0.5	1.7	448275.64	4450173.92	FP, S4
OCKPC2	T4	24	0.7	0	448275.64	4450175.62	VL edge, toe of terrace
OCKPC2	T5	8	0.7	12.7	448282.82	4450161.13	VR edge, FP
OCKPC2	T5	20	0.3	10	448282.78	4450163.83	BF, FP
OCKPC2	T5	0	0	9.6	448282.78	4450164.23	REW
OCKPC2	T5	0	0.3	3.1	448282.68	4450170.73	LEW
OCKPC2	T5	32	0.5	2.9	448282.68	4450170.93	BF, ToC
OCKPC2	T5	17	0.9	1.3	448282.66	4450172.53	FP, S5
OCKPC2	T5	14	1	0	448282.64	4450173.83	FP, VL edge
OCKPC2	T6	10	0.7	10.7	448289.43	4450159.31	VR edge
OCKPC2	T6	54	0.4	9.6	448289.38	4450160.41	BF RR
OCKPC2	T6	0	0	9.2	448289.37	4450160.81	REW
OCKPC2	T6	0	0.1	4.2	448289.17	4450165.80	LEW
OCKPC2	T6	21	0.3	4.2	448289.17	4450165.80	BF RL
OCKPC2	T6	19	0.6	2.3	448289.09	4450167.70	S6, FP
OCKPC2	T6	16	0.7	0	448289.00	4450170.00	VL edge
OCKPC2	T7	8	0.7	13.1	448297.46	4450158.22	VR edge
OCKPC2	T7	23	0.3	12.1	448297.36	4450159.22	BF RR
OCKPC2	T7	0	0	11.6	448297.31	4450159.72	REW
OCKPC2	T7	0	0.1	5.6	448296.72	4450165.69	LEW
OCKPC2	T7	25	0.4	4.7	448296.63	4450166.58	BF RL
OCKPC2	T7	18	0.5	2.5	448296.41	4450168.77	S7, FP
OCKPC2	T7	15	0.8	0	448296.16	4450171.26	VL edge toe of terrace
OCKPC2	T8	21	0.6	16.4	448303.21	4450157.85	VR edge
OCKPC2	T8	0	0.4	14.9	448303.08	4450159.34	BF RR
OCKPC2	T8	0	0.1	14.3	448303.03	4450159.94	REW
OCKPC2	T8	0	0	7.5	448302.48	4450166.72	LEW
OCKPC2	T8	0	0.3	6.9	448302.43	4450167.31	BF RL
OCKPC2	T8	33	0.5	6.5	448302.40	4450167.71	ToC
OCKPC2	T8	7	0.7	3.4	448302.14	4450170.80	S8, FP

OCKPC2	T8	4	0.9	0	448301.87	4450174.19	FP, VL edge, toe of terrace
OCKPC2	T9	3	0.7	14.2	448308.00	4450159.06	VR edge
OCKPC2	T9	53	0.4	13.8	448307.97	4450159.46	BF RR
OCKPC2	T9	0	0	13.3	448307.93	4450159.96	REW
OCKPC2	T9	0	0.3	7.6	448307.52	4450165.64	LEW
OCKPC2	T9	72	0.7	6.8	448307.47	4450166.44	BF RL
OCKPC2	T9	6	1	3.4	448307.22	4450169.83	S9 on cobs
OCKPC2	T9	12	1.1	0	448306.98	4450173.22	VL edge
OCKPC2	T10	0	0.7	15.3	448314.97	4450158.44	VR edge, B
OCKPC2	T10	0	0.2	12.8	448314.56	4450160.90	BF B
OCKPC2	T10	0	0	12.1	448314.45	4450161.59	REW
OCKPC2	T10	0	0.1	6.4	448313.51	4450167.22	LEW
OCKPC2	T10	14	0.3	6.2	448313.48	4450167.41	BF RL
OCKPC2	T10	5	0.6	2.4	448312.86	4450171.16	FP, S10, duff on cobbles
OCKPC2	T10	24	0.5	0	448312.46	4450173.53	VL edge
OCKPC2	T11	21	0.9	18.4	448321.02	4450157.91	VR edge
OCKPC2	T11	8	0.7	16.6	448320.68	4450159.68	S12
OCKPC2	T11	19	0.8	15.8	448320.53	4450160.46	berm, log on B
OCKPC2	T11	20	0.3	14.7	448320.32	4450161.55	BF
OCKPC2	T11	0	0	14.5	448320.28	4450161.74	REW
OCKPC2	T11	0	0	8.9	448319.23	4450167.24	LEW
OCKPC2	T11	25	0.3	8.8	448319.21	4450167.34	BF RL
OCKPC2	T11	9	0.7	3.9	448318.29	4450172.15	FP, S11
OCKPC2	T11	27	0.7	0	448317.55	4450175.98	VL edge, FP
OCKAB2	T1	29	0.2	46.5	447587.91	4450410.61	VR edge, S1
OCKAB2	T1	0	0	45.3	447588.17	4450411.78	side channel\
OCKAB2	T1	53	0.5	44.4	447588.37	4450412.66	top of berm island, E
OCKAB2	T1	51	0.2	42	447588.89	4450415.00	REW edge of island/side channel
OCKAB2	T1	46	0	40.7	447589.17	4450416.27	LEW side channel, grasses
OCKAB2	T1	22	0.4	34.2	447590.58	4450422.61	veg island, E
OCKAB2	T1	38	0.5	28.8	447591.75	4450427.89	veg island, E
OCKAB2	T1	19	0.6	21.1	447593.42	4450435.40	log mossy hummock

OCKAB2	T1	19	0.2	18	447594.10	4450438.43	mian stem, berm, ToC
OCKAB2	T1	0	0.1	17.9	447594.12	4450438.53	REW
OCKAB2	T1	0	0.1	11.9	447595.42	4450444.38	LEW
OCKAB2	T1	58	0.4	11.7	447595.46	4450444.58	ToC RL
OCKAB2	T1	35	0.3	3.5	447597.24	4450452.58	grassy BM
OCKAB2	T1	0	0.4	0	447598.00	4450456.00	VL edge, cobs
OCKAB2	T2	2	0.3	46	447596.02	4450410.10	VR edge, S2
OCKAB2	T2	30	0	43.9	447596.48	4450412.15	REW
OCKAB2	T2	19	0.2	40.4	447597.24	4450415.56	LEW
OCKAB2	T2	33	0.4	35.8	447598.23	4450420.05	S3, veg island, ES
OCKAB2	T2	15	0.4	28.6	447599.80	4450427.08	veg island, wet grassy BM, old growth
OCKAB2	T2	33	0.4	27.5	447600.03	4450428.15	S4, wet grassy BM vegetated island
OCKAB2	T2	46	0.6	19.5	447601.77	4450435.96	grassy meadow berm, REW, main stem
OCKAB2	T2	0	0.7	11.5	447603.51	4450443.77	OB flow, grassy BM
OCKAB2	T2	58	1.1	10.2	447603.79	4450445.04	LEW
OCKAB2	T2	83	1.3	4.2	447605.09	4450450.90	grassy BM
OCKAB2	T2	18	1.3	0	447606.00	4450455.00	VL edge
OCKAB2	T3	18	0.2	36.3	447604.07	4450412.37	ES, old VR edge
OCKAB2	T3	49	0	34.2	447604.47	4450414.43	on logs downed wood, Esside channel, REW
OCKAB2	T3	39	0	31.5	447604.99	4450417.08	LEW, side channel
OCKAB2	T3	47	0.2	25.1	447606.21	4450423.36	
OCKAB2	T3	31	0.3	19.2	447607.34	4450429.15	log tree hummock, grassy berm
OCKAB2	T3	27	0.7	14.6	447608.21	4450433.67	REW main stem, grass berm
OCKAB2	T3	8	0.7	11.2	447608.86	4450437.01	LEW island
OCKAB2	T3	44	0.9	9.7	447609.15	4450438.48	island, S5
OCKAB2	T3	46	1	8.4	447609.40	4450439.75	REW island
OCKAB2	T3	24	1.1	8.3	447609.42	4450439.85	wet BM, LEW side channel
OCKAB2	T3	46	1.5	5	447610.05	4450443.09	grassy hummock
OCKAB2	T3	11	1.2	0	447611.00	4450448.00	grassy BM, VL edge
OCKAB2	T4	9	0.3	43.4	447606.81	4450405.35	VR edge
OCKAB2	T4	48	0.2	41.7	447607.29	4450406.98	FP, S6
OCKAB2	T4	0	0	41.1	447607.46	4450407.55	REW side channel

OCKAB2	T4	0	0	39.1	447608.02	4450409.47	LEW
OCKAB2	T4	62	0.5	36.5	447608.75	4450411.97	grassy island, ES, old growth
OCKAB2	T4	46	0.6	33.4	447609.62	4450414.94	S7, grassy edge of old growth ES and burn area
OCKAB2	T4	17	0.4	25.2	447611.92	4450422.81	burn area, grassy
OCKAB2	T4	0	0.3	25.1	447611.95	4450422.91	REW
OCKAB2	T4	0	0.3	7.7	447616.84	4450439.61	LEW
OCKAB2	T4	45	0.4	7.6	447616.87	4450439.71	wet grassy BM
OCKAB2	T4	55	0.5	4.7	447617.68	4450442.49	wet grassy BM
OCKAB2	T4	1	0.5	0	447619.00	4450447.00	VL edge
OCKAB2	T5	22	0.5	45.8	447614.12	4450401.51	VR slope
OCKAB2	T5	59	0.6	43.9	447614.58	4450403.36	top of grassy hummock, burn
OCKAB2	T5	23	0.1	41.5	447615.15	4450405.69	ToC
OCKAB2	T5	0	0	41.4	447615.17	4450405.78	side channel, REW
OCKAB2	T5	0	0	40.4	447615.41	4450406.76	LEW, side channel
OCKAB2	T5	26	0.3	39.6	447615.60	4450407.53	grassy meadow, burn
OCKAB2	T5	45	0.4	31	447617.64	4450415.89	grassy meadow, burn
OCKAB2	T5	49	0.4	26.5	447618.71	4450420.26	grassy meadow, burn, ToC
OCKAB2	T5	0	0.1	26.2	447618.78	4450420.55	REW, main stem
OCKAB2	T5	0	0	20.8	447620.06	4450425.79	LEW, main stem
OCKAB2	T5	73	0.7	19.9	447620.27	4450426.67	island
OCKAB2	T5	0	0.2	19.5	447620.37	4450427.06	REW, side channel
OCKAB2	T5	0	0.2	16.5	447621.08	4450429.97	LEW, side channel
OCKAB2	T5	62	0.4	14.5	447621.56	4450431.91	island
OCKAB2	T5	55	0.4	12.4	447622.06	4450433.95	ToC RR
OCKAB2	T5	0	0.3	12.3	447622.08	4450434.05	REW
OCKAB2	T5	0	0.3	9.1	447622.84	4450437.16	LEW
OCKAB2	T5	38	0.4	9	447622.86	4450437.26	Wet grassy BM
OCKAB2	T5	19	0.5	5.8	447623.62	4450440.37	Wet grassy BM
OCKAB2	T5	6	0.7	0	447625.00	4450446.00	VL edge
OCKAB2	T6	35	0.5	55.4	447617.08	4450394.25	VR edge
OCKAB2	T6	18	0.4	49.4	447618.91	4450399.96	FP, grassy meadow, ES
OCKAB2	T6	33	0.3	42.4	447621.05	4450406.63	ToC, RR

OCKAB2	T6	0	0.2	41.8	447621.23	4450407.20	REW, side channel
OCKAB2	T6	0	0.2	40.9	447621.51	4450408.05	LEW side channel
OCKAB2	T6	19	0.6	37.9	447622.42	4450410.91	grassy meadow burn
OCKAB2	T6	26	0.6	31.7	447624.32	4450416.81	grassy meadow burn
OCKAB2	T6	42	0.5	27.1	447625.72	4450421.19	grassy meadow burn
OCKAB2	T6	0	0.2	26.9	447625.78	4450421.39	REW main stem
OCKAB2	T6	0	0	18	447628.50	4450429.86	LEW main stem
OCKAB2	T6	44	0.5	17.6	447628.62	4450430.24	ToC RL, island
OCKAB2	T6	40	0.5	15.4	447629.30	4450432.34	S11, island
OCKAB2	T6	31	0.5	11.2	447630.58	4450436.34	ToC, RR
OCKAB2	T6	0	0.1	10.9	447630.67	4450436.62	REW main stem
OCKAB2	T6	0	0.1	6.3	447632.08	4450441.00	LEW main stem
OCKAB2	T6	70	0.4	5.6	447632.29	4450441.67	ToC, RL
OCKAB2	T6	35	0.3	1.9	447633.42	4450445.19	OB channel, grassy BM
OCKAB2	T6	25	0.5	0	447634.00	4450447.00	VL edge
OCKAB2	T7	12	0.9	55.1	447626.73	4450391.06	VR edge, grassy meadow, W, ES
OCKAB2	T7	51	0.8	46.5	447629.11	4450399.32	FP, grassy meadow
OCKAB2	T7	16	0.5	43.4	447629.97	4450402.30	OB channel
OCKAB2	T7	32	0.8	39.5	447631.05	4450406.05	ToC
OCKAB2	T7	0	0.7	39.1	447631.16	4450406.43	REW side channel
OCKAB2	T7	0	0.7	38.1	447631.44	4450407.39	LEW, side channel
OCKAB2	T7	20	1.1	37.5	447631.61	4450407.97	ToC
OCKAB2	T7	10	0.5	31.4	447633.30	4450413.83	grassy meadow
OCKAB2	T7	16	0.4	25.1	447635.04	4450419.88	R bank, side channel
OCKAB2	T7	0	0.3	24.7	447635.15	4450420.27	REW side channel
OCKAB2	T7	0	0.3	23.2	447635.57	4450421.71	LEW, side channel
OCKAB2	T7	35	0.5	22.6	447635.74	4450422.29	ToC, RL island
OCKAB2	T7	47	0.5	21.7	447635.99	4450423.15	ToC RR, island
OCKAB2	T7	0	0.3	21.4	447636.07	4450423.44	REW side channel
OCKAB2	T7	0	0.3	19.8	447636.51	4450424.98	LEW, side channel
OCKAB2	T7	25	0.4	19.4	447636.62	4450425.36	island ToC, RL
OCKAB2	T7	30	0.5	16.9	447637.32	4450427.76	island, ToC, RR

OCKAB2	T7	0	0.3	16.2	447637.51	4450428.43	REW, main stem
OCKAB2	T7	0	0.1	10.9	447638.98	4450433.53	LEW main stem
OCKAB2	T7	24	0.3	10.9	447638.98	4450433.53	ToC RL
OCKAB2	T7	34	0.2	9.9	447639.26	4450434.49	ToC RR
OCKAB2	T7	0	0.3	9.8	447639.28	4450434.58	REW
OCKAB2	T7	0	0	7.5	447639.92	4450436.79	LEW
OCKAB2	T7	83	0.2	7.3	447639.98	4450436.99	ToC, RL
OCKAB2	T7	3	0.3	4.2	447640.84	4450439.96	grassy BM, W
OCKAB2	T7	3	0	0	447642.00	4450444.00	VL edge
OCKAB2	T8	34	0.7	39.7	447637.47	4450402.72	VR edge, W
OCKAB2	T8	22	0.9	34.9	447638.75	4450407.35	ToC, FP, boulder berm
OCKAB2	T8	23	0.5	30.8	447639.83	4450411.30	ToB, RR, side channel, S8
OCKAB2	T8	0	0.2	30.3	447639.97	4450411.78	REW, side channel
OCKAB2	T8	0	0.2	28	447640.58	4450414.00	LEW side channel
OCKAB2	T8	18	0.5	27.3	447640.76	4450414.68	ToC, RL, grassy BM
OCKAB2	T8	12	0.2	20.4	447642.59	4450421.33	wet BM with grass, W
OCKAB2	T8	69	0.6	15	447644.02	4450426.54	ToC, RR, side channel
OCKAB2	T8	0	0.2	14.6	447644.13	4450426.92	REW
OCKAB2	T8	0	0	10.7	447645.16	4450430.68	LEW
OCKAB2	T8	56	0.7	7.9	447645.91	4450433.38	Top of grassy island
OCKAB2	T8	0	0.5	6	447646.41	4450435.21	REW, side channel
OCKAB2	T8	0	0.5	5	447646.67	4450436.18	LEW side channel
OCKAB2	T8	27	1	3.8	447646.99	4450437.34	top of island
OCKAB2	T8	0	0.3	2.7	447647.28	4450438.40	REW, main stem
OCKAB2	T8	38	0.6	2.7	447647.28	4450438.40	ToC
OCKAB2	T8	6	0.7	0	447648.00	4450441.00	grassy BM, VL edge
OCKAB2	T9	21	1.8	46.5	447642.19	4450396.60	VR ege, S9
OCKAB2	T9	21	1.5	41.9	447643.55	4450400.99	grassy, BM
OCKAB2	T9	10	1.4	39.3	447644.33	4450403.47	ToC, RR
OCKAB2	T9	0	1	39	447644.41	4450403.76	REW, side channel
OCKAB2	T9	0	1	36.2	447645.25	4450406.43	LEW, side channel
OCKAB2	T9	33	1.1	36	447645.31	4450406.63	ToC, RL, W

OCKAB2	T9	30	0.8	29.4	447647.27	4450412.93	grassy BM, W
OCKAB2	T9	56	0.8	27.4	447647.86	4450414.84	ToC, RR, W
OCKAB2	T9	0	0.5	27.3	447647.89	4450414.93	REW, side channel
OCKAB2	T9	0	0.3	24.6	447648.69	4450417.51	LEW, side channel
OCKAB2	T9	33	0.4	24.5	447648.72	4450417.61	tToC, RL bank, grassy, W
OCKAB2	T9	68	0.7	17.1	447650.92	4450424.67	grassy BM island, W
OCKAB2	T9	10	0.4	14.8	447651.60	4450426.87	grassy BM island, W
OCKAB2	T9	0	0.3	14.7	447651.63	4450426.96	REW, main stem
OCKAB2	T9	0	0	6.7	447654.01	4450434.60	LEW, main stem
OCKAB2	T9	29	0.4	6.6	447654.04	4450434.70	TOC, RL
OCKAB2	T9	10	0.5	1.4	447655.58	4450439.66	grassy BM, W
OCKAB2	T9	2	0.6	0	447656.00	4450441.00	VL edge
OCKAB2	T10	6	1.2	38.5	447649.19	4450402.46	VR edge, S10
OCKAB2	T10	25	0.8	33.2	447651.23	4450407.35	grassy BM, W
OCKAB2	T10	0	0.6	32.9	447651.35	4450407.63	REW side channel
OCKAB2	T10	0	0.6	31.8	447651.77	4450408.65	LEW side channel
OCKAB2	T10	38	0.8	30.3	447652.35	4450410.03	top of grassy BM island
OCKAB2	T10	14	0.3	27.5	447653.42	4450412.62	ToC, RR
OCKAB2	T10	0	0	27.3	447653.50	4450412.80	REW side channel
OCKAB2	T10	0	0	22.8	447655.23	4450416.95	LEW side channel
OCKAB2	T10	22	0.3	22.6	447655.31	4450417.14	ToC, RL
OCKAB2	T10	87	0.7	18.3	447656.96	4450421.11	grassy BM island
OCKAB2	T10	27	0.9	16.5	447657.65	4450422.77	ToC, bank
OCKAB2	T10	0	0.6	16.3	447657.73	4450422.95	REW main stem
OCKAB2	T10	0	0.6	10.8	447659.85	4450428.03	LEW main stem
OCKAB2	T10	83	0.8	10.5	447659.96	4450428.31	ToC, bank
OCKAB2	T10	3	0.9	6	447661.69	4450432.46	grassy BM
OCKAB2	T10	3	0.6	0	447664.00	4450438.00	VL edge, grassy BM
OCKAB2	T11	14	0.5	33.9	447658.10	4450402.26	VR edge
OCKAB2	T11	0	0.2	32.4	447658.62	4450403.66	REW side channel, BK
OCKAB2	T11	0	0.2	31.6	447658.90	4450404.41	LEW side channel
OCKAB2	T11	22	0.6	31.6	447658.90	4450404.41	ToC, RL island

OCKAB2	T11	41	0.4	28.5	447659.99	4450407.31	ToC RR, island
OCKAB2	T11	0	-0.2	28.4	447660.03	4450407.41	REW side channel
OCKAB2	T11	0	-0.2	24.8	447661.29	4450410.78	LEW side channel
OCKAB2	T11	64	0.4	24.3	447661.47	4450411.25	ToC, RL
OCKAB2	T11	21	0.7	17.9	447663.71	4450417.24	Top grassy BM, island
OCKAB2	T11	69	0.6	14.6	447664.87	4450420.33	ToC, RR, main stem
OCKAB2	T11	0	0	14.1	447665.05	4450420.80	REW
OCKAB2	T11	0	0.4	9.4	447666.70	4450425.20	LEW
OCKAB2	T11	77	0.7	8.8	447666.91	4450425.76	ToC, RL island
OCKAB2	T11	45	0.8	5.4	447668.10	4450428.94	ToC RR island
OCKAB2	T11	0	0.5	5	447668.24	4450429.32	REW side channel
OCKAB2	T11	0	0.5	4.2	447668.53	4450430.07	LEW side channel
OCKAB2	T11	32	0.6	3.7	447668.70	4450430.54	S13, FP bank
OCKAB2	T11	4	0.6	0	447670.00	4450434.00	VL edge
GCKUC2	T1	35	0.4	24.6	445676.58	4459134.98	VR edge
GCKUC2	T1	55	0.4	19.8	445671.78	4459134.79	FP, ToC
GCKUC2	T1	0	0	19.6	445671.58	4459134.78	REW
GCKUC2	T1	0	0	15.1	445667.09	4459134.60	LEW, diagonal across channel
GCKUC2	T1	46	0.5	15	445666.99	4459134.60	ToC
GCKUC2	T1	40	0.6	13.3	445665.29	4459134.53	Fp, grassy meadow
GCKUC2	T1	37	0.3	4.5	445656.50	4459134.18	S4, meadow
GCKUC2	T1	46	0.3	0	445652.00	4459134.00	VL edge
GCKUC2	T2	29	0.5	31	445681.98	4459142.00	S1, VR edge
GCKUC2	T2	51	0.7	24.5	445675.49	4459141.79	FP, grassy meadow
GCKUC2	T2	38	0.5	22.9	445673.89	4459141.74	ToC
GCKUC2	T2	0	0	22.7	445673.69	4459141.73	REW
GCKUC2	T2	0	0	17.9	445668.89	4459141.58	LEW, diagonal across channel
GCKUC2	T2	52	0.6	17.6	445668.59	4459141.57	ToC
GCKUC2	T2	38	0.6	10.5	445661.49	4459141.34	FP, grassy meadow
GCKUC2	T2	30	0.6	0	445651.00	4459141.00	VL edge
GCKUC2	T3	69	0.5	34.8	445682.74	4459147.99	VR edge
GCKUC2	T3	99	0.8	26.1	445674.06	4459147.49	FP, wet grassy meadow

GCKUC2	T3	74	0.5	25.3	445673.26	4459147.44	ToC
GCKUC2	T3	0	0	23.6	445671.56	4459147.35	REW
GCKUC2	T3	0	0	20	445667.97	4459147.14	LEW
GCKUC2	T3	49	0.6	19.4	445667.37	4459147.11	ToC, FP
GCKUC2	T3	37	0.6	12.8	445660.78	4459146.73	FP
GCKUC2	T3	35	0.1	5.6	445653.59	4459146.32	OB channel
GCKUC2	T3	18	0.4	0	445648.00	4459146.00	VL edge, FP edge, S5
GCKUC2	T4	16	0.8	41.8	445684.38	4459154.91	SAMPLE, VR edge, S2
GCKUC2	T4	81	0.9	32.8	445675.47	4459153.64	FP, wet meadow
GCKUC2	T4	89	0.6	29	445671.71	4459153.10	ToC, FP
GCKUC2	T4	0	0	28.8	445671.51	4459153.07	Toe of cutbank, dry sand channel
GCKUC2	T4	0	0	25.9	445668.64	4459152.66	REW
GCKUC2	T4	0	0	22.6	445665.37	4459152.20	LEW
GCKUC2	T4	48	0.5	22.5	445665.27	4459152.18	ToC, FP
GCKUC2	T4	35	0.4	12.5	445655.37	4459150.77	FP
GCKUC2	T4	60	0.4	5.4	445648.35	4459149.76	FP
GCKUC2	T4	46	0.3	0	445643.00	4459149.00	VL edge
GCKUC2	T5	0	0.8	35.9	445678.77	4459158.07	S3, VR edge
GCKUC2	T5	47	0.5	30.4	445673.29	4459157.60	ToC
GCKUC2	T5	0	0	30.3	445673.19	4459157.59	REW
GCKUC2	T5	0	0	22.6	445665.52	4459156.93	LEW, small spring input
GCKUC2	T5	36	0.4	22.3	445665.22	4459156.90	ToC, FP, adjacent to spring
GCKUC2	T5	57	0.6	12.5	445655.45	4459156.07	FP, tree roots and hummock
GCKUC2	T5	63	0.6	0	445643.00	4459155.00	VL edge
GCKUC2	T6	44	0.3	35.5	445679.37	4459163.03	VR edge alluvial fan
GCKUC2	T6	36	0.3	33	445676.88	4459162.82	FP, ToC
GCKUC2	T6	0	0	32.9	445676.78	4459162.81	REW
GCKUC2	T6	0	0	28	445671.90	4459162.39	LEW
GCKUC2	T6	56	0.3	27.9	445671.80	4459162.38	ToC, FP
GCKUC2	T6	48	0.5	26.5	445670.40	4459162.26	FP
GCKUC2	T6	35	0.7	17.7	445661.64	4459161.51	FP
GCKUC2	T6	48	0.6	14.1	445658.05	4459161.20	S6, FP

GCKUC2	T6	97	0.8	5.3	445649.28	4459160.45	FP
GCKUC2	T6	60	0.8	0	445644.00	4459160.00	FP, OB channel, VL edge
GCKUC2	T7	58	0.5	35.2	445676.15	4459166.95	VR edge, fan
GCKUC2	T7	66	0.5	34.8	445675.75	4459166.93	ToC, RR
GCKUC2	T7	0	0	34.8	445675.75	4459166.93	REW
GCKUC2	T7	0	0	29.9	445670.85	4459166.66	LEW
GCKUC2	T7	59	0.4	29.8	445670.75	4459166.65	ToC, RL
GCKUC2	T7	46	0.5	19.8	445660.77	4459166.10	FP
GCKUC2	T7	58	0.6	9.8	445650.78	4459165.54	FP
GCKUC2	T7	35	0.6	0	445641.00	4459165.00	S7, VL edge, OB channel
GCKUC2	T8	79	0.7	33.1	445674.10	4459170.00	VR edge, fan, ToC
GCKUC2	T8	0	0	33	445674.00	4459170.00	REW
GCKUC2	T8	0	0	27.9	445668.90	4459170.00	LEW
GCKUC2	T8	36	0.3	27.8	445668.80	4459170.00	ToC RL
GCKUC2	T8	47	0.5	21.9	445662.90	4459170.00	S8, FP
GCKUC2	T8	36	0.5	11.9	445652.90	4459170.00	FP
GCKUC2	T8	119	0.6	3.3	445644.30	4459170.00	FP, standing water
GCKUC2	T8	93	0.5	0	445641.00	4459170.00	VL edge, OB channel
GCKUC2	T9	83	0.5	27.9	445671.90	4459175.00	VR edge, fan, ToC
GCKUC2	T9	0	0	27.7	445671.70	4459175.00	REW, diagonally across channel parrellel with
GCKUC2	T9	0	0	18	445662.00	4459175.00	LEW, diagonally across channel parrellel with
GCKUC2	T9	58	0.5	17.8	445661.80	4459175.00	ToC, RL, FP
GCKUC2	T9	53	0.7	16	445660.00	4459175.00	FP, grassy meadow
GCKUC2	T9	64	0.7	10.2	445654.20	4459175.00	FP, tree hummock
GCKUC2	T9	109	0.6	5.8	445649.80	4459175.00	FP, wet meadow
GCKUC2	T9	34	0.6	0	445644.00	4459175.00	VL edge, S9
GCKUC2	T10	39	0.4	22.3	445669.30	4459181.00	VR edge, fan
GCKUC2	T10	59	0.4	18.1	445665.10	4459181.00	FP, ToC
GCKUC2	T10	0	0	18	445665.00	4459181.00	REW
GCKUC2	T10	0	0	14.4	445661.40	4459181.00	LEW
GCKUC2	T10	81	0.5	14	445661.00	4459181.00	ToC, RL, FP
GCKUC2	T10	57	0.5	12.3	445659.30	4459181.00	S10, FP

GCKUC2	T10	60	0.4	7	445654.00	4459181.00	FP
GCKUC2	T10	34	0.5	0	445647.00	4459181.00	VL edge
GCKUC2	T11	59	0.5	26.8	445672.80	4459186.00	VR edge, fan
GCKUC2	T11	37	0.4	20.7	445666.70	4459186.00	FP, ToC, wet grassy meadow
GCKUC2	T11	0	0	20.6	445666.60	4459186.00	REW
GCKUC2	T11	0	0	16.4	445662.40	4459186.00	LEW
GCKUC2	T11	60	0.5	16.1	445662.10	4459186.00	ToC, RL
GCKUC2	T11	42	0.5	8.5	445654.50	4459186.00	FP, grassy meadow
GCKUC2	T11	27	0.8	0	445646.00	4459186.00	S11, VL edge, OB channel
OCKCF2	T1	43	0.7	11.1	447745.00	4450389.90	VR edge
OCKCF2	T1	23	0.6	9.6	447745.00	4450391.40	S6, FP
OCKCF2	T1	64	0.4	7.9	447745.00	4450393.10	BF, FP, ToC
OCKCF2	T1	0	0	7.7	447745.00	4450393.30	REW
OCKCF2	T1	0	0.4	2	447745.00	4450399.00	LEW
OCKCF2	T1	26	0.6	1	447745.00	4450400.00	BF RL
OCKCF2	T1	10	0.8	0	447745.00	4450401.00	VL edge
OCKCF2	T2	28	0.6	10.3	447750.07	4450390.74	VR edge, FP
OCKCF2	T2	23	0.3	9.3	447750.16	4450391.74	BF RR, cutbank
OCKCF2	T2	0	0	9.1	447750.18	4450391.94	REW
OCKCF2	T2	0	0.4	2	447750.82	4450399.01	LEW
OCKCF2	T2	46	1.1	1.6	447750.86	4450399.41	BF, ToC
OCKCF2	T2	15	0.8	0.6	447750.95	4450400.40	S1, FP, OB channel
OCKCF2	T2	30	1	0	447751.00	4450401.00	VL edge
OCKCF2	T3	23	0.9	11.7	447756.00	4450389.30	VR edge, FP
OCKCF2	T3	6	0.6	10.7	447756.00	4450390.30	S7
OCKCF2	T3	49	0.4	9.6	447756.00	4450391.40	BF RR
OCKCF2	T3	0	0	8.9	447756.00	4450392.10	REW
OCKCF2	T3	0	0.7	1.7	447756.00	4450399.30	LEW
OCKCF2	T3	31	0.9	1.4	447756.00	4450399.60	ToC, RL
OCKCF2	T3	25	1.1	0.4	447756.00	4450400.60	BF RL
OCKCF2	T3	48	1.2	0	447756.00	4450401.00	VL edge
OCKCF2	T4	16	0.7	10.5	447756.60	4450390.00	VR edge

OCKCF2	T4	11	0.6	9.7	447757.01	4450390.68	FP
OCKCF2	T4	20	0.4	8.7	447757.52	4450391.54	BF RR
OCKCF2	T4	0	0	8.4	447757.68	4450391.80	REW
OCKCF2	T4	0	0	1.7	447761.13	4450397.54	LEW
OCKCF2	T4	20	0.3	1.1	447761.43	4450398.06	BF RL
OCKCF2	T4	31	0.5	0.6	447761.69	4450398.49	S2, bank
OCKCF2	T4	31	0.8	0	447762.00	4450399.00	VL edge
OCKCF2	T5	16	0.4	9.3	447764.98	4450387.92	VR edge, FP
OCKCF2	T5	26	0.1	7.9	447765.29	4450389.29	FP, S8
OCKCF2	T5	70	0.3	6.5	447765.59	4450390.65	BF RR
OCKCF2	T5	0	0	6.3	447765.63	4450390.85	REW
OCKCF2	T5	0	0.2	1.1	447766.76	4450395.93	LEW
OCKCF2	T5	43	0.5	0.6	447766.87	4450396.41	BF RL
OCKCF2	T5	27	0.6	0	447767.00	4450397.00	VL edge
OCKCF2	T6	52	0.9	9.6	447769.96	4450385.89	VR edge
OCKCF2	T6	12	0.6	8.1	447770.44	4450387.32	FP
OCKCF2	T6	40	0.3	6.7	447770.88	4450388.64	BF RR
OCKCF2	T6	0	0	6.4	447770.98	4450388.93	REW
OCKCF2	T6	0	0.2	1.6	447772.49	4450393.48	LEW
OCKCF2	T6	39	0.4	1	447772.68	4450394.05	BF RL
OCKCF2	T6	15	0.4	0	447773.00	4450395.00	VL FP, S3
OCKCF2	T7	5	0.4	9.5	447774.14	4450383.32	VR edge
OCKCF2	T7	6	0.1	8.7	447774.47	4450384.05	S9, FP
OCKCF2	T7	22	0.2	7.8	447774.83	4450384.87	BF
OCKCF2	T7	0	0	7.7	447774.87	4450384.96	REW
OCKCF2	T7	0	0	2.6	447776.94	4450389.62	LEW
OCKCF2	T7	41	0.4	2.1	447777.15	4450390.08	BF RL
OCKCF2	T7	0	0.2	1	447777.59	4450391.09	OB side channel
OCKCF2	T7	27	0.6	0	447778.00	4450392.00	VL edge
OCKCF2	T8	22	0.7	8.9	447777.21	4450380.24	VR edge
OCKCF2	T8	16	0.4	8.1	447777.73	4450380.85	BF, RR
OCKCF2	T8	0	0.2	8.1	447777.73	4450380.85	REW

OCKCF2	T8	0	0	1.5	447782.02	4450385.86	LEW
OCKCF2	T8	44	0.4	1.2	447782.22	4450386.09	BF RL
OCKCF2	T8	26	0.4	0.7	447782.54	4450386.47	FP, S4
OCKCF2	T8	31	0.7	0	447783.00	4450387.00	VL edge
OCKCF2	T9	17	0.7	7.6	447781.63	4450376.63	VR edge
OCKCF2	T9	0	0.3	5.5	447783.11	4450378.11	BF RR, undercut
OCKCF2	T9	0	0	5.3	447783.25	4450378.25	REW
OCKCF2	T9	0	0.1	1	447786.29	4450381.29	LEW
OCKCF2	T9	51	0.5	0.5	447786.65	4450381.65	FP, S5
OCKCF2	T9	39	0.6	0	447787.00	4450382.00	VL edge
OCKCF2	T10	8	0.4	8.5	447783.08	4450372.06	VR edge
OCKCF2	T10	24	0	7.2	447784.14	4450372.82	FP, OB channel, S10
OCKCF2	T10	22	0.5	5.6	447785.44	4450373.75	RR, ToC
OCKCF2	T10	0	0	4.9	447786.01	4450374.15	REW
OCKCF2	T10	0	0.4	1.7	447788.62	4450376.01	LEW
OCKCF2	T10	41	0.8	1.1	447789.10	4450376.36	BF RL
OCKCF2	T10	23	1.1	0	447790.00	4450377.00	VL edge
OCKCF2	T11	14	0.4	6.7	447787.43	4450368.28	VR edge
OCKCF2	T11	18	0.2	5.7	447788.26	4450368.84	FP, S11
OCKCF2	T11	35	0.3	4.7	447789.09	4450369.39	BF RR, ToC
OCKCF2	T11	0	0	4.4	447789.34	4450369.56	REW
OCKCF2	T11	0	0.1	0.7	447792.42	4450371.61	LEW
OCKCF2	T11	75	0.5	0.6	447792.50	4450371.67	YoC, RL
OCKCF2	T11	60	0.9	0	447793.00	4450372.00	VL edge
GCKPC3	T1	24	1.4	43.2	446376.28	4463016.81	VR edge, overbank channel
GCKPC3	T1	20	1.7	36.8	446370.93	4463020.31	S1, FP
GCKPC3	T1	10	2.1	30.9	446365.99	4463023.54	FP or trrace
GCKPC3	T1	12	2	26.8	446362.55	4463025.78	FP or trrace
GCKPC3	T1	13	1.2	16.8	446354.18	4463031.25	BF
GCKPC3	T1	0	0	16.5	446353.93	4463031.42	REW
GCKPC3	T1	0	0	7.5	446346.40	4463036.34	LEW
GCKPC3	T1	49	0.3	5.9	446345.06	4463037.21	S14, BF, FP

GCKPC3	T1	44	0.3	1.3	446341.21	4463039.73	FP
GCKPC3	T1	20	0.6	0	446340.12	4463040.44	VL edge
GCKPC3	T2	31	0.5	42.2	446387.66	4463022.58	VR edge, overbank channel
GCKPC3	T2	15	0.8	33	446379.97	4463027.63	FP, berm/island
GCKPC3	T2	24	0.4	25.4	446373.62	4463031.80	Overbank channel
GCKPC3	T2	17	0.6	23.1	446371.70	4463033.06	S2, FP island
GCKPC3	T2	50	0.5	16	446365.76	4463036.96	FP, island/berm
GCKPC3	T2	13	0.4	13.1	446363.34	4463038.55	BF
GCKPC3	T2	0	0	12.5	446362.84	4463038.88	REW
GCKPC3	T2	0	0	1.5	446353.64	4463044.92	LEW
GCKPC3	T2	0.7	0.3	0.8	446353.06	4463045.30	BF
GCKPC3	T2	12	0.6	0	446352.39	4463045.74	VL edge
GCKPC3	T3	8	0.7	39	446395.21	4463030.59	VR edge
GCKPC3	T3	12	0.4	37.3	446393.78	4463031.51	overbank channel
GCKPC3	T3	19	0.8	34.6	446391.51	4463032.96	FP, berm
GCKPC3	T3	17	0.6	26.9	446385.03	4463037.12	overbank channel
GCKPC3	T3	11	0.9	21.1	446380.15	4463040.25	S3, FP island
GCKPC3	T3	24	0.6	17.4	446377.03	4463042.25	overbank channel
GCKPC3	T3	21	0.9	13.6	446373.83	4463044.30	FP, terrace
GCKPC3	T3	21	0.4	12.2	446372.66	4463045.06	BF
GCKPC3	T3	0	0	11.5	446372.07	4463045.44	REW
GCKPC3	T3	0	0	1.5	446363.65	4463050.84	LEW
GCKPC3	T3	10	0.3	0.6	446362.89	4463051.32	BF
GCKPC3	T3	18	0.5	0	446362.39	4463051.65	VL edge
GCKPC3	T4	12	0.2	33.3	446397.39	4463039.75	VR edge, toe pf terrace
GCKPC3	T4	20	-0.1	30.9	446395.37	4463041.05	OB channl
GCKPC3	T4	20	0.3	28.4	446393.27	4463042.39	S4, OB channel FP
GCKPC3	T4	15	0.4	27.4	446392.42	4463042.93	overbank channel
GCKPC3	T4	25	0.2	25.5	446390.82	4463043.96	overbank channel, interfluve
GCKPC3	T4	10	0.5	22.4	446388.21	4463045.63	FP, terrace, cobs>B
GCKPC3	T4	4	0.3	21.6	446387.54	4463046.06	BF, pebs>cobs
GCKPC3	T4	0	0	21.2	446387.20	4463046.27	REW

GCKPC3	T4	0	0	11.7	446379.20	4463051.39	LEW
GCKPC3	T4	8	0.3	11.1	446378.69	4463051.71	BF, gravel
GCKPC3	T4	3	0.6	9.8	446377.60	4463052.41	, possible debris flo levee, gravel>B, grassy, S, F
GCKPC3	T4	12	0.8	6.6	446374.90	4463054.14	DF lobe, dead standing tree
GCKPC3	T4	17	0.7	4.7	446373.30	4463055.16	S13, DF, FP
GCKPC3	T4	74	1	0	446369.34	4463057.69	VL edge
GCKPC3	T5	20	0.7	26.3	446399.25	4463050.97	VR edge
GCKPC3	T5	40	0.5	24.4	446397.64	4463051.99	S5, FP
GCKPC3	T5	0	0.5	23.5	446396.88	4463052.47	on logs, driftwood (beaver den?)
GCKPC3	T5	0	0.2	23.1	446396.54	4463052.68	BF, RR, logs/beaver den
GCKPC3	T5	0	0	22.5	446396.03	4463053.00	REW
GCKPC3	T5	0	0	13.6	446388.50	4463057.75	LEW
GCKPC3	T5	26	0.2	13.5	446388.42	4463057.80	BF, grassy FP
GCKPC3	T5	84	0.6	9.9	446385.37	4463059.72	berm
GCKPC3	T5	34	0.3	2.6	446379.20	4463063.61	OB channel
GCKPC3	T5	26	0.5	0	446377.00	4463065.00	VL edge
GCKPC3	T6	21	0.5	23.6	446404.26	4463061.88	Wood, soil, VR edge
GCKPC3	T6	0	0.3	22.6	446403.40	4463062.38	BF, large boulder
GCKPC3	T6	0	0	22.6	446403.40	4463062.38	REW
GCKPC3	T6	0	0	16.8	446398.37	4463065.28	LEW
GCKPC3	T6	23	0	15.8	446397.51	4463065.78	grassy bank, birch, surface water
GCKPC3	T6	34	0.3	15.3	446397.07	4463066.03	BF, grassy FP, S, A
GCKPC3	T6	5	0.6	13.9	446395.86	4463066.73	FP, wood on 5 cm of soil
GCKPC3	T6	20	0	9.4	446391.96	4463068.97	S12, OB channel, FP
GCKPC3	T6	26	0.7	4.6	446387.80	4463071.37	berm on FP
GCKPC3	T6	43	0.3	1.7	446385.29	4463072.82	OB channel
GCKPC3	T6	20	0.6	0	446383.81	4463073.66	VL edge
GCKPC3	T7	13	0.8	20.9	446408.70	4463070.88	VR edge
GCKPC3	T7	36	0.6	20.3	446408.19	4463071.20	S6, VR
GCKPC3	T7	56	0.5	19.7	446407.68	4463071.52	BF, grasses
GCKPC3	T7	0	0	19.4	446407.43	4463071.68	REW
GCKPC3	T7	0	0	13.6	446402.52	4463074.77	LEW

GCKPC3	T7	25	0.3	13.4	446402.35	4463074.87	BF, grassy FP, aspen, juniper, spruce, DF
GCKPC3	T7	38	0.5	10.7	446400.06	4463076.31	FP
GCKPC3	T7	4	0.3	6.8	446396.76	4463078.38	FP
GCKPC3	T7	21	0.1	3.4	446393.88	4463080.19	overbank channel FP, RE pool
GCKPC3	T7	38	0.1	1.9	446392.61	4463080.99	FP
GCKPC3	T7	50	0.8	0	446391.00	4463082.00	VL edge, wood
GCKPC3	T8	13	0.8	14.7	446413.14	4463080.13	FP, VR edge, toe of terrace
GCKPC3	T8	13	1	13.4	446412.12	4463080.94	FP
GCKPC3	T8	35	1	12.1	446411.10	4463081.75	BF
GCKPC3	T8	0	0.8	11.8	446410.86	4463081.93	REW
GCKPC3	T8	0	0.8	4.2	446404.90	4463086.65	LEW
GCKPC3	T8	31	1.2	3.9	446404.67	4463086.84	BF, grassy FP, Aspen, Doug fir, spruce
GCKPC3	T8	11	1.1	2.2	446403.34	4463087.89	S11, FP
GCKPC3	T8	11	1.3	0	446401.61	4463089.26	VL edge
GCKPC3	T9	20	0	23.5	446429.05	4463080.96	VR edge
GCKPC3	T9	27	0	19.4	446425.90	4463083.58	OB channel
GCKPC3	T9	18	0.3	15	446422.52	4463086.40	S7, FP
GCKPC3	T9	22	0.4	12.9	446420.91	4463087.74	FP
GCKPC3	T9	22	0.2	10.2	446418.84	4463089.47	FP
GCKPC3	T9	40	0.2	9	446417.91	4463090.24	BF
GCKPC3	T9	0	0	8.9	446417.84	4463090.30	REW
GCKPC3	T9	0	0	2.3	446412.77	4463094.53	LEW
GCKPC3	T9	0	0.3	2.2	446412.69	4463094.59	on B, BF
GCKPC3	T9	5	0.9	0	446411.00	4463096.00	VL edge, litter, mineral soil
GCKPC3	T10	42	0.3	43.1	446454.59	4463074.68	VR edge
GCKPC3	T10	11	0.1	33.5	446447.56	4463081.21	S8, Grassy meadow FP
GCKPC3	T10	5	0.1	29.9	446444.92	4463083.66	OB channel
GCKPC3	T10	7	0.7	17.4	446435.75	4463092.16	Top edge of FP island
GCKPC3	T10	13	0.1	13.8	446433.12	4463094.61	FP, toe of raised FP terrace
GCKPC3	T10	23	0.2	11.9	446431.72	4463095.91	BF, RR, FP
GCKPC3	T10	0	0	11.4	446431.36	4463096.25	REW
GCKPC3	T10	0	0	2.4	446424.76	4463102.37	LEW

GCKPC3	T10	11	0.3	1.3	446423.95	4463103.12	BF, RL
GCKPC3	T10	12	0.7	0	446423.00	4463104.00	VL edge
GCKPC3	T11	50	0.4	39	446462.87	4463080.72	FP, VR edge, toe of terrace
GCKPC3	T11	60	0.2	37.2	446461.58	4463081.98	S10, overbank channel
GCKPC3	T11	43	0.5	34.4	446459.58	4463083.94	edge of sloped uppaer surface
GCKPC3	T11	15	0.9	19.8	446449.15	4463094.15	S9, FP
GCKPC3	T11	15	0.9	12.5	446443.93	4463099.26	top edge of veg island
GCKPC3	T11	15	0.5	10.3	446442.36	4463100.80	BF, RR, toe of FP veg island w? pine
GCKPC3	T11	0	0	9.7	446441.93	4463101.21	REW
GCKPC3	T11	0	0	0.9	446435.64	4463107.37	LEW
GCKPC3	T11	8	0.4	0.6	446435.43	4463107.58	BF, cobs
GCKPC3	T11	1	0.7	0	446435.00	4463108.00	VL edge
GCKCF3	T1	0	0.2	18.2	445752.10	4461780.91	VR edge, B, BK, at log jam
GCKCF3	T1	0	0	17.4	445751.30	4461780.82	BF RR, B
GCKCF3	T1	0	0.3	17.3	445751.20	4461780.81	REW
GCKCF3	T1	0	0.3	1	445734.99	4461779.10	LEW, large pool, log jam and 2ndary channel
GCKCF3	T1	0	0.5	0.4	445734.40	4461779.04	BF gravel on B
GCKCF3	T1	0	0.8	0	445734.00	4461779.00	BF, gravel on B, VL edge
GCKCF3	T2	24	0.6	13.1	445748.07	4461785.07	VR edge
GCKCF3	T2	54	0.4	12.1	445747.07	4461785.14	BF, RR, S6
GCKCF3	T2	0	0	12	445746.97	4461785.15	REW
GCKCF3	T2	0	0	1	445736.00	4461785.93	LEW
GCKCF3	T2	7	0.4	0.7	445735.70	4461785.95	litter on roots and gravel
GCKCF3	T2	0	0.7	0	445735.00	4461786.00	VL edge
GCKCF3	T3	0	0.7	9.6	445750.20	4461789.24	VR edge
GCKCF3	T3	0	0.2	8.1	445748.76	4461789.67	BF, RR
GCKCF3	T3	0	0	7.4	445748.09	4461789.87	REW
GCKCF3	T3	0	0.4	2.1	445743.01	4461791.40	LEW
GCKCF3	T3	0	0.6	1.6	445742.53	4461791.54	BF, litter on B
GCKCF3	T3	0	1	1	445741.96	4461791.71	B
GCKCF3	T3	0	0.8	0.6	445741.57	4461791.83	edge of B
GCKCF3	T3	0	0.9	0	445741.00	4461792.00	VL edge

GCKCF3	T4	0	0.5	8.5	445750.96	4461794.02	VR edge
GCKCF3	T4	0	0.2	7.7	445750.21	4461794.30	BF, RR
GCKCF3	T4	0	0	6.6	445749.18	4461794.68	REW
GCKCF3	T4	0	0	1.1	445744.03	4461796.61	LEW
GCKCF3	T4	0	0.3	0.5	445743.47	4461796.82	BF, RL, gravel on BK & cons
GCKCF3	T4	25	0.5	0	445743.00	4461797.00	VL edge, S1
GCKCF3	T5	0	0.5	12.9	445757.33	4461799.21	VR edge
GCKCF3	T5	0	0.2	12.4	445756.85	4461799.35	BF RR, pebs on BK
GCKCF3	T5	0	0	11.8	445756.28	4461799.53	REW
GCKCF3	T5	0	0.1	5.5	445750.26	4461801.38	LEW
GCKCF3	T5	0	0.3	5.2	445749.97	4461801.47	Wood & litter on sand
GCKCF3	T5	0	0.2	3.3	445748.15	4461802.03	Litter & sand, toe of large B
GCKCF3	T5	0	0.5	2.7	445747.58	4461802.21	large B
GCKCF3	T5	0	1.2	1.5	445746.43	4461802.56	large B
GCKCF3	T5	15	1	1.3	445746.24	4461802.62	toe of B
GCKCF3	T5	15	1.1	0	445745.00	4461803.00	VL edge, S2
GCKCF3	T6	0	0.8	9.2	445757.73	4461806.09	VR edge, B
GCKCF3	T6	0	0.5	8.6	445757.16	4461806.28	BF, BK
GCKCF3	T6	0	0	8.2	445756.78	4461806.41	REW
GCKCF3	T6	0	0	1.9	445750.80	4461808.40	LEW
GCKCF3	T6	0	1.1	1.2	445750.14	4461808.62	BF, BK
GCKCF3	T6	0	1.3	0	445749.00	4461809.00	VL edge, B
GCKCF3	T7	0	0.6	10.6	445763.96	4461812.38	VR edge, gravel slope
GCKCF3	T7	0	0.1	9.1	445762.55	4461812.89	BK/gravel slope, BF RR
GCKCF3	T7	0	0	8	445761.52	4461813.27	REW
GCKCF3	T7	0	0.5	1.4	445755.32	4461815.52	LEW
GCKCF3	T7	0	0.7	0.1	445754.09	4461815.97	BF RL, B
GCKCF3	T7	0	0.9	0	445754.00	4461816.00	VL edge
GCKCF3	T8	0	0.1	11.1	445765.77	4461819.31	VR edge & BF, litter on Gravel
GCKCF3	T8	0	0	10	445764.70	4461819.57	REW
GCKCF3	T8	0	0	1.8	445756.75	4461821.56	LEW
GCKCF3	T8	17	0.1	1.4	445756.36	4461821.66	S3, BF

GCKCF3	T8	9	0.3	0	445755.00	4461822.00	VL edge, base of large B
GCKCF3	T9	0	0.5	12.8	445769.47	4461825.12	VR edge
GCKCF3	T9	20	0.3	12.5	445769.18	4461825.19	FP edge
GCKCF3	T9	55	0.2	12.1	445768.79	4461825.28	S5, FP
GCKCF3	T9	0	0.2	11.4	445768.11	4461825.44	BF, edge of FP
GCKCF3	T9	0	0	11.3	445768.01	4461825.46	REW
GCKCF3	T9	0	0.1	5.4	445762.26	4461826.79	LEW
GCKCF3	T9	0	1.1	3.4	445760.31	4461827.24	ToB
GCKCF3	T9	8	1.9	2.2	445759.14	4461827.51	BF, S4
GCKCF3	T9	0	1.9	0.9	445757.88	4461827.80	BF
GCKCF3	T9	0	2.5	0	445757.00	4461828.00	VL slope
GCKCF3	T10	0	0.5	6	445765.69	4461832.10	B, VR
GCKCF3	T10	0	0.2	5	445764.74	4461832.42	B
GCKCF3	T10	0	0	4.7	445764.46	4461832.51	REW
GCKCF3	T10	0	0	0	445760.00	4461834.00	LEW
GCKCF3	T10	0	0.4	0	445760.00	4461834.00	VL edge
GCKCF3	T11	0	0.6	6.5	445768.41	4461840.93	VR edge, B
GCKCF3	T11	0	0	6.4	445768.31	4461840.95	BF, B
GCKCF3	T11	0	0.3	6.3	445768.21	4461840.96	REW
GCKCF3	T11	0	0.3	1.6	445763.58	4461841.74	LEW
GCKCF3	T11	0	0.7	0.8	445762.79	4461841.87	BF, BK
GCKCF3	T11	0	1.3	0	445762.00	4461842.00	VL edge, BK
MCKUC3	T1	68	1.05	80	446013.10	4464547.50	VR edge
MCKUC3	T1	53	0.65	69.9	446011.22	4464557.42	FP, dry OB chan
MCKUC3	T1	61	0.55	62.1	446009.77	4464565.08	FP, dry OB chan
MCKUC3	T1	96	0.45	54	446008.26	4464573.04	FP, dry OB chan
MCKUC3	T1	98	0.35	47	446006.96	4464579.92	FP, dry OB chan
MCKUC3	T1	50	0.15	43.9	446006.38	4464582.97	ToC, RR main stem
MCKUC3	T1	0	0	43.8	446006.36	4464583.06	REW
MCKUC3	T1	0	0	38.2	446005.32	4464588.57	LEW
MCKUC3	T1	78	0.4	37.9	446005.27	4464588.86	ToC, RL
MCKUC3	T1	76	0.4	28.1	446003.44	4464598.49	gassy meadow

MCKUC3	T1	43	0.4	17.9	446001.55	4464608.51	grassy meadow w/ standing water
MCKUC3	T1	80	0.3	11.8	446000.41	4464614.51	S1, bank of channel RL, channel bends
MCKUC3	T1	56	0.2	10.5	446000.17	4464615.78	ToC, RL, bend in chan
MCKUC3	T1	0	0.1	10.3	446000.13	4464615.98	REW, bend in chan
MCKUC3	T1	0	0	1	445998.40	4464625.12	LEW bend in chan
MCKUC3	T1	56	0.3	0.9	445998.38	4464625.22	ToC, RL
MCKUC3	T1	42	0.4	0	445998.22	4464626.10	VL edge
MCKUC3	T2	63	0.7	71.6	446014.66	4464557.23	VR edge
MCKUC3	T2	27	1	62.7	446013.35	4464566.03	FP, tree hummock
MCKUC3	T2	71	0.9	53	446011.92	4464575.62	FP, tree hummock
MCKUC3	T2	33	0.7	46.1	446010.91	4464582.45	FP, tree hummock
MCKUC3	T2	68	0.7	39.6	446009.95	4464588.88	S2, FP, tree hummock
MCKUC3	T2	0	0.4	37.5	446009.64	4464590.96	REW
MCKUC3	T2	0	0	0.8	446004.24	4464627.26	LEW, channel flows perp
MCKUC3	T2	49	0.3	0	446004.12	4464628.05	VL edge, RB, SAF edge of forest
MCKUC3	T3	18	1	61.5	446018.22	4464563.89	VR edge
MCKUC3	T3	33	0.8	54.8	446017.26	4464570.52	FP, conifer on wet FP hummock
MCKUC3	T3	139	1	49.2	446016.46	4464576.06	FP, conifer on wet FP hummock
MCKUC3	T3	51	0.4	41.8	446015.40	4464583.38	FP grassy meadow
MCKUC3	T3	53	0.6	33.6	446014.23	4464591.50	FP grassy meadow
MCKUC3	T3	107	0.9	25.1	446013.01	4464599.91	tree hummock
MCKUC3	T3	92	0.7	18.5	446012.07	4464606.45	S3 @ 43 m, grassy meadow
MCKUC3	T3	23	0.8	13.8	446011.40	4464611.10	tree berm
MCKUC3	T3	84	0.5	8.1	446010.59	4464616.74	grassy meadow, FP
MCKUC3	T3	58	0.3	4.5	446010.07	4464620.30	ToC, RR
MCKUC3	T3	0	0	4.4	446010.06	4464620.40	REW
MCKUC3	T3	0	0	0.8	446009.54	4464623.96	LEW
MCKUC3	T3	64	0.5	0	446009.43	4464624.76	VL edge
MCKUC3	T4	48	0.9	59.1	446024.54	4464566.39	VR edge
MCKUC3	T4	17	0.8	56.1	446024.09	4464569.36	S4, VR
MCKUC3	T4	23	0.4	46.9	446022.71	4464578.45	FP, OB channel
MCKUC3	T4	117	0.6	41.2	446021.86	4464584.09	tree hummock

MCKUC3	T4	64	0.4	34.9	446020.91	4464590.32	FP grassy OB channel
MCKUC3	T4	44	0.3	29.2	446020.06	4464595.95	FP grassy OB channel
MCKUC3	T4	73	0.5	20.5	446018.75	4464604.56	FP, grassy meadow
MCKUC3	T4	53	0.5	14.4	446017.84	4464610.59	Tree hummock
MCKUC3	T4	36	0.8	10	446017.18	4464614.94	Tree hummock
MCKUC3	T4	68	0.3	4.4	446016.34	4464620.47	ToC RR, grassy meadow
MCKUC3	T4	0	0	4.2	446016.31	4464620.67	REW
MCKUC3	T4	0	0	0.7	446015.79	4464624.13	LEW
MCKUC3	T4	41	0.4	0	446015.68	4464624.82	VL edge
MCKUC3	T5	8	0.4	46.1	446028.78	4464575.47	VR edge, S5
MCKUC3	T5	50	0.1	40.3	446027.79	4464581.18	OB chan
MCKUC3	T5	58	0.1	31.3	446026.26	4464590.05	FP grassy meadow
MCKUC3	T5	62	0.1	23.1	446024.86	4464598.13	FP grassy meadow
MCKUC3	T5	61	0.3	18.1	446024.01	4464603.06	OB chan, tree hummock
MCKUC3	T5	46	0.1	11.9	446022.95	4464609.17	OB chan, tree hummock
MCKUC3	T5	62	0.3	7.4	446022.19	4464613.60	grassy bank
MCKUC3	T5	0	0	5.2	446021.81	4464615.77	REW
MCKUC3	T5	0	0	1.1	446021.11	4464619.81	LEW
MCKUC3	T5	99	0.3	1	446021.10	4464619.91	TOC
MCKUC3	T5	58	0.5	0	446020.93	4464620.89	VL edge
MCKUC3	T6	66	0.4	32.3	446033.23	4464586.30	VR edge
MCKUC3	T6	98	0.4	25.3	446031.67	4464593.13	S6, edge of tree cluster, grassy meadow
MCKUC3	T6	57	0.2	15.5	446029.48	4464602.68	grassy meadow
MCKUC3	T6	98	0.7	8.9	446028.01	4464609.11	tree hummock
MCKUC3	T6	64	0.2	5.6	446027.27	4464612.33	ToC RR
MCKUC3	T6	0	0	5.5	446027.25	4464612.43	REW
MCKUC3	T6	0	0	2.1	446026.49	4464615.74	LEW
MCKUC3	T6	49	0.5	0	446026.02	4464617.79	VL edge, grassy bank, RB, SAF
MCKUC3	T7	57	0.3	32.6	446039.50	4464586.28	VR edge of grassy meadow
MCKUC3	T7	73	0.3	22.4	446037.16	4464596.20	grassy meadow
MCKUC3	T7	44	0	20.3	446036.67	4464598.25	OB chan, standing water
MCKUC3	T7	76	0.5	15.6	446035.59	4464602.82	S7, tree hummock, SAF, ES

MCKUC3	T7	24	0.1	8.8	446034.03	4464609.44	OB chan
MCKUC3	T7	81	0.4	6.8	446033.57	4464611.38	ToC, RR
MCKUC3	T7	0	0.9	6.5	446033.50	4464611.67	REW
MCKUC3	T7	0	0.9	1.4	446032.32	4464616.64	LEW
MCKUC3	T7	62	1.2	0	446032.00	4464618.00	VL edge
MCKUC3	T8	71	0.5	30.9	446044.40	4464590.26	S8, VR edge grassy edge of trees
MCKUC3	T8	92	0.6	25.8	446043.01	4464595.17	tree hummock
MCKUC3	T8	58	0.2	18	446040.89	4464602.68	stadning water depth 10 cm, OB chan
MCKUC3	T8	83	0.6	14.1	446039.83	4464606.43	tree hummock
MCKUC3	T8	60	0.5	12.4	446039.37	4464608.07	tree hummock, ToC, RR
MCKUC3	T8	0	0	12.3	446039.34	4464608.16	REW
MCKUC3	T8	0	0	4.3	446037.17	4464615.86	LEW
MCKUC3	T8	91	0.4	4.1	446037.11	4464616.05	ToC RL
MCKUC3	T8	33	0.4	0	446036.00	4464620.00	VL edge
MCKUC3	T9	33	0.5	31.8	446048.56	4464593.01	VR edge, standing water, OB chan
MCKUC3	T9	87	0.8	25.1	446046.34	4464599.33	Tree hummock
MCKUC3	T9	65	0.5	16.4	446043.45	4464607.53	ToC
MCKUC3	T9	0	0	16.2	446043.38	4464607.72	REW
MCKUC3	T9	0	0	13.9	446042.62	4464609.89	LEW. Sie chan
MCKUC3	T9	66	0.4	13.8	446042.58	4464609.98	REW island, ToC, RL
MCKUC3	T9	68	0.4	11.6	446041.85	4464612.06	LEW island
MCKUC3	T9	0	0.2	11.5	446041.82	4464612.15	REW, side chan
MCKUC3	T9	0	0.2	9.8	446041.26	4464613.76	LEW side chan
MCKUC3	T9	58	0.5	9.5	446041.16	4464614.04	ToC, RL
MCKUC3	T9	74	0.6	7.8	446040.59	4464615.64	S9
MCKUC3	T9	28	0.6	0	446038.00	4464623.00	VL edge
MCKUC3	T10	50	0.5	27	446052.05	4464597.94	VR edge, grassy meado
MCKUC3	T10	86	0.4	20.3	446049.56	4464604.16	OB chan, standing water
MCKUC3	T10	63	0.5	13.8	446047.14	4464610.19	Toc RR
MCKUC3	T10	0	0.1	13.6	446047.06	4464610.38	REW, sdie chan
MCKUC3	T10	0	0.1	10.4	446045.87	4464613.35	LEW side chan
MCKUC3	T10	53	0.5	10.3	446045.83	4464613.44	ToC, RL island

MCKUC3	T10	62	0.4	7	446044.61	4464616.50	ToC, RR island
MCKUC3	T10	0	0	6.8	446044.53	4464616.69	REW, side chan
MCKUC3	T10	0	0	5.2	446043.94	4464618.17	LEW side chan
MCKUC3	T10	79	0.3	5	446043.86	4464618.36	ToC, RL grassy meadow
MCKUC3	T10	24	0.3	0	446042.00	4464623.00	S10, VL edge
MCKUC3	T11	18	0.4	28.3	446057.49	4464599.95	VR edge wet standing water, grassy meadow
MCKUC3	T11	70	0.5	20.2	446054.30	4464607.39	wet standing water, grassy meadow
MCKUC3	T11	72	0.5	17.3	446053.16	4464610.06	S11, standing water, grassy meadow
MCKUC3	T11	64	0.4	16.3	446052.77	4464610.98	Grassy meadow
MCKUC3	T11	0	0	16.2	446052.73	4464611.07	REW
MCKUC3	T11	0	0.1	11.4	446050.84	4464615.48	LEW
MCKUC3	T11	26	0.3	11.3	446050.80	4464615.58	ToC RL, grassy meadow
MCKUC3	T11	2	0.4	5.4	446048.48	4464621.00	ToC RL, grassy meadow
MCKUC3	T11	21	0.4	0	446046.36	4464625.96	VL edge of meadow
OCKMT3	T1	29	2	52.6	447327.99	4450429.81	VR edge
OCKMT3	T1	0	1.6	51.8	447328.03	4450430.61	ToC, Bk
OCKMT3	T1	0	1.1	51.2	447328.06	4450431.21	REW
OCKMT3	T1	0	1.1	46.5	447328.29	4450435.91	LEW
OCKMT3	T1	38	1.3	46.4	447328.30	4450436.01	ToC
OCKMT3	T1	45	1.8	42.9	447328.47	4450439.50	tree berm on bank
OCKMT3	T1	19	1.4	38.7	447328.67	4450443.70	OB chan (not active)
OCKMT3	T1	34	1.4	32.7	447328.97	4450449.69	OB chan (not active)
OCKMT3	T1	11	1.1	25.8	447329.31	4450456.58	S1, OB overflow interfluve
OCKMT3	T1	24	1.2	22.4	447329.47	4450459.98	tree hummock
OCKMT3	T1	17	0.7	16.1	447329.78	4450466.27	wet OB chn
OCKMT3	T1	14	0.6	8.9	447330.14	4450473.46	
OCKMT3	T1	32	0	0	447330.57	4450482.35	VL edge
OCKMT3	T2	22	1.5	50.2	447334.00	4450428.97	VR edge
OCKMT3	T2	30	0.9	49.4	447334.04	4450429.77	ToC
OCKMT3	T2	0	0.5	48.8	447334.07	4450430.37	REW, small island ~1 m wide
OCKMT3	T2	0	0.5	41.4	447334.45	4450437.76	LEW small island
OCKMT3	T2	56	1	41.2	447334.46	4450437.96	ToC on tree hummock

OCKMT3	T2	18	0.8	38.2	447334.61	4450440.96	OB chan	
OCKMT3	T2	19	0.9	32.5	447334.90	4450446.65	high FP	
OCKMT3	T2	12	1	29.8	447335.04	4450449.34	high FP, herbaceous	
OCKMT3	T2	20	0.5	26.4	447335.22	4450452.74	OB chan	
OCKMT3	T2	23	0.4	21.2	447335.48	4450457.93	RR top of OB chan	
OCKMT3	T2	36	0	16.3	447335.73	4450462.83	S2, RR top of OB chan	
OCKMT3	T2	70	0.2	14.7	447335.81	4450464.43	tree hummock	
OCKMT3	T2	12	0	10.3	447336.04	4450468.82		70
OCKMT3	T2	47	0.4	7.4	447336.19	4450471.72	grassy FP meadow hummock	
OCKMT3	T2	7	0.3	4.7	447336.33	4450474.41	OB chan	
OCKMT3	T2	17	0.4	0	447336.57	4450479.11	VL edge	
OCKMT3	T3	12	1.2	54.2	447342.00	4450431.42	VR edge	
OCKMT3	T3	0	0.8	53.3	447342.00	4450432.32	ToC B/cobs, small FP	
OCKMT3	T3	0	0.3	53	447342.00	4450432.62	REW	
OCKMT3	T3	0	0.3	48.4	447341.98	4450437.22	LEW	
OCKMT3	T3	54	0.9	46.9	447341.98	4450438.72	top of bank, ES, SAF	
OCKMT3	T3	35	1	45.6	447341.98	4450440.02	tree hummock/bank	
OCKMT3	T3	13	0.6	38.7	447341.96	4450446.92	OB chan	
OCKMT3	T3	7	0.8	34.8	447341.95	4450450.82	gravely berm	
OCKMT3	T3	7	0.4	31.9	447341.94	4450453.72	low OB chan	
OCKMT3	T3	13	0.1	26.3	447341.92	4450459.32	standing water OB chan	
OCKMT3	T3	36	0	20.8	447341.91	4450464.82	S3, bog, edge of stagnant water	
OCKMT3	T3	30	0	16.4	447341.90	4450469.22	standing stagnant pool	
OCKMT3	T3	51	0.3	10.7	447341.88	4450474.92	wet grassy meadow	
OCKMT3	T3	20	0.3	3.8	447341.86	4450481.82		
OCKMT3	T3	29	0.6	0	447341.85	4450485.62	VL edge	
OCKMT3	T4	27	1.1	48.9	447349.27	4450441.85	VR edge	
OCKMT3	T4	20	0.7	48.1	447349.27	4450442.65	ToC	
OCKMT3	T4	0	0.3	47.9	447349.26	4450442.85	REW	
OCKMT3	T4	0	0.3	43.4	447349.22	4450447.35	LEW	
OCKMT3	T4	59	0.8	43.1	447349.22	4450447.65	ToC tree hummock, ES	
OCKMT3	T4	2	0.6	38.3	447349.18	4450452.45	OB chan w/ tall gras, herbaceous veg	

OCKMT3	T4	13	0.3	30.9	447349.11	4450459.85	wet OB chan w/ grass, herbaceous, SAF
OCKMT3	T4	6	0	23.5	447349.05	4450467.25	standing water
OCKMT3	T4	54	0.3	17.1	447348.99	4450473.65	grassy hummock w/ SAF
OCKMT3	T4	32	0.2	10.8	447348.94	4450479.95	grassy meadow on edge of berm
OCKMT3	T4	38	0.4	2.9	447348.87	4450487.85	S4, grassy wet meadow on edge of berm
OCKMT3	T4	67	0.5	0	447348.84	4450490.75	VL edge
OCKMT3	T5	36	1.2	57.1	447355.00	4450489.16	VL edge, grassy meadow, edge of berm, ES
OCKMT3	T5	47	0.8	46.7	447354.96	4450478.76	wet grassy meadow w/ still water holes, bog
OCKMT3	T5	77	1	39.9	447354.93	4450471.96	grassy hummock in meadow
OCKMT3	T5	22	0.6	31.7	447354.89	4450463.76	wet grassy meadow
OCKMT3	T5	27	0.4	21	447354.85	4450453.06	small OB channel
OCKMT3	T5	35	0.6	18.8	447354.84	4450450.86	wet OB chan, FP
OCKMT3	T5	0	0	14.7	447354.82	4450446.76	side channel pebs >sd
OCKMT3	T5	20	0.3	13.1	447354.82	4450445.16	S5, tall grassy herbaceous FP
OCKMT3	T5	0	0.1	9.4	447354.80	4450441.46	OB chan
OCKMT3	T5	14	0.4	7.7	447354.79	4450439.76	top of bank
OCKMT3	T5	0	0.8	6.9	447354.79	4450438.96	LEW
OCKMT3	T5	0	0.8	1.6	447354.77	4450433.66	REW
OCKMT3	T5	32	1	1.3	447354.77	4450433.36	ToC
OCKMT3	T5	41	1.6	0	447354.76	4450432.06	VR edge
OCKMT3	T6	14	1.4	56.4	447363.70	4450431.43	VR edge
OCKMT3	T6	0	0.7	55.9	447363.69	4450431.93	REW
OCKMT3	T6	0	0.7	49.6	447363.65	4450438.23	LEW
OCKMT3	T6	40	1	47.2	447363.64	4450440.63	top of island bank
OCKMT3	T6	36	1.1	44	447363.62	4450443.83	tree hummock w/ downed trres
OCKMT3	T6	0	0.6	38.9	447363.58	4450448.93	OB chan
OCKMT3	T6	23	0.7	32.5	447363.54	4450455.33	grassy, herbaceous FP
OCKMT3	T6	30	0.5	24.3	447363.49	4450463.53	S6, herbaceous meadow
OCKMT3	T6	9	0.1	20.4	447363.46	4450467.43	abandoned OB chan
OCKMT3	T6	55	0.3	15.8	447363.43	4450472.03	grassy meadow FP
OCKMT3	T6	52	0	10.2	447363.39	4450477.63	wet grassy meadow w. standing water
OCKMT3	T6	25	0.3	4.2	447363.36	4450483.63	wet grassy meadow w. standing water

OCKMT3	T6	34	0	0	447363.33	4450487.83	VL edge
OCKMT3	T7	14	0.3	55.2	447371.00	4450484.02	VL edge, grassy meadow
OCKMT3	T7	16	0.2	49.8	447371.07	4450478.62	grassy meadow
OCKMT3	T7	9	0.1	46.1	447371.12	4450474.92	tree hummock, young ES
OCKMT3	T7	0	0	35.5	447371.26	4450464.32	channel
OCKMT3	T7	63	0.4	32.5	447371.30	4450461.32	tree hummock w/ grass
OCKMT3	T7	0	0.1	28.1	447371.36	4450456.92	side channel, herbaceous
OCKMT3	T7	47	1	24.6	447371.41	4450453.42	high tree/grassyhummokc
OCKMT3	T7	0	0.5	21.3	447371.45	4450450.12	cob>B side chan
OCKMT3	T7	11	1	16.3	447371.52	4450445.12	veg island w/ herbs & ES
OCKMT3	T7	12	0.9	12.6	447371.57	4450441.42	OB chan
OCKMT3	T7	35	1	10.2	447371.60	4450439.02	S7, on grassy veg island w/ ES and flowers,
OCKMT3	T7	34	1.1	7.5	447371.64	4450436.32	top of bank
OCKMT3	T7	0	0.7	6.3	447371.65	4450435.12	LEW
OCKMT3	T7	0	0.7	2	447371.71	4450430.82	REW
OCKMT3	T7	0	1.5	1	447371.72	4450429.82	on B
OCKMT3	T7	26	1.9	0	447371.74	4450428.82	VR edge
OCKMT3	T8	41	1.2	52.8	447378.35	4450430.40	VR edge
OCKMT3	T8	36	0.7	51.8	447378.38	4450431.40	ToC RR
OCKMT3	T8	0	0.4	51.6	447378.38	4450431.60	REW
OCKMT3	T8	0	0.4	47.1	447378.48	4450436.10	LEW
OCKMT3	T8	41	0.8	45.4	447378.52	4450437.80	S8, herbaceous FP
OCKMT3	T8	9	0.5	42.6	447378.58	4450440.60	herbaceous FP
OCKMT3	T8	0	0.3	38	447378.68	4450445.20	side chan
OCKMT3	T8	18	0.2	32.1	447378.82	4450451.10	OB chan
OCKMT3	T8	58	0.6	28.6	447378.89	4450454.60	tree hummock, tall grass
OCKMT3	T8	8	0	25.5	447378.96	4450457.70	side cha, cobs
OCKMT3	T8	19	0.1	21.6	447379.05	4450461.60	OB chan, gras & flow
OCKMT3	T8	82	0.5	17.9	447379.13	4450465.30	tree hummock, edge of berm
OCKMT3	T8	0	0.1	14	447379.22	4450469.19	side chan
OCKMT3	T8	34	0.5	9.8	447379.31	4450473.39	grassy meadow
OCKMT3	T8	10	0.4	0	447379.53	4450483.19	VL edge, grassy wet meadow, w/ W & bunr

OCKMT3	T9	24	1.4	50.9	447384.73	4450436.15	VR edge
OCKMT3	T9	3	0.9	49.4	447384.79	4450437.65	ToC RR, main stem
OCKMT3	T9	0	0.2	48.8	447384.82	4450438.25	REW
OCKMT3	T9	0	0.2	44.5	447385.01	4450442.54	LEW
OCKMT3	T9	47	0.7	44.2	447385.03	4450442.84	ToC RL
OCKMT3	T9	27	0.9	41.9	447385.13	4450445.14	S9, veg island w. ES & SAF
OCKMT3	T9	26	0.7	39.7	447385.23	4450447.34	veg island w. ES and SAF
OCKMT3	T9	0	0.3	35.9	447385.40	4450451.14	dry side chan
OCKMT3	T9	29	1	32.2	447385.56	4450454.83	tree hummock
OCKMT3	T9	26	0.6	29.2	447385.70	4450457.83	veg island
OCKMT3	T9	44	0.4	25	447385.88	4450462.02	veg island
OCKMT3	T9	0	0	22.4	447386.00	4450464.62	side chan, some standing water
OCKMT3	T9	18	0.4	21.5	447386.04	4450465.52	side chan, bank grassy FP
OCKMT3	T9	38	0.3	15.3	447386.32	4450471.72	grassy meadow
OCKMT3	T9	20	0.2	9.9	447386.56	4450477.11	muddy wet meadow chan
OCKMT3	T9	30	0.5	6.5	447386.71	4450480.51	grassy meadow FP
OCKMT3	T9	11	0.4	5.1	447386.77	4450481.91	grassy meadow chan
OCKMT3	T9	23	0.2	0	447387.00	4450487.00	VL edge, grassy meadow w/ W
OCKMT3	T10	40	0.2	48.5	447394.99	4450487.85	S10, VL edge
OCKMT3	T10	17	0	44	447394.84	4450483.35	wet grassy mneadow
OCKMT3	T10	57	0.3	39.1	447394.67	4450478.46	wet grassy mneadow
OCKMT3	T10	40	0.4	34.9	447394.52	4450474.26	wet grassy meadow hummock
OCKMT3	T10	0	0.1	32.3	447394.43	4450471.66	side chan w/ stading water
OCKMT3	T10	0	0.3	28.4	447394.29	4450467.76	side chan w/ stading water
OCKMT3	T10	41	0.7	25.8	447394.20	4450465.17	tree hummock w/ logs
OCKMT3	T10	26	0.4	23.6	447394.13	4450462.97	dry OB chan
OCKMT3	T10	19	0.6	19.7	447393.99	4450459.07	dry OB chan
OCKMT3	T10	0	0.5	13.7	447393.78	4450453.07	large dry side ch
OCKMT3	T10	30	0.8	10.2	447393.66	4450449.58	org debris, soil under inlet of side chan
OCKMT3	T10	0	0.5	7.4	447393.56	4450446.78	LEW
OCKMT3	T10	0	0.5	3.2	447393.41	4450442.58	REW
OCKMT3	T10	38	1.2	2.1	447393.38	4450441.48	ToC, RR, main stem

OCKMT3	T10	12	1.9	0	447393.30	4450439.38	VR edge
OCKMT3	T11	13	3	49.66	447402.22	4450436.37	VR edge
OCKMT3	T11	8	2.2	48.06	447402.28	4450437.97	ToC
OCKMT3	T11	0	1.9	47.06	447402.32	4450438.97	REW
OCKMT3	T11	0	1.9	40.26	447402.56	4450445.77	LEW
OCKMT3	T11	51	2.6	40.2	447402.56	4450445.83	Toc
OCKMT3	T11	0	1.8	37.2	447402.67	4450448.82	wet side chan center
OCKMT3	T11	0	1.7	32.2	447402.85	4450453.82	standing H2O side ch
OCKMT3	T11	39	1.1	28.3	447402.99	4450457.72	grassy meadow, FP
OCKMT3	T11	19	0.7	24.8	447403.11	4450461.22	dray grassy OB chan
OCKMT3	T11	61	1.1	22.7	447403.19	4450463.31	grassy hummokc
OCKMT3	T11	0	0.5	19.2	447403.31	4450466.81	OB chan with standing water
OCKMT3	T11	72	1	18.4	447403.34	4450467.61	Rl bank of chan, grassy meadow
OCKMT3	T11	33	0.5	14.5	447403.48	4450471.51	grassy meadow, OB chan, S11
OCKMT3	T11	36	0.3	10.8	447403.61	4450475.21	grassy meadow, OB chan
OCKMT3	T11	12	0	8.4	447403.70	4450477.61	grassy meadow, OB chan
OCKMT3	T11	37	0.3	5.2	447403.81	4450480.80	OB chan
OCKMT3	T11	26	0.3	2	447403.93	4450484.00	OB chan
OCKMT3	T11	22	0.4	0	447404.00	4450486.00	VL edhe, IB chan
NSVAB4	T1	21	1.3	222.9	453193.58	4451503.62	VL edge
NSVAB4	T1	50	1.5	202.9	453203.83	4451486.45	S1, BM FP
NSVAB4	T1	24	1.5	186.9	453212.03	4451472.71	ToC
NSVAB4	T1	0	1.2	186.8	453212.08	4451472.63	River bank, LEW
NSVAB4	T1	0	1.2	173.2	453219.05	4451460.95	REW
NSVAB4	T1	62	1.5	172.4	453219.46	4451460.26	top of bank
NSVAB4	T1	36	1.7	170.4	453220.48	4451458.54	grassy FP w/ W
NSVAB4	T1	104	1.8	163.2	453224.17	4451452.36	adjacent stagnant OB chann;
NSVAB4	T1	52	1.2	161.3	453225.15	4451450.73	OB channel water depth 24 cm
NSVAB4	T1	72	1.7	157.9	453226.89	4451447.81	Beaver mound
NSVAB4	T1	110	1.4	154.1	453228.84	4451444.55	FP adjacent to OB channel
NSVAB4	T1	53	1.3	148.9	453231.50	4451440.08	FP adjacent to OB channel
NSVAB4	T1	89	1.3	144	453234.02	4451435.87	FP w/ W, RB

NSVAB4	T1	97	1.4	140.8	453235.66	4451433.13	next to OB channel
NSVAB4	T1	74	0.9	138.1	453237.04	4451430.81	standing water/beaver pond water depth 27cm
NSVAB4	T1	77	1.4	133.4	453239.45	4451426.77	wet meadow w/ W, grass
NSVAB4	T1	87	1.4	129.8	453241.29	4451423.68	wet meadow w/ W, grass
NSVAB4	T1	89	1.3	121.7	453245.44	4451416.72	wet meadow w/ W, grass
NSVAB4	T1	43	1.4	114.3	453249.24	4451410.37	upland, next to spruce
NSVAB4	T1	46	1.3	106.1	453253.44	4451403.33	upland, next to spruce
NSVAB4	T1	79	0.7	97.6	453257.80	4451396.03	lowland OB channel
NSVAB4	T1	31	0.8	88.3	453262.56	4451388.04	Meadow grass, W
NSVAB4	T1	24	0.5	76.1	453268.81	4451377.57	edge of beaevr pond, water depth 8cm
NSVAB4	T1	16	0.3	67.7	453273.12	4451370.36	edge of beaevr pond, water depth 12cm
NSVAB4	T1	17	0.2	56.8	453278.71	4451361.00	edge of beaevr pond, water depth 10cm
NSVAB4	T1	22	0.2	49.3	453282.55	4451354.56	edge of beaevr pond, water depth 9cm
NSVAB4	T1	19	0.3	41.7	453286.44	4451348.03	upland dry meadow
NSVAB4	T1	66	0.3	34.9	453289.93	4451342.19	upland dry meadow, edge of spruce
NSVAB4	T1	76	0.4	26.9	453294.03	4451335.32	spruce forested upland
NSVAB4	T1	96	0.5	20.1	453297.52	4451329.48	edge of spruce/RB
NSVAB4	T1	43	0	11.5	453301.92	4451322.10	lowland swampy wet backwater, depth 5 cm
NSVAB4	T1	154	0	4.7	453305.41	4451316.26	edge of beave rpond, wet water, 4cm
NSVAB4	T1	72	0.1	0	453307.82	4451312.22	VR edge
NSVAB4	T2	19	0.6	225.2	453214.82	4451513.10	VL edge
NSVAB4	T2	59	0.5	222.2	453216.29	4451510.48	S2, wt at 9cm, VL
NSVAB4	T2	80	0.5	220.6	453217.07	4451509.09	LEW
NSVAB4	T2	68	0.5	219.1	453217.81	4451507.78	REW, side channel
NSVAB4	T2	32	0.4	212	453221.29	4451501.59	wet meadow
NSVAB4	T2	71	0.2	210.1	453222.22	4451499.94	LEW, side channel
NSVAB4	T2	65	0.3	207.7	453223.40	4451497.85	REW side channel
NSVAB4	T2	70	0.6	201	453226.69	4451492.01	wet meadow
NSVAB4	T2	86	0.9	198.6	453227.86	4451489.91	top high pt of wet meadow
NSVAB4	T2	44	0.6	197.7	453228.31	4451489.13	LEW, main stem
NSVAB4	T2	0	0.6	186.4	453233.85	4451479.28	REW main stem
NSVAB4	T2	40	0.7	184.4	453234.83	4451477.54	

NSVAB4	T2	117	0.5	179.5	453237.23	4451473.27	Willow hell
NSVAB4	T2	57	0	177.1	453238.41	4451471.18	OB chan, water depth @ 30cm
NSVAB4	T2	27	0.9	172.3	453240.76	4451466.99	grassy FP w/ W
NSVAB4	T2	69	1	167.8	453242.97	4451463.07	grassy FP w/ W
NSVAB4	T2	75	1	160.8	453246.40	4451456.97	grassy FP w/ W
NSVAB4	T2	66	0.8	154.1	453249.69	4451451.13	OB chan depression, beaver trail
NSVAB4	T2	60	0.9	148	453252.68	4451445.82	OB chan depression, beaver trail
NSVAB4	T2	84	1.2	143.8	453254.74	4451442.16	grassy wet meadow w/ W
NSVAB4	T2	74	0.9	137.8	453257.68	4451436.93	grassy WBM, beaver trail/OB chan
NSVAB4	T2	97	1.2	131.7	453260.67	4451431.61	upward toward pond
NSVAB4	T2	33	1.8	125.2	453263.86	4451425.95	grassy upland w/ conifer
NSVAB4	T2	37	1.7	119	453266.90	4451420.54	grassy upland w/ conifer
NSVAB4	T2	35	1.9	109.4	453271.61	4451412.18	grassy upland w/ conifer
NSVAB4	T2	53	1.9	101.9	453275.29	4451405.64	grassy upland w/ conifer
NSVAB4	T2	82	1.9	92.4	453279.95	4451397.36	grassy upland w/ conifer, W
NSVAB4	T2	78	1.7	83.3	453284.41	4451389.43	grassy upland w/ conifer, lots of W, next to
NSVAB4	T2	57	1.8	72.9	453289.51	4451380.37	adjacent to small marshy pond
NSVAB4	T2	69	1.8	63.3	453294.22	4451372.00	in small swamp, 30cm depth
NSVAB4	T2	46	1.1	51.9	453299.81	4451362.07	small swamp, 18 cm depth
NSVAB4	T2	7	1.2	44.7	453303.34	4451355.79	water edge of small marsh
NSVAB4	T2	18	1.4	40.2	453305.54	4451351.87	edge of water, pond
NSVAB4	T2	42	1.5	32.4	453309.37	4451345.07	in edge of pond, water depth 14cm
NSVAB4	T2	34	1.3	22.2	453314.37	4451336.18	in edge of pond, water depth 32 cm
NSVAB4	T2	28	1.1	13.7	453318.54	4451328.78	in pond on U/S end, water depth 20cm
NSVAB4	T2	41	1.2	6.7	453321.97	4451322.68	In pond, depth 20cm
NSVAB4	T2	58	1.2	0	453325.26	4451316.84	south edge of pond, VR edge
NSVAB4	T3	32	0.4	243.1	453230.12	4451533.76	VL edge, LEW (stadning pool/side channel)
NSVAB4	T3	92	0.4	238.7	453232.16	4451529.86	grassy meadow, OB soland
NSVAB4	T3	56	0.6	235.7	453233.55	4451527.21	REW, side channel, ToB
NSVAB4	T3	23	0.8	228.5	453236.90	4451520.83	sandy FP
NSVAB4	T3	0	0.6	226.2	453237.96	4451518.79	LEW, mainstem
NSVAB4	T3	0	0.6	214	453243.62	4451507.98	REW main stem

NSVAB4	T3	64	0.4	207.2	453246.78	4451501.96	sandy FP w/ wood on edge of OB chan
NSVAB4	T3	33	0.5	196.3	453251.84	4451492.30	grassy FP w/ W
NSVAB4	T3	46	0.6	188.2	453255.60	4451485.13	grassy FP w? W
NSVAB4	T3	71	0.6	178.6	453260.05	4451476.63	grassy FP w/ W
NSVAB4	T3	20	0	176.6	453260.98	4451474.85	OB chan, water depth 0.55m
NSVAB4	T3	111	0.8	173.2	453262.56	4451471.84	Grassy hummocky, FP w/ W
NSVAB4	T3	51	0.8	165.8	453265.99	4451465.29	Grassy hummocky, FP w/ W
NSVAB4	T3	54	1.1	155.7	453270.68	4451456.34	Grassy hummocky, FP w/ W
NSVAB4	T3	68	1.2	144.8	453275.73	4451446.69	Grassy hummocky, FP w/ W
NSVAB4	T3	89	1.3	137.1	453279.31	4451439.86	Grassy hummocky, FP w/ W
NSVAB4	T3	35	1.1	130.4	453282.42	4451433.93	buried cob bar on up slope toward grassy
NSVAB4	T3	46	0.8	121.7	453286.45	4451426.22	buried cob upland mound with conifers
NSVAB4	T3	35	1.2	113.2	453290.40	4451418.69	buried cob upland mound with conifers
NSVAB4	T3	54	1.3	103.7	453294.81	4451410.28	buried cob upland mound with conifers
NSVAB4	T3	73	1	96.3	453298.24	4451403.72	moving down off upland into meadow
NSVAB4	T3	71	1.1	88.4	453301.91	4451396.72	moving down off upland into meadow
NSVAB4	T3	76	1	81.2	453305.25	4451390.35	wet BM
NSVAB4	T3	112	1.5	80.8	453305.43	4451389.99	S11, wet BM
NSVAB4	T3	123	1.6	72.9	453309.10	4451382.99	wet BM, upslope toward B pond
NSVAB4	T3	70	1.4	63.7	453313.37	4451374.85	wet BM, depression w/ water
NSVAB4	T3	19	2.5	60	453315.08	4451371.57	cobble bar, upland rise cob mound toward B
NSVAB4	T3	21	2.4	51	453319.26	4451363.60	cobble bar, upland rise cob mound toward B
NSVAB4	T3	42	2.3	43.8	453322.60	4451357.22	upland adjacent to pond
NSVAB4	T3	34	2.1	40	453324.36	4451353.85	north edge of pond
NSVAB4	T3	5	1.6	34	453327.15	4451348.54	In pond, decaying algae on cobs
NSVAB4	T3	10	1.5	27.9	453329.98	4451343.13	In pond, decaying algae on cobs
NSVAB4	T3	10	1.5	21.1	453333.14	4451337.11	In pond, decaying algae on cobs
NSVAB4	T3	30	1.4	14.6	453336.15	4451331.35	in pond decaying algae with minerl seds
NSVAB4	T3	30	1.5	7.7	453339.35	4451325.24	in pond, mushy gook
NSVAB4	T3	10	2.1	0	453342.93	4451318.42	South edge of pond, VR edge
NSVAB4	T4	112	1.9	267.5	453242.84	4451550.58	VL edge, LEW side channel
NSVAB4	T4	110	1.7	262	453245.48	4451545.76	inunndated surface, flowing water, sandy FP

NSVAB4	T4	55	1.7	258.3	453247.26	4451542.52	inunndated surface, flowing water, sandy FP
NSVAB4	T4	139	2	252.1	453250.24	4451537.08	inunndated surface, flowing water, sandy FP
NSVAB4	T4	89	1.5	244.8	453253.76	4451530.68	REW ToC
NSVAB4	T4	0	0.9	244	453254.14	4451529.98	LEW at BF? BF edge of water, all under water!
NSVAB4	T4	0	0.9	232.2	453259.82	4451519.63	REW @ BF
NSVAB4	T4	0	0.6	225.6	453262.99	4451513.85	Gravel pt bar on U/S side RR w/ sand, W, flow
NSVAB4	T4	69	0.7	221.2	453265.11	4451509.99	
NSVAB4	T4	64	0.8	218	453266.65	4451507.18	OB channel flowing over grass
NSVAB4	T4	74	1	213.5	453268.81	4451503.24	hummocky bank w/ grass, W
NSVAB4	T4	50	0.7	205.8	453272.51	4451496.49	hummocky bank w/ grass, W
NSVAB4	T4	58	0.7	203.9	453273.43	4451494.82	hummocky bank w/ grass, W
NSVAB4	T4	109	0.6	200	453275.30	4451491.40	hummocky bank w/ grass, W
NSVAB4	T4	93	0.6	196.4	453277.04	4451488.25	hummocky bank w/ grass, W
NSVAB4	T4	57	0.6	192.9	453278.72	4451485.18	hummocky bank w/ grass, W
NSVAB4	T4	0	0.1	190.9	453279.68	4451483.43	OB channel, sand bed
NSVAB4	T4	51	0.6	188.4	453280.88	4451481.23	muddy bank
NSVAB4	T4	0	0	187.4	453281.36	4451480.36	OB channel, sand, bed
NSVAB4	T4	0	0.6	184.9	453282.57	4451478.17	EW, OB channel
NSVAB4	T4	56	1	184.2	453282.90	4451477.55	top of bank
NSVAB4	T4	0	0.3	181.1	453284.39	4451474.83	OB chan, 0.5m depth
NSVAB4	T4	48	0.6	178.5	453285.65	4451472.55	baqnk of OB channel
NSVAB4	T4	96	0.9	173.6	453288.00	4451468.26	FP, grassy meadow
NSVAB4	T4	82	1	169.1	453290.17	4451464.31	FP, grassy meadow
NSVAB4	T4	36	0.3	164.1	453292.57	4451459.93	OB channel stagnant water, depth 0.6m
NSVAB4	T4	98	1.1	159	453295.02	4451455.46	bank adjacent to OB chan, S10
NSVAB4	T4	75	1	151.7	453298.54	4451449.06	beaver pond inlet adjacent to channel on bank
NSVAB4	T4	37	0.8	146.7	453300.94	4451444.67	beaver pond (BP), depth 0.17m
NSVAB4	T4	61	0.7	141.7	453303.35	4451440.29	BP, 0.32m
NSVAB4	T4	71	0.6	135.1	453306.52	4451434.50	BP, 0.4m
NSVAB4	T4	32	0.8	129.3	453309.31	4451429.42	BP, 0.16m
NSVAB4	T4	84	1	122.8	453312.44	4451423.72	BP, 0.01m
NSVAB4	T4	64	1.2	116.2	453315.61	4451417.93	upland meadow, grass, W

NSVAB4	T4	62	1.1	110.3	453318.45	4451412.76	wet upland meadow, grass, W
NSVAB4	T4	62	1.2	104.3	453321.33	4451407.50	wet upland meadow, grass, W
NSVAB4	T4	64	1.3	98	453324.37	4451401.98	wet upland meadow, grass, W
NSVAB4	T4	108	1.4	89.3	453328.55	4451394.35	wet upland meadow, grass, W
NSVAB4	T4	87	1.4	82	453332.06	4451387.95	wet upland meadow, grass, W
NSVAB4	T4	8.3	1.5	75.5	453335.19	4451382.25	wet upland meadow, grass, W
NSVAB4	T4	90	1.6	69.5	453338.07	4451376.99	wet upland meadow, grass, W
NSVAB4	T4	61	1.7	62.7	453341.34	4451371.03	wet upland meadow, grass, W
NSVAB4	T4	38	2.1	53.1	453345.96	4451362.61	Toe of berm/beaver dam at pond
NSVAB4	T4	41	2.5	43.4	453350.63	4451354.11	Toe of berm/beaver dam at pond
NSVAB4	T4	42	2.5	38.1	453353.18	4451349.46	north edge of water & pond
NSVAB4	T4	46	2.45	37.2	453353.61	4451348.67	beaver pond, water depth 5cm
NSVAB4	T4	15	1.95	32.4	453355.92	4451344.46	in pond, lots of silt and clay
NSVAB4	T4	15	1.85	26.8	453358.61	4451339.56	S13, in pond, lots of silt and clay
NSVAB4	T4	51	1.85	21.6	453361.11	4451335.00	in pond, lots of silt and clay
NSVAB4	T4	12	1.95	15.7	453363.95	4451329.82	in pond, lots of silt and clay. S12
NSVAB4	T4	53	2.35	3.5	453369.82	4451319.13	south edge of water & pond
NSVAB4	T4	28	2.35	0	453371.50	4451316.06	VR edge
NSVAB4	T5	46	0	244	453260.38	4451567.99	VL edge, running water
NSVAB4	T5	0	0.1	243	453260.84	4451567.10	LEW (side channel)
NSVAB4	T5	0	0.5	237.6	453263.34	4451562.32	REW, side channel
NSVAB4	T5	29	0.6	229.1	453267.28	4451554.78	FP wet
NSVAB4	T5	28	0.6	223.6	453269.83	4451549.91	edge of FP, side channel, S3
NSVAB4	T5	42	0.6	217.3	453272.75	4451544.33	running water, wet meadow
NSVAB4	T5	88	0.2	210.5	453275.90	4451538.30	running water, wet meadow
NSVAB4	T5	82	0.1	209	453276.59	4451536.97	running water, wet meadow
NSVAB4	T5	90	0.1	205.3	453278.30	4451533.69	sandy/grassy island hummock (dry)
NSVAB4	T5	122	0.1	205	453278.44	4451533.43	rapid flowing water on outside of river bend
NSVAB4	T5	0	0.2	203	453279.37	4451531.65	LEW @ BF, knee high water
NSVAB4	T5	0	0.3	202	453279.83	4451530.77	REW main stem
NSVAB4	T5	43	0.7	196.6	453282.33	4451525.98	ToC grassy hummock
NSVAB4	T5	38	0.8	188.1	453286.27	4451518.45	grassy sloppy FP W

NSVAB4	T5	78	0.8	182.6	453288.82	4451513.58	grassy sloppy FP W
NSVAB4	T5	0	0.8	176.3	453291.74	4451507.99	bed of side channel, gravel bed
NSVAB4	T5	74	0.4	169.5	453294.89	4451501.97	small island in side channel
NSVAB4	T5	0	0.4	126.5	453314.81	4451463.86	sidec hannel gravel bed
NSVAB4	T5	21	0.4	126.4	453314.86	4451463.77	top of bank, grassy tree hummock with spruce
NSVAB4	T5	60	0.4	117.8	453318.84	4451456.15	edge of stagnant OB channel
NSVAB4	T5	72	0.7	111.7	453321.67	4451450.74	OB channel, beaver pond outflow
NSVAB4	T5	58	0	110.2	453322.36	4451449.41	OB channel, beaver pond outflow
NSVAB4	T5	54	0.8	109.1	453322.87	4451448.44	grassy W
NSVAB4	T5	101	0.4	107.3	453323.70	4451446.84	edge of pond shallow pond
NSVAB4	T5	57	1	105.7	453324.45	4451445.43	edge of pond shallow pond
NSVAB4	T5	42	1.2	99.5	453327.32	4451439.93	in pond water depth, 25cm
NSVAB4	T5	88	1.5	91.7	453330.93	4451433.02	in pond, water depth 21cm
NSVAB4	T5	55	1.6	83.8	453334.59	4451426.02	edge of pond, water depth 3 cm
NSVAB4	T5	42	1.7	79.9	453336.40	4451422.56	sloppy grassy meadow w/ RB, W
NSVAB4	T5	140	1.8	73.5	453339.36	4451416.89	sloppy grassy meadow w/ RB, W
NSVAB4	T5	75	1.7	68.7	453341.59	4451412.63	tree berm in wet meadow
NSVAB4	T5	81	1.4	59.5	453345.85	4451404.48	sloppy grassy meadow w/ RB, W
NSVAB4	T5	98	1.4	52	453349.32	4451397.84	in meadow next to pond
NSVAB4	T5	74	1.7	41.5	453354.19	4451388.53	near pond drainage outlet
NSVAB4	T5	30	1.9	30.9	453359.10	4451379.14	wet BM, W
NSVAB4	T5	43	2.2	23.4	453362.57	4451372.49	wet BM, W
NSVAB4	T5	79	2.5	16.5	453365.77	4451366.37	wet BM, W
NSVAB4	T5	33	2.7	8.7	453369.38	4451359.46	D/S of beaver pond
NSVAB4	T5	86	3	0	453373.41	4451351.75	VR egde
NSVAB4	T6	86	0.3	260.8	453282.78	4451579.46	VL edge
NSVAB4	T6	52	0.4	251.1	453287.03	4451570.74	grassy meadow, FP
NSVAB4	T6	61	0.3	245.3	453289.57	4451565.52	ToC, RL side channel
NSVAB4	T6	0	0	245.2	453289.61	4451565.43	LEW side channel
NSVAB4	T6	0	0	211.9	453304.19	4451535.50	REW side channel
NSVAB4	T6	66	0.4	211.3	453304.46	4451534.96	Island TOC, W hell
NSVAB4	T6	82	0.1	204.5	453307.44	4451528.84	island with small chanenls, W, RR edge of

NSVAB4	T6	0	0.1	200.2	453309.32	4451524.98	LEW side channel
NSVAB4	T6	125	0.4	200.1	453309.36	4451524.89	RL edge of island
NSVAB4	T6	100	0.3	198.1	453310.24	4451523.09	RR edge of osland, ToC
NSVAB4	T6	0	0.1	198	453310.28	4451523.00	REW side channel
NSVAB4	T6	0	0.1	190.7	453313.48	4451516.44	LEW side channel
NSVAB4	T6	46	0.2	190.6	453313.52	4451516.35	REW edhe of island
NSVAB4	T6	44	0	186.9	453315.14	4451513.02	standing water isolated side pool/side channel
NSVAB4	T6	35	0.2	177.1	453319.44	4451504.21	ToC RR edge of island
NSVAB4	T6	0	0	176.8	453319.57	4451503.94	LEW side channel
NSVAB4	T6	0	0	172	453321.67	4451499.63	REW RL, edge of island
NSVAB4	T6	34	0.1	171.2	453322.02	4451498.91	Top of island, main stem, RR edge of island
NSVAB4	T6	0	0	170.4	453322.37	4451498.19	LEW main stem
NSVAB4	T6	0	0	142	453334.81	4451472.66	REW main stem
NSVAB4	T6	37	0.3	141.6	453334.98	4451472.30	Top bank
NSVAB4	T6	6	0.2	137.4	453336.82	4451468.52	dry OB channel
NSVAB4	T6	30	0.5	131.2	453339.54	4451462.95	dry upland, W
NSVAB4	T6	19	0.7	125.1	453342.21	4451457.46	little grassy meadow next to RB and W
NSVAB4	T6	64	0.1	118.1	453345.28	4451451.17	Standing water, OB channel, 18cm deep
NSVAB4	T6	38	0.4	110.7	453348.52	4451444.52	
NSVAB4	T6	30	0.2	103.7	453351.58	4451438.23	adjacent to standing orange water and OB
NSVAB4	T6	110	0.2	97.8	453354.17	4451432.92	OB channel, standing water RB, W
NSVAB4	T6	73	0.2	91.2	453357.06	4451426.99	wet meadow,RB, W, grass
NSVAB4	T6	88	0.2	86.3	453359.20	4451422.58	wet meadow,RB, W, grass
NSVAB4	T6	101	0.3	78.1	453362.79	4451415.21	wet meadow,RB, W, grass
NSVAB4	T6	97	0.3	71.4	453365.73	4451409.19	floating grass matt
NSVAB4	T6	77	0.3	63.1	453369.36	4451401.73	floating ground held together by root matt
NSVAB4	T6	82	0.4	55.8	453372.56	4451395.16	floating ground held together by root matt
NSVAB4	T6	87	0.4	45.5	453377.07	4451385.90	wet meadow
NSVAB4	T6	79	0.4	37.3	453380.66	4451378.53	wet meadow
NSVAB4	T6	93	0.3	30.4	453383.69	4451372.33	wet meadow
NSVAB4	T6	103	0.4	23.1	453386.88	4451365.77	wet meadow
NSVAB4	T6	135	0.5	18	453389.12	4451361.18	wet meadow

NSVAB4	T6	93	0.4	12	453391.74	4451355.79	wet, meadow, OB channel
NSVAB4	T6	104	0.4	8.3	453393.36	4451352.46	standing orange water, wet meadow, W, grass,
NSVAB4	T6	132	0.5	4.2	453395.16	4451348.78	S9, edge of sloping meadow
NSVAB4	T6	134	0.6	0	453397.00	4451345.00	VR edge
NSVAB4	T7	59	1.3	214	453416.53	4451360.38	VR edge
NSVAB4	T7	102	1.2	205.8	453412.80	4451367.68	berm between interfluv and side channel
NSVAB4	T7	107	1.1	199.9	453410.12	4451372.94	wet grassy M with W, RB, standing water
NSVAB4	T7	82	1.2	194.9	453407.84	4451377.39	wet grassy M with W, RB, standing water
NSVAB4	T7	98	1.3	185.7	453403.66	4451385.58	wet grassy M with W, RB, standing water
NSVAB4	T7	58	1.3	175.9	453399.20	4451394.31	OB channel, wet meadow, W, RB
NSVAB4	T7	79	1.4	170.6	453396.79	4451399.03	wet meadow W, RB
NSVAB4	T7	112	1.6	162.9	453393.28	4451405.88	S8, hummock w/ RB, wet meadow, S8
NSVAB4	T7	84	1.7	157.8	453390.96	4451410.43	wet grassy M with W, RB, standing water
NSVAB4	T7	54	1.7	151	453387.87	4451416.48	standing water, wet grassy M with W, RB,
NSVAB4	T7	71	1.7	143.6	453384.50	4451423.07	standing water, wet grassy M with W, RB,
NSVAB4	T7	82	1.7	140.6	453383.14	4451425.74	standing water, wet grassy M with W, RB,
NSVAB4	T7	87	1.6	132	453379.23	4451433.40	standing water, wet grassy M with W, RB,
NSVAB4	T7	97	1.4	122.4	453374.86	4451441.95	standing water, wet grassy M with W, RB,
NSVAB4	T7	97	0.8	113.2	453370.67	4451450.14	OB channel, wet grassy meadow
NSVAB4	T7	15	1.2	110	453369.22	4451452.99	standing water, wet grassy M with W, RB,
NSVAB4	T7	41	1	104.9	453366.90	4451457.53	standing water, wet grassy M with W, RB,
NSVAB4	T7	84	1.1	99.9	453364.62	4451461.99	standing water, wet grassy M with W, RB,
NSVAB4	T7	25	1.3	96.9	453363.26	4451464.66	Dry hummock
NSVAB4	T7	34	1.1	92.7	453361.35	4451468.40	
NSVAB4	T7	0	1	92.1	453361.07	4451468.93	REW
NSVAB4	T7	0	1	83.5	453357.16	4451476.59	LEW main stem)
NSVAB4	T7	24	1.2	81.6	453356.30	4451478.28	top of sloped bank
NSVAB4	T7	22	1.1	79.3	453355.25	4451480.33	left edge island, REW
NSVAB4	T7	40	0.8	71.1	453351.52	4451487.63	FP, OB channel
NSVAB4	T7	100	1.1	69.3	453350.70	4451489.24	LEW OB Channel
NSVAB4	T7	103	1.4	65.4	453348.92	4451492.71	FP w/ W hell
NSVAB4	T7	102	1.2	59	453346.01	4451498.41	FP w/ W hell

NSVAB4	T7	36	0.7	53	453343.28	4451503.75	OB channel stagnent
NSVAB4	T7	19	0	48.1	453341.05	4451508.11	OB channel stagnent
NSVAB4	T7	76	0.8	38.7	453336.78	4451516.48	grassy meadow, W hell
NSVAB4	T7	68	0.7	30.9	453333.23	4451523.43	grassy meadow, W hell
NSVAB4	T7	47	0.8	23.4	453329.82	4451530.11	top of grassy meadow, W hell
NSVAB4	T7	46	0.6	22.1	453329.22	4451531.27	L edge of island sie channel ToC
NSVAB4	T7	0	0.3	22	453329.18	4451531.36	REW, side channel
NSVAB4	T7	0	0.3	16.1	453326.49	4451536.61	LEW side channel
NSVAB4	T7	73	0.7	15.2	453326.08	4451537.41	Top of island
NSVAB4	T7	54	0.6	11.2	453324.26	4451540.97	Wet meadow
NSVAB4	T7	50	0.8	5.1	453321.49	4451546.41	OB channel
NSVAB4	T7	33	1	0	453319.17	4451550.95	VL edge
NSVAB4	T8	53	0.3	234.2	453343.13	4451559.62	VL edge
NSVAB4	T8	27	0.1	228.7	453345.39	4451554.60	OV channel
NSVAB4	T8	55	0.5	228.1	453345.64	4451554.06	FP, grassy meadow
NSVAB4	T8	0	0.2	224.7	453347.03	4451550.96	LEW side channel
NSVAB4	T8	0	0.2	215.6	453350.78	4451542.66	REW side channel
NSVAB4	T8	50	0.4	215.3	453350.90	4451542.39	ToC
NSVAB4	T8	68	0.2	207.7	453354.03	4451535.46	grassy meadow, FP, standing water
NSVAB4	T8	16	0	201.2	453356.70	4451529.54	grassy meadow, FP,
NSVAB4	T8	114	0.7	195.8	453358.92	4451524.62	grassy meadow, FP,
NSVAB4	T8	71	0.8	190.6	453361.06	4451519.88	grassy meadow, FP,
NSVAB4	T8	102	1.5	185.3	453363.24	4451515.05	Top of cutbank, island
NSVAB4	T8	66	1.4	179.9	453365.47	4451510.12	grassy Willow, FP, meadow
NSVAB4	T8	0	0.8	176.6	453366.82	4451507.12	LEW
NSVAB4	T8	0	0.8	164.2	453371.92	4451495.81	REW
NSVAB4	T8	47	1.2	162.3	453372.71	4451494.08	FP
NSVAB4	T8	85	1.2	155.8	453375.38	4451488.16	FP, grass, W
NSVAB4	T8	110	1.2	150.7	453377.48	4451483.51	FP, grass, W
NSVAB4	T8	74	1.1	146.3	453379.29	4451479.50	FP, W, grass, adjacent to sdie channel
NSVAB4	T8	110	1.3	138.8	453382.37	4451472.66	grass, W, adjacent to stagnant orange water
NSVAB4	T8	62	1.2	132.5	453384.97	4451466.92	grass, W, adjacent to stagnant orange water

NSVAB4	T8	84	1.2	125.3	453387.93	4451460.36	grass, W, adjacent to stagnant orange water
NSVAB4	T8	58	1.1	114.6	453392.33	4451450.61	grass, W, side channel adjacent to stagnant
NSVAB4	T8	31	1.1	108.6	453394.80	4451445.14	grass, W, adjacent to stagnant orange water
NSVAB4	T8	40	1.1	102.7	453397.23	4451439.76	grass, W, adjacent to stagnant orange water
NSVAB4	T8	61	0.9	94.4	453400.64	4451432.19	wet grass & RB with standing water
NSVAB4	T8	70	0.7	88.3	453403.15	4451426.63	wet grass & RB with standing water
NSVAB4	T8	74	0.6	80	453406.56	4451419.07	wet grass & RB with standing water
NSVAB4	T8	78	0.4	71.2	453410.18	4451411.05	WBM adjacent to beaver pond
NSVAB4	T8	112	0.4	60.9	453414.42	4451401.66	WBM adjacent to beaver pond
NSVAB4	T8	103	0.4	53.8	453417.34	4451395.19	WBM adjacent to beaver pond
NSVAB4	T8	111	0.4	45.9	453420.59	4451387.99	WBM adjacent to beaver pond
NSVAB4	T8	61	0.4	40.1	453422.98	4451382.70	edge of bog
NSVAB4	T8	90	0.5	36	453424.67	4451378.97	upland island with grass, W, RB
NSVAB4	T8	147	0.6	24.6	453429.36	4451368.58	upland edge of bog, RB, grasses
NSVAB4	T8	85	0.4	16.5	453432.69	4451361.19	S6, between standing water interfluves
NSVAB4	T8	64	0.5	13.2	453434.05	4451358.18	next to standing water
NSVAB4	T8	129	0.8	5.9	453437.05	4451351.53	upland berm between standing water fallen
NSVAB4	T8	44	0.7	0	453439.48	4451346.15	VR edge
NSVAB4	T9	150	2	235.1	453457.69	4451358.59	VR edge
NSVAB4	T9	107	2.1	226.3	453454.07	4451366.61	Wet W field standing water
NSVAB4	T9	100	1.8	217.9	453450.62	4451374.27	Wet W field standing water
NSVAB4	T9	122	1.5	211.6	453448.03	4451380.01	S7, Next to standing orange water
NSVAB4	T9	99	1.5	206.3	453445.86	4451384.85	adjacent to beaver pond outflow
NSVAB4	T9	97	1.6	205	453445.32	4451386.03	adjacent to Beaver pond, on berm/dam
NSVAB4	T9	130	1.7	198.1	453442.49	4451392.32	adjacent to Beaver pond, on berm/dam, P301-
NSVAB4	T9	134	1.8	187.9	453438.30	4451401.62	on beaver dam/berm, P301-304
NSVAB4	T9	97	1.7	178.8	453434.56	4451409.92	on beaver dam/berm
NSVAB4	T9	84	1.7	168.7	453430.41	4451419.13	on berm with wood beneath soil
NSVAB4	T9	101	1.6	159	453426.43	4451427.97	adjacent to pond on beaver dam/berm
NSVAB4	T9	108	1.7	149.9	453422.69	4451436.27	adjacent to pond on beaver dam/berm
NSVAB4	T9	55	1.4	141.2	453419.11	4451444.20	moving away from pond, down off berm on
NSVAB4	T9	51	1.5	132.3	453415.46	4451452.31	dry grassy meadow

NSVAB4	T9	62	1.6	123.8	453411.97	4451460.06	dry grassy meadow
NSVAB4	T9	34	1	114.4	453408.10	4451468.63	OB channeladjacent to standing pond
NSVAB4	T9	28	1.2	106.1	453404.70	4451476.20	upland grassy FP with W
NSVAB4	T9	63	1	98.3	453401.49	4451483.31	grassy FP slope to channel
NSVAB4	T9	35	1	92.2	453398.99	4451488.87	OB channel, grassy FP slope to channel
NSVAB4	T9	48	0.8	85.8	453396.36	4451494.71	grassy FP slope to channel
NSVAB4	T9	108	0.6	81	453394.38	4451499.09	ToC
NSVAB4	T9	0	0.4	80.9	453394.34	4451499.18	REW
NSVAB4	T9	0	0.4	61.3	453386.29	4451517.05	LEW, main stem (better to us LEW from other
NSVAB4	T9	52	0.7	57	453384.53	4451520.97	grassy meadow, top of sklope
NSVAB4	T9	51	0.8	50.2	453381.73	4451527.17	grassy meadow, top of sklope
NSVAB4	T9	69	0.4	44.2	453379.27	4451532.64	ToC, grassy meadow
NSVAB4	T9	0	0.1	43.1	453378.82	4451533.64	REW side channel
NSVAB4	T9	0	0.1	41.5	453378.16	4451535.10	RR edge of small island
NSVAB4	T9	90	0.9	40.9	453377.91	4451535.65	Top of island
NSVAB4	T9	0	0.1	40.3	453377.67	4451536.19	RL edge of small grassy island
NSVAB4	T9	0	0.1	23.1	453370.60	4451551.88	Many active side channels, LEW
NSVAB4	T9	77	0.4	22.7	453370.44	4451552.24	Top of cutbank, FP, grassy meadow
NSVAB4	T9	90	0.4	15.9	453367.64	4451558.44	Grassy, W hell, FP
NSVAB4	T9	51	0	8.7	453364.69	4451565.00	OB channel (dry)
NSVAB4	T9	66	0.4	4.5	453362.96	4451568.83	W hummock
NSVAB4	T9	15	0.2	0	453361.11	4451572.94	VL edge
NSVAB4	T10	12	0.8	255.5	453376.22	4451590.52	Vl edge
NSVAB4	T10	56	0.6	248.4	453379.18	4451584.06	Grassy meadow
NSVAB4	T10	0	0.2	248.2	453379.27	4451583.88	LEW stagnant OB channel
NSVAB4	T10	0	0.2	244.4	453380.85	4451580.43	REW, algae
NSVAB4	T10	34	0.8	241.4	453382.10	4451577.70	S4, grassy meadow hummock
NSVAB4	T10	36	0.9	234.2	453385.10	4451571.16	grassy meadow hummmock
NSVAB4	T10	71	0.9	227	453388.10	4451564.61	ToC, grassy meadow
NSVAB4	T10	0	0.5	226.8	453388.19	4451564.43	LEW side channel
NSVAB4	T10	0	0.5	222.3	453390.06	4451560.34	REW side chanenl
NSVAB4	T10	69	0.9	221.7	453390.31	4451559.79	ToC RR side channel

NSVAB4	T10	26	0.5	218.1	453391.82	4451556.52	
NSVAB4	T10	72	0.9	216.4	453392.52	4451554.98	Toc RL side channel
NSVAB4	T10	0	0.5	216.2	453392.61	4451554.80	LEW, edge of channel
NSVAB4	T10	0	0.5	206.1	453396.82	4451545.62	REW
NSVAB4	T10	42	0.8	205.5	453397.07	4451545.07	ToC
NSVAB4	T10	106	0.6	199.5	453399.57	4451539.62	grassy OB channel
NSVAB4	T10	88	0.9	193.3	453402.16	4451533.98	grassy hummock, FP
NSVAB4	T10	39	0.6	184.7	453405.74	4451526.16	grassu OC channel
NSVAB4	T10	30	0.7	176.9	453408.99	4451519.07	sandy grass meadow
NSVAB4	T10	37	0.4	168.2	453412.62	4451511.17	grassy willow FP
NSVAB4	T10	31	0.6	164	453414.37	4451507.35	grassy willow FP
NSVAB4	T10	0	0.4	161.8	453415.29	4451505.35	LEW main stem
NSVAB4	T10	0	0.4	144.2	453422.63	4451489.35	REW main stem, diagonally across the channel
NSVAB4	T10	70	1	144	453422.71	4451489.17	ToC, grassy hummock, W
NSVAB4	T10	59	0.8	137.3	453425.50	4451483.08	upper FP, grass with W
NSVAB4	T10	49	0.8	129.8	453428.63	4451476.26	upper FP, grass with W
NSVAB4	T10	57	1	122.2	453431.80	4451469.36	upper FP, grass with W
NSVAB4	T10	68	1.2	116.7	453434.09	4451464.36	upper FP, grass with W
NSVAB4	T10	31	1.1	106.2	453438.47	4451454.81	upper FP, grass with W
NSVAB4	T10	28	0.9	100.4	453440.89	4451449.54	upper FP, grass with W
NSVAB4	T10	59	0.6	91.7	453444.52	4451441.63	OB, channel, upper FP, grass with W
NSVAB4	T10	62	0.4	85.1	453447.27	4451435.63	upper FP, grass with W
NSVAB4	T10	42	0.4	75.6	453451.23	4451427.00	upper FP, grass with W
NSVAB4	T10	37	0.5	68.2	453454.32	4451420.27	upper FP, grass with W
NSVAB4	T10	21	0	60.9	453457.36	4451413.64	OB channel w standing black water
NSVAB4	T10	47	0.4	50.3	453461.78	4451404.00	Grassy wet meadow with W
NSVAB4	T10	40	0.3	44.3	453464.28	4451398.55	Grassy wet meadow with W
NSVAB4	T10	72	0.1	37.2	453467.24	4451392.10	orange standing water, grassy wet meadow, OB
NSVAB4	T10	70	0.1	29.9	453470.28	4451385.46	orange standing water, grassy wet meadow, OB
NSVAB4	T10	83	0.1	24.1	453472.70	4451380.19	orange standing water, grassy wet meadow, OB
NSVAB4	T10	48	0.1	16.2	453476.00	4451373.01	Grassy wet meadow, W
NSVAB4	T10	81	0.2	8.8	453479.08	4451366.28	Grassy wet meadow, W

NSVAB4	T10	108	0.2	2.5	453481.71	4451360.56	Grassy wet meadow, W
NSVAB4	T10	100	0.1	0	453482.75	4451358.28	VR egde
NSVAB4	T11	48	0.4	268.5	453511.25	4451359.41	VR edge, wet meadow with W, grass at W/pine
NSVAB4	T11	57	0.3	262.6	453508.68	4451364.72	S5, wet grassy meadow with W
NSVAB4	T11	46	0.2	258.3	453506.81	4451368.59	WM with W & grass
NSVAB4	T11	72	0.1	248.8	453502.68	4451377.15	WM with W & grass, orange stagnant water, OB
NSVAB4	T11	47	0.2	240.2	453498.94	4451384.89	WM with W & grass, orange stagnant water
NSVAB4	T11	82	0.1	233.6	453496.07	4451390.84	WM with W & grass, orange stagnant water, OB
NSVAB4	T11	73	0	224.1	453491.94	4451399.39	WM with W & grass, orange stagnant water
NSVAB4	T11	29	0.2	217.8	453489.20	4451405.06	upland meadow or grass & W
NSVAB4	T11	70	0.2	208.2	453485.02	4451413.71	upland meadow or grass & W
NSVAB4	T11	43	0.3	198.5	453480.81	4451422.44	upland meadow or grass & W
NSVAB4	T11	67	0.4	188.9	453476.63	4451431.09	upland meadow or grass & W
NSVAB4	T11	35	0.2	180.6	453473.02	4451438.56	grassy, W, OB channel
NSVAB4	T11	43	0.3	170	453468.41	4451448.11	grassy, W, OB channel
NSVAB4	T11	33	0.6	161	453464.50	4451456.21	grassy, W, OB channel
NSVAB4	T11	54	0.6	151	453460.15	4451465.22	grass, W, FP
NSVAB4	T11	38	0.7	141.1	453455.84	4451474.13	grass, W, FP
NSVAB4	T11	71	0.3	131.2	453451.54	4451483.05	ToC
NSVAB4	T11	0	0.3	131.2	453451.54	4451483.05	REW main stem
NSVAB4	T11	0	0.3	123.9	453448.36	4451489.62	LEW main stem
NSVAB4	T11	32	0.4	123.8	453448.32	4451489.71	ToC, FP
NSVAB4	T11	105	0.4	116.5	453445.15	4451496.28	FP
NSVAB4	T11	64	0.8	108.6	453441.71	4451503.40	upland FP, grassy W
NSVAB4	T11	35	0.8	101.1	453438.45	4451510.15	OB channel
NSVAB4	T11	45	1	96	453436.23	4451514.74	Tall grass willow upland
NSVAB4	T11	65	1.1	90.9	453434.01	4451519.34	Tall grass willow upland
NSVAB4	T11	55	0.9	85.5	453431.66	4451524.20	OB channel, grassy willow
NSVAB4	T11	32	1	78.4	453428.58	4451530.59	OB channel, grassy willow
NSVAB4	T11	63	1	69.5	453424.71	4451538.61	OB channel, grassy willow
NSVAB4	T11	107	1.2	60.8	453420.92	4451546.44	OB channel, grassy willow
NSVAB4	T11	94	1.4	56.5	453419.05	4451550.31	upland berm

NSVAB4	T11	78	1.4	51.8	453417.01	4451554.54	upland berm
NSVAB4	T11	34	1.1	46.3	453414.62	4451559.50	FP
NSVAB4	T11	0	1	45	453414.05	4451560.67	REW side channel
NSVAB4	T11	0	1	37.3	453410.70	4451567.60	LEW side channel
NSVAB4	T11	60	1.6	30	453407.53	4451574.18	hummocky island
NSVAB4	T11	55	1.4	25.2	453405.44	4451578.50	hummocky island
NSVAB4	T11	57	1.4	18.8	453402.66	4451584.26	hummocky island
NSVAB4	T11	0	1.1	18.7	453402.61	4451584.35	hummocky island
NSVAB4	T11	0	1.1	6	453397.09	4451595.79	REW side channel
NSVAB4	T11	13	0.9	5.4	453396.83	4451596.33	LEW
NSVAB4	T11	0	1.6	0	453394.48	4451601.19	VL edge
NSVCF4	T1	0	1.2	9.2	447280.16	4451059.61	VR edge
NSVCF4	T1	0	0.9	8.3	447280.84	4451060.20	BF, RR, BK
NSVCF4	T1	0	0.3	6.2	447282.42	4451061.58	REW, BK
NSVCF4	T1	0	0	0.3	447286.86	4451065.47	LEW, BK
NSVCF4	T1	0	1	0	447287.08	4451065.67	VL edge, BK
NSVCF4	T2	18	0.6	10.1	447284.61	4451054.13	VR edge, Bk
NSVCF4	T2	9	0.3	9.8	447284.83	4451054.33	BF, RR
NSVCF4	T2	0	0.1	8.5	447285.77	4451055.23	REW
NSVCF4	T2	0	0	2.1	447290.40	4451059.65	LEW
NSVCF4	T2	15	0.3	1.7	447290.69	4451059.93	BF, RL
NSVCF4	T2	14	0.2	0.9	447291.26	4451060.48	S1, FP
NSVCF4	T2	20	0.4	0	447291.91	4451061.10	VL edge
NSVCF4	T3	0	1.1	7.5	447291.62	4451051.68	VR edge, BK, B
NSVCF4	T3	0	0.5	6	447292.80	4451052.62	BF, RR, BK, B
NSVCF4	T3	0	0	6	447292.80	4451052.62	REW, BK
NSVCF4	T3	0	0.1	0.5	447297.09	4451056.05	LEW
NSVCF4	T3	0	0.9	0.5	447297.09	4451056.05	ToC
NSVCF4	T3	8	1.1	0	447297.48	4451056.37	FP, VL edge, S2
NSVCF4	T4	24	0.7	9.3	447295.87	4451046.27	VR edge
NSVCF4	T4	6	0.4	8.4	447296.55	4451046.86	BF, RR, FP, S10
NSVCF4	T4	0	0	7.7	447297.09	4451047.31	REW

NSVCF4	T4	0	0.2	3.5	447300.30	4451050.02	LEW
NSVCF4	T4	0	0.3	2.3	447301.21	4451050.80	ToB
NSVCF4	T4	0	0.3	0	447302.97	4451052.28	VL edge, B
NSVCF4	T5	8	0.3	11.5	447296.99	4451039.08	VR edge, BF, RR
NSVCF4	T5	0	0	10.9	447297.46	4451039.46	REW
NSVCF4	T5	0	0	4.6	447302.39	4451043.38	LEW
NSVCF4	T5	15	0.3	4.3	447302.62	4451043.56	ToC, RL
NSVCF4	T5	7	0.4	2.7	447303.87	4451044.56	BF, RL
NSVCF4	T5	34	0.4	2.2	447304.27	4451044.87	FP, S3
NSVCF4	T5	19	0.5	0	447305.99	4451046.24	VL edge
NSVCF4	T6	0	1	10.5	447303.16	4451034.06	VR edge, BF, RR, BK
NSVCF4	T6	0	0.7	10.1	447303.39	4451034.38	REW
NSVCF4	T6	0	0.9	3.1	447307.41	4451040.11	LEW
NSVCF4	T6	44	1.2	2.4	447307.82	4451040.68	BF, RL, ToC
NSVCF4	T6	16	1.3	1.2	447308.51	4451041.66	FP, S4
NSVCF4	T6	23	1.8	0	447309.20	4451042.64	VL edge
NSVCF4	T7	0	0.3	9.1	447311.36	4451032.83	VR edge, BF, RR, BK
NSVCF4	T7	0	0	8.5	447311.57	4451033.40	REW
NSVCF4	T7	0	0	1.4	447313.96	4451040.08	LEW
NSVCF4	T7	29	0.4	1.1	447314.06	4451040.36	ToC, RL
NSVCF4	T7	46	0.5	0.6	447314.23	4451040.83	FP, S5
NSVCF4	T7	34	0.6	0	447314.44	4451041.40	VL edge
NSVCF4	T8	16	0.5	10.5	447319.05	4451031.69	VR edge
NSVCF4	T8	37	0.3	8.8	447319.43	4451033.35	BF RR
NSVCF4	T8	0	0	8.4	447319.52	4451033.74	REW
NSVCF4	T8	0	0.2	2.9	447320.75	4451039.10	LEW
NSVCF4	T8	23	0.3	2	447320.95	4451039.98	FP
NSVCF4	T8	36	0.4	1.2	447321.13	4451040.76	BF RL, S6
NSVCF4	T8	29	0.4	0	447321.40	4451041.93	FP, VL edge
NSVCF4	T9	10	0.6	10.5	447325.18	4451029.68	VR edge, FP
NSVCF4	T9	32	0.4	9.3	447325.65	4451030.79	S11, FP
NSVCF4	T9	40	0.3	8.3	447326.04	4451031.71	BF RR, FP, ToC

NSVCF4	T9	0	0	7.7	447326.28	4451032.26	REW
NSVCF4	T9	0	0.1	2.1	447328.47	4451037.41	LEW
NSVCF4	T9	39	0.3	1.8	447328.59	4451037.69	BF RL
NSVCF4	T9	36	0.4	1.3	447328.78	4451038.15	FP, S7
NSVCF4	T9	10	0.7	0	447329.29	4451039.34	VL edge
NSVCF4	T10	0	0.5	9.4	447331.70	4451027.45	BF, RR, VR edge
NSVCF4	T10	0	0	9.1	447331.87	4451027.70	REW
NSVCF4	T10	0	0.2	4.3	447334.55	4451031.69	LEW
NSVCF4	T10	0	0.7	2.6	447335.49	4451033.10	ToB
NSVCF4	T10	19	0.8	1.2	447336.27	4451034.26	FP, ToB
NSVCF4	T10	17	0.7	0.6	447336.61	4451034.76	S8, VL
NSVCF4	T10	32	0.8	0	447336.94	4451035.25	VL edge
NSVCF4	T11	46	0.8	12.3	447334.11	4451020.01	VR edge
NSVCF4	T11	18	0.7	11.3	447334.80	4451020.74	ToC, FP
NSVCF4	T11	0	0	10.5	447335.34	4451021.32	REW
NSVCF4	T11	0	0.2	3.1	447340.39	4451026.73	LEW
NSVCF4	T11	51	0.5	2.8	447340.60	4451026.95	ToC RL, BF
NSVCF4	T11	47	0.5	1.3	447341.62	4451028.05	S9, FP
NSVCF4	T11	4	0.6	0	447342.51	4451029.00	VL edge
HCKPC4	T1	8	0.3	12.2	449714.06	4452520.84	VR edge
HCKPC4	T1	44	0.2	11.8	449714.09	4452521.23	BF RR
HCKPC4	T1	0	0	11.2	449714.14	4452521.83	REW
HCKPC4	T1	37	0	7.1	449714.46	4452525.92	LEW
HCKPC4	T1	41	0.2	6.3	449714.52	4452526.72	BF RL
HCKPC4	T1	57	0.3	4.1	449714.69	4452528.91	S3, FP
HCKPC4	T1	31	0.4	0	449715.00	4452533.00	VL edge
HCKPC4	T2	22	0.1	15.3	449718.10	4452517.82	VR edge
HCKPC4	T2	35	0.1	14.3	449718.23	4452518.81	S1, FP
HCKPC4	T2	21	0.2	12	449718.51	4452521.09	ToC
HCKPC4	T2	0	0.1	11.7	449718.55	4452521.39	BF RR
HCKPC4	T2	0	0	11.7	449718.55	4452521.39	REW
HCKPC4	T2	0	1	7.2	449719.11	4452525.86	LEW

HCKPC4	T2	64	1.5	6.6	449719.18	4452526.45	ToC, FP
HCKPC4	T2	53	1.7	5.1	449719.37	4452527.94	FP
HCKPC4	T2	15	2	0	449720.00	4452533.00	VL edge
HCKPC4	T3	69	1	12.9	449721.04	4452518.25	VR edge, FP
HCKPC4	T3	24	0.8	11.3	449721.28	4452519.83	BF RR
HCKPC4	T3	0	0.4	10.6	449721.39	4452520.52	REW
HCKPC4	T3	0	0	6.5	449722.01	4452524.58	LEW
HCKPC4	T3	40	0.3	6.1	449722.07	4452524.97	BF
HCKPC4	T3	29	0.7	4.9	449722.25	4452526.16	FP edge
HCKPC4	T3	25	0.7	4.7	449722.29	4452526.35	S4, FP
HCKPC4	T3	48	0.6	2.1	449722.68	4452528.92	FP, OB channel
HCKPC4	T3	69	0.7	0	449723.00	4452531.00	VL edge
HCKPC4	T4	23	0.7	15.3	449723.16	4452516.49	VR edge
HCKPC4	T4	37	0.7	14	449723.57	4452517.72	FP
HCKPC4	T4	33	0.4	12.8	449723.95	4452518.86	
HCKPC4	T4	21	0.3	12.2	449724.14	4452519.43	BF RR
HCKPC4	T4	0	0	12.1	449724.17	4452519.52	REW
HCKPC4	T4	0	0	9.3	449725.06	4452522.18	LEW
HCKPC4	T4	22	0.4	9.3	449725.06	4452522.18	BF RL
HCKPC4	T4	4	0.7	8.1	449725.44	4452523.32	FP, S5
HCKPC4	T4	40	0.8	5.8	449726.17	4452525.50	FP
HCKPC4	T4	46	0.5	3	449727.05	4452528.15	FP, OB channel
HCKPC4	T4	48	0.7	0	449728.00	4452531.00	VL edge
HCKPC4	T5	32	0.8	14.8	449726.02	4452516.06	VR edge, S2
HCKPC4	T5	38	0.8	13.6	449726.43	4452517.19	FP
HCKPC4	T5	42	0.3	11.9	449727.00	4452518.79	BF RR, ToC
HCKPC4	T5	0	0.1	11.9	449727.00	4452518.79	REW
HCKPC4	T5	0	0	8.9	449728.01	4452521.62	LEW
HCKPC4	T5	71	0.5	8.8	449728.04	4452521.71	ToC, BF RL
HCKPC4	T5	13	1	6.2	449728.91	4452524.16	FP
HCKPC4	T5	7	0.7	3.1	449729.96	4452527.08	FP, OB channel
HCKPC4	T5	57	0.4	0	449731.00	4452530.00	VL edge

HCKPC4	T6	40	0.5	14.6	449729.08	4452514.15	VR edge
HCKPC4	T6	36	0.3	13.1	449729.79	4452515.47	BF, FP, ToC
HCKPC4	T6	0	0	13.1	449729.79	4452515.47	REW
HCKPC4	T6	0	0	9.8	449731.35	4452518.37	LEW
HCKPC4	T6	48	0.3	9.7	449731.40	4452518.46	BR RL, ToC
HCKPC4	T6	31	0.5	7.4	449732.49	4452520.48	FP
HCKPC4	T6	58	0.7	1.6	449735.24	4452525.59	S6, FP
HCKPC4	T6	45	0.8	0	449736.00	4452527.00	VL edge
HCKPC4	T7	32	0.7	17.2	449732.57	4452512.01	VR edge
HCKPC4	T7	52	0.3	16.8	449732.76	4452512.36	BR, ToC
HCKPC4	T7	0	0	16.8	449732.76	4452512.36	REW
HCKPC4	T7	0	0.1	14.2	449734.04	4452514.62	LEW
HCKPC4	T7	43	0.4	13.8	449734.23	4452514.97	BF RL, ToC
HCKPC4	T7	57	0.7	12.3	449734.97	4452516.28	FP
HCKPC4	T7	34	0.7	7.4	449737.37	4452520.55	
HCKPC4	T7	40	0.9	1.2	449740.41	4452525.95	S7, VL
HCKPC4	T7	43	1	0	449741.00	4452527.00	VL edge
HCKPC4	T8	25	0.6	15	449736.00	4452511.00	VR edge
HCKPC4	T8	56	0.3	14.6	449736.24	4452511.32	BF, ToC
HCKPC4	T8	0	0.1	14.6	449736.24	4452511.32	REW
HCKPC4	T8	0	0	11.1	449738.34	4452514.12	LEW
HCKPC4	T8	25	0.4	10.9	449738.46	4452514.28	BF RL, ToC
HCKPC4	T8	52	0.6	8.8	449739.72	4452515.96	FP
HCKPC4	T8	24	0.5	7	449740.80	4452517.40	S8, FP
HCKPC4	T8	68	0.7	4.9	449742.06	4452519.08	FP
HCKPC4	T8	0	0.3	3.7	449742.78	4452520.04	Center of small trib
HCKPC4	T8	34	0.6	2	449743.80	4452521.40	ToC, trib
HCKPC4	T8	71	0.4	0	449745.00	4452523.00	VL edge
HCKPC4	T9	48	0.7	16.2	449738.54	4452509.54	VR edge
HCKPC4	T9	37	0.6	15.2	449739.25	4452510.25	ToC
HCKPC4	T9	0	0.4	15.2	449739.25	4452510.25	BF RR ToC
HCKPC4	T9	0	0.1	15.1	449739.32	4452510.32	REW

HCKPC4	T9	0	0	11.4	449741.94	4452512.94	LEW
HCKPC4	T9	50	0.3	11.1	449742.15	4452513.15	BF RL, ToC
HCKPC4	T9	40	0.5	9	449743.64	4452514.64	FP, S9
HCKPC4	T9	63	0.3	6.1	449745.69	4452516.69	
HCKPC4	T9	42	0.7	0	449750.00	4452521.00	VL edge
HCKPC4	T10	27	0.6	12.7	449741.56	4452507.50	VR edge
HCKPC4	T10	56	0.5	12.4	449741.78	4452507.70	ToC
HCKPC4	T10	0	0.3	12.3	449741.86	4452507.77	BF ToC
HCKPC4	T10	0	0	12.3	449741.86	4452507.77	REW
HCKPC4	T10	0	0	8.8	449744.46	4452510.11	LEW
HCKPC4	T10	36	0.4	8.5	449744.68	4452510.31	BF RL
HCKPC4	T10	23	0.5	7.7	449745.28	4452510.85	S10, FP
HCKPC4	T10	24	0.5	4.2	449747.88	4452513.19	FP
HCKPC4	T10	11	0.7	0	449751.00	4452516.00	VL edge
HCKPC4	T11	47	0.8	14.1	449742.27	4452505.18	VR edge
HCKPC4	T11	52	0.7	13.5	449742.77	4452505.51	ToC
HCKPC4	T11	0	0.4	13.5	449742.77	4452505.51	BF, RR
HCKPC4	T11	0	0	13.5	449742.77	4452505.51	REW
HCKPC4	T11	0	0	9.1	449746.43	4452507.95	LEW
HCKPC4	T11	7	0.5	8.7	449746.76	4452508.17	BF RL
HCKPC4	T11	25	1	8.4	449747.01	4452508.34	ToC, trail
HCKPC4	T11	17	1.1	7.1	449748.09	4452509.06	S11, FP
HCKPC4	T11	19	1.2	0	449754.00	4452513.00	VL edge
BTRAB5	T1	115	0.6	183	447460.35	4467328.63	VR edge, conifers, RB
BTRAB5	T1	148	0.7	173	447461.96	4467338.50	grassy meadow w/ RB
BTRAB5	T1	75	0.7	163.9	447463.42	4467347.48	grassy meadow w/ RB
BTRAB5	T1	65	0.6	154	447465.02	4467357.25	S1, outside exclosure
BTRAB5	T1	49	0.5	144.9	447466.48	4467366.23	grassy meadow, exclosure
BTRAB5	T1	59	0.7	135.1	447468.06	4467375.90	grassy meadow, exclosure
BTRAB5	T1	106	0.5	125.5	447469.61	4467385.38	grassy meadow, exclosure
BTRAB5	T1	74	0.4	115.5	447471.22	4467395.25	ToC
BTRAB5	T1	0	0.1	115.4	447471.24	4467395.35	REW, edge of channel

BTRAB5	T1	75	0.1	96.9	447474.22	4467413.60	LEW, diagonal across measuring chan bend
BTRAB5	T1	53	0.4	96.4	447474.30	4467414.10	ToC, Left edge of channelEW
BTRAB5	T1	93	0.6	87.5	447475.73	4467422.88	grassy meadow
BTRAB5	T1	89	0.5	77.3	447477.37	4467432.95	grassy meadow
BTRAB5	T1	77	0.6	68.2	447478.84	4467441.93	grassy meadow
BTRAB5	T1	54	0.5	58.3	447480.43	4467451.70	grassy meadow
BTRAB5	T1	44	0.6	48.1	447482.07	4467461.77	grassy meadow
BTRAB5	T1	58	0.6	38.9	447483.56	4467470.85	grassy meadow
BTRAB5	T1	76	0.7	30	447484.99	4467479.63	Grassy meadow
BTRAB5	T1	82	0.5	24.3	447485.91	4467485.26	Grassy meadow, against fence
BTRAB5	T1	55	0.3	21.7	447486.33	4467487.82	grassy meadow, ToC, enclosure RR
BTRAB5	T1	0	0	21.5	447486.36	4467488.02	REW main stem at road
BTRAB5	T1	0	0	1.8	447489.53	4467507.46	LEW, main stem
BTRAB5	T1	0	0.9	0	447489.82	4467509.24	ToC, RL, VL edge, nect to rd
BTRAB5	T2	130	0.2	201.5	447475.25	4467314.86	VR edge
BTRAB5	T2	129	0.5	192.5	447476.81	4467323.72	grassy meadow w/ RB
BTRAB5	T2	86	0.5	183.1	447478.44	4467332.98	grassy meadow with RB, next to stagnant pool
BTRAB5	T2	81	0.5	172.8	447480.23	4467343.12	grassy meadow, burned RB
BTRAB5	T2	118	0.7	164.5	447481.67	4467351.29	grassy meadow, burned RB
BTRAB5	T2	88	0.8	155.9	447483.17	4467359.76	grassy meadow, burned RB
BTRAB5	T2	102	0.8	151	447484.02	4467364.59	grassy meadow, burned RB
BTRAB5	T2	90	0.5	140.1	447485.91	4467375.32	started 7/1, grassy meadow
BTRAB5	T2	97	0.5	130.6	447487.56	4467384.68	grassy meadow, standing pools
BTRAB5	T2	134	0.6	122.1	447489.04	4467393.05	grassy meadow, standing pools
BTRAB5	T2	77	0.5	111.7	447490.84	4467403.29	grassy meadow, standing pools
BTRAB5	T2	105	0.5	101.6	447492.60	4467413.24	grassy meadow, standing pools
BTRAB5	T2	51	0.5	92.8	447494.12	4467421.91	grassy meadow, standing pools
BTRAB5	T2	80	0.3	84.3	447495.60	4467430.28	S2, water table at 36cm depth, against south
BTRAB5	T2	86	0.3	37.8	447503.67	4467476.07	at North side of fence of 2nd exclosure (shot
BTRAB5	T2	71	0.2	35.5	447504.07	4467478.34	against fence (1st exclosure)
BTRAB5	T2	57	0.2	25.1	447505.88	4467488.58	grassy meadow on N side of fence
BTRAB5	T2	41	0.3	15.4	447507.56	4467498.13	grassy meadow on N side of fence

BTRAB5	T2	0	0	13.2	447507.95	4467500.30	REW
BTRAB5	T2	0	0	1.8	447509.92	4467511.52	LEW
BTRAB5	T2	0	0.3	1.1	447510.05	4467512.21	ToC, RL
BTRAB5	T2	0	0.8	0	447510.24	4467513.30	VL edge, road edge fill
BTRAB5	T3	104	0.7	194.4	447494.11	4467322.40	VR edge, grassy meadow, w/ RB, spruce on VR
BTRAB5	T3	112	1	185.9	447495.55	4467330.78	grassy meadow w/ RB
BTRAB5	T3	131	1	178.2	447496.85	4467338.37	grassy meadow w/ RB
BTRAB5	T3	125	1	170.8	447498.10	4467345.66	grassy meadow w/ RB, P1012 looking to Valley
BTRAB5	T3	102	1.1	160.5	447499.85	4467355.81	grassy meadow w/ RB
BTRAB5	T3	189	1	151.2	447501.42	4467364.98	grassy meadow w/ RB
BTRAB5	T3	77	0.9	142.4	447502.91	4467373.65	grassy meadow w/ RB
BTRAB5	T3	67	0.8	132.7	447504.55	4467383.21	grassy meadow w/ standing water
BTRAB5	T3	135	0.8	122.2	447506.33	4467393.56	S3, grassy meadow w/ standing water
BTRAB5	T3	96	0.6	112.8	447507.92	4467402.83	grassy meadow w/ standing water
BTRAB5	T3	77	0.5	102.7	447509.63	4467412.78	grassy meadow w/ standing water
BTRAB5	T3	9	0.1	95.4	447510.86	4467419.98	OB chan. grassy meadow w/ standing water
BTRAB5	T3	33	0.1	87	447512.28	4467428.25	against fence, grassy meadow w/ standing
BTRAB5	T3	109	0.3	77.8	447513.84	4467437.32	arouns SE corner of fence surveying along E
BTRAB5	T3	39	0.3	68.3	447515.44	4467446.68	wet grassy meadow
BTRAB5	T3	78	0	58.9	447517.04	4467455.95	along fence, grassy meadow
BTRAB5	T3	103	0.4	49.2	447518.68	4467465.51	along fence, grassy meadow
BTRAB5	T3	80	0.6	40.2	447520.20	4467474.38	end 2nd exclosure, wet grassy meadow
BTRAB5	T3	25	0.4	35.9	447520.93	4467478.62	N side of 2nd exclosure
BTRAB5	T3	42	0.6	27.6	447522.33	4467486.80	N side of exclosure fence, grassy meadow w/
BTRAB5	T3	45	0.8	17.9	447523.97	4467496.36	high point natural levee w/ RB
BTRAB5	T3	34	0.7	13.3	447524.75	4467500.89	ToC, RR
BTRAB5	T3	0	0.36	13.2	447524.77	4467500.99	REW
BTRAB5	T3	0	0.36	0.9	447526.85	4467513.11	LEW
BTRAB5	T3	0	1.16	0	447527.00	4467514.00	ToC, RL, VL edge
BTRAB5	T4	92	1	188.3	447514.59	4467324.01	VR edge, grassy meadow w. RB
BTRAB5	T4	7	0.1	178.7	447516.09	4467333.49	standing pool, water depth, 41cm
BTRAB5	T4	105	0.8	167.7	447517.80	4467344.36	grassy meadow w/ RB

BTRAB5	T4	129	0.9	159.6	447519.07	4467352.36	grassy meadow w/ RB
BTRAB5	T4	73	1.1	151.1	447520.40	4467360.75	grassy meadow w/ RB
BTRAB5	T4	64	1.1	143	447521.66	4467368.76	grassy meadow w/ RB
BTRAB5	T4	73	0.9	134.3	447523.02	4467377.35	grassy meadow w/ RB
BTRAB5	T4	49	1	126.2	447524.29	4467385.35	grassy meadow w/ RB
BTRAB5	T4	90	1.1	118	447525.57	4467393.45	grassy meadow w/ RB
BTRAB5	T4	25	0.9	107.8	447527.16	4467403.52	grassy meadow w/ RB
BTRAB5	T4	33	1	98.7	447528.58	4467412.51	grassy meadow w/ RB
BTRAB5	T4	0	0	89	447530.10	4467422.09	OB chan, water depth 38 cm
BTRAB5	T4	21	2	79	447531.66	4467431.97	grassy wet meadow
BTRAB5	T4	27	1.6	70.1	447533.05	4467440.76	S4, adjacent to back-flow chan, wet grassy
BTRAB5	T4	0	0.8	61.1	447534.46	4467449.65	grassy wet meadow
BTRAB5	T4	48	1.6	51	447536.03	4467459.63	grassy wet meadow
BTRAB5	T4	60	1.9	44.9	447536.99	4467465.65	grassy wet meadow
BTRAB5	T4	64	1.3	39.2	447537.88	4467471.28	OB chan, H20 at 10cm
BTRAB5	T4	69	2	34.4	447538.63	4467476.02	next to fence exclosure
BTRAB5	T4	44	2.3	24.5	447540.17	4467485.80	N side of exclosure
BTRAB5	T4	0	1.8	17.3	447541.30	4467492.91	REW
BTRAB5	T4	0	1.8	1.9	447543.70	4467508.12	LEW
BTRAB5	T4	60	2.6	1.7	447543.73	4467508.32	ToC
BTRAB5	T4	30	3	0	447544.00	4467510.00	VL edge, adjacent to road
BTRAB5	T5	42	1.3	190.1	447531.96	4467318.75	VR edge
BTRAB5	T5	114	1.1	186.1	447532.64	4467322.69	S5 - water depth 29cm, grassy meadow, S, RB,
BTRAB5	T5	89	1.3	175.7	447534.43	4467332.94	grassy meadow, stagnant pond, S, RB
BTRAB5	T5	84	1.2	166.2	447536.06	4467342.30	grassy meadow, stagnant pond, S, RB
BTRAB5	T5	65	1.2	156	447537.81	4467352.35	grassy meadow, stagnant pond, S, RB
BTRAB5	T5	147	1.3	145.4	447539.63	4467362.79	grassy meadow, stagnant pond, S, RB, tree
BTRAB5	T5	69	1.4	136.5	447541.16	4467371.56	grassy meadow w/ RB
BTRAB5	T5	10	1	128.7	447542.50	4467379.24	OB chan, low point (S of fence)
BTRAB5	T5	46	1.2	121.7	447543.70	4467386.14	grassy meadow w/ RB, N of fence
BTRAB5	T5	62	1	113.9	447545.04	4467393.82	grassy meadow RB
BTRAB5	T5	32	1.1	104.3	447546.68	4467403.28	grassy meadow RB

BTRAB5	T5	41	0.8	94.2	447548.42	4467413.23	grassy meadow RB
BTRAB5	T5	0	0	88.6	447549.38	4467418.75	OB chan, backwater chan, water depth 30cm
BTRAB5	T5	57	0.5	85.6	447549.89	4467421.70	upland adjacent to H2O
BTRAB5	T5	50	0.3	75.6	447551.61	4467431.55	edge of backwater chan
BTRAB5	T5	0	0.7	66.1	447553.24	4467440.91	upland sand & gravel
BTRAB5	T5	53	0.9	57	447554.80	4467449.88	upland, sand grassy meadow
BTRAB5	T5	0	0.7	46	447556.69	4467460.71	lowland, OB chan
BTRAB5	T5	89	1.2	36.1	447558.39	4467470.47	grassy meadow, against fence exclosure
BTRAB5	T5	0	0.8	26.1	447560.11	4467480.32	REW, gradual sloping point bar
BTRAB5	T5	0	0.8	13.7	447562.24	4467492.54	LEW
BTRAB5	T5	96	1.2	13.3	447562.30	4467492.93	ToC, RL
BTRAB5	T5	72	0.9	6.8	447563.42	4467499.33	FP, wet grassy meadow
BTRAB5	T5	108	1.2	1.6	447564.31	4467504.46	FP, wet grassy meadow
BTRAB5	T5	71	1.5	0	447564.59	4467506.03	VL edge
BTRAB5	T6	75	1.3	175.8	447559.52	4467321.98	VR edge, grassy meadow
BTRAB5	T6	145	1.1	168	447560.40	4467329.73	grassy meadow w/ RB
BTRAB5	T6	79	1	160.9	447561.21	4467336.78	grassy meadow w/ stagnant pools
BTRAB5	T6	60	1	150.1	447562.43	4467347.51	grassy meadow w/ RB
BTRAB5	T6	74	1.2	141.2	447563.44	4467356.36	grassy meadow w/ RB
BTRAB5	T6	107	1.1	132.9	447564.38	4467364.60	OB chan, grassy meadow w/ RB
BTRAB5	T6	58	0.7	126.6	447565.09	4467370.86	grassy meadow w/ RB
BTRAB5	T6	113	1	118	447566.07	4467379.41	grassy meadow w/ RB
BTRAB5	T6	129	1.1	110.2	447566.95	4467387.16	grassy meadow w/ RB
BTRAB5	T6	114	1	100.2	447568.09	4467397.09	OB chan, grassy meadow w/ RB
BTRAB5	T6	98	0.5	94.1	447568.78	4467403.15	grassy meadow w/ RB
BTRAB5	T6	55	0.7	85.1	447569.80	4467412.09	grassy meadow w/ RB
BTRAB5	T6	57	0.6	78.8	447570.51	4467418.35	S6, near backwater chan, lower most floodplain
BTRAB5	T6	80	0.9	74.4	447571.01	4467422.73	ToC, RR
BTRAB5	T6	0	0.5	74	447571.06	4467423.12	REW
BTRAB5	T6	0	0.5	54.7	447573.24	4467442.30	LEW
BTRAB5	T6	52	0.9	45.9	447574.24	4467451.04	cobble point bar w/ Grass
BTRAB5	T6	60	1	40.1	447574.90	4467456.80	GM, running parellel adjacent to channel bend

BTRAB5	T6	114	1	32.5	447575.76	4467464.36	GM, running parellel adjacent to channel bend
BTRAB5	T6	114	1.1	24.1	447576.71	4467472.70	GM, running parellel adjacent to channel bend
BTRAB5	T6	0	0	18.5	447577.35	4467478.27	OB chan, sd>cobs, depth water 35 cm
BTRAB5	T6	90	1	10.8	447578.22	4467485.92	GM
BTRAB5	T6	0	0	5	447578.88	4467491.68	OB chan, H2O depth 12cm
BTRAB5	T6	43	0.6	0.6	447579.38	4467496.05	edge of OB chan
BTRAB5	T6	78	1.1	0	447579.45	4467496.65	VL edge
BTRAB5	T7	32	0.9	165.3	447580.42	4467322.75	VR edge
BTRAB5	T7	54	0.9	158	447581.25	4467330.00	grassy meadow w/ RB
BTRAB5	T7	8	0.4	149.9	447582.16	4467338.05	OB chan, stagnant water 1cm deep
BTRAB5	T7	92	0.9	140.1	447583.26	4467347.79	grassy meadow w/ RB
BTRAB5	T7	102	0.8	130.7	447584.31	4467357.13	grassy meadow w/ RB
BTRAB5	T7	112	0.9	121.8	447585.31	4467365.97	grassy meadow w/ RB
BTRAB5	T7	94	0.5	111.6	447586.46	4467376.11	OB chan, grassy meadow w/ RB
BTRAB5	T7	68	0.7	102.5	447587.48	4467385.15	grassy meadow w/ RB
BTRAB5	T7	96	0.6	94.5	447588.38	4467393.10	grassy meadow w/ RB
BTRAB5	T7	25	0.7	84.7	447589.48	4467402.84	ToC, RR
BTRAB5	T7	0	0.2	84.1	447589.55	4467403.43	REW at BF diagonally up channel at meaander
BTRAB5	T7	0	0.2	56.6	447592.64	4467430.76	LEW
BTRAB5	T7	39	0.7	56	447592.71	4467431.35	ToC, RL
BTRAB5	T7	71	0.9	55.1	447592.81	4467432.25	GM
BTRAB5	T7	37	1.2	44.1	447594.04	4467443.18	Gm
BTRAB5	T7	77	1.2	33.7	447595.21	4467453.51	GM
BTRAB5	T7	28	1.3	23.9	447596.31	4467463.25	GM
BTRAB5	T7	41	1.2	22.2	447596.51	4467464.94	S7, dry GM
BTRAB5	T7	29	0.6	14.7	447597.35	4467472.39	wet grassy meadow & side chan
BTRAB5	T7	75	0.9	10.9	447597.78	4467476.17	wet grassy meadow & side chan
BTRAB5	T7	0	0	8.5	447598.04	4467478.55	OB chan, wet, water depth 35cm
BTRAB5	T7	22	0	3.7	447598.58	4467483.32	edge of OB chan
BTRAB5	T7	23	1.1	0	447599.00	4467487.00	VL edge
BTRAB5	T8	28	1.9	172.4	447599.05	4467315.36	VR edge
BTRAB5	T8	18	1.5	164.2	447600.17	4467323.48	edge of small terrace grassy upland

BTRAB5	T8	39	1.1	156.4	447601.23	4467331.21	grassy meadow w/ RB
BTRAB5	T8	74	1	151.6	447601.88	4467335.96	stagnant pond depth 20 cm
BTRAB5	T8	68	1.2	141.8	447603.22	4467345.67	grassy meadow w/ RB
BTRAB5	T8	56	1.4	133.5	447604.35	4467353.89	grassy meadow w/ RB
BTRAB5	T8	48	1.4	124.4	447605.59	4467362.91	S8, dry upland grassy meadow
BTRAB5	T8	61	1.2	114.7	447606.91	4467372.52	grassy meadow
BTRAB5	T8	137	1.1	108.7	447607.73	4467378.46	grassy meadow, ToC, RR
BTRAB5	T8	0	0.5	108	447607.82	4467379.15	REW
BTRAB5	T8	0	0.5	90.7	447610.18	4467396.29	LEW
BTRAB5	T8	14	0.6	84.8	447610.98	4467402.14	point bar
BTRAB5	T8	31	0.7	75.5	447612.25	4467411.35	GM
BTRAB5	T8	64	0.7	65.9	447613.56	4467420.86	Gm
BTRAB5	T8	27	0.2	56.9	447614.78	4467429.78	GM, dry OB chan
BTRAB5	T8	27	0.8	46.9	447616.15	4467439.69	GM
BTRAB5	T8	26	0.4	35.9	447617.65	4467450.58	Gm dry OB chan
BTRAB5	T8	40	1.1	25.4	447619.08	4467460.98	G<
BTRAB5	T8	61	1.1	14.8	447620.52	4467471.49	GM
BTRAB5	T8	0	0	6.7	447621.62	4467479.51	flowing OB chan depth 24 cm
BTRAB5	T8	33	0.3	0.8	447622.43	4467485.36	edge of small OB chan FP
BTRAB5	T8	12	0.6	0	447622.54	4467486.15	VL edge
BTRAB5	T9	24	0.98	175.2	447616.80	4467307.91	VR edge, conifer aspen, grassy upland terrace
BTRAB5	T9	110	1.18	165.3	447617.94	4467317.74	conifer, aspen, grassy uppland terrace
BTRAB5	T9	56	0.28	154.3	447619.21	4467328.67	lower FP, grassy meadow
BTRAB5	T9	38	0.58	146.6	447620.10	4467336.32	grassy meadoww/ RB
BTRAB5	T9	12	0.08	140.2	447620.84	4467342.67	OB chan
BTRAB5	T9	51	0.48	134.3	447621.52	4467348.53	upland grassy meadow
BTRAB5	T9	57	0.58	124.5	447622.64	4467358.27	upland grassy meadow
BTRAB5	T9	88	0.68	114.4	447623.81	4467368.30	upland grassy meadow
BTRAB5	T9	150	0.68	107.1	447624.65	4467375.55	ToC, RR
BTRAB5	T9	0	0.28	107.1	447624.65	4467375.55	REW
BTRAB5	T9	0	0.58	90	447626.62	4467392.54	LEW
BTRAB5	T9	25	0.28	83.6	447627.36	4467398.90	BF side channel, wet, no flow

BTRAB5	T9	40	0.48	74	447628.46	4467408.43	Moist GM
BTRAB5	T9	73	0.48	66	447629.39	4467416.38	Moist GM
BTRAB5	T9	32	0.48	58.3	447630.27	4467424.03	Moist GM
BTRAB5	T9	70	0.18	48.8	447631.37	4467433.47	Moist GM
BTRAB5	T9	109	0.88	39.6	447632.43	4467442.60	GM
BTRAB5	T9	26	0.68	29.4	447633.60	4467452.74	GM
BTRAB5	T9	68	0.48	24.4	447634.18	4467457.70	S9, moist GM
BTRAB5	T9	78	0.6	16.3	447635.11	4467465.75	moist GM
BTRAB5	T9	26	0.1	12.3	447635.57	4467469.72	moist GM
BTRAB5	T9	19	0	4.8	447636.44	4467477.17	moist GM, OB chan
BTRAB5	T9	50	0.3	0	447636.99	4467481.94	VL edge
BTRAB5	T10	47	0.8	161.3	447643.82	4467318.24	VR edge
BTRAB5	T10	46	0.9	152.1	447644.53	4467327.42	grassy meadow w/ RB
BTRAB5	T10	6	0	142.2	447645.28	4467337.29	OB chan in GM, water depth 17 cm
BTRAB5	T10	112	0.8	134.3	447645.88	4467345.16	GM w/ RB
BTRAB5	T10	42	0.8	125.2	447646.58	4467354.24	GM w/ RB
BTRAB5	T10	85	0.8	114.7	447647.38	4467364.71	dry GM
BTRAB5	T10	42	0.9	105.2	447648.10	4467374.18	dry GM
BTRAB5	T10	91	1	101.3	447648.40	4467378.07	S10, dry GM, FP
BTRAB5	T10	83	0.9	99.6	447648.53	4467379.76	ToC
BTRAB5	T10	0	0.5	99.5	447648.54	4467379.86	REW
BTRAB5	T10	0	0.5	79.9	447650.04	4467399.41	LEW, gently sloping bank
BTRAB5	T10	55	0.7	77	447650.26	4467402.30	FP, grassy w/ alder & RB
BTRAB5	T10	78	1	69.5	447650.83	4467409.78	upper FP surface, hummock
BTRAB5	T10	71	1.1	61.4	447651.45	4467417.85	upper FP surface, grass, RB
BTRAB5	T10	29	1.2	51.1	447652.23	4467428.12	upper FP surface, grass, RB
BTRAB5	T10	10	0.4	43.3	447652.83	4467435.90	standing water depth at 20 cm
BTRAB5	T10	48	1	37	447653.31	4467442.18	bank of water hole
BTRAB5	T10	39	1.3	28	447654.00	4467451.15	upland grass FP meadow
BTRAB5	T10	14	0.5	20.2	447654.59	4467458.93	standing water depth 12 cm
BTRAB5	T10	84	1.4	11.9	447655.22	4467467.21	grassy FP meadow, upland
BTRAB5	T10	42	1.4	4.2	447655.81	4467474.89	grassy FP meadow, upland

BTRAB5	T10	0	1.2	0	447656.13	4467479.07	VL edge
BTRAB5	T11	23	0.4	169.2	447656.50	4467309.61	VR edge, sloping fan surface, dry GM
BTRAB5	T11	41	0.4	160.4	447657.36	4467318.36	dry GM
BTRAB5	T11	17	0.7	152	447658.18	4467326.72	dry GM, OB chan
BTRAB5	T11	55	0.8	142.4	447659.11	4467336.28	dry GM
BTRAB5	T11	34	0	133.5	447659.98	4467345.14	dry GM
BTRAB5	T11	16	0.7	126.2	447660.69	4467352.40	dry GM, OB chan
BTRAB5	T11	115	0.8	121.1	447661.19	4467357.48	dry GM
BTRAB5	T11	77	1	112.3	447662.05	4467366.24	dry GM
BTRAB5	T11	57	0.8	103.7	447662.89	4467374.79	dry GM w/ RB
BTRAB5	T11	73	0.3	96.6	447663.58	4467381.86	dry GM w/ RB
BTRAB5	T11	56	0.3	91.1	447664.12	4467387.33	Top of sloping FP surface
BTRAB5	T11	0	0.7	86	447664.61	4467392.41	REW
BTRAB5	T11	0	0.9	67.7	447666.40	4467410.62	LEW
BTRAB5	T11	61	0.1	67.4	447666.43	4467410.92	S11 ToC, grassy meadow bank
BTRAB5	T11	124	0.7	57.8	447667.36	4467420.48	
BTRAB5	T11	67	0.1	50.1	447668.11	4467428.14	standing water depth 27cm
BTRAB5	T11	88	1.1	49.9	447668.13	4467428.34	grassy bank w/ side chan
BTRAB5	T11	18	1	39.2	447669.18	4467438.99	standing water side chan depth 30 cm
BTRAB5	T11	63	0.5	29	447670.17	4467449.14	gassy meadow w/ RB
BTRAB5	T11	48	0.3	18.3	447671.22	4467459.79	gassy meadow w/ RB
BTRAB5	T11	0	0.8	11.4	447671.89	4467466.65	standing water side channel depth 22cm
BTRAB5	T11	4.1	2.3	1.3	447672.87	4467476.71	standing water side channel depth 18cm
BTRAB5	T11	64	2.3	0	447673.00	4467478.00	VL edge
NSVCF5	T1	0	0.5	15.8	462807.68	4450967.35	VR edge. B
NSVCF5	T1	0	0.1	15.1	462807.20	4450967.87	BF RR, cobs>B
NSVCF5	T1	0	0	14.7	462806.93	4450968.16	REW
NSVCF5	T1	0	0	2.9	462798.96	4450976.86	LEW
NSVCF5	T1	0	0.3	1.3	462797.88	4450978.04	BF RL, B
NSVCF5	T1	3	0.4	0.7	462797.47	4450978.48	S8
NSVCF5	T1	50	0.6	0	462797.00	4450979.00	VL edge
NSVCF5	T2	0	0.5	15.6	462815.48	4450981.21	VR edge

NSVCF5	T2	0	0.2	15.1	462815.02	4450981.39	BF RR
NSVCF5	T2	0	0	14.8	462814.74	4450981.50	REW
NSVCF5	T2	0	0	2.1	462802.95	4450986.22	LEW
NSVCF5	T2	25	0.2	0.8	462801.74	4450986.70	BF RL
NSVCF5	T2	15	0.4	0.4	462801.37	4450986.85	S9
NSVCF5	T2	21	0.5	0	462801.00	4450987.00	VL edge
NSVCF5	T3	0	1	15.6	462817.46	4450994.94	VR edge, tallace, B
NSVCF5	T3	0	0.5	14.8	462816.67	4450995.04	BF RR, B
NSVCF5	T3	0	0.1	14.1	462815.98	4450995.14	REW
NSVCF5	T3	0	0	3	462804.97	4450996.60	LEW
NSVCF5	T3	0	0.2	1.8	462803.78	4450996.76	BF RL, snd>cobs
NSVCF5	T3	0	0.6	0	462802.00	4450997.00	VL edge
NSVCF5	T4	0	0.6	20.1	462825.90	4451010.16	VR edge
NSVCF5	T4	0	0.2	19.7	462825.50	4451010.21	BF RR, B
NSVCF5	T4	0	0	19.7	462825.50	4451010.21	REW
NSVCF5	T4	0	0	4.1	462810.06	4451012.42	LEW
NSVCF5	T4	0	0.2	3.6	462809.56	4451012.49	pebs>cobs
NSVCF5	T4	0	0.5	2.5	462808.47	4451012.65	pebs>cobs
NSVCF5	T4	0	1.1	0	462806.00	4451013.00	VL edge
NSVCF5	T5	0	1.4	16.8	462824.50	4451026.86	VR edge
NSVCF5	T5	5	1	16.1	462823.82	4451026.99	
NSVCF5	T5	6	0.7	15.7	462823.42	4451027.06	S1
NSVCF5	T5	23	0.6	15.3	462823.03	4451027.14	BF RR
NSVCF5	T5	0	0.3	14.7	462822.44	4451027.25	REW
NSVCF5	T5	0	0	1.6	462809.57	4451029.70	LEW
NSVCF5	T5	0	0.3	0.8	462808.79	4451029.85	BF RL, cobs
NSVCF5	T5	0	0.6	0	462808.00	4451030.00	VL edge, cobs
NSVCF5	T6	13	0.8	19.9	462825.51	4451043.10	VR edge
NSVCF5	T6	51	0.6	19.2	462824.83	4451043.23	S2, VR
NSVCF5	T6	36	0.4	18.4	462824.04	4451043.39	BF RR, ToC
NSVCF5	T6	0	0.1	18.2	462823.85	4451043.43	sand
NSVCF5	T6	0	0	17.6	462823.26	4451043.55	REW

NSVCF5	T6	0	0	3.2	462809.14	4451046.37	LEW
NSVCF5	T6	10	0.2	2.5	462808.45	4451046.51	BF RL
NSVCF5	T6	18	0.4	1.2	462807.18	4451046.76	S10. FP
NSVCF5	T6	22	0.5	0	462806.00	4451047.00	FP, VL edge
NSVCF5	T7	7	0.7	22.3	462830.97	4451057.18	VR edge
NSVCF5	T7	4	0.6	21.1	462829.79	4451057.38	S3
NSVCF5	T7	40	0.3	19.9	462828.61	4451057.59	BF RR
NSVCF5	T7	0	0	18.9	462827.62	4451057.76	REW
NSVCF5	T7	0	0	2.6	462811.56	4451060.55	LEW
NSVCF5	T7	19	0.1	1.8	462810.77	4451060.69	
NSVCF5	T7	12	0.2	1	462809.99	4451060.83	S11, VL
NSVCF5	T7	5	0.4	0	462809.00	4451061.00	VL
NSVCF5	T8	62	0.9	20.1	462837.71	4451069.06	VR edge
NSVCF5	T8	58	0.7	18.1	462835.75	4451069.45	S4, FP
NSVCF5	T8	33	0.5	16.1	462833.79	4451069.84	BF RR, ToC
NSVCF5	T8	0	0.2	16.1	462833.79	4451069.84	REW
NSVCF5	T8	0	0	1.7	462819.67	4451072.67	LEW
NSVCF5	T8	0	0.5	0.8	462818.78	4451072.84	BF, cobs>B
NSVCF5	T8	0	0.9	0	462818.00	4451073.00	VL ege, cobsd>B, edge of terrace
NSVCF5	T9	8	0.9	18.5	462841.40	4451085.94	VR edge
NSVCF5	T9	61	0.8	16.6	462839.51	4451085.74	S5, FP
NSVCF5	T9	39	0.5	14.8	462837.72	4451085.55	BF RR, ToC
NSVCF5	T9	0	0.3	14.5	462837.42	4451085.52	REW
NSVCF5	T9	0	0	1.5	462824.49	4451084.16	LEW
NSVCF5	T9	0	0.2	0.7	462823.70	4451084.07	BF RL, cobs>B
NSVCF5	T9	0	0.7	0	462823.00	4451084.00	VL edge
NSVCF5	T10	12	0.6	17.2	462841.20	4451101.00	VR edge
NSVCF5	T10	58	0.6	16.2	462840.20	4451101.00	S6, FP
NSVCF5	T10	28	0.3	15	462839.00	4451101.00	BF RR
NSVCF5	T10	0	0.1	14.2	462838.20	4451101.00	REW
NSVCF5	T10	0	0	1.7	462825.70	4451101.00	LEW
NSVCF5	T10	0	0.3	1.2	462825.20	4451101.00	BF RL, cobs>B

NSVCF5	T10	0	0.7	0	462824.00	4451101.00	VL edge
NSVCF5	T11	13	0.4	19.7	462842.68	4451115.02	VR edge
NSVCF5	T11	18	0.3	18.8	462841.78	4451115.06	S7, bank
NSVCF5	T11	0	0.2	18	462840.98	4451115.10	BF RR, ToC
NSVCF5	T11	0	0	17.7	462840.68	4451115.12	REW
NSVCF5	T11	0	0.1	2.6	462825.60	4451115.87	LEW
NSVCF5	T11	0	0.2	1.7	462824.70	4451115.92	BF RL, cobs>B
NSVCF5	T11	0	0.4	0	462823.00	4451116.00	VL edge
NSVPC5	T1	9	0.8	17.8	461201.13	4451727.19	VR edge
NSVPC5	T1	5	0.4	16.8	461201.68	4451728.02	BF
NSVPC5	T1	0	0	15.6	461202.35	4451729.02	REW
NSVPC5	T1	0	0	3.1	461209.28	4451739.42	LEW
NSVPC5	T1	33	0.5	2.2	461209.78	4451740.17	BF
NSVPC5	T1	44	0.7	0.7	461210.61	4451741.42	S1, FP
NSVPC5	T1	38	0.8	0	461211.00	4451742.00	VL edge
NSVPC5	T2	17	0	29.3	461208.29	4451714.32	VR edge
NSVPC5	T2	25	0.6	27	461209.84	4451716.02	FP, S5
NSVPC5	T2	80	0.6	21.1	461213.81	4451720.39	FP
NSVPC5	T2	81	0.4	18.5	461215.56	4451722.31	FP, BF
NSVPC5	T2	0	0.1	17.1	461216.50	4451723.35	REW
NSVPC5	T2	0	0.1	1.6	461226.92	4451734.82	LEW
NSVPC5	T2	3	0.6	0.4	461227.73	4451735.70	BF
NSVPC5	T2	22	0.9	0	461228.00	4451736.00	VL edge
NSVPC5	T3	24	0	30.3	461219.62	4451704.57	VR edge
NSVPC5	T3	71	0.1	28.3	461221.10	4451705.92	FP, S6
NSVPC5	T3	52	0.3	23	461225.01	4451709.49	FP
NSVPC5	T3	32	0.2	21.8	461225.90	4451710.30	BF
NSVPC5	T3	0	0	21.2	461226.34	4451710.71	REW
NSVPC5	T3	0	0.1	14.4	461231.37	4451715.29	LEW, island
NSVPC5	T3	0	0.1	10.9	461233.95	4451717.65	REW, island
NSVPC5	T3	0	0.1	2.7	461240.01	4451723.18	LEW
NSVPC5	T3	0	0.5	1.2	461241.11	4451724.19	BF

NSVPC5	T3	7	0.9	0	461242.00	4451725.00	VL edge, duff on B
NSVPC5	T4	71	0.7	26	461232.52	4451696.35	VR sedge, FP, OB channel
NSVPC5	T4	55	0.9	19.2	461238.14	4451700.18	FP
NSVPC5	T4	16	0.9	17	461239.95	4451701.42	FP, S7
NSVPC5	T4	32	0.3	12.8	461243.42	4451703.79	ToC, BF
NSVPC5	T4	0	0	12.6	461243.59	4451703.90	Toe of cutbank, channel, cobs
NSVPC5	T4	0	0	11.4	461244.58	4451704.58	REW
NSVPC5	T4	0	0.1	1	461253.17	4451710.44	LEW
NSVPC5	T4	0	0.4	0.8	461253.34	4451710.55	BF
NSVPC5	T4	0	1.3	0	461254.00	4451711.00	VL edge
NSVPC5	T5	44	0.5	36	461238.00	4451681.51	VR edge
NSVPC5	T5	56	0.6	27.5	461245.55	4451685.41	FP
NSVPC5	T5	41	0.5	22.1	461250.35	4451687.88	Fp
NSVPC5	T5	42	0.4	18.5	461253.55	4451689.53	BF
NSVPC5	T5	0	0	17.2	461254.71	4451690.12	REW
NSVPC5	T5	0	0	2.7	461267.60	4451696.76	LEW
NSVPC5	T5	24	0.2	2	461268.22	4451697.08	BF
NSVPC5	T5	42	0.3	1	461269.11	4451697.54	S2, FP
NSVPC5	T5	35	0.4	0	461270.00	4451698.00	VL edge
NSVPC5	T6	29	0.3	30.4	461247.40	4451670.09	VR edge
NSVPC5	T6	46	0.1	25.5	461252.17	4451671.21	FP
NSVPC5	T6	28	0.2	24.5	461253.14	4451671.43	FP, S8
NSVPC5	T6	26	0	19.1	461258.40	4451672.66	BF
NSVPC5	T6	0	0.3	18.8	461258.69	4451672.73	REW
NSVPC5	T6	0	0.3	2.3	461274.76	4451676.48	LEW
NSVPC5	T6	0	0.8	0.6	461276.42	4451676.86	pebs>cobs, BF
NSVPC5	T6	43	1.3	0	461277.00	4451677.00	ToC, VL edge
NSVPC5	T7	57	0.7	26.3	461252.78	4451652.98	VR edge, S9
NSVPC5	T7	35	0.5	20.4	461258.66	4451653.44	FP
NSVPC5	T7	27	0.4	16.8	461262.25	4451653.71	BF, ToC
NSVPC5	T7	0	0	16.7	461262.35	4451653.72	REW
NSVPC5	T7	0	0	2.5	461276.51	4451654.81	LEW

NSVPC5	T7	11	0.4	1.6	461277.40	4451654.88	BF
NSVPC5	T7	0	0.9	0	461279.00	4451655.00	VL edge
NSVPC5	T8	52	0.7	35	461248.05	4451635.94	VR edge
NSVPC5	T8	67	0.6	32	461251.05	4451635.78	
NSVPC5	T8	46	0.3	27.3	461255.74	4451635.51	BF
NSVPC5	T8	0	0	27.2	461255.84	4451635.51	REW
NSVPC5	T8	0	0.1	12	461271.02	4451634.67	LEW
NSVPC5	T8	10	0.5	11.5	461271.52	4451634.64	BF, cobs
NSVPC5	T8	17	0.9	10.6	461272.42	4451634.59	ToL
NSVPC5	T8	5	0.9	10	461273.02	4451634.55	S3, bank
NSVPC5	T8	25	0.7	5.7	461277.31	4451634.32	FP
NSVPC5	T8	97	0.1	0	461283.00	4451634.00	FP, VL edge
NSVPC5	T9	61	0.6	26.7	461244.59	4451621.91	VR edge
NSVPC5	T9	38	0.6	22.5	461248.74	4451621.30	S10, FP
NSVPC5	T9	47	0.7	17.2	461253.99	4451620.52	ToL, cutbank
NSVPC5	T9		0.4	15.7	461255.47	4451620.30	BF
NSVPC5	T9	0	0	14	461257.15	4451620.05	REW
NSVPC5	T9	0	0	1.7	461269.32	4451618.25	LEW
NSVPC5	T9	11	0.5	1	461270.01	4451618.15	BFm cobs>B
NSVPC5	T9	9	0.9	0	461271.00	4451618.00	VL edge
NSVPC5	T10	17	0.5	25.6	461234.37	4451608.85	VR edge, S11
NSVPC5	T10	14	0.4	23.3	461236.49	4451607.96	BF
NSVPC5	T10	0	0	21.9	461237.78	4451607.42	REW
NSVPC5	T10	0	0	10.7	461248.12	4451603.12	LEW
NSVPC5	T10	14	0.3	10.1	461248.68	4451602.88	BF
NSVPC5	T10	9	0.8	8.8	461249.88	4451602.38	terrace, OB levee
NSVPC5	T10	27	0.7	5.2	461253.20	4451601.00	OB levee
NSVPC5	T10	17	0.4	0	461258.00	4451599.00	VL edge, FP, OB channel
NSVPC5	T11	27	0.6	18	461235.43	4451590.10	VR edge
NSVPC5	T11	0	0.5	16.9	461236.50	4451590.33	BF, cobs>B
NSVPC5	T11	0	0	16.4	461236.99	4451590.44	REW
NSVPC5	T11	0	0	6.8	461246.36	4451592.52	LEW

NSVPC5	T11	15	0.4	5.5	461247.63	4451592.81	BF
NSVPC5	T11	78	0.7	2.6	461250.46	4451593.44	FP, S4
NSVPC5	T11	59	0.5	0	461253.00	4451594.00	VL edge
SFPAB6	T1	108	0.3	59.2	455668.89	4496270.14	VL edge, moist OB channel from peak runoff
SFPAB6	T1	81	0.3	49.7	455676.45	4496275.90	FP, organics, sd, grassy meadow, BS
SFPAB6	T1	52	0.4	42.2	455682.42	4496280.44	S1, FP, grassy meadow
SFPAB6	T1	35	0.2	35.4	455687.83	4496284.56	FP, grassy meadow
SFPAB6	T1	34	0.4	28.8	455693.08	4496288.56	berm, FP, levee
SFPAB6	T1	0	0.1	25.9	455695.39	4496290.31	edge of soil, BF, gravel bar
SFPAB6	T1	0	0	22.4	455698.18	4496292.43	LEW
SFPAB6	T1	0	0	13.5	455705.26	4496297.82	REW
SFPAB6	T1	60	0.4	13.4	455705.34	4496297.88	ToC, bank of FP, W, RB
SFPAB6	T1	60	0.9	9	455708.84	4496300.55	FP bank, W, RB
SFPAB6	T1	67	0.8	4.4	455712.50	4496303.34	OC chan, st>sd, BS, W, RB
SFPAB6	T1	35	1	0	455716.00	4496306.00	VR edge
SFPAB6	T2	41	0.6	60	455663.06	4496281.31	VL edge, OB chan, moist sd>slt
SFPAB6	T2	34	0.6	50.7	455670.04	4496287.46	OB chann, wet sd>st, BS
SFPAB6	T2	43	0.5	42	455676.57	4496293.21	FP, grass, wood and debris, W
SFPAB6	T2	59	0.3	35.5	455681.45	4496297.50	S2, W, sand, grassy FP
SFPAB6	T2	0	0	30.9	455684.90	4496300.54	soil/cob contact, ~BF, LEW
SFPAB6	T2	0	0	16.6	455695.63	4496310.00	BF, REW
SFPAB6	T2	25	0.6	15.1	455696.76	4496310.99	Top of sloped bank, all sand, RB, W
SFPAB6	T2	39	0.8	9.9	455700.66	4496314.43	sandy FP, w/ RB, W, BS
SFPAB6	T2	76	0.7	4.3	455704.86	4496318.13	sandy OB chan, FP, RB, W, BS
SFPAB6	T2	60	0.9	0	455708.09	4496320.97	VR edge, grassy
SFPAB6	T3	43	0.9	63.7	455657.08	4496290.71	S3, VL edge, OB chan, FP
SFPAB6	T3	53	1	54.7	455663.61	4496296.90	FP w/ grass, sd>clay
SFPAB6	T3	55	0.9	48.3	455668.25	4496301.31	FP w/ grass, sd>clay
SFPAB6	T3	82	0.4	41.2	455673.40	4496306.20	grassy hummock/berm
SFPAB6	T3	40	0.5	36.7	455676.67	4496309.30	OB chan, W, RB, BS
SFPAB6	T3	0	0.1	33.5	455678.99	4496311.50	soil/cob contact, ~BF RL, W, RB
SFPAB6	T3	0	0	32.1	455680.00	4496312.46	LEW

SFPAB6	T3	0	0	20.4	455688.49	4496320.52	REW
SFPAB6	T3	13	0.6	20.1	455688.71	4496320.72	ToC, RR, W, RB, BS
SFPAB6	T3	49	0.7	12.2	455694.44	4496326.16	sandy FP w/ BS, RB
SFPAB6	T3	34	0.7	5.8	455699.08	4496330.57	med sd, FP w/ BS, ES, W, RB
SFPAB6	T3	101	0.7	0	455703.28	4496334.56	VR edge
SFPAB6	T4	77	0.5	68.8	455647.92	4496296.17	VL edge, RB, BS
SFPAB6	T4	52	0.5	60.2	455653.90	4496302.35	FP, evidence of flow, grass, ES, W, RB
SFPAB6	T4	43	0.3	51.7	455659.81	4496308.46	FP, evidence of flow, grass, ES, W, RB
SFPAB6	T4	22	0.5	46.8	455663.22	4496311.98	FP, grassy berm w? BS
SFPAB6	T4	30	0.5	40.7	455667.47	4496316.36	Top of bank RL, RB, W, tall grass
SFPAB6	T4	0	0	40.4	455667.67	4496316.58	sandy channel
SFPAB6	T4	0	0.1	37.1	455669.97	4496318.95	LEW
SFPAB6	T4	0	0.2	28.5	455675.95	4496325.13	REW
SFPAB6	T4	34	1.1	28.2	455676.16	4496325.34	ToC grassy, FP, RW, W, BS
SFPAB6	T4	26	1.1	25.6	455677.97	4496327.21	S4 , grassy FP, RB, W, BS
SFPAB6	T4	31	1.2	20.9	455681.24	4496330.59	
SFPAB6	T4	48	1.3	12.8	455686.87	4496336.41	Grassy FP, RB, W, BS
SFPAB6	T4	81	1.3	5.9	455691.67	4496341.36	Grassy FP, RB, W, BS
SFPAB6	T4	42	1.2	0	455695.78	4496345.60	VR edge
SFPAB6	T5	83	0.7	73.7	455640.35	4496305.39	VL edge, ES, RB
SFPAB6	T5	83	0.5	68.3	455643.94	4496309.42	OB chan, wet meadow, sand, RB, ES
SFPAB6	T5	95	0.7	67.1	455644.74	4496310.32	S5, FP, grassy, wet sand
SFPAB6	T5	51	0.6	59.9	455649.53	4496315.69	OB chan, snady FP, grass, W, RB, ES
SFPAB6	T5	36	0.7	54.3	455653.25	4496319.88	higher OB levee, tall grass
SFPAB6	T5	38	0.5	51.5	455655.11	4496321.97	ToC, RL
SFPAB6	T5	0	0	51.2	455655.31	4496322.19	edge of chan, LEW
SFPAB6	T5	0	0	39.5	455663.09	4496330.93	REW
SFPAB6	T5	80	0.6	38.2	455663.95	4496331.90	ToC, very large BS, RB, W
SFPAB6	T5	81	0.5	33.5	455667.08	4496335.41	Grassy FP, BS, W, RB
SFPAB6	T5	18	0.6	27.2	455671.27	4496340.12	grassy FP w/ sd, W, RB, BS
SFPAB6	T5	57	0.7	17.8	455677.52	4496347.14	Tall grassy meadow, Road disturbance?
SFPAB6	T5	25	0.5	8.6	455683.64	4496354.01	Tall grassy meadow, Road disturbance?

SFPAB6	T5	28	0.5	0	455689.35	4496360.43	VR edge, very large BS, RB, aspen, tall grass
SFPAB6	T6	44	0.7	76.6	455635.39	4496316.89	VL edge, RB, ES, BS
SFPAB6	T6	6	0.5	70.6	455639.23	4496321.51	OB chan, st>sd, grass
SFPAB6	T6	0	0.6	67.1	455641.46	4496324.20	berm, FP levee, BS, RB, W
SFPAB6	T6	0	0	64.4	455643.19	4496326.28	LEW
SFPAB6	T6	0	0	52.2	455650.98	4496335.67	REW
SFPAB6	T6	53	0.7	51.9	455651.17	4496335.90	ToC, BS, RB, W
SFPAB6	T6	97	0.9	46	455654.94	4496340.44	sandy FP, RB, W
SFPAB6	T6	79	0.7	38.6	455659.66	4496346.13	sandy FP, RB, W, BS
SFPAB6	T6	60	0.8	31.8	455664.01	4496351.37	sandy FP, RB, W, BS
SFPAB6	T6	55	0.4	22.3	455670.07	4496358.68	S6, sandy FP, in group of BS w. tall grass
SFPAB6	T6	32	0.2	14.5	455675.06	4496364.68	sandy FP in BS w/ tall grass, OB channel
SFPAB6	T6	53	0.3	7	455679.85	4496370.45	sandy FP in BS w/ tall grass, OB channel
SFPAB6	T6	43	0.8	0	455684.32	4496375.84	VR edge, grassy edge w/ aspen, RB
SFPAB6	T7	26	0.8	81.5	455623.88	4496325.86	VL edge, ES, BS, RB
SFPAB6	T7	38	0.6	77.1	455626.73	4496329.21	FP moist sd &st, ES, RB, W
SFPAB6	T7	0	0	74.2	455628.60	4496331.42	LEW
SFPAB6	T7	0	0	64.3	455635.01	4496338.97	REW
SFPAB6	T7	74	0.7	63.8	455635.34	4496339.35	ToC, RR, large RB, ES, BS
SFPAB6	T7	35	0.8	59.1	455638.38	4496342.93	FP w/ sd, BS, RB
SFPAB6	T7	26	0.9	49.8	455644.40	4496350.02	FP w/ sd, BS, RB
SFPAB6	T7	48	0.7	43.5	455648.48	4496354.82	OB chan, FP, sd & W
SFPAB6	T7	37	0.9	39.9	455650.81	4496357.56	sd mound from OB flow through W
SFPAB6	T7	120	0.7	32.5	455655.60	4496363.20	S7, sandy interfluve, OB chan, RB, BS, FP
SFPAB6	T7	48	0.5	24.5	455660.78	4496369.30	next to large BS
SFPAB6	T7	26	0.1	15.4	455666.67	4496376.24	sandy OB chan w/ cobs present, standing
SFPAB6	T7	56	0.2	7.6	455671.72	4496382.18	
SFPAB6	T7	31	0.5	5.3	455673.21	4496383.93	edge of valley
SFPAB6	T7	0	0.8	0	455676.64	4496387.97	VR slope edge, toe of road slop
SFPAB6	T8	16	0.6	82	455617.63	4496333.79	VL edge, mini FP
SFPAB6	T8	15	0.5	81.3	455618.09	4496334.32	ToC, RL
SFPAB6	T8	0	0	81.3	455618.09	4496334.32	LEW

SFPAB6	T8	0	0	70.7	455624.99	4496342.36	REW
SFPAB6	T8	54	0.4	70.4	455625.19	4496342.59	ToC, grassy bank w/ RB, sd?cob
SFPAB6	T8	43	0.9	62.5	455630.34	4496348.58	sandy tree cover w/ BS
SFPAB6	T8	95	0.8	55	455635.23	4496354.27	sandy FP w/ RB, W, OB flow
SFPAB6	T8	106	0.7	47.7	455639.98	4496359.81	sandy FP w/ RB, W, OB flow
SFPAB6	T8	52	0.4	41.7	455643.89	4496364.36	S8, low grassy area w/ evidence of OB flow next
SFPAB6	T8	46	0.8	35.9	455647.67	4496368.76	grassy FP, RB, W, andy
SFPAB6	T8	36	0.7	29.2	455652.04	4496373.84	sandy grassy FP, BS, RB, W
SFPAB6	T8	51	0.6	21.4	455657.12	4496379.75	litter filled tree berm, BS, W, Aspen
SFPAB6	T8	54	0	13.9	455662.01	4496385.44	standing water in OB channel, 10 cm depth
SFPAB6	T8	53	0.2	6.4	455666.90	4496391.13	low wet OB channel
SFPAB6	T8	14	0.5	0	455671.07	4496395.98	VR edge, grassy FP, BS, A
SFPAB6	T9	11	0.6	86.9	455609.07	4496340.08	VL edge, on B
SFPAB6	T9	61	0.5	85.9	455609.72	4496340.84	Toc, RL
SFPAB6	T9	0	0	85.7	455609.85	4496340.99	LEW
SFPAB6	T9	0	0	76.6	455615.76	4496347.90	REW
SFPAB6	T9	54	0.6	74.8	455616.93	4496349.27	Top of bank, grassy w/ RB
SFPAB6	T9	57	0.8	66.7	455622.20	4496355.43	tall grassy FP w/ BS, RB
SFPAB6	T9	130	1.2	58.9	455627.27	4496361.35	litter riddled tree cluster of BS
SFPAB6	T9	83	1.2	53.9	455630.52	4496365.15	edge of tree cluster/grassy meadow
SFPAB6	T9	32	1.2	47.9	455634.42	4496369.71	S9 grassy meadow
SFPAB6	T9	88	1.2	38.5	455640.53	4496376.85	grassy meadow surrounding BS
SFPAB6	T9	55	0.1	30.5	455645.73	4496382.93	other side of grassy meadow berm, OB channel
SFPAB6	T9	44	0.5	22.5	455650.93	4496389.01	higher tree cluster of BS
SFPAB6	T9	29	0.1	15.4	455655.55	4496394.41	wet muddy OB channel
SFPAB6	T9	60	0.3	8.2	455660.23	4496399.88	herbacious, wet FP, W, RB, BS, evidence of
SFPAB6	T9	66	0.5	0	455665.56	4496406.11	VR edge
SFPAB6	T10	64	0.7	94.5	455599.17	4496346.21	VL edge
SFPAB6	T10	47	0.3	93.5	455599.81	4496346.97	ToC
SFPAB6	T10	0	0	93.4	455599.88	4496347.05	LEW
SFPAB6	T10	0	0	83.6	455606.17	4496354.56	REW
SFPAB6	T10	35	0.6	83.1	455606.49	4496354.94	ToC, RR, grassy bark w/ BS, RB

SFPAB6	T10	93	0.6	76.1	455610.99	4496360.31	sand FP depsoits on herbacious FP, RB, BS
SFPAB6	T10	93	0.7	70.3	455614.71	4496364.76	cluster of BS w/ RB
SFPAB6	T10	91	1.1	64.8	455618.24	4496368.97	slope berm edge of grassy upland
SFPAB6	T10	30	1.2	55.1	455624.47	4496376.41	grassy meadow upland
SFPAB6	T10	48	1.4	44.5	455631.28	4496384.54	pine trees in meadow
SFPAB6	T10	63	0.8	37.1	455636.03	4496390.21	downslope off grassy meadow in group of BS &
SFPAB6	T10	46	0.3	29.5	455640.91	4496396.04	S10, toe of sloped grassy berm
SFPAB6	T10	33	0.2	22.7	455645.28	4496401.25	FP, w/ W, RB & BS
SFPAB6	T10	64	-0.1	16.6	455649.19	4496405.92	FP, w/ W, RB & BS, sd>peb OB chan
SFPAB6	T10	80	0	10.4	455653.17	4496410.68	wet FP w/ grass, RB, W, BS
SFPAB6	T10	59	0	3.3	455657.73	4496416.12	wet FP w/ grass, RB, W, BS
SFPAB6	T10	27	0.1	0	455659.85	4496418.65	VR ege, RB, W, BS
SFPAB6	T11	0	1.3	99.1	455591.25	4496360.27	VL edge, Bk
SFPAB6	T11	0	0.3	97.9	455592.06	4496361.15	LEW, BK
SFPAB6	T11	0	0.3	88.3	455598.59	4496368.19	REW
SFPAB6	T11	42	0.7	88	455598.79	4496368.41	ToC, RR grassy w? RB, BS
SFPAB6	T11	62	0.7	80.3	455604.02	4496374.06	sand FP w/ grass, RB, BS
SFPAB6	T11	110	0.7	72.1	455609.59	4496380.08	S11, sandy grassy FP w/ RB, BS, W
SFPAB6	T11	107	1	66	455613.74	4496384.55	bunch of BS on edgge of meadow
SFPAB6	T11	10	1.2	57.5	455619.52	4496390.79	in grassy meadow
SFPAB6	T11	73	1.4	46.9	455626.72	4496398.56	in grassy meadow
SFPAB6	T11	120	1.3	38.2	455632.63	4496404.95	Top edge of berm/ downslopeof meadow
SFPAB6	T11	14	0.3	28.6	455639.15	4496411.99	toe of berm, OB chan, RB, W
SFPAB6	T11	58	0.2	20.1	455644.93	4496418.23	Wet FP, OB chan, W, RB
SFPAB6	T11	69	0	15	455648.39	4496421.97	wet OB chan, standing water
SFPAB6	T11	28	0.3	7.5	455653.49	4496427.47	herbacious FP w/ RB, W, BS
SFPAB6	T11	79	0.4	0	455658.59	4496432.97	VR edge, tow of road winrow
GCKPC6	T1	58	0.4	15.1	445794.10	4458363.00	VR edge, meadow
GCKPC6	T1	54	0.4	14.1	445793.10	4458363.00	S1, meadow
GCKPC6	T1	3	0.5	8.8	445787.80	4458363.00	Top of tree island, meadow
GCKPC6	T1	2	0.3	8	445787.00	4458363.00	BF
GCKPC6	T1	0	0	7.8	445786.80	4458363.00	REW

GCKPC6	T1	0	0	2.9	445781.90	4458363.00	LEW
GCKPC6	T1	0	0.3	2.9	445781.90	4458363.00	BF
GCKPC6	T1	41	0.4	2.7	445781.70	4458363.00	ToC
GCKPC6	T1	53	0.4	1.4	445780.40	4458363.00	
GCKPC6	T1	27	0.6	0	445779.00	4458363.00	VL edge
GCKPC6	T2	60	0.6	11.6	445790.57	4458366.11	VR edge, S2, meadow
GCKPC6	T2	26	0.4	8.6	445787.57	4458366.34	OB channel, FP
GCKPC6	T2	14	0.4	5.5	445784.48	4458366.58	ToC
GCKPC6	T2	34	0.3	5.4	445784.38	4458366.59	BF, undercut bank
GCKPC6	T2	0	0	5.4	445784.38	4458366.59	REW
GCKPC6	T2	0	0	1.6	445780.60	4458366.88	LEW
GCKPC6	T2	0	0.3	1.6	445780.60	4458366.88	BF
GCKPC6	T2	54	0.4	1.5	445780.50	4458366.88	ToC
GCKPC6	T2	22	0.4	0	445779.00	4458367.00	VL edge
GCKPC6	T3	64	0.6	12	445790.84	4458370.03	VR edge, OB channel
GCKPC6	T3	23	0.2	7.7	445786.60	4458370.73	BF
GCKPC6	T3	0	0	7.5	445786.40	4458370.77	REW
GCKPC6	T3	0	0	4.4	445783.34	4458371.28	LEW
GCKPC6	T3	52	0.3	4.3	445783.24	4458371.29	BF
GCKPC6	T3	71	0.5	3.6	445782.55	4458371.41	FP
GCKPC6	T3	29	0.4	1	445779.99	4458371.84	S3, VL
GCKPC6	T3	20	0.4	0	445779.00	4458372.00	VL edge
GCKPC6	T4	64	0.7	11.8	445794.45	4458373.14	VR edge
GCKPC6	T4	48	0.7	10.8	445793.48	4458373.38	S4, VR
GCKPC6	T4	20	0.4	7.8	445790.57	4458374.11	ToC, BF
GCKPC6	T4	0	0	7.7	445790.47	4458374.13	REW
GCKPC6	T4	0	0	4.5	445787.37	4458374.91	LEW
GCKPC6	T4	28	0.2	4.4	445787.27	4458374.93	ToC, BF
GCKPC6	T4	34	0.8	3	445785.91	4458375.27	ToC, hummock
GCKPC6	T4	39	0.6	1.6	445784.55	4458375.61	OB channel, FP
GCKPC6	T4	32	0.7	0	445783.00	4458376.00	VL edge
GCKPC6	T5	66	0.6	11	445796.61	4458378.11	S5, VR edge

GCKPC6	T5	13	0.4	6.6	445792.37	4458379.26	ToC, BF
GCKPC6	T5	0	0	6.5	445792.27	4458379.29	REW
GCKPC6	T5	0	0	2.9	445788.80	4458380.24	LEW
GCKPC6	T5	15	0.2	2.5	445788.41	4458380.34	ToC, FP
GCKPC6	T5	35	0.5	1	445786.96	4458380.74	FP
GCKPC6	T5	44	0.5	0	445786.00	4458381.00	VL edge
GCKPC6	T6	14	0.7	9.2	445795.98	4458383.00	VR edge
GCKPC6	T6	7	0.4	6.2	445793.05	4458383.66	S6, ToC, BF
GCKPC6	T6	0	0	5.9	445792.76	4458383.72	REW
GCKPC6	T6	0	0	0.7	445787.68	4458384.85	LEW
GCKPC6	T6	0	0.3	0.7	445787.68	4458384.85	BF
GCKPC6	T6	55	0.8	0.6	445787.59	4458384.87	ToC
GCKPC6	T6	45	1.1	0	445787.00	4458385.00	VL edge, trees next to Bk
GCKPC6	T7	9	1.1	11.4	445798.00	4458387.00	VR edge, FP, OB flow
GCKPC6	T7	11	0.3	8	445794.72	4458387.90	ToC, BF
GCKPC6	T7	0	0	7.9	445794.62	4458387.92	REW
GCKPC6	T7	0	0	2	445788.93	4458389.47	LEW
GCKPC6	T7	0	0.2	2	445788.93	4458389.47	BF
GCKPC6	T7	35	0.4	1.9	445788.83	4458389.50	ToC
GCKPC6	T7	73	0.7	1.4	445788.35	4458389.63	S11, FP
GCKPC6	T7	71	0.9	0	445787.00	4458390.00	VL edge
GCKPC6	T8	0	0.7	12.6	445799.28	4458392.17	VR edge on cobs
GCKPC6	T8	47	0.4	10.2	445796.94	4458392.71	ToC, BF
GCKPC6	T8	0	0	9.3	445796.06	4458392.91	REW
GCKPC6	T8	0	0	4.8	445791.68	4458393.92	LEW
GCKPC6	T8	0	0.2	4.8	445791.68	4458393.92	BF
GCKPC6	T8	58	0.5	4.7	445791.58	4458393.94	ToC
GCKPC6	T8	60	0.6	2.6	445789.53	4458394.42	S10, FP, meadow at top of fan
GCKPC6	T8	77	0.7	0	445787.00	4458395.00	VL edge
GCKPC6	T9	20	1	17.5	445804.26	4458396.12	VR edge, FP, grassy wetland meadow, OB
GCKPC6	T9	40	1.1	11.5	445798.34	4458397.11	S7, FP, OB channel
GCKPC6	T9	108	1.2	8.6	445795.48	4458397.59	Tree hummock

GCKPC6	T9	83	1	7.5	445794.40	4458397.77	ToC, BF
GCKPC6	T9	0	0.4	7	445793.90	4458397.85	REW
GCKPC6	T9	0	0.4	3.6	445790.55	4458398.41	LEW
GCKPC6	T9	11	0.8	3.6	445790.55	4458398.41	TOC
GCKPC6	T9	20	1	3.1	445790.06	4458398.49	Hummock
GCKPC6	T9	67	0.9	0	445787.00	4458399.00	grassy meadow, fan, VL edge
GCKPC6	T10	124	0.8	16.4	445803.29	4458401.08	VR edge, wet meadow with grass
GCKPC6	T10	97	0.8	10.2	445797.13	4458401.81	
GCKPC6	T10	63	0.5	7.6	445794.55	4458402.11	ToC, BF
GCKPC6	T10	0	0	7.5	445794.45	4458402.12	REW
GCKPC6	T10	0	0	3.2	445790.18	4458402.63	LEW
GCKPC6	T10	12	0.3	3.1	445790.08	4458402.64	ToC, BF
GCKPC6	T10	52	0.3	1.4	445788.39	4458402.84	S9, FP
GCKPC6	T10	41	0.3	0	445787.00	4458403.00	FP, VL edge
GCKPC6	T11	103	0.9	25.9	445810.73	4458404.03	VR edge, FP, OB channel, Wet Grassy meadow
GCKPC6	T11	91	1.1	17.7	445802.58	4458404.97	FP, OB channel
GCKPC6	T11	88	0.7	10.9	445795.83	4458405.75	FP, Tree island, S8
GCKPC6	T11	37	0.5	8.3	445793.25	4458406.05	ToC, BF
GCKPC6	T11	0	0	8.1	445793.05	4458406.07	REW
GCKPC6	T11	0	0	4.1	445789.07	4458406.53	LEW
GCKPC6	T11	24	0.2	4	445788.97	4458406.54	BF,
GCKPC6	T11	55	0.4	0	445785.00	4458407.00	FP, grassy meadow, VL edge
NSVPC7	T1	61	0.7	41.1	452228.08	4451083.76	VR edge
NSVPC7	T1	60	0.4	33.4	452225.79	4451091.11	RR edge, ToC
NSVPC7	T1	0	0	33.1	452225.71	4451091.40	REW
NSVPC7	T1	0	0	17.8	452221.17	4451106.01	LEW
NSVPC7	T1	76	0.3	17.7	452221.14	4451106.10	ToC
NSVPC7	T1	59	0.3	11.3	452219.25	4451112.22	sandy FP depsoits, soft, conifers
NSVPC7	T1	40	0.4	6.3	452217.77	4451116.99	S1, higher sandy surface on FP
NSVPC7	T1	8	0.4	0	452215.90	4451123.01	VL edge
NSVPC7	T2	19	0	37.4	452241.32	4451088.54	VR edge
NSVPC7	T2	63	1	35.2	452240.83	4451090.68	river right BF

NSVPC7	T2	0	0.9	33.8	452240.52	4451092.05	REW
NSVPC7	T2	0	1.1	14.7	452236.27	4451110.67	LEW
NSVPC7	T2	29	1.3	14.6	452236.25	4451110.77	ToC, grassy meadow
NSVPC7	T2	40	1.2	14.6	452236.25	4451110.77	S2, grassy bank, change F, RP, LP
NSVPC7	T2	76	1.1	10	452235.22	4451115.25	grassy FP
NSVPC7	T2	76	1.1	6.7	452234.49	4451118.47	grassy FP
NSVPC7	T2	28	0.9	1.5	452233.33	4451123.54	grassy FP, OB chan, satnding water
NSVPC7	T2	41	1.2	0	452233.00	4451125.00	VL edge
NSVPC7	T3	58	0.6	31.9	452258.07	4451090.20	VR edge
NSVPC7	T3	8	0	29.5	452257.49	4451092.53	stagnant H2O, OB chan, water depth 35cm
NSVPC7	T3	79	0	28.9	452257.35	4451093.11	S3, stangant water OB channel
NSVPC7	T3	69	0.7	23.3	452256.00	4451098.54	ToC, RR, BF
NSVPC7	T3	0	0.3	22.5	452255.80	4451099.32	REW
NSVPC7	T3	0	0.3	10.9	452253.00	4451110.57	LEW
NSVPC7	T3	34	0.7	8.7	452252.47	4451112.71	ToC, of side channel, RB, W, hummocky island
NSVPC7	T3	0	0.2	8.5	452252.42	4451112.90	REW, side chan
NSVPC7	T3	0	0.2	7	452252.06	4451114.36	LEW side chan
NSVPC7	T3	73	0.6	6.9	452252.03	4451114.46	ToC RL
NSVPC7	T3	45	0.5	2.9	452251.07	4451118.34	grassy open meadow, ES
NSVPC7	T3	49	0.3	0	452250.36	4451121.15	OB chan, VL edge
NSVPC7	T4	70	1	42.8	452273.08	4451091.72	VR sgde
NSVPC7	T4	124	0.5	37.2	452271.58	4451097.12	FP, hummock between stagnant pools
NSVPC7	T4	52	0.9	33.1	452270.49	4451101.07	stagnant water depth 15cm
NSVPC7	T4	21	0.5	29.5	452269.53	4451104.54	BF hummock on log
NSVPC7	T4	0	0.5	27.9	452269.11	4451106.08	REW
NSVPC7	T4	0	0.7	18.1	452266.49	4451115.53	LEW
NSVPC7	T4	29	0.6	18	452266.47	4451115.63	ToC, Rl under old growth, ES
NSVPC7	T4	63	0.4	13.1	452265.16	4451120.35	sandy FP island w/ ES
NSVPC7	T4	53	0.3	8.2	452263.86	4451125.07	Top edge of terrace
NSVPC7	T4	55	0.2	4.2	452262.79	4451128.93	S4, water table at 24cm, FP
NSVPC7	T4	53	0	3.3	452262.55	4451129.79	REW, sandy bank & bed
NSVPC7	T4	30	0	2.3	452262.28	4451130.76	center of chn, depth of water 16cm

NSVPC7	T4	22	0.6	1.2	452261.99	4451131.82	LEW depth of water 18cm
NSVPC7	T4	42	0.6	1.2	452261.99	4451131.82	ToC, RL
NSVPC7	T4	41	1	0	452261.67	4451132.97	VL edge
NSVPC7	T5	54	0.4	56.2	452286.42	4451085.10	VR edge, next to stagnant pond
NSVPC7	T5	80	0.5	48.3	452284.90	4451092.86	FP, hummmocky area w/ confier
NSVPC7	T5	100	0.5	42.6	452283.80	4451098.45	FP, hummmocky area w/ confier
NSVPC7	T5	92	0.1	39	452283.11	4451101.98	ToC, edge of bankFP, hummmocky area w/
NSVPC7	T5	0	0	38.6	452283.03	4451102.38	REW
NSVPC7	T5	0	0	22.8	452279.99	4451117.88	LEW
NSVPC7	T5	13	0.2	21.6	452279.76	4451119.06	bank of island w/ sand conifers and beaver den
NSVPC7	T5	51	0.3	17.6	452278.99	4451122.98	bank of island w/ sand conifers and beaver den
NSVPC7	T5	45	0	14.7	452278.43	4451125.83	REW side chan
NSVPC7	T5	55	0	12.1	452277.93	4451128.38	LEW suide chan
NSVPC7	T5	69	0.2	12	452277.91	4451128.48	Grassy bank of side chan
NSVPC7	T5		0.3	8.2	452277.18	4451132.21	S5, grassy FP w/ ES
NSVPC7	T5	34	0.2	3	452276.18	4451137.31	grassy Fp w/ ES
NSVPC7	T5	32	0.1	0	452275.60	4451140.25	VL edge
NSVPC7	T6	124	1	53.4	452299.50	4451079.00	VR edge
NSVPC7	T6	68	0.8	43.8	452298.33	4451088.53	grassy meadow FP w/ standing water hole
NSVPC7	T6	74	0.8	35.8	452297.36	4451096.47	wet meadow w/ standing water
NSVPC7	T6	49	0.4	27	452296.29	4451105.20	wet meadow w/ standing water
NSVPC7	T6	0	0.3	26.9	452296.28	4451105.30	REW
NSVPC7	T6	0	0.3	11.6	452294.41	4451120.49	LEW, river bend & W
NSVPC7	T6	32	0.4	10.9	452294.33	4451121.18	grassy meadow island w/ DF & ES
NSVPC7	T6	12	0.6	7.4	452293.90	4451124.66	grassy meadow island w/ DF & ES
NSVPC7	T6	86	0.5	4.1	452293.50	4451127.93	ToC, RR side chan, grassy meadow island
NSVPC7	T6	0	0	3.4	452293.41	4451128.63	REW side chan s/ sd>cobs
NSVPC7	T6	0	0	2.1	452293.26	4451129.92	LEW w/ sd>cobs
NSVPC7	T6	106	0.4	2	452293.24	4451130.01	ToC
NSVPC7	T6	60	0.4	1.3	452293.16	4451130.71	S6, grassy meadow, FP
NSVPC7	T6	50	0.3	0	452293.00	4451132.00	VL edge
NSVPC7	T7	29	0.5	65.4	452314.10	4451072.55	VR edge

NSVPC7	T7	72	0.4	56.4	452312.92	4451081.47	sloppey wet meadow
NSVPC7	T7		0.3	50.7	452312.17	4451087.12	S7, w meadow
NSVPC7	T7	84	0	41.2	452310.92	4451096.54	wet meadow
NSVPC7	T7	70	0.2	35.1	452310.12	4451102.59	edge of sandy FP
NSVPC7	T7	31	0.1	28.2	452309.21	4451109.43	ToC, RR
NSVPC7	T7	0	0.1	28	452309.18	4451109.62	REW
NSVPC7	T7	0	0.3	9.7	452306.77	4451127.77	LEW
NSVPC7	T7	30	0.5	8.4	452306.60	4451129.05	Gassy meadow island
NSVPC7	T7	30	0	6.7	452306.38	4451130.74	Top of island
NSVPC7	T7	0	0	5.9	452306.27	4451131.53	REW, RR side channel, sd.pebs
NSVPC7	T7	0	0	3.9	452306.01	4451133.52	against large B
NSVPC7	T7	22	0.3	1.1	452305.64	4451136.29	LEW, against B
NSVPC7	T7	55	2.6	0	452305.50	4451137.38	VL edge
NSVPC7	T8	30	0.9	49.2	452324.72	4451079.75	VR edge
NSVPC7	T8	74	0.9	39.2	452323.69	4451089.70	wet meadow w/ stadning water
NSVPC7	T8	60	0.4	33.4	452323.09	4451095.47	wet meadow w/ stadning water
NSVPC7	T8	31	0	25	452322.22	4451103.83	ToB, next to rock RR
NSVPC7	T8	0	0	24.9	452322.21	4451103.93	REW
NSVPC7	T8	0	0	1.6	452319.81	4451127.10	LEW
NSVPC7	T8	20	0.4	0	452319.65	4451128.69	S8, VL edge
NSVPC7	T9	0	0.1	29	452336.83	4451093.30	VR egde
NSVPC7	T9	72	0	23.9	452336.98	4451098.40	Wet meadow w/ grass, W
NSVPC7	T9	26	0	20.6	452337.07	4451101.70	bank RR
NSVPC7	T9	0	0	20.5	452337.07	4451101.80	REW
NSVPC7	T9	0	0	15.3	452337.22	4451107.00	LEW, diagonal across chan
NSVPC7	T9	66	0.2	13.8	452337.26	4451108.50	sandy bank w/ ES & RB
NSVPC7	T9	30	0.6	6.9	452337.46	4451115.39	sandy bank w/ ES & RB, aspen, juniper, LP, DF
NSVPC7	T9	49	0.7	2.5	452337.58	4451119.79	sandy bank w/ ES & RB, aspen, juniper, LP, DF
NSVPC7	T9	47	0.7	1	452337.62	4451121.29	S9, VL
NSVPC7	T9	33	0.8	0	452337.65	4451122.29	VL edge
NSVPC7	T10	46	0.3	27	452348.97	4451084.83	VR edge
NSVPC7	T10	40	0.3	25.7	452349.21	4451086.11	FP

NSVPC7	T10	19	0.1	23.8	452349.56	4451087.98	Top of bank
NSVPC7	T10	0	0	23.7	452349.58	4451088.07	REW
NSVPC7	T10	0	0	12.6	452351.63	4451098.98	LEW
NSVPC7	T10	37	0.4	11.3	452351.87	4451100.26	Top of bank, sandy FP point bar
NSVPC7	T10	42	0.4	7.2	452352.63	4451104.29	S10,W, Aspen, ES, DF, LP, FP
NSVPC7	T10	17	0.7	0	452353.96	4451111.37	VL edge, surface sand in Aspen
NSVPC7	T11	55	-0.9	24	452363.04	4451076.12	VR edge
NSVPC7	T11	92	-0.8	21.6	452363.79	4451078.40	FP
NSVPC7	T11	44	-0.8	18.4	452364.79	4451081.44	ToC
NSVPC7	T11	0	-1.6	16.7	452365.32	4451083.06	REW
NSVPC7	T11	0	-1.6	6.2	452368.59	4451093.03	LEW
NSVPC7	T11	85	-1.2	3.7	452369.37	4451095.41	sandy FP/pt bar w/ A, W, ES, LP, DF, bank
NSVPC7	T11	13	-1	2.7	452369.68	4451096.36	S11, duff on B
NSVPC7	T11	28	-0.9	0	452370.52	4451098.93	VL edge
GCKCF7	T1	0	0.4	15.4	445748.75	4458853.28	VR edge, Bk
GCKCF7	T1	0	0	15	445748.37	4458853.14	REW
GCKCF7	T1	0	0	3	445737.17	4458848.85	LEW
GCKCF7	T1	19	0.1	2.6	445736.79	4458848.70	ToC, RL
GCKCF7	T1	22	0.2	1.1	445735.39	4458848.17	S1
GCKCF7	T1	26	0.1	0	445734.37	4458847.77	VL edge
GCKCF7	T2	0	2.1	8.6	445744.01	4458861.01	VR edge, Bk
GCKCF7	T2	0	0.2	6.2	445741.81	4458860.06	BF, RR, REW
GCKCF7	T2	0	0	2.9	445738.78	4458858.76	LEW
GCKCF7	T2	27	0.3	2.3	445738.23	4458858.52	BF, RL
GCKCF7	T2	12	0.5	1.2	445737.21	4458858.09	RL, S2
GCKCF7	T2	17	1.2	0	445736.11	4458857.61	VL edge
GCKCF7	T3	16	0.3	12	445741.98	4458871.41	VR edge, grassy FP/B
GCKCF7	T3	21	0.1	8.5	445738.71	4458870.17	S3, FP, back eddy around very LB
GCKCF7	T3	23	0.2	5.3	445735.72	4458869.03	ToC, BF RR
GCKCF7	T3	0	0	5.1	445735.53	4458868.96	REW
GCKCF7	T3	0	0	0	445730.77	4458867.14	LEW, VL edge
GCKCF7	T4	23	1.3	13.3	445740.23	4458880.07	VR edge

GCKCF7	T4	79	0.7	10.9	445737.95	4458879.32	S4, FP
GCKCF7	T4	27	0.2	7.1	445734.34	4458878.14	ToC, BF RR
GCKCF7	T4	0	0	6.9	445734.15	4458878.07	REW
GCKCF7	T4	0	1	0	445727.59	4458875.92	LEW, VL edge, Bk
GCKCF7	T5	10	0.5	9.3	445736.98	4458887.47	VR edge, liter on Bk
GCKCF7	T5	0	0.5	8.3	445736.04	4458887.14	top of B
GCKCF7	T5	7	0.2	7.5	445735.28	4458886.88	BF, ToC, S5
GCKCF7	T5	0	0	7.4	445735.19	4458886.85	REW
GCKCF7	T5	0	0.1	0	445728.20	4458884.40	LEW. VL edge, BK
GCKCF7	T6	7	0.8	13.6	445732.93	4458894.20	VR edge
GCKCF7	T6	19	0.5	12.8	445732.17	4458893.94	S6R, RR bank
GCKCF7	T6	0	0.4	10.9	445730.38	4458893.31	VF on BK, RR
GCKCF7	T6	0	0.1	9.8	445729.34	4458892.95	REW, BK
GCKCF7	T6	0	0.1	4.7	445724.52	4458891.29	LEW, BK
GCKCF7	T6	38	0.4	4.6	445724.42	4458891.25	BF, RL soil on BK
GCKCF7	T6	0	0	2.1	445722.06	4458890.44	left Bank, wood
GCKCF7	T6	43	0	0	445720.08	4458889.75	S6L, VL edge
GCKCF7	T7	0	0.2	8.2	445730.56	4458900.77	VR edge, sd>peds
GCKCF7	T7	0	0.2	6.4	445728.85	4458900.20	pebs>sd
GCKCF7	T7	0	0	5.3	445727.81	4458899.84	REW
GCKCF7	T7	0	0	1.1	445723.83	4458898.50	LEW
GCKCF7	T7	30	0.4	1	445723.74	4458898.47	ToC, BF RL
GCKCF7	T7	32	0.4	0.4	445723.17	4458898.28	S7, FP, grass
GCKCF7	T7	34	0.4	0	445722.79	4458898.15	VL edge
GCKCF7	T8	7	0.1	7.7	445731.05	4458908.01	VR edge, base of BK, FP
GCKCF7	T8	5	0.2	6.3	445729.70	4458907.63	FP
GCKCF7	T8	6	0.2	5.7	445729.13	4458907.46	BF, ToC
GCKCF7	T8	0	0	5.4	445728.84	4458907.38	REW
GCKCF7	T8	0	0	1.4	445725.00	4458906.27	LEW
GCKCF7	T8	12	0.2	1.1	445724.71	4458906.19	BF, ToC, RL
GCKCF7	T8	20	0.4	0.5	445724.13	4458906.03	S8, FP
GCKCF7	T8	13	0.6	0	445723.65	4458905.89	VL edge

GCKCF7	T9	32	1.9	8.61	445730.74	4458914.08	S9, VR edge, litter on Bk
GCKCF7	T9	0	1.4	6.51	445728.74	4458913.45	litter edge on Bk
GCKCF7	T9	3	0.9	5.4	445727.68	4458913.12	litter edge on BK
GCKCF7	T9	0	0.2	4.7	445727.01	4458912.91	REW
GCKCF7	T9	0	0	0	445722.53	4458911.51	LEW, VL edge
GCKCF7	T10	18	0.7	5.1	445727.96	4458918.99	VR edge
GCKCF7	T10	9	0.4	4.5	445727.39	4458918.80	S10, bank
GCKCF7	T10	0	0.2	4	445726.92	4458918.65	Top of B, BF
GCKCF7	T10	0	0	3.8	445726.73	4458918.58	REW
GCKCF7	T10	0	0.1	0	445723.11	4458917.40	LEW, VL edge
GCKCF7	T11	0	0.9	5.2	445724.93	4458925.97	VR edge, B
GCKCF7	T11	0	0.1	4.7	445724.47	4458925.78	REW, pebs>cobs on Bk
GCKCF7	T11	0	0	0	445720.12	4458923.99	LEW, BK bank, VL edge

Table 7.2. Wood survey data for large downed wood on the floodplain of 24 study reaches.

NSVCF1			NSVCF1 (cont.)			OCKCF2			NSVCF4		
Length (m)	Width 1 (cm)	width 2 (cm)	Length (m)	Width 1 (cm)	width 2 (cm)	Length (m)	Width 1 (cm)	width 2 (cm)	Length (m)	Width 1 (cm)	width 2 (cm)
9	20	25	10.9	10	30	2.9	27	37	2.4	12	14
5.6	15	20	5.6	3	25	2.9	14	13	3.8	7	12
8.7	10	30	12.5	10	35	4.6	38	18	2.2	26	32
8.2	10	30	10	10	15	2.5	12	16	4.4	10	12
7.3	10	25	6	20	40	3.7	16	18	4.8	20	26
8.6	7	22	9.4	10	30	2.3	15	13	5.2	17	30
5.5	5	20	5.5	10	15	1.5	17	12	3.5	12	19
2.9	10	15	7	10	23	4.3	21	13	4.4	10	12
13.6	10	40	9	6	35	4.7	7	19	2.8	21	44
2.5	15	20	7.5	15	25	2.6	7	28	4.8	5	11
12.4	20	60	7.6	10	38	2.8	10	55	8.4	9	22
3	10	25	GCKCF3			5	10	22	14.7	5	45
6	25	35	Length (m)	Width 1 (cm)	width 2 (cm)	2.6	26	20	7.2	5	18
7	20	35	6.7	8	22	2.5	55	28	2	19	20
8	15	25	1.5	10	12	3.6	19	22	NSVCF5		
6	10	25	1.2	10	11	3.1	18	45	Length (m)	Width 1 (cm)	width 2 (cm)
4	15	20	2	10	10	3.3	20	21	1.9	9	14
3	10	15	4.3	7	17	3.2	18	20	2.4	8	12
11.1	5	20	4.1	10	18	2.1	45	40	2.7	10	14
7	10	20	2	10	15	3.8	17	32	2.7	7	12
3	15	20	1.5	15	16	5.1	16	20	3.7	10	20
6	10	20	3.1	10	15	9.7	17	13	3.5	8	13
5.5	20	30	3	11	14	4.3	24	12	3.8	6	10
10	15	35	4.9	12	20	1.8	18	20	3.4	10	15
8.5	15	25	2	12	15	2.1	10	21	3.6	10	18
10	15	40	2.7	5	14	2.8	8	29	4.2	19	26
9.5	15	30	1.8	20	22	2	19	29	2.4	9	15
10.9	10	30	1.2	10	18	3.2	17	31	4	3	23
5.6	3	25	0.9	12	17	2.2	22	30	1	20	20
12.5	10	35				11.1	15	25	2	5	7
10	10	15				3.2	24	30	2	6	13
6	6	40				2	20	31	2	7	25
9.4	9.4	30				1	19	15	3	4	11
5.5	5.5	15				3	24	40	3	11	24
7	7	23				2	18	31	5	7	20
9	9	35				2	12	17	GCKCF7		
7.5	7.5	25				1.5	33	12	Length (m)	Width 1 (cm)	width 2 (cm)
7.6	7.6	38				2.5	20	17	12	15	45
6	25	35				3	12	25			
7	20	35				2.5	10	36			
8	15	25				2	15	15			
6	10	25				3	19	17			
4	15	20				1	34	15			
3	10	15				3	10	34			
11.1	5	20				4.5	10	31			
7	10	20				4	9	32			
3	15	20				3	29	18			
6	10	20				2.5	28	42			
5.5	20	30				1.5	17	27			
10	15	35				2	14	21			
8.5	15	25				3	38	47			
10	15	40				3	18	20			
9.5	15	30				5	11	31			

NSVPC1			OCKPC2			OCKPC2 (cont.)			NSVPC7 (cont.)		
Length (m)	Width 1 (cm)	width 2 (cm)	Length (m)	Width 1 (cm)	width 2 (cm)	Length (m)	Width 1 (cm)	width 2 (cm)	Length (m)	Width 1 (cm)	width 2 (cm)
3.4	10	15	2	13	14	2	27	28	10.8	13	34
9.1	10	28	4.5	6	14	3.5	17	22	9.1	5	37
5.2	7	20	7.1	24	35	14	30	48	5.9	6	20
10.5	8	25	14.4	10	18	4	18	22	4.5	3	11
2.3	20	33	3.4	10	18	4	35	49	6.1	8	23
5.2	10	25	2.9	13	22	2.5	26	28	4.7	4	12
5.8	5	15	2.9	10	12	4	10	15	5.6	3	18
3.5	10	15	3.8	14	16	4	10	17	8.5	6	21
4	10	15	6.5	8	14	6	26	30	9.4	25	40
3.9	10	18	7.4	8	17	9	15	24	6.3	8	16
9.4	15	24	2.1	10	11	3	20	21	2.7	15	20
2.9	22	25	3.6	14	23	3.5	6	15	3.5	7	13
18	23	55	2	10	10	11.7	10	26	10.2	7	30
4.8	20	25	6	10	23	6.4	24	37	2	30	32
5	5	15	2.8	14	18	**GCKPC6**			3	28	30
6.2	8	20	3.5	8	14	**Length (m)**	**Width 1 (cm)**	**width 2 (cm)**	1.5	10	13
6	20	25	12.6	6	20	4.5	33	50	6.1	6	20
3.1	25	40	2.3	14	21	2.5	5	10	1.5	11	12
1.5	35	60	5.5	26	34	3.5	14	17	2.5	10	13
8.5	15	25	6.3	6	12	3.1	24	27	2.2	15	18
6.4	10	20	6.2	10	15	2.6	12	15	2	5	14
13.8	15	35	7.3	13	21	2.7	12	17	2.3	9	11
14.6	15	37	1.5	25	28	2	16	17	1.7	10	13
12.3	17	43	2	10	12	4.1	18	21	2.1	13	14
13.4	10	40	9.3	10	19	**NSVPC7**			3.2	9	15
12.7	15	50	6.3	10	14	**Length (m)**	**Width 1 (cm)**	**width 2 (cm)**	2.9	30	30
12.2	10	30	1.9	16	20	2.7	4	11	1.3	10	11
10.6	15	50	4.5	18	22	2.7	10	40	2.7	19	21
9.7	5	35	3.4	10	12	3.3	11	20	2.2	13	19
9.8	15	45	8.1	20	28	14.7	10	47	3	5	12
11.6	10	20	5.3	20	26	13.3	3	15	7.6	10	21
8.2	10	22	3	15	20	3.9	33	38	1.4	20	28
7.3	15	30	2	15	25	6.2	12	22	11.8	6	24
11.9	10	23	2	13	25	10.6	11	35	3.9	4	13
6	20	25	6	7	19				10.3	20	32
3	18	27	3.5	8	12				12.5	18	28
3	12	15	4	25	35				9.2	15	22
4	30	34	9	22	33				4	6	15
7.5	10	20	6	30	40				5.7	9	27
4.5	23	35	8	25	42				6.3	4	13
5.3	20	25	5	10	15				4.5	10	25
3.4	28	30	4.5	10	30				6.1	6	23
2	10	16	8	16	27				6.5	5	17
4	5	10	7	30	35				14.5	10	31
9.5	30	45	3	18	22				13.3	11	31
11.4	10	30	4	10	16				6.7	4	10
4	20	25	10	10	30				4.4	2	10
3.2	10	15	5	13	22				19.5	5	42
13.2	10	35	4	8	14						
9.4	10	27	16	10	20						
8.3	10	35	13	23	45						
6	35	50	15	30	60						
GCKPC3			**HCKPC4**			**NSVPC5**			**NSVPC7 (cont)**		
Length (m)	**Width 1 (cm)**	**width 2 (cm)**	**Length (m)**	**Width 1 (cm)**	**width 2 (cm)**	**Length (m)**	**Width 1 (cm)**	**width 2 (cm)**	**Length (m)**	**Width 1 (cm)**	**width 2 (cm)**
2	15	20	4.1	22	25	3.7	10	18	5.7	3	10
2	15	15	3.5	10	11	4.7	15	25	13.7	7	27
3	10	18	7.3	20	33	3.4	5	12	6.6	3	14
4	10	20	7.6	20	27	3.3	7	10	3.7	5	17

2	10	10	2	36	37	4.3	10	18	5.5	4	13
2.5	5	10	2.4	49	51	4.9	9	12	6	6	17
2	5	12	2.1	30	32	3.7	6	12	4.7	3	18
4.2	5	17	10.8	20	29	5.8	12	19	5.7	3	10
5.4	10	34	4.7	17	22	6.3	22	35	14.4	9	45
11.4	10	26	2	12	13	6.9	10	23	8.1	4	22
6.2	15	22	3.9	22	24	4.5	6	10	8.3	6	23
5.4	12	20	4.9	10	15	4.8	8	12	6.5	5	18
3.8	12	16	6.6	12	17	5.2	11	17	6.1	3	12
3.4	10	12	2	26	28	3	6	10	6.5	45	50
4	15	20	5.6	13	20	7	1	20	4.3	3	14
1.3	20	22	5.7	8	18	1.5	20	24	5.9	3	11
3	10	15	3.9	15	19	5	5	16	5.1	4	10
9.9	15	48	20.5	10	38	2	5	10	5.2	3	10
9.1	10	35	8.8	16	23	2	7	12	12.4	8	22
3	10	15	3	12	16	1.5	3	9	6.7	19	29
3	10	15	13.1	24	43	4	11	16	6.2	17	23
7	10	45	4.1	40	47	6	5	14	6.9	15	20
7	10	17	5.2	7	15	7	7	17	10.9	18	27
12.8	10	38	5.6	27	35	3	4	12	9.6	20	29
14	10	30	10	16	24	3	18	31	4.2	12	17
2.9	10	12	3.5	15	20	2	10	16	9.4	4	19
5	10	10	11.5	6	18	2.5	24	36	3.8	19	24
11.5	5	30	2.5	15	17	9	19	57	5.9	7	26
2.5	10	13	6.8	15	23	3	21	33	4.9	5	26
2.6	10	11	6.5	20	28	4	2	12	7.1	4	27
2.6	10	15	5.4	26	28	6	7	13	12.4	5	25
4.4	8	18	4.6	20	25	3	2	10	3.8	6	14
2.4	5	11	2	46	48	7	8	14	11.4	15	37
3.8	4	12	2.2	16	18	4	4	15	3.5	13	18
10	10	326	4.7	48	51	3	1	12	11.1	5	29
3	5	10	4.4	10	15	6	1	7	7.5	10	32
3.9	6	12	6.5	11	15	4	1	13	13.8	12	35
9	5	12	5.3	20	30	4	2	15	8.1	10	36
0.5	13	13	8.3	25	34	2	8	10	9.8	5	28
6.7	23	30	4.5	21	27	7	5	23	11	4	17
2.3	8	12				3	2	8	2.3	11	13
6	5	10									
1.2	30	30									
5.2	10	23									
3.3	47	50									
4	7	12									
4.2	10	20									
4.9	15	17									

CCKUC1			GCKUC2			MCKUC3		
Length (m)	Width 1 (cm)	width 2 (cm)	Length (m)	Width 1 (cm)	width 2 (cm)	Length (m)	Width 1 (cm)	width 2 (cm)
5	20	25	2	10	12	7.4	7	16
3	28	31	5.2	18	21	2.5	11	14
2	16	18	2.3	25	28	2.7	5	12
3	3	10	9.5	5	34	2.2	10	11
4	24	32	2.2	5	12	1.6	21	24
1	30	32	3.9	45	50	3.8	15	18
9	8	26	3.6	12	18	5.7	28	39
6	8	23	3.1	10	17	1.2	10	8
5	42	53	6.6	29	44	7.9	17	30
1	27	30	3.3	28	35	11.1	43	4
3.5	18	23	9.2	11	21	19.8	38	6
12	21	42	7.8	26	35	5.6	12	9
6	31	56	9.4	10	32	5.3	8	12
14	19	33	4.1	8	14	6.8	13	10
7	14	20	6.1	13	20	2.8	9	12
6	14	29	5.8	10	12	5.9	19	31
5	10	17	4.9	13	20	6.2	18	8.5
2	9	27	2.8	29	38	9	13	6
2	33	47	10.6	12	29	12.7	22	52
2	13	17	5.2	29	34	15.3	3	34
9	22	38	2.1	12	16	3.4	6	12
18	48	56	3.3	5	15	4.6	11	15
5	3	15	3	25	30	1.2	34	71
9	22	24				1.2	41	36
7	25	43				5.7	12	4
9	18	31				7.6	9	42
3	42	43				1.6	48	70
9	16	35				2.8	5	31
12	11	43				3.2	7	12
5	19	40				4	6	18
9	42	64				13.8	16	48
1.5	51	58				3.7	5	14
14	12	30						
5	19	30						
8	17	34						
6	24	37						
3	54	61						
4	3	12						
5	5	16						
6	16	27						
3	18	23						
4	3	15						

NSVAB1			NSVAB1			BTRAB5 (cont.)			BTRAB5 (cont.)		
Length (m)	**Width 1 (cm)**	**width 2 (cm)**	**Length (m)**	**Width 1 (cm)**	**width 2 (cm)**	**Length (m)**	**Width 1 (cm)**	**width 2 (cm)**	**Length (m)**	**Width 1 (cm)**	**width 2 (cm)**
4.6	12	19	10.7	15	34	1.5	10	30	3	10	10
6.6	10	25	2.2	10	18	2	10	15	1	20	30
2	20	20	10.5	31	36	1.5	5	10	3	15	15
9.6	25	31	6.8	6	16	1.5	20	25	4	15	20
3.4	8	12	5.4	8	12	3	10	10	7	20	20
7.9	16	44	4.2	10	13	2.5	10	15	4	10	15
5.5	16	28	6.2	22	36	2	10	10	3	10	10
3.5	10	15	3.9	27	45	4	2	10	6	5	10
3.3	10	17	3.3	16	19	1.3	9	10	5	10	15
11.7	20	46	4	20	30	1.8	4	80	8	20	20
5.6	31	45	2	30	50	2	5	10	6	5	10
5.4	11	19	17	10	35	3	10	20	3	30	30
10	15	32	20	5	40	1	30	30	1	40	40
5.8	51	68	16	20	33	1.5	5	10	1	10	20
3.6	12	25	3.5	20	40	2	20	30	3	10	10
6.6	25	50	5.9	30	40	2	40	40	2	10	15
7.3	24	30	4	10	15	3	10	30	1	10	30
9.3	12	31	2.5	20	25	2	5	10	2	20	20
3.2	8	14	7	20	30	1	30	30	6	5	25
8.5	15	35	BTRAB5			1.5	5	10	20	5	70
3	38	41	**Length (m)**	**Width 1 (cm)**	**width 2 (cm)**	2	20	30	1	10	40
4	15	25	1	21	21	2	40	40	10	25	40
2	40	45	2.2	13	15	3	10	30	4	20	30
3	25	30	7.7	16	23	2	5	10	3	20	20
4.5	15	35	1.1	7	12	1	15	15	2	10	15
10.7	10	28	1.5	20	31	1.5	8	20	1	10	10
9	15	35	1	10	20	3	3	11	2	5	15
3.3	28	34	1	20	20	2.5	3	10	2	10	20
2	48	49	10	5	20	2	10	10	1	10	20
3.2	15	19	2	10	10	1	10	25	1	5	10
6.3	13	26	3	10	15	6	25	35	1	15	20
3.8	16	28	1	10	10	4	20	30	1.2	15	16
4.3	15	26	2.5	10	10	10	5	30	1.5	11	42
5.9	24	42	1.5	10	20	5	30	40	1.7	13	14
2	26	28	20	10	60	2	20	20	1.9	13	15
3.3	48	55	8	10	20	8	10	20	1	12	21
4.3	28	36	10	10	20	1	5	20	1.5	13	20
6.8	6	16	16	12	40	2	5	10	4.6	15	18
5.4	8	15	1	5	10	1	5	20	1.8	8	12
6.4	10	15	5	5	25	4	10	10	1.3	15	16
3.4	5	12	2	10	10	3	3	10	20	27	28
5.7	11	23	2.5	10	10	3	4	10	2.9	12	14
4.2	18	23	1	5	20	1	15	35	1.1	15	16
3.8	35	69	1.5	5	20	3	10	10	1	12	14
5	20	27	1	10	20	2	10	20	1.4	20	21
2.8	35	50	5	10	15	5	5	20	4.4	8	11
9.5	19	37	5	5	15	7	5	20	1.2	18	19
2.6	17	21	1.5	5	20	15	3	20	2.2	16	18
3.5	10	13	4	5	15	13	10	30	2.1	5	11
12.4	22	34	5	20	35	5	15	15	2.4	5	10
8.5	10	23	3	10	15	3	20	25	1.5	10	11
5.9	14	24	4	5	25	6	5	10	3.1	10	11
2	8	12	4	15	20	2	5	40	2.1	10	23
2.3	8	10	2.5	5	20	4	10	10	2.5	9	13
5.5	12	19	3.5	10	30	7	10	15	2.1	10	15
5.1	10	40	2	20	20	2	10	20	1.6	11	12
									1.5	18	19
									1.6	12	14

NSVAB4	
Length (m)	Ave (Mid) Width (cm)
2.16	14
6.4	20
2.9	10
2.4	12
2.7	10
2.3	10
2.1	10
8.3	16
6.9	19
1.3	12
8.7	45
1.1	13
1.3	29
2.2	16
6.9	25
2.7	12
4.3	12
4.1	11
5.7	30
9.6	31
2.7	10
6.8	23
10	29
1.7	10
2.3	12
3.1	14
4.7	15
5.6	11
2.9	13
3.1	11
4.1	14
4.3	12
3.8	11
9.5	28
3.1	11
2.6	10
4	13
7.9	22
6.5	26
10	28
9.6	34
1.7	14
3.1	19
1.1	21
6.1	35
2.15	19
3.3	10
3	13
1.1	13
1.4	10
2.1	16
3.2	14
1	15
1.8	11
2.9	26
2.6	22

NSVAB4 (cont.)	
Length (m)	Ave (Mid) Width (cm)
1.8	12
1.1	15
1.2	12
2.1	21
2.9	20
1.1	13
2.6	28
1.3	11
1.3	16
4.3	21
1.6	28
4.1	14
1.4	16
1.7	31
3.9	11
3.7	22
2.8	26
2.1	30
1.9	13
1.8	12
2.6	11
1.7	19
3.3	22
3.1	12
1	27
1.4	13
3.2	30
1.2	16
1.1	16
3.1	16
3.6	10
1.2	17
1	10
1.1	12
2.1	11
1.5	17
2.2	11
4.1	38
1.3	12
1.6	13
1.8	16
2.3	27
1.1	33
1.2	17
2.1	22
1.1	12
1	11
1.6	10
1	16
1.9	36
2.2	18
2.1	11
3.1	10
2.2	21
1.56	13
1.3	12

NSVAB4 (cont.)	
Length (m)	Ave (Mid) Width (cm)
1.2	15
1.5	27
1.9	15
1	13
2.3	20
1.1	11
1.1	14
2.1	10
2.2	18
2.6	38
1.6	16
1.8	14
3	10
3.2	19
3.6	17
1.9	20
2.8	10
1.3	12
1.9	18
1.2	11
1.8	17
1.1	26
3.4	21
1.8	16
2.1	24
1.3	11
1.4	13
2.1	47
2.2	16

SFPAB6		
Length (m)	Width 1 (cm)	width 2 (cm)
4.9	18	30
4.1	16	28
3.8	23	28
4.5	13	24
2.9	11	19
5.3	3	13
4.8	17	24
4.6	19	28
5.6	27	39
4.6	4	12
3.3	19	21
5.8	11	40
3.4	5	10
15.4	32	54
20	16	60
3	10	10
1	10	10
2	10	10
22	4	10
1	15	10

SFPAB6 (cont.)		
Length (m)	Width 1 (cm)	width 2 (cm)
2	10	5
2	25	20
3	15	10
1.5	12	15
3.5	15	10
4	15	15
3	10	5
1	15	15
2	10	10
4	20	10
2	30	30
3	10	10
3	20	20
2	50	20
2	12	15
5	30	30
21	60	20
2	12	10
3	10	5
4	20	10
10	25	10
10	40	30
2.5	15	10
2	30	30
10	35	20
1	20	20
2	20	20
3	10	5
1	15	10
3	10	5
5	50	30
1	10	5
25	15	10
6	25	10
2.5	10	5
1.5	10	10
1	10	10
1	10	5
9	20	5
7.5	20	5
3	15	5
1	15	15
1	30	20
1	10	5
1	10	5
1.5	10	10
3	20	15
1	25	20
1.5	15	10
1	20	10
1.5	20	20
2.5	15	10
1	15	15
3	10	5
2	10	5
3	25	25

OCKAB2			OCKAB2 (cont)			OCKAB2 (cont)			OCKAB2 (cont)		
Length (m)	**Width 1 (cm)**	**width 2 (cm)**	**Length (m)**	**Width 1 (cm)**	**width 2 (cm)**	**Length (m)**	**Width 1 (cm)**	**width 2 (cm)**	**Length (m)**	**Width 1 (cm)**	**width 2 (cm)**
2	13	15	12.4	7	24	8	32	56	5	22	28
3.5	18	31	11.6	24	32	12.4	10	56	3	19	21
1	12	13	4.5	5	15	12.2	20	54	6	6	25
2	34	45	6	5	17	10.7	13	31	4	46	58
3	8	17	5.5	4	15	6.5	10	18	3.5	31	62
2	9	15	3.4	14	18	6.9	23	42	5	13	30
2	8	11	6.7	17	24	9.6	17	24	3	4	9
17	15	45	8	25	35	14	10	33	4	7	14
1.5	27	34	15	25	40	10.1	10	43	4	5	12
2	24	34	5.2	5	15	1.7	10	15	5	8	17
3.5	21	26	7.8	14	23	10.8	13	36	2.5	5	10
18	6	45	6.5	26	33	6.9	35	42	7	10	23
4	7	20	5.6	5	18	10.4	8	18	3.5	12	16
7	58	98	6.5	16	23	8.6	6	17	6	18	37
2	12	18	12	15	32	7.4	22	34	4	26	43
10	28	63	8.6	12	21	6.5	6	13	5	9	25
6	37	56	6.5	26	37	11.7	4	16	3.5	24	35
7	17	31	7	28	36	12.8	6	18	5	17	30
9	12	30	6.4	10	28	14.1	13	36	5	14	34
11	16	49	4.7	20	32	13.6	12	28	4	16	30
3	10	15	3	13	16	11.8	11	26	6	28	53
12	33	66	3.6	17	20	8	6	24	10	16	49
5	17	33	7.4	5	19	11.2	7	25	12	14	53
6	4	23	6.2	4	15	9.9	5	19	3	18	22
5	9	14	4.7	11	22	9.1	7	17	3.5	17	24
3	23	29	7.1	20	28	8.5	16	23	6	7	20
4	8	14	12.4	22	48	9.7	20	36	5	6	18
2	10	13	8.6	20	24	10.8	11	24	7	19	40
9	8	29	15.8	14	44	6.9	5	14	16	3	42
8	22	49	15.2	13	39	6.2	7	20	7	14	21
7	9	21	23.5	9	56	5.6	8	16	5	22	32
6	23	42	6.6	6	20	13.7	6	25	8	2	23
5	14	22	7.8	25	33	8.1	5	15	2	10	12
5	4	17	15.7	12	48	8.4	5	17	9	6	27
6	38	57	19	16	51	11	15	24	6	2	31
2	14	17	13.7	11	36	7.8	19	23	4	27	30
3	22	30	12.6	4	29	4.5	20	33	8	13	24
9	27	49	5.9	13	20	5.1	24	30	8	12	36
3	19	24	10.9	7	28	11.4	18	26	9	35	49
8.4	18	30	12.2	11	27	3.8	10	17	6	6	12
10.2	8	30	8.8	25	33	3.6	51	54	4	24	29
7.3	10	23	5.4	29	41	9.7	7	21	16	8	47
8.5	5	32	5.3	25	30	8.8	13	29	12	7	20
8.1	9	29	7.5	3	15	6.1	6	17	10	8	36
2.6	11	18	5.3	45	52	8.4	24	37	11	12	46
5.8	5	17	3.9	5	14	18.4	10	36	4	13	27
2.5	18	32	7.3	5	16	11.1	8	25	5	16	21
6.3	10	25	10.7	4	23	8.2	26	38	7	31	47
9	25	36	9.3	4	20	9.1	27	36	8	16	42
10.9	19	40	9.2	12	21	9.8	22	30	2	31	34
5.4	7	13	4	34	41	8	23	32	3.5	21	24
7.5	14	20	3	5	17	8	15	62	3	35	40
4.5	35	42	2	15	18	14	6	51	3	16	22
						7	8	31	4	7	17

NSVMT1			NSVMT1 (cont.)			NSVMT1 (cont.)			NSVMT1 (cont.)		
Length (m)	**Width 1 (cm)**	**width 2 (cm)**	**Length (m)**	**Width 1 (cm)**	**width 2 (cm)**	**Length (m)**	**Width 1 (cm)**	**width 2 (cm)**	**Length (m)**	**Width 1 (cm)**	**width 2 (cm)**
5.5	45	51	4	24	37	5.5	40	48	2	33	36
2.5	30	35	10.9	22	39	2	31	38	2	19	22
2.6	13	17	10.9	18	37	7.1	16	25	3	28	34
4.2	14	28	9.5	10	18	3.1	10	15	9	25	40
6.3	19	28	7.4	30	38	2.5	10	13	3	13	22
3.5	10	15	3.1	37	41	5.7	15	21	4.5	28	36
6.7	44	52	2	10	12	2.6	38	45	2.5	14	37
5.6	10	22	3.4	8	11	4.8	42	50	2	27	33
2.8	33	34	7.6	13	24	2.2	24	30	7	13	24
2	23	25	10.6	18	32	6.7	25	29	7	30	45
3.9	11	17	2.3	12	14	2.8	10	15	2	17	23
5.2	10	17	5.8	10	14	1.8	28	35	4	26	38
2.1	14	15	6.8	11	25	5.9	15	24	3	17	26
3.2	25	30	3	27	32	5.1	24	27	3	22	25
2.4	22	23	6	26	32	6.1	33	38	8	8	39
4.8	11	22	2.6	24	25	4.2	5	14	5	12	23
3.7	16	21	5.9	14	21	2	18	23	11	13	45
4.4	23	26	6.9	15	29	4.1	13	20	13	17	51
6.8	16	24	2.7	17	23	4.6	12	16	2	20	29
4.9	11	20	3.4	30	34	2.7	22	29	3.5	6	10
2.8	17	23	10.5	13	27	2.8	18	22	19	5	44
7.3	18	27	8	35	48	3.1	16	19	11	11	60
9.7	23	38	12	20	32	4.8	18	25	7	13	23
7.4	24	40	16.5	14	60	2.4	15	19	2	30	45
6.4	21	32	4.5	8	14	1.7	36	39	6	16	31
6.4	22	25	9.9	10	21	3.3	19	23	7	27	35
13.8	18	35	4.8	16	27	10.1	25	44	16	7	30
5.7	15	20	5.5	5	13	4.7	9	14	13	16	39
4	18	22	4.7	6	20	5.1	11	15	8	13	29
6.9	19	38	11.5	23	51	9.7	17	33	5	31	41
11.8	18	38	5.4	10	15	5.4	5	13	2	28	37
10.5	8	36	3.2	10	13	2	26	28	10	15	16
15.4	6	39	2	18	20	9.2	15	25	12	4	25
10.7	5	25	3	6	13	14.6	15	38	4	9	13
6.4	12	18	4.8	12	19	6.2	12	18	3	5	22
7.1	17	32	2.4	30	33	6	7	14	4	19	26
5	15	19	2	30	34	8.4	8	16	4	15	20
18.7	11	31	2.3	28	30	4.5	25	30	2.5	20	31
7.7	15	26	6.6	14	19	7.3	18	24	3	19	32
2.5	16	21	9.9	25	51	11.7	26	34	4.5	17	21
3.2	9	16	3.5	14	18	10.8	5	21	4	14	19
9.8	16	32	4.1	5	13	2.8	20	25	9	13	18
3.2	8	14	5.8	10	15	9.2	26	39	3	32	54
2	37	41	9.3	13	33	7.6	15	33	4	14	21
3	6	14	6.7	5	13	3.1	10	15	3	15	18
3	25	27	9.6	5	28	2	21	23	2	18	19
1.7	10	13	7.7	14	26	2.8	20	25	9	9	30
4	9	19	6.4	23	37	3	15	18	2	16	24
4.2	15	15	2.5	17	22	17.3	14	42	8	26	48
4	17	25	7.7	15	34	13.9	25	31	10	12	31
17	10	55	4.9	8	15	7.5	22	31	11	14	42
11.1	10	20	3.5	19	24	9.9	15	21	2.5	22	26
8.9	21	28	7.3	10	14	8.4	30	42	6	4	13
6.6	28	44	9.2	25	42	17.1	21	39	5	11	27
5.5	10	29	12.2	10	25	6.9	16	19	6	9	34
2.7	38	45	4.9	12	19	8.6	14	22	9	19	51
9.3	30	64	4.1	15	20	5.9	14	21	7	6	19
14.7	29	43	3.9	18	25	13	20	35	3	8	19
7.2	18	23	6.6	12	23	3.2	24	36	4	4	16
13.1	12	35	14.7	7	39	9.1	13	28	8	15	24

3.1	9	12	7.2	26	35	7	25	40	9.2	7	27
5	15	17	3.7	25	33	4.8	5	15	10	7	22
3.5	41	57	6.4	11	16	5.3	5	17	8	4	17
5.4	14	25	9.1	28	32	5.5	28	33	4	31	33
4.5	5	11	2.7	30	35	10.1	24	37	5	37	53
13.2	20	47	6.4	30	40	7	20	29	3	17	42
14.3	6	23	6.4	29	38	9.3	20	25	5	11	32
2.8	19	34	7.8	19	26	2.9	32	35	3	3	10
6.8	15	20	15.8	10	35	9.5	25	30	2.5	32	37
3	34	43	10.4	5	22	7.3	20	28	5	28	43
16.8	17	57	6.7	18	20	13.7	13	56	3	11	17
3.3	16	19	4.4	29	38	3.5	20	24	6	23	28
2.9	17	21	3.2	28	33	9.8	12	25	7	24	48
7.8	7	26	5.8	35	44	4.9	17	24	12	14	33
3.9	29	31	4.5	29	32	8.8	7	17	4	16	24
17.1	15	42	3.4	14	22	6.1	18	24	13	21	41
7.4	48	57	5.2	26	28	5.7	4	13	4	17	28
2.9	10	19	2.2	12	15	9.5	10	20	16	26	53
2.9	35	50	3.9	26	34	6	10	22	15.5	8	47
									14	14	32

GCKMT2			GCKMT2 (cont.)			GCKMT2 (cont.)			OCKMT3		
Length (m)	**Width 1 (cm)**	**width 2 (cm)**	**Length (m)**	**Width 1 (cm)**	**width 2 (cm)**	**Length (m)**	**Width 1 (cm)**	**width 2 (cm)**	**Length (m)**	**Width 1 (cm)**	**width 2 (cm)**
4.5	59	72	3.8	11	16	2.5	15	24	2.1	14	16
2.5	56	61	15.9	19	58	10.3	8	14	2.4	10	12
3	58	65	9.6	13	18	10.4	6	12	1.3	9	12
1.4	23	26	7.7	12	20	9.8	55	72	15.1	8	18
3.8	39	44	2	40	43	2.4	18	20	14.8	25	37
2.2	38	41	3.4	15	22	2.1	8	13	13.5	12	36
1.8	16	19	2	58	76	2.3	9	12	5	17	25
1.4	10	13	2.2	10	12	2.5	12	16	13.3	11	37
4.2	6	21	3.3	48	62	1.8	10	13	4.1	19	26
4.6	13	23	2.4	31	34	6.8	32	14	12.7	20	51
3.5	9	14	5.9	13	21	11	14	55	2.5	10	13
3.8	30	39	12.4	11	26	2.5	15	20	7.3	26	38
3.1	12	15	11.6	12	34	7.5	10	30	9.4	12	20
1.9	12	15	1.3	24	26	2	10	10	4.1	20	41
7.2	27	59	1.1	27	48	3	15	20	3.2	10	14
1.2	25	28	8.1	38	67	11	15	20	12.6	18	36
1.9	15	18	3.8	16	25	14	10	35	11	15	31
3.2	40	54	1.5	8	10	10.5	70	25	8.5	5	18
3.1	24	30	4	8	17	11.5	30	50	8.8	7	20
6.1	27	32	2.5	25	32	8.5	12	25	2.2	36	38
1.9	6	11	13.2	22	95	13	20	60	3.7	15	20
5.5	11	24	3.5	14	11	1	20	20	7.1	16	21
5.3	5	13	1.2	10	10	8	5	25	8.7	25	25
1	13	17	2.8	14	22	9	20	20	2	34	34
4.3	6	13	1.1	6	11	7	10	15	9.4	18	18
2.3	11	14	1.4	31	39	6	10	15	2	40	40
2.7	10	16	11.6	21	32	4.5	15	25	3.5	18	18
1	10	11	1	15	32	2	10	10	11	12	12
1.3	7	11	2.7	38	55	9.5	15	25	6	9	9
7	4	18	2.5	10	44	11.5	5	25	4.2	20	20
2.1	8	11	2.3	12	18	10	25	35	2.8	13	13
2	28	31	11.2	11	28	2	15	20	10	7	7
12.5	16	48	12	8	25	1.5	10	15	7.7	19	19
9.8	14	47	3.2	38	45	9	10	20	2.1	10	10
7.8	12	29	4	6	22	2	40	55	5.2	10	10
21.9	4	48	1.8	34	38	5	15	30	7.8	12	12
27.3	13	50	10.5	18	43	7.5	5	25	5.1	23	23
17.3	8	52	4.5	14	28	2.5	20	35	6.6	13	13
1.8	34	36	2.8	35	16	6	55	65	10.2	20	20
13.3	15	57	1.6	10	11	4.5	10	20	7.6	10	10

7.8	17	24	21.6	8	74	5	10	15	11.5	23	23
1.2	12	15	8.3	11	32	2	10	10	7.6	18	18
11.7	12	42	10.3	12	41	10	35	50	6.7	25	25
2	12	16	8.9	13	28	14	25	40	7.8	12	12
2.8	10	13	3.2	16	33	4	40	55	2.2	13	13
2.6	2.7	30	7.3	8	19	9	55	60	6.8	8	20
1	12	20	3.7	6	11	11	10	25	6.6	7	17
2.4	53	89	2.4	33	41	11	5	20	7	8	13
3.1	8	14	4.6	13	24	1.5	20	20	8	16	21
3.3	7	11	12.5	17	35	3.5	25	35	4.5	20	24
2.3	11	12	16.7	10	84	2	40	40	3	12	16
3.5	11	16	2.4	1	10	3.5	5	20	5	20	24
4	54	67	12.3	14	61	1.5	25	30	4	25	30
2.1	31	38	2.6	10	12	2.5	10	10	1	16	18
1	17	26	1.2	10	5	15	45	5	8.5	14	20
2.8	65	82	1	31	46	3.5	5	15	7.4	12	16
12.2	23	50	1.4	11	18	4	40	50	5.5	10	17
1.6	26	31	1.8	4	10	17	10	35	3.5	7	13
2.2	10	12	8.1	5	14	3	5	15	10.9	18	34
4.6	22	34	11.4	22	68	8	15	20	6.5	5	18
4.4	5	10	5.1	35	44				12.5	20	36
4.7	10	19	6.3	11	41				3	13	16
9.7	8	42	1.3	69	66				2.3	5	10
10.1	27	58	3.5	51	38				9.6	18	30
3.7	42	49	1.8	13	24				5.9	15	20
4.8	21	60	1.1	18	22				4	7	13
3.1	18	32	3.1	35	64				4.1	14	20
1.8	20	34	3.4	10	15				6.5	30	40
1.4	8	14	3.6	12	14				10.6	18	25
1.5	10	28	1.2	18	21				5.9	15	22
5.8	17	36	3.8	14	23				9.5	13	25
2.1	25	28	4.1	11	25				10	8	16
3.7	21	36	12.5	8	45				2.3	12	15
1.8	18	27	1.3	10	12				2	7	10
4.7	12	21	1.3	14	22				4	7	14
8.6	8	26	2.5	10	16				8.1	16	32
13.4	4	20	3.8	8	14				3.2	15	20
2.8	11	27	2.1	12	32				8.3	23	31
1.9	23	30	3.5	14	27				12	14	52
2.3	9	12	4.4	20	21						

7.2 Appendix B. Litter, humus, and soil data

Table 7.3. Litter and humus bulk density data

Sample ID	Depth (cm)	Depth (m)	Dry weight (g)	Burned weight (g)	Volume (cm^3)	Density (g cm^{-3})
AB1S1.0	13	0.13	24.14	3.94	251.00	0.09617687
AB1S10.0L	25	0.25	30.31	9.81	418.33	0.072455367
AB1S11.0L	20	0.2	73.37	43.25	501.99	0.146157766
AB1S12.0L	57	0.57	28.77	8.52	669.32	0.04298377
AB1S2.0R	44	0.44	39.85	23.43	334.66	0.11907565
AB1S3.0R	30	0.3	51.67	34.23	334.66	0.154394952
AB1S4.0	28	0.28	48.67	24.59	292.83	0.166206471
AB1S5.0	122	1.22	38.66	17.03	251.00	0.15402642
AB1S6.0L	60	0.6	32.05	12.09	334.66	0.095768497
AB1S7.0L	9	0.09	68.88	45.94	376.49	0.182951196
AB1S8.0L	70	0.7	36.45	4.12	460.16	0.079211725
AB1S9.0L	55	0.55	46.1	11.86	501.99	0.091834169
AB2S1.0R	29	0.29	28.28	6.62	209.16	0.135205396
AB2S10.0R	6	0.06	63.23	53.61	167.33	0.377874698
AB2S11.0i	40	0.4	30.61	6.33	292.83	0.104532157
AB2S13.0	32	0.32	29.32	9.66	334.66	0.087610993
AB2S2.0R	2	0.02	29.54	9.58	501.99	0.058845583
AB2S3.0R	33	0.33	29.78	11.43	501.99	0.059323678
AB2S4.0	33	0.33	28.92	4.34	543.82	0.053178926
AB2S5.0i	44	0.44	32.35	14.06	334.66	0.096664926
AB2S6.0R	48	0.48	20.88	6.14	376.49	0.055459073
AB2S7.0R	46	0.46	18.86	1.74	292.83	0.064406288
AB2S8.0	23	0.23	26	17.14	585.66	0.044394578
AB2S9.0	21	0.21	55.65	30.83	334.66	0.166287577
AB4S1.0R	50	0.5	9.41	6.82	41.83	0.224943913
AB4S10.0	98	0.98	92.71	55.33	418.33	0.22162115
AB4S11.0	112	1.12	76.97	51.61	292.83	0.262850053
AB4S2.0	59	0.59	5.14	3.36	41.83	0.122870533
AB4S3.0	28	0.28	2.18	0.84	41.83	0.052112405
AB4S4.0	34	0.34	94.36	74.49	167.33	0.563913594
AB4S5.0	57	0.57	33.48	17.9	167.33	0.20008295
AB4S6.0	85	0.85	38.25	23.85	167.33	0.228589391
AB4S7.0	30	0.3	40.52	17.85	209.16	0.19372428
AB4S8.0	112	1.12	34.67	14.42	167.33	0.20719462
AB4S9.0	132	1.32	41.04	16.21	209.16	0.196210376
AB5S1.0	65	0.65	80.34	72.94	167.33	0.480127365
AB5S10.0R	91	0.91	25.81	21.22	83.67	0.308491095
AB5S2.0	80	0.8	92.27	78.5	209.16	0.44113868
AB5S4.0	27	0.27	28.66	22.98	83.67	0.342555396
AB5S5.0R	114	1.14	41.09	29.16	209.16	0.196449424
AB5S6.0	57	0.57	32.49	24.48	125.50	0.258888691
AB5S7.0	41	0.41	30.64	22.86	83.67	0.366221122
AB5S8.0R	48	0.48	51.48	41.19	83.67	0.615308856

AB5S9.0	68	0.68	67.26	56.75	209.16	0.321567006
AB6S1.0	52	0.52	7.82	7	41.83	0.186935324
AB6S10.0	46	0.46	3.28	2.5	41.83	0.078407655
AB6S11.0	110	1.1	9.36	6.21	41.83	0.223748675
AB6S2.0	59	0.59	5.5	4.68	41.83	0.131476251
AB6S4.0	26	0.26	38.67	36.38	41.83	0.92439757
AB6S6.0	55	0.55	15.47	13.6	83.67	0.184903419
AB6S8.0	52	0.52	30.45	25.21	41.83	0.727900336
AB6S9.0	32	0.32	5.83	4.89	41.83	0.139364826
CF2S1.0L	15	0.15	95.79	61.12	418.33	0.22898382
CF2S10.0L	24	0.24	176.86	159.93	334.66	0.528474768
CF2S10.0R	24	0.24	68.17	48.03	460.16	0.148144397
CF2S11.0R	18	0.18	54.89	19.68	543.82	0.100933307
CF2S2.0	31	0.31	32.78	20.25	334.66	0.097949807
CF2S3.0L	15	0.15	114.18	91.83	292.83	0.389920996
CF2S4.0L	26	0.26	65.49	51.06	376.49	0.173947064
CF2S5.0	51	0.51	174.38	144.74	334.66	0.521064288
CF2S6.0R	23	0.23	47.01	26.95	501.99	0.093646948
CF2S7.0R	6	0.06	30.37	12.24	251.00	0.120997992
CF2S8.0R	26	0.26	33.34	15.04	418.33	0.079698513
CF2S9.0R	6	0.06	77.83	48.16	251.00	0.310084746
CF3S1.0L	25	0.25	16.14	1.93	167.33	0.096455759
CF3S1.1L	25	0.25	20.15	1.8	627.49	0.032112078
CF3S2.0L	15	0.15	56.74	35.22	334.66	0.169544602
CF3S3.0L	17	0.17	51.77	42.26	251.00	0.206258349
CF3S4.0L	8	0.08	78.76	58.01	334.66	0.23534249
CF3S5.0R	8	0.08	71.13	61.3	209.16	0.3400693
CF3S6.0R	54	0.54	55.02	34.33	251.00	0.219206768
CF4S1.0	14	0.14	62.45	21.24	585.66	0.106632362
CF4S10.0R	6	0.06	79.44	66.69	251.00	0.316499194
CF4S11.0R	32	0.32	41.04	18.91	376.49	0.109005765
CF4S2.0	8	0.08	18.36	2.27	334.66	0.054861454
CF4S3.0R	34	0.34	54.69	35.44	334.66	0.163419004
CF4S4.0R	16	0.16	24.56	5.02	418.33	0.058710122
CF4S5.0R	46	0.46	22.78	5.73	418.33	0.054455073
CF4S6.0R	36	0.36	25.85	4.95	543.82	0.047533722
CF4S7.0R	36	0.36	59.36	38.6	334.66	0.177373415
CF4S8.0R	17	0.17	119.23	97.19	376.49	0.31668512
CF4S9.0R	47	0.47	65.58	38.02	334.66	0.195959376
CF5S1.0R	6	0.06	165.62	153.39	251.00	0.659851416
CF5S10.0	18	0.18	56.77	53.97	125.50	0.452357987
CF5S11L	12	0.12	21.81	17.81	83.67	0.260681549
CF5S2.0R	51	0.51	112.81	93.49	209.16	0.539339487
CF5S3.0R	4	0.04	133.14	110.84	167.33	0.795670368
CF5S4.0R	58	0.58	74.14	62.2	209.16	0.354459973
CF5S5.0R	61	0.61	38.13	32.83	167.33	0.227872248
CF5S6.0	58	0.58	70.51	60.12	209.16	0.337105108
CF5S7.0R	18	0.18	56.26	43.83	209.16	0.268976505
CF5S8.0L	3	0.03	59.75	51.48	125.50	0.476103395

CF5S9.0L	15	0.15	50.88	39.26	209.16	0.24325497
CF7S1.0	22	0.22	61.31	47.87	251.00	0.244266938
CF7S10	9	0.09	7.34	1.98	41.83	0.175461033
CF7S2.0	12	0.12	51.35	44.01	167.33	0.306877523
CF7S3.0	21	0.21	80.96	65.41	209.16	0.387066084
CF7S4.0	79	0.79	43.09	20.55	209.16	0.206011333
CF7S5.0	7	0.07	42.69	29.03	292.83	0.145784965
CF7S6.0L	43	0.43	30.51	16.19	167.33	0.182333656
CF7S6.0R	19	0.19	39.87	10.67	209.16	0.190616659
CF7S7.0	32	0.32	40.35	24.2	334.66	0.120569699
CF7S8.0	20	0.2	38.63	25.41	167.33	0.230860345
CF7S9.0	32	0.32	30.11	3.27	334.66	0.089971589
CF7S9.1	32	0.32	36.73	15.08	1003.98	0.036584263
MT2S2.0	19		81.19	68.63	794.82	0.102148869
MT2S1.0	49	0.49	40.28	23.71	209.16	0.192576851
MT2S3.0		0	37.22	21.04	83.67	0.444867825
MT2S4.0	220	2.2	32.76	8.92	627.49	0.052208024
MT2S5.0	24	0.24	79.74	55.92	376.49	0.211796288
MT2S7.0	32	0.32	15.7	4.62	251.00	0.062550823
MT2S8.0	26	0.26	71.56	14.21	627.49	0.114041703
MT2S9.0	6	0.06	2.14	1.4	41.83	0.051156214
MT3S1.0	11	0.11	68.63	4.84	125.50	0.546861522
MT3S10.0	40	0.4	73.74	60.41	543.82	0.135595227
MT3S11.0	33	0.33	36.16	11.14	543.82	0.066492045
MT3S2.0	36	0.36	12.49	5.21	209.16	0.059714123
MT3S3.0	36	0.36	46	20.8	585.66	0.078544254
MT3S4.0	38	0.38	13.71	2.17	1045.82	0.013109377
MT3S5.0	20	0.2	35.8	25.07	251.00	0.142631812
MT3S6.0	30	0.3	13.73	3.37	292.83	0.046887505
MT3S7.0	35	0.35	77.92	41.16	711.16	0.10956823
MT3S8.0	41	0.41	48.35	23.57	669.32	0.072237236
MT3S9.0	27	0.27	38.57	8.57	627.49	0.06146714
PC2S1.0	55	0.55	39.25	15.7	543.82	0.072174026
PC2S10.0L	5	0.05	65.46	55.75	209.16	0.312961287
PC2S11.0L	9	0.09	79.01	66.09	251.00	0.314786018
PC2S12.0R	8	0.08	215.26	196.51	334.66	0.643217678
PC2S2.0L	30	0.3	44.16	10.74	627.49	0.070375652
PC2S3.0	29	0.29	45.11	19.21	585.66	0.077024593
PC2S4.0L	12	0.12	13.05	6.68	251.00	0.051992881
PC2S5.0L	17	0.17	39.29	25.05	292.83	0.134174076
PC2S6.0L	19	0.19	21.42	10.9	251.00	0.085340039
PC2S7.0L	18	0.18	70.48	47.81	292.83	0.240686914
PC2S8.0L	7	0.07	89.94	55.36	292.83	0.307142183
PC2S9.0L	6	0.06	65.39	42.76	251.00	0.260522184
PC3S1.0R	20	0.2	128.61	103.4	292.83	0.439198978
PC3S11.0L	11	0.11	129.01	114.23	292.83	0.440564965
PC3S12.0L	20	0.2	81.95	57.77	334.66	0.244874518
PC3S13.0L	17	0.17	140.02	123.63	251.00	0.557857718
PC3S14.0L	49	0.49	86.31	63.09	376.49	0.229246773

PC3S2.0R	17	0.17	50.42	27.76	418.33	0.120527865
PC3S4.0R	20	0.2	78.31	55.97	334.66	0.233997846
PC3S5.0R	40	0.4	28.53	12.46	418.33	0.068200317
PC3S6.0R	36	0.36	99.41	82.56	376.49	0.264041498
PC3S7.0R	18	0.18	20.29	1.9	209.16	0.097005569
PC3S8.0R	11	0.11	143.85	120.17	334.66	0.429837699
PC3S9.0R	15	0.15	81.67	67.98	167.33	0.488075702
PC4S1.0R	35	0.35	51.3	27.09	292.83	0.175187836
PC4S10.0L	23	0.23	41.12	13.84	376.49	0.109218252
PC4S11.0L	17	0.17	61.38	43.1	292.83	0.209610709
PC4S2.0R	32	0.32	29.49	4.47	292.83	0.100707393
PC4S3.0L	57	0.57	17.9	6.7	209.16	0.085579087
PC4S4.0L	25	0.25	54.81	24.05	418.33	0.131022061
PC4S5.0L	4	0.04	83.32	53.78	167.33	0.49793642
PC4S6.0	58	0.58	49.22	18.41	460.16	0.106962993
PC4S7.0L	40	0.4	23.97	8.38	251.00	0.095499568
PC4S8.0L	24	0.24	43.25	11.43	460.16	0.093989221
PC4S9.0L	40	0.4	45.66	9.35	418.33	0.109149193
PC6S1.0R	54	0.54	11.85	3.55	209.16	0.056654312
PC6S10.0	60	0.6	7.89	1.2	83.67	0.094304329
PC6S11.0L	73	0.73	13.04	2.84	209.16	0.062343648
PC6S2.0R	60	0.6	2.95	0.45	83.67	0.03525954
PC6S3.0	29	0.29	5.58	0.57	83.67	0.066694317
PC6S4.0R	48	0.48	7.04	1.32	125.50	0.056096534
PC6S5.0R	66	0.66	10.18	1.02	251.00	0.040558431
PC6S6.0R	7	0.07	8.83	3.06	83.67	0.105539573
PC6S8.0	88	0.88	11.16	1.16	83.67	0.133388633
PC6S9.0	52	0.52	5.22	1.14	83.67	0.062391457
PC7S1.0	40	0.4	228.14	194.21	418.33	0.54536349
PC7S11.0L	13	0.13	306.8	244.97	543.82	0.564152642
PC7S2.0	40	0.4	104.8	80.44	418.33	0.25052202
PC7S5.0		0	170.93	139.22	418.33	0.408604284
PC7S6.0L	60	0.6	93.52	79.26	125.50	0.745191455
PC7S7.0		0	57.9	29.53	334.66	0.173010794
UC1S1.0R	10	0.1	44.55	35.42	83.67	0.532478817
UC1S10.0	57	0.57	15.2	3.51	125.50	0.121117516
UC1S11.0L	31	0.31	50.09	40.78	125.50	0.399130026
UC1S2.0R	12	0.12	24.25	14.27	41.83	0.579690744
UC1S3.0R	54	0.54	21.2	5.27	125.50	0.168927062
UC1S4.0R	31	0.31	13.13	0.89	334.66	0.039233709
UC1S5.0R	21	0.21	24.97	2.07	292.83	0.08527174
UC1S6.0	24	0.24	15.83	8.72	83.67	0.189206278
UC1S7.0R	0	0	17.49	2.32	125.50	0.139364826
UC1S8.0	23	0.23	14.88	6.06	209.16	0.071140604
UC1S9.0R	12	0.12	13.92	5.95	83.67	0.16637722
UC2S1.0R	29	0.29	18.62	2.35	209.16	0.089021374
UC2S10.0L	57	0.57	18.33	5.08	334.66	0.054771811
UC2S11.0	27	0.27	11.91	1.06	501.99	0.023725487
UC2S2.0	16	0.16	17.36	2.88	209.16	0.082997372

UC2S3.0R	0	0	14.52	4.95	167.33	0.086774326
UC2S4.0L	37	0.37	9.65	4.4	125.50	0.076893686
UC2S5.0L	18	0.18	14.04	3.18	125.50	0.111874337
UC2S6.0L	48	0.48	10.53	4.01	125.50	0.083905753
UC2S7.0L	35	0.35	44.03	1.05	376.49	0.116947461
UC2S8.0L	47	0.47	12.21	4.26	125.50	0.097292426
UC2S9.0L	34	0.34	7.21	1.09	167.33	0.043088353
UC3S11.0	72	0.72	96.85	42.25	627.49	0.154345151
UC3S2.0	68	0.68	41.39	13.06	334.66	0.123677319
UC3S3.0	92	0.92	30.79	15.07	334.66	0.092003495
UC3S4.0	17	0.17	38.47	10.25	292.83	0.131373802
UC3S5.0	8	0.08	29.25	5.05	292.83	0.099887801
UC3S6.0	98	0.98	21.29	6.44	167.33	0.127233154
UC3S7.0	76	0.76	42.58	8.16	501.99	0.084822103
UC3S8.0	71	0.71	38.74	14.82	251.00	0.154345151
UC3S9.0	74	0.74	37.43	18.57	334.66	0.111844456

DUFF can	
diameter	7.3
radius	3.65
height	10.7
Volume of can (cm3)	447.8363813

Min	0.013109377
Median	0.144208389
Max	0.92439757
Mean	0.204053655
Standard deviation	0.169018508

Table 7.4. Organic carbon content (%) of litter and humus.

Sample ID	Max depth (cm)	Dry weight (g)	Burned weight (g)	Organic matter (g)	Carbon (g)	Organic Carbon (%)
AB1S1.0	6	24.14	3.94	20.20	10.10	41.84
AB1S10.0L	10	30.31	9.81	20.50	10.25	33.82
AB1S11.0L	12	73.37	43.25	30.12	15.06	20.53
AB1S12.0L	16	28.77	8.52	20.25	10.13	35.19
AB1S2.0R	8	39.85	23.43	16.42	8.21	20.60
AB1S3.0R	8	51.67	34.23	17.44	8.72	16.88
AB1S4.0	7	48.67	24.59	24.08	12.04	24.74
AB1S5.0	6	38.66	17.03	21.63	10.82	27.97
AB1S6.0L	8	32.05	12.09	19.96	9.98	31.14
AB1S7.0L	9	68.88	45.94	22.94	11.47	16.65
AB1S8.0L	11	36.45	4.12	32.33	16.17	44.35
AB1S9.0L	12	46.10	11.86	34.24	17.12	37.14
AB2S1.0R	5	28.28	6.62	21.66	10.83	38.30
AB2S10.0R	4	63.23	53.61	9.62	4.81	7.61
AB2S11.0i	7	30.61	6.33	24.28	12.14	39.66
AB2S13.0	8	29.32	9.66	19.66	9.83	33.53
AB2S2.0R	12	29.54	9.58	19.96	9.98	33.78
AB2S3.0R	12	29.78	11.43	18.35	9.18	30.81
AB2S4.0	13	28.92	4.34	24.58	12.29	42.50
AB2S5.0i	8	32.35	14.06	18.29	9.15	28.27
AB2S6.0R	9	20.88	6.14	14.74	7.37	35.30
AB2S7.0R	7	18.86	1.74	17.12	8.56	45.39
AB2S8.0	14	26.00	17.14	8.86	4.43	17.04
AB2S9.0	8	55.65	30.83	24.82	12.41	22.30
AB4S1.0R	1	9.41	6.82	2.59	1.30	13.76
AB4S10.0	10	92.71	55.33	37.38	18.69	20.16
AB4S11.0	7	76.97	51.61	25.36	12.68	16.47
AB4S2.0	1	5.14	3.36	1.78	0.89	17.32
AB4S3.0	1	2.18	0.84	1.34	0.67	30.73
AB4S4.0	4	94.36	74.49	19.87	9.94	10.53
AB4S5.0	4	33.48	17.90	15.58	7.79	23.27
AB4S6.0	4	38.25	23.85	14.40	7.20	18.82
AB4S7.0	5	40.52	17.85	22.67	11.34	27.97
AB4S8.0	4	34.67	14.42	20.25	10.13	29.20
AB4S9.0	5	41.04	16.21	24.83	12.42	30.25
AB5S1.0	4	80.34	72.94	7.40	3.70	4.61
AB5S10.0R	2	25.81	21.22	4.59	2.30	8.89
AB5S2.0	5	92.27	78.50	13.77	6.89	7.46
AB5S4.0	2	28.66	22.98	5.68	2.84	9.91
AB5S5.0R	5	41.09	29.16	11.93	5.97	14.52
AB5S6.0	3	32.49	24.48	8.01	4.01	12.33
AB5S7.0	2	30.64	22.86	7.78	3.89	12.70
AB5S8.0R	2	51.48	41.19	10.29	5.15	9.99
AB5S9.0	5	67.26	56.75	10.51	5.26	7.81

AB6S1.0	1	7.82	7.00	0.82	0.41	5.24
AB6S10.0	1	3.28	2.50	0.78	0.39	11.89
AB6S11.0	1	9.36	6.21	3.15	1.58	16.83
AB6S2.0	1	5.50	4.68	0.82	0.41	7.45
AB6S4.0	1	38.67	36.38	2.29	1.15	2.96
AB6S6.0	2	15.47	13.60	1.87	0.94	6.04
AB6S8.0	1	30.45	25.21	5.24	2.62	8.60
AB6S9.0	1	5.83	4.89	0.94	0.47	8.06
CF1S1.0L	10	55.61	36.64	18.97	9.49	17.06
CF1S2.0L	9	253.03	219.21	33.82	16.91	6.68
CF1S3.0	6	79.12	64.03	15.09	7.55	9.54
CF1S5.0L	12	80.39	60.60	19.79	9.90	12.31
CF1S1.0R	12	211.07	125.29	85.78	42.89	20.32
CF1S10.0R	6	222.20	171.07	51.13	25.57	11.51
CF1S11.0R	13	138.87	98.69	40.18	20.09	14.47
CF1S2.0R	9	207.46	141.03	66.43	33.22	16.01
CF1S3.0R	18	220.70	106.72	113.98	56.99	25.82
CF1S4.0R	8	152.64	124.67	27.97	13.99	9.16
CF1S5.0R	7	335.05	302.62	32.43	16.22	4.84
CF1S6.0R	8	267.61	204.93	62.68	31.34	11.71
CF1S7.0R	4	116.93	99.53	17.40	8.70	7.44
CF1S8.0R	7	272.61	211.65	60.96	30.48	11.18
CF1S9.0R	8	168.61	126.96	41.65	20.83	12.35
CF1S4.0L	6	97.79	73.23	24.56	12.28	12.56
CF2S1.0L	10	95.79	61.12	34.67	17.34	18.10
CF2S10.0L	8	176.86	159.93	16.93	8.47	4.79
CF2S10.0R	11	68.17	48.03	20.14	10.07	14.77
CF2S11.0R	13	54.89	19.68	35.21	17.61	32.07
CF2S2.0	8	32.78	20.25	12.53	6.27	19.11
CF2S3.0L	7	114.18	91.83	22.35	11.18	9.79
CF2S4.0L	9	65.49	51.06	14.43	7.22	11.02
CF2S5.0	8	174.38	144.74	29.64	14.82	8.50
CF2S6.0R	12	47.01	26.95	20.06	10.03	21.34
CF2S7.0R	6	30.37	12.24	18.13	9.07	29.85
CF2S8.0R	10	33.34	15.04	18.30	9.15	27.44
CF2S9.0R	6	77.83	48.16	29.67	14.84	19.06
CF3S1.0L	4	16.14	1.93	14.21	7.11	44.02
CF3S1.1L	19	20.15	1.80	18.35	9.18	45.53
CF3S2.0L	8	56.74	35.22	21.52	10.76	18.96
CF3S3.0L	6	51.77	42.26	9.51	4.76	9.18
CF3S4.0L	8	78.76	58.01	20.75	10.38	13.17
CF3S5.0R	5	71.13	61.30	9.83	4.92	6.91
CF3S6.0R	6	55.02	34.33	20.69	10.35	18.80
CF4S1.0	14	62.45	21.24	41.21	20.61	32.99
CF4S10.0R	6	79.44	66.69	12.75	6.38	8.02
CF4S11.0R	9	41.04	18.91	22.13	11.07	26.96
CF4S2.0	8	18.36	2.27	16.09	8.05	43.82
CF4S3.0R	8	54.69	35.44	19.25	9.63	17.60
CF4S4.0R	10	24.56	5.02	19.54	9.77	0.40

CF4S5.0R	10	22.78	5.73	17.05	8.53	37.42
CF4S6.0R	13	25.85	4.95	20.90	10.45	40.43
CF4S7.0R	8	59.36	38.60	20.76	10.38	17.49
CF4S8.0R	9	119.23	97.19	22.04	11.02	9.24
CF4S9.0R	8	65.58	38.02	27.56	13.78	21.01
CF5S1.0R	6	165.62	153.39	12.23	6.12	3.69
CF5S10.0	3	56.77	53.97	2.80	1.40	2.47
CF5S11L	2	21.81	17.81	4.00	2.00	9.17
CF5S2.0R	5	112.81	93.49	19.32	9.66	8.56
CF5S3.0R	4	133.14	110.84	22.30	11.15	8.37
CF5S4.0R	5	74.14	62.20	11.94	5.97	8.05
CF5S5.0R	4	38.13	32.83	5.30	2.65	6.95
CF5S6.0	5	70.51	60.12	10.39	5.20	7.37
CF5S7.0R	5	56.26	43.83	12.43	6.22	11.05
CF5S8.0L	3	59.75	51.48	8.27	4.14	6.92
CF5S9.0L	5	50.88	39.26	11.62	5.81	11.42
CF7S1.0	6	61.31	47.87	13.44	6.72	0.11
CF7S10	1	7.34	1.98	5.36	2.68	36.51
CF7S2.0	4	51.35	44.01	7.34	3.67	7.15
CF7S3.0	5	80.96	65.41	15.55	7.78	9.60
CF7S4.0	5	43.09	20.55	22.54	11.27	26.15
CF7S5.0	7	42.69	29.03	13.66	6.83	16.00
CF7S6.0L	4	30.51	16.19	14.32	7.16	23.47
CF7S6.0R	5	39.87	10.67	29.20	14.60	36.62
CF7S7.0	8	40.35	24.20	16.15	8.08	20.01
CF7S8.0	4	38.63	25.41	13.22	6.61	17.11
CF7S9.0	8	30.11	3.27	26.84	13.42	44.57
CF7S9.1	32	36.73	15.08	21.65	10.83	29.47
MT1S1.0	10	29.15	11.83	17.32	8.66	0.30
MT1S2.0	3	30.15	23.79	6.36	3.18	0.11
MT1S3.0	3	59.11	40.14	18.97	9.49	0.16
MT1S4.0	27	149.30	46.42	102.88	51.44	0.34
MT1S4T5	13	212.47	163.09	49.38	24.69	0.12
MT1S5.0	10	27.67	10.57	17.10	8.55	0.31
MT1S6.0	12	99.78	90.13	9.65	4.83	0.05
MT1S7.0	10	43.80	17.53	26.27	13.14	0.30
MT1S8.0	13	65.97	31.81	34.16	17.08	0.15
MT1S10	10	91.16	61.07	30.09	15.05	0.17
MT1S11.0	15	47.32	19.46	27.86	13.93	0.29
MT1S12.0	9	65.35	26.51	38.84	19.42	0.30
MT1S9.0	14	41.51	13.47	28.04	14.02	0.34
MT1S14.0	14	60.09	19.95	40.14	20.07	0.33
MT1S15.0	10	37.51	16.25	21.26	10.63	0.28
MT1S16.0	17	74.60	45.50	29.10	14.55	0.20
MT1S17	5	74.56	28.10	46.46	23.23	0.31
MT1S18.0	10	41.94	12.85	29.09	14.55	0.35
MT1S19.0	10	43.58	23.98	19.60	9.80	0.22
MT1S20.0	8	37.95	19.00	18.95	9.48	0.25
MT1S21.0	16	67.61	38.86	28.75	14.38	0.21

MT1S22.0	12	66.59	26.15	40.44	20.22	0.30
MT1S23.0	15	54.17	24.08	30.09	15.05	0.28
MT1S24.0	11	99.58	65.92	33.66	16.83	0.17
MT1S25.0	4	45.12	27.33	17.79	8.90	0.20
MT1S26.0	14	53.91	11.85	42.06	21.03	0.39
MT1S34.0	12	29.80	8.14	21.66	10.83	0.36
MT1S28.0	5	22.25	7.27	14.98	7.49	0.34
MT1SS29	18	71.20	28.44	42.76	21.38	0.30
MT1S31.0	7	42.93	16.58	26.35	13.18	0.31
MT1S32.0	8	37.09	20.94	16.15	8.08	0.22
MT1S33	19	67.18	38.57	28.61	14.31	0.21
MT2S2.0	19	81.19	68.63	12.56	6.28	0.08
MT2S1.0	5	40.28	23.71	16.57	8.29	20.57
MT2S3.0	2	37.22	21.04	16.18	8.09	21.74
MT2S4.0	15	32.76	8.92	23.84	11.92	36.39
MT2S5.0	9	79.74	55.92	23.82	11.91	14.94
MT2S7.0	6	15.70	4.62	11.08	5.54	35.29
MT2S8.0	15	71.56	14.21	57.35	28.68	40.07
MT2S9.0	1	2.14	1.40	0.74	0.37	17.29
MT3S1.0	3	68.63	4.84	63.79	31.90	46.47
MT3S10.0	13	73.74	60.41	13.33	6.67	9.04
MT3S11.0	13	36.16	11.14	25.02	12.51	34.60
MT3S2.0	5	12.49	5.21	7.28	3.64	29.14
MT3S3.0	14	46.00	20.80	25.20	12.60	27.39
MT3S4.0	25	13.71	2.17	11.54	5.77	42.09
MT3S5.0	6	35.80	25.07	10.73	5.37	14.99
MT3S6.0	7	13.73	3.37	10.36	5.18	37.73
MT3S7.0	17	77.92	41.16	36.76	18.38	23.59
MT3S8.0	16	48.35	23.57	24.78	12.39	25.63
MT3S9.0	15	38.57	8.57	30.00	15.00	38.89
PC1S1.0L	11	338.75	280.14	58.61	29.31	8.65
PC1S2.0L	12	107.18	84.94	22.24	11.12	10.38
PC1S3.0L	9	124.90	95.21	29.69	14.85	11.89
PC1S4.0L	1	4.05	0.89	3.16	1.58	39.01
PC1S6.0L	9	216.55	189.33	27.22	13.61	6.28
PC1S7.0L	7	220.17	192.89	27.28	13.64	6.20
PC1S8.0L	9	168.73	145.76	22.97	11.49	6.81
PC1S9.0L	3	69.62	63.07	6.55	3.28	4.70
PC1S1.0	7	128.20	86.70	41.50	20.75	16.19
PC1S2.0R	6	150.25	123.81	26.44	13.22	8.80
PC1S4.0R	3	69.58	61.71	7.87	3.94	5.66
PC1S5.0R	6	150.03	125.07	24.96	12.48	8.32
PC1S6.0R	7	148.14	125.43	22.71	11.36	7.67
PC1S7.0R	7	232.54	197.04	35.50	17.75	7.63
PC2S1.0	13	39.25	15.70	23.55	11.78	30.00
PC2S10.0L	5	65.46	55.75	9.71	4.86	7.42
PC2S11.0L	6	79.01	66.09	12.92	6.46	8.18
PC2S12.0R	8	215.26	196.51	18.75	9.38	4.36
PC2S2.0L	15	44.16	10.74	33.42	16.71	37.84

PC2S3.0	14	45.11	19.21	25.90	12.95	28.71
PC2S4.0L	6	13.05	6.68	6.37	3.19	24.41
PC2S5.0L	7	39.29	25.05	14.24	7.12	18.12
PC2S6.0L	6	21.42	10.90	10.52	5.26	24.56
PC2S7.0L	7	70.48	47.81	22.67	11.34	16.08
PC2S8.0L	7	89.94	55.36	34.58	17.29	19.22
PC2S9.0L	6	65.39	42.76	22.63	11.32	17.30
PC3S1.0R	7	128.61	103.40	25.21	12.61	9.80
PC3S11.0L	7	129.01	114.23	14.78	7.39	5.73
PC3S12.0L	8	81.95	57.77	24.18	12.09	14.75
PC3S13.0L	6	140.02	123.63	16.39	8.20	5.85
PC3S14.0L	9	86.31	63.09	23.22	11.61	13.45
PC3S2.0R	10	50.42	27.76	22.66	11.33	22.47
PC3S4.0R	8	78.31	55.97	22.34	11.17	14.26
PC3S5.0R	10	28.53	12.46	16.07	8.04	28.16
PC3S6.0R	9	99.41	82.56	16.85	8.43	8.48
PC3S7.0R	5	20.29	1.90	18.39	9.20	45.32
PC3S8.0R	8	143.85	120.17	23.68	11.84	8.23
PC3S9.0R	4	81.67	67.98	13.69	6.85	8.38
PC4S1.0R	7	51.30	27.09	24.21	12.11	23.60
PC4S10.0L	9	41.12	13.84	27.28	13.64	33.17
PC4S11.0L	7	61.38	43.10	18.28	9.14	14.89
PC4S2.0R	7	29.49	4.47	25.02	12.51	42.42
PC4S3.0L	5	17.90	6.70	11.20	5.60	31.28
PC4S4.0L	10	54.81	24.05	30.76	15.38	28.06
PC4S5.0L	4	83.32	53.78	29.54	14.77	17.73
PC4S6.0	11	49.22	18.41	30.81	15.41	31.30
PC4S7.0L	6	23.97	8.38	15.59	7.80	32.52
PC4S8.0L	11	43.25	11.43	31.82	15.91	36.79
PC4S9.0L	10	45.66	9.35	36.31	18.16	39.76
PC5S1.0L	2	26.90	19.96	6.94	3.47	12.90
PC5S10.0R	1	63.24	54.84	8.40	4.20	6.64
PC5S11.0R	2	74.78	59.34	15.44	7.72	10.32
PC5S2.0L	2	69.36	57.51	11.85	5.93	8.54
PC5S3.0	2	8.74	5.90	2.84	1.42	16.25
PC5S4.0L	6	89.42	71.88	17.54	8.77	9.81
PC5S5.0R	1	54.24	41.45	12.79	6.40	11.79
PC5S6.0R	1	67.99	56.72	11.27	5.64	8.29
PC5S7.0R	1	19.24	14.40	4.84	2.42	12.58
PC5S8.0	3	41.01	28.02	12.99	6.50	15.84
PC5S9.0R	1	48.05	40.78	7.27	3.64	7.57
PC6S1.0R	5	11.85	3.55	8.30	4.15	35.02
PC6S10.0	2	7.89	1.20	6.69	3.35	42.40
PC6S11.0L	5	13.04	2.84	10.20	5.10	39.11
PC6S2.0R	2	2.95	0.45	2.50	1.25	42.37
PC6S3.0	2	5.58	0.57	5.01	2.51	44.89
PC6S4.0R	3	7.04	1.32	5.72	2.86	40.63
PC6S5.0R	6	10.18	1.02	9.16	4.58	44.99
PC6S6.0R	2	8.83	3.06	5.77	2.89	32.67

PC6S8.0	2	11.16	1.16	10.00	5.00	44.80
PC6S9.0	2	5.22	1.14	4.08	2.04	39.08
PC7S1.0	10	228.14	194.21	33.93	16.97	7.44
PC7S11.0L	13	306.80	244.97	61.83	30.92	10.08
PC7S2.0	10	104.80	80.44	24.36	12.18	11.62
PC7S3.0R	1	56.76	48.64	8.12	4.06	7.15
PC7S5.0	10	170.93	139.22	31.71	15.86	9.28
PC7S6.0L	3	93.52	79.26	14.26	7.13	7.62
PC7S7.0	8	57.90	29.53	28.37	14.19	24.50
PC7S9.0L	1	77.40	69.18	8.22	4.11	5.31
UC1S1.0R	2	44.55	35.42	9.13	4.57	10.25
UC1S10.0	3	15.20	3.51	11.69	5.85	38.45
UC1S11.0L	3	50.09	40.78	9.31	4.66	9.29
UC1S2.0R	1	24.25	14.27	9.98	4.99	20.58
UC1S3.0R	3	21.20	5.27	15.93	7.97	37.57
UC1S4.0R	8	13.13	0.89	12.24	6.12	46.61
UC1S5.0R	7	24.97	2.07	22.90	11.45	45.86
UC1S6.0	2	15.83	8.72	7.11	3.56	22.46
UC1S7.0R	3	17.49	2.32	15.17	7.59	43.37
UC1S8.0	5	14.88	6.06	8.82	4.41	29.64
UC1S9.0R	2	13.92	5.95	7.97	3.99	28.63
UC2S1.0R	5	18.62	2.35	16.27	8.14	43.69
UC2S10.0L	8	18.33	5.08	13.25	6.63	36.14
UC2S11.0	12	11.91	1.06	10.85	5.43	45.55
UC2S2.0	5	17.36	2.88	14.48	7.24	41.71
UC2S3.0R	4	14.52	4.95	9.57	4.79	32.95
UC2S4.0L	3	9.65	4.40	5.25	2.63	27.20
UC2S5.0L	3	14.04	3.18	10.86	5.43	38.68
UC2S6.0L	3	10.53	4.01	6.52	3.26	30.96
UC2S7.0L	9	44.03	1.05	42.98	21.49	48.81
UC2S8.0L	3	12.21	4.26	7.95	3.98	32.56
UC2S9.0L	4	7.21	1.09	6.12	3.06	42.44
UC3S11.0	15	96.85	42.25	54.60	27.30	28.19
UC3S2.0	8	41.39	13.06	28.33	14.17	34.22
UC3S3.0	8	30.79	15.07	15.72	7.86	25.53
UC3S4.0	7	38.47	10.25	28.22	14.11	36.68
UC3S5.0	7	29.25	5.05	24.20	12.10	41.37
UC3S6.0	4	21.29	6.44	14.85	7.43	34.88
UC3S7.0	12	42.58	8.16	34.42	17.21	40.42
UC3S8.0	6	38.74	14.82	23.92	11.96	30.87
UC3S9.0	8	37.43	18.57	18.86	9.43	25.19

Table 7.5. Soil bulk density

Sample ID	Sampler	sampler radius (cm)	Sample length (cm)	volume (cm3)	Mass (g)	dry bulk density (g/cm3)
AB2S1b	Soil probe	0.65	17	22.55	20.32	0.90
AB5S1.0	Soil probe	0.65	15	19.90	21.4	1.08
AB5S1.1	Soil probe	0.65	10	13.27	13.72	1.03
AB5S11.1	Soil tube	3.65	7	292.83	262.88	0.90
AB5S11.1a	Soil tube	3.65	7	292.83	288.82	0.99
AB5S2.0	Soil tube	3.65	7	292.83	153.29	0.52
AB5S20.1	Soil tube	3.65	7	292.83	266.06	0.91
AB5S20.2	Soil tube	3.65	7	292.83	234.28	0.80
AB5S7.1	Soil tube	3.65	7	292.83	240.27	0.82
AB5S7.2	Soil tube	3.65	7	292.83	269.89	0.92
AB5S9.1	Soil tube	3.65	7	292.83	284.67	0.97
AB5S9.2	Soil tube	3.65	7	292.83	353	1.21
AB6S1.0	Soil tube	3.65	7	292.83	356.49	1.22
AB6S1.1	Soil tube	3.65	7	292.83	376.5	1.29
AB6S10.0	Soil tube	3.65	7	292.83	268.78	0.92
AB6S3.0	Soil tube	3.65	7	292.83	244.7	0.84
AB6S3.1	Soil tube	3.65	7	292.83	328.3	1.12
AB6S6.0	Soil tube	3.65	7	292.83	288.92	0.99
AB6S7.0	Soil tube	3.65	7	292.83	248.92	0.85
IMT2S1.0	Soil tube	3.65	7	292.83	258.13	0.88
MT1S2	Soil tube	3.65	7	292.83	146.12	0.50
MT2S1.0	Soil tube	3.65	7	292.83	260.48	0.89
PC1S21.1	Soil tube	3.65	7	292.83	379.9	1.30
PC1S21.2	Soil tube	3.65	7	292.83	283.36	0.97
PC2S4.1	Soil probe	0.65	12	15.92	17.99	1.13
PC7S1.1	Soil probe	0.65	15	19.90	18.89	0.95
UC3S11.0	Soil tube	3.65	7	292.83	139.98	0.48
UC3S11.0a	Soil tube	3.65	7	292.83	135.96	0.46
UC3S11.1	Soil tube	3.65	7	292.83	286.11	0.98
UC3S11.1a	Soil tube	3.65	7	292.83	282.35	0.96
UC3S8.0	Soil tube	3.65	7	292.83	181.56	0.62
UC3S8.0	Soil tube	3.65	7	292.83	174.39	0.60
				Mean		0.91
				Standard Deviation		0.22

Table 7.6. Grain size analysis of soil samples

Sample ID	Total (g)	>2mm (g)	0.5 - 2 mm (g)	0.062 - 0.5 mm (g)	< 0.062 (g)
AB1S11.1	37.61	0	9.91	20.23	7.55
AB1S2.1	32.95	1.07	5.55	20.93	3.52
AB1S2.2	106.77	29.42	33.14	37.65	5.57
AB1S4.1	253.76	13.72	101	119.14	16.6
AB1S4.2	356.56	7.31	123.07	202.49	21.47
AB1S4.3	386.63	23.02	138.11	185.53	39.21
AB2S13.1	35.2	0	6.22	18.82	9.95
AB2S13.2	101.24	6.1	41.61	40.06	13.25
AB2S6.1	17.52	0	1.83	9.43	6.14
AB2S8.1	21.01	0	3.78	14.15	3.13
AB4S11.1	105.29	0	12.7	56.62	31.71
AB4S11.2	252.84	0	52.54	129.01	69.74
AB4S11.3	255.35	2.47	76.8	113.62	61.5
AB4S11.4	459.47	85.4	142.43	170.53	60.79
AB4S11.5	491.25	217.85	162.35	92.2	18.11
AB4S3.1	210.58	2.16	22.64	137.16	48.34
AB4S3.2	232.1	19.63	17	152.63	42.63
AB4S8.1	83.95	0	8.04	36.12	39.16
AB4S8.3	371.64	10.51	136.78	220.36	0
AB5S11.0	231.55	0	8.69	223.61	0
AB5S11.1	231.8	0	13.95	167.65	50.21
AB5S11.1	409.05	4.01	36.33	324.34	43.78
AB5S11.2	285.55	13.4	40.35	176.13	55.5
AB5S11.2	267.89	8.75	25.24	191.05	42.56
AB5S2.0	134.26	0.23	17.49	93.49	23.5
AB5S2.1A	73.59	0	5.81	54.25	13.46
AB5S2.2a	269.43	0.31	36.81	204.56	25.16
AB5S2.3A	352.9	3.01	13.67	234.69	100.96
AB5S2.4	185.83	0.48	20.03	147.23	16.56
AB5S2.5a	386.36	0.23	15.39	314.79	54.49
AB5S3.0	27.41	0	0	18.99	8.27
AB5S3.1	151.71	0	37.34	90.09	18.18
AB5S3.6	415.94	0.38	91.47	309.64	11.2
AB5S3.7	329.97	0	25.05	282.35	22.28
AB5S4.1	138.93	0	0.28	102.4	36.1
AB5S4.2	265.46	2.68	12.78	210.41	32.05
AB5S4.3	342.54	0.34	11.87	296.01	31.98
AB5S4.4	380.8	22.79	41.85	280.08	35.53
AB5S4.5	320.54	79.48	102.34	124.88	13.78
AB5S5.1	180.98	0.6	96.98	46.06	34.48
AB5S5.2	280.58	39.66	85.53	87.67	66.93
AB5S5.3	361.89	2.72	73.72	143.1	141.88
AB5S5.4	424.13	7.72	63.7	262.19	89.46
AB5S5.5	375.01	2.98	49.96	239.5	82.41
AB5S5.6	476.26	13.61	55.3	289.88	116.18

AB5S5.7	414.83	24.51	81.81	262.35	45.86
AB5S7.1	210.96	2.43	59.1	126.31	23.24
AB5S7.2	253.22	42.45	65.36	123.13	21.81
AB5S7.3	208.22	24.78	58.61	104.78	20.18
AB5S7.4	409.85	49.67	115.29	216.13	27.18
AB5S9.2	354	17.69	61.44	248.54	25.71
AB5S9.3	322.83	54.08	65.61	174.27	27.85
AB6S1.0	335.73	2.97	45.11	233.04	54.49
AB6S1.1	360.36	6.94	53.63	255.83	43.64
AB6S10.0pb	263.12	0	15.53	175.37	72.23
AB6S3.0	204	0.62	55.58	106.45	41.1
AB6S3.0	218.37	0	14.31	154.22	49.74
AB6S3.1	263.25	8.18	68.76	144.07	42.02
AB6S3.1	300.43	3.05	21.51	210.56	65.43
AB6S3.3	414.29	196.75	90.4	113.8	10.12
AB6S4.1	204.18	0	4.11	162.27	37.26
AB6S4.2	225.8	0	64.81	131.48	28.34
AB6S4.3	446.82	105.54	165.6	138.03	37.08
AB6S6.0	258.61	0	30.37	170.15	57.64
AB6S7.0	219.71	16.85	86.94	89.97	25.56
CF1S1.1	99.01	28.36	35.15	30.79	4.75
CF1S1.1	104.85	0	19.95	69.86	14.76
CF1S1.2	251.97	3.08	116.37	118.98	10.86
CF1S1.3	152.26	5.06	81.88	58.27	7.08
CF1S10.1	251.99	10.17	75.26	137.39	25.93
CF1S10.2	355.58	21.55	162.86	147.38	22.05
CF1S10.3	204.88	9.72	68.2	109.02	16.25
CF1S5.1	168.97	5.84	55.01	92.89	13.24
CF1S5.1	208.96	25.26	44.88	117.06	21.68
CF1S8.1	123.85	2.51	54.45	61.63	4.94
CF2S1.1	91.49	18.07	23.94	38.19	11.01
CF2S2.1	147.32	15.19	30.9	72.69	28.52
CF3S1.2	23.21	0	0	7.01	1.4
CF3S2.1	39.01	6.73	15.14	14.15	2.88
CF3S3.1	133.67	37.27	57.35	31.43	3.59
CF4S11.1	61.23	0	7.02	43.46	10.71
CF4S11.2	302.63	45.11	119.47	126.55	11.34
CF4S4.0	5.18	0	0	3.24	1.99
CF5S5.1	215.84	0.77	37.13	156.78	18.73
CF5S5.2	390.71	3.28	124.06	232.47	26.72
CF5S5.3	357.74	2.8	73.7	238.23	42.9
CF5S5.4	436.36	9.45	76.89	305.82	44.06
CF7S1.0	48.34	4.27	8.84	27.88	7.3
CF7S2.1	52.55	0.62	12.92	34.09	5
CF7S3.1	314.37	86.27	80.5	136.88	7.17
CF7S6.1	74.95	11.19	13.65	27.5	22.39
CF7S6.1	71.56	2.5	27.63	40.15	0
CF7S6.3	74.54	1.01	15.66	40.15	17.34
CF7S8.1	145.37	29.55	58.03	53.17	4.08

LC2S1.0	119.17	1.83	23.24	56.78	36.84
LC2S1.1	190.36	0.24	52.46	90.45	46.9
LC2S1.2	117.16	1.25	37.53	53.13	24.77
M1S11.1	71.49	0	8.86	33.25	29.2
M1S11.2	73.03	0	13.7	29.74	29.35
M1S11.4	132.61	0	29.42	64.26	38.85
M1S12.2	245.21	136.5	65.37	35.28	8.05
M1S12.3	150.98	100.67	30.26	16.18	3.9
M1S3.2	30.71	0	2.71	20.05	7.84
M1S3.3	193.22	0.89	19.17	146.83	26.56
M1S6.1	50.3	0	13.34	23.38	13.63
M1S7.1	111.59	0	17.93	72.39	21.04
M1S9.3	90.5	0	12.84	64.34	13.14
M1S9.4	136.42	0.97	23.39	98.38	13.15
MT1S17.2	146.57	3.7	28.8	96.26	18.07
MT1S3.3	209.85	20.78	72.76	97.19	18.88
MT1S6.2	35.95	0	6.56	17.29	12.07
MT1S8.0	25.87	0	7.23	15.18	3.47
MT2S1.0	240.02	80.16	107.94	42.65	9.88
MT2S1.2	105.42	0.88	10.14	78.92	15.39
MT2S1.3	223.2	6.1	45.9	142.82	28.25
MT2S1.4	149.95	8.03	64.27	57.82	19.67
MT2S9.1	123.68	0	9	91.62	22.89
MT3S10.1	176.83	0.8	89.71	55.88	29.78
MT3S2.1	66.3	0.52	24.4	30.37	10.79
MT3S5.1	74.4	0.94	24.95	36.13	12.14
MT3S7.1	202.78	1.89	92.26	84.48	23.88
MT1S9.2	102.12	35.47	20.9	33.88	12.01
MT1S11.3	67.78	0	7.66	32.8	27.09
PC1S1.1	326.8	18	100.7	190.81	17.07
PC1S1.1	228.47	0	14.69	154.56	54.17
PC1S1.2	396.45	65.7	183.5	118.44	28.44
PC1S1.3	102.17	24.48	36.6	34.48	6.74
PC1S8.2	408.2	36.82	174.93	180.19	16.08
PC1S8.4	600	219.58	260.47	110.73	8.77
PC2S1.1	28.97	0.85	9.92	12.94	5.26
PC2S1.2	156.36	14.38	49.17	71.34	21.69
PC2S1.3	204.99	48.3	67.84	74.07	14.78
PC2S11.1	50.46	4.14	11.55	28.35	5.28
PC2S7.1	244.9	37.21	64.74	113.19	29.49
PC3S14.1	209.29	0	62.15	121.85	16.31
PC3S14.2	323.71	21.63	70.59	205.19	24.92
PC3S14.3	343.51	104.82	77.79	147.12	13.73
PC3S4.1	142.19	32.94	46.8	52.71	9.63
PC3S5.1	267.8	7.78	165.78	81.16	9.59
PC3S5.2	329.52	2.57	113.89	167.91	44.95
PC4S10.1	103.03	5.07	36.3	57.38	3.92
PC4S4.1	116.53	1.08	44.49	54.96	15.32
PC4S7.1	246.79	55.98	134.28	47.49	5.19

PC4S7.2	420.75	61.4	267.18	82.08	8.63
PC4S7.3	284.61	125.63	105.11	47.52	6.18
PC5S5.1	180.75	0	75.71	87.32	14.59
PC5S5.2	182.75	11.46	76	82.14	12.46
PC5S7.1	157.66	11.62	66.87	63.03	5.93
PC5S9.1	197.22	1.93	39.98	139.01	16.33
PC5S9.2	328.15	7.44	83.92	213.03	23.68
PC5S9.3	424.05	4.68	134.91	258.46	25.74
PC5S9.4	359.32	18.29	142.03	166.5	31.8
PC6S10.1	11.98	0	0.37	8.2	3.44
PC6S10.2	70.45	0	1.39	43.67	25.16
PC6S10.3	66.06	0	3.55	36.59	25.63
PC6S10.4	41.63	0	1.77	20.13	19.65
PC6S6.1	79.07	51.19	18.26	7.88	1.65
PC6S9.1	317.99	5.51	90.85	197.81	23.64
PC6S9.2	172.08	0.51	6.5	113.18	51.71
PC6S9.4	130.9	39.71	33.74	44.51	12.89
PC7S3.4	389.22	0	2.62	277.9	108.01
PC7S4.0	558.35	0.22	290.85	265.91	2.22
PC7S4.1	246.94	2.05	87.33	137.74	19.03
PC7S4.2	271.58	9.84	67.7	169.98	16.86
PC7S4.3	363.3	25.79	122.2	194.04	18.83
PC7S5.1	216.89	0.07	5.26	210.58	0
PC7S5.2	337.11	2.04	40.24	259.67	30.12
PC7S5.3	462.41	3.71	119.82	309.96	27.48
PC7S5.4	528.72	42.16	253.47	214.94	16.83
PC7S5.5	480.51	25.3	214.61	221.93	14.45
PC7S6.1	84.26	0	0.45	67.27	16.39
PC7S6.2	168.18	0.99	5.6	140.75	20.89
PC7S6.3	476.72	82.19	80.33	281.44	32.49
PC7S6.4	415.4	33.84	20.38	312.56	48.5
PC7S9.1	230.82	21.05	79.02	111.77	18.14
PC7S9.2	267.47	47.55	89.31	111.38	18.52
PC7S9.3	494.87	46.24	106.78	276.03	65.03
UC1S11.1	165.02	65.87	34.53	48.51	16.14
UC1S11.2	233.09	44.08	63.75	109.07	16
UC1S4.1	17.36	1.43	4.67	6.49	3.89
UC1S4.2	48.01	0	10.58	21.1	14.9
UC1S7.1	23.21	0	1.13	11.49	10.44
UC1S7.2	145.83	39.73	40.1	52.32	13.72
UC2S1.1	14.12	0	0.61	8.09	5.42
UC2S1.2	30.83	0.14	2.66	16.49	11.47
UC2S2.0	29.38	0	10	16.2	3.02
UC2S2.1	28.1	2.26	12.74	10.1	2.81
UC2S3.1	32.29	0	1.12	16.23	14.84
UC2S3.2	348.74	265.46	15.26	36.9	30.55
UC2S3.3	133.02	0	31.18	57.62	43.44
UC2S3.4	239.66	0	76.48	110.44	52.06
UC2S3.5	235.58	0.52	53.04	120.52	61.24

UC2S3.6	239.52	36.59	104.6	83.78	14.23
UC2S3.7	348.43	145.09	119.37	67.59	14.54
UC2S3.8	256.73	101.53	92.97	50.61	11.69
UC2S8.2	76.96	0	1.19	38.53	37.09
UC2S8.3	65.16	0	7.57	34.52	22.88
UC3S11.0	109.65	0	25.66	48.11	35.08
UC3S11.1	264.94	4.18	13.54	196.79	50.3
UC3S11.2	298	2.58	49.58	178.7	66.6
UC3S11.3	312.83	1.02	98.59	188.1	24.75
UC3S11.4	294.24	12.09	83.55	148.29	49.73
UC3S2.1	239.99	1.89	63.54	142.69	31.39
UC3S2.2	238.84	0.69	40.63	129.39	67.42
UC3S2.3	324.23	4.48	67.52	176.74	75.23
UC3S2.4	334.34	24.07	62.34	169.57	78.3
UC3S2.5	480.02	70.67	152.82	170.31	85.61
UC3S2.6	572.35	89.35	235.78	191.67	55.54
UC3S5.1	65.45	0.15	25.34	22.2	17.7
UC3S8.0	147.94	16.67	66.14	34.57	30.75
UC3S8.1	164.52	1.66	66.97	52.16	43.47
UC3S8.2	349.44	8.12	126.96	108.47	105.46
UC3S8.3	374.42	1.11	134.5	133.41	104.84
UC3S8.4	495.93	0	196.53	177.01	121.88

Table 7. 7. Soil organic carbon content

Sample ID	Min depth (cm)	Max depth (cm)	gravimetric moisture content (%)	Total Carbon (%)	CaCO3 (%)	Inorganic C (%)	Organic C (%)	NREL Lab No.
AB1S1.1	6	13	25.22	4.17	0.36	0.04	4.13	R3824
AB1S10.1	10	25	81.00	31.34	0.51	0.06	31.28	R3825
AB1S10.2	25	45	86.14	23.61	0.52	0.06	23.55	R3826
AB1S11.1	12	20	71.41	15.12	0.16	0.02	15.10	R3827
AB1S12.1	16	32	8.50	1.72	0.72	0.09	1.63	R3829
AB1S12.2	32	47	85.71	31.63	0.81	0.10	31.53	R3830
AB1S12.3	47	65	80.91	24.11	0.67	0.08	24.03	R3831
AB1S12.4	65	82	47.53	5.50	0.47	0.06	5.45	R3828
AB1S2.1	8	23	24.42	14.29	0.53	0.06	14.23	R3832
AB1S2.2	25	44	33.88	12.54	0.55	0.07	12.47	R3833
AB1S3.1	8	23	48.97	9.39	0.33	0.04	9.35	R3834
AB1S3.2	23	30	23.38	0.61	0.27	0.03	0.58	R3835
AB1S4.1	7	22	20.06	1.28	0.40	0.05	1.23	R3836
AB1S4.2	22	36	14.72	0.25	0.42	0.05	0.20	R3837
AB1S4.3	36	48	22.74	0.44	0.66	0.08	0.36	R3838
AB1S5.1	6	22	62.67	14.30	0.84	0.10	14.20	R3839
AB1S5.2	22	37	55.99	5.54	0.64	0.08	5.46	R3840
AB1S5.3	37	44	64.50	1.20	0.59	0.07	1.13	R3841
AB1S6.1	8	23	68.83	15.18	0.55	0.07	15.11	R3842
AB1S6.2	23	38	72.03	19.48	0.18	0.02	19.46	R3843
AB1S6.3	38	53	75.45	8.75	0.37	0.04	8.71	R3844
AB1S6.4	53	60	70.41	0.12	0.22	0.03	0.10	R3845
AB1S7.1	9	20	77.46	4.54	0.92	0.11	4.43	R3846
AB1S8.1	11	20	28.57	25.54	0.52	0.06	25.48	R3848
AB1S8.2	43	58	60.67	9.58	0.44	0.05	9.53	R3847
AB1S8.3	58	70	66.74	9.42	0.42	0.05	9.37	R3849
AB1S9.1	12	30	82.70	29.30	0.49	0.06	29.24	R3850
AB1S9.2	30	47	85.34	13.93	0.44	0.05	13.88	R3851
AB2S1.1	5	20	74.16	21.22	0.17	0.02	21.20	R3785
AB2S1.2	20	29	60.37	15.27	0.15	0.02	15.25	R3786
AB2S11.1	7	18	77.51	15.94	0.00	0.00	15.94	R3800
AB2S13.1	8	23	60.81	10.69	0.18	0.02	10.67	R3801
AB2S13.2	23	32	45.52	8.34	0.20	0.02	8.31	R3802
AB2S3.1	12	27	67.12	11.42	0.04	0.01	11.41	R3787
AB2S3.2	27	34	70.94	10.00	0.01	0.00	10.00	R3788
AB2S4.1	13	30	81.82	25.23	0.01	0.00	25.23	R3789
AB2S4.2	30	33	80.76	19.59	0.32	0.04	19.55	R3790
AB2S5.1	8	20	80.80	14.37	0.08	0.01	14.36	R3791
AB2S6.1	9	24	64.93	24.76	0.06	0.01	24.75	R3792
AB2S6.2	24	40	45.77	11.22	0.19	0.02	11.20	R3793
AB2S6.3	40	47	65.63	8.16	0.02	0.00	8.15	R3794
AB2S7.1	7	22	79.12	11.80	0.01	0.00	11.80	R3795
AB2S7.2	22	37	56.58	2.88	0.01	0.00	2.88	R3796
AB2S7.3	37	46	34.89	1.12	0.01	0.00	1.12	R3797

AB2S8.1	14	22	62.91	10.68	0.01	0.00	10.68	R3798
AB2S9.1	8	21	52.13	6.73	0.02	0.00	6.73	R3799
AB4S1.1	1	16	43.69	8.21	0.27	0.03	8.17	R875
AB4S1.2	16	31	30.63	0.91	0.37	0.04	0.86	R876
AB4S1.3	31	46	26.72	1.77	0.01	0.00	1.77	R877
AB4S1.4	46	50	46.66	4.77	0.75	0.09	4.68	R878
AB4S10.1	10	25	46.70	8.98	0.26	0.03	8.95	R4722
AB4S10.2	25	40	46.30	5.00	0.16	0.02	4.98	R4723
AB4S10.3	40	55	36.60	4.33	0.27	0.03	4.30	R4724
AB4S10.4	55	70	37.90	3.97	0.30	0.04	3.94	R4725
AB4S10.5	70	95	17.80	1.28	0.34	0.04	1.24	R4726
AB4S10.6	95	102	18.80	1.87	0.37	0.04	1.83	R4727
AB4S11.1	7	22	48.20	4.61	0.52	0.06	4.55	R4728
AB4S11.2	22	37	47.90	8.41	0.16	0.02	8.39	R4729
AB4S11.3	37	52	51.30	9.04	0.35	0.04	9.00	R4730
AB4S11.4	52	67	33.50	2.82	0.47	0.06	2.76	R4731
AB4S11.5	67	82	20.80	0.85	0.37	0.04	0.81	R4732
AB4S12	0	15	58.30	6.64	0.24	0.03	6.61	R4733
AB4S13	0	15	59.40	3.89	0.72	0.09	3.80	R4734
AB4S2.1	1	18	49.00	14.04	0.48	0.06	13.98	R4735
AB4S2.2	18	33	61.70	6.92	0.25	0.03	6.89	R4736
AB4S2.3	33	48	43.40	3.60	0.66	0.08	3.52	R4737
AB4S3.1	1	20	34.90	3.89	0.48	0.06	3.83	R4738
AB4S3.2	20	28	38.00	3.12	0.22	0.03	3.10	R4739
AB4S4.1	4	19	39.30	7.14	0.25	0.03	7.11	R4740
AB4S4.2	19	26	41.10	5.53	0.33	0.04	5.49	R4741
AB4S5.1	4	23	43.60	7.25	0.28	0.03	7.21	R4742
AB4S5.2	23	41	24.20	1.11	0.12	0.01	1.09	R4743
AB4S5.3	41	50	30.10	0.56	0.09	0.01	0.55	R4744
AB4S6.1	4	19	38.70	7.54	0.12	0.01	7.52	R4745
AB4S6.2	19	37	40.90	4.97	0.06	0.01	4.97	R4746
AB4S6.3	37	54	45.50	7.58	0.25	0.03	7.55	R4747
AB4S6.4	54	69	46.90	3.61	0.11	0.01	3.60	R4748
AB4S6.5	69	85	42.70	1.34	0.11	0.01	1.33	R4749
AB4S6.6	85	98	18.90	0.41	0.24	0.03	0.38	R4750
AB4S7.1	5	20	59.50	15.64	0.08	0.01	15.63	R4751
AB4S7.2	20	35	60.50	13.90	0.12	0.01	13.89	R4752
AB4S7.3	35	50	67.10	18.38	0.26	0.03	18.35	R4753
AB4S7.4	50	65	62.30	5.86	0.10	0.01	5.85	R4754
AB4S7.5	65	90	23.20	0.56	0.11	0.01	0.55	R4755
AB4S7.6	90	99	20.30	0.35	0.08	0.01	0.34	R4756
AB4S8.1	4	23	63.70	13.32	0.14	0.02	13.30	R4757
AB4S8.2	23	38	46.80	4.22	0.08	0.01	4.21	R4758
AB4S8.3	38	54	32.36	1.91	0.52	0.06	1.85	R565
AB4S9.1	5	20	54.10	7.37	0.07	0.01	7.36	R4760
AB4S9.2	20	35	34.80	5.37	0.10	0.01	5.36	R4761
AB4S9.3	35	50	45.20	5.32	0.08	0.01	5.31	R4762
AB4S9.4	50	65	36.20	2.31	0.16	0.02	2.29	R4763
AB4S9.5	65	80	17.00	0.37	0.08	0.01	0.36	R4764

AB4S9.6	80	95	22.20	0.93	0.11	0.01	0.91	R4765
AB4S9.7	95	110	20.30	0.63	0.00	0.00	0.63	R4766
AB5S1.1a	4	15	19.43	5.55	0.38	0.05	5.50	2014R605
AB5S1.2a	15	30	27.04	2.03	0.36	0.04	1.98	2014R606
AB5S1.3	30	45	21.98	0.90	0.19	0.02	0.88	2014R607
AB5S1.4	45	54	16.48	0.53	0.25	0.03	0.50	2014R608
AB5S1.5	54	65	12.66	0.43	0.12	0.01	0.41	2014R609
AB5S10.1	2	16	27.46	4.19	0.20	0.02	4.16	2014R610
AB5S10.2	16	31	30.29	3.84	0.09	0.01	3.83	2014R611
AB5S10.3	31	46	32.19	2.20	0.24	0.03	2.17	2014R612
AB5S10.4	46	65	31.85	1.57	0.10	0.01	1.55	2014R613
AB5S10.5	65	86	29.43	0.84	0.20	0.02	0.81	2014R614
AB5S10.6	86	103	24.43	0.34	0.12	0.01	0.32	2014R615
AB5S11.0	0	15	37.56	3.89	0.60	0.07	3.82	2014R651
AB5S11.1	15	30	28.00	2.03	0.22	0.03	2.01	2014R652
AB5S11.2	30	45	34.39	1.49	0.20	0.02	1.46	2014R653
AB5S2.1	5	20	44.12	7.82	0.45	0.05	7.77	2014R616
AB5S2.2	20	35	37.22	3.46	0.40	0.05	3.41	2014R617
AB5S2.3	35	50	40.97	2.34	0.00	0.00	2.34	2014R618
AB5S2.4	50	65	46.80	1.76	0.36	0.04	1.72	2014R619
AB5S2.5	65	80	31.73	0.95	0.36	0.04	0.91	2014R620
AB5S3.1	3	18	37.11	5.47	0.18	0.02	5.45	2014R621
AB5S3.2	18	33	36.05	3.69	0.04	0.01	3.69	2014R622
AB5S3.3	33	48	44.28	4.04	0.33	0.04	4.00	2014R623
AB5S3.4	48	63	40.15	2.36	0.01	0.00	2.35	2014R624
AB5S3.5	63	83	35.59	1.26	0.32	0.04	1.22	2014R625
AB5S3.6	83	103	22.61	0.35	0.16	0.02	0.34	2014R626
AB5S3.7	103	120	27.25	0.63	0.42	0.05	0.58	2014R627
AB5S4.1	2	17	31.79	5.33	0.23	0.03	5.30	2014R628
AB5S4.2	17	31	23.41	3.61	0.39	0.05	3.56	2014R629
AB5S4.3	31	46	32.33	1.36	0.06	0.01	1.35	2014R630
AB5S4.4	46	61	27.86	0.91	0.20	0.02	0.88	2014R631
AB5S4.5	61	70	18.61	0.42	0.71	0.08	0.34	2014R632
AB5S5.1	5	20	46.01	7.65	0.07	0.01	7.64	2014R633
AB5S5.2	20	35	33.63	2.69	0.04	0.01	2.68	2014R634
AB5S5.3	35	50	34.75	1.70	0.01	0.00	1.70	2014R635
AB5S5.4	50	68	35.74	0.94	0.15	0.02	0.92	2014R636
AB5S5.5	68	87	30.27	0.71	0.32	0.04	0.67	2014R637
AB5S5.6	87	107	23.80	0.49	0.36	0.04	0.45	2014R638
AB5S5.7	107	115	18.51	0.31	0.34	0.04	0.27	2014R639
AB5S6.1	3	20	37.45	4.53	0.48	0.06	4.47	2014R640
AB5S6.2	20	33	30.37	2.36	0.20	0.02	2.34	2014R641
AB5S6.3	33	50	23.60	1.37	0.39	0.05	1.32	2014R642
AB5S7.3	20	28	3.01	2.15	0.16	0.02	2.13	2014R644
AB5S7.4	28	38	3.53	1.11	0.36	0.04	1.07	2014R643
AB5S8.1	2	19	17.23	4.54	0.08	0.01	4.53	2014R645
AB5S8.2	19	33	22.86	3.79	0.42	0.05	3.73	2014R646
AB5S8.3	33	46	27.58	1.98	0.32	0.04	1.94	2014R647
AB5S9.1	2	17	18.19	0.87	0.47	0.06	0.81	2014R648

AB5S9.2	17	32	26.97	0.91	0.34	0.04	0.87	2014R649
AB5S9.3	30	40	23.01	2.01	0.49	0.06	1.95	2014R650
AB6S1.1	0	15	25.32	2.50	0.65	0.08	2.43	R566
AB6S1.2	15	30	23.33	1.76	0.43	0.05	1.71	R567
AB6S10.1	0	15	33.58	6.95	0.60	0.07	6.88	R594
AB6S10.2	15	30	29.93	1.93	0.55	0.07	1.87	R595
AB6S10.3	30	46	26.84	1.36	0.82	0.10	1.26	R596
AB6S11.1	0	15	30.10	4.67	0.67	0.08	4.59	R597
AB6S11.2	15	30	24.07	2.53	0.96	0.11	2.41	R598
AB6S11.3	30	45	24.58	1.63	0.60	0.07	1.56	R599
AB6S11.4	45	60	29.66	1.63	0.72	0.09	1.55	R600
AB6S11.5	60	80	25.88	1.56	0.34	0.04	1.52	R601
AB6S11.6	80	100	40.24	8.46	0.65	0.08	8.39	R602
AB6S11.7	100	118	51.97	4.20	0.68	0.08	4.12	2014R603
AB6S11.8	118	128	22.48	0.50	0.08	0.01	0.49	2014R604
AB6S2.1	0	15	34.35	4.12	0.30	0.04	4.08	R568
AB6S2.2	15	30	24.16	1.10	0.43	0.05	1.05	R569
AB6S3.0	0	15	35.18	5.10	0.56	0.07	5.03	R570
AB6S3.1	15	30	27.34	3.29	0.59	0.07	3.22	R571
AB6S3.2	30	45	21.98	1.39	0.33	0.04	1.35	R572
AB6S3.3	45	55	11.61	0.23	0.60	0.07	0.16	R573
AB6S4.1	1	16	16.60	4.20	0.50	0.06	4.14	R574
AB6S4.2	16	31	25.03	3.31	0.40	0.05	3.26	R575
AB6S4.3	31	46	21.98	1.90	4.16	0.50	1.40	R576
AB6S5	0	15	41.67	6.91	0.53	0.06	6.85	R577
AB6S5.1	15	30	33.33	5.48	0.32	0.04	5.44	R578
AB6S5.2	30	45	21.42	0.26	0.58	0.07	0.19	R579
AB6S5.3	45	60	24.25	0.99	0.60	0.07	0.91	R580
AB6S5.4	60	80	27.50	0.89	0.73	0.09	0.81	R581
AB6S5.5	80	90	17.51	0.26	0.59	0.07	0.19	R582
AB6S6.1	0	15	25.20	5.13	0.81	0.10	5.03	R583
AB6S6.2	15	30	12.72	2.73	0.83	0.10	2.63	R584
AB6S7	0	15	26.21	5.74	0.65	0.08	5.67	R585
AB6S7.1	15	30	19.87	3.74	0.53	0.06	3.67	R586
AB6S7.2	30	45	21.62	2.27	0.44	0.05	2.21	R587
AB6S7.3	45	60	15.94	1.00	0.59	0.07	0.93	R588
AB6S8.1	1	16	22.88	5.14	0.60	0.07	5.07	R589
AB6S8.2	16	31	18.30	3.10	0.71	0.08	3.02	R590
AB6S9.1	1	15	10.26	1.41	0.60	0.07	1.34	R591
AB6S9.2	15	30	8.51	1.39	0.61	0.07	1.31	R592
AB6S9.3	30	42	9.12	0.89	0.71	0.08	0.80	R593
CF1LS1.1	10	23	14.63	4.48	0.43	0.05	4.42	R471
CF1RS1.1	12	27	23.28	6.88	0.28	0.03	6.85	R470
CF1RS1.2	27	42	34.81	5.99	0.28	0.03	5.95	R472
CF1RS1.3	42	48	40.00	1.94	0.19	0.02	1.92	R473
CF1RS10.1	6	21	11.21	2.86	0.33	0.04	2.82	R474
CF1RS10.2	21	36	17.40	1.15	0.04	0.01	1.15	R475
CF1RS10.3	36	41	13.89	1.36	0.14	0.02	1.34	R476
CF1RS11.1	13	28	9.75	1.78	0.36	0.04	1.73	R477

CF1RS11.2	28	43	10.36	1.34	0.23	0.03	1.31	R478
CF1RS11.3	43	58	8.58	1.14	0.24	0.03	1.11	R479
CF1RS11.4	58	70	13.94	0.73	0.01	0.00	0.73	R480
CF1LS2.1	9	24	5.59	1.31	0.23	0.03	1.28	R482
CF1RS2.1	9	19	15.02	4.65	0.36	0.04	4.60	R481
CF1S2.2	24	39	7.95	1.42	0.22	0.03	1.39	R983
CF1S2.3	39	43	10.53	1.37	0.08	0.01	1.36	R975
CF1LS3.1	6	23	21.80	4.15	0.26	0.03	4.12	R483
CF1RS3.1	18	29	11.90	3.89	0.23	0.03	3.86	R484
CF1LS3.2	23	41	16.08	1.62	0.07	0.01	1.61	R485
CF1LS3.3	41	63	17.53	0.65	0.02	0.00	0.65	R486
CF1LS3.4	63	75	23.21	0.49	0.18	0.02	0.46	R487
CF1RS4.1	8	24	16.14	4.03	0.16	0.02	4.01	R488
CF1S4.1	6	21	6.88	1.39	0.18	0.02	1.36	R986
CF1RS4.2	24	39	14.03	2.25	0.42	0.05	2.20	R489
CF1S4.2	21	35	9.41	6.74	0.18	0.02	6.72	R978
CF1RS4.3	39	49	13.92	1.63	0.27	0.03	1.60	R490
CF1LS5.1	12	24	9.57	3.57	0.20	0.02	3.55	R491
CF1RS5.1	7	22	20.35	3.46	0.14	0.02	3.45	R492
CF1RS6.1	8	23	21.54	3.42	0.30	0.04	3.38	R493
CF1RS6.2	23	38	25.35	2.70	0.18	0.02	2.68	R494
CF1RS7.1	4	19	18.00	2.87	0.12	0.01	2.86	R495
CF1RS7.2	19	34	19.47	0.51	0.42	0.05	0.46	R496
CF1RS7.3	34	39	13.36	0.44	0.24	0.03	0.41	R497
CF1RS8.1	7	22	16.70	5.22	0.10	0.01	5.21	R498
CF1RS8.2	22	37	21.10	5.16	0.50	0.06	5.10	R499
CF1RS8.3	37	52	17.08	4.82	0.39	0.05	4.78	R500
CF1RS8.4	52	65	16.22	0.45	0.27	0.03	0.42	R501
CF1RS9.1	8	23	11.34	3.46	0.49	0.06	3.40	R502
CF1RS9.2	23	32	19.77	3.02	0.36	0.04	2.97	R503
CF2S1.1	10	15	25.88	7.34	0.02	0.00	7.34	R3803
CF2S10.1	11	24	57.76	7.41	0.02	0.00	7.41	R3812
CF2S11.1	13	18	50.44	10.56	0.01	0.00	10.56	R3813
CF2S2.1	8	23	26.91	5.19	0.06	0.01	5.19	R3804
CF2S2.2	23	31	23.45	1.74	0.01	0.00	1.74	R3805
CF2S3.1	7	15	31.96	7.40	0.14	0.02	7.38	R3806
CF2S4.1	9	26	31.40	6.47	0.01	0.00	6.47	R3807
CF2S5.1	8	24	34.34	10.94	0.08	0.01	10.93	R3808
CF2S5.2	24	39	22.94	0.40	0.02	0.00	0.40	R3809
CF2S6.1	12	23	30.31	5.37	0.07	0.01	5.36	R3810
CF2S8.1	10	26	49.23	5.67	0.02	0.00	5.67	R3811
CF3S1.2	19	25	44.05	41.96	0.42	0.05	41.91	2013R518
CF3S2.1	8	15	20.81	19.20	0.26	0.03	19.17	2013R519
CF3S3.1	6	17	30.72	5.28	0.73	0.09	5.19	2013R520
CF3S5.1	5	23	36.47	5.69	0.09	0.01	5.68	R987
CF3S5.2	23	38	19.94	0.22	0.60	0.07	0.15	R3852
CF3S5.3	38	51	29.99	1.30	0.71	0.08	1.22	2013R521
CF3S5.4	51	55	34.43	0.01	0.52	0.06	-0.05	R3853
CF3S6.1	6	22	32.02	6.25	0.57	0.07	6.18	R3854

CF3S6.2	22	37	36.91	3.26	0.53	0.06	3.19	2013R517
CF3S6.3	37	54	52.14	2.36	0.47	0.06	2.30	2013R516
CF4S11.1	9	24	44.92	8.14	0.18	0.02	8.11	R879
CF4S11.2	24	37	22.18	2.41	0.51	0.06	2.34	R880
CF4S3.1	8	23	11.79	3.13	0.31	0.04	3.10	R427
CF4S3.2	23	34	15.88	2.38	0.28	0.03	2.34	R428
CF4S4.1	10	16	80.00	29.50	0.27	0.03	29.47	R429
CF4S5.1	10	25	58.10	30.52	0.35	0.04	30.48	R430
CF4S5.2	25	40	38.32	5.18	0.43	0.05	5.13	R431
CF4S5.3	40	46	35.59	6.45	0.52	0.06	6.38	R432
CF4S6.1	13	28	60.83	10.72	0.42	0.05	10.67	R433
CF4S6.2	28	36	37.67	3.90	0.26	0.03	3.87	R434
CF4S7.1	18	25	57.01	12.18	0.22	0.03	12.15	R435
CF4S7.2	25	32	52.11	5.33	0.31	0.04	5.29	R436
CF4S8.1	9	17	16.51	7.27	0.48	0.06	7.21	R437
CF4S9.1	8	23	31.40	3.81	0.33	0.04	3.77	R438
CF4S9.2	23	38	21.79	2.01	0.55	0.07	1.95	R439
CF4S9.3	38	47	29.21	2.37	0.57	0.07	2.30	R440
CF5S10.1	3	18	6.64	0.32	0.16	0.02	0.30	R882
CF5S11.1	2	12	20.31	0.95	0.15	0.02	0.93	R883
CF5S2.1	5	20	12.59	3.62	0.02	0.00	3.62	R884
CF5S2.2	20	35	19.64	3.01	0.58	0.07	2.94	R885
CF5S2.3	35	51	23.70	2.91	0.41	0.05	2.86	R886
CF5S4.1	5	20	19.95	4.70	0.14	0.02	4.68	R888
CF5S4.2	20	35	20.72	2.43	0.33	0.04	2.39	R889
CF5S4.3	35	50	21.28	2.02	0.15	0.02	2.00	R890
CF5S4.4	50	58	24.90	2.10	0.18	0.02	2.08	R891
CF5S5.1	4	19	11.29	2.62	0.19	0.02	2.60	R892
CF5S5.2	19	34	14.86	1.55	0.35	0.04	1.51	R893
CF5S5.3	34	49	23.85	1.93	0.10	0.01	1.92	R894
CF5S5.4	49	61	23.42	0.58	0.22	0.03	0.55	R895
CF5S6.1	5	20	23.24	3.73	0.19	0.02	3.70	R896
CF5S6.2	20	35	24.61	3.72	0.18	0.02	3.69	R897
CF5S6.3	35	50	22.31	1.12	0.39	0.05	1.07	R898
CF5S6.4	50	58	20.06	1.66	0.07	0.01	1.65	R899
CF5S7.1	5	18	9.39	4.23	0.27	0.03	4.19	R900
CF5S9.1	5	15	36.06	5.51	0.51	0.06	5.45	R901
CF7S1.1	6	22	63.32	12.80	0.12	0.01	12.79	R515
CF7S10.1	1	9	42.21	17.85	0.45	0.05	17.80	2014R520
CF7S2.1	4	12	29.65	5.07	0.09	0.01	5.06	2014R516
CF7S3.1	5	21	30.98	1.21	0.07	0.01	1.20	2014R517
CF7S4.1	5	19	42.26	9.80	0.23	0.03	9.77	2014R518
CF7S6.1L	4	19	45.13	9.78	0.17	0.02	9.75	R522
CF7S6.1R	5	23	38.39	7.45	0.27	0.03	7.42	2014R519
CF7S6.3L	19	31	46.86	8.03	0.03	0.00	8.03	R523
CF7S7.1	8	19	51.90	12.10	0.20	0.02	12.08	2014R514
CF7S8.1	4	20	32.01	3.05	0.26	0.03	3.02	2014R521
M1T1S1.2	10	20	75.00	5.53	0.37	0.04	5.49	2012R603
M1T6S10	10	25	49.00	3.15	1.00	0.12	3.03	2012R628

M1T3S10.2	10	25	29.90	2.06	0.34	0.04	2.02	2012R617
M1T10S11	18	32	50.24	4.42	0.49	0.06	4.36	2012R644
M1T6S11	25	33	50.83	2.26	0.47	0.06	2.20	2012R629
M1T3S11.2	15	30	30.83	9.21	0.43	0.05	9.16	2012R618
M1T3S12.2	9	24	10.23	0.64	0.26	0.03	0.61	2012R619
M1T3S12.3	24	28	10.29	4.13	0.26	0.03	4.09	2012R620
M1T10S13	11	25	35.30	6.55	0.24	0.03	6.52	2012R645
M1T6S13	8	25	55.96	4.66	0.53	0.06	4.60	2012R630
M1T6S14	25	35	51.65	3.77	0.71	0.08	3.69	2012R631
M1T2S14.2	15	30	39.90	12.48	0.67	0.08	12.40	2012R621
M1T4S14.3	30	45	54.49	3.54	0.44	0.05	3.48	2012R622
M1T11S15	7	22	53.37	5.99	0.42	0.05	5.94	2012R646
M1T4S15			39.83	12.73	0.42	0.05	12.68	2012R623
M1T11S16	22	37	55.25	5.73	0.36	0.04	5.69	2012R647
M1T7S16	16	31	52.83	4.46	0.41	0.05	4.41	2012R632
M1T11S17	37	54	64.76	3.84	0.61	0.07	3.76	2012R648
M1T7S17	31	45	42.69	3.29	0.65	0.08	3.22	2012R633
M1T11S18	54	76	65.07	3.84	0.32	0.04	3.80	2012R649
M1T7S19	12	27	34.09	1.42	0.53	0.06	1.36	2012R634
M1T5S2	17	32	45.60	4.76	0.47	0.06	4.70	2012R624
M1T9S2	4	14	14.55	1.60	0.68	0.08	1.52	2012R639
M1T1S2.2	3	8	38.18	0.72	0.26	0.03	0.69	2012R604
M1T7S20	27	43	18.76	0.57	0.41	0.05	0.52	2012R635
M1T11S21	8	15	40.44	6.44	0.58	0.07	6.37	2012R650
M1T11S22	15	25	30.61	0.52	0.34	0.04	0.48	2012R651
M1T8S22	15	30	20.47	0.23	0.35	0.04	0.18	2012R636
M1T11S24	19	35	47.24	2.73	0.55	0.07	2.66	2012R652
M1T8S24	11	26	35.68	4.06	0.95	0.11	3.95	2012R637
M1T11S25	35	40	34.41	0.68	0.82	0.10	0.58	2012R653
M1T8S25	26	41	35.47	3.37	0.82	0.10	3.27	2012R638
M1T5S3	32	40	54.29	2.20	0.68	0.08	2.12	2012R625
M1T1S3.2	3	18	39.09	1.39	0.36	0.04	1.34	2012R605
M1T1S3.3	18	33	65.27	6.12	0.57	0.07	6.05	2012R606
M1T1S3.4	33	44	40.54	1.25	0.49	0.06	1.19	2012R607
M1T9S4	14	24	56.23	6.78	0.84	0.10	6.68	2012R640
M1T1S4.2	27	34	49.77	11.64	0.19	0.02	11.62	2012R608
M1T2S5.2	10	25	65.01	5.43	0.19	0.02	5.41	2012R609
M1T2S5.3	25	28	48.54	2.09	0.07	0.01	2.08	2012R610
M1T2S6	0	12	55.09	2.14	0.44	0.05	2.09	2012R611
M1T9S6	12	27	59.18	7.18	0.67	0.08	7.10	2012R641
M1T5S6	5	20	29.86	13.52	0.33	0.04	13.48	2012R626
M1T5S7	20	35	32.34	9.69	0.34	0.04	9.65	2012R627
M1T9S7	27	38	64.91	7.67	1.02	0.12	7.55	2012R642
M1T2S7.2	10	15	42.21	9.04	0.49	0.06	8.98	2012R612
M1T2S8.2	13	30	61.29	4.11	0.48	0.06	4.05	2012R613
M1T9S9	5	15	38.19	18.52	0.27	0.03	18.49	2012R643
M1T3S9.2	14	29	53.63	5.44	0.22	0.03	5.41	2012R614
M1T3S9.3	29	44	58.97	3.65	0.61	0.07	3.58	2012R615
M1T3S9.4	44	51	41.61	0.71	0.42	0.05	0.66	2012R616

MT2ILC1S1.0	0	5	24.80	8.13	1.14	0.14	7.99	R4752
MT2ILC1S1.1	5	13	16.20	3.35	0.90	0.11	3.24	R4760
MT2ILC1S2.0	0	5	58.80	17.82	0.82	0.10	17.72	R4771
MT2ILC2S1.0	0	5	52.40	8.91	0.76	0.09	8.82	R4770
MT2ILC2S1.1	5	20	46.30	5.10	0.61	0.07	5.02	R4757
MT2ILC2S1.2	20	34	29.50	2.19	0.58	0.07	2.12	R4769
MT2ILC2S2.0	0	8	28.60	1.65	0.82	0.10	1.55	R4753
MT2ILC2S2.1	5	20	47.40	5.99	0.85	0.10	5.88	R4762
MT2ILC2S2.1	5	20	45.10	8.45	0.77	0.09	8.36	R4766
MT2ILC2S2.2	20	35	66.90	31.88	2.10	0.25	31.63	R4763
MT2IM1S1.0	0	5	74.40	14.61	2.23	0.27	14.34	R4759
MT2IM1S1.1	5	13	31.80	2.95	0.95	0.11	2.84	R4767
MT2IM1S2.0	0	19	34.10	6.99	0.74	0.09	6.90	R4754
MT2IM2S1.0	0	5	69.20	12.66	0.67	0.08	12.58	R4768
MT2IM2S1.1	5	15	46.20	5.92	0.63	0.08	5.84	R4761
MT2IM2S1.2	15	32	23.50	3.11	0.76	0.09	3.02	R4765
MT2IM2S1.3	32	43	45.20	5.78	0.92	0.11	5.67	R4751
MT2IM2S2.0	0	11	20.70	0.27	0.47	0.06	0.21	R4756
MT2IUC1S1.0	0	11	42.90	15.39	0.90	0.11	15.28	R4758
MT2IUC2S1.0	0	10	61.90	19.97	0.82	0.10	19.87	R4755
MT2IUC2S1.1	10	20	68.80	30.13	1.08	0.13	30.00	R4764
MT2S1.1	5	20	17.30	1.43	0.72	0.09	1.34	R4746
MT2S1.2	20	36	33.70	2.46	0.75	0.09	2.37	R4747
MT2S1.3	36	50	34.40	1.91	0.79	0.09	1.81	R4748
MT2S1.4	50	63	39.10	1.35	0.74	0.09	1.26	R4749
MT2S1.5	63	73	34.30	1.07	0.73	0.09	0.98	R4750
MT2S3.1	2	19	81.40	29.21	1.71	0.21	29.00	R4745
MT2S4.0	0	15	35.90	33.50	1.87	0.22	33.28	R4742
MT2S4.1	15	25	9.40	23.28	0.83	0.10	23.18	R4743
MT2S4.2	25	40	12.90	27.25	0.69	0.08	27.17	R4744
MT2S5.1	9	25	37.10	3.67	0.73	0.09	3.58	R4741
MT2S6.0	0	15	45.20	6.09	0.56	0.07	6.02	R4739
MT2S6.1	15	34	23.10	2.24	0.77	0.09	2.15	R4740
MT2S7.0	0	6	66.00	29.81	1.39	0.17	29.64	R4736
MT2S7.1	6	21	50.50	7.51	0.40	0.05	7.46	R4737
MT2S7.2	21	35	38.20	3.83	0.50	0.06	3.77	R4738
MT2S9.1	1	13	32.00	3.41	0.75	0.09	3.32	R4735
OCKILC1IS1.0	4	8	24.30	1.59	0.64	0.08	1.51	R4460
OCKILC1IS1.1	8	16	28.30	2.00	0.87	0.10	1.89	R4459
OCKILC1IS2.1	4	11	37.30	3.64	0.61	0.07	3.57	R4458
OCKILC2IS1.0	0	15	19.50	3.31	0.66	0.08	3.23	R4457
OCKILC2IS1.1	15	30	53.10	13.70	0.75	0.09	13.61	R4456
OCKILC2IS1.2	30	42	51.90	20.53	0.72	0.09	20.44	R4455
MT2S1.0	0	5	87.50	33.01	0.97	0.12	32.89	R4477
MT2S1.1	5	15	83.10	25.72	0.67	0.08	25.64	R4476
OCKIUC2IS1.1	7	27	83.80	30.26	0.57	0.07	30.19	R4454
OCKIUC2IS1.2	27	36	35.10	6.35	0.68	0.08	6.27	R4453
OCKIUC2IS2.0	0	10	54.30	16.26	0.48	0.06	16.20	R4447
OCKIUC2IS2.1	10	19	54.60	31.81	0.63	0.08	31.73	R4452

OCKIUC2IS3.0	0	16	77.90	34.26	0.56	0.07	34.19	R4451
OCKIUCIS1.0	0	20	65.40	26.54	0.56	0.07	26.47	R4450
OCKIUCIS1.1	20	27	77.30	35.76	0.60	0.07	35.69	R4449
OCKIUCIS2.0	2	12	69.50	26.14	0.57	0.07	26.07	R4448
MT3S1.1	3	11	62.80	18.04	0.66	0.08	17.96	R4475
MT3S10.1	13	32	42.90	3.50	1.04	0.12	3.38	R4474
MT3S11.1	15	27	74.50	7.55	0.60	0.07	7.47	R4473
MT3S2.1	5	14	49.60	4.96	0.79	0.09	4.86	R4472
MT3S3.1	14	30	57.10	9.30	0.43	0.05	9.24	R4471
MT3S3.2	30	36	69.20	19.62	0.83	0.10	19.52	R4470
MT3S4.1	25	40	61.70	4.94	0.74	0.09	4.85	R4469
MT3S4.2	40	55	54.30	4.23	0.58	0.07	4.16	R4468
MT3S5.1	6	22	50.10	3.75	0.90	0.11	3.65	R4467
MT3S6.1	7	22	51.10	10.25	0.81	0.10	10.15	R4466
MT3S6.2	22	32	47.50	3.33	0.65	0.08	3.25	R4465
MT3S7.1	17	31	43.30	2.65	0.56	0.07	2.58	R4464
MT3S8.1	16	33	42.30	12.78	0.83	0.10	12.68	R4463
MT3S9.1	15	30	44.10	24.57	0.79	0.09	24.48	R4462
MT3S9.2	30	37	43.00	15.61	0.72	0.09	15.52	R4461
PC1LS1.1	11	25	24.12	1.83	0.08	0.01	1.82	R444
PC1RS1.1	7	22	13.19	2.94	0.02	0.00	2.93	R442
PC1RS1.2	22	37	6.13	1.69	0.22	0.03	1.66	R441
PC1RS1.3	37	39	7.69	3.39	0.44	0.05	3.33	R443
PC1LS10.1	8	23	8.28	3.41	0.10	0.01	3.40	R445
PC1LS10.2	23	38	17.88	3.84	0.23	0.03	3.81	R446
PC1L10.3	38	53	30.87	2.70	0.40	0.05	2.65	R448
PC1LS10.4	53	69	34.58	1.87	0.32	0.04	1.83	R447
PC1LS2.1	12	23	48.71	4.94	0.47	0.06	4.89	R452
PC1RS2.1	6	22	23.70	6.35	0.35	0.04	6.31	R453
PC1S3.0	0	4	13.33	20.95	0.09	0.01	20.94	R977
Pc1RS4.1	3	13	27.35	5.20	0.34	0.04	5.16	R460
PC1S5.0	0	18	26.39	4.70	0.59	0.07	4.63	R990
PC1LS5.1	18	33	31.72	3.08	0.59	0.07	3.01	R454
PC1RS5.1	6	22	16.15	4.89	0.31	0.04	4.85	R467
PC1LS5.2	33	40	34.60	1.39	0.39	0.05	1.35	R455
PC1RS5.2	22	37	21.01	4.01	0.33	0.04	3.97	R466
PC1RS5.4	37	57	20.80	1.11	0.16	0.02	1.09	R465
PC1RS5.5	57	74	22.86	0.76	0.23	0.03	0.73	R468
PC1RS5.6	74	83	25.65	0.61	0.37	0.04	0.56	R469
PC1LS6.1	9	24	12.63	1.97	0.40	0.05	1.93	R457
PC1RS6.1	7	22	16.94	3.14	0.23	0.03	3.12	R449
PC1RS6.2	22	33	16.91	2.20	0.18	0.02	2.17	R450
PC1S6.2	24	41	25.98	2.71	0.22	0.03	2.68	R985
PC1LS6.3	41	60	21.44	0.55	0.44	0.05	0.49	R456
PC1LS7.1	8	22	9.04	3.05	0.35	0.04	3.00	R458
PC1RS7.1	7	22	14.50	3.58	0.31	0.04	3.54	R451
PC1LS7.2	22	35	8.19	1.34	0.20	0.02	1.31	R459
PC1S7.2	22	25	12.06	4.30	0.19	0.02	4.28	R973
PC1S7.3	35	47	21.10	2.37	0.20	0.02	2.34	R979

PC1LS8.1	9	24	26.78	1.92	0.24	0.03	1.89	R462
PC1LS8.2	24	39	21.02	0.67	0.36	0.04	0.62	R461
PC1LS8.3	39	53	24.57	0.51	0.58	0.07	0.44	R464
PC1S8.4	53	60	11.97	0.56	0.08	0.01	0.55	R974
PC2S1.1	13	28	44.12	8.68	0.08	0.01	8.67	R3814
PC2S1.2	28	43	33.02	7.92	0.02	0.00	7.92	R3815
PC2S1.3	43	55	31.72	5.63	0.06	0.01	5.62	R3816
PC2S12.1	6	9	78.41	33.09	0.03	0.00	33.09	R3817
PC2S2.1	15	30	55.46	8.75	0.02	0.00	8.74	R3818
PC2S3.1	14	29	56.76	5.18	0.20	0.02	5.16	R3819
PC2S4.1	6	12	37.80	20.55	0.02	0.00	20.55	R3820
PC2S4.1	6	12	35.07	7.36	0.37	0.04	7.32	R504
PC2S5.1	7	18	18.52	0.31	0.01	0.00	0.31	R3821
PC2S6.1	6	19	14.42	3.29	0.01	0.00	3.29	R3822
PC2S7.1	7	18	7.77	1.78	0.66	0.08	1.70	R3823
PC3S1.1	7	20	6.71	2.06	0.23	0.03	2.03	R506
PC3S10.0	0	15	32.44	6.84	0.40	0.05	6.79	R3855
PC3S10.1	15	30	28.24	1.79	0.59	0.07	1.72	R3856
PC3S10.2	30	45	33.69	1.65	0.04	0.01	1.64	R976
PC3S10.3	45	60	36.40	0.73	0.24	0.03	0.70	R989
PC3S11.1	7	11	40.76	2.17	0.53	0.06	2.11	R3857
PC3S12.1	8	20	50.39	14.65	0.96	0.11	14.54	2013R514
PC3S13.1	6	17	17.08	2.33	0.41	0.05	2.28	R512
PC3S14.1	9	24	42.39	8.66	0.74	0.09	8.57	R505
PC3S14.2	24	39	32.72	0.91	0.59	0.07	0.84	R3858
PC3S14.3	39	51	52.64	0.91	0.50	0.06	0.85	R3859
PC3S2.1	10	17	8.24	2.75	0.44	0.05	2.70	R509
PC3S3.0	0	3	3.21	3.62	0.52	0.06	3.56	R510
PC3S3.1	3	11	4.10	1.29	0.81	0.10	1.19	R511
PC3S4.1	8	20	21.35	6.77	0.45	0.05	6.72	R513
PC3S5.1	10	25	27.74	4.31	0.40	0.05	4.27	R980
PC3S5.2	25	40	28.57	5.62	0.10	0.01	5.60	R984
PC3S6.1	9	26	34.69	3.61	0.08	0.01	3.60	R982
PC3S6.2	26	36	31.74	2.90	0.18	0.02	2.88	R981
PC3S7.1	5	13	14.65	2.80	0.17	0.02	2.78	R988
PC3S8.1	8	11	7.76	5.86	1.00	0.12	5.74	R507
PC3S9.1	9	15	3.20	1.20	0.88	0.11	1.09	R508
PC4S1.1	7	22	25.51	5.56	0.26	0.03	5.52	R902
PC4S1.2	22	35	7.13	0.47	0.15	0.02	0.45	R903
PC4S10.1	9	23	33.23	4.59	0.20	0.02	4.56	R904
PC4S11.1	7	17	26.09	6.18	0.49	0.06	6.12	R905
PC4S2.1	7	22	52.68	9.04	0.15	0.02	9.03	R906
PC4S2.2	22	32	23.71	2.08	0.26	0.03	2.05	R907
PC4S3.1	5	20	22.87	1.47	0.15	0.02	1.45	R908
PC4S3.2	20	35	41.75	1.28	0.34	0.04	1.24	R909
PC4S3.3	35	50	31.70	2.27	0.10	0.01	2.25	R910
PC4S3.4	50	57	31.67	1.99	0.16	0.02	1.97	R911
PC4S4.1	10	25	42.70	4.64	0.33	0.04	4.60	R912
PC4S6.1	11	26	9.71	0.53	0.12	0.01	0.52	R913

PC4S6.2	26	41	46.62	1.85	0.55	0.07	1.78	R914
PC4S6.3	41	58	35.19	2.78	0.01	0.00	2.78	R915
PC4S7.1	6	21	33.94	1.35	0.17	0.02	1.33	R916
PC4S7.2	21	36	21.05	0.77	0.16	0.02	0.75	R917
PC4S7.3	36	40	12.90	0.82	0.42	0.05	0.77	R918
PC4S8.1	11	24	38.46	2.07	0.53	0.06	2.01	R919
PC4S9.1	10	25	44.05	3.48	0.49	0.06	3.42	R920
PC4S9.2	25	40	18.90	0.68	0.31	0.04	0.64	R921
PC5S1.1	2	18	20.09	4.90	0.35	0.04	4.85	R922
PC5S1.2	17	32	17.86	1.89	0.22	0.03	1.86	R923
PC5S1.3	32	44	19.75	2.18	0.11	0.01	2.17	R924
PC5S10.1	1	16	16.47	3.71	0.02	0.00	3.71	R925
PC5S10.2	16	31	12.55	2.69	0.10	0.01	2.67	R926
PC5S10.3	31	38	8.40	1.49	0.24	0.03	1.46	R927
PC5S10a	0	47	14.96	2.36	0.35	0.04	2.32	R564
PC5S11.1	2	17	17.63	3.45	0.14	0.02	3.43	R928
PC5S2.1	2	17	30.20	4.56	0.24	0.03	4.53	R929
PC5S2.2	17	32	17.99	1.13	0.36	0.04	1.09	R930
PC5S2.3	32	42	17.04	0.78	0.26	0.03	0.75	R931
PC5S3.1	2	5	9.11	1.19	0.32	0.04	1.15	R932
PC5S4.1	6	21	18.64	4.15	0.30	0.04	4.11	R934
PC5S4.2	21	37	19.95	2.56	0.40	0.05	2.51	R935
PC5S4.3	37	52	21.38	2.41	0.14	0.02	2.39	R936
PC5S4.4	52	69	21.88	1.30	0.49	0.06	1.24	R937
PC5S4.5	69	78	26.63	1.44	0.34	0.04	1.40	R938
PC5S4a	0	34	32.93	5.21	0.31	0.04	5.17	R558
PC5S5.1	1	17	40.25	8.07	0.31	0.04	8.04	R939
PC5S5.2	17	25	31.80	3.41	0.30	0.04	3.37	R940
PC5S5a	0	44	15.00	0.28	0.47	0.06	0.22	R559
PC5S6.1	1	16	32.45	5.21	0.69	0.08	5.12	R941
PC5S6.2	16	31	36.47	2.38	0.40	0.05	2.33	R942
PC5S6.3	31	46	25.93	2.30	0.51	0.06	2.24	R943
PC5S6.4	46	62	23.97	1.69	0.24	0.03	1.66	R944
PC5S6.5	62	71	40.56	0.62	0.11	0.01	0.60	R933
PC5S6a	0	45	30.35	2.31	0.32	0.04	2.27	R560
PC5S7.1	1	16	29.55	2.80	0.15	0.02	2.78	R945
PC5S7a	0	42	37.55	3.67	0.41	0.05	3.62	R561
PC5S8.1	3	20	24.85	5.99	0.60	0.07	5.92	R946
PC5S8.2	20	28	19.47	3.51	0.26	0.03	3.48	R947
PC5S8a	0	42	29.26	1.90	0.38	0.05	1.86	R562
PC5S9.1	1	16	21.85	5.39	0.23	0.03	5.36	R948
PC5S9.2	16	31	20.74	3.70	0.55	0.07	3.63	R949
PC5S9.3	31	47	25.20	1.10	0.66	0.08	1.02	R950
PC5S9.4	47	57	24.68	1.14	0.36	0.04	1.10	R951
PC5S9a	0	54	22.92	2.98	0.40	0.05	2.93	R563
PC6S1.2	5	20	62.60	23.13	0.04	0.01	23.12	R4649
PC6S1.3	20	35	86.20	74.15	0.08	0.01	74.14	R4650
PC6S1.4	35	54	83.50	30.13	0.34	0.04	30.09	R4651
PC6S10.1	2	17	64.40	15.76	0.28	0.03	15.73	R4652

PC6S10.2	17	32	57.50	12.79	0.03	0.00	12.79	R4653
PC6S10.3	32	50	71.50	18.95	0.18	0.02	18.93	R4654
PC6S10.4	50	60	71.20	19.55	0.00	0.00	19.55	R4655
PC6S11.1	5	20	67.70	17.82	0.31	0.04	17.78	R4656
PC6S11.2	20	35	55.47	13.51	0.14	0.02	13.49	R4657
PC6S11.4	50	65	47.10	12.90	0.25	0.03	12.87	R4659
PC6S11.5	65	67	48.00	12.86	0.06	0.01	12.85	R4660
PC6S2.1	2	17	77.60	19.76	0.42	0.05	19.71	R4661
PC6S2.2	17	32	81.90	28.74	0.26	0.03	28.71	R4662
PC6S2.3	32	47	76.70	28.85	0.41	0.05	28.80	R4663
PC6S2.4	47	60	81.80	27.41	0.16	0.02	27.39	R4664
PC6S3.1	2	17	62.80	14.08	0.31	0.04	14.04	R4665
PC6S3.2	17	31	61.30	11.58	0.37	0.04	11.54	R4666
PC6S4.1	3	18	10.30	1.69	0.14	0.02	1.68	R4667
PC6S4.2	18	33	11.50	1.36	0.18	0.02	1.33	R4668
PC6S4.3	33	48	32.40	14.63	0.31	0.04	14.59	R4669
PC6S5.1	6	21	11.50	1.61	0.23	0.03	1.58	R4670
PC6S5.2	21	36	9.30	2.89	0.20	0.02	2.87	R4671
PC6S5.3	36	47	29.70	4.62	0.26	0.03	4.59	R4672
PC6S6.1	2	7	6.00	3.78	0.18	0.02	3.75	R4673
PC6S7.1	15	30	33.80	4.04	0.35	0.04	3.99	R4674
PC6S7.2	30	40	65.40	16.88	0.20	0.02	16.86	R4675
PC6S8.1	2	17	14.00	3.56	0.26	0.03	3.53	R4676
PC6S8.2	17	32	13.70	0.57	0.50	0.06	0.51	R4677
PC6S8.3	32	47	28.70	4.12	0.49	0.06	4.06	R4678
PC6S8.4	47	62	41.60	6.93	0.18	0.02	6.91	R4679
PC6S8.5	62	77	36.50	4.17	0.43	0.05	4.12	R4680
PC6S8.6	77	88	32.20	1.99	0.43	0.05	1.94	R4681
PC6S9.1	2	17	18.10	2.17	0.33	0.04	2.13	R4682
PC6S9.2	17	32	64.10	4.92	0.24	0.03	4.89	R4683
PC6S9.3	32	47	64.90	13.40	0.19	0.02	13.38	R4684
PC6S9.4	47	52	35.90	3.37	0.26	0.03	3.33	R4685
PC7S1.2	25	40	29.55	2.65	0.33	0.04	2.61	R524
PC7S10	0	15	17.06	2.33	0.34	0.04	2.29	R555
PC7S10.1	15	30	20.06	2.41	0.34	0.04	2.37	R556
PC7S10.2	30	38	22.73	1.76	0.26	0.03	1.73	R557
PC7S2.1A	9	25	40.85	7.65	0.23	0.03	7.62	R525
PC7S2.2	25	40	33.76	1.43	0.20	0.02	1.40	R526
PC7S3.1	1	16	37.99	5.89	0.31	0.04	5.85	R527
PC7S3.2	16	31	24.32	0.62	0.41	0.05	0.58	R528
PC7S3.3	31	46	31.83	2.32	0.39	0.05	2.27	R529
PC7S3.4	46	61	40.13	2.05	0.17	0.02	2.03	R530
PC7S3.5	61	79	32.36	0.88	0.23	0.03	0.85	R531
PC7S4.1	10	25	26.12	0.68	0.10	0.01	0.67	R532
PC7S4.2	25	40	37.92	2.49	0.20	0.02	2.47	R533
PC7S4.3	40	55	27.89	1.35	0.32	0.04	1.31	R534
PC7S5.1	10	25	33.12	6.26	0.45	0.05	6.21	R535
PC7S5.2	25	40	30.73	2.91	0.41	0.05	2.86	R536
PC7S5.3	40	55	30.50	1.73	0.16	0.02	1.71	R537

PC7S5.4	55	72	23.71	0.62	0.26	0.03	0.59	R538
PC7S5.5	72	92	33.47	1.02	0.14	0.02	1.00	R539
PC7S6.1	3	18	36.95	7.27	0.27	0.03	7.23	R540
PC7S6.2	18	33	31.21	4.94	0.36	0.04	4.90	R541
PC7S6.3	33	48	23.68	0.75	0.15	0.02	0.73	R542
PC7S6.4	48	60	18.37	0.75	0.30	0.04	0.71	R543
PC7S7.1	8	23	70.72	12.92	0.25	0.03	12.89	R544
PC7S7.2	23	38	80.27	20.65	0.24	0.03	20.62	R545
PC7S7.3	38	53	84.65	14.72	0.49	0.06	14.66	R546
PC7S7.4	53	68	48.46	3.79	0.33	0.04	3.75	R547
PC7S7.5	68	83	68.93	13.99	0.25	0.03	13.96	R548
PC7S7.6	83	92	64.05	3.31	0.28	0.03	3.27	R549
PC7S8.0	0	15	10.06	1.90	0.23	0.03	1.87	R550
PC7S8.1	15	20	10.52	1.44	0.26	0.03	1.41	R551
PC7S9.1	1	16	14.83	2.47	0.33	0.04	2.43	R552
PC7S9.2	16	31	12.46	1.53	0.18	0.02	1.51	R553
PC7S9.3	31	47	16.12	0.68	0.51	0.06	0.62	R554
UC1S1.1	2	10	58.55	6.86	0.52	0.06	6.80	R952
UC1S10.1	3	20	81.18	55.20	0.55	0.07	55.13	R953
UC1S10.2	20	35	82.22	19.98	0.39	0.05	19.93	R954
UC1S10.3	35	51	60.61	3.06	0.39	0.05	3.02	R955
UC1S11.1	3	20	41.26	3.65	0.15	0.02	3.63	R956
UC1S11.2	20	31	21.50	2.66	0.16	0.02	2.64	R957
UC1S2.1	1	12	78.76	17.87	0.26	0.03	17.84	R958
UC1S3.1	3	20	66.16	45.03	0.45	0.05	44.98	R959
UC1S3.2	20	35	68.07	30.98	0.50	0.06	30.92	R960
UC1S3.3	35	47	66.88	9.29	0.72	0.09	9.20	R961
UC1S4.1	8	23	76.32	29.42	0.55	0.07	29.35	R962
UC1S4.2	23	31	77.89	25.87	0.05	0.01	25.86	R1209
UC1S5.1	7	21	56.29	47.65	0.26	0.03	47.62	R963
UC1S6.1	2	17	62.41	37.48	0.34	0.04	37.44	R964
UC1S6.2	17	32	44.25	5.10	0.69	0.08	5.02	R965
UC1S6.3	32	47	34.99	2.39	0.10	0.01	2.37	R966
UC1S6.4	47	69	37.17	2.32	0.02	0.00	2.32	R967
UC1S6.5	69	71	33.47	1.98	0.10	0.01	1.96	R968
UC1S7.1	3	18	61.34	33.00	0.25	0.03	32.97	R969
UC1S7.2	18	26	45.85	6.13	0.06	0.01	6.12	R970
UC1S8.1	5	18	48.67	3.80	0.10	0.01	3.79	R971
UC1S9.1	2	12	68.72	18.01	0.01	0.00	18.01	R972
UC2S1.1	5	20	61.00	28.50	0.54	0.06	28.44	R4686
UC2S1.2	20	29	52.20	13.95	0.34	0.04	13.91	R4687
UC2S10.1	8	23	62.70	15.19	0.40	0.05	15.14	R4688
UC2S10.2	23	38	63.70	10.40	0.14	0.02	10.38	R4689
UC2S10.3	38	53	62.80	5.32	0.19	0.02	5.30	R4690
UC2S10.4	53	57	37.70	6.66	0.27	0.03	6.63	R4691
UC2S11.1	12	27	75.20	18.60	0.34	0.04	18.56	R4692
UC2S11.2	27	43	34.20	3.64	0.40	0.05	3.59	R4693
UC2S11.3	43	58	34.60	2.13	0.14	0.02	2.11	R4694
UC2S2.1	5	16	73.60	26.49	0.26	0.03	26.46	R4695

UC2S3.1	4	19	75.30	21.05	0.12	0.01	21.04	R4696
UC2S3.10	146	161	23.40	2.35	0.07	0.01	2.34	R4697
UC2S3.11	161	165	22.90	1.26	0.18	0.02	1.23	R4698
UC2S3.2	19	34	75.20	17.22	0.09	0.01	17.21	R4699
UC2S3.3	34	49	61.20	12.04	0.44	0.05	11.99	R4700
UC2S3.4	49	64	64.00	4.09	0.11	0.01	4.08	R4701
UC2S3.5	64	79	39.40	5.77	0.22	0.03	5.75	R4702
UC2S3.6	79	94	30.40	4.67	0.07	0.01	4.67	R4703
UC2S3.7	94	112	26.60	1.51	0.07	0.01	1.50	R4704
UC2S3.8	112	127	45.20	2.49	0.35	0.04	2.44	R4705
UC2S3.9	127	146	27.20	3.28	0.16	0.02	3.26	R4706
UC2S4.1	3	18	64.20	5.33	0.37	0.04	5.28	R4707
UC2S4.21	18	33	50.00	4.21	0.20	0.02	4.18	R4708
UC2S4.3	33	37	71.90	1.68	0.22	0.03	1.66	R4709
UC2S5.1	3	18	51.40	9.98	0.17	0.02	9.96	R4710
UC2S6.1	3	18	57.90	5.96	0.14	0.02	5.94	R4711
UC2S6.2	18	33	56.70	13.78	0.19	0.02	13.76	R4712
UC2S6.3	33	48	52.70	8.79	0.33	0.04	8.75	R4713
UC2S7.1	9	24	77.30	21.88	0.44	0.05	21.83	R4714
UC2S7.2	24	35	60.10	11.68	0.32	0.04	11.64	R4715
UC2S8	3	18	54.80	11.56	0.12	0.01	11.55	R4716
UC2S8.1	18	33	59.40	15.87	0.31	0.04	15.83	R4717
UC2S8.2	33	47	63.90	16.67	0.22	0.03	16.64	R4718
UC2S9.1	4	19	79.40	21.35	0.35	0.04	21.31	R4719
UC2S9.2	19	34	56.30	23.81	0.58	0.07	23.74	R4720
UC3S1.1	16	33	54.50	5.27	1.38	0.17	5.10	R3810
UC3S1.2	33	50	41.10	3.37	1.20	0.14	3.23	R3811
UC3S1.3	50	65	56.70	6.38	1.17	0.14	6.24	R3812
UC3S1.5	65	80	50.90	6.00	12.72	1.53	4.47	R3813
UC3S10.1	6	21	41.00	5.88	1.87	0.22	5.66	R3814
UC3S10.2	21	28	31.00	1.78	1.50	0.18	1.60	R3815
UC3S11.1	15	30	57.20	9.94	2.03	0.24	9.69	R3816
UC3S11.2	30	45	39.20	4.05	1.26	0.15	3.90	R3817
UC3S11.3	45	60	38.00	0.92	1.17	0.14	0.78	R3818
UC3S11.4	60	78	58.40	5.65	1.10	0.13	5.52	R3819
UC3S2.1	8	26	36.20	4.74	1.41	0.17	4.57	R3820
UC3S2.2	26	41	41.30	4.87	0.99	0.12	4.75	R3821
UC3S2.3	41	56	39.40	4.53	0.99	0.12	4.41	R3822
UC3S2.4	56	72	40.30	4.56	1.21	0.15	4.41	R3823
UC3S2.5	72	83	40.30	3.87	1.39	0.17	3.70	R3824
UC3S2.6	83	92	33.30	0.73	1.29	0.15	0.57	R3825
UC3S3.1	8	25	26.20	6.72	1.45	0.17	6.54	R3826
UC3S3.2	25	43	25.90	5.64	1.25	0.15	5.49	R3827
UC3S3.3	43	60	39.30	4.11	1.30	0.16	3.95	R3828
UC3S3.4	60	75	40.40	4.66	1.85	0.22	4.44	R3829
UC3S3.5	75	90	48.70	4.82	1.71	0.21	4.61	R3830
UC3S3.7	90	110	45.30	5.35	1.44	0.17	5.18	R3831
UC3S3.8	110	120	51.10	6.84	1.64	0.20	6.64	R3832
UC3S4.1	7	27	42.50	6.72	1.22	0.15	6.57	R3833

UC3S5.1	7	20	53.20	13.49	1.71	0.21	13.28	R3834
UC3S6.1	4	19	55.30	11.15	1.15	0.14	11.01	R3835
UC3S6.2	19	38	32.20	2.58	1.16	0.14	2.44	R3836
UC3S6.3	38	58	30.30	2.37	1.37	0.16	2.20	R3837
UC3S6.4	58	75	37.90	3.99	1.40	0.17	3.82	R3838
UC3S6.5	75	91	26.60	0.84	0.93	0.11	0.73	R3839
UC3S6.6	91	100	37.50	1.27	1.12	0.13	1.14	R3840
UC3S7.1	12	29	54.50	11.35	1.31	0.16	11.19	R3841
UC3S7.2	29	44	31.80	1.67	1.71	0.21	1.47	R3842
UC3S7.3	44	60	29.80	2.12	0.81	0.10	2.02	R3843
UC3S7.4	60	75	31.10	1.63	1.18	0.14	1.48	R3844
UC3S8.1	6	15	57.40	8.17	1.12	0.13	8.03	R3845
UC3S8.2	7	34	34.20	3.10	1.25	0.15	2.95	R3846
UC3S8.3	34	51	42.20	4.35	1.37	0.16	4.18	R3847
UC3S8.4	51	71	36.70	3.55	1.29	0.15	3.39	R3848

7.3 Appendix C. Radiocarbon age data

Table 7.8. Un-calibrated radiocarbon ages

Sample ID	Delta ^{13}C (per mil)	Radiocarbon age (y BP)	1 sigma error
AB4S6.3	-19.3	1110	29
AB4S10.4	-15.4	1887	24
AB4S12	-15.6	581	25
UC1S8.1	-25	350	69
UC1S6.4	-22.5	1931	31
MT1S2.0	-21.1	1332	22
MT1S2.1	-18.9	1274	24
MT1S2.2	-19.6	1831	23
MT1S2.3	-17.1	1952	23
MT1S3.0	-17.4	538	22
MT1S4.1	-17.9	657	27
MT1S5.0	-18.5	602	22
MT1S6.0	-19.4	595	23
MT1S6.1	-21.4	870	25
MT1S7.2	-17.6	1968	26
MT1S12	-18.7	1654	24
MT1S14	-24.1	2009	23
MT1S16	-23.2	1872	25
MT1S17	-18.4	1876	25
MT1S20	-22.1	1761	22
AB1S2.2	-20.2	909	23
AB1S3.1	-23.1	121	23
AB1S4.2	-21.6	2989	23
AB1S4.3	-18.8	5267	28
AB1S6.2	-21.2	1256	23
AB1S8.3	-20.7	2131	23
PC1RS1.1	-24.9	300	23
PC1RS1.3	-22.8	324	22
PC1RS5.2	-24.9	1665	28
PC1LS8.3	-22.3	1208	21
PC1LS10.3	-24.5	599	23
PC1S7.2	-28.7	201	26
PC1RS6.2	-23.9	524	23
PC1RS5.5	-17.7	1089	29
PC1LS10.4	-14.5	342	32
PC2S1.3	-20.7	84	28
PC2S3.1	-18.4	134	30
PC2S4.1	-22.6	337	27
PC4S3.3	-22.2	1780	22
PC4S4.1	-24.8	1875	21
PC4S6.2	-20.3	370	21
PC4S3.4	-22.9	1695	31
PC4S6.3	-20.8	1503	25
PC4S7.2	-22.8	1116	28
PC5S6.2	-21.1	48	20
PC5S6.3	-24.5	68	21
PC5S8.1	-21.7	225	22
PC5S10.1	-27.6	861	29
PC5S10.2	-23.4	279	24
PC5S8.2	-14.6	181	28
PC5S1.3	-19.9	1240	27
PC5S9.2	-22.3	1240	29

Table 7.9. Calibrated radiocarbon ages using OxCal calibration software and the IntCal13 calibration curve.

Sample ID	Maximum age (y BP)	Minimum age (y BP)	Mean calibrated age (y BP)	sigma error (y BP)	Mean calibrated age (y BP)	Elevation (m)
AB1S2.2	914	765	844	44	852	2905
AB1S3.1	270	12	135	78	114	2905
AB1S4.2	3232	3075	3164	46	3170	2905
AB1S4.3	6179	5939	6053	70	6052	2905
AB1S6.2	1278	1090	1214	38	1220	2905
AB1S8.3	2296	2008	2117	60	2115	2905
PC1RS1.1	453	300	378	44	390	2469
PC1RS1.3	461	308	385	44	386	2469
PC1RS5.2	1690	1522	1572	38	1567	2469
PC1LS8.3	1223	1065	1130	40	1128	2469
PC1LS10.3	651	543	601	31	604	2469
PC1S7.2	300	55	172	93	176	2469
PC1RS6.2	622	511	540	25	534	2469
PC1RS5.5	1058	936	1000	36	995	2469
PC1LS10.4	484	310	396	52	392	2469
PC4S3.3	1809	1618	1691	47	1697	3027
PC4S4.1	1875	1735	1818	40	1827	3027
PC4S6.2	500	320	421	58	445	3027
PC4S3.4	1696	1538	1607	44	1598	3027
PC4S6.3	1517	1327	1388	39	1382	3027
PC4S7.2	1171	955	1019	38	1017	3027
PC5S6.2	253	33	85	66	53	2219
PC5S6.3	255	31	111	76	69	2219
PC5S8.1	308	55	211	88	185	2219
PC5S10.1	901	695	774	47	765	2219
PC5S10.2	432	286	357	56	370	2219
PC5S8.2	297	55	163	89	180	2219
PC5S1.3	1265	1075	1184	54	1197	2219
PC5S9.2	1266	1074	1182	55	1192	2219
PC2S1.3	260	25	125	77	105	2927
PC2S3.1	278	8	142	81	134	2927
PC2S4.1	476	311	392	49	388	2927
AB4S6.3	1071	938	1015	37	1013	2547
AB4S10.4	1888	1737	1833	37	1840	2547
AB4S12	647	536	594	33	605	2547
UC1S8.1	516	288	396	75	399	3054
UC1S6.4	1949	1817	1878	37	1879	3054
MT1S2.0	1300	1186	1269	28	1278	3035

MT1S2.1	1276	1180	1226	32	1229	3035
MT1S2.2	1824	1708	1768	35	1769	3035
MT1S2.3	1969	1827	1902	28	1901	3035
MT1S3.0	627	517	554	33	541	3035
MT1S4.1	671	559	613	38	601	3035
MT1S5.0	652	545	602	30	604	3035
MT1S6.0	651	541	600	31	605	3035
MT1S6.1	904	709	783	47	772	3035
MT1S7.2	1989	1870	1919	31	1917	3035
MT1S12	1617	1445	1558	33	1555	3035
MT1S14	2001	1896	1957	29	1958	3035
MT1S16	1875	1730	1811	43	1820	3035
MT1S17	1878	1733	1817	42	1826	3035
MT1S20	1731	1605	1666	35	1662	3035